23rd edition

HERVEX

ISSN 1454 - 8003

Proceedings of International Conference on HYDRAULICS, PNEUMATICS, TOOLS, SEALING ELEMENTS, FINE MECHANICS, SPECIFIC ELECTRONIC EQUIPMENT & MECHATRONICS

HERVEX 2017

November 8-10 | Băile Govora, ROMANIA

November 2017
23rd Edition

INTERNATIONAL CONFERENCE

HERVEX 2017

Hydraulics| Pneumatics| Sealing Elements| Fine Mechanics| Tools| Specific Electronic Equipment & Mechatronics

Baile Govora, ROMANIA | November 8 - 10, 2017

HERVEX 2017

ORGANIZERS

HYDRAULICS AND PNEUMATICS RESEARCH INSTITUTE
BUCHAREST, ROMANIA

CHAMBER OF COMMERCE AND INDUSTRY VALCEA, ROMANIA

PARTNERS

WROCLAW UNIVERSITY OF TECHNOLOGY, POLAND

TECHNICAL UNIVERSITY OF MOLDOVA IN CHISINAU, REPUBLIC OF MOLDOVA

“POLITEHNICA” UNIVERSITY OF BUCHAREST, ROMANIA

NATIONAL INSTITUTE OF RESEARCH & DEVELOPMENT FOR MACHINES AND INSTALLATIONS DESIGNED TO AGRICULTURE AND FOOD INDUSTRY – INMA BUCHAREST, ROMANIA

“POLITEHNICA” UNIVERSITY OF TIMISOARA, ROMANIA

TECHNICAL UNIVERSITY OF CLUJ-NAPOCA, ROMANIA

MEDIA PARTNERS

HIDRAULICA
HYDRAULICS-PNEUMATICS-TRIBOLOGY-ECOLOGY-SENSORICS-MECHATRONICS

Partener European

CONFERENCE HELD UNDER HONORARY AEGIS OF

Comité Européen des Transmissions Oléohydrauliques et Pneumatiques
CETOP

Published by - Hydraulics and Pneumatics Research Institute, Bucharest, Romania
- Chamber of Commerce and Industry Valcea, Romania

INTERNATIONAL CONFERENCE

HERVEX 2017

IS SUPPORTED BY:

MINISTRY OF RESEARCH AND INNOVATION

NATIONAL PROFESSIONAL ASSOCIATION OF HYDRAULICS AND PNEUMATICS IN ROMANIA - "FLUIDAS"

Conference Proceedings is indexed by:

COMMITTEES

HONORARY COMMITTEE

Dr. Stefan KÖNIG – President of European Fluid Power Committee – CETOP

Prof. PhD.Eng. Henryk CHROSTOWSKI – Wroclaw University of Technology, Poland

PhD.Eng. Hubertus MURRENHOFF – Institute for Fluid Power Drives and Controls at Aachen University, Germany

PhD.Eng. Petrin DRUMEA – President of National Professional Association of Hydraulics and Pneumatics – FLUIDAS, Romania

ORGANIZING COMMITTEE

Dipl. Eng. Gheorghe RIZOIU – General Manager of Chamber of Commerce and Industry Valcea, Romania

PhD. Eng. Gabriela MATACHE – Hydraulics and Pneumatics Research Institute in Bucharest, Romania

Assoc.Prof. PhD.Eng. Constantin RÂNEA – Romanian Ministry of National Education and Scientific Research

Prof. PhD. Eng. Viorel BOSTAN – Rector of Technical University of Moldova, Republic of Moldova

PhD. Eng. Krzysztof KEDZIA – Wroclaw University of Technology, Poland

Prof. PhD. Eng. Dan OPRUȚA – Technical University of Cluj-Napoca, Romania

Prof. PhD. Eng. Ilare BORDEAȘU – Politehnica University of Timisoara, Romania

Prof. PhD. Eng. Adrian CIOCĂNEA – Politehnica University of Bucharest, Romania

PhD.Eng. Sergiu NICOLAIE – General Manager of R&D National Institute for Electrical Engineering ICPE-Advanced Researches, Bucharest, Romania

PhD.Eng. Nicolae-Valentin VLĂDUȚ – General Manager of National Institute of Research and Development for Machines and Installations Designed to Agriculture and Food Industry – INMA Bucharest, Romania

SCIENTIFIC PROGRAMMEE COMMITTEE

PhD.Eng. Mohamed HAJJAM – University of Poitiers – IUT Angouléme, France

PhD.Eng. Zygmunt DOMAGALA – Wroclaw University of Technology, Poland

Prof. PhD.Eng. Pavel MACH – Technical University of Praga, Czech Republic

Prof. PhD.Eng. Vasile JAVGUREANU – Technical University of Moldova, Republic of Moldova

Phd.Eng. Catalin DUMITRESCU – Director of Hydraulics and Pneumatics Research Institute in Bucharest, Romania

PhD.Eng. Ioan LEPADATU – Hydraulics and Pneumatics Research Institute in Bucharest, Romania

PhD.Eng. Wilhelm KAPPEL – Scientific Manager of R&D National Institute for Electrical Engineering ICPE-Advanced Researches, Bucharest, Romania

Prof. PhD.Eng. Gheorghe I. GHEORGHE – General Manager of National Institute of Research and Development in Mechatronics and Measurement Technique (INCDMTM), Bucharest, Romania

Dipl.Eng. Valentin CISMARU – President of Chamber of Commerce and Industry Valcea, Romania

Prof.Dr.Ing. Andrzej SOBCZYK – Cracow University of Technology, Poland

Prof. PhD.Eng. Mihai AVRAM – Politehnica University of Bucharest, Romania

Prof. PhD.Eng. Cristian PAVEL – Technical University of Civil Engineering in Bucharest, Romania

PhD.Eng. Cornelia MURARU-IONEL – National Institute of Research and Development for Machines and Installations Designed to Agriculture and Food Industry – INMA Bucharest, Romania

PhD.Eng. Diana BADEA – National Institute of Research and Development in Mechatronics and Measurement Technique (INCDMTM), Bucharest, Romania

Prof. PhD.Eng. Alexandru MARIN – Politehnica University of Bucharest, Romania

Prof. PhD.Eng. Liviu VAIDA – Technical University of Cluj-Napoca, Romania

Prof. PhD.Eng. Doru Dumitru PALADE – National Institute of Research and Development in Mechatronics and Measurement Technique (INCDMTM), Bucharest, Romania

PhD.Eng. Andrei DRUMEA – Politehnica University of Bucharest, Romania

Prof. PhD.Eng. Doru CALARASU – Technical University “Gheorghe Asachi” in Iasi, Romania

Prof. PhD.Eng. Ion DAVID – Technical University of Civil Engineering in Bucharest, Romania

Prof. PhD.Eng. Gheorghe VOICU – Politehnica University of Bucharest, Romania

Prof. PhD.Eng. Edmond MAICAN – Politehnica University of Bucharest, Romania

PhD.Eng. Mihai Gabriel MATACHE – National Institute of Research – Development for Machines and Installations Designed to Agriculture and Food Industry – INMA, Bucharest- Romania

PhD.Eng. Mircea PRICOP - S.C. HESPER S.A., Bucharest, Romania

PhD.Eng. Ioan Lucian MARCU – Technical University of Cluj-Napoca, Romania

Prof. PhD.Eng. Valeriu BANU – S.M.C. Romania

Dipl. Eng. Ioan CAMPEAN – S.C. HIDROSIB S.A. Sibiu, Romania

Dipl. Eng. Mircea DANCIU – PARKER HANNIFIN Corporation, Romania

Dipl. Eng. Leopold LUPUSANSCHI - S.C. CEROB S.R.L. Bucharest, Romania

PhD.Eng. Daniel MARIN - S.C. FAST ECO S.A., Bucharest, Romania

PhD.Eng. Adrian MIREA – S.C. FAST ECO S.A., Bucharest, Romania

Dipl. Eng. Ioan MOLDOVEANU – Festo S.R.L., Bucharest, Romania

Dipl. Eng. Nicolae TASU – HANSA FLEX Romania

Phd.Eng. Iulian-Claudiu DUȚU – Politehnica University of Bucharest, Romania

CONTENTS

SECTION II: MOBILE HYDRAULICS, PNEUMAICS AND TRIBOLOGY

SECTION III: HYDRAULIC SYSTEMS, STANDS AND COMPLEX EQUIPMENT

ISSN 1454 - 8003
Proceedings of 2017 International Conference on Hydraulics and Pneumatics - HERVEX
November 8-10, Băile Govora, Romania

EXPERIMENTAL DESIGN, MODELLING AND NUMERICAL CALIBRATION OF A HIGH SPEED SHPB MECHATRONIC SYSTEM USING A PNEUMATIC PROPULSION DEVICE

Adinel GAVRUS[1], Fabien MARCO[2], Sylvain GUEGAN[3]

[1]INSA Rennes, LGCGM-EA3913, University Bretagne Loire, Rennes, France, adinel.gavrus@insa-rennes.fr

[2]fabien.marco@insa-rennes.fr

[3]sylvain.guegan@insa-rennes.fr

Abstract: *This research paper focus on the experimental design and analytical/numerical analysis of a high speed pneumatic compression SHPB bench performed at INSA Rennes (France) – LGCGM Laboratory. The main goals are to present details concerning an improved mechatronic data acquisition system, the performances of the air propulsion system in terms of impact velocities prediction and measurement, together with a novel hybrid analytical-numerical calibration method. This proposed SHPB calibration and numerical analysis method is based on a complete finite element simulation starting from a dynamic elastic equilibrium model and the dynamic mechanical interactions at the interfaces between the striker bar undergoing high pressure air-impact speed propulsion, the incident and the sending bars. As real application of proposed complete FE model has been mentioned the previous and actual research works at INSA Rennes on the use of a two-step inverse analysis technique to identify thermo-mechanical constitutive equations of materials subjected to high strain rates and important gradients of plastic strain, strain-rate and temperature.*

Keywords*: Pneumatic SHPB Device, Mechatronic Design, Impact Velocity Estimation, Analytical-Numerical Calibration, Complete SHPB Finite Element Modelling, Hybrid Analytical-Numerical Model Validation*

1. Introduction

During many manufacturing processes or industrial applications developed in the second half of the 20th century, various metallic or non-metallic structures are subjected to high rates of loadings, severe elastoplastic strains, strain rates and temperatures or localized gradients of strain-stress developed during an impact, choc or crash. The modelling of corresponding material thermos-mechanical behavior becomes a real scientific key which requires design of corresponding dynamic experimental tests together with the use of a rigorous calibration method and reliable data analysis via improved analytical or numerical models. According to the high strain rates which occur during these dynamic tests, elastic waves propagate in the system bench and specimen material at speeds of several kilometers per second. Therefore it is difficult to have an intuitive understanding of the observed physical phenomena. In order to perform quality measurements during the dynamic deformations obtained from rapid loadings, it is nevertheless necessary to take account the description of elastic wave propagation phenomena. The first high-speed mechanical stress tests were conducted around 1870 by John Hopkinson who developed a type of apparatus based on a specific mechanisms to impact a cylindrical bar. In 1914, Bertram Hopkinson [1] introduced a pressure bar to study dynamic events such as the explosive detonation or the impact of different types of projectiles. Essentially, the Hopkinson pressure bar uses the propagation of elastic strain wave's theory to predict strains and stress developed in a material sample. Hopkinson discovered that the small local displacements in the bar are directly related to the length of the elastic wave obtained during the very short times of the impact caused by the material sound celerity. In the case of materials subjected to an impact through a projectile Davies [2] shows in 1948 that it is possible to measure the temporal form of the generated elastic wave using strain gauges instrumented bar. Starting from these previous old studies the first Split Hopkinson Pressure Bars system (SHPB) was introduced in 1949 by Kolsky [3] which has used a gas propulsion device to obtain high speed of a projectile bar and add two other metallic bars (named incident and sending bars) to realize a dynamic compression. Typically the SHPB device offers material testing capabilities for speeds up to 30-40 m/s at strain rates in the range of 10^2 to 10^4 s^{-1}. A lot of other dynamic experimental set-up has been developed further: the Taylor test (gas or explosive propulsion around of 100 m/s), Crossbow device (speed up to 10-30 m/s), Weight Falling, traction or torsion Hopkinson Bars and more recently specific hydraulic press using particular actuators and control devices (speed up to 10 m/s).

The main purpose of this scientific paper is to describe a mechatronic SHPB compression test designed on GCGM Laboratory (INSA Rennes) using a pneumatic propulsion with a robust control of air pressure, laser camera measurement of projectile bar speed, automatic electronic data acquisition of bar's elastic deformations and a calibration method developed from a hybrid analytical and numerical finite element system modelling.

2. Experimental Principle of Pneumatic SHPB System

Kolsky found that the stress and the deformation of an impacted specimen can be directly related to the displacements of the incident and sending bars. Contrary of the Hopkinson pressure bar, in the SHPB device the projectile does not strike directly the specimen. It is first a receiving or incident bar that receives the impact of the projectile (striker bar) and that is subjected to a lot of dynamic elastic deformation pulse. The obtained elastic wave of the receiving bar it is more intense as the speed of projectile is high and is lasts time longer as the projectile is long. This wave is reflected partially by the material sample, the other part passes through it and is subsequently transmitted to a second bar (named sending or transmitter bar) [4-7].

2.1 Framework and design characteristics

The SHPB system designed at GCGM Laboratory of INSA Rennes is presented in the Figure 1.

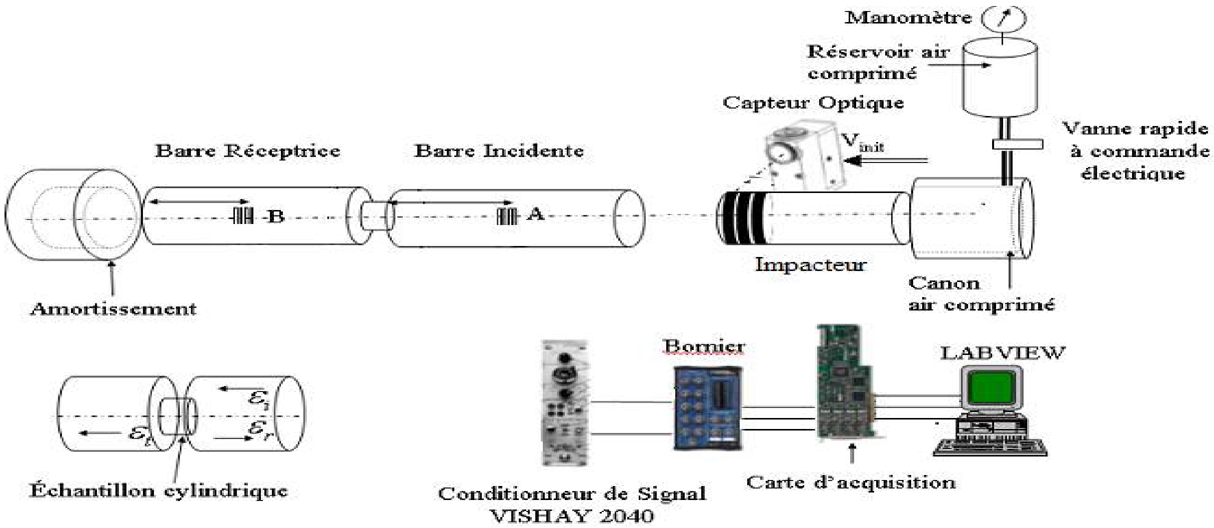

Fig.1. General schema of the compression Split Hopkinson Pressure Bars (SHPB) bench: pneumatic propulsion bars design with automatic acquisition of laser camera and strain gauges A/B signals (incident $\varepsilon_i(t)$, reflected $\varepsilon_r(t)$ and transmitted $\varepsilon_t(t)$ elastic deformations) performed with a Labwiew program, true stress - true strain curves of material specimen obtained from David code [8].

According to the general theory of elastic wave propagation [4-8], to the type of specimen's materials and to the desired obtained strain and strain rate, the choice of the material and bars geometric size requires to take into account some physical conditions. In a first time it is necessary to have similar elastic impedances of the bars as those of tested material specimens. In particular for steels, aluminum or titan alloys, the hardened high strength steel MARVAL18 is used (Table 1).

Table 1: Mechanical end elastic properties of the MARVAL 18 steel bars

Temperature 20°C	E_b [GPa]	υ	$R_{0,2}$ [MPa]	ρ_b [Kg /m^3]	$c_b = \sqrt{E_b / \rho_b}$ [m/s]	$Z_b = \rho_b c_b = \sqrt{\rho_b E_b}$ [Kg/m^{2}s]
MARVAL 18	186	0,33	1840	8000	4821,82	$38{,}57 \cdot 10^6$

To avoid superposition of measured elastic strain gauges by incident and sending bars [7-8] it is necessary to take into account the minimum measurement time using the following relationships:

$$\Delta t_{measure} = t_i = \frac{2 l_{bimp}}{c_b} \le \frac{l_{bi}}{c_b} \quad \text{and} \quad \frac{l_{bt}}{c_b} \ge \frac{0.5 l_{bi}}{c_b} \tag{1}$$

It is then required to have $l_{bi} \ge 2 l_{bimp}$ and $l_{bt} \ge 0.5 l_{bi}$. Taking into account the maximal average plastic strain of material specimen estimated from the large displacements compression theory by $\bar{\varepsilon} \approx \ln\left[1-(2v_{imp} l_{b_{mp}i} / l_0 c_b\right]^{-1}$, for a specimen length l_0 = 10 *mm* and an impact velocity v_{imp} = 10 *m/s*, a value around of 25%-50% can be obtained for $l_{bimp} \in [0.5m, 1m] \Rightarrow l_{bi} \ge 1m \div 2m$ and $l_{bt} \ge 0.5m \div 1m$. Furthermore to minimize the effect of the dispersion elastic waves and to have conditions close to the infinite bar wave propagation theory [7], the bars diameters d_b must to be very small as compared to the twist of striker lengths i.e. $d_b \ll c_b t_i = 2 l_{bimp}$. Table 2 synthetizes the chosen geometric characteristics of the Hopkinson bars in order to perform compression impact tests with large plastic deformations of material specimen.

Table 2: SHPB bars geometric characteristics (total length of table support ≈ 5,5 m)

Bars	Air Gun	Striker Bar	Receiving Bar	Sending Bar
Material	MARVAL 18	MARVAL 18	MARVAL 18	MARVAL 18
Diameter [mm]	ϕ_{in} 30.0 and ϕ_{out} 40.0	ϕ 16.0	ϕ 16.0	ϕ 16.0
Length [m]	2.0	0.602 (0.5÷1)	2.0	1.3

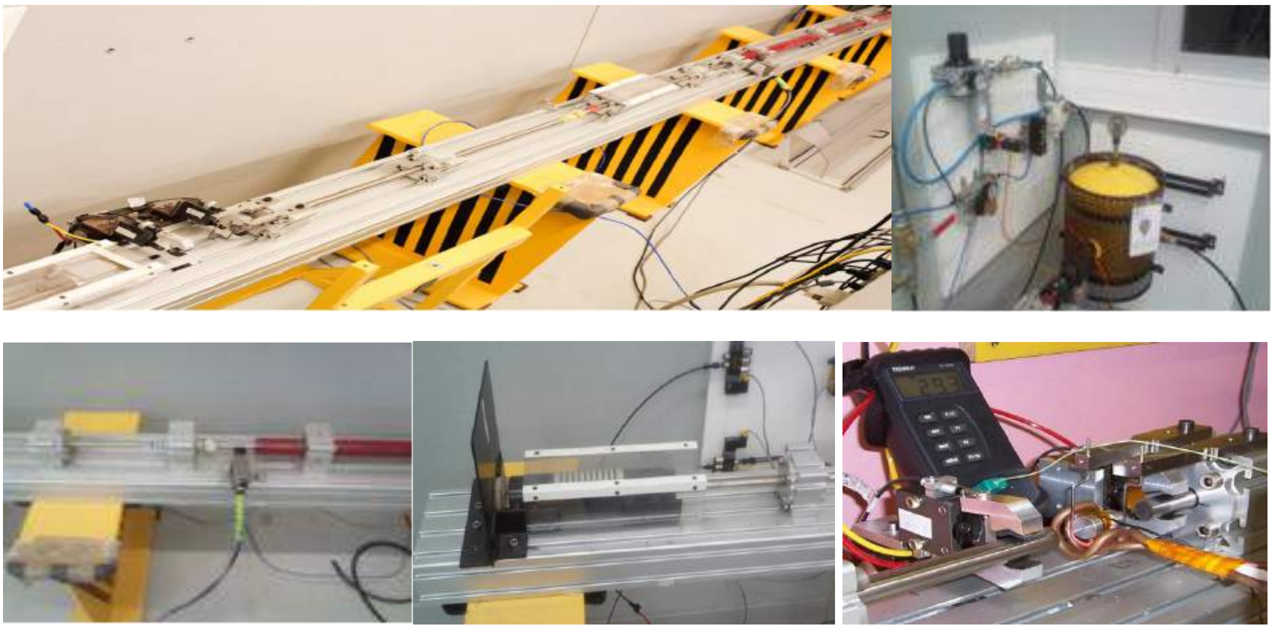

Fig. 2. General view pictures of experimental pneumatic SHPB bench with presentation of principal control and measurement devices

As can be shown in the Figure 2 the striker bar is driven by a pneumatic device using a tank with a volume V_0 of *20* l coupled on a pressurized air via a circuit of rapid control, regulate and secure valves. Using a lot of plastic collars mounted on the striker bar, this one is moved in axial translation by the air pression propulsion on a distance of *1 m* inside the gun undergoing a small friction effect. The axial impact velocity is measured by a laser camera reading a barcode of *50 mm* large with a length of $\lambda_v = 5mm$ for each uniform ditributed white/black slotes, glued on the end of impactor bar surface. So the initial impact speed value is obtained by division of the slote length λ_v with the corresponding measured period times T_v recorded from a specific Labview programm coupled on a high speed NI PCI 6110 acquition card (5 *MHz*). This program is also performed to record in Volt the signals of the twice strain full bridges mounted on the half part of the incident bar and half part of the sending bar using a digital conditionner VISHAY (Figure 1). So the incident $\varepsilon_i(t)$, reflected $\varepsilon_r(t)$ and transmitted $\varepsilon_t(t)$ elastic deformations of the bars can be estimated from a direct conversion or from calibration techniques. Computation of interfaces velocities and loads can be performed from analytical relationships based on the general dynamic elastic deformations propagation inside the bars [7] using David software [8]. An infrared camera and inductive heating coil toghether with a thermal control device, able to keep the initial metallurgical structure of metal specimen and to measure the material self-heating, was provided to make possible tests at different initial temperature [9-11]. It is then possible to identify the thermo-mechanical material specimen behaviour in terms of true stress-elasto-plastic strain for differents strain rates and temperatures using plasticity theory, analytical methods and inverse analysis strategy [9-14].

2.2 Details of pneumatic circuit and Labview data acquisition program

As shown in Figure 3, the propulsion control system of SHPB bench is fully pneumatic and in open loop. When the desired pressure is reached, the air gun is triggered manually by the operator. This operation is sufficient for the tests performed and presented in this article.

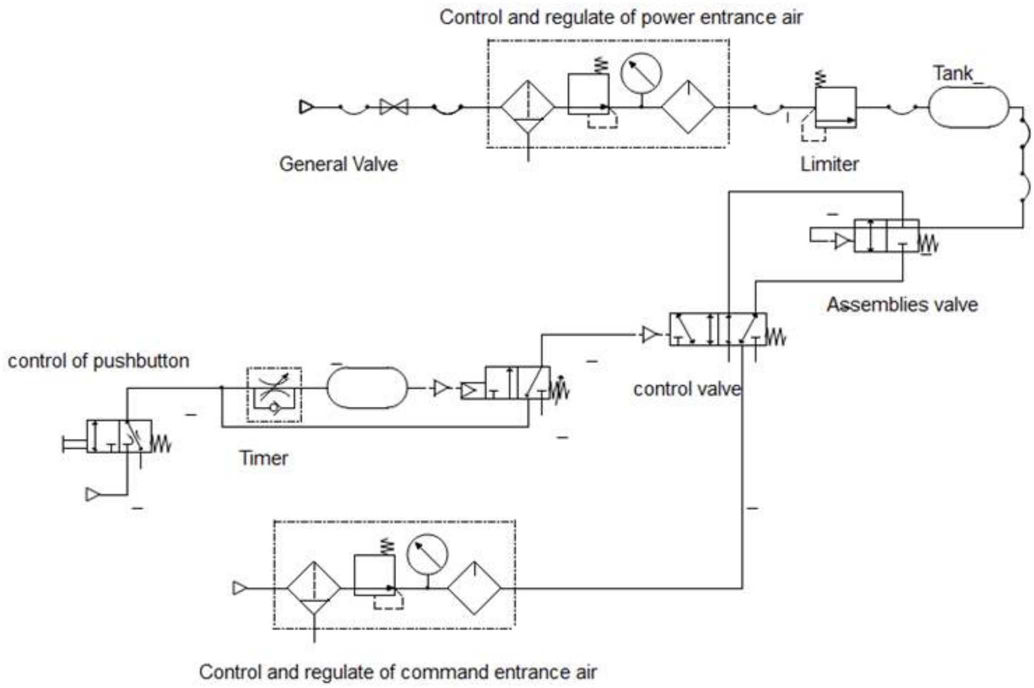

Fig. 3. Pneumatic control circuit used for propulsion of experimental SHPB bench

However, the implementation of a digital control system with feedback of different states of the system will improve its control allow precise and constant pressures when start the move of the striker bar inside the air gun. To resume, with an automatic control system, the pressure keep constant value on the time gap between value pressure regulation and the launch of the test, the repeatability and robustness of the experiments guaranteed and more rigorous studies will be possible. After starting and triggering of the rapid control valve, the air gun projects the striker against the receiving bar. Before the shock, the laser sensor captures on the front of the incident bar the variation of a signal from an uniform succesion of black and white slots with a length of λ_v. Thus is generate a square-shaped signal of period T_v, where the first rising edge acts as a trigger for optical sensor acquisition. The impact speed is deduced there from the ratio λ_v / T_v. The Labview language program developed for a real time acquisition of the optic sensor and gauge full bridges raw signals (Figure 4) allows adjustment of the acquisition frequency f_a and of the scanning number b_s. The product $f_a \cdot b_s$ determines the total acquisition duration.

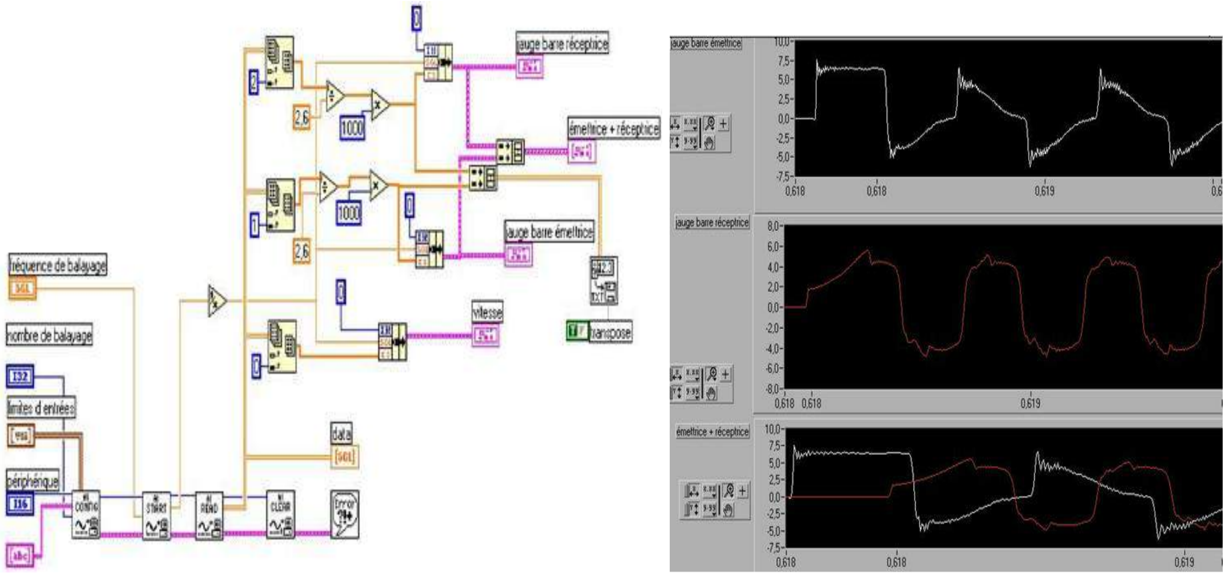

a)

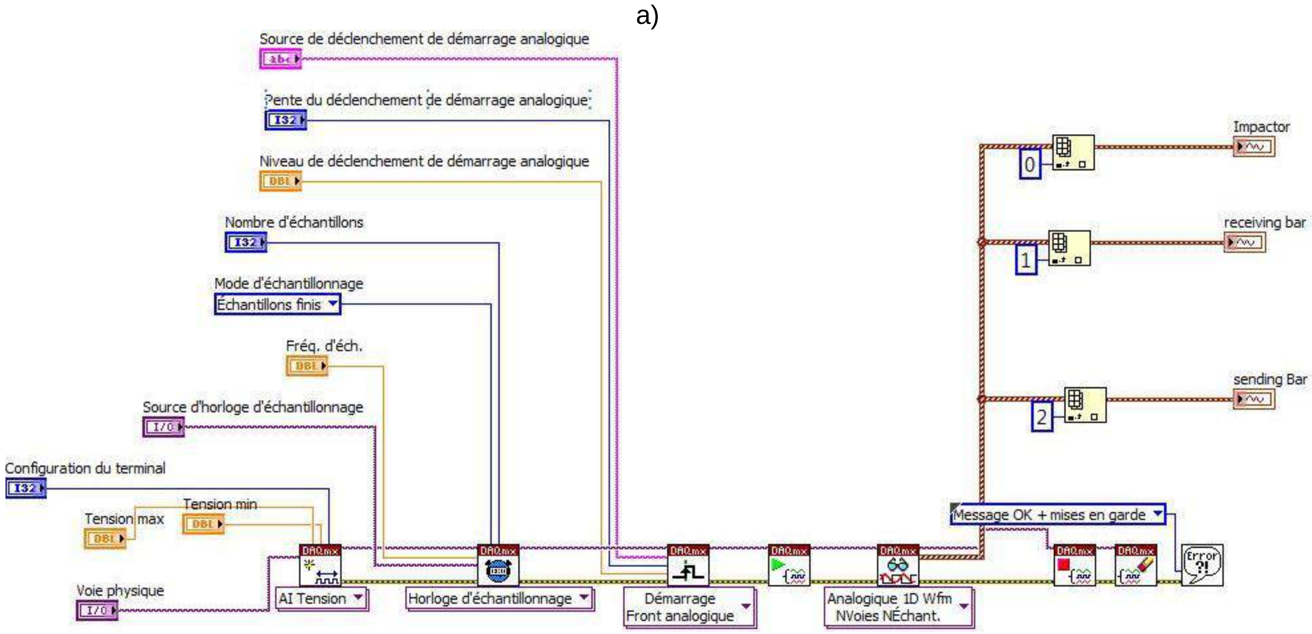

b)

Fig. 4. Labview program of experimental data acquisition a) version using gauge bridges calibration factor to recorded elastic strains signals $\varepsilon_i(t)$, $\varepsilon_r(t)$, $\varepsilon_t(t)$ in μdef, b) version using automatic triggering and record of gauge bridges tensions expressed in Volt

2.3 Theoretical estimation of initial impact velocity

Using theorem of mechanical energy balance the kinetic energy variation of the striker ΔE_c is equal to the work *W* of the bar surface force generated by air pressure i.e.:

$$\Delta E_c = \frac{1}{2} m v^2 = W = \int_0^l \left(\iint p(x) dS \right) dx \text{ with } m = \rho g l_{imp} \pi d_b^2 / 4 \quad (2)$$

where *m* is the mass of the striker bar, *v* the impact velocity obtained after the move on a distance equal to *l* and *p(x)* represents the air pressure value of each axial bar position *x*.

Or if p_c is the initial absolute pressure inside the tank of volume V_0, taking into account the atmospheric pressure p_0 and the isothermal perfect gas law the axial pressure variation is obtained from:

$$p(x)\left(V_0 + Sx\right) = p_r V_0 \text{ with } p_r = p_c - p_0 \quad (3)$$

Consequently, assuming a uniform pressure distribution on the plastic collar glued on the bars along its section *S,* the corresponding mechanical work can be computed by:

$$W = \int_0^l p(x) S dx = \int_0^l \left(\frac{p_r V_0 S}{V_0 + Sx} \right) dx = p_r V_0 \ln\left(1 + \frac{lS}{V_0}\right) \quad (4)$$

Starting from Eq. 2 the obtained impact velocity can be obtained from the following relationship:

$$v = \sqrt{\frac{2V_0}{m} \ln\left(1 + \frac{lS}{V_0}\right)} \cdot \sqrt{(p_c - p_0)} \text{ or } v = \left(\alpha / \sqrt{l_{imp}}\right) \sqrt{(p_c - p_0)} \quad (5)$$

Here α is a variable depending of tank capacity, inner section $S = \pi \Phi^2 / 4$ of the gun, material and geometry of the bars. Starting from the SHPB material properties and geometric characteristics given on Table 1 and 2 the tank volume is $V_0 = 20\, l = 2 \cdot 10^{-2} m^3$, the displacement is *l=1m* and the collar surface glued on the front of the striker bar has a surface $S = \pi \cdot 30^2 / 4 \times 10^{-6} m^2 = 706{,}86 \times 10^{-6} m^2$ which approximate $\ln\left[1 + (lS / V_0)\right] = 0{,}035$ and $\alpha \approx 0{,}029$.

Variations of estimated impact velocities for different striker bar lengths l_{imp} from 0.5 *m* to 1 *m* are presented in Figure 5 together with a comparison between the experimental values and the theoretical ones for the case of l_{imp} = 0,602 *m*.

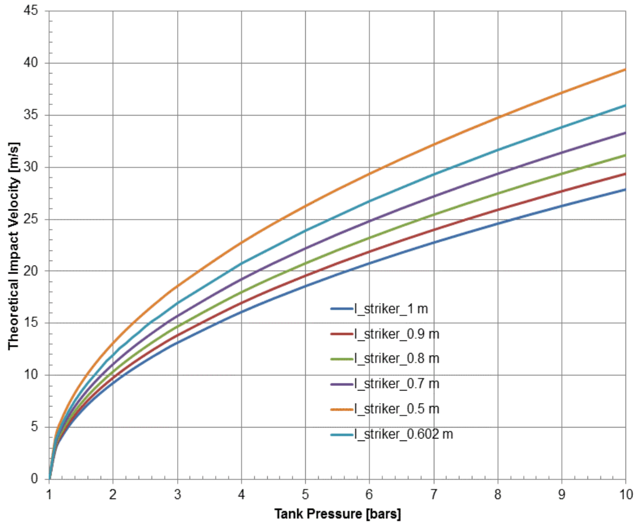

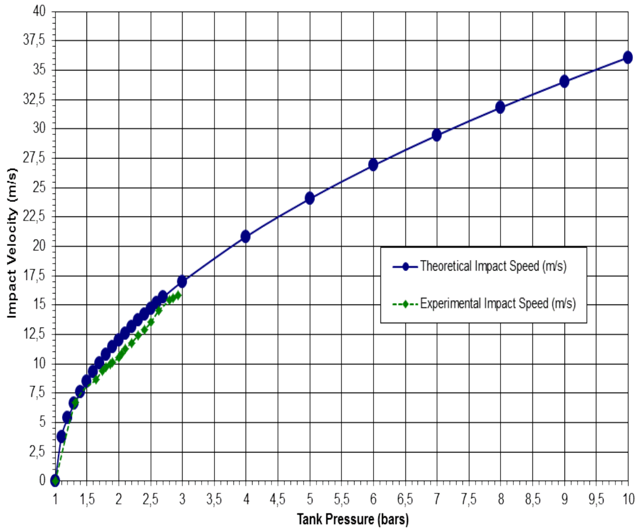

Fig. 5. a) Variation of theoretical impact speed with the absolute tank pressure for different length of striker bars (0,5 m to 1 m) b) Comparison between the theoretical impact speed and experimental values obtained for the striker with a length of 0,602 m.

It can be observed that using a maximal tank pressure of 8 bars for impactors with short length (0,5 m à' 0,6 m) the impact velocity varied from 5 *m/s* to 30-35 *m/s* as compared to an impactor with a length of 1 *m* where the maximum impact speed is limited to 25 *m/s*. The use of a striker with the length of 0,602 *m* (mass $m \approx 0,96 Kg$), if the tank pressure is expressed in bars an estimation of impact velocity can be obtained by $v \approx 11,82\sqrt{(p_c - p_0)}$.

Table 3: Theoretical and experimental impact speed obtaned from different values of tank pressure for the striker with a length of 0,602 m

Tank Pressure (bars)	Theoretical Impact Speed (m/s)	Tank Pressure (bars)	Exp Impact Speed (m/s)
1	0	1	0
1,1	3,73	-	-
1,2	5,29	-	-
1,3	6,47	1,32	6,68
1,4	7,48	1,55	6,86
1,5	8,35	1,64	8,67
1,6	9,15	1,74	9,41
1,7	9,89	1,8	9,7
1,8	10,57	1,87	10
1,9	11,21	1,9	10,1
2	11,82	2	10,56
2,1	12,39	2,05	10,84
2,2	12,94	2,1	11,3
2,3	13,47	2,2	11,8
2,4	13,98	2,3	12,4
2,5	14,47	2,4	12,9
2,6	14,95	2,5	13,52
2,7	15,41	2,63	14,54
3	16,71	2,8	15,4
4	20,47	2,85	15,6
5	23,63	2,93	15,82
6	26,42	-	-
7	28,95	-	-
8	31,27	-	-
9	34,43	-	-
10	35,46	-	-

The experimental values of initial impact velocities measured by laser camera for a lot of tank pressures show very good correlation with the curve of theoretical variation plotted in Figure 5b and values detailed in Table 3. An average estimation error of 10 % is obtained due essentially to the friction phenomena caused by the local contact of a striker bar with the inside surface of the gun through the mounted plastic collars.

3. Finite Element Modelling and Numerical Calibration of SHPB System

In a classical way the full bridge gauge tension *U* (μV) is expressed in function of the corresponding elastic deformation value ε (μdef) starting from the formula:

$$U = U_0 \left[\frac{F_g \varepsilon (1+\upsilon)}{2 + F_g \varepsilon (1-\upsilon) 10^{-6}} \right] \tag{6}$$

Here U_0 is the bridge supply voltage expressed in Volt and F_g the gauge factor. Starting from an acquisition frequency of 1 *MHz* caused by the very short time of the impact around of 1 *ms* it is required to record 1*μV/μdef*. Consequently to obtain a reliable sensitive recorded tension, the dynamic conditioner amplifier uses a gain factor *G* ($\widehat{U} = GU$) and the equation (6) gives:

$$\varepsilon = \frac{2\widehat{U}\cdot 10^6}{U_0 G F_g\left(1+\upsilon\right) - \hat{U} F_g\left(1-\upsilon\right)} \approx \frac{2\widehat{U}\cdot 10^6}{U_0 G F_g\left(1+\upsilon\right)} \tag{7}$$

where $\widehat{U}$ (expressed in Volt) represents the tension values recorded by the output of Labview program (Figure 4) and $U_0 G \gg \widehat{U}$ i.e. $U_0 \gg U$.

As can be seen, the variation of gauge deformation with the recorded tension is quasi-linear, consequently it is possible to define the calibration factor K_{exp} by the ratio between the corresponding gauge deformation value and the recorded tension i.e.:

$$K_{exp} = \varepsilon / \widehat{U} \quad (\mu def\ /Volt) \tag{8}$$

For a gauge factor F_g equal to 2.09, a gain *G* around of 250 and a supply voltage of the bridge of 7.5 *V* it is obtained K_{exp} = 1000/2,6 = 384,62 *μdef /Volt*. If an empty experimental SHPB test is performed at an initial impact velocity v_{imp}, an analytical estimation of calibration factor K_{an} can be obtained from the ratio of values corresponding to incident elastic deformation $\hat{\varepsilon}_i$ and tension $\widehat{U}_i$:

$$K_{an} = \hat{\varepsilon}_i / \widehat{U}_i \quad (\mu def\ /Volt) \tag{9}$$

Or the general theory of bar's elastic wave propagation shown that for an impact velocity *v* $\hat{\sigma}_i = \frac{1}{2}\rho c_b v \cong E_b \hat{\varepsilon}_i$ and $\hat{\varepsilon}_i = \frac{\rho c_b}{2E_b} v = \frac{v}{2c_b}$. So:

$$K_{an} = \frac{v}{2c_{\exp}\widehat{U}_i}\cdot 10^6 \ (\mu def\ /Volt) \tag{10}$$

where the bar's celerity c_{exp} can be estimated using the expression (1) from the time period $t_{i_{\exp}}$ of the first slot of the recorded incident signal $\widehat{U}_i(t)$ by $c_{\exp} = 2l_{imp} / t_{i_{\exp}}$.

The Figure 6 plot the recorded experimental tensions obtained from laser camera reading the striker barcode and from the full gauge bridges for a tank pressure around of 1,9-2 bars and an acquisition frequency f_a = 1 *MHz*.

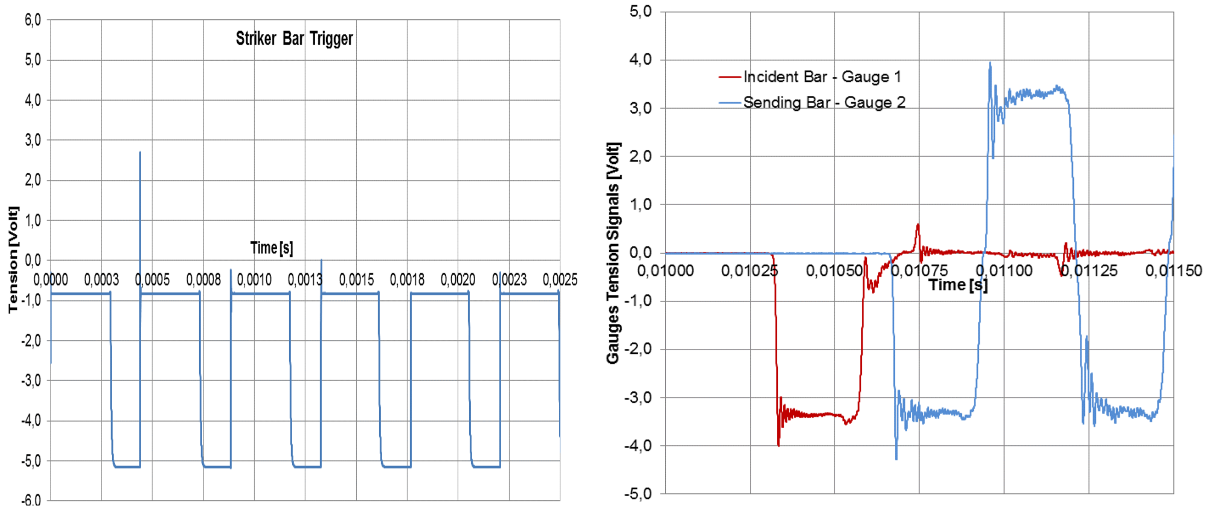

a) b)

Fig. 6. a) Square-shaped signal of laser camera recorded by triggering option of Labview program, b) Gauges tension signal variation corresponding to the elastic deformation of the bars for a tank pressure of 1,9-2 bars

Starting from the square-shape signal corresponding to the succesion of black and white slots with a constant length of λ_v = 5 mm the time period T_v is estimated to be equal to 0,5138 *ms* and consequently the obtained impact velocity is $v = \lambda_v / T_v \approx 10\, m/s$. The signal of incident deformation measured in Volts has a value close to $\hat{U}_i = 3,33V$ with a time broadness $t_i = 0,254\, ms$ and the experimental celerity can be evaluated as $c_{\exp} = 2 l_{imp} / t_{i_{\exp}} = 2 \cdot 10^3 \cdot 0,602/0,254 \approx 4740\ m/s$. As compared to a previous estimation about of 4821 *m/s* [11] the error of the sound celerity is smallest that 2.5%. Using the equation (10), the analytical calibration factor becomes K_{an} = 317 μ*def /Volt* i.e. 17% differences as compared to the classical strain gauge's calibration method.

To improve the calibration procedure in order to avoid approximations of gauge factor, gain choice and measurements errors, a robust and more general numerical calibration method is proposed. This numerical method is based on a lot of empty SHPB experimental tests without specimen performed for different initial impact velocities and on a finite element modelling of the entire bar's system. The following steps must be followed:

1. Empty experimental compression SHPB test (without any sample or specimen) with contact of incident and sending bar and at a desired initial impact velocity *v* chosen with respect to the diagram impact velocity-pressure. In this case it can be proved that $\varepsilon_i < 0, \varepsilon_r = 0, \varepsilon_t = \varepsilon_i < 0$ [14];

2. Time variations recorded of tensions $\widehat{U}_i(t)$, $\widehat{U}_r(t)$ and $\widehat{U}_t(t)$ (corresponding to the experimental gauge elastic deformations $\varepsilon_i(t)$, $\varepsilon_r(t)$ and $\varepsilon_t(t)$) found using Labview program);

3. Estimation of the real initial impact speed $\hat{v}$ from the time period T_v of the first square-shaped signal of the recorded laser camera signal using the formula $\hat{v} = \lambda_v / T_v$;

4. Estimation of the celerity c_{exp} from the time period $t_{i_{\exp}}$ of the first slot of the recorded incident signal $\widehat{U}_i(t)$ by $c_{\exp} = 2 l_{imp} / t_{i_{\exp}}$;

5. Finite Element simulation of the entire SHPB system based on same conditions as the experimental one (using same celerity speed value and same impact velocity) and extraction of elastic strains $\varepsilon_{i_{num}}(t)$, $\varepsilon_{r_{num}}(t)$ and $\varepsilon_{t_{num}}(t)$ corresponding to geometric positions of the two gauge bridges (one on the half part of the incident bar and other on the half part of the sending bar).

6. Computation of the calibration factor K_{num} = $\mathrm{Max}\left|\varepsilon_{i_{num}}(t)\right| / \mathrm{Max}\left|\widehat{U}_i(t)\right| = \hat{\varepsilon}_{i_{num}} / \widehat{U}_i$

7. Comparisons of the whole time variation of incident, reflected and transmitted elastic strains for both experimental and numerical values.

An axisymmetric dynamic Finite Element Modelling of SHPB test choosing an initial impact velocity of 10 *m/s* and an incremental time of 10^{-6}s is performed using Cast3M code [15] based on tridimensional elastic properties of the bars, inertial effect and QUAD4 mesh (Figure 7).

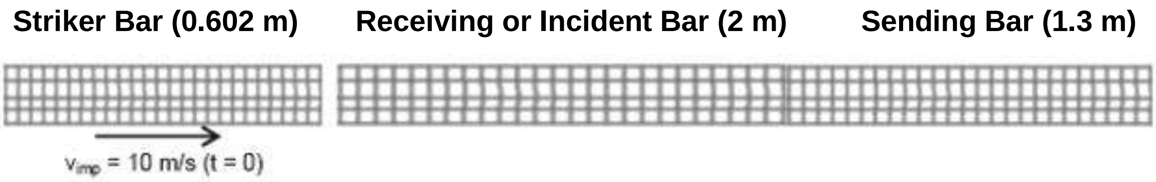

Fig. 7. Mesh of the striker, receiving (incident) and sending bars used for a Dynamic Finite Element Simulation of the SHPB device using Cast3m code

Results concerning the elastic deformations and axial stress obtained from gauge bridges positions are illustrated in Figure 8. Same numerical results are obtained using Abaqus or LsDyna FEM as has been proven in a previous scientific research [14].

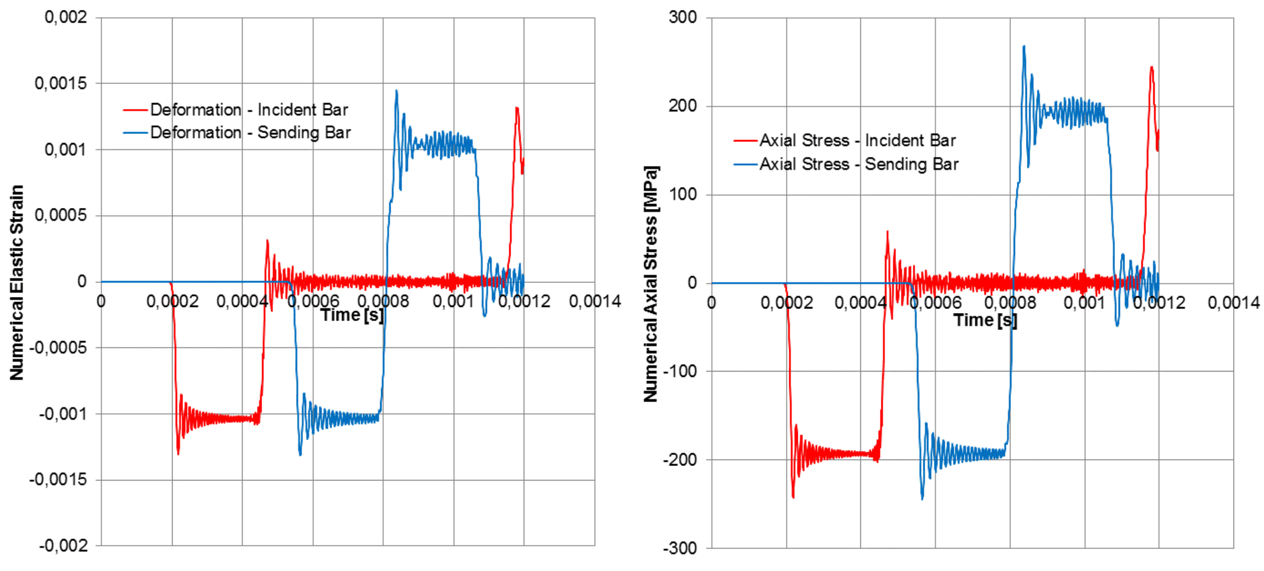

a) b)

Fig. 8. Numerical results corresponding to the gauge bridges position obtained from the Dynamic Finite Element Simulation using Cast3M code a) Elastic Strains, b) Axial Stress

It can be observed that $\mathrm{Max}\left|\varepsilon_{i_{num}}(t)\right|$ = 1034,7 *μdef* and $\mathrm{Max}\left|\sigma_{i_{num}}(t)\right|$ = 191 *MPa* values close to the analytical estimations gived by $\hat{\varepsilon}_{i_{an}} = v/2c_b \cong$ 1054,9 *μdef* and $\hat{\sigma}_{i_{an}} = 0{,}5\rho c_b v \cong$ 189,6 *MPa*. Taking into account the experimental tension value obtained from the incident deformation signal the numerical calibration factor can be estimated by K_{num} = 310,7 *μdef /Volt.* As compared to the analytical calibration factor the error is around of 2%. Despite the validation of the proposed calibration method it is possible to conclude that this numerical strategy can be performed for more complex conditions as for example in the case of viscoelastic or non-metallic materials bars, to see for optic fibbers measurements of elastic deformations where analytical computation models are too approximate or no more valid. Furthermore the entire finite element model can be used to simulate SHPB tests using different shape of specimens undergoing complex strain path especially used to identify by inverse analysis non-linear thermo-mechanical material behavior and valid them by comparisons of numerical-experimental elastic deformations of the bars as can be shown in previous works of Gavrus et al. [9-14].

4. Conclusions

The experimental design and quantitative description of the pneumatic compression SHPB bench confirms the robustness of impact speed control together with experimental validations of theoretical dependency on tank pressure set point. A new hybrid analytical-numerical calibration method has been proposed to estimate the elastic strains of the incident and sending bars. A complete dynamic finite element simulation of the SHPB system without specimen has been performed to establish a more rigorous conversion of the gauge full bridge tensions based on information obtained from the incident elastic wave signal. Comparisons with analytical formulas based on elastic wave propagation theory of infinite bars have shown the high precision of the finite element modelling results and permits to valid the calibration methodology. It is also possible to confirm again the rightness of the two-step inverse analysis technique developed in previous research works at INSA Rennes to identify thermo-mechanical constitutive equations of metallic materials under severe loadings. Based on the generality of the proposed numerical calibration method this one will be applied in a future work to improve the SHPB acquisition system using local optic fibers sensors to measure with a more accuracy the elastic deformations of the bars.

References

[1] B. Hopkinson, “A method of measuring the pressure produced in the detonation of high explosives or by the impact of bullets”, Philosophical Trans. of the Royal Society of London, Vol. A213, pp. 437-452, 1914;
[2] R.M. Davies, “A critical study of Hopkinson pressure bar”, Philosophical Transactions of the Royal Society of London, Vol. A240, N° 821, pp. 375-457,1948;
[3] H. Kolsky, “An investigation of the mechanical properties of materials at a very high rate of loading”, Proceedings of the Physical Society of London, Vol. B62, pp.676-701, 1949;
[4] H. Kolsky, “Stress Waves in Solids”, Clarendon Press, Oxford, 1953.
[5] D. J. Parry, P. R. Dixon, S. Hodson, N. A. Maliky, “Stress equilibrium effects within Hopkinson bar specimens’, Department of Physics, Loughborough, 1994.
[6] G. Gary, H. Zhao, “Dépouillement de l'essai aux barres de Hopkinson par une technique de calcul inverse”, Journal de Physique I (supplément J. of Physique III), Colloque C8, Vol. 4, septembre 1994;
[7] H. Zhao, “Analyse de l’essai aux barres d’Hopkinson:Aplication a la mesure du comportement dynamique des materiaux“, PhD Thesis, Ecole Polytehnique, Paris, France, 1992;
[8] DAVID software, Ecole Polytehnique, LMS, Paris, France;
[9] A. Gavrus, P. Caestecker, E. Ragneau, B; Davoodi, “Analysys of the dynamic SHPB test using the finite element simulation”, Journal de PhysiqueIV, 110, 2003;
[10] A. Gavrus, A., B. Davoodi, E. Ragneau, “An experimental and numerical analysis of heat transfer problem in SHPB at elevated temperatures”, Meas.Sci.Technol, 16, pp. 2101-2108, 2005;
[11] A. Gavrus, B. Davoodi, E. Ragneau, “A study of material constitutive behaviour at elevated temperature from compressive SHPB test using an inverse analysis method”, Journal de Physique IV, EDP Sciences (Eur. Phys. J), 134, pp.661-666, 2006;
[12] A. Rotariu, “Contributii privind determinarea experimentală a proprietătilor mecanice ale unor materiale în regim dynamic”, PhD Thesis, Academia Tehnica Militara, Bucuresti 2007;
[13] S. Diot, D. Guines, A. Gavrus, E. Ragneau , “Two step procedure for identification of metal behaviour from dynamic compression tests”, Int. Journal of Impact Engineering, Vol. 34, pp. 1163-1184, 2007;
[14] A. Gavrus, F. Bucur, A. Rotariu, S. Cananau; “Mechanical Behavior Analysis of Metallic Materials using a Finite Element Modeling of the SHPB Test, a Numerical Calibration of the Bar’s Elastic Strains and an Inverse Analysis Method“, International Journal of Material Forming, vol. 8, Issue 4, pp.567-579, 2015;
[15] CAST3M – Finite Element Code developed by Center of Atomic Energy CEA – France.

CONTROL CONCEPT FOR A NOVEL INTEGRATED PRESSURE BOOSTER

Stephan MERKELBACH[1], Olivier REINERTZ[2], Hubertus MURRENHOFF[3]

[1] RWTH Aachen University, Institute for Fluid Power Drives and Controls (IFAS), stephan.merkelbach@ifas.rwth-aachen.de

[2] RWTH Aachen University, Institute for Fluid Power Drives and Controls (IFAS), olivier.reinertz@ifas.rwth-aachen.de

[3] RWTH Aachen University, Institute for Fluid Power Drives and Controls (IFAS), post@ifas.rwth-aachen.de

Abstract: *The paper proposes a novel concept for pressure boosters based on rotational equipment. Instead of double piston boosters as they are common in industrial applications today, the proposed concept is based on a pneumatic radial piston motor. During one cycle, all cylinder chambers act as actuator and compressor as well. The paper shows a mathematical model of the cycle and its simulative implementation. A control concept using fast switching valves is proposed. To evaluate the efficiency, a parameter variation is undertaken. This includes the number and size of the pistons as well as pressure levels for input and output respectively. The thermodynamic concept of exergy is used to compare the different system configurations.*

Keywords*: Pneumatics, Pressure Booster, Energy Efficiency, Simulation*

1. Introduction

Pneumatic drives are used in a great variety of applications, especially in manufacturing and process engineering. Since compressed air is an expensive form of energy, recent developments show a tendency to lower the overall system pressure in compressed air systems. This improvement should lead to higher efficiency in the compressor while larger drives are needed to provide equivalent driving forces [1]. On the other hand, some applications require compact drives and therefore a higher driving pressure. To ensure the applicability of these drives while maintaining the energy efficiency, a suitable option is to implement pressure boosters. Current concepts for pressure boosters feature double piston linear transformers which have a limited efficiency. To enhance the efficiency of pneumatic transformers, the paper proposes a novel concept based on a rotating unit. The concept consists of a radial piston motor which is used in a combined cycle as motor and compressor to boost the pressure.

2. Working principle of the novel booster concept

Pressure transducers based on rotational units have been around in hydraulics for several years. So called hydro transformers built from a separate pump and hydraulic motor are used for energy recovery in many different applications (see e.g. [2]). On the other hand, there are concepts using only one integrated rotational unit which serves as a combined motor and pump. Concepts like the Innas Hydraulic Transformer are based on an axial piston pump whose valve plate has three instead of the common two openings connecting the ports to high pressure, tank pressure and transfomation pressure lines [3]. The novel booster concept proposed in this paper applies this working principle to pneumatics.

As air having a much lower viscosity than hydraulic fluids, an actuation of the cylinders using a valve plate would lead to very high leakage and therewith low efficiency of the booster. Therefore, a concept using a radial piston motor with actuation by switching and check valves is proposed.

Fig. 1 shows a schematic of this integrated pressure booster concept and the p-V-diagram of the cycle within one cylinder. The booster consists of three to six cylinders in radial layout. The pistons are connected through a crank drive with the crank length l_{crank} and the rod length l_{rod}. Each cylinder is actuated using two switching valves connecting the chamber to the pressure supply and the environment, respectively. Connection to the higher output pressure p_{out} is carried out via a check valve.

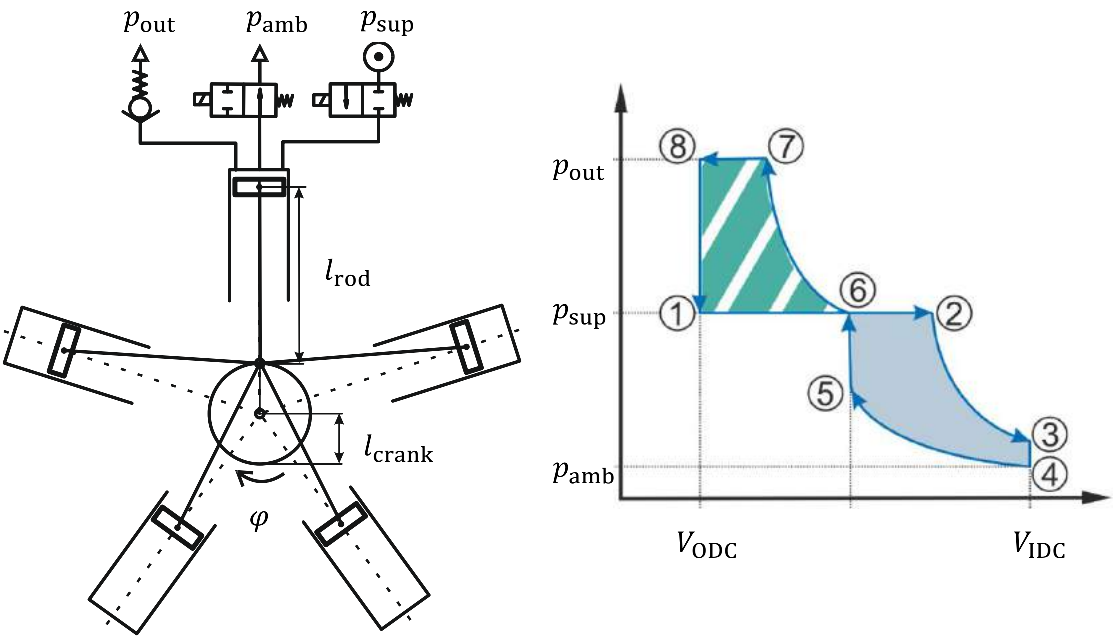

Fig. 1: Schematic and p-V-diagram of the integrated booster concept

At the beginning of the cycle, the piston is in the outer dead center (ODC) and the cylinder chamber is connected to the supply pressure p_{sup}. The piston acts in motor mode. At a certain point during the piston stroke, the valve connecting the cylinder and the supply is closed to use the expansion energy contained in the air. When the piston reaches its inner dead center (IDC), the cylinder chamber is connected to the environment for a short period of time to exhaust the chamber. Now, both magnetic valves are closed and the air within the chamber is compressed. This reduces the air mass added to the chamber between points 5 and 6 in the p-V-diagram. At point 5, the supply valve opens briefly and the cylinder chamber is filled with supply air again. The valve closes at point 6, and the compression cycle starts. When the pressure in the chamber reaches the outlet pressure of the booster (point 7), the check valve opens and the air is pushed out. At the ODC (point 8), the check valve closes again due to the pressure drop caused by the forced piston movement and the cycle restarts. In an optimal booster cycle, the work of the motoring cycle (solid blue area in the p-V-diagram) equals the work needed to conduct the compression cycle (green dashed area).
In a simulation study the number of cylinders of the unit, the bore size and stroke length as well as the ratio between supply and outlet pressure are varied. The influence of these parameters on the overall efficiency of the transducer is examined. The switching points of the valves considerably influence the efficiency of the booster. Therefore, an optimization of these points is carried out.
Additionally, losses caused by friction between piston and cylinder as well as leakage are evaluated and their influence on the overall efficiency is identified.
To allow a comparison of the efficiency at different pressure levels and pressure ratios, the thermodynamic concept of exergy is used to assess the efficiency of the different configurations (see e.g. [4]).

2.1 Configurations

Different configurations of the booster were examined in the simulation study to obtain a good knowledge of the main impact on the efficiency. This includes the number and size of the cylinders as well as the leakage mass flow between the pistons and the cylinder wall.
Table 1 shows an overview of the 9 different pressure transducer configurations that were examined in the study. Off-the-shelf radial piston motors were taken as basis for the geometrical values. This includes configurations 1, 2 and 5. Additionally, scaled versions were simulated as well. Configuration 4 represents a five cylinder motor with the piston diameter and lengths of configuration 1. Configurations 3, 6 and 9 were obtained by scaling the piston diameter, rod length and crank length of the smaller builds 1, 4 and 7. Configurations 7 to 9 represent a six cylinder version, which corresponds to two of the three cylinder motors mounted on a single shaft.

Table 1: Overview over the different configurations examined in the study

Configuration	Number of cylinders	Piston diameter	Crank length	Length of connecting rod	Angle between 2 cylinders
1	3	22 mm	7 mm	56 mm	120°
2	3	32 mm	9.25 mm	61.25 mm	120°
3	3	44 mm	14 mm	112 mm	120°
4	5	22 mm	7 mm	56 mm	72°
5	5	32 mm	9.25 mm	61.25 mm	72°
6	5	44 mm	14 mm	112 mm	72°
7	6	22 mm	7 mm	56 mm	60°
8	6	32 mm	9.25 mm	61.25 mm	60°
9	6	44 mm	14 mm	112 mm	60°

3. Simulation model

To examine the efficiency of the different configurations, a simulation model was implemented in the lumped parameter simulation environment DSHplus. This includes mathematical models for the pistons and the actuation by valves as well as the kinematics of the crank shaft.

3.1 Mathematical description

Fig. 2 shows a schematic of one cylinder including the crank drive which converts the linear movement of the piston into a rotational movement of the shaft.

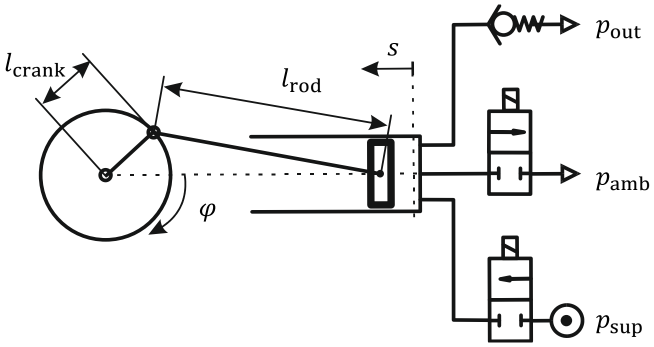

Fig. 2: Schematic of the crank and valves for one cylinder

The crank length l_{crank} and the length of the piston rod l_{rod} and their ratio $\lambda_{\text{s}} = \frac{l_{\text{crank}}}{l_{\text{rod}}}$ have a large influence on the dynamic behaviour of the booster. The piston position $s(\varphi)$ and the piston velocity $\dot{s}(\varphi)$ can be estimated using the equations (1) and (2) for $\lambda_{\text{s}}^2 \ll 1$, which is valid for all configurations examined in the study.

$$s(\varphi) = l_{\text{crank}} \cdot \left[1 - \cos(\varphi) + \frac{1}{4} \cdot \lambda_s \cdot (1 - \cos(2\varphi))\right] \tag{1}$$

$$\dot{s}(\varphi) = \frac{ds(\varphi)}{dt} = \frac{ds(\varphi)}{d\varphi}\omega = l_{\text{crank}} \cdot \omega \cdot \sin(\varphi) + \frac{1}{2} \cdot \lambda_s \cdot \sin(2\varphi) \tag{2}$$

The torque applied on the shaft by each piston depends on the angular position and the pressure in the cylinder chamber. The torque M_{press} applied by each piston can be calculated by equation (3) using the pressure force $F_{\text{G}} = \Delta p \cdot A_{\text{piston}}$ with $\gamma = \arcsin\left(\frac{l_{\text{crank}}}{l_{\text{rod}}} \cdot \sin\varphi\right)$.

$$M_{\text{Press}} = F_{\text{TG}} \cdot l_{\text{crank}} = \frac{\cos(90° - \varphi - \gamma)}{\cos\gamma} \cdot F_{\text{G}} \cdot l_{\text{crank}} \tag{3}$$

Using the conservation of angular momentum leads to equation (4) for the calculation of the angular acceleration.

$$\sum_{i=1}^{n=n_{\text{piston}}} M_{\text{press},i} - M_{\text{load}} = J_{\text{Mot}} \cdot \ddot{\varphi} \tag{4}$$

These equations form a kinematic model of the booster from which the compression and expansion during the cycle can be derived. The change of pressure inside each chamber is calculated according to equation (5). Therein $\dot{p}_{\dot{m}}$ represents the pressure change by mass transfer, $\dot{p}_{\text{HE}}$ represents the pressure change by heat exchange with the environment and $\dot{p}_{\dot{V}}$ represent the pressure change by volume change. [5]

$$\dot{p} = \dot{p}_{\dot{m}} + \dot{p}_{HE} + \dot{p}_{\dot{V}} \tag{5}$$

The mass flow in and out of each chamber is calculated within the valves. Leakage losses between the cylinder chambers are considered as well (cf. paragraph 4.3). To calculate the heat exchange between air and cylinder walls, a heat transfer coefficient of $\alpha = 3\,\frac{\text{W}}{\text{m}^2\text{K}}$ is assumed. The change of chamber volume is calculated with the axial piston velocity (eq. (2)).

3.2 Exergy efficiency

To assess the efficiency of the novel booster concept, the thermodynamic concept of exergy is used. The concept of exergy allows the comparison of different forms of energy. Exergy describes the ability to conduct work of different forms of energy when brought into equilibrium with the environment. As described by Krichel in [6], this is advantageous for the efficiency assessment of pneumatic systems.

According to equation (6), the exergy of an air mass flow can be calculated from its specific enthalpy h and its entropy s. [7]

$$\begin{aligned}\dot{E}_{\mathrm{air}} &= \dot{m}_{\mathrm{air}} \cdot \Big(h(T_{\mathrm{air}}) - h(T_{\mathrm{amb}}) - T_{\mathrm{amb}} \cdot \big(s(T_{\mathrm{air}}, p_{\mathrm{air}}) - s(T_{\mathrm{amb}}, p_{\mathrm{amb}})\big)\Big) \\ &= \dot{m}_{\mathrm{air}} \cdot \big[c_{\mathrm{p,air}} \cdot (T_{\mathrm{air}})\big]\end{aligned} \tag{6}$$

The exergy efficiency can be calculated as the ratio between the exergy flow $\dot{E}_{\mathrm{out}}$ out of the booster and the exergy flow $\dot{E}_{\mathrm{in}}$ fed to the booster (caf. equation (7)) subsequently.

$$\xi = \frac{\dot{E}_{\mathrm{out}}}{\dot{E}_{\mathrm{in}}} \tag{7}$$

Assuming an isothermal change of state between the inlet and the outlet of the booster leads to equation (8) for the exergy efficiency of the booster. This assumption is valid for the whole booster system if the output air flow is fed into an accumulator where it cools down to ambient temperature.

$$\xi = \frac{\dot{m}_{\mathrm{out}} \cdot \ln\left(\frac{p_{\mathrm{out}}}{p_{\mathrm{amb}}}\right)}{\dot{m}_{in} \cdot \ln\left(\frac{p_{\mathrm{in}}}{p_{\mathrm{amb}}}\right)} \tag{8}$$

This definition of the exergy efficiency is used throughout the simulation study presented in paragraph 4.

3.3 Implementation in DSHplus

Fig. 3 shows an excerpt of the simulation model implemented in DSHplus for one cylinder. The cylinder creates a force on the thrust crank which represents the connecting rod and the excentricity of the crank shaft. Within the crank, the torque built up by each cylinder is calculated.

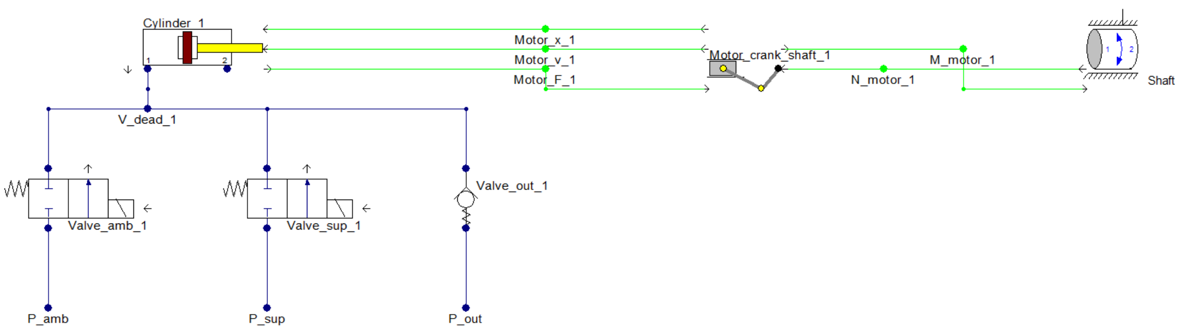

Fig. 3: Excerpt of the simulation model for one cylinder

The torque leads to an acceleration of the rotating mass ("Shaft") on the right hand side of Fig. 3. Therewith, the rotational position and speed are calculated and fed back to the crank where they are transmitted into the position and velocity of the cylinder.
In dependence on the rotational position of the shaft, the valves connecting the cylinder chamber to the environment and the pressure supply are switched. The check valve to the high pressure outlet opens automatically at a pressure difference of 0.1 bar. To gain maximum efficiency, the switching points of the 2/2-way-valves are varied for each configuration and have to be adapted to the pressure ratio between supply and target pressure. The opening and closing time of the valves is 10 ms which is in the range of typical fast switching valves.

4. Results

In the following section, some exemplary results of the simulation study are shown. To illustrate the process in one cylinder chamber, fig. 4 shows the valve signals for both switching valves for one cylinder in comparison to the normalised piston stroke. Additionally, the chamber pressure and the output mass flow through the check valve connecting the chamber to the output volume are shown.

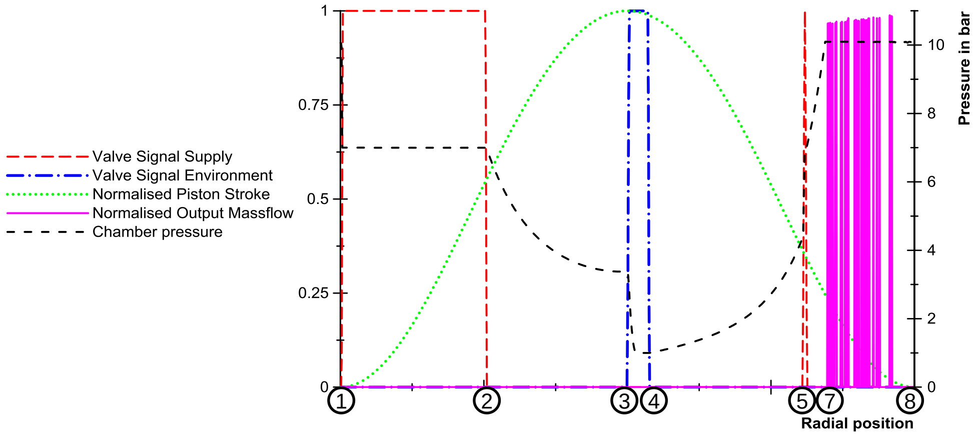

Fig. 4: Valve signals, piston stroke, output massflow and chamber pressure for one cylinder during one load cycle

As long as the supply valve is open (between points 1 and 2), the chamber pressure equals supply pressure (here: 7 bar). At point 2, the valve closes and the pressure decreases while the piston keeps on moving out until it reaches its inner dead center at point 3 where the valve to the environment opens. Now, the chamber is exhausted and the pressure falls to ambient pressure. Closing the valve at point 4 starts the precompression of the air volume inside the chamber. At point 5, the supply valve opens again for a brief period of time and the chamber is filled with air at supply pressure. The angular position of point 5 is subject to optimisation so that the amount of work executed during motoring and the energy needed by the compression are adjusted. The air inside the chamber is compressed, until the output pressure (here: 10 bar) is reached at point 7. Now, the air inside the chamber is pushed out through the check valve. This causes a pressure drop in the chamber which leads to closing of the check valve. Due to its small opening pressure in combination with a relatively high conductance the check valve opens and closes in a high frequency which shows in strong oscillations of the output mass flow.
Dependent on the supply and output pressure, the switching points of the supply valve have to be altered to gain maximum efficiency. Filling the chamber for a longer period of time increases the maximum output pressure and the maximum output mass flow because the mean driving torque increases. On the downside, more supply air is needed, which lowers the efficiency. Later refilling of the chamber during outward movement decreases the high pressure output because a smaller volume is filled with air at supply pressure and therewith, less air mass is compressed. A longer connection to the environment lowers the driving torque needed, as the mean pressure during outward movement decreases. Due to the smaller amount of precompressed air, the air mass

which has to be filled to the chamber during the second opening of the supply valve increases. All these different impacts have to be considered to gain maximum efficiency.
Automatic optimisation of the switching points would require a closed loop control concept for the booster considering the input and output pressure as well as the rotational speed. In the study presented here, no such concept was implemented. Instead of mathematical optimisation, iterative adjustment of the switching points was executed for each load and booster configuration.
Fig. 5 shows the p-V-diagram for the pressure build up phase for a three piston booster in comparison to a six piston configurations. Both configurations feature the same piston diameter.

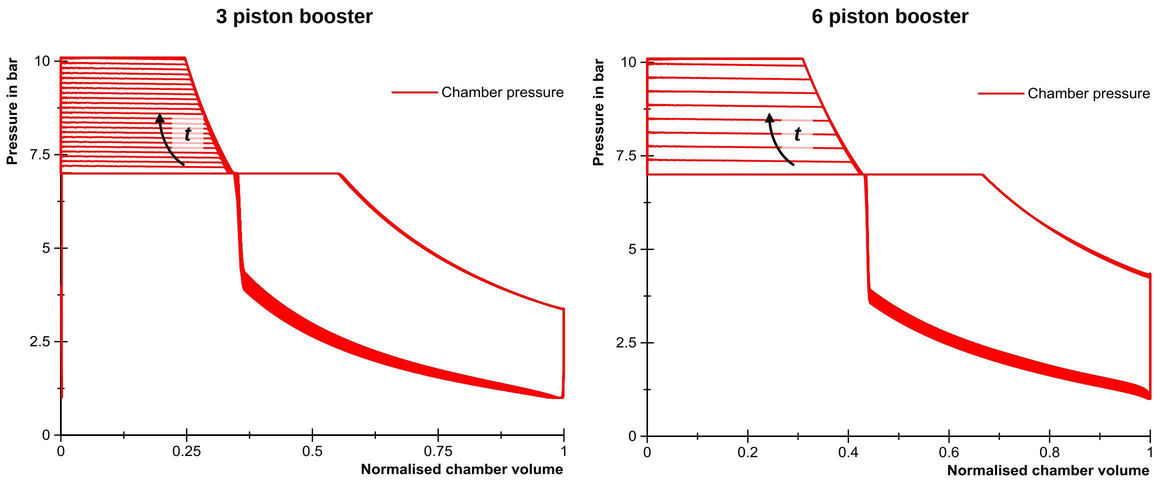

Fig. 5: Comparison of p-V-diagrams for 3- and 6-piston booster

The output pressure rises with each rotational cycle which is to be seen in the lines in the upper part of the diagram. Due to the lower cylinder number, the smaller booster needs a higher number of revolutions to reach the pressure of 10 bar in the accumulator. In the simulations shown in fig. 5, the switching points for the valves controlling the motoring cycle and the start of the compression cycle have been adapted to the load for maximum performance. This leads to different switching points for the three and six piston booster.

4.1 Influence of the piston diameter and cylinder number

Results of the different simulations show, that the efficiency of the booster increases with the piston diameter when all other parameters are kept constant. The maximum exergy efficiency is 60.5 % for the scaled geometry in a six-cylinder-configuration.
Table 2 and fig. 6 show exemplary results of the simulation study for the different configurations explained in table 1. These show a large influence of the number of cylinders. Especially the dynamic behaviour of the booster differs between the different configurations. A larger number of cylinders reduces the fluctuations in driving torque at the shaft which leads to a smoother rotation.

Table 2: Results of the simulation study

Confi-guration	Maximum Efficiency	No. of Revolutions until p_{max} is reached	Annotations
1	21.5 %	86	Bad dynamic behaviour
2	45.0 %	22	Bad dynamic behaviour
3	45.8 %	10	Bad dynamic behaviour
4	32.5 %	37	High fluctuation in rotational speed
5	42.0 %	11	High fluctuation in rotational speed
6	59.9 %	4	High fluctuation in rotational speed
7	29.4 %	30	
8	42.8 %	8	
9	60.5 %	2	

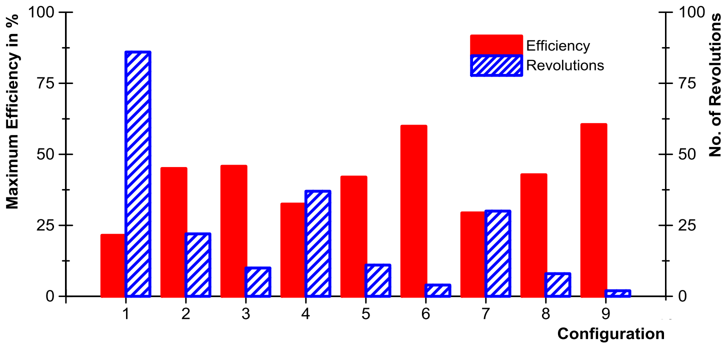

Fig. 6: Maximum exergy efficiency and number of revolutions needed to reach output pressure for the different configurations

Additionally, the number of revolutions needed until the desired maximum pressure in the output volume is reached, decreases with the number of cylinders as well as with the piston diameter. An increase in piston diameter is beneficial for the efficiency, because friction and leakage losses have a lower impact in comparison to the driving torque and mass flow in and out of the cylinder chamber.

4.2 Sensitivity on valve switching points

The sensitivity of the exergy efficiency on the valve switching points is examined in the following section. Fig. 7 shows a comparison of three p-V-diagrams for configuration 9 (6 pistons, 44 mm piston diameter). The air supply during motoring mode is switched off at three different rotational positions of the crank shaft: 91°, 95° and 100°. Due to the kinematics of the motion, this leads to a relatively large difference in the chamber volume filled with air at supply pressure. Therefore, the chamber pressure Δp_{IDC} at the inner dead center shows a difference of around 0.6 bar.

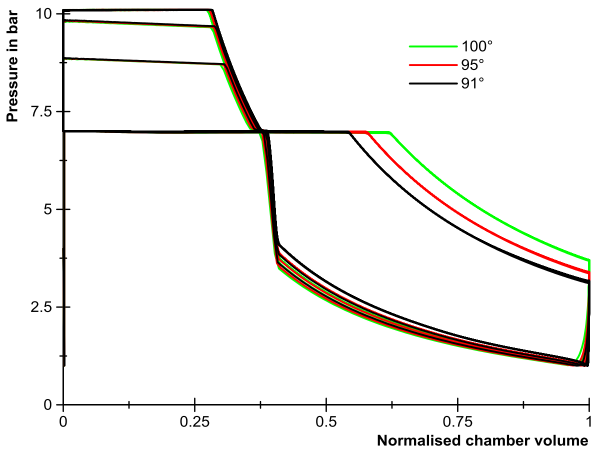

Fig. 7: Comparison of the p-V-diagrams for different switching points for the supply valve

The influence of the different switching points on the exergy efficiency of the booster is shown in fig. 8. It is obvious that later switching reduces the exergy efficiency by about 7 %.

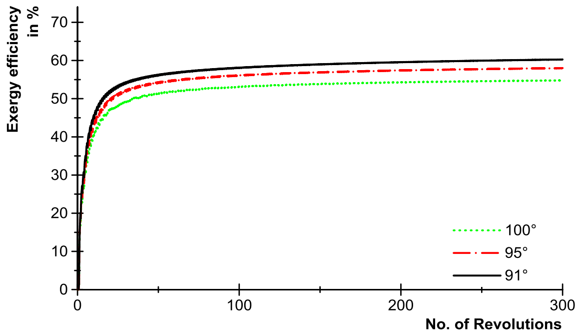

Fig. 8: Slope of the efficiency for different switching angles

Due to the smaller driving torque resulting from the lower mean pressure during the motoring cycle, it is not possible to reduce the angle at which the air is switched off infinitely. At a switching angle of 90°, the dynamics of the booster deteriorate and the booster frequently stops rotating. A higher driving torque also increases the rotating speed and therewith the output mass flow of the booster.

4.3 Sensitivity on leakage mass flow

The leakage between pistons and cylinder walls has large influence on the obtainable efficiency of the transformer. This is shown exemplarily for a six cylinder booster with large piston diameter (configuration 9 in Table 1) in Fig. 9. The conductances used to compute the shown diagram equal maximum gap heights of 9 µm, 11 µm and 19 µm, respectively.

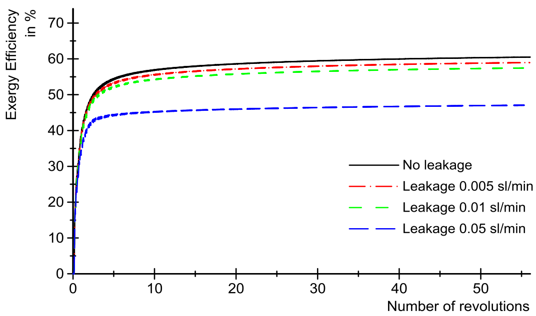

Fig. 9: Slope of the efficiency for different leakage flow coefficients

The higher the leakage flow, the lower the efficiency will be. Considering zero leakage the maximum efficiency of the booster is 60 % whereas a high leakage conductance reduces the efficiency to 47 %. If a conductance of 0.01 sl/min/bar is assumed, the total leakage mass flow equals 3.9 % of the supply mass flow or 8.5 % of the high pressure output flow. This is within the typical range for piston compressors (cf. e.g. [6]) and leads to a maximum efficiency of 57.5 % for the pressure transducer.

5. Conclusions & Outlook

A novel concept for pneumatic pressure boosters using radial piston motors is shown in the paper. These boosters have a large potential to increase the efficiency of local pressure adjustment in industrial applications if losses due to friction and leakage can be kept low. The simulation of the exergetic efficiency of the proposed booster concept shows results up to 60 %.
The influence of the switching points of the different valves is shown in one example. By adapting these switching points to the desired output mass flow and pressure, the efficiency can be kept high.
It is shown that especially the reduction of the leakage mass flow through the gap between the pistons and the cylinder wall has great influence on the efficiency. If the leakage flow increases, the efficiency decreases by far due to the larger amount of air which has to be supplied in motor mode as well as the lower amount of air discharged to the high pressure side.
In the next step, a working model of the integrated pressure transducer will be designed and built. Additionally, a different concept featuring two separate rotating units for motor and compressor mode working on a single shaft is currently under investigation at IFAS. A closed loop control concept for the automatic adaption of the switching points of the different valves may be developed to gain maximum efficiency depending on the output pressure and mass flow needed in industrial applications.

Acknowledgements

The authors thank the Research Association for Fluid Power of the German Engineering Federation VDMA for its financial support. Special gratitude is expressed to the participating companies and their representatives in the accompanying industrial committee for their advisory and technical support.

References

[1] Krichel, S., Gauchel, W., Kefer, J., Genauer hinsehen lohnt sich! Niederdruckpneumatik ist kein Garant für verbesserte Energieeffizienz, O+P Ölhydraulik und Pneumatik (in German language), 2014, pp. 20–27.
[2] Vukovic, M., Sgro, S., Murrenhoff, H.: STEAM – A Mobile Hydraulic System with Engine Integration. In: Proceedings of the ASME/BATH 2013 Symposium on Fluid Power & Motion Control FPMC2013 October 6-9, 2013, Sarasota, Florida, USA.
[3] Achten, P., van den Brink, T., Potma, J., Schellekens, M., Vael, G.: A four-quadrant hydraulic transformer for hybrid vehicles. In: The 11th Scandinavian International Conference on Fluid Power, SICFP'09, June 2-4, 2009, Linköping, Sweden.
[4] Merkelbach, S., Murrenhoff, H., et al.: Pneumatic or electromechanical drives – a comparison regarding their exergy efficiency. In: 10th International Fluid Power Conference (10th IFK). 8th - 10th March 2016, Dresden, Germany, 2016, pp. 103–115.
[5] Murrenhoff, H., Reinertz, O.: Fundamentals of fluid power – Part 2: Pneumatics, Shaker, 2014, Aachen, Germany.
[6] Krichel S. V., Sawodny O., Hülsmann S., Hirzel S. and Elsland R., 2012,"Exergy Flow Diagrams as Novel Approach to Discuss the Efficiency of Compressed Air Systems," *Proceedings of the 8th International Fluid Power Conference IFK*.
[7] Baehr H. D., and Kabelac S., 2012. *Thermodynamik*, Springer Berlin Heidelberg, Berlin, Heidelberg.

ISSN 1454 - 8003
Proceedings of 2017 International Conference on Hydraulics and Pneumatics - HERVEX
November 8-10, Băile Govora, Romania

ADJUSTMENT OF HYDROSTATIC PARAMETERS TO A HYDRAULIC INSTALLATION SYSTEM OF LAMINAR CYLINDER CASSETTE - LABORATORY VERSION

Nicușor BAROIU[1], Elena Felicia BEZNEA[2], Gabriel Marcel BOGHIAN[3]

[1] Department of Manufacturing Engineering, ”Dunărea de Jos” University of Galaţi, Romania
Nicusor.Baroiu@ugal.ro

[2] Mechanical Engineering Department, ”Dunărea de Jos” University of Galaţi, Romania
Elena.Beznea@ugal.ro

[3] Mechanical Engineering Department, ”Dunărea de Jos” University of Galaţi, Romania
boghian.marcel92@yahoo.ro

Abstract: *The intensive development of the industrial branches, the explosion in the design and execution of the new installations and equipment in machines building field, determined the same dynamics in the evolution of their components. The design of a hydrostatic operation system involves the structural design of the installation and the calculation of the numerical values for the functional and dimensional parameters of the component elements, so that the installation fulfils one or more required conditions in working. In this paper, there are highlighted the main components of a hydrostatic plant, which is also a miniaturized and readapted version of an installation existing in the ArcelorMittal Steel Factory Galati, which aims to provide the auxiliary operations necessary for mounting the laminar cylinder cassette on the spindles. It has been studied the behaviour of the plate (working table) that can support various weights as part of the device. Maximum deformation and equivalent stress was determined for the case the plate is being at the "minimum stroke", but also for the case where the plate is at the "maximum stroke". Analysis were made for the plate to support a weight of between 10 kg and 100 kg in the race in empty or the race in load.*

Keywords*: hydraulic cylinder, finite element analysis (FEA), functional analysis*

1. Introduction

The hydraulic drive systems have a significant weight in manufacturing field and it is necessary, by concrete examples, to make a technical calculation of these systems, starting from the fundamental relations regarding the calculation of the mechanical and hydraulic parameters that interfere with the operation of the hydrostatic systems [1,2] as well as modeling using the finite element method, as a general method of approximate solving of some mathematical equations describing physical phenomena [3,4]. The basic function of a hydraulic system is to transmit the mechanical energy from one place to another. This is done by the system by assembling the functions of the component elements and circulating a hydraulic medium between them, acting as energy and information carrier. The energy is transferred from a force element, a conducting element, to a running element, conducted. The energy, respectively the mechanical power provided by the conducting element, is transmitted to a primary element at which a first mechanical-hydraulic conversion occurs, the mechanical taken over energy being transmitted to the fluid. In the end, it arrives to the secondary element, where the inverse, hydro-mechanical energy conversion, takes place. Regardless of its function and design, every hydraulic system has a minimum number of basic components (pump, reservoir, valves, actuators and filter etc.) in addition to a means through which the fluid is transmitted [5]. Among the characteristic parameters of the most important hydraulic installations, can be mentioned: nominal working pressure - p; the maximum flow crossing the system, limited in its functional scheme by the effective working pressure, the pressure drop and the forces required for switching - Q; nominal diameter (diameter), conventional size that defines the nominal section of flow through pipes - DN etc. [6, 7].

2. Hydrostatic installation for the auxiliary operations required for mounting the rolling cylinders on the spindle shafts

In the case of the miniaturized and readapted version of the installation, Figure 1, the choice of the components of the installation has been made taking into account a number of technical parameters necessary to ensure preliminary sizing conditions to satisfy the technological cycles, starting from the practical model that best meets the technical and economic requirements imposed on the system - stationary performance, dynamic performance, stability, etc., as well as a number of hydrostatic criteria. Thus, it has been discussed: a) calculation of mechanical-hydraulic parameters for elements composing the system, selection or designing the component elements; b) designing and realizing the assembly of the connection and bonding elements, comprising the assembly of elements forming part of the installation, the designing of the electric motor-pump energy group (calculation and selection of the couplings), the selection of the connecting elements (fittings, joints, etc.) structuring and drawing up the execution designs and the overall drawing of the installation; c) the recalculation of some hydraulic parameters - only if, after finishing of the execution drawings, there are some differences from the initial situation offered by the assembly scheme (the length of the pipes changed, the number and type of the hydraulic resistances changed, the structure of some hydraulic elements changed, etc.). In this situation, the pressure and flow losses are reevaluated, and then corrections are made on the calculations in which the respective sizes occur.

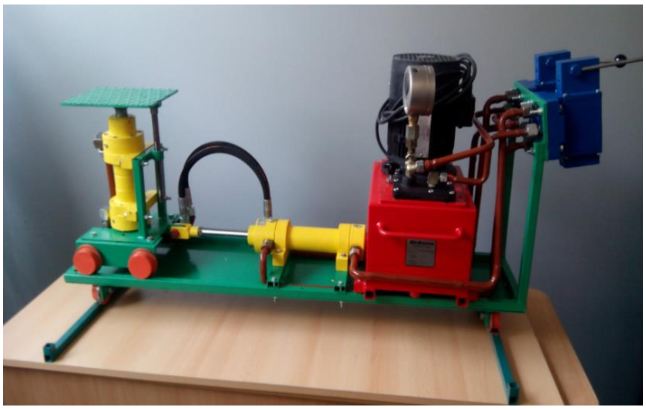

a. **b.**

Fig. 1. Hydraulic mounting system of laminar cylinder cassette
ArcelorMittal version (a); laboratory version (b)

In accordance with the engineering design cycle imposed by the projection, it has been chosen a constructive version containing a gear pump, two hydraulic cylinders, one of them making a horizontal movement, Figure 2 and the other for vertical movement, Figure 3, other components of the installation of cylinder cassette assembly, are: the rolling path, the tank, the manual distributors, the electric motor, the pressure gauge, the pressure regulator, the guides, the work table, etc. The pipes for the hydraulic cylinder performing the horizontal displacement of the mobile cart are fix. Also, the hydraulic cylinder is fixed in the metal frame with support.

Fig. 2. Hydraulic cylinder for horizontal movement

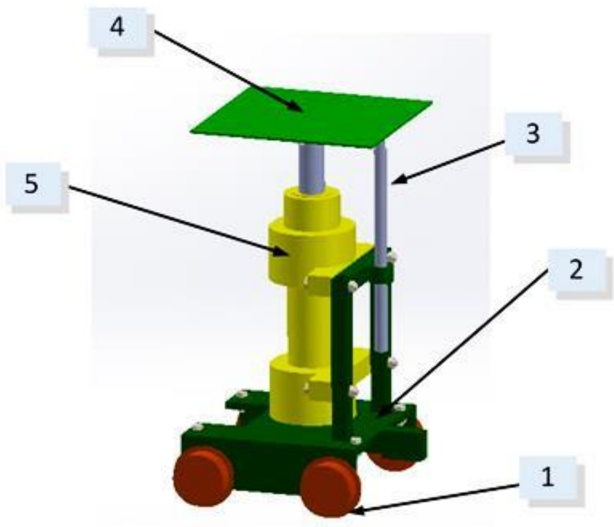

Fig. 3. Hydraulic cylinder for vertical movement

The horizontal displacement of the hydraulic cylinder is nailed by the moving cart through an ear tapped onto the cylinder stem, or by a bolt that passes through the mobile cart's ear. A working table is attached to the head of the hydraulic cylinder that performs the vertical displacement to which a guide is added. The guide assists in the horizontal movement of the entire rod stroke and does not allow the table to rotate. The supply pressure must have a value so that the force of the hydrostatic pressure created by the engine overcomes the sum of the resistances that oppose the drive. The components of the mobile assembly are: 1 - wheels; 2 - metal frame; 3 - guide; 4 - work table (plate); 5 - vertical displacement hydraulic cylinder.

3. Determination of working parameters for the adjustment system of the hydrostatic parameters

The list of hydrostatic parameters that occur in the calculation of the control system for vertical and horizontal displacement hydraulic cylinders are defined in Table 1.

Table 1: Working parameters for horizontal and vertical displacement hydraulic cylinders

Horizontal hydraulic cylinder		**Vertical hydraulic cylinder**	
Parameter	**Value**	**Parameter**	**Value**
p [bar] – working pressure	10–100	p [bar] – working pressure	10–100
L [mm] – rod stroke length	125	L [mm] – rod stroke length	125
D [mm] – piston diameter	40	D [mm] – piston diameter	40
d [mm] – rod diameter	28	d [mm] – rod diameter	28
g [kg] – working load	10–100	g [kg] – working load	10–100

Calculation of hydraulic cylinder surfaces

$$S_a = \frac{\pi \cdot D^2}{4} \tag{1}$$

$$S_p = \frac{\pi \cdot (D^2 - d^2)}{4} \tag{2}$$

S_a [mm^2] – surface of the active stroke;

S_p [mm^2] – surface of the passive stroke.

Calculation of forces at minimum and maximum stroke

$$F_{ag} = p \cdot S_a \tag{3}$$

$$F_{pg} = p \cdot S_p \tag{4}$$
$$F_{as} = p \cdot S_a \tag{5}$$
$$F_{ps} = p \cdot S_p \tag{6}$$

F_{ag} [daN] – the active force at the minimum stroke;

F_{pg} [daN] – the passive force at the minimum stroke;

F_{as} [daN] – the active force at the maximum stroke;

F_{ps} [daN] – the passive force at the maximum stroke.

Table 2 shows the tabular layout and variations in the minimum and maximum stroke force for the vertical displacement cylinder.

Table 2: Calculation of hydrostatic parameters - variations of the force with the minimum stroke, respectively for the maximum stroke

p [bar]	L [mm]	g [kg]	D [mm]	d [mm]	S_a [mm^2]	S_p [mm^2]	F_{ag} [daN]	F_{pg} [daN]	F_{as} [daN]	F_{ps} [daN]
10	70	10	40	32	1256	452	125,6	45,2	126,6	46,2
20	70	20	40	32	1256	452	251,2	90,4	253,2	92,4
30	70	30	40	32	1256	452	376,8	135,6	379,8	138,6
40	70	40	40	32	1256	452	502,4	180,8	506,4	184,8
50	70	50	40	32	1256	452	628	226	633	231
60	70	60	40	32	1256	452	753,6	271,2	759,6	277,2
70	70	70	40	32	1256	452	879,2	316,4	886,2	323,4
80	70	80	40	32	1256	452	1004,8	361,6	1012,8	369,6
90	70	90	40	32	1256	452	1130,4	406,8	1139,4	415,8
100	70	100	40	32	1256	452	1256	452	1266	462

4. Determination of total deformations and equivalent stress to vertical plate loading

The finite element analysis software series that supports the design and validation of products in a virtual environment that analyzes complex physical phenomena correlated with each other and offers a wide range of technologies for exploring dynamic behavior. It has been studied the behaviour of the plate (working table) that can support various weights as part of the device. Maximum deformation and equivalent stress was determined for the case the plate is being at the "minimum stroke", but also for the case where the plate is at the "maximum stroke". Analysis were made for the plate to support a weight of between 10 kg and 100 kg in the race in empty or the race in load.

4.1 Deformations and stresses at the minimum stroke of the vertical cylinder

The emphasis is on the analysis of the loading situations of the plate moved by the vertical hydraulic cylinder through a study of the total deformations and the equivalent stress that arise as a result of the distributed applied forces in the form of pressure by gradually loading the plate with different weights. The vertical cylinder is at the end of the stroke in the lower minimum position of the piston. With the Ansys Workbench software package, which performs the finite element

analysis, the structural static analysis is considered, the gravitational acceleration value taken into account being 9806,6 mm/s^2. Figure 4 shows the model of the plate in the minimum stroke.
Figure 5 shows the embedded plate on the contour and loaded with a weight of 1 kg. Figures 6 ÷ 11 show the variation maps of the total deformation, as well as the map of equivalent stress variation if the plate was loaded with a weight of 10, 50, 100 kg).

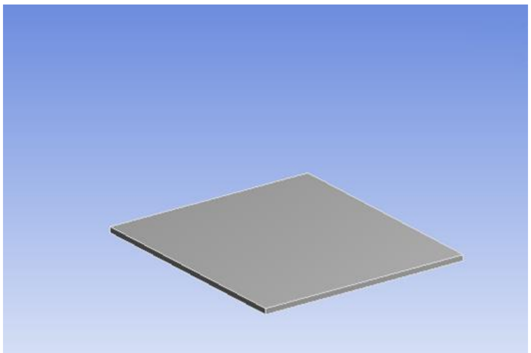

Fig. 4. Plate in the minimum stroke

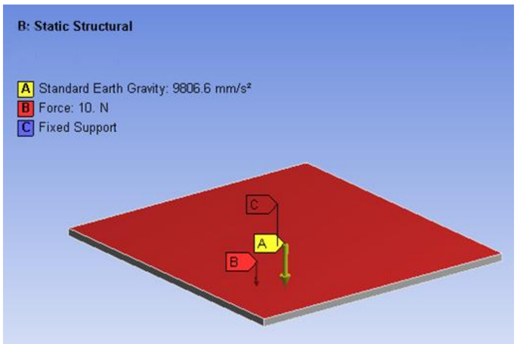

Fig. 5. Plate loaded with 1kg

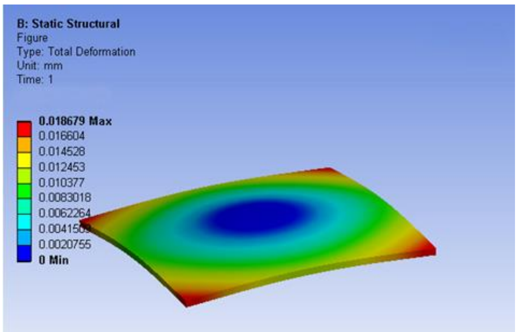

Fig. 6. Variation map of total deformation-10kg

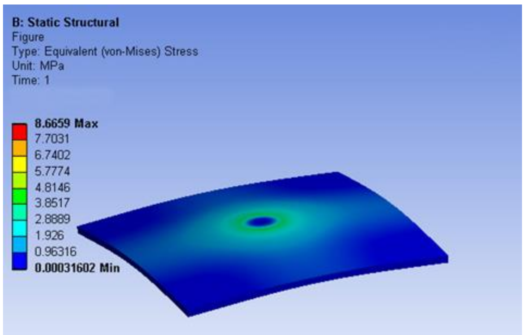

Fig. 7. Variation map of equivalent stress-10kg

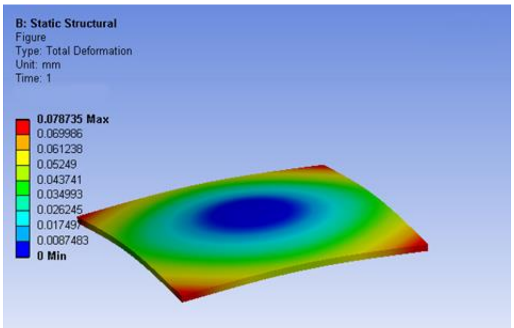

Fig. 8. Variation map of total deformation-50kg

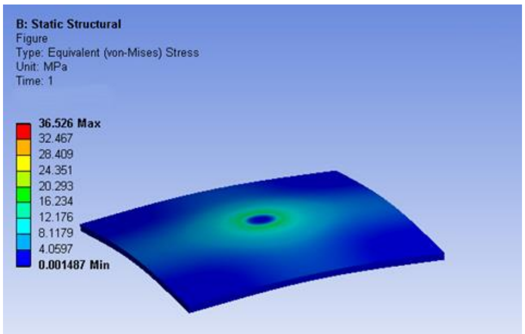

Fig. 9. Variation map of equivalent stress-50kg

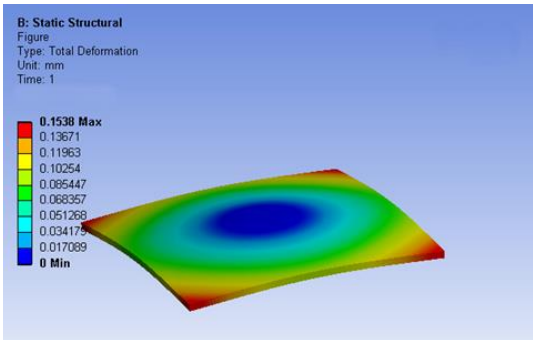

Fig. 10. Variation map of total deformation-100kg

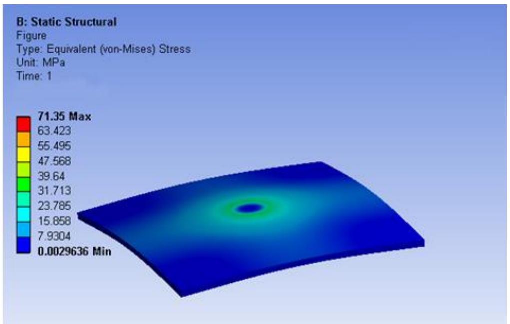

Fig. 11. Variation map of equivalent stress-100kg

4.2 Deformations and stresses at the maximum stroke of the vertical cylinder

The same loading conditions are considered, but in the case where the vertical cylinder is at the end of the stroke, in the upper maximum position of the piston. Figure 12 shows the model of the plate at the maximum stroke. Figure 13 - the embossed board on the contour and loaded with a weight of 1 kg.

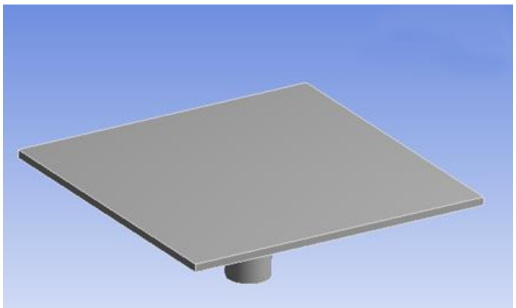

Fig. 12. Plate in maximum stroke

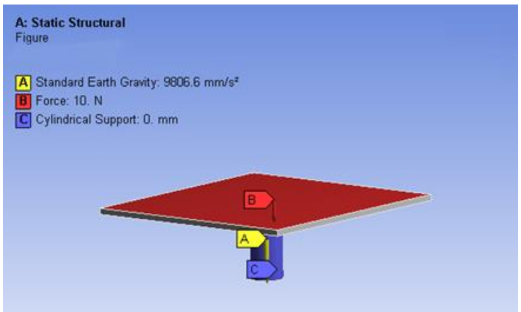

Fig. 13. Plate loaded with 1kg

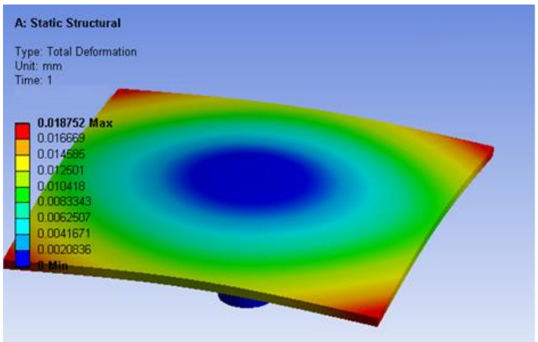

Fig. 14. Variation map of total deformation-10kg

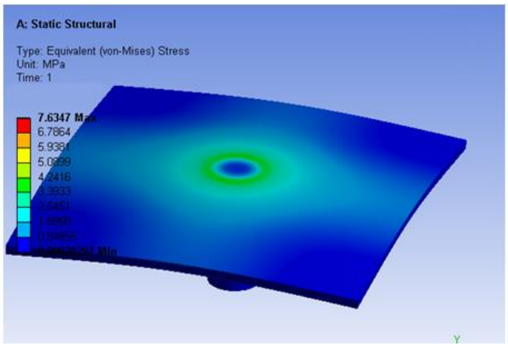

Fig. 15. Variation map of equivalent stress-10kg

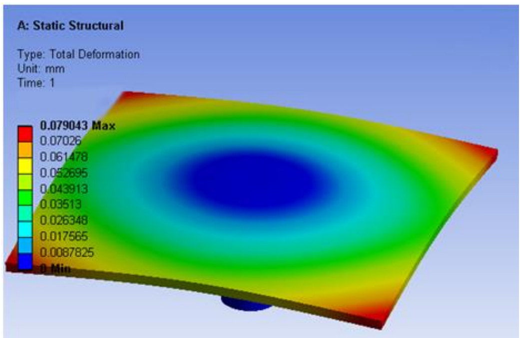

Fig. 16. Variation map of total deformation-50kg

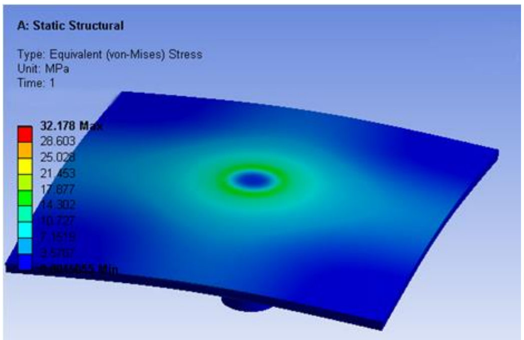

Fig. 17. Variation map of equivalent stress-50kg

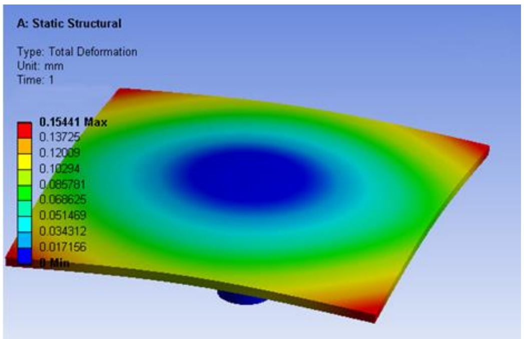

Fig. 18. Variation map of total deformation-100kg

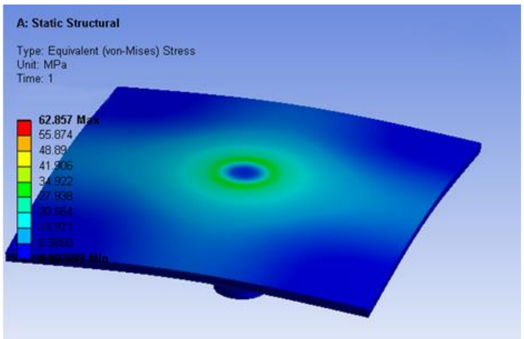

Fig. 19. Variation map of equivalent stress-100kg

Figures 14 ÷ 19 show the variation maps of the total deformation and the equivalent stress in case the plate was loaded with 10, 50 and 100 kg.
Figure 20 shows the variation of the total deformation at successive loadings of the vertical moving mobile unit plate weighing from 10-100 kg and in Figure 21 the variance of the von Mises stress under the same loading conditions.

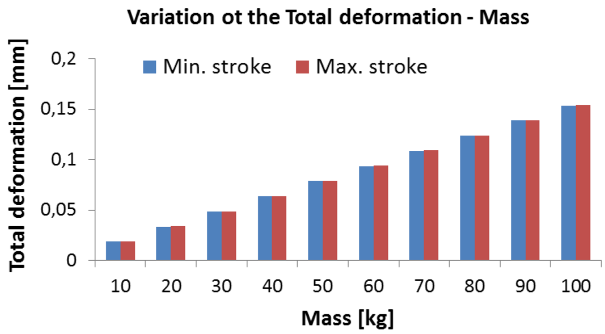

Fig. 20. Variation of total deformation by mass

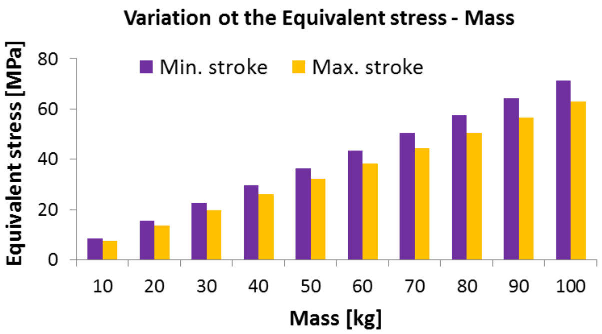

Fig. 21. Variation of total equivalent stress by mass

5. Conclusions

As a result of modeling the finite element of the work table in the minimum stroke, work table loaded with weights ranging from 10-100 kg, it can be noticed that both the total deformation and the equivalent tension register a linear increase. When loading the work table with 10 kg, the total deformation is 0.0118679 mm, and when loading the work table with 100 kg of 0.1538 mm. Von Mises equivalent stress for a 10 kg load are 8.6659 MPa and 100.00 kg loading table are 71.35 MPa. Similarly, at maximum stroke, the total deformation varies from 0.018752 when loading the work table of 10 kg to 0.15441 when loading the work table by 100 kg. The equivalent von Mises stress range from 7,63347 MPa for a load of 10 kg to 62,857 MPa for a 100 kg load table.

References

[1] G. Axinti, A.S. Axinti, "Acţionări hidraulice şi pneumatice. Dinamica echipamentelor şi sistemelor", Ed. Tehnica-Info, Chişinău, 2008;
[2] N. Baroiu, C.L. Popa, V.G. Teodor, S. Berbinschi, F. Susac, "Pompe și compresoare elicoidale - profilări CAD și analitice ale sculelor generatoare, Ed. Academica, ISBN 978-606-606-004-2, 2017;
[3] E.F. Beznea, C.A. Vasilache, I. Chirică, "FEM buckling behavior studies on composite plates with initial imperfections", The4-th International Conference "Advanced Composite Materials Engineering", COMAT, Brașov, 2012;
[4] Baroiu N., Teodor V.G., Costin G.A., "Constructive-functional analysis of single-rod double-acting hydraulic cylinders", TEHNOMUS Journal - New Technologies and Products in Machine Manufacturing Technologies, ISSN-1224-029X, pp. 126-131, 2017.
[5] http://www.monografias.com/trabajos97/anteproyecto-tesis-diseno-sistemas-scada-sitemas-oleohidraulicos/anteproyecto-tesis-diseno-sistemas-scada-sitemas-oleohidraulicos.shtml;
[6] O.D. Ciocan, "Acţionări hidraulice şi pneumatice", Ed. Tehnica-Info, Chişinău, 2008;
[7] F. Stan, N. Baroiu, O.D. Ciocan, "Hidrostatică tehnologică – Aplicaţii", Ed. Didactică şi Pedagogică, Bucureşti, ISBN 978-973-30-3600-5, 2014.

ISSN 1454 - 8003
Proceedings of 2017 International Conference on Hydraulics and Pneumatics - HERVEX
November 8-10, Băile Govora, Romania

USING LOGIC GATES IN FLUID POWER SYSTEMS CONTROL (Part 1)

Eugen DOBÂNDĂ[1], Ilare BORDEAŞU[1]

[1] POLITEHNICA University of Timişoara; eugen.dobanda@upt.ro**,** ilare.bordeasu@upt.ro

Abstract: *The control of fluid power systems refers especially to flow (speed) and pressure (force) and is realized by several methods, from mechanical to electro-electronic-mechanic solutions. In this paper we present the possibility to use hydraulic components to simulate logic gates (logic functions) in order to control fluid power systems.*

Keywords*: Fluid, power, logic, gate, automation.*

1. Elementary logic gates

A logic gate (function) is an elementary block, having at least one input (gate) (named in the following "A", "B",) and one output (named "y". At this moment, we will consider login gates having two inputs.
At any gate should have one of the two Boolean conditions: zero (0) – meaning no signal – 1 (one) – meaning existence of a signal.
For the beginning, will take into consideration the most three common logic gates: AND, OR and NOT.
In figure 1 are presented this logic gates, their representation, the truth tables and the hydraulic representations.

AND

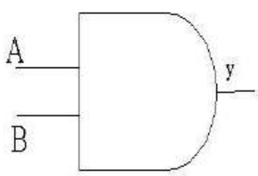

A	B	Y
0	0	0
0	1	0
1	0	0
1	1	1

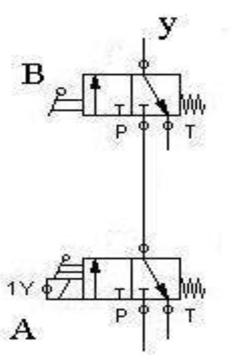

OR

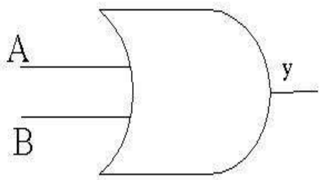

A	B	Y
0	0	0
0	1	1
1	0	1
1	1	1

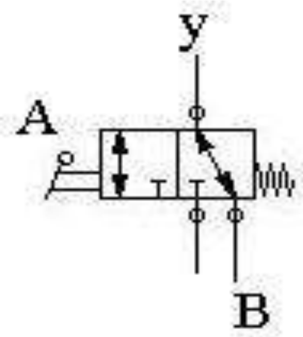

NOT

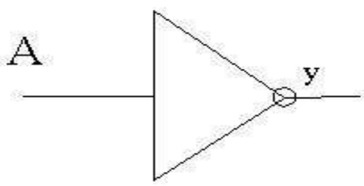

Ā	y
0	1
1	0

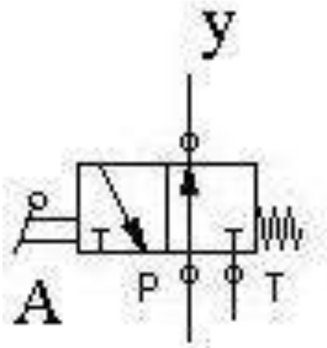

Fig. 1. Basic logic gates

2. The use of OR logic gate

In figure 4 there is presented an example of using the OR logic gate. As can be observed, the fluid parameters – pressure, i.e. the force at the cylinder - will be modified by acting the pressure relief valves. In case that in circuit is placed a throttle valve, the flow could be modified, i.e. the speed of the cylinder rod.
In figure 2 is presented a hydraulic circuit containing an OR logic gate. In figures 3 there are presented the hydraulic circuit, and the truth table for logic gate OR.

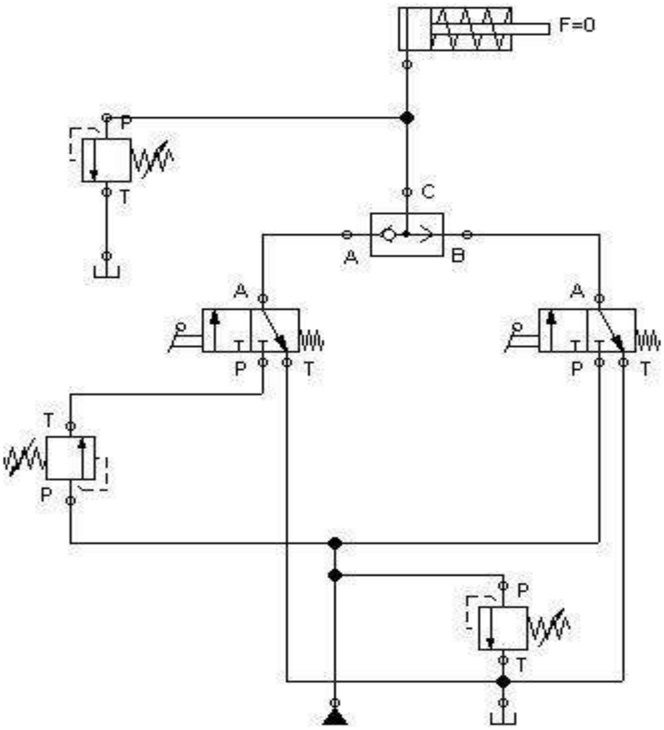

Fig. 2. The hydraulic circuit for OR gate

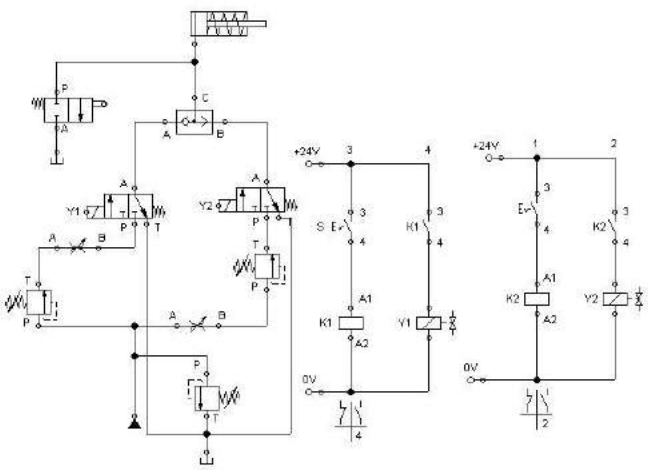

Fig. 3.a. OR truth table : A = 0, B = 0, y = 0

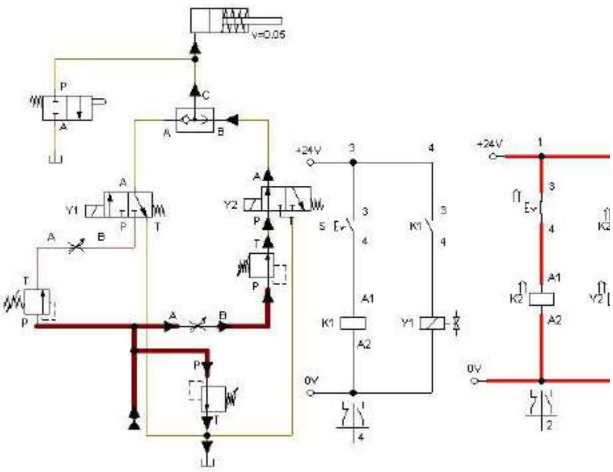

Fig. 3.b. OR truth table : A = 0, B = 1, y = 1

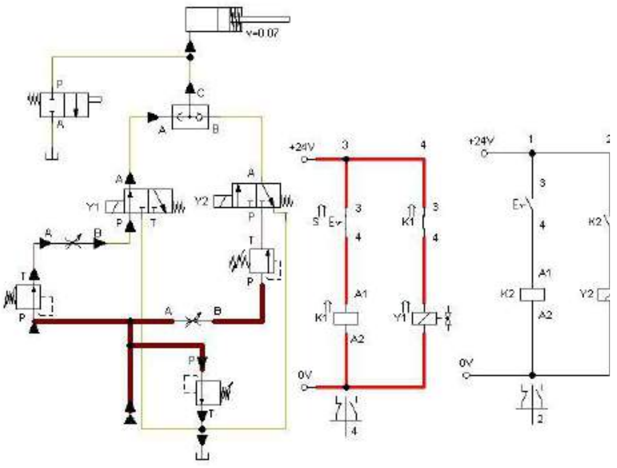

Fig. 3.c. OR truth table : A = 1, B = 0, y = 0

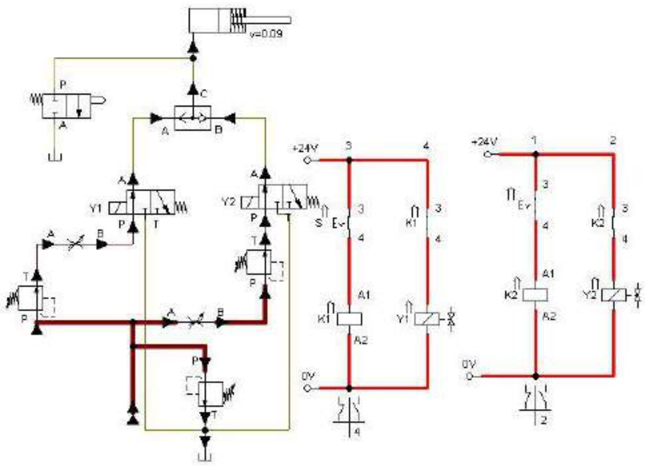

Fig. 3.d. OR truth table : A = 1, B =1, y = 1

3. The use of AND logic gate

Figure 4 presents the use of AND logic gate. Figures 5 there are presented the hydraulic circuit, and the truth table for logic gate AND.

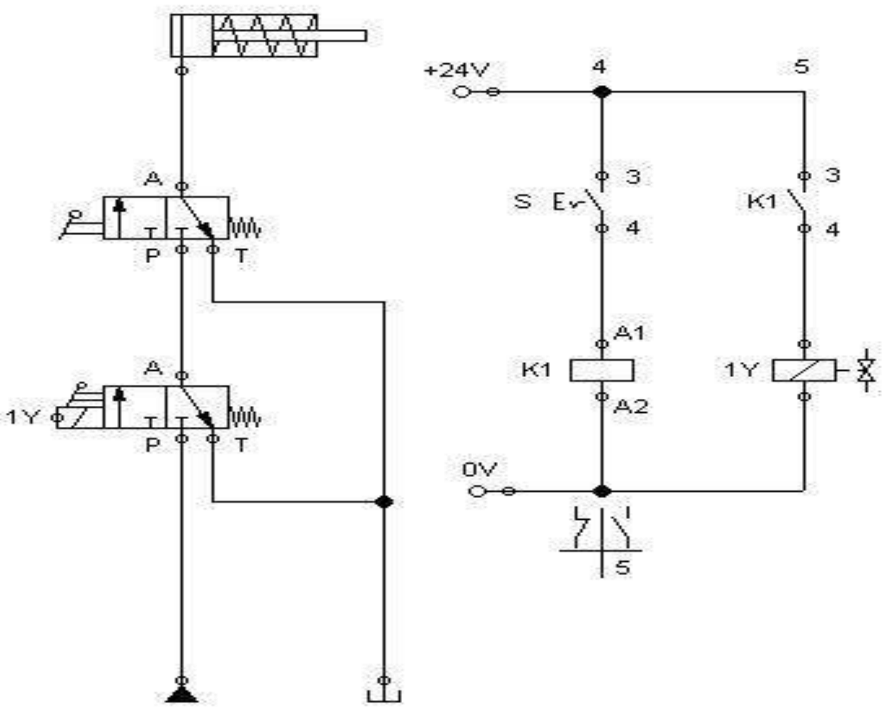

Fig. 4. The hydraulic circuit for AND gate

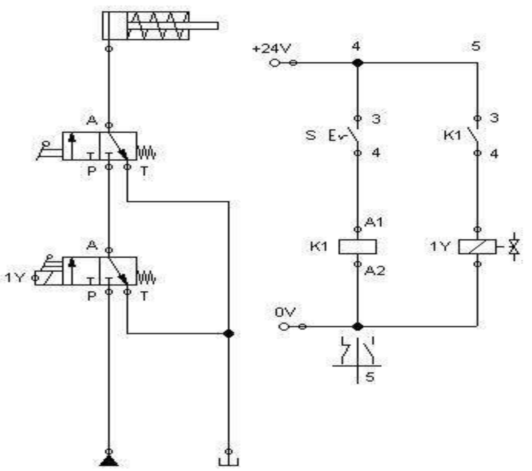

Fig. 5.a. AND truth table : A = 0, B = 0, y = 0

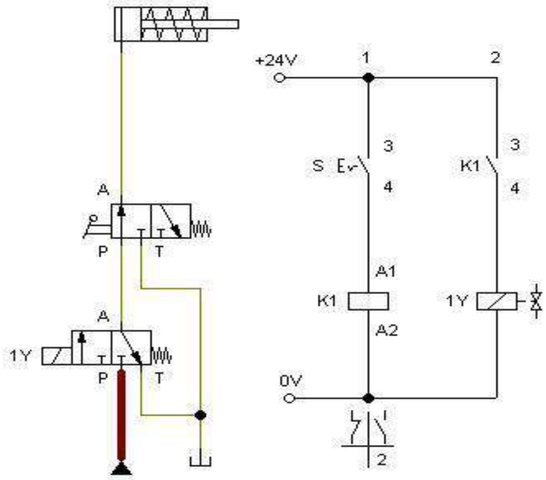

Fig. 5.b. AND truth table : A = 0, B = 1, y = 0

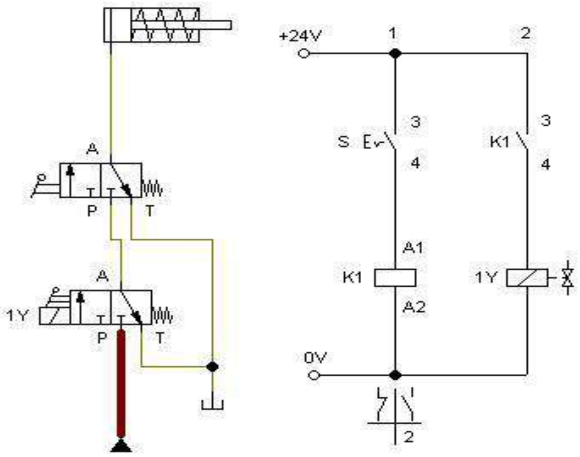

Fig. 5.c. AND truth table : A = 1, B = 0, y = 0

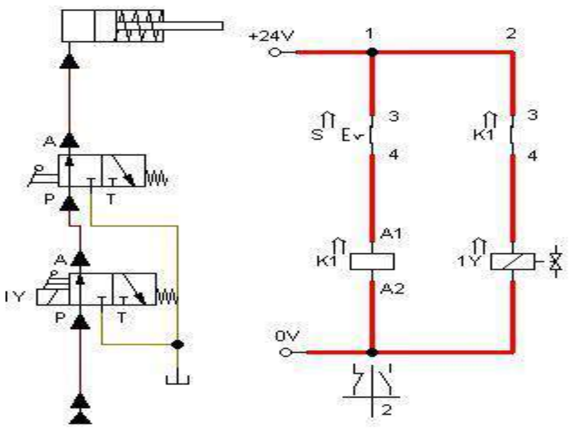

Fig. 5.d. AND truth table : A = 1, B =1, y = 1

4. The use of NOT logic gate

Figure 6 presents the use of NOT logic gate. Figures 7 there are presented the hydraulic circuit, and the truth table for logic gate NOT.

5. Combined logic gates

Logical gates can be, also combined in order to obtain more complex functions.
So, if gates NOT and OR are combined, will be obtained NOR logic gate. Figure 8 presents the use of NOR logic gate, the correspondent hydraulic circuit, and the truth table.
If gates NOT and AND are combined, will be obtained NAND logic gate. Figure 9 presents the use of NOR logic gate, the correspondent hydraulic circuit, and the truth table.

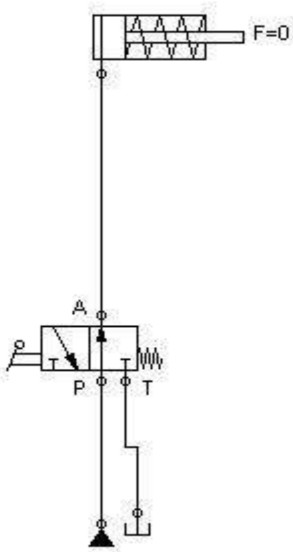

Fig. 6. The hydraulic circuit for NOT gate

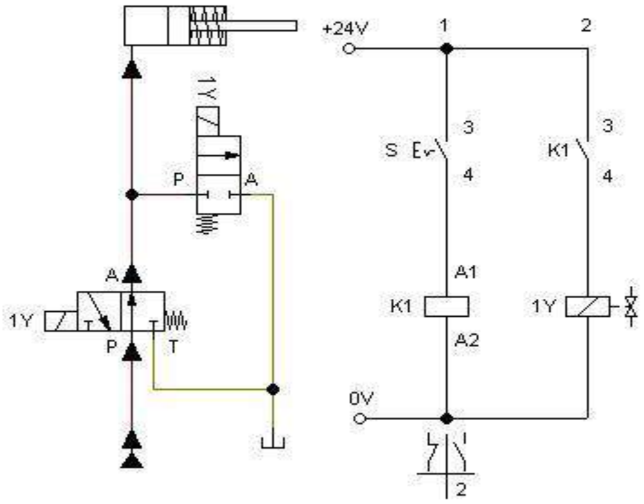

Fig. 7.a. NOT Truth table : Ā = 0, y = 1

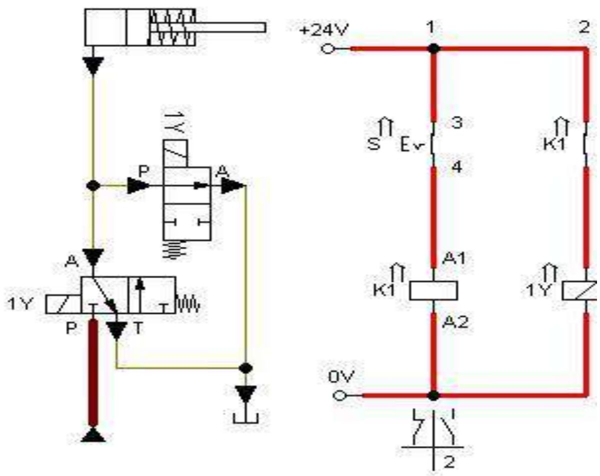

Fig. 7.b. NOT Truth table : Ā = 1, y = 0

NOR (= NOT + OR)

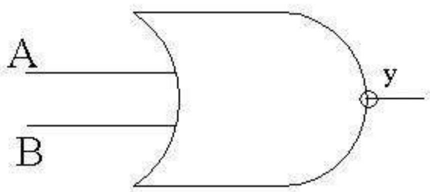

A	*B*	*y*
0	*0*	*1*
0	*1*	*0*
1	*0*	*0*
1	*1*	*0*

NAND (= NOT + AND)

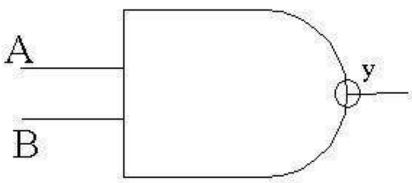

A	*B*	*y*
0	*0*	*1*
0	*1*	*1*
1	*0*	*1*
1	*1*	*0*

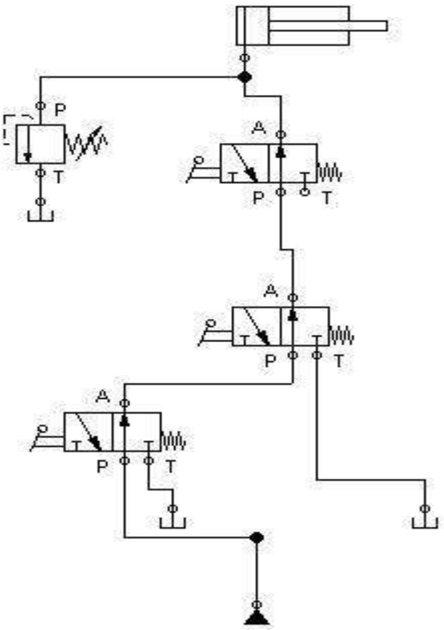

Fig. 8. NOR gate representations

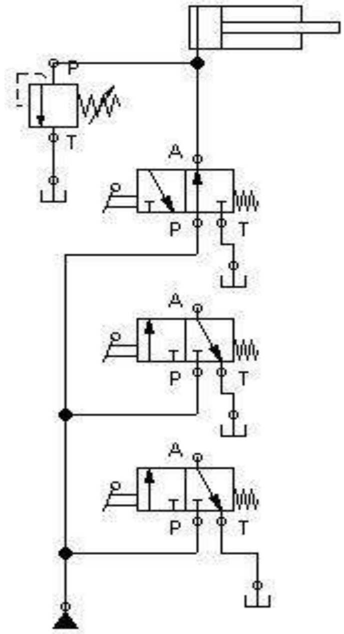

Fig. 9. NAND gate representations

6. Conclusions

The paper presented the possibility to generate logic gates, using fluid power components.
There are presented the hydraulic scheme equivalents of logic gates in correspondence with truth tables.

References

[1] V. Radcenco, N. Alexandrescu, E. Ionescu, M. Ionescu., "Calculation and design of pneumatic automation elements and schemes" („Calculul si proiectarea elementelor si schemelor pneumatice de automatizare"), Technical Publishing House, Bucharest, 1985;
[2] https://en.wikipedia.org/wiki/Logic_gate;
[3] V. Alexa, S. Ratiu, C. Birtok-Baneasa, "Simulating pneumatic logic functions using pneumatic FluidSIM software" ("Simularea functiilor logice pneumatice utilizand softul FluidSIM pneumatic"), ISSN 2067-7138, Bucharest 2011, Proc. Science and Engineering, vol. 19, pp. 569-574;
[4] E. Dobândă, „Hydraulic actuation and automation systems" (Sisteme de acţionare şi automatizare hidropneumatică), courese notes, 2010 – 2017.

ISSN 1454 - 8003
Proceedings of 2017 International Conference on Hydraulics and Pneumatics - HERVEX
November 8-10, Băile Govora, Romania

THE STATE FEEDBACK CONTROL OF WATER HYDRAULIC SERVO MOTOR SYSTEM BY POLE PLACEMENT

Yusuf ALTUN

Duzce University, Engineering Faculty, Computer Engineering, yusufaltun@duzce.edu.tr

Abstract: *The state feedback control is presented by pole placement for the water hydraulic servo motor system in this paper, which is a choice of driving source for many applications. Although the system is highly nonlinear and has uncertainty parameters, it can be linearized around the working points. The pole placement method is used for the velocity control because it has simpler structure and low-cost contrary to advanced controllers or dynamic controllers. In addition, the control enables to place the desired poles. Therefore, the oscillation, settling time and overshoot are regulated to the disturbances thanks to the controller. The simulation results are presented for the control performance.*

Keywords*: hydraulic servo motor, control design, fluid system.*

1. Introduction

Nowadays, water hydraulic servo motor systems, where a hydraulic motor is combined with a servo valve, are a prominent position because of environment-friendly. The system fluid is water because it has prominent features such as clean, non-combustible, cheap, and easily available. Moreover, water hydraulics have a faster reaction according to oil hydraulics. These properties give high opportunity to use for the industry such as food, chemical, forestry. Yet, they have uncertain parameters, highly nonlinearities and disturbances in addition to the leakage flow and friction in valves or actuators, wide friction torque during the lower motor velocity to oil hydraulics, so their applications can be still rather limited. Accordingly, the researchers have studied on the controller design of the systems to improve the motion performance. Many controller designs are performed up to now. In [1], the gain scheduling PID controller is proposed for the wide overshoot and steady-state error. In [2], a sliding mode control together with the disturbance observer is performed for the angle of the system. In [3], some robust control methods including disturbance observer are observed for the system by comparing. In [4], a simple adaptive control is implemented to the system for the control of both angle and speed, which is simple, lower orderly and has fewer adaptive variables. In [5], it is proposed that the PID funnel control together distance approximation aimed to generate the controller signal is proposed for the speed control of the system. In [6], an adaptive output feedback controller design is proposed for the position of hydraulic servo system under uncertain parameters without measuring the states. In [7], a PID control, whose parameters are tuned by genetic algorithm, is designed for the angular motion control of electrohydraulic servo system. In [8], the position control based on the feedback linearization of an electrohydraulic servo system. In [9], a robust adaptive control is implemented for the hydraulic actuators with single-rod. In [10], an adaptive robust controller based on back-stepping technique based is proposed for the electrohydraulic servo systems with uncertain parameters and unknown dead zone. [11], a nonlinear adaptive feedback controller is designed for the position of the system by using Lyapunov approach according to load disturbances and frictions. In [12], an adaptive neural controller is designed for the velocity of the system via feedback linearization. The above studies are either complex or costly for the applications. So, this paper presents that the velocity control of the system via pole placement method for the water hydraulic servo motor systems this paper. Therefore, the success is gained by regulating the system poles against the disturbances.

2. The Water Hydraulic Servo Motor System Model

Figure 1 shows the servo motor system to be controlled. It contains some basic elements. They are a flywheel attached to a servo motor which generates the outputs the rotational $\theta(t)$ angle and spool displacement of $x_v(t)$ servo valve. Therefore, the controller purposes the angle $\theta(t)$ or speed $\dot{\theta}(t)/\omega(t)$ by producing the $u(t)$ control signal in voltage and so it brings about the spool displacing of servo valve.

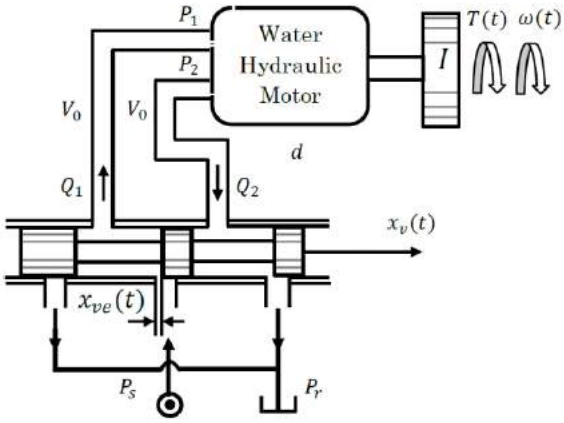

Fig. 1. Water hydraulic servo motor system [4], [5]

The $x_v(t)$ is regarded to u(t) as follows where k_v and τ_v are the gain and time constant of the servo valve dynamics, respectively.

$$\tau_v \dot{x}_v(t) = x_v(t) + k_v u(t) \tag{1}$$

The other nonlinear dynamic equations are detailed in from (2) to (9) in [4]. Where, the of the system is linearized to design the linear controller. Thus, the linearized transfer functions are used in this paper. Accordingly, the friction and leakage flows are omitted and the flow-gain coefficients of the related to servo valves are assumed to equivalent. $k_q = k_{q1} = k_{q2}$. By defining the load pressure (P_L) and the load discharge flow (Q_L), the below equations are obtained.

$$P_L = P_1 - P_2 \tag{2}$$

$$Q_L = \frac{Q_1 + Q_2}{2} = \frac{k_q x_{ve}}{\sqrt{2}} \sqrt{P_s - P_r - sign(x_{ve}) P_L} \tag{3}$$

The Taylor series of (3) are as in (4) where k_x, k_p are determined by test around linearization points.

$$Q_L = k_x x_{ve} - k_p P_L \tag{4}$$

From (8) and (9) in [4], the expression is deducted with neglecting the load flow and all leakages.

$$Q_L = \frac{V_0}{2E} \dot{P}_L + \frac{D_M}{2\pi} \dot{\theta} \tag{5}$$

the dead- zone character and valve dynamics are ignored for the system linearized, and so the x_{ve} spool motion is directly regarded to the $u(t)$ control signal ($x_{ve}(t) = k_v u(t)$). From the other equations in [4], a transfer function from the control input u(t) to the output $\omega(t)$ is obtained as in (6) for which the whole leakages and frictions are omitted. State space form can be derived from the transfer function for the controller design.

$$\frac{\omega(t)}{u(t)} = \frac{\left(ED_M k_v k_x / \pi V_0 I_{fw}\right)}{s^2 + \left(ED_M^2 / 2\pi^2 V_0 I_{fw}\right)s + \left(2Ek_p / V_0\right)} \tag{6}$$

Also, the transfer function from the control input *u*(t) to the output *θ*(t) is obtained as in (7).

$$\frac{\theta(t)}{u(t)} = \frac{\left(ED_M k_v k_x / \pi V_0 I_{fw}\right)}{s^3 + \left(ED_M^2 / 2\pi^2 V_0 I_{fw}\right)s^2 + \left(2Ek_p / V_0\right)s} \tag{7}$$

3. The Controller Design for with Pole Placement

The pole placement method has been used for the linear control design in the literature. The controller structure is simple for practical implementation. It places the poles of closed loop system. Thus, it can provide stability, disturbance rejection, convergence rate, command tracking, noise dispensation etc. therefore, the controller is designed against the disturbances thanks to the effectiveness by the placing of desired poles.
For the linear system in (8), the controller signal is given by (9), where *r* is the reference signal. The negative sign is used to indicate a negative feedback that is the general status.

$$\begin{aligned} \dot{x}(t) &= Ax(t) + Bu(t) \\ y(t) &= Cx(t) \end{aligned} \tag{8}$$

$$u(t) = -Kx + K_r r \tag{9}$$

So, the closed loop system is obtained as in (10) if the controller signal *u*(t) in(9) is replaced into (8). Accordingly, the closed loop system matrices are in (11). Thus, the matrix *K* provides the stability and K_f provides the reference tracking.

$$\begin{aligned} \dot{x}(t) &= Ax - BKx + BK_r r \\ &= (A - BK)x + BK_r r \end{aligned} \tag{10}$$

$$\begin{aligned} A_{cl} &= (A - BK) \\ B_{cl} &= BK_r \end{aligned} \tag{11}$$

It is tried to appoint the feedback gain *K* in order that the characteristic equation of closed-loop system in (12) is adjusted. This control design via regulating the poles is called as pole assignment or placement.

$$p(s) = s^n + p_1 s^{n-1} + \ldots + p_{n-1} s^{n-1} s + p_n \tag{12}$$

The transfer function from reference signal *r* to output signal y of the closed-loop system is

$$G_{yr}(s) = C(sI - A + BK)^{-1} BK_r \tag{13}$$

So, the static-gain K_r from reference signal *r* to output signal y is equal to (13).

$$K_r = \frac{1}{C(-A + BK)^{-1} B} = \frac{1 + LA^{-1}B}{CA^{-1}B} \tag{14}$$

The given K_r is related to the values of parameters. Therefore, the system is calibrated regarding to reference signal. This case is different from a system with integral action, in which the static-gain is not dependent on the values of parameters.

4. Simulation Studies

The whole computations via Matlab™ are performed for the simulation studies. The parameters of the system are as in Table 1 for the simulation studies [5]. The block diagram of control system simulation is as in Figure 2.

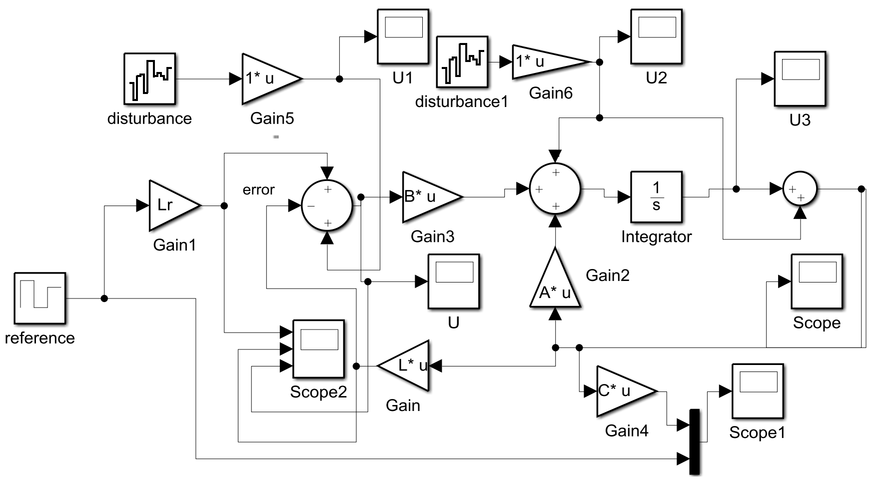

Fig. 2. Simulation block diagram.

Table 1: The values of parameters for the tank system

Parameter	Symbol	Value
Valve time-constant	τ_v	0.02 s
Servo gain	k_v	$1.153 x 10^{-4}$ m/V
Right valve dead zone	b_r	$0.3 x 10^{-4}$ m
Left valve dead zone	b_l	$0.4 x 10^{-4}$ m
Discharge coefficient	C_d	0.61
Bulk modulus	E	$2.2 x 10^{9}$ Pa
Displacement volume of motor	D_M	$15 x 10^{-6}$ m^3
Leakage coefficient	C_{Li}	10^{-12} m^3/s Pa
The moment of inertia for flywheel	I_{fw}	4.5 kgm^2
Volume of pipe	V_0	$5 x 10^{-2}$ m3
Flow gain coefficients	$k_{q1} = k_{q2}$	$0.858 X 10^{-3}$ $m^2/\sqrt{Pa}$s

In accordance with the simulation results, the outputs are as in Figure 3, Figure 4 and Figure 5. According to the references which are stairs type, Figure 3 shows the response of the system output angular velocity without disturbances. The output signal reaches successfully the desired velocity. When is applied the disturbances, which affect the input and output signals, Figure 4 shows the response of the system. Accordingly, the successful of rotational velocity response is decreased in point of reaching the desired reference signal due to oscillation and overshoot. Therefore, the obtained output response is as in Figure 5 when the controller matrices are constructed by changing poles in the design. Thus, the disturbances are attenuated and so the response is improved in point of reaching the desired reference signal. According to results, the system performance is successful despite the disturbances in system.

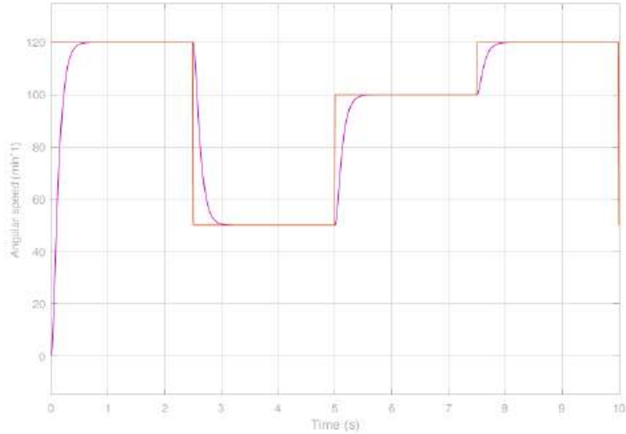

Fig. 3. The angular velocity of the system without disturbances.

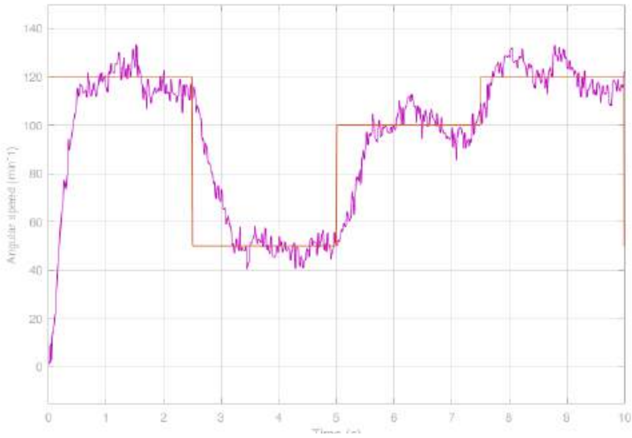

Fig. 4. The angular velocity of the system under disturbances.

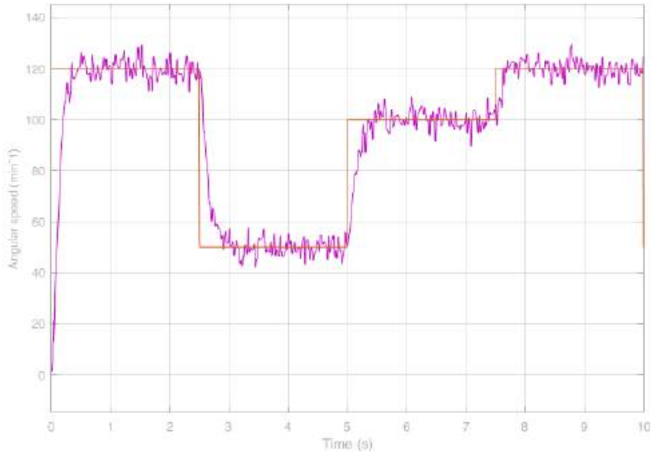

Fig. 5. The angular velocity of the system under disturbances.

5. Conclusions

This paper presents that the state feedback control via pole placement is designed method for water hydraulic servo motor system. The controller is designed by regulating the poles of closed-loop. The design includes the regulation of closed-loop poles against to disturbances for the system. The simulation results show that the controller gives a good performance despite the disturbances which affect input and output of the system. Thus, the simulation results demonstrate that the controller attenuates the disturbances by regulating the poles. Finally, the controller is both simple for the industry and successful against the disturbances.

References

[1] K. Ito and S. Ikeo, "PID control performance of a water hydraulic servomotor system," in *Proceedings of the 41st SICE Annual Conference. SICE 2002.*, 2002, vol. 3, pp. 1732–1735.

[2] K. Ito, H. Takahashi, S. Ikeo, and K. Takahashi, "Robust Control of Water Hydraulic Servo Motor System Using Sliding Mode Control with Disturbance Observer," in *2006 SICE-ICASE International Joint Conference*, 2006, pp. 4659–4662.

[3] K. Ito, H. Takahashı, and S. Ikeo, "Comparative Study of Robust Control for a Water Hydraulic Servo Motor System (2nd report: Disturbance Observer and/or Sliding Mode Control Design Approach)," *Transactions of the Japan Fluid Power System Society*, vol. 38, no. 2, pp. 21–28, 2007.

[4] P. N. Pham, K. Ito, and S. Ikeo, "The application of simple adaptive control for simulated water hydraulic servo motor system," in *Proceedings of the IEEE International Conference on Industrial Technology*, 2013, pp. 204–209.

[5] C. Khajorntraidet and K. Ito, "Water Hydraulic Servo Motor Velocity Control Using PID Funnel Control with Future Distance Estimation," *JFPS International Journal of Fluid Power System*, vol. 10, no. 1, pp. 1–8, 2017.

[6] H.-P. Ren and P.-F. Gong, "Adaptive control of hydraulic position servo system using output feedback," *Proceedings of the Institution of Mechanical Engineers, Part I: Journal of Systems and Control Engineering*, vol. 231, no. 7, pp. 527–540, Aug. 2017.

[7] A. A. Aly, "PID Parameters Optimization Using Genetic Algorithm Technique for Electrohydraulic Servo Control System," *Intelligent Control and Automation*, vol. 2, no. 2, pp. 69–76, 2011.

[8] H. Angue Mintsa, R. Venugopal, J. P. Kenn, and C. Belleau, "Feedback linearization-based position control of an electrohydraulic servo system with supply pressure uncertainty," *IEEE Transactions on Control Systems Technology*, vol. 20, no. 4, pp. 1092–1099, 2012.

[9] B. Yao, F. Bu, J. Reedy, and G. T. C. Chiu, "Adaptive robust motion control of single-rod hydraulic actuators: Theory and experiments," *IEEE/ASME Transactions on Mechatronics*, vol. 5, no. 1, pp. 79–91, 2000.

[10] Y. He, J. Wang, and R. Hao, "Adaptive robust dead-zone compensation control of electro-hydraulic servo systems with load disturbance rejection," *Journal of Systems Science and Complexity*, vol. 28, no. 2, pp. 341–359, 2015.

[11] H. Angue-Mintsa, R. Venugopal, J.-P. Kenné, and C. Belleau, "Adaptive Position Control of an Electrohydraulic Servo System With Load Disturbance Rejection and Friction Compensation," *Journal of Dynamic Systems, Measurement, and Control*, vol. 133, no. 6, p. 64506, Nov. 2011.

[12] Z. Alzahra, S. Dashti, M. Gholami, and M. A. Shoorehdeli, "Neural – Adaptive Control Based on Feedback Linearization for Electro Hydraulic Servo System," *IOSR Journal of Electrical and Electronics Engineering*, vol. 8, no. 1, pp. 2278–1676.

ISSN 1454 - 8003
Proceedings of 2017 International Conference on Hydraulics and Pneumatics - HERVEX
November 8-10, Băile Govora, Romania

NOISE CONTROL IN OIL HYDRAULIC SYSTEM

Basavaraj HUBBALLI[1], Vilas SONDUR[2]

[1] Jain College of Engineering, Belagavi Karnataka India, bvhubliabhi@gmail.com

[2] Visvesvarayya Technological University, Belagavi Karnataka India, vbsondur@gmail.com

Abstract: *This paper reviews the techniques for analyzing the Noise Control in Hydraulic System components. Hydraulic power transmission was quieter than the gears, cams, connecting rods, and cables that replaced. However, as economics led to higher pressures and speeds, it also led to less beefy components. Power levels of machines also grew rapidly. All of these factors increased noise. Hydraulic machines generally have a number of noise sources. This paper explains how Pumps, Motors and Valves generate airborne, structure-borne, and fluid-borne noises. It identifies hydraulic parameters that influence noise and guide planning programs for designing and developing of some quiet hydraulic components. Economics requires that all quieting efforts be focused on identifying and controlling the key noise generator.*

Keywords: *Cavitation, fluidborne, noise, pump, valve*

1. Introduction

Sources of noise in hydraulic systems are the pump and its driver, the distribution lines, control elements and actuators. Of these, the pump is normally the main source of noise, but this can usually be reduced to moderate levels by suitable acoustic treatment. The main aim at this end of the system should be to minimize pump-generated noise and vibration and any associated resonance. At the same time it is highly desirable to isolate the distribution line(s) so that vibration generated by the pump unit is not transmitted through the pipe work, with the possibility of resonance occurring at other connecting points. This does not, however, eliminates the possibility of pressure pulsations being transmitted by the fluid to the pipe work system and attached components, which phenomenon may need separate treatment.
Noise in fluid power systems is generally caused by pressure waves in the fluid stream. The pumps in general use are positive displacement types and employ pistons, vanes, or gear teeth to move the fluid. Since the fluid moves in sequential packets, pressure waves are set up in the fluid stream. These pulses of fluid are a cause of noise and system instability.
All pump and motor noise standards require that only the sound radiated from the test unit be measured. This is difficult and a whole technology has evolved for excluding unwanted noises from support brackets, bed plates, drive shafts, and hydraulic lines. Valves present a different problem. Their noise is due to a cavitation plume streaming downstream from the valve. For this reason the sound radiated by the first few feet of line as well as that of the valve must be included in the measurement.
Cavitation is an undesirable phenomenon in fluid power systems, which not only changes the fluid characteristics like density and compressibility, but also induces vibration, noise and erosion. In oil hydraulic systems, cavitation most frequently occurs in valves, pumps and actuators, inside which the pressure plays an important role in formation and development of cavitation. It is clear that when the local hydrostatic pressure drops below the fluid vapor pressure at the actual temperature, cavitation occurs.
Cavitation inception was investigated a lot in various cavitation models and by various ways, and several engineering methods were proposed. As in pump cases, detection of the net positive suction head (*NPSH*) and paint erosion were usually used as direct index for cavitation inception judgment. In some cases, the measurement of static pressures on the volute-casing wall was used as evidences for cavitation distributions. Sound and vibration were mostly used for cavitations' detection. Acoustical signals are used to judge the thresholds of cavitation inception. The

interferences from environmental noise can be easily eliminated based on the spectrum method. The cavitation distribution states play an important role on the cavitation noise [1].

2. Types of noise

Vibrations are called structure borne noise and fluid pulsations are called fluid borne noise. Pump commonly generate as much as 1000 times more energy in the form of structureborne or fluidborne noise than they do in the form of airborne noise. These forms act on other machine elements and frequently end up generating more airborne noise than that coming directly from the pump. Because of this, it is important to control all three forms of noise. Controls for the three types noise are different [2].

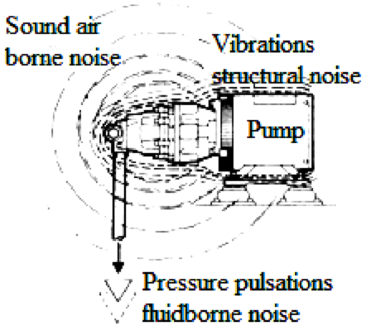

Fig. 1. Three forms of noise

2.1 Fluidborne Noise

Fluidborne noise is that it has as much as a thousand times the energy of pump airborne noise. It therefore poses the risk of exciting other machine components to produce high airborne noise levels. Even when the conversion is relatively inefficient, it can produce louder than the pump itself. Pulsations generate vibrations as well as sound. They are responsible for hydraulic line vibrations that cause metal lines to fail in fatigue and flexible lines to fail by chaffing. Often, these fluidborne noise-induced vibrations, in turn, also generate sound. Fluidborne noise is generally more important in mobile machinery than in industrial. There is a new and growing concern over fluidborne noise. Pulsations can interfere with the electronic controls that are finding wider use in hydraulic systems. Most of these depend on pressure oscillations generally require more sophisticated electronics for signal processing and may also limit the system’s sensitivity.

<u>Fluidborne Noise Mechanics</u>

It is periodic fluid flow perturbations or pulsations. When these encounter flow resistance, they result in pressure pulsations as well. For this reason it generally considers fluidborne noise to be pressure pulsations or waves. The major difference in airborne and fluidborne noise is the medium in which they exist. Because fluids have higher stiffness or bulk moduli, fluid waves travel faster than air waves. The sound velocity in a fluid is:

$$C=\sqrt{\frac{\beta}{\rho}}$$, where β = bulk modulus, ρ = mass density

It follows that the length of fluidborne waves, the distance between like points on successive waves, is

Wavelength, λ = C / f , where c = sonic velocity , f = frequency

It is often necessary to deal with fractions of a wavelength. In this we consider wavelength in terms of angles, with one wavelength equal to 2π rad. Angular fractions of a wavelength are found by multiplying distances by a coefficient equal to:

$$\beta = \frac{2\pi}{\lambda}, rad\ /m$$

This quantity is called the phase shift constant because the phase difference in pressures at two points is determined by multiplying it by the distance between the points.
It may be necessary to analyze the various possible sources of noise in the complete hydraulic system in detail in order to arrive at satisfactory noise treatment. In this case the possible sources of noise generation are, in decreasing order of significance:

(i) Pump Noise
(ii) Appliance noise
(iii) Control element noise
(iv) Water hammer
(v) Chatter
(vi) Cavitation
(vii) Resonance
(viii) Pipework noise
(ix) Thermal effects

Pump Noise and Vibration can be minimized by mounting by the pump and motor on a common base (or Mounting the motor integral with the pump) and isolating the complete unit on a resilient mount. A general recommendation is that the natural frequency of the isolated mount should not exceed on-quarter of the shaft speed (frequency), although it may be permissible to approach one-third of the shaft speed if a stiffer mount is required. If further acoustic treatment is required the whole pump/motor unit can be fitted with a suitable enclosure. The majority of hydraulic pumps are driven by electric motors, so no special problems are involved other than ensuring an adequate airflow for cooling the electric motor. If necessary a forced draught ventilating system can be used with a completely sealed enclosure, employing dust silencers of the absorptive type.

3. Measuring Pump Fluidborne Noise

The pump pressure pulsations are influenced by discharge line parameters. Because the discharge line has this much influence, there is a problem in finding a measurement that accurately scales a pump's intrinsic fluidborne noise without being affected by the test circuit.

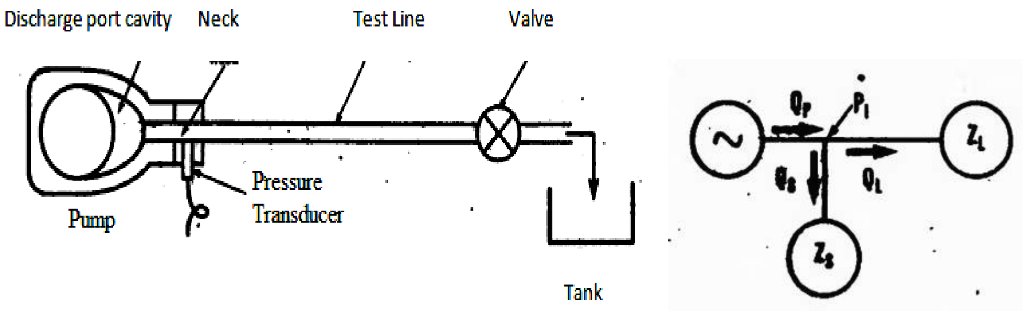

Fig. 2. Schematic diagram of pump circuit

A cavity in the pump represents the fluid volume in the discharge passages. This volume is the primary factor in determining the pump impedance.
The periodic flow generated by the pump, at each frequency, is divided between the pump and test circuit impedances inverse proportion to their magnitudes.
The flow then is:

$$Q_P = P_1\left[\frac{1}{Z_L}+\frac{1}{Z_S}\right]$$

Where P_1 = measured pressure at interface, Z_s = pump internal impedance , Z_L = test circuit impedance at interface

Solving this for the pressure measured at the interface

$$P_1 = \frac{Q_P Z_S}{1 + {Z_S}/{Z_L}}$$

The numerator consists of two inherent pump parameters. Their product is called the blocked pressure because it is the pressure pulsation that would be generated if the pump only produced its noise flow and its outlet was blocked. It is an inherent property of the pump that is analogous to the open-circuit voltage of an electrical generator.
Although pump flow perturbations are the basic cause of fluidborne noise, it is generally agreed that the blocked pressure is the best measure of this noise. The principal reason is that dynamic pressures are easily measured, whereas dynamic flows are very difficult to measure.
The locked pressure is measured by the transducer at the pump interface if the test circuit impedance is much higher than the pump impedance.
The impedance of the test circuit is:

$$Z_L = Z_o \frac{Z_T \cos\beta 1 + jZ_o \sin\omega 1}{Z_o \cos\beta 1 + jZ_T \sin\beta 1}$$

Where Z_T = load valve impedance, Z_O = test line characteristic impedance
B = phase shift constant, l =test-line length

In most pumps, the compressibility of the fluid in the discharge passages and the pumping chambers in communication with the discharge port account for most of the pump impedance.

4. Hydraulic Components

4.1 Decoupling of pump vibrations

The flexible pump carrier is used to connect the hydraulic pump to the drive motor, whereby the transfer of component vibrations and oscillations is avoided to a large extent. The pump vibrations are isolated and damped by a temperature and fluid stable rubber ring which transfers all the forces. By using a rotary flexible coupling there is no metallic connection between the pump and motor. The noise level within a hydraulic system may be reduced considerably by this means.

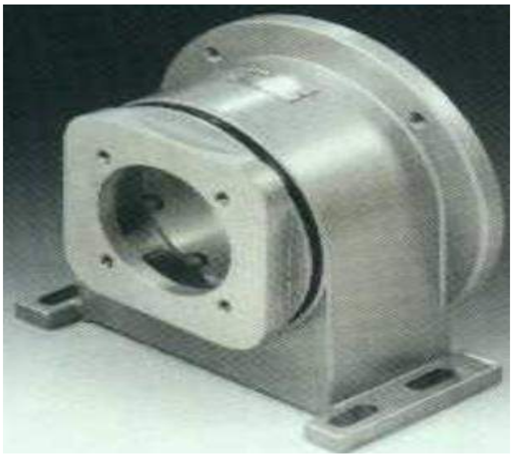

Fig. 3. Pump carrier with damping of vibrations (Flexible pump carrier)

The possible reduction in the noise level depends on many factors (type of pump, operating pressure, type of pipes, construction, etc).Hence exact values cannot be provided. In general noise levels may be reduced by up to 6 dB (A). The damping materials used in the pump combinations.

Figure shows the measuring arrangement and typical noise reduction for an flexible pump carrier in comparison with a rigid pump carrier [3].

4.2 Valves

Noise due to the operation of valves, regulators and control elements is transient and related to the degree of turbulence or cavitation produced, although in specific designs and certain circumstances individual elements may be subject to vibration and generate a continuous noise. So much depends on the design and finish of the flow passages involved that no general analysis can be attempted. The noise level of such devices is dependent on the design and localized flow velocities produced and also on the response time, where applicable.
The latter effect can be minimized by arranging that the response time is shorter than that required by the system, This will result in minimum 'hammer', 'Water hammer', in fact depends on the switching velocity of the valve-i.e. on the spool-switching velocity in the case of spool valves. Valves operated by dry solenoids have in fact; uncontrolled response and so often produce 'hammer'. Wet solenoids are cushioned by the hydraulic fluid so move more smoothly and open the valve passages more gradually.
Many of the valves used to control hydraulic systems are constrained with steel coil springs. The valves are free to move within the valve housing and are biased on one or both ends with springs. The valve and spring effectively act as a spring-mass system. The valve may then oscillate at its own natural frequency and is also subject to the forcing function provided by the pressure waves in the fluid stream. Pressure waves in hydraulic systems can cause control valves to become unstable during operation and also contribute to vibration and noise. Therefore, it becomes desirable to filter out or at least reduce the magnitude of the pulses, in order to optimize the performance of fluid power systems and their controls. Reduction in pressure wave amplitude also reduces wear and damage to system parts. The fluid pump is usually the primary source of pressure pulsations. These waves travel throughout the fluid system. Therefore, it becomes advantageous to reduce the amplitude of the pressure waves as close to the source as possible.

Cavitation in valves

Cavitation is a breakdown inflow caused by the localized fluid falling below the vapour pressure of the fluid. Consequently, vapour bubbles are formed resulting in irregular and noisy flow. Such a reduction in pressure can occur in regions of localized high flow velocities, such as are caused by restrictions to the flow path. Accurate prediction of cavitation conditions is most difficult, and usually impossible, in the design of valves and fittings, and problems have to be tackled on empirical lines. If the flow rate is sufficiently restricted cavitation and noisy flow can be expected.
Thus partially closed tap or valve is nearly always noisier than when fully opened; also quiet a small change in position, and thus flow rate can cause a change from cavitating to non cavitating flow. It is also a characteristic of many valves, that for flow rates (valve openings) below that which produces cavitation, cavitation noise increases with increasing frequency: whilst for higher flow rates, where flow is non-cavitating, cavitation noise does not vary greatly with frequency.
Cavitation is by far the leading noise generating mechanisms in valves. It is quite common in pressure-regulating and pressure relief valves. When these valves cavitate for a long time, there may be more of an erosion problem than a noise problem. When the erosion occurs, it not only reduces valve life but pollutes the fluid within metal particles, which cause pump damage. Valves control fluid flow by constructing the flow path. This causes the fluid to speed up in passing through the construction. Since friction losses in turbulent flow are proportional to the square of velocity, the needed energy loss is then achieved in a relatively short distance.
In the case of high pressure systems, or valves subject to high pressure drops, it is desirable to utilize flow paths designed to eliminate cavitation as this can cause physical damage to the valve components as well as excessive noise. The problem, basically, is one of preventing the pressure in the valve throat from falling below the fluid vapour pressure in order to prevent cavitation occurring.

4.3 Cavitation Noise

Cavitation itself does not cause noise. It is the collapse of the cavities that causes noise. With valves this occurs when the jet dissipates into a more normal flow and pressure recovery takes place. Often this happens in the discharge line, outside the valve. Bubble collapse releases a surprising amount of energy. When it occurs at a solid surface, it is capable of causing surface fatigue failures, pitting, in all but the hardest materials. The energy also causes structural vibration that can end up as a loud noise. In addition, the reaction with the rest of the fluid results in high levels of fluidborne noise.

Cavitation generated fluidborne noise is confined to the downstream side of the valve orifice. While the impedance of the orifice is sufficiently different from that of the downstream passage, to reflect much of this noise downstream, it is believed that the cavitation bubbles do most of the reflecting. Cavitation noise is random, like the bubble collapse that causes it. Fluidborne noise exists at all frequencies but is strongest in the range 4 to 8 kHz. Because of its strong high frequencies, it is efficiently radiated as airborne noise. It is generally described as a hissing sound.

4.4 Cavitation Control

A good way to avoid cavitation is to design the throttling device so that it has laminar flow. The advantage of this type of flow is that It uses viscous friction to achieve fairly good energy loss with low velocities and it does not generate vortices. This type of flow occurs when the Reynolds number of the flow is below about 2000.
The Reynolds number is: N =2500vR /v
where v = fluid velocity, R= hydraulic radius, v =kinematic viscosity
The hydraulic radius, in this equation, depends on the shape of the flow cross section. It is defined as R = cross-sectional area / perimeter.
In case of passages that are round or whose cross-sectional dimensions remain proportional, their areas decrease as the square of their size while their allowable velocity changes only linearity. It would seem desirable to keep the passages as large as possible to keep from having to provide large numbers to handle a given flow. However, as velocities are reduced, the passage length must also be increased, to achieve a given pressure drop. It can be shown that pressure drop for laminar flow.

$\Delta P = k\frac{lV^3}{N_R}$, where k = a constant, l= path length

V = average flow velocity, N_R = Reynolds number
From this it can be seen that the real advantage is in reducing passage size and increasing velocity, because this rapidly reduces the length needed for a given pressure drop. Porous materials are sometimes used to achieve laminar flow. Both compacted stainless steel wool and sintered powdered metal have been used. These not only provide small pore sizes, they also offer paths with many turnings which are good for energy loss. However, they erode easily and shed debris if velocities are too high or if some cavitation occurs.
A difficulty with using this material is in making the valve adjustable. Figure 4 and 6, shows the general idea of an adjustment scheme. With this configuration, either the porous plug of the outer port sleeve can be moved back and forth to change the flow path length. A similar throttling mechanism utilizes flow paths etched in the faces of washers. Multiple paths are provided by stacking many washers together to form a porous sleeve.
Since cavitation is caused by low pressure, it seems reasonable to except that it could be suppressed by increasing a valve's back pressure. Increasing back pressure increases sound power. It has been observed that increasing back pressure shifts the bubble collapse zone upstream. From this it is concluded that the sound increase is due to having more bubbles collapse near the solid valve surfaces. The maximum occurs when the collapse zone reaches the valve. The fact that this maximum noise occurs at back pressures that increase with flow appears to

support this theory. Noise reductions occurring when back pressure is increased above the maximum noise pressure are probably due to reduced cavitation.

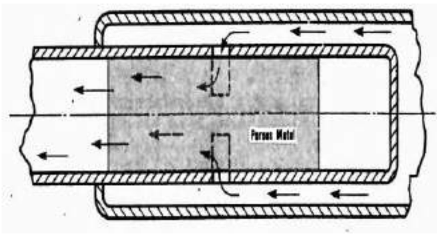

Fig. 4. Porous metal valve concept

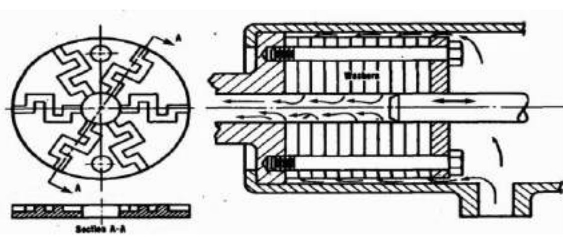

Fig. 5. Etched washer valve concept

Some noise reduction is achieved by using a series of pressure drops, with the downstream ones providing back pressure to suppress cavitation in their upstream counterparts. A pilot operated valve was built with two poppet valves in series with the control, dividing the pressure drop equally between the two stages. This valve produced less noise than that of a comparable valve of conventional design.
Reductions of sound levels have been made by recontouring the throttling device and valve passages. The objective of these modifications is to move cavitation collapse farther from solid surfaces and to smooth discharge flow to reduce vortex formation. It is believed that noise reductions achieved by contouring the spool valve shown in Fig is due to this factor. Throttling element modification can produce larger noise reductions. Test results shows that , there was a definite increase in noise as the poppet angle was increased. The quietest seat was the straight sided orifice shown. Convergent and divergent orifices had little effect on noise levels for the low-angle poppets. It was found that part of the reason for the high noise levels with the large angle poppets was due to the flow restriction that they caused. Reducing the poppet diameter to provide a more generous downstream passage reduced the noise level.

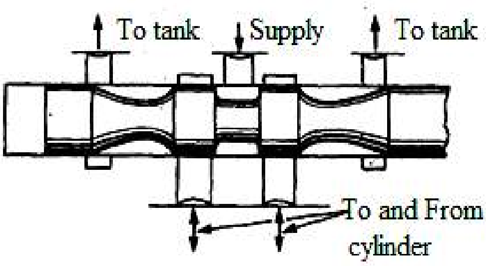

Fig. 6. DCV spool contoured for low noise

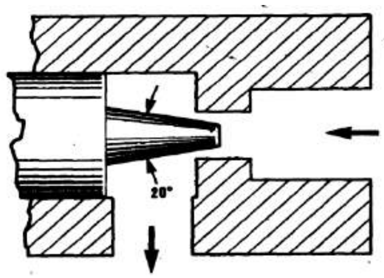

Fig. 7. Quietest poppet and seat assembly

4.5 Valve Oscillation

This noise is a single-frequency or pure tone sound, generally described as a squeal or whistle. Single-stage poppet valves are the most liable to be unstable. This can be due either ability to react more quickly or because they have less damping than that of spool or pilot operated valves.
The fact that valve instability produces a pure tone shows that a resonance is involved. Research has shown that valves are capable of generating self-sustaining oscillations. One source of these oscillations is a flow instability called hydraulic jet flip.
At lower pressure drops, jets tend to cling to a wall. At higher pressures it takes on a more independent form. There is a transient pressure range where it exists in either form and may flip back and forth from one to the other. Each time it flips, the flow is perturbed and the valve begins to oscillate. Squeal from such sources occurs at some operating conditions and not others.
Flow and acceleration forces that tend to open the valve further than called for provide another motivation for valve oscillation. The onset of vibration is related to the strength of these forces in comparison to other parameters, such as stiffness, damping, and how much the ports open for a

given valve movement. These forces increase with pressure drop through the valve, which explains why some valves provide good service at some pressures but begin to squeal at higher pressures.
The system in which the valve operates may have natural frequencies that are excited by transients and cause the valve to sustain the oscillations. This occurs with valves having just a little more than border line stability. Valves with even greater inherent stability succumb if their natural frequency nearly matches that of the circuit. These valves operates satisfactorily in some circuits and squeal in others. Sometimes, changing the line connected to a valve makes this difference.
Long lines increase the likelihood of an unfavorable match with a valve because these have a larger number of resonant frequencies in the range of valve natural frequencies. For that reason instabilities are sometimes avoided by using shorter lines. Valve inner chamber volume has an effect similar to adding line length, so reducing this volume is another option. Another way of discouraging this type of instability is to use lines composed of two different diameters so that reflections from the change in diameters interferes with the organ pipeline resonances.
Analyzing valves and their circuits to determine what factors must be changed to avoid instability requires considerable effort. Literature on this process universally prescribes replacing a squealing valve with one of a different design. Where the offender is a single-stage valve, it is best replaced with a pilot operated valve.
Pilot operated valves have instabilities, although these are relatively rare. When it occurs after operating without trouble for a long time, it is usually cured by replacing worn seats or poppets. One unstable poppet valve problem was cured by installing guides that prevented sideways poppet motion. Such motion will produce flow perturbations as well as axial motions. This suggests that some valve instabilities are due to lateral vibration, which does not appear to have been considered in past research [4].

4.6 Reservoir

Reservoirs should be designed to avoid the entrainment of air in the fluid, and the recommendations given in the following paragraphs are intended to assist in this. Return lines should enter and suction lines should leave the reservoir well below the surface of the fluid when at its lowest permissible level. Return lines should be fitted with a pepper pot and suction lines with a bell mouth entry or a suction strainer where they enter the reservoir. A baffle should be fitted between the suction and return lines. Variable capacity systems require special attention. The reservoir should be fitted with a bubble separator. This may be a single 60 mesh wire gauze set between the return and suction tank openings. Maximum effect is obtained when the gauze lies at an angle of 30^o to the horizontal.
Where a reservoir is pressurized with air, there should be a separator at the oil-air interface. The pressure drop across the entire suction line should not exceed 0.3 bar regardless of reservoir pressure, nor should suction pressure at the pump inlet be less than 0.2 bar. Suction line velocities should not exceed 1.5 m/s. Working and return line velocities should not exceed 4.5 m/s. Reservoirs should be flexibly mounted and isolated from surrounding structures.

4.7 Pipelines

A simple method of isolating or decoupling the pump from the delivery line is by a flexible hose connection. Isolation can be further improved by suing two such hose lengths in close proximity and mounted at 90^o to each other. Ideally, isolation by flexible pipe should include bends in two mutually perpendicular directions with equal distances between bends. In general, isolation of the pump and motor from the tank by suitable mountings and decoupling from the pipework will free the rest of the system from the transmission of mechanical vibrations and the consequent possibility that these would be amplified. Care must be taken to ensure that there is no short-circuiting of the isolation or decoupling employed.
Noise produced in hydraulic lines may be pump generated (changes in power and pressure, or varying amplitudes of pressure pulsations) or fluid generated (flow instability, turbulence or simple fluid friction). Fluid generated noise in small bore pipes with low to moderate flow rates is generally

negligible, unless pressure pulsations are present. Thus pipe vibration, and consequent radiation of airborne noise, is usually due to the higher level of noise generated by fittings; pipe resonance is due to mechanical vibration or resonant noise generated in supporting systems.

4.8 Suction Line

The suction line is a first suspect in a hydraulic installation which proves noisy, and where the noise cannot be directly attributed to pump or components. Suction lines can generate noise if there is an excessive pressure drop when the pump is sucking at sub-atmospheric pressure and drawing air out of solution. The resulting formation of air bubbles, and their subsequent collapse, can cause ‘mechanical’ noise which is often erroneously diagnosed as pump noise. Suction line noise can also be caused by a partially blocked or undersized suction filter, poor placement of the outlet pipe in the reservoir or entrained air.

4.9 Delivery Lines

Delivery lines can carry mechanical vibrations to distant parts of the circuit. These vibrations may be amplified at local points by the resonance of supporting structures or components directly connected to the pipework. Resonance can be eliminated by decoupling connections. All pipework installations should be designed on the basis of avoiding abrupt changes of section which could lead to large flow velocity changes and generation of turbulence.

5. Components to Reduce Noise

Hydraulic systems include components which agitate fluid and air and these effects influence each other. In order to reduce noise in hydraulic power units various measures are available. Due to the large surfaces and the thin metal walls used, oil tanks are very good resonators. By using materials which damp vibrations it is possible to decouple noise from the tank. Measures which help in this are: Placing pump on an anti vibration element , Installing a vibration damping pump carrier, Using pipe ducts made of rubber, Fixing lines with noise damping fixing clamps. Vibrations occur in fluids especially when pressure pulses are present. Measures which help in this are the use of accumulators which remove pressure pulses and creation of opposing pulses, which neutralize the pulses within the complete system. Decoupling of air vibrations is only possible by using an acoustic absorption cover over the hydraulic unit.
The vibration and noise damping characteristics of these clamps are the most important, as transfer of component vibrations to the complete system may be avoided in this way. Components for the decoupling of vibrations in fluids. Accumulators are mainly used to decouple vibrations in fluids. It is only possible to decouple the noise travelling in air in hydraulic systems by using noise absorbing covers.
Sufficient damping for pipes is usually provided by suitable supports, or pipe clips spaced at regular intervals, the supports having resilient linings so that vibration in the pipe is not transmitted directly to the surface to which the supports are fixed.

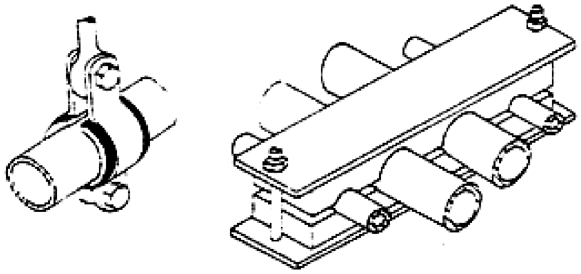

Fig. 8. Vibrating and isolating pipe clip and Pipe clamp block with vibrating isolating material

<u>Shock Preventers</u>
Shock preventers are pulsation dampers (or accumulators) characterized by having very large flow inlet apertures which are partially closed off by liquid trying to flow back out of them. They are

not shock absorbers, as they prevent shock or surge occurring. For the same reason , they do not attenuate shock.

Shock Removers
These are sensitive hydro devices which prevent a standing wave from passing farther down a system or from bouncing back through them. They are normally of tubular or sleeve form with a flexible membrane.

Acoustic Filters
Acoustic filters can be fitted to systems where pressure ripple is high. These are essentially tuned silencers which are critical in design and are usually effective over only very narrow frequency bands, although the attenuation achieved can be quite high. Untuned silencers simply comprise an expansion chamber with broader coverage but reduced attenuation. An accumulator is, in effect, an unturned hydraulic acoustic silencer and is most effective at lower frequencies.

Conclusion

The cheapest quiet machines are those that initially were planned, designed and developed to be quiet. Many noise controls can be incorporated into a new design for little cost but are expensive when added to an existing machine. It is important to set these goals for machines while they are still in their planning stage. Having a clear noise-level goal saves time in making other planning decisions. If it indicates the need for noise controls such as isolators or enclosures, other planning factors can be adjusted to accommodate these without losing time.
A machine can have almost any noise level, from a very high one to a very low one, depending on how much noise control is built into it. In planning a new machine, estimate its noise level for some known degree of noise control. Operating parameters such as size, speed, and pressure all affect noise, so selecting the optimum combination of these three parameters is the first step in finding a quiet pump. Since speed has the greatest influence. This is because, as speed increases, more of the strong, lower pumping harmonics move into the frequency range where they radiated efficiently.
Noise increases equally with both pressure and pump size, so there is no advantage of trading off one against the other. For quietness, the optimum operating parameters are the slowest practical speed and any combination of pressure and displacement that provides the needed hydraulic power. Unit selection has to be on the basis of airborne noise ratings. There is not enough data on structure and fluidborne noise for making comparisons. It is generally assumed that steps that reduced audible noise of a pump also reduced the other two noises as well. This is a reasonable assumption when comparing pumps and motors of the same type but may not be valid when comparing different types.
The leading noise generator provides a basis for estimating a proposals machine's noise level. Usually, it is a pump, but it could just as well be a hydraulic motor or, in rare cases, a valve. The noise source's sound pressure rating is useful because it approximates numerically the noise level that the unit will generate in a machine that utilizes normal machine design practices and does not have any special noise control features. Since pumps, motors and valves are the leading noise sources, it follows that selecting the quietest ones is the first step in producing a quiet machine. To generalize, noise levels of industrial and mobile machines should not exceed 85 dB.

References

[1] Fu. Xin et.al., "Noise Properties in Spool Valves with Cavitating Flow", State Key Laboratory of Fluid Power Transmission and Control, Zhejiang University, Hangzhou, China, 2008;
[2] S. Skaistis, M. Dekker, "Noise control of Hydraulic Machinery", New York, 1988;
[3] H. Exner et.al, "Basic Principles and Components of Fluid Technology", Hydraulic Trainer, Volume I, 1991;
[4] R.H .Warring, "Hydraulic Handbook", Trade and Technical Press Ltd, England, 1983.

NEW MECHATRONICS AND CYBER-MIX MECHATRONICS SYSTEMS AND ECO-SYSTEMS DESIGNED BY THE RESEARCH INFRASTRUCTURE ECOSIN-MECATRON

Gheorghe Ion GHEORGHE

[1] National Institute of Research and Development in Mechatronics and Measurement Technique, Bucharest, Romania

Abstract: *Within the framework of the "ECOSIN – MECATRON" Research Infrastructure project, INCDMTM - Bucharest develops Intelligent Mechatronics and Cyber - Mix - Mechatronics Intelligent Eco Systems, which is the foundation for the Intelligent Mechatronics Industries for the Intelligent Field of Specialization and for Mechatronics and Cyber – Mechatronics, by presenting advanced solutions and intelligent technologies related to the economic, industrial and social sustainability in Romania.*

Keywords*: Intelligent ecosystems, mechatronics and cyber-mechatronics systems, research infrastructure, ecosin-mecatron*

1. I.C. ECOSIN-MECATRON

- **I.C. ECOSIN-MECATRON** = New MECHATRONICS and CYBER-MIXMECHATRONICS MULTIAPLICATIVE Intelligent Systems, is currently research infrastructure I.C. national and distributed and in the future European / international and distributed.
- **Coordinator partners**
  INCDMTM – coordinator and initiator of I.C.);
  Partners (and participants):
    INCD-ICPECA; INCD-IMT; INCD-TP; INCD-INMA; INCD-INOE 2000; INFLPR; IMS-AR; ISSR; S.C. OPTOELECTRONICA 2001; INCD- Victor Babeș; I.N. Fundeni; IPA-CIFAT, Craiova; U.P.B.; U.Gh. Asachi-Iași; U.Tr.-Brașov; U.V. Târgoviște; U. Dunărea de Jos-Galați; U. Ovidiu- Constanța, U. Lucian Blaga- Sibiu; U.T. Cluj-Napoca; U.P.-Timișoara; U. Ștefan cel Mare- Suceava; U.T.- Craiova; U.- Pitești; U.M.F. Carol Davila- București; R.T.R. București; S.C. Automobile Renault- Dacia, Pitești; AroTT;
- **Location:** distributed, at the headquarters of the coordinator and partners and participants (currently- from România and in the future – from Romania and Europe). Headquarters of the coordinator institution is: București, România, șos. Pantelimon, nr. 6-8, sector 2; web: www.incdmtm.ro;
- **Short description**: I.C. ECOSIN-MECATRON, develop Smart Specialized Intelligent Domain Eco-Nano-Technologies and Advanced Materials from SNCDI by Physical Sciences and Engineering correlated and focused with the field of science, Mechatronics and Cyber Mechatronics.
- Due to advances in automation of manufacturing and processes, mechatronics and cyber-mechatronics are gaining more and more importance, and its demands result in the need for advanced intelligent systems. Due to the increasing importance of automation and manufacturing and processes, the automation and cybernetic technology industry takes on an increasingly important role in industrial processes (intelligent manufacturing, intelligent integrated control). The basis of any intelligent mechatronic and / or cyber mechatronic closed loop control system is to detect states and variables of intelligent coloring or data processes that are then remote configured, remote manipulated and remote monitoring.
- **Scientific context and relevance:** I. C. ECOSIN-MECHATRON is relevant in the context of major societal challenges, this project being unique to Romania's industrial and economic construction and to many countries in the world. In Romania, INCDMTM has developed intelligent

and cyber-mechatronic systems and products already implemented in the Romanian industry (ex SC Automobile Renault-Dacia, Pitesti). Since 2000, INCDMTM has created and developed other evolutionary engineering branches, such as Integronics and Adaptronics, as scientific steps to Cyber-Mechatronics and Multi-Media Cyber-Mechatronics, with adaptations to the new working conditions of the intelligent industry and the performing economy. INCDMTM, collaborates in this intelligent specialized field with other national institutes, technical and polytechnical universities and other companies, in the fields of: Mechatronics and Micro-Nano-Mechatronics; Cyber-Mechatronics and Cyber-Micro Nano Mechatronics; Advanced intelligent materials; Mechatronics in Robotics, Mechatronics in Agriculture 4.0; Mechatronics in Industry 4.0; Automobile Mechatronics [Autotronics]; and so on The ECOSIN-MECATRON project contributes to the achievement of the objectives of the National Strategy for RDI 2020, namely general strategic objectives: increasing the competitiveness of the Romanian economy through innovation, increasing the Romanian contribution to the knowledge programs; increasing the role of science in society and specific objectives: increasing the level and efficiency of knowledge in correlation with the public priority: New and emerging technologies.

- **The state of implementation in Romania:** I. C. ECOSIN-MECATRON, includes a National Strategic Consortium (Universities and Research Entities), which will expand its European / international strategy (with existing Mechatronics and Cyber-Mecatronics entities in Europe). The implementation steps are: p1 - the development of the National Consortium (achieved) and the International Strategic Consortium (to be achieved); p2 - offering projects in the fields of I.C., by national and European programs (partially implemented); p3 - project execution (in progress); p4- monitoring of construction and equipment related to projects and infrastructure (in progress); p5- monitoring of national and European project financing (to be achieved); p6-enrollment of I.C. in Networks (national and European / International), completing the National and European Values Chain (to be achieved); p7-value contribution of I.C. (to be achieved). I.C. highlights the achievements already begun with socio-economic impact, as follows: achieving over 250 intelligent mechatronic products implemented in industry (e.g. Automotive Industry – SC Automobile Renault-Dacia, SC Componente Auto Topoloveni, SC Renault Technologie Roumanie, etc.).), the creation of new jobs (about 120); increasing labor productivity, increasing the quality of manufacturing, etc.
- **Socio-economic Impact**: (a) the chronology of events: established in 2010, and based on the SOPE projects. The initiative started with the projects won at the POSCCE competitions, as early as 2010, for the intelligent domains: CENTERS: Sedcontrol, Bio mechatronics, Certim, Cermiso, Knowledge Transfer and Mechatronic Products. (b) the type of service they provide or they will provide: industrial and laboratory; for intelligent manufacturing; new and advanced materials; micro-nanotechnologies; automation and cybernetization of manufacturing, etc.
- The socio-economic impact in Romania will be sustainable and developed for a Romanian information society with a modern and competitive 4.0 industry with intelligent agriculture, etc.
- Socio-economic impact in the E.U. and in the world will be globally sustainable and developed for a society of intelligent knowledge and a neural society, with intelligent industries and economies, with superior and performing social, cultural and communication relations and with societal transformations and changes, corresponding to the level of the 21st century.
- **Unique character of I.C. ECOSIN-MECATRON:**

- radical societal changes (industry 4.0 - intelligence and cybernetics, agriculture 4.0 - intelligent and cybernetics, intelligent medicine, advanced aerospace industry - mechatronic and cyber-mechatronic systems and technologies for adaptive and multifunctional aerospace systems (e.g. drone systems and networks for agriculture - control of crops and agricultural production), etc.

The ECOSIN-MECATRON project contributes to the achievement of the objectives of the National Strategy for CDI2020, namely general strategic objectives:

- ECOSIN-MECATRON, contributes to the achievement of the main and specific objectives of the National RDI Strategy 2020 at national level and the Europe 2020 and Europe 2030 Strategy at European / International level.
- **Financial Information:**

Construction costs and infrastructure for the European component: 280 mil. Euro

Construction costs and infrastructure for the Romanian component: 56 mil. Euro
(of which spent and provided in contracted projects, 7.009 mil. Euro);
Total operating costs: 38 mil. Euro
Operating costs, Romanian contribution:19 mil. Euro

- **Representative image:**

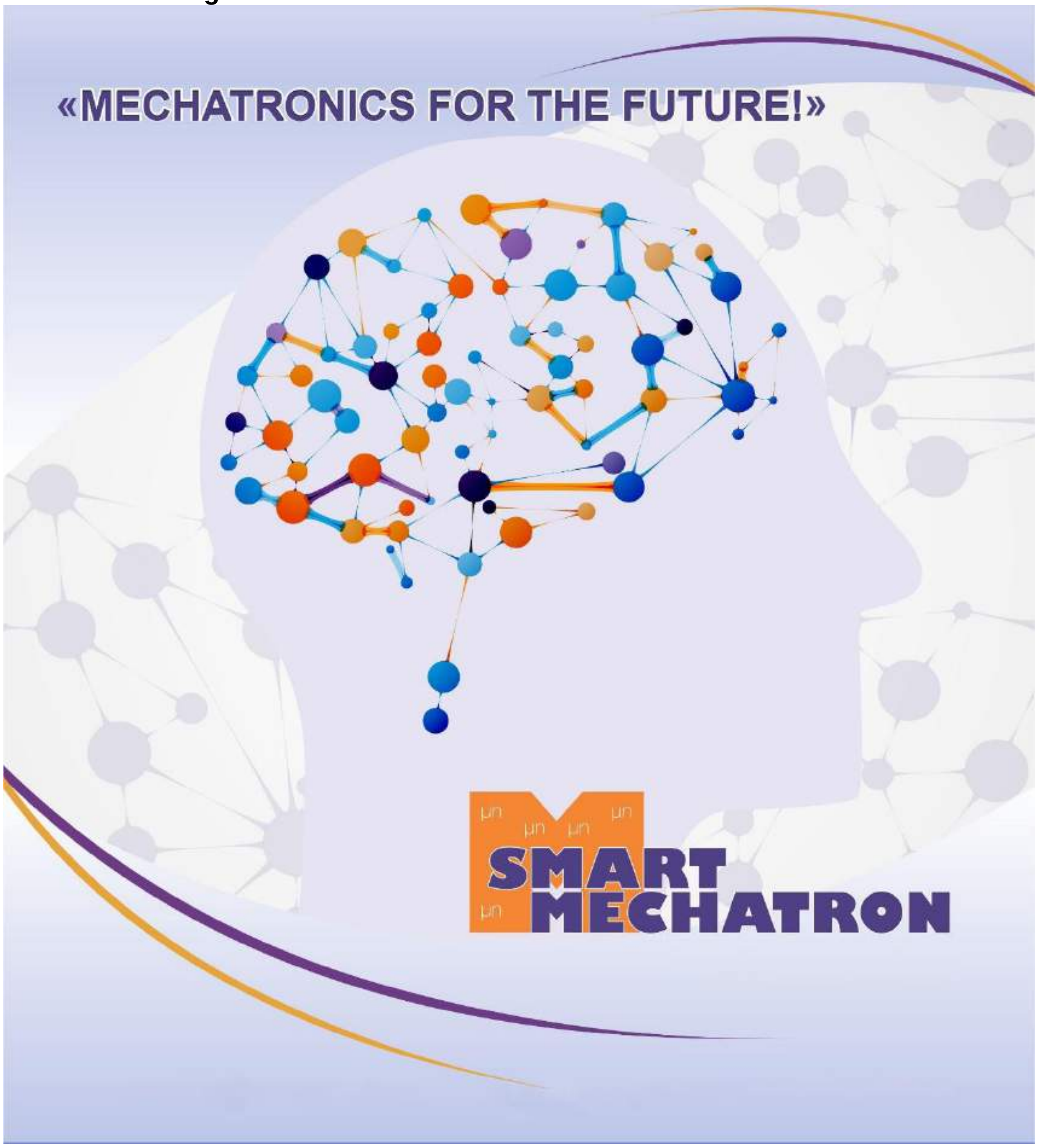

2. Preamble

The new Intelligent Specialization Mecatronica, Mix - Mechatronics and Cyber - MixMecatronica, addresses the philosophy of education in the new Engineering for the Future and Future Cognitive Society, as well as the holistic multidisciplinarity of it.
Depending on the new requirements of the process, product, materials, technology, energy, application and effect in industry, economy and society, this new field has been developed, upgraded and adapted to meet various operational criteria such as reducing material resources , energy and finance, high-level operation, optimal ergonomics, and cost-cutting at the limit.
In this sense, the concept and the evolutionary structure of the intelligent specialized field develops

towards a generative evolution, by adding new structural, functional elements and components and subsystems, on new principles and adapted accordingly to the new scientific discoveries, in order to obtain technical facilities and effects, technological and economic demands required by the concrete applications of intelligent mechatronic products, technologies and services.
The concepts of the mechatronic and cyber-mixmechatronic experimental models are involved in selective scenarios and variants and in support of their construction, through engineering challenges, as follows:
➢ selected scenarious on “monitoring system of controllers from distance;
➢ selected scenarious on “actuator detection control system”;
➢ selected scenarious on “ Automated Traffic Control and Monitoring System”;
➢ selected scenarious on “ mobile surveillance system for automobile survival”;
➢ selected scenarious on “monitoring system of communication channel”;
➢ the concept of a "cyber-mecatronic robot system with telemonitoring and telecontrol" and modularised programming and coordination systems in cyberspace;
➢ the concept of a “the concept of a "intelligent 3D mecatronic system with two grippers and two 3D sensors for measurement, integrated control and industrial services" and monitored programming and coordination subsystems in cyberspace;
➢ the concept of a “ the concept of a "cyber-mecatronic technological instrument system with telemonitoring and telecontrol and modularized programming and coordinating subsystems in cyberspace;
➢ the modular structure of a “mechatronic and cyber-mecatronic intelligent control system of castings in the automotive industry by telecontrol and telemonitoring" and the modularized programming and coordination subsystems in cyberspace;
➢ the concept of “ convergence of complexity in cyber-mechatronics’;
➢ “microcontroller programming and interfacing to intelligent mechatronic and cyber-mixmechronic systems”;
➢ “ Intelligent Mechatronic 3D Equipment for Processes of Measurement, Control and Industrial Services”;
➢ “intelligent mecatronic intelligent 3D equipment, dual in triple axes”;
➢ “ hardware and software structures for mechatronic and cyber-mechatronic systems”;
➢ “ creating virtual prototypes that increase the speed of development of mechatronic and cyber-mechatronic machines”;
➢ “conceptual design of the magnetic suspension for the suspension system”;
➢ the structure of cyber-mixmecatronic 3D multi-application system with telecontrol and telemonitoring”;
➢ “magneto-rheological damping system for railway vehicle suspensions”;
➢ etc.
It is presented in ECOSIN-MECATRON, in original concept, foundation of cyber-mixmechatronics multiaplicative systems as parts of cyber-physical systems (cyber-physical / cyber-mechatronics and intelligent virtual solutions in construction. The paper focuses on the basics of cyber-physical systems supported by the world's great strategists, with specific examples and concepts, with potential societal applications - intelligent mechatronic systems and in the future, clatronics, systems in virtual reality, with some major challenges on reliability and uncertainty, abstraction and physical-cybernetic matching, as well as design software, time-sensitive programming languages and networking for superdense time.
The Universe of Cyber Physics (or Physical Cybernetics / Cyber-Mechatronics) includes, in its program of development and implementation, the main stages, step by step, to materialize and implement them in society, to ensure innovative national, European and international strategies for a post-informational and neural society.
Thus, they are based on the "bases of cyber-physical systems" created and grounded by the great strategists of the world regarding:
> **The concepts** of cyber-physical systems (supported by global strategists Christopher Chadwick, Sarah Betzig și Fei Hu);

> **The design challenges of cyber-physical systems** (supported by global strategists Cameron Patterson, Roger Vasquez și Fei Hu);
> **Creating** mobile cyber-physical systems (supported by global strategists Yeqing Wu și Fei Hu),
Follows the "design principles of cyber-physical systems":
> Cyber-physical systems controllers (supported by Tony Huynh, Ahmed Alsadah and Fei Hu);
> Learning apprenticeship on the Physical-Cybernetic Intelligent System (supported by Kassie mccarley, Joseph Pivscan and Fei Hu);
> **Application** of HDP-HMM for the dynamic recognition of "hand gestures" (supported by world strategies Lv Wu Ting Zhang and Fei Hu);
> **Modeling problems** in Cyber-Physics Systems (supported by global strategies Michael Johnson, Tony Randolph and Fei Hu);
> **Modeling** Cyber-Physics Systems (Cognitive Vehicles - Remote Airplane), (backed by global strategy Meng Cheng Ong, Fei Hu and Yang-Ki Hong);
> **Security** of Cyber-Physics Systems (supported by Steven Guy, Erica Boyle and Fei Hu);
> **Physical Cyber Security Systems** - Smart Smart Network example (supported by Rebecca Landrum, Sarah Pace and Fei Hu),
Continuing with "Intelligent Sensor Architecture - the basis of Cyber-Physics Systems, on:
> **Wireless sensors** and wireless actuators for applications in Cyber-Physics (supported by Kassie mccarley, Joseph Pierson and Fei Hu);
> **Communication detection** (supported by Trenton Bennet, John Har and Fei Hu);
> **Integrated / Deployed Wireless Microsystem Architecture and Security** (supported by Derek Chandler, Jonathan Pittman, Jaber Abu-Qahouq, and Fei Hu);
> **Application** of a learning machine in physical sensing activity monitoring (Wenlong Tang, Ting Zhong and Edward Sezonov)
Finally, it concludes with "Cyber-Physical Civil Applications Applications" for:
> Creating efficient energy (supported by great strategists Preston Arnett, Jan Wolfe and Fei Hu);
> Creating cyber-physical systems for smart grid smart applications (supported by great strategists Matei Rell, Loilim Muirhead and Fei Hu);
> Creating Video in Unmanned Aircraft for Cyber-Physical Systems (supported by great strategists Meng Cheng Ong, Fei Hu, Yang-Ki Hong, Kenneth Rieks, and Jaber Abu-Qahouq).

3. Conception and realization of mechatronics and cyber-mix mechatronics experimental models by research infrastructure ECOSIN-MECATRON

• **3D cyber-mix-mecatronic System ultraprecise multiaplicative for remote control and remote monitoring** (fig. 1).

- According to figure 1, the matrix structure physical (mixmechatronics) and cybernetical (IT&C) of the system, enables automation, computerization and remote communication, intelligent control and monitoring, thereby contributing to raising the quality level and reducing operating costs specific to the automotive industry.
- The 3D axis system (x, y, z) 1.1 with ultraprecise remote control is ordered by PC with specific software 1.4 and 1.5 for the realization of measuring function of a part 1.3 with 3D ultraprecise probe 1.2. The system is protected with lasser protection barrier 1.6 and communicate with special equipments from the electronic unit 1.7 in PLC 2.1 and Internet GPRS 4G. This communication connection is linked with remote control center 3 provided with a computing station 3.2 and 3.3 connected to the router 3.1 and on which specialized software 3.4 runs.
- In the 3D mode of travel, the cyber-mix-mechatronic system is designed to be operated locally using a program preinstalled on PC equipped with display and control software and modeling and emulating remote position. Switching between the two operating modes can be done anytime and measurement (3D control) points may be stored in the memory functioning in the automatic PLC mode.

- Thus, all these complex functions may be implemented by integrating several functional testing and smart subsystems.

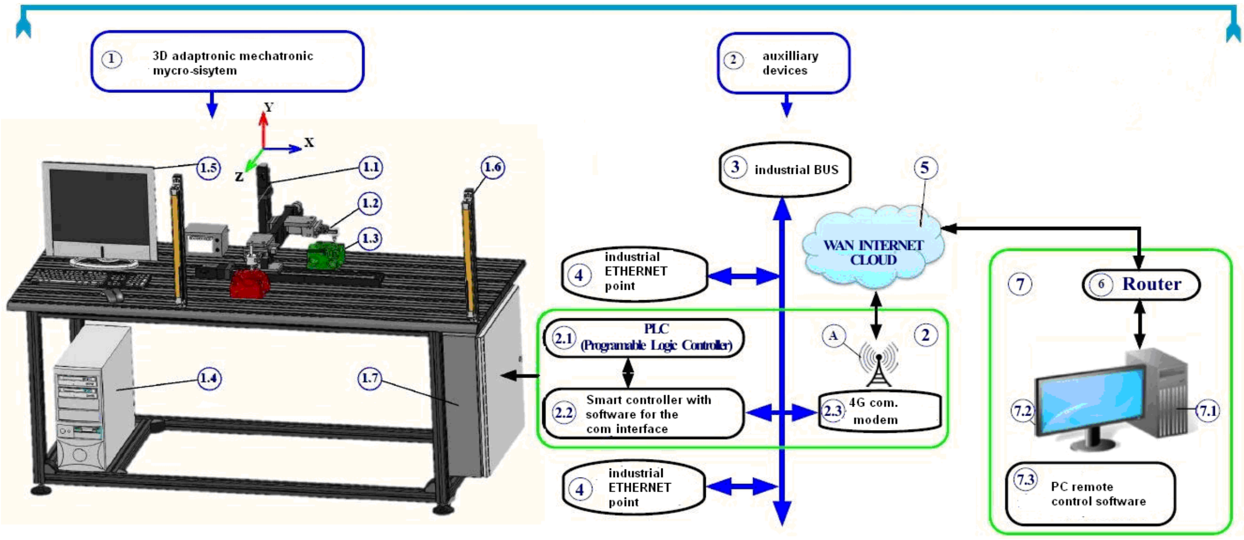

Fig. 1

Caption:

1. 3 D cyber-mix-mechatronic system:
1.1 Ultra-precise 3D measuring system / measuring robot / ultra precise control robot (x-300mm; y=200mm; z=250mm; accuracy:0.1-1nm);
1.2 3D ultra precise probe (accuracy: 0.1 nm);
1.3 Control / measurement part;
1.4 PC local host;
1.5 Display and local user interface;
1.6 Laser protection barrier
1.7 Unit with command system, driving system and telecommunications system;

2. Auxiliary equipments:
2.1 PLC (Programmable Logic Controller);
2.2 Smart controller with software for communication interface;
2.3 4G communication modem;
3. Industrial BUS;
4. Industrial ETHERNET point;
5. WAN INTERNET CLOUD access;
6. 802,1 lb/g router
7. Control Centre
7.2 PC Display
7.3 PC Remote monitoring software

At the same time, this cyber-mixmecatronic system does not require the continued presence of the qualified and costly human operator and aims to ensure operating parameters at nominal values, along with the advantages of cyber technology, such as:
- minimizing operating – troubleshooting time;
- preventive strategies in the operation and maintenance process;
- modularity, flexibility and security.

The 3D multiaplicative cyber-mixmechatronic system, for remote control and monitoring provides connection of remote process stations to one or more centarl control systems , using various public or private networks for event-driven take-backs caused by an event or cyclical data processing performed using special protocols and effectively managed. The cyber-mixmechatronic system uses one or more software to connect it to the "remote control and monitoring center" based on modern GPRS technologies and multiple PLCs. The cyber-mixmecatronic system can also do the teleservice that offers data exchange via the telephone line or via the Internet and Intranet, using remote equipment and systems such as computers, machines, installations and lines production, error detection, diagnostics, activity optimization, maintenance, repairs, etc.
Thus, the cyber-mixmecatronic system makes significant contributions to minimizing the cost and increasing the efficiency and productivity of industrial activities.
The main system servicies consist of:
- remote control - remote control and monitoring of a system;
- remote maintenace, consist of:

- ➢ remote monitoring – determining of the status of the system;
- ➢ remote diagnosis – identifying the causes of malfunction;
- ➢ remote maintenace – eliminating causes;
- ➢ acquisition of geometric and mechanical parameters.
- **The cyber-mixmechatronic system with remote control and remote monitoring (fig. 2)**
- ➢ According to figure 2, the physical (mechatronics) and cybernetics (IT&C) matrix structure of the system, enables automation and computerization of remote processes (telecontrol and telemonitoring) of the industrial manufacturing line.
- ➢ The system performs the function of protecting workstations from human errors specific to fabrication lines (1.1) in the series in the industry, such as automotive parts in the manufacturing industry. Parts (1.2) call feature tags with unique ID RFID (1.3) communicating bi-directionally with a drive (2.4) with automation equipment and telecommunication local but also a smart bracelet (2.3) situated on the hand of the operator who is using the device (2.2) equipped with RFID tag and bidirectional communication. Intercommunication between elements listed (part, device, operator) is collected and transmitted using antennas (2.5) and (4.1) through the Internet to a (4.2) computing station at the center of remote monitoring and remote control (4).
- ➢ The computer center remote monitoring and remote control (4.2) running special software designed to synchronize tasks on a database technology and eliminate errors caused by real-time tracking and manufacturing through a comprehensive analysis and forecasts.

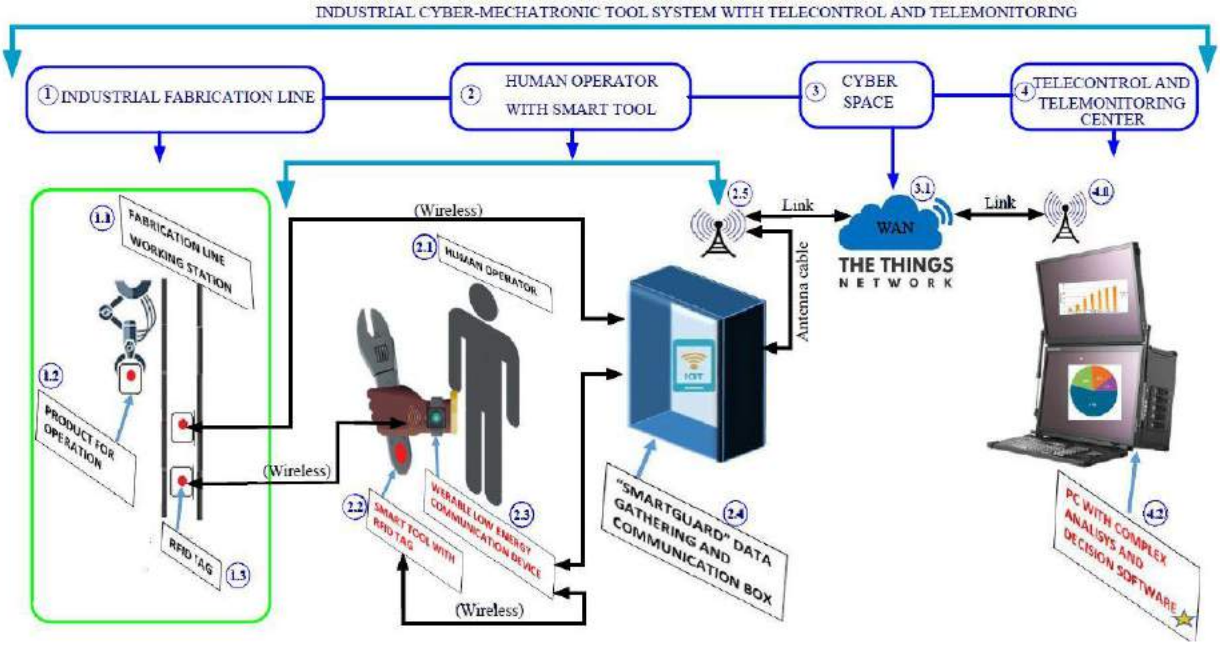

Fig. 2

Caption:				
	1. Industrial manufacturing line 1.1 Workstation on the fabrication line 1.2 Product for technological applications 1.3 Unique identification system with RFID	2. Human operator with smart instruments 2.1 Human operator 2.2 Unique identification system with RFID 2.3 Smart communication and warning bracelet 2.4 Unit with system for data acquisition and communication 2.5 Antenna	3. Cyber space 3.1 Internet WAN	4. Remote control and remote monitoring centre 4.1 Antenna 4.2 PC with software for complex analysis and decision

- **Smart multi-application cyber-mixmechatronic device type industrial robot for remote control and remote monitoring of operational and service processes (fig.3).**

➢ According to the mentioned figure, the structure of the physical matrix [Mechatronics and Cybernetics (IT & C)] of the system allows the cybernetization and remote communication of technological operational processes and of processes that service the industry, thus contributing to a higher increase in productivity and of quality of smart industrial. The cyber-mixmechatronic multi-application system performs a remote control and remote monitoring of an industrial robot (1) connected to the cyberspace via the control unit 1.2 and the interface 1.3 with both the internal industrial bus (2.1) and Internet via a 4G GPRS modem. Through this communication connection is made the link to a centre of remote control and remote monitoring (3) provided with a computing station (3.2) and (3.3) connected to the router (3.1) and running specialized software for robot control (3.4).

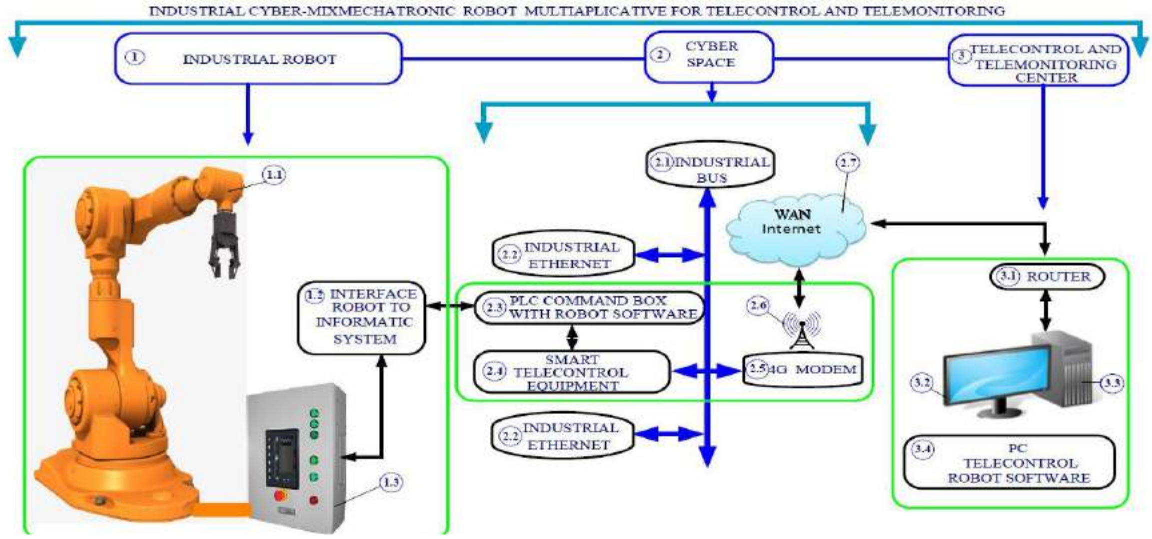

Fig. 3

Caption:			
	1. Industrial robot 1.1Universal robotic arm (with gripper / 3D feeler) 1.2Interface between the robot and the informatic environment 1.3Command tools	2. Cyber space 2.1Industrial communication bus 2.2Industrial ETHERNET network 2.3Programmable PLC with ROBOT software 2.4Smart devices for remote control and remote communication 2.54D GPRS modem 2.6Internet WAN	3. Center of remote control and remote monitoring 3.1 Router linking to WAN Internet 3.2 PC monitor 3.3 Central unit 3.4 UPC with ROBOT remote control software

- **Cyber-mixmechatronic system for dampening for automotives and with remote control and remote monitoring functions (fig.4).**

According to the mentioned figure, the structure of the physical matrix (damper and cybernetics (IT & C) of the cyber-mixmechatronic system for dampening for automotives allows the smart computerization and cybernetization of the automotive and of the automotive industry, by raising the quality and increasing productivity of the automotive industry.

The cyber-mixmechatronic system for dampening for automotives allows the function of remote monitoring and remote control of a smart damper (1) provided with an electromagnet (1.1) powered by a high voltage source (1.6) in order to modulate the degree of viscosity of the rheologic fluid (1.3).

To obtain information on the global acceleration of the cyber-mechatronic assembly attached to a tire of a vehicle uses the sensor (1.4) and the interface (1.5) connected to an intelligent control and remote control equipment (1.7).
Internet wan network connection is performed using a specialized 4g gprs modem (1.9) provided with an antenna (1.8).
Through this communication connection is made the link to a centre of remote control and remote monitoring (3) provided with a computing station (3.2) and (3.3) connected to the router (3.1) and running specialized software for robot control (3.4).

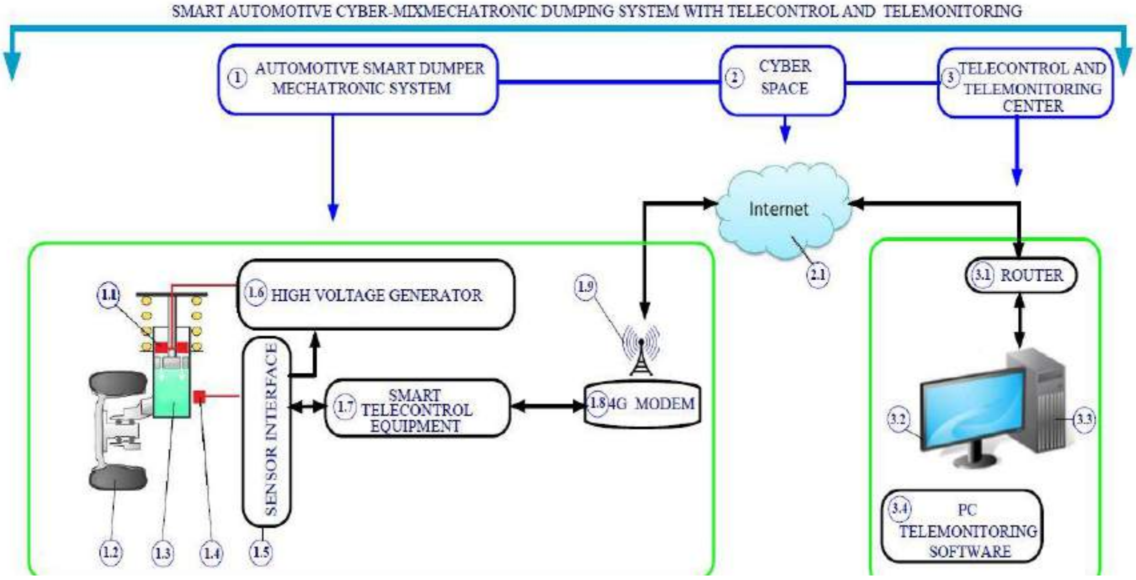

Fig. 4

Caption:

1. Smart cyber mix-mechatronic system for dampening
1.1 Electromagnet or coil
1.2 Section of a tire
1.3 Rheological fluid
1.4 Acceleration sensor
1.5 Interface between sensor and acceleration
1.6 High tension source
1.7 Smart remote control device
1.8 4D GPRS modem
Antenna

2. Cyber space
2.1 Internet WAN

3. Centre of remote control and remote monitoring
3.1 Router linking with WAN Internet
3.2 PC monitor
3.3 Central PC unit
3.4 PC with software for remote monitoring and remote control smart DAMPER

4. Scientific results

The scientific results obtained in the paper are synthesized as follows:
• **concepts of virtual models** in variants and scenarios for mechatronic and cyber-mechatronic systems, with applications in industry (eg automobile industry - SC Automobile Renault - Dacia SA Pitesti, SC Componente Auto SA Topoloveni, SC Comis SRL Valenii de munte etc) in medicine (eg smart mechatronic technologies for selective sintering with laser beam - Hospitals in Bucharest, etc.)
• Physical models in original solutions for mechatronic and cyber-mix-mechatronics systems with industrial applications (eg the fine mechanics and mechatronics industry - Mechatronics and Cyber - Mix - Mechatronics Laboratory at INCDMTM Bucharest, for measurements, micro and nano technologies for PhD thesis, from the Doctoral School of Mechanical Engineering and Mechatronics of UPB and UVT, etc);

• real parametric values for remote metered and mechatronic systems: telecontrol, telemonitoring, teleservice and teleconfiguration;
• process validation and mechatronic and cyber-mix-mecatronic system in real industrial applications.

5. Conclusions

By carrying out this scientific work” Systems and Intelligent mechatronics and cyber-mixmechatronics ecosystems developed in”ECOSIN-MECATRON”, research infrastructure”, the author presented:
• the creation and development of a new, specialized 21st century intelligent specialized domain to ensure the sustainable development of the national and international economy and industry, the field of Mechatronics and Cyber-Mix-Mechatronics;
• creation and development of new mechatronic and cyber-mixmechronic systems, in original and multi-purpose applications in many industrial, economic and societal environments;
• substantial contributions to solving the scientific paradigm Mechatronics, MixMecatronics and Cyber-MixMecatronics;
• Original contributions to research, development and innovation in the intelligent specialized fields of Mechatronics, MixMecatronics (Integral and Adaptronics) and Cyber-MixMecatronics.

References

[1] Gh. Gheorghe, ”Mechatronics & Cyber-Mechatronics Systems*”*, CEFIN, București, România, 2015;
[2] Gh.Gheorghe, *”*Smart Adaptronic Micronanoengineering*”*, CEFIN, București, România, 2014;
[3] Gh. Gheorghe et al., *”*Mechatronics and Micro – Mechatronics Concepts and Techniques for Intelligent Integrating Micro Engineering*”*, *The 19th International DAAAM Symposium „Inteligent Manufacturing & Automation: Focus on Focus on Next Generation of Intelligent Systems and Solutions”*, 22 – 25th October 2008;
[4] V. Giurgiutiu, S.E. Lyshevski, ”Micromechatronics: Modeling, Analysis and Design with MATLAB**”**, CRC Press, ISBN 084931593X, 856 pages;
[5] M. Gronau, ”Technologien fur Mikrosystems”, VDI-verlang GmbH, Dusseldorf, 1993;
[6] P. Jănker, F. Hermle, T. Lorkowski, S. Storm, M. Wettemann, M. Gerle, *”*Actuator Technology based on smart materials for adaptive systems in aerospace”, *Proc: ICAS 2000*, Harrogate/UK (2000).

ISSN 1454 - 8003
Proceedings of 2017 International Conference on Hydraulics and Pneumatics - HERVEX
November 8-10, Băile Govora, Romania

LQR CONTROL OF LIQUID LEVEL AND TEMPERATURE CONTROL FOR COUPLED-TANK SYSTEM

Melih AKTAŞ[1], Yusuf ALTUN[2], Oğuz EROL[3]

[1] Duzce University, Engineering Faculty, Electrical and Electronics Engineering, Duzce, Turkey.

[2] Duzce University, Engineering Faculty, Computer Engineering, Duzce, Turkey.

[3] Duzce University, Mechatronics Engineering, Duzce, Turkey.

Abstract: *This paper shows the linear-quadratic regulator (LQR) control of coupled-tank system based on the linearized mathematical model. Although the system is nonlinear, it can be linearized at the operating points. Therefore, the temperature and level controller is designed via the method, which is applicable in practical. Also, the control method is known as an optimal control and it has good performance is obtained by determining some matrices of and designing of control for liquid level and temperature controls.*

Keywords*: Two tanks, level and temperature control, LQR control, optimal control.*

1. Introduction

Liquid tanks which are generally used in industrial facilities have strategic importance because of significance of storage which are highly important for human life. In the process of industrial applications, frequently it is essential to may be store up in tanks and transferred to other tanks as per requirement. It is often necessary to keep the liquid at a certain height or within a certain range[1]. For industrial applications, liquid-level and temperature are important parameter, and widely applied in various field, such as, product tank, water tanks, chemical process systems, liquid storage tanks are important components of lifeline and industrial facilities. The coupled-tank liquid level and temperature controls are typical representative of process control, are hot research topics in control field [2]. The coupled-tank liquid-level control system has nonlinear and complex characteristics, in which the control accuracy is directly affected by system status, system parameters and the control algorithm [3]. Because of that the Linear Quadratic Regulator (LQR) is suitable controller for the coupled tank liquid system. LQR is an optimal controller that requires a state-space linear approximation of the non-linear system but generally has superior performance. LQR measures all states and produces a plant input as a function. LQR stabilizes the system using full state feedback [4]. Because of its characteristics, it is also one of the most important benchmark control problem. The goal of the control is to ensure that the liquid levels in the tanks are maintained at the desired level during the transfer. The coupled tank control systems are a multi-input multi output (MIMO) systems, where input is a control voltage and the output is water level. Tanks have an important place for mixing processes in important industries such as petrochemical industry, paper industry, water treatment industry. Therefore, the liquid level control system is noted in the literature. The control of a nonlinear coupled three tank system is dealt, and the aim is to control the temperature and level of water in tanks by using feedback linearization method [5]. Fractional Order Proportional Integral (FOPI) controllers along with conventional feedforward controllers work better than PI/PID/2DOF-PI/3DOF-PI with feedforward controllers in such situation. FOPI controller is designed using the frequency domain approach. Effectiveness of the controllers is tested to maintain a constant level in the first tank while making the level of the second tank to follow a sinusoidal and square wave reference signals. Experimental results validate the objective of the study [6]. Fuzzy logic control is adopted to liquid tank system which has three coupled tanks together [7]. An adaptive fuzzy control (AFC) system has been proposed to realize level control of two coupled water tanks[8]. Real-time experimental and simulation results with an interval type-II fuzzy logic systems (IT2FLS) are compared with those of a linear quadratic regulator (LQR) for level control of three-tank hybrid system [9]. An observer-based control design has been implemented for a combined four-tank liquid level system [10]. In this paper, LQR control based on optimal control method is designed for the two tanks system.

2. The Coupled-Tank Process Model

The water tank process model [11] is shown in Figure 1. Tank 1 and Tank 2 are coupled as shown. Cold water and warm water can be pumped into the left tank via two control input signals U1 and U2 driving control valves. The flows capacity and the temperatures are Tw, Tc, Qw and Qc, respectively. The flow between the tanks is Qr and the flow out of the outlet valve of tank 2 is Qb. The water levels in the Tank 1 and Tank 2 are H1 and H2, respectively, and the tanks have the same cross-sectional field A. This second valve has the variable opening area Av. Water is rapidly blended in both tanks, and for this reason, it is assumed that the temperature is constant throughout the entire volume of the tank. So, the whole volume is homogeneous in terms of temperature.

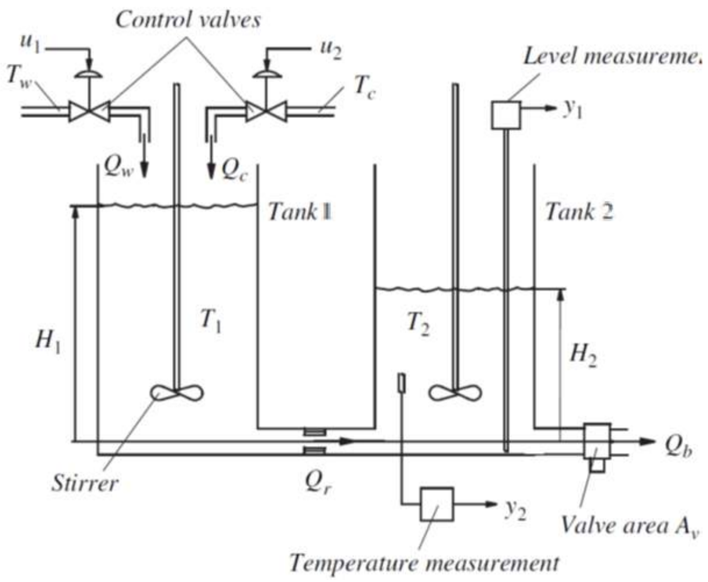

Fig. 1. Water Tank System [11]

Two variables can be measured on the system: the liquid level and the temperature of Tank 2. The measurable variables are as in (1), where k_h and k_t are transducer gains.

$$\begin{aligned} y_1 &= k_h H_2 \\ y_2 &= k_t T_2 \end{aligned} \tag{1}$$

The system equations are as in (2). They are attained from linear equations and therefore they are linearized near a localized working point by the basic linearization technique [11]. Hence, if the left sides of the expressions in (2) are equal to zero, the linear equations are obtained at the stationary operating point. Thus, the linearized state-space equation of the system is as in (3) where Δx (Δx_1, Δx_2, Δx_3, Δx_4) defines ΔH_1, ΔH_2, ΔT_1, ΔT_2, Δu defines Δu_1, Δu_2, and Δv (Δv_1, Δv_2, Δv_3) defines ΔA_v, ΔT_w, ΔT_c. The matrices of state-space are as in (5) and (6). In addition, Δ defines the deviations from the values of stationary. Thus, states are calculated with including deviations in values of stationary as in (4) to the states' working points. As for the system parameters; c is heat capacity of water, k_a is the flow coefficient, ρ is mass density, $D_v = C_d\sqrt{2g}$, A_o is the area of orifice, C_d is a constant loss coefficient and g is gravitational acceleration. In addition, it is assumed that $H_1 \succ H_2$.

$$\begin{aligned}
\frac{dx_1}{dx} &= \frac{1}{A}\left[k_a\left(u_1+u_2\right)-C_0\sqrt{x_1-x_2}\right] \\
\frac{dx_2}{dx} &= \left(\frac{1}{A}C_0\sqrt{x_1-x_2}-D_v\sqrt{x_2}v_1\right) \\
\frac{dx_3}{dx} &= \frac{1}{Ax_1}\left[\left(v_2-x_3\right)k_a u_1-\left(v_3-x_3\right)k_a u_2\right] \\
\frac{dx_4}{dx} &= \frac{1}{Ax_2}\left(x_3-x_4\right)C_0\sqrt{x_1-x_2} \\
y &= \begin{pmatrix} y_1 \\ y_2 \end{pmatrix} = \begin{pmatrix} 0 & k_h & 0 & 0 \\ 0 & 0 & 0 & k_t \end{pmatrix}
\end{aligned} \tag{2}$$

The added subscript-zero defines the fix operating points.

$$\begin{aligned}
\Delta\dot{x}(t) &= A\Delta x(t)+B_1\Delta w(t)+B_2\Delta u(t) \\
\Delta y(t) &= C\Delta x(t)
\end{aligned} \tag{3}$$

$$H_1 = H_{10}+\Delta H_1(t) \tag{4}$$

$$A=\begin{pmatrix}
\frac{-C_0}{2A\sqrt{x_{10}-x_{20}}} & \frac{C_0}{2A\sqrt{x_{10}-x_{20}}} & 0 & 0 \\
\frac{C_0}{2A\sqrt{x_{10}-x_{20}}} & \frac{-C_0}{2A\sqrt{x_{10}-x_{20}}}-\frac{D_v v_{10}}{2A\sqrt{x_{20}}} & 0 & 0 \\
0 & 0 & -\frac{k_a\left(u_{20}+u_{10}\right)}{Ax_{10}} & 0 \\
0 & 0 & \frac{C_0\sqrt{x_{10}-x_{20}}}{Ax_{20}} & -\frac{C_0\sqrt{x_{10}-x_{20}}}{Ax_{20}}
\end{pmatrix} \tag{5}$$

$$B_1=\begin{pmatrix}
0 & 0 & 0 \\
-\frac{D_v\sqrt{x_{20}}}{A} & 0 & 0 \\
0 & \frac{k_a u_{10}}{Ax_{10}} & \frac{k_a u_{20}}{Ax_{10}} \\
0 & 0 & 0
\end{pmatrix}, B_2=\begin{pmatrix}
\frac{k_a}{A} & \frac{k_a}{A} \\
0 & 0 \\
\frac{k_a\left(v_{20}-x_{30}\right)}{Ax_{10}} & \frac{k_a\left(v_{30}-x_{30}\right)}{Ax_{10}} \\
0 & 0
\end{pmatrix}, C=\begin{bmatrix} 0 & k_h & 0 & 0 \\ 0 & 0 & 0 & k_t \end{bmatrix} \tag{6}$$

3. The Controller Design

LQR is an optimal controller that requires a state-space linear approximation of the non-linear system but generally has superior performance. LQR measures all states and produces a plant input as a function. LQR stabilizes the system using full state feedback. Suppose that state space equations of linear time invariant system is;

$$\dot{x}(t) = Ax(t) + Bu(t) \tag{7}$$

$$y(t) = Cx(t) + Du(t) \tag{8}$$

Performance index of the LQR controller is introduced as follows, where u(t) is input and x(t) is the state of the system.

$$J = \frac{1}{2}\int_0^\infty [x(t)\,\mathrm{Q}\mathrm{x}(t) + \mathrm{u}(t)\,\mathrm{R}\mathrm{u}(t)]dt \tag{9}$$

J must be minimal in order to achieve an optimal control. Q and R denote the weighting matrix of the state variable and input variable. An optimal control is dependent on Q and R matrix. However, there is no common method in tuning those parameters. Usually simulation trial and error method is used for arranging the correct parameters. However, note that to implement an optimal control an optimal control input must be found u(t). (9) could be written as (10).

$$J = J_0 + \frac{1}{2}\int_0^\infty \left[\left(\mathrm{u(t)} - \mathrm{u_0(t)}\right)' \mathrm{R}\left(\mathrm{u(t)} - \mathrm{u_0(t)}\right)\right]dt \tag{10}$$

Let P be a symmetric matrix, there exists such relation:

$$\int_0^\infty \left[\mathrm{x}'(\mathrm{A}'\mathrm{P} + \mathrm{PA})\,\mathrm{x} + 2x\,\mathrm{PBu}\right]dt = -x(0)'Px(0) \tag{11}$$

By adding and subtracting (11) to (9), (12) is obtained.

$$\mathrm{J} = x(0)'Px(0) + \int_0^\infty \left[\mathrm{x}'(\mathrm{A}'\mathrm{P} + \mathrm{PA} + \mathrm{Q})\,\mathrm{x} + u'Ru + 2x'(\mathrm{PB} + \mathrm{N})\,\mathrm{u}\right]dt \tag{12}$$

Then the optimal control input which minimizes the cost function J is found in (12) by (10) and (11).

$$u_0 = -R^{-1}(B'P + N')x \tag{13}$$

Moreover, Q and R have significant effect on the system performance, if R is large than a smaller input will be applied to stabilize the system. Also, if the error in a certain state needs to be small, the corresponding column of Q needs to be larger. Also keeping Q need and reducing R; results a decrease in transition time and maximum overshoot and an increase in rise time and steady state error.

$$u(t) = -Kx(t) \tag{14}$$

$$K = R^{-1}(B'P + N') \tag{15}$$

The optimal control input is also be found by the help of MATLAB function K =lqr(A,B,Q,R) where K is the LQR gain of the controller. Where the input is being as in (14).

Accordingly, the obtained controller matrix is given by

$$K = \begin{bmatrix} 12.206 & 8.5194 & 17.763 & 12.67 \\ 11.19 & 7.8927 & -9.5695 & -6.7384 \end{bmatrix}$$

4. Simulation Results

For the simulation, Matlab-Simulink is used for the system performance analysis. Table 1 shows that the parameters of the system. According to this, the level and temperature results od second tank are as in Figure 3 and 4 for the initial conditions ΔH_2=0.4m, ΔT_2= 3°C. The references are zero. It means that it is desired that the changes of level and temperature for second tank should be zero. Figure 3 presents the changing of ΔH_2 while Figure 4 presents the changing of output ΔT_2. Regarding the results, the control performance is good response as shown in Figure 2 and Figure 3.

Table 1: The values of parameters for the tank system

The stationary points in the linearization	Value	Parameters	Value
A_{v0}	0.0122m^2	k_h	2 volt/m;
T_{w0}	60°C	k_t	0.1 volt/°C
T_{c0}	30°C		
x_{10}	2.03m	A	0.785 m^2
x_{20}	1.519m	D_v	2.66 m$^{1/2}$/sec
x_{30}=x_{40}	45°C	C_0	0.056 m$^{5/2}$/sec
u_{10}=u_{20}	5volt	k_a	0.004 m^3/volt.sec;

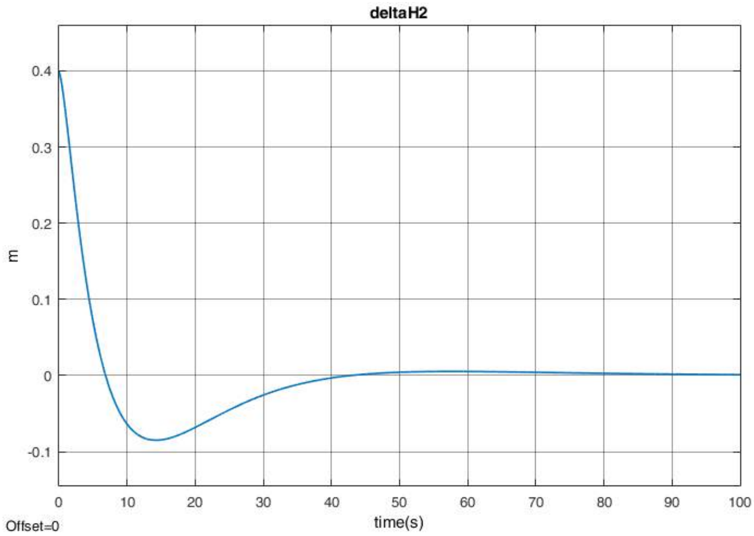

Fig. 2. The level of the tank 2

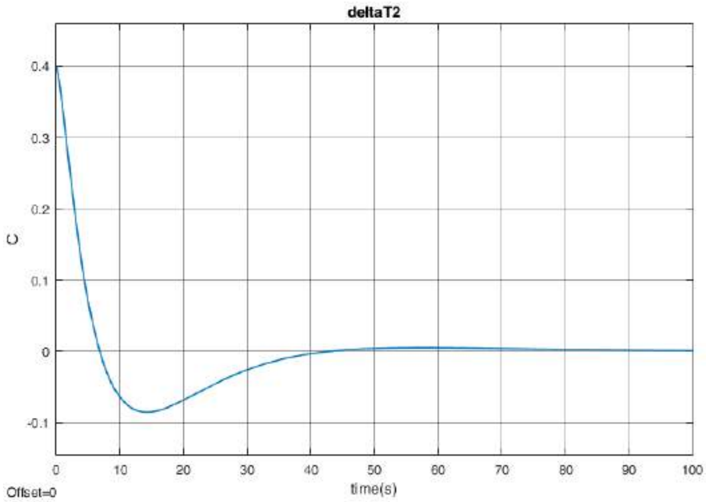

Fig. 3. The temperature of the tank 2

5. Conclusions

This paper shows that LQR control of two water tanks is fulfilled. The controller is designed via optimization software. the controller is an optimal control method. The simulation results show that the controller gives a satisfactory performance according to desired states. The simulation results prove that the controller performance is very good for level and temperature of tank. Finally, there is good settling- time and no overshoot for the two water tank system.

References

[1] H. Abbas, S. Asghar, and S. Qamar, “Sliding Mode Control for Coupled-Tank Liquid Level Control,” *10th Int. Conf. Front. Inf. Technol. (Fit 2012)*, pp. 325–330, 2012.

[2] T. Timur, “Evaluation Of Seismic Behaviour Of Base Isolated Cylindrical Liquid Storage Tanks,” İstanbul Teknik Üniversitesi, 2010.

[3] L. Li, “The application of fuzzy PID controller in coupled-tank liquid-level control system,” *2011 Int. Conf. Electron. Commun. Control. ICECC 2011 - Proc.*, pp. 2894–2897, 2011.

[4] Y. Tekn, “Matlab ve simulink kullanarak lqr ve kutup yerleşimi metotlari ile tepe vinci kontrolü,” 2006.

[5] F. Tahir, N. Iqbal, and G. Mustafa, “Control of a Nonlinear Coupled Three Tank System using Feedback Linearization,” *2009 Third Int. Conf. Electr. Eng.*, pp. 1–6, 2009.

[6] K. Sundaravadivu, V. Jeyakumar, and K. Saravanan, “Design of Fractional Order PI controller for liquid level control of spherical tank modeled as Fractional Order System,” in *Proceedings - 2011 IEEE International Conference on Control System, Computing and Engineering, ICCSCE 2011*, 2011, pp. 522–525.

[7] M. Abid, “Fuzzy logic control of coupled liquid tank system,” in *Proceedings of 1st International Conference on Information and Communication Technology, ICICT 2005*, 2005, vol. 2005, pp. 144–147.

[8] A. Başçi and A. Derdiyok, “Implementation of an adaptive fuzzy compensator for coupled tank liquid level control system,” *Meas. J. Int. Meas. Confed.*, vol. 91, pp. 12–18, 2016.

[9] H. Sahu and R. Ayyagari, “Interval fuzzy type-II Controller for the level control of a three tank system,” in *IFAC-PapersOnLine*, 2016, vol. 49, no. 1, pp. 561–566.

[10] H. Gouta, S. Hadj Saïd, N. Barhoumi, and F. M’Sahli, “Generalized predictive control for a coupled four tank MIMO system using a continuous-discrete time observer,” *ISA Trans.*, vol. 67, pp. 280–292, 2017.

[11] E. Hendricks, O. Jannerup, and P. H. Sørense, “Linear Systems Control,” *Linear Syst. Control*, vol. 0, no. 1, p. 555, 2008.

ISSN 1454 - 8003
Proceedings of 2017 International Conference on Hydraulics and Pneumatics - HERVEX
November 8-10, Băile Govora, Romania

DISTRIBUTED SYSTEM FOR MONITORING ELECTRO-HYDRAULIC DRIVES

Ioana ILIE[1], Marian BLEJAN[1], Alexandru HRISTEA[1]

[1] Hydraulics and Pneumatics Research Institute – INOE 2000-IHP Bucharest, ilie.ihp@fluidas.ro

Abstract: *The paper presents a short-overview of a distributed monitoring system designed for hydraulic drives that allows immediate access to system performance measurements, behaviour analysis over time, and maintaining the hydraulic systems in the most efficient working manner. The monitoring system was implemented on various applications in industry (metallurgic field), in training equipment for aircraft personal and in laboratory equipment.*

Keywords*: Monitoring, process data, programmable controller*

1. Introduction

Monitoring hydraulic equipment, respective components, can be achieve in two different ways: a simple approach that mean simple measures for component monitoring, and an advanced way based on the methods of signal acquisition and conditioning.
Conceptually, the monitoring system was designed as a distributed system which allows users and other applications outside it to interact with it in a uniform and coherent manner. The system components are placed on interconnected processing units, in both hydraulic and informatics levels, and their actions are communicate and coordinate by messaging. The convenient and secure online access to system condition allows taking the best decisions regarding system operation.
The monitoring system functionality is implemented on a programmable controller at hydraulic level, on computers network at information system level and the software application created is based on event-driven approach.

2. The monitoring system architecture

The monitoring system is designed for electro-hydraulic drives so the main support for it is a processing unit placed on hydraulics, that mean electronics, microprocessors, PLCs or process computers. These process units have implemented both control and monitoring application for hydraulic drives using.
At the information system level there is a one or more PCs running a software application - Operator Console and standard DBMS. The operator console provides data reception from the hydraulic drive, stores the data in the database, and displays the process data locally in numeric or graphic form.

2.1 Hardware architecture

The system concept was implemented on various applications and for each one on the hydraulic level the hardware support chosen was a common PLC (figure no. 1). For the informatics system it was used a PC running the operator console and one or more PCs running the DBMS. The process data transmission at the PLC level was ensured by a serial data line: Ethernet, RS485, and Wi-Fi.

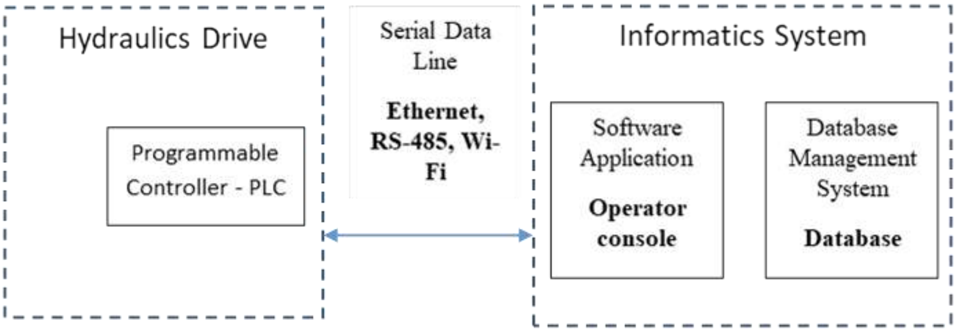

Fig. 1. Hardware architecture

2.2 Software architecture

The functionality of the monitoring software is provided by three components: first is the monitoring level running on Programmable Controller, the second component is Operator Console that's running on the PC System and the third component is the DBMS. It have to say that this paper refers only to the first two components mentioned below (figure no. 2).

The monitoring software running at the programmable controller level consists of a program loop that runs at within 20ms. This allows a monitoring rate of 50 samples/s for each monitored process quantity. Within these loops are packed the process data that will be transmitted to the operator console application.

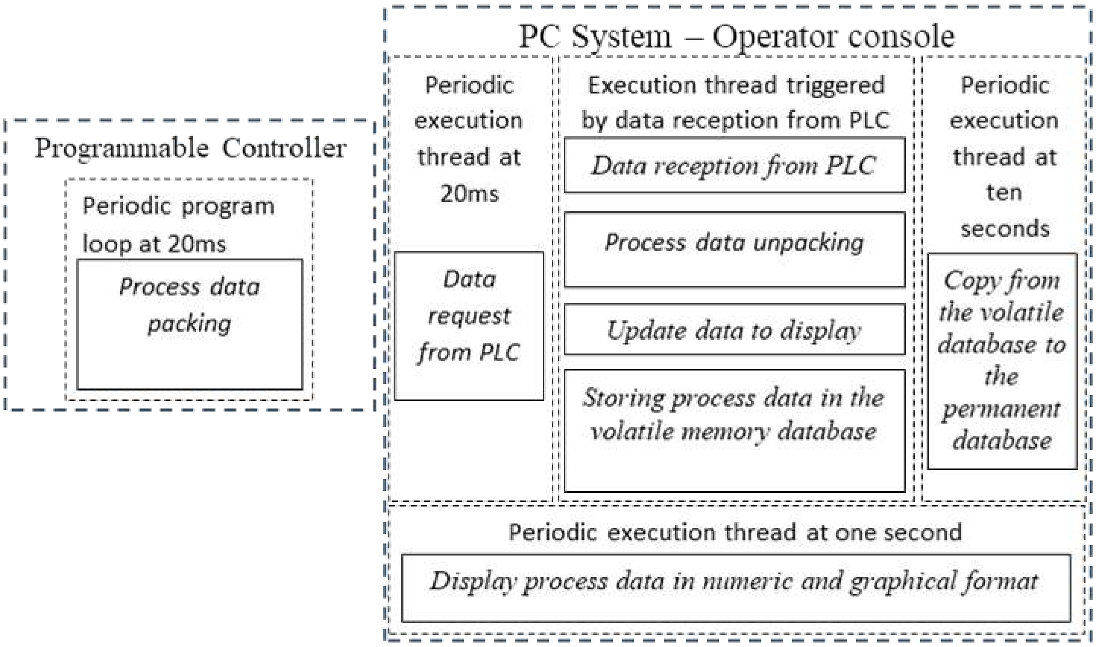

Fig. 2. Software architecture

The operator console software application has a 4-thread parallel execution structure. A thread executes periodically at 20ms to make a data request to the PLC through the data line. The second thread is triggered by PLC data reception and its functions is to unpacks the received process data, prepares data for display (PLC formats in real units), and stores data in a local database in volatile memory and PC. The third thread executes periodically at a time of 1 second, displays the process data in numeric or graphical format in the application panel. The fourth thread is executed periodically at a time interval of 10 seconds copies the data from the temporary database to the permanent one.

3. Practical implementation of the monitoring system

3.1 Electrohydraulic system for winding rolled wire

The concept of distributed monitoring system was implemented on various applications in industry, in training equipment for aircraft personal and in laboratory equipment.

In the metallurgy field the monitoring concept was used on the electrohydraulic system for winding rolled wire (figure no. 3). This ensures wire stringing on spool coil by coil, by controlling movements of the debugger head, adapting itself to changes in spool rotational speed; spool rotational speed is dictated by the rolling process parameters and also the wire load of the spool that is diameter of the coil being wound[1].

This electrohydraulic system contains a linear axis consisting of a bilateral rod hydraulic cylinder, on its liner being located the debugger head, controlled with a proportional flow distributor. H*ardware components* of the monitoring system contains *sensors* for monitoring spool rotational speed and the speed of the debugger head, *electronics* necessary for interfacing the execution elements and transducers with the *programmable controller* (figure no. 4)

Software components consist of *software* application that running on PLC and the operator console and the DBMS. The PLC software implements both the control of the mechatronic system and the monitoring features. This application has two data communication lines, a serial RS485 line with MODBUS protocol implemented to connect the PLC with the operator console, and an Ethernet line, that allows TCP / IP networks connection between the operator console and the company server where the DBMS was implemented [1].

Fig. 3. Winding roller

Fig. 4. Electric cabinet

The operator console (figure no.5) displays the process data locally in numeric or graphic form and allows connection with the DBMS to stores the process data in the database. The graphic shown in figure no. 6 is obtained with DBMS stored data.

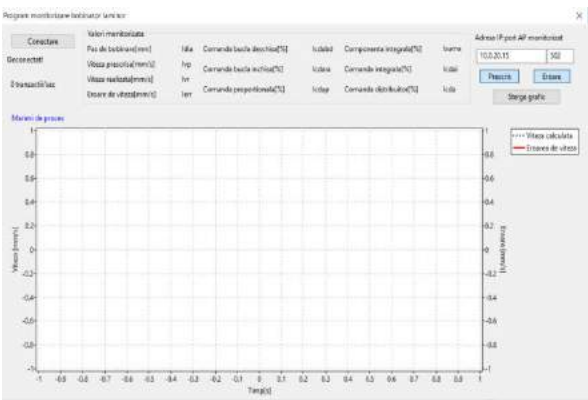

Fig. 5. Operator console

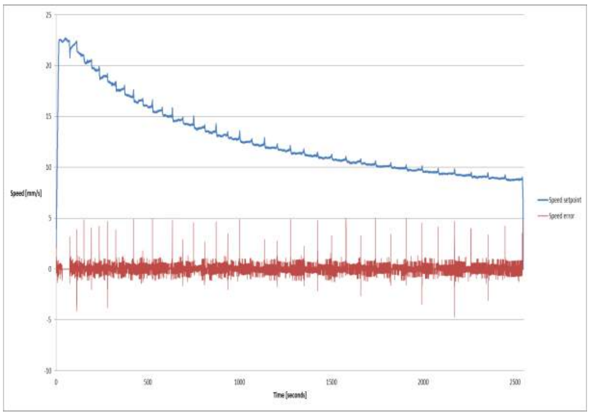

Fig. 6. Data process for one coil

3.2 Electrohydraulic actuation system for Cabin Emergency and Escape Trainer CEET B732

The electro-hydraulic actuation system is used on the Cabin Emergency and Escape Trainer CEET B732 for the Sea Survival School Tuzla (figure no 7) [3], and also implements the concept of distributed monitoring system. The monitoring system hardware contains sensors and PLC (figure no 8) at the and a single PC that contains the operator console and DBMS. Interfaces with data communication networks, namely the master-slave network implemented on RS485 communication line and the TCP/IP network implemented on Ethernet line. The PLC software application allows parameterization of the control system and updates both pseudo-analog (Pulse Width Modulation) and discrete outputs. The arithmetic on PLC is based on 16 and 32 bits words; for this application the calculus is made only with 16 bits signed words. Taking into account that the PLC arithmetic operation has only two operands, for the calculus of the error value (one of the monitored parameter) was used the PLC feature that could execute the program loop in fixed program execution time (for this application it was used 50ms scan time)[2].

Fig. 7. The Cabin Emergency and Escape Trainer

Fig. 8. Electric cabinet

The electro-hydraulic system has been tested for two command inputs types: for a ramp type and for a step type and the monitored value was positioning error. In figure no 9 is shown the experimental results obtained for a ramp type excitation signal (the dashed line) with a 17mm/s speed value. The positioning error (the continuous line) is 4 mm for a positioning range of 500mm; this error can be minimized by introducing in program a derivative component of error. In the figure no 10 is shown the results obtained for a step type input signal. The settling time for a 250mm step value is 2.5s. In this case introducing in command a derivative component of error would worsen the system response; respectively the settling time and the overshooting value would increase [2].

Fig. 9. The operator console – ramp type input signal

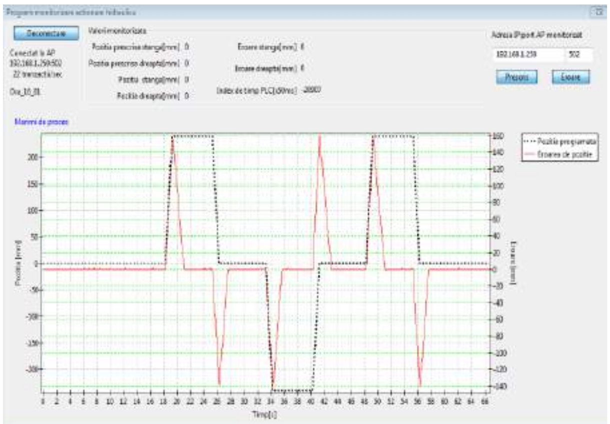

Fig. 10. The operator console – step type input signal

4. Conclusions

The distributed system for monitoring electrohydraulic drives is designed to be used in various application in different field form heavy industry to laboratory equipment, and its main advantages are:

- Changing and adjusting the operating algorithm, for each kind of application, only requires rewriting software in the PLC, operator console and updating DBMS;

- Due its communication capabilities via Ethernet it can be integrated in a tracking IT system;

- Using new devices coupled to the serial bus, additional functions can be implemented on the process units, namely new parameters monitoring or control;

- The PLC that implements the monitoring program may be equipped with HMI console (human machine interface).
- Continuous monitoring allows early detection of potential issues and prevents unnecessary downtime for unneeded maintenance.

Acknowledgments

This paper has been developed in INOE 2000-IHP, with the financial support of the Executive Agency for Higher Education, Research, Development and Innovation Funding (UEFISCDI), under PN III, Programme 2-Increasing the competitiveness of the Romanian economy through research, development and innovation, Subprogramme 2.1- Competitiveness through Research, Development and Innovation - Innovation Cheques, project title: *Computerizing the technological process of heat treatment of metallic materials*, Financial Agreement no. 126CI/2017.

References

[1] T. C. Popescu, M. Blejan, D. Vasiliu, “Innovative solution of energy efficiency and management for the production of aluminum wires”, *14th International Multidisciplinary Scientific GeoConference SGEM 2014*, www.sgem.org, SGEM2014 Conference Proceedings, ISBN 978-619-7105-15-5 / ISSN 1314-2704, June 19-25, 2014, Book 4, Vol. 1, 315-322 pp - DOI: 10.5593/SGEM2014/B41/S17.041;

[2] M. Blejan, I. Ilie, C. Cristescu “ Electronics for Electro-Hydraulic Actuation System “ („Acţionări hidraulice şi pneumatice”), *2015 IEEE 21st International Symposium for Design and Technology in Electronic Packaging (SIITME)*, 22-25 Oct 2015, Brasov, Romania, 978-1-5090-0332-7/15/$31.00 ©2015 IEEE;

[3] http://www.sea-survival.ro/en/news/105-simulator-improvement .

ISSN 1454 - 8003
Proceedings of 2017 International Conference on Hydraulics and Pneumatics - HERVEX
November 8-10, Băile Govora, Romania

CONSIDERATIONS REGARDING THE HYDRODOYNAMIC STRESSES FOR DIRECTIONAL SPOOL VALVES

Victor BĂLĂȘOIU[1], Rodica BĂDĂRĂU[2], Ilare BORDEAȘU[3], Mircea O. POPOVICIU[4], Dorin BORDEAȘU[5]

[1]Polytechnic University of Timisoara, Mihai Viteazul No.1, 300222, Timisoara, Romania, E-mail: balasoiu89@yahoo.com
[2]Polytechnic University of Timisoara, Mihai Viteazul No.1, 300222, Timisoara, Romania, E-mail: rodica.badarau@upt.ro
[3]Polytechnic University of Timisoara, Mihai Viteazul No.1, 300222, Timisoara, Romania, E-mail: ilarica59@gmail.com
[4]Academy of Romanian Scientists, Mihai Viteazul Street, Nr. 1, 300222 Timisoara, Romania, E-mail: mpopoviciu@gmail.com
[5]Aalborg University Esbjerg, Denmark, E-mail: dorin_craiova@yahoo.com

Abstract: *The dynamic analyzes of directional spool valves as well as the employed coefficients is an objective of great importance for understanding their running performances. The paper presents a synthesis of the manner in which must be determined for directional spool valves, the working characteristics taking into consideration the pressure and flow capacity losses. The established relations as well as the realized analyzes put into evidence most of the elements which must be taken into account for the design, fabrication and running of those devices.*

Keywords*: Directional spool valves, impulse hydrodynamic forces, angle, edge.*

1. Introduction

By way of operation hydraulic directional valves, no matter how they work, are subject to random dynamic stress produced by hydrodynamic forces induced by the hydraulic flow regime [1, 3, 4, 8, 15, 16, 17, 18]. Hydrodynamic parameters which influence the stress value are mainly the pressure, the flow and respectively the speed of the oil through the interstices created between the spool shoulders and the hole in the valve body. Because the application range is very wide, it is very important to know the hydrodynamic behavior of valves, depending on the pressure level, the flow rate, and the type of actuation scheme used [1, 3, 4, 8, 15, 16, 17, 18].

2. Impulse hydrodynamic forces

When passing the fluid through the valve sections as a result of spool displacement with the $\mathbf{Y_S}$ distance, an impulse force emerges which opposes its movement and seeks to bring it back to its original position. The hydrodynamic impulse force has two components: a stationary component, associated with the instantaneous flow through the spool, and a transient component determined by the transient variation of the flow rate [1, 3, 4, 8, 15, 16, 17, 18].
In Fig.1 is shown the flow distribution into the spool - valve body assembly for two $\mathbf{Y_S}$ positions (openings) made between the shoulder of the spool and the hole in the valve body, which lead to different passage angles through the annular space of the spool valve.

For spools with straight edges and for certain values of the ratio $\frac{\mathbf{Y_S}}{\mathbf{J}}$ (Fig.2), Von Misses sets the values of the angles under which the jet enters or exits relative the axis of the valve, for θ = 21 - 69°. For θ = 21...45°, the ratio is $0 < \frac{\mathbf{Y_S}}{\mathbf{J}} < 1.0$, respectively $\mathbf{Y_S} = \mathbf{J}$, for θ = 45° (Fig.1). The

ISSN 1454 - 8003
Proceedings of 2017 International Conference on Hydraulics and Pneumatics - HERVEX
November 8-10, Băile Govora, Romania

deduction is based on the impulse theorem applied for a non-stationary flow in the annular control volume of the axial section “**abcdef**” (Fig.2) in the form:

$$\frac{d}{dt}\sum(M_s\ \dot{\vec{Y}}_s) = \sum \vec{F}_e \tag{1}$$

which becomes:

$$\sum \vec{F}_e = \int_{cd} \rho\ \dot{\vec{Y}}_s\ dQ\ -\ \int_{ab} \rho\ \dot{\vec{Y}}_s\ dQ\ -\ \int_{abcdef} \frac{\partial\,(\rho\ \dot{\vec{Y}}_s)}{dt}\, dW_d \tag{2}$$

where: $\mathbf{W_d}$ - the volume element in the ring zone of the spool.

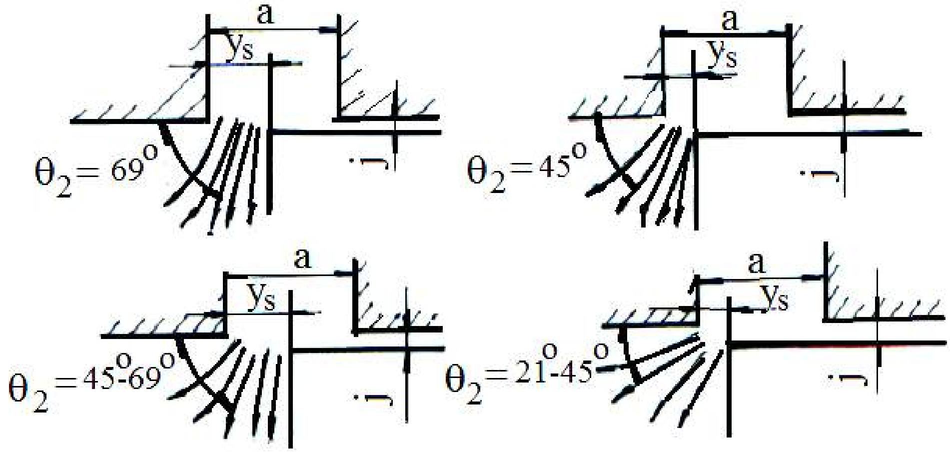

Fig.1

From the point of view of the power required for the displacement of the spool, it is useful to know only the axial component of the hydrodynamic impulse force on the hydraulic spool. For this purpose, equation (2) is projected along the axis of symmetry of the spool (OX axis), the radial forces being canceled due to axial symmetry. Thus, we obtain the force with which the liquid acts on the spool (in two hypotheses) (Fig.2, correlated with Fig.1):

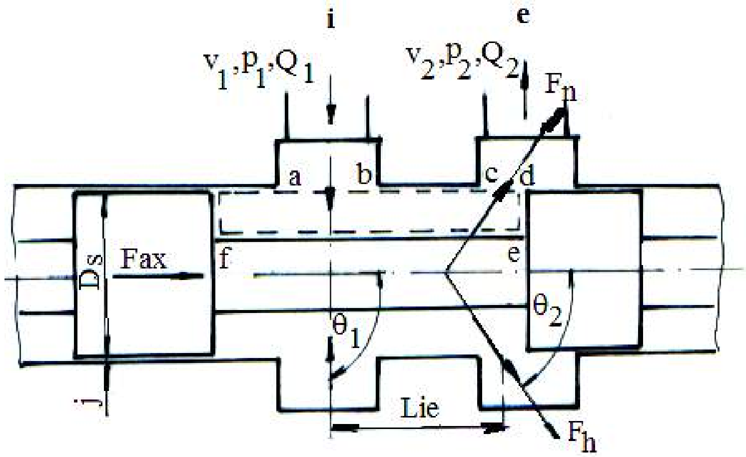

Fig. 2. Highlighting hydrodynamic forces in the spool - valve assembly

a) the fluid inlet is done from **i** to **e**, at the control edge of the spool:

$$F_{hax} = \rho\, \dot{Y}_{s_2}\; Q \cos\theta_e - \rho\, \dot{Y}_{s_1}\; Q \cos\theta_i - \rho\, L_{ie} \frac{dQ}{dt} \qquad (3)$$

where to: $\boldsymbol{\theta_e} = \boldsymbol{\theta}_2 = 90\,°$; $\mathbf{cos\,\theta_2} = 0$

$$\boldsymbol{\theta_i} = \theta_1 + 180^{\mathbf{o}} \;;\quad \mathbf{cos\,\theta_i = cos(\theta_1} + 180^{\mathbf{o}}\mathbf{) = -cos\,\theta_1}$$

we will have:

$$\mathbf{F_{hax} = \rho\, Q\, \dot{Y}_{s1}\; cos\;\; \theta_1 - \rho\, L_{ie} \frac{dQ}{dt}} \qquad (4)$$

b) the fluid inlet is done from **e** to **i,** at the control edge of the spool:

$$\mathbf{F_{hax} = \rho\, \dot{Y}_{s1}\, Q \cos\theta_e - \rho\, \dot{Y}_{s2}\, Q \cos\theta_i + \rho\, L_{ie} \frac{dQ}{dt}} \qquad (5)$$

where to: $\mathbf{\theta_e = \theta_1;\;\; \theta_i = \theta_2 + 180^{\circ} = 270^{\circ}\;;\;\; cos\;\; \theta_i = 0}$ we will have:

$$\mathbf{F_{hax} = \rho\, \dot{Y}_{s1}\, Q \cos\theta_1 + \rho\, L_{ie} \frac{dQ}{dt}} \qquad (6)$$

In both cases, the stationary component of the hydrodynamic impulse force has the same value and acts in the direction of closure of the wiper slot. The angle $\boldsymbol{\theta_1}$ depends on the size of the radial play and the ratio $\mathbf{\frac{Y_S}{J}}$ and varies within the limits $\boldsymbol{\theta}$ = 0°... 69° (Fig.1). Considering that the valve is working on a pressure $\mathbf{\Delta p}$ = const., we will have:

$$\mathbf{\dot{Y}_{s1} = C_v \sqrt{\frac{2\,\Delta p}{\rho}}} \qquad (7)$$

From [1] it follows:

$$\mathbf{Q = C_d\; \pi\; D_s\;\; Y_s \sqrt{\frac{2\;\Delta p}{\rho}}} \qquad (8)$$

from which, the stationary component of the axial hydrodynamic force, $\mathbf{F_{haxs}}$, under the conditions of constant pressure operation, becomes:

$$\mathbf{F_{haxs} = \rho\, Q\, \dot{Y}_{s1}\, cos\;\; \theta_1 = 2\, C_d\, C_v\; \pi\, D_s\;\, Y_s\; \Delta p\, cos\;\; \theta_1 = K_{hp}\;\; Y_s} \qquad (9)$$

respectively

$$F_{haxs} = \rho\, Q\, \dot{Y}_{S1} \cos\theta_1 = B_F\; Q \sqrt{\Delta p} \qquad (10)$$

where different forms of the hydrodynamic force coefficients are presented in the expressions (9) and (10).

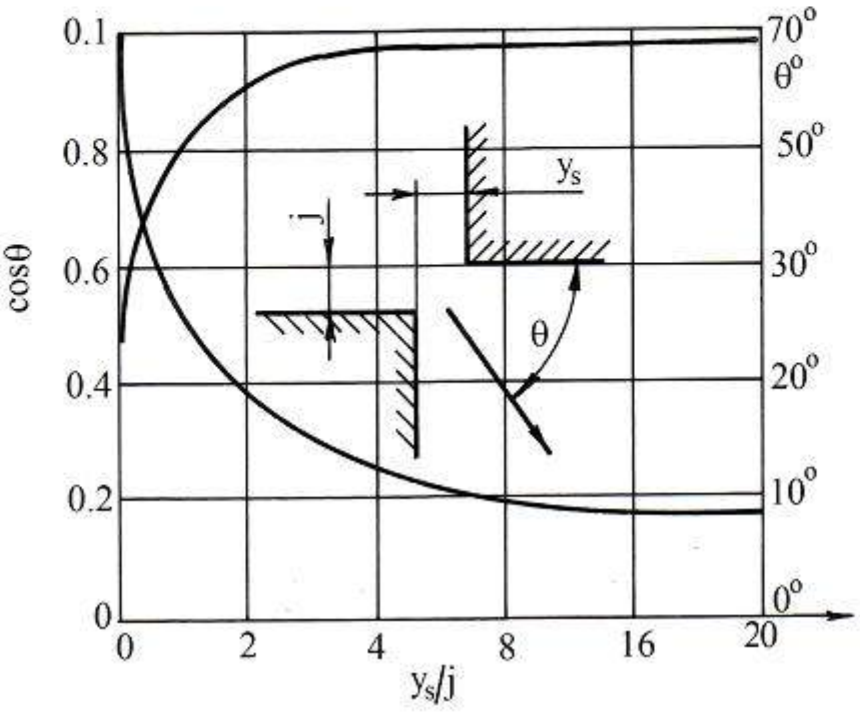

Fig.3

Under constant flow operation regime, we will have:

$$F_{haxs} = \frac{\rho\, Q^2 \cos\ \theta_1}{C_d\ \pi\, D_s\ Y_s} = K_{hq}\ \frac{1}{Y_s} \tag{11}$$

Here we noted: **C_d, C_v** - flow and speed coefficients (**C_d** = 0.61 – 0.7; **C_v** = 0.95 – 0.98); **K_{hp}**, **K_{hq}**, $\mathbf{B_F = \sqrt{2\,\rho}\cos\theta_1}$ - coefficients of axial hydrodynamic forces. In the general case, for **n_m** circuits that pass through the valve, relations coeficienţii forţelor hidrodinamice axiale (9, 10) become:

$$F_{haxs} = 2\, n_m\ C_d\ C_v\ \pi\, D_s\ Y_S \Delta p \cos\ \theta_1 \tag{12}$$

$$F_{haxs} = \frac{\rho\, n_m\ Q^2 \cos\ \theta_1}{C_d\ \pi\, D_s Y_s} \tag{13}$$

For the real situation, where the radial play is also considered, the hydrodynamic force becomes (Fig.2):

$$F_{haxs} = 2\, n_m\ C_d\ C_v\ \pi\, D_s \Delta p\ \sqrt{Y_s^2 + J^2}\ \cos\ \theta_1 \tag{14}$$

where:

$$\frac{\mathbf{Y_s}}{\mathbf{J}} = \frac{1 + \frac{\pi}{2}\sin\ \theta_1 - \ln\left[\ tg\frac{\pi - \theta_1}{2}\right]\cos\ \theta_1}{1 + \frac{\pi}{2}\cos\ \theta_1 + \ln\left[\ tg\frac{\pi - \theta_1}{2}\right]\sin\ \theta_1} \tag{15}$$

The relations (9 ... 14) show that in the case of feeding a hydraulic resistance (specific to the spool - body valve assembly) at constant pressure (Fig.4c), the hydrodynamic force **F_{haxs}** increases with the **Y_S**, opening up to the saturation of the source, until all the flow provided by the pump passes by resistance, which causes the safety valve to be closed and as result the constant feeding pressure condition to be canceled (Fig.4b).

The stationary component $\mathbf{F_{haxs}}$ of the axial hydrodynamic force on the spool always tends to close the slot of the throttle and is calculated with the same relation regardless the location of the hydraulic spool control edge.

The relations (9 ... 14) show that in the case of feeding a hydraulic resistance at constant flow (Fig.4d), the hydrodynamic force $\mathbf{F_{haxs}}$ increases with the decrease of $\mathbf{Y_S}$ opening up to the saturation of the source, when the safety valve opens and a part of the pump flow is discharge to the tank, thus canceling the feeding condition at constant flow (Fig.4a).

Therefore, at reaching the saturation limits, a hydraulic resistance feeded at constant pressure passes into a steady flow feed and vice versa.

The values of the stationary hydrodynamic force component, calculated with relations (9 ... 14) for a DN 10 distributor, are shown in Figures 4a and b. For small openings, the curves can be approximated by straight lines. For the larger $\mathbf{Y_S}$ openings, the impulse hydrodynamic force decreases because the pressure $\mathbf{\Delta p}$ on the control edge becomes smaller.

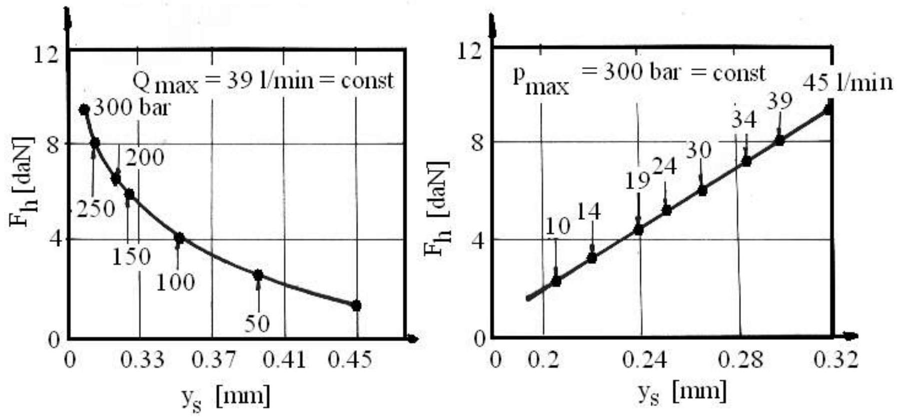

a) under constant flow regime; b) under constant pressure regime

Fig.4

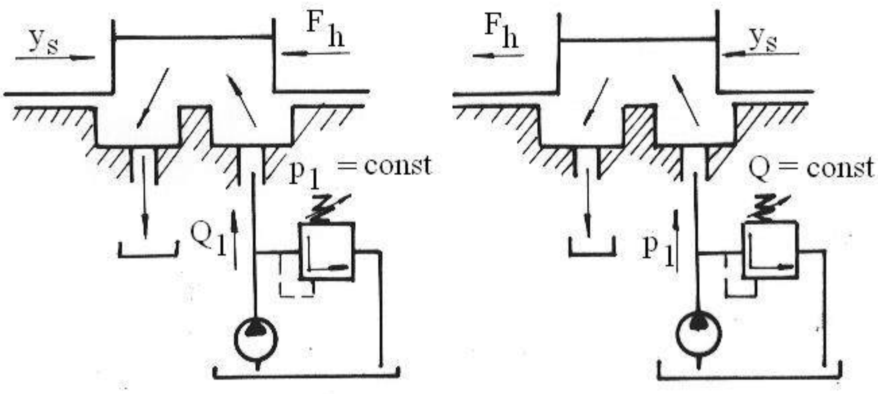

c) d)

Fig.4

The compensation of hydrodynamic forces can be achieved by:

- properly fitting of the spool and of the valve body (Fig.5). The hydrodynamic force becomes:

$$\mathbf{F_{haxs}} = \rho\, Q - \dot{Y}_{s1}\ \cos\ \theta_1 - \rho\, Q\, Y_{s2}\ \cos\ \theta_2 = \rho\, Q\, \dot{Y}_{s1}\left[1 - \frac{\dot{Y}_{s2}\ \cos\ \theta_2}{\dot{Y}_{s1}\ \cos\ \theta_1}\right] \qquad (16)$$

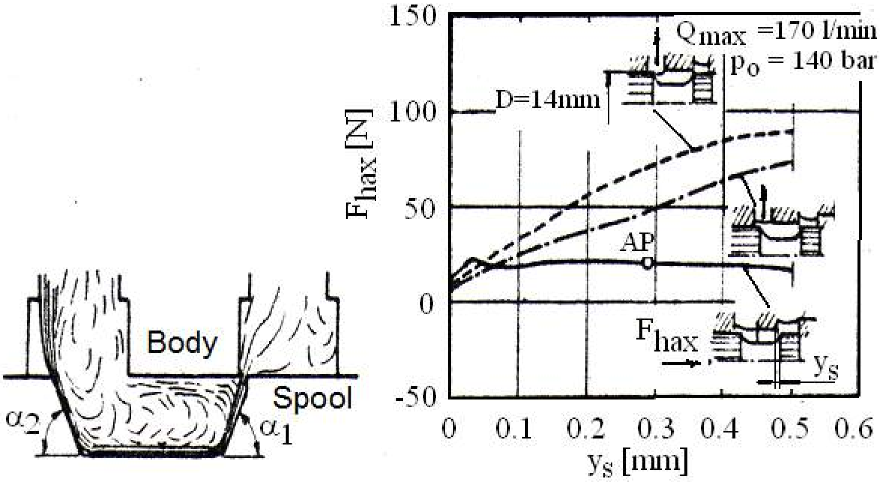

Fig.5.a. The effect of the fluid flow on the hydrodynamic force for the inlet and outlet edge

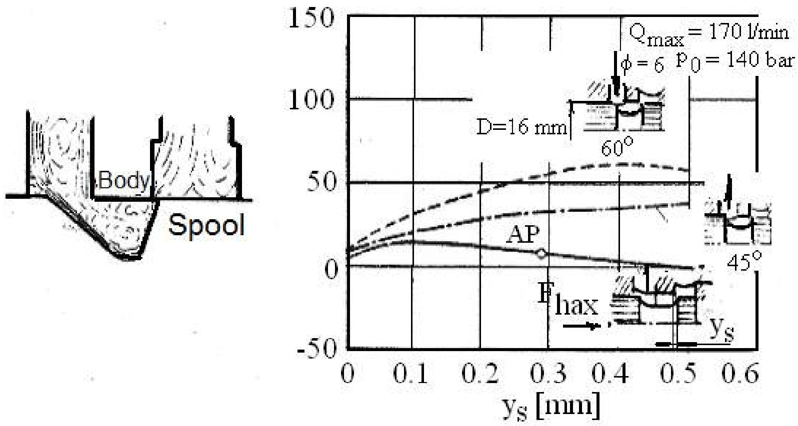

Fig.5.b. The influence of spool angle in the flow area on the impulse hydrodynamic forces

The data from Figures 5a and b suggest that by selecting the contour of the spool the constructor has the possibility to control the hydrodynamic forces on the spool both in size and direction, but within certain limits. This is also possible by further processing of the spool shoulders, which will lead to a corresponding adjustment of the hydrodynamic forces for the inlet and outlet edges.
Typical output angle is $\theta_1 \approx 69°$. The lower values of θ_1 slightly influence the hydrodynamic force, having a more pronounced effect at the large openings of the spool. Biger angular values for θ_1 will lead to detachment of the flow within the valve and high pressure losses due to direction changes, which require lower angle values for θ_2. This method is an effective means of compensation, although it is not possible to define an optimal profile of the spool or valve body.

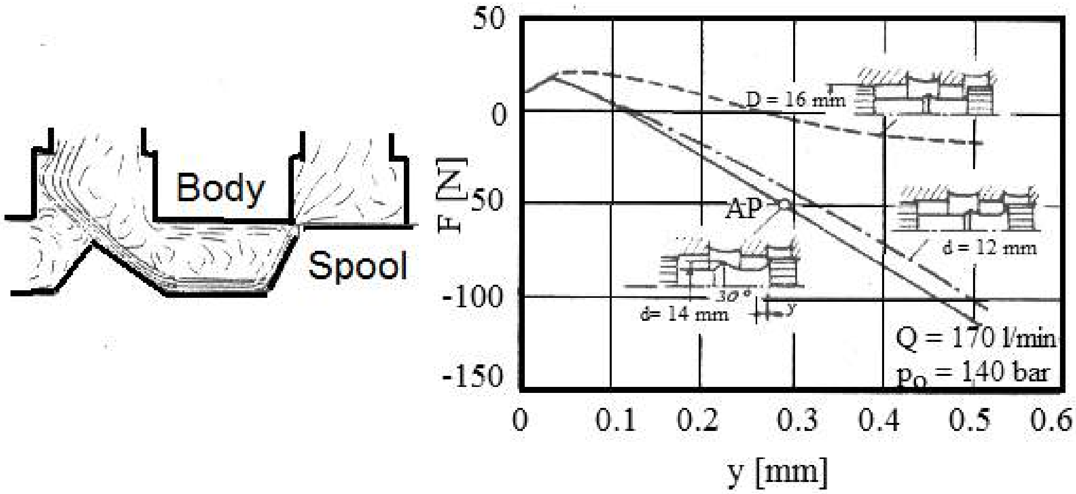

Fig.5.c. The compensation of hydrodynamic force on a flow edge through a conical shoulder in the spool chamber

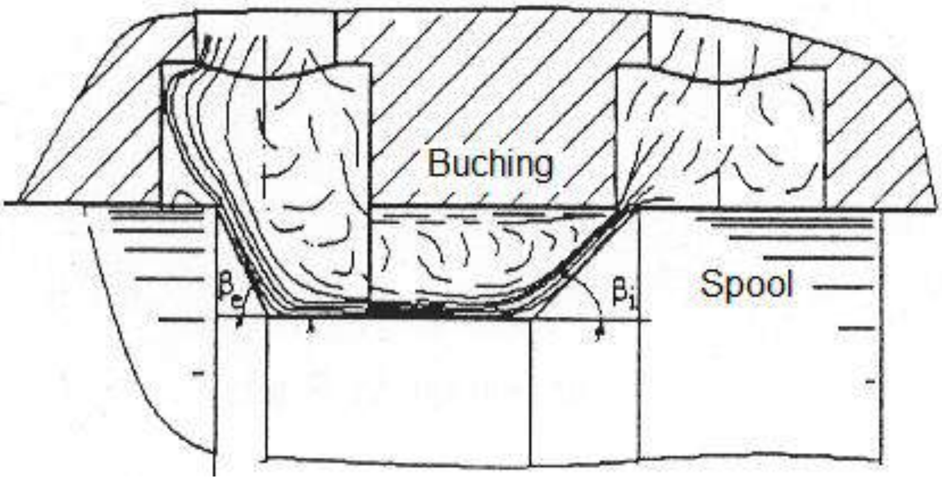

Fig. 6

The method of jet deviation at inlet and outlet spool edges aims to compensate the axial component of the impulse hydrodynamic forces caused by the inlet jet by means of the flow at the outlet, or vice versa, which is done by the geometry of the spool shoulders. The jet in the hydraulic resistance (Fig.5) breaks a little in the spool chamber, which, at angles $\theta > 60^0$, allows for good compensation.
Experimentally, it has been demonstrated that a sufficient reduction of hydrodynamic forces can be achieved for different geometries of the spool - valve body assembly (Fig.5.b). By concentrating the fluid flow near the spool rod, the desired flow of the current is possible with relatively small shoulders of the spool.
The combination of channel bushing and spool with an additional 30 ° angle in the outlet area leds at the action of the force in the direction of opening the spool (induced impuls hydrodynamic force) (Fig.5.c). The insertion of a double conic threshold allows the use of the inertia force of the "sticky" jet to divert it, providing a sufficient flow section to the tank (Fig.6).

ISSN 1454 - 8003
Proceedings of 2017 International Conference on Hydraulics and Pneumatics - HERVEX
November 8-10, Băile Govora, Romania

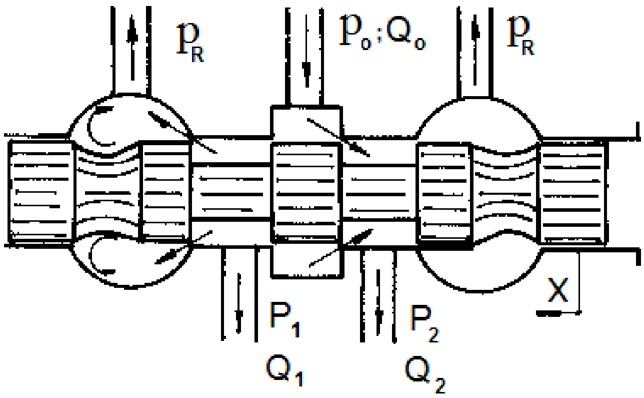

Fig. 7

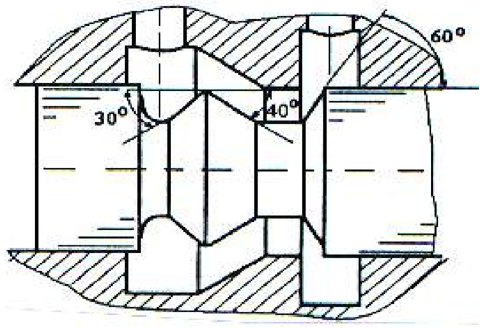

Fig. 8

The corresponding profiling of both the spool and the valve body, Figs. 7-8, has the effect of reducing axial hydrodynamic forces but is technologically high in complexity. For this case, the resulting force will have the value:

$$F_{hd\,ax} = Q\,\dot{Y}_S\,\rho(\cos\theta_1 - \cos\theta_2) \tag{17}$$

According to this relation if $\cos\theta_2 > \cos\theta_1$, the axial hydrodynamic force becomes negative, provide a positive effect on the spool control system, i.e. it tends to move the spool in the direction of the opening of the adjustment section (participates in the opening or closing of the spool). Increasing the angle θ_1 can be done by means of a bevelled edge on the spool (Fig.6). As the angle tends to values $\theta_1 > 69°$, the axial component of the hydrodynamic force acts in the radial direction, leading to its compensation, ie the value of the hydrodynamic force tends to zero (Fig.9).

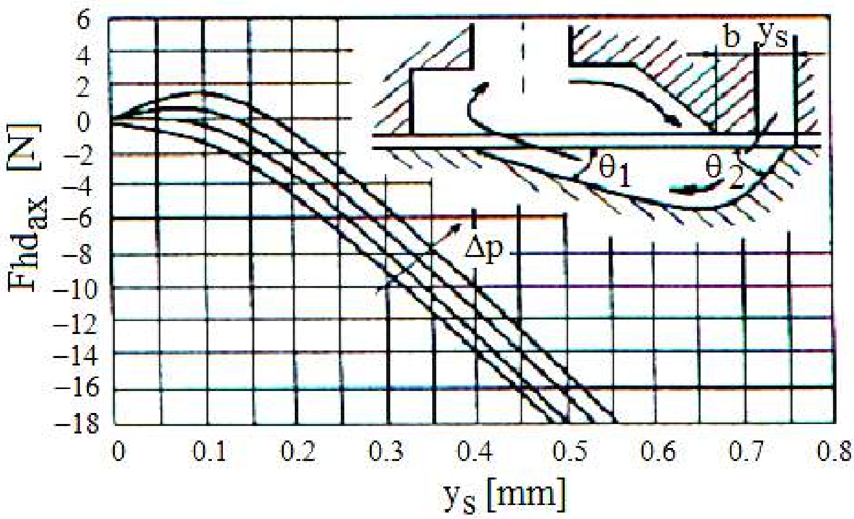

Fig. 9

The compensation of the impulse hydrodynamic forces by changing the angle of the jet or the resistance force is achieved by dividing the total section of the current into several partial sections, which will operate in succession (Fig.10.a). This solution leads to large spool strokes and nonlinear features, plus: the high cost price and the phenomenon of clogging. At a high amplifier coefficient of the valve, limited compensation is achieved (Fig.10.a).
The introduction of a hydraulic resistance force (Fig.10.b), by creating a pressure drop compared to the first solution, that of the corresponding profiling of the spool and the valve body, highlights

that the first method (Fig.10.a) is more efficient. The pressure loss that occurs by the insertion of an additional step on the spool shoulder (Fig.11) is due to the discontinuous section enlargements (determined with the Borda-Carnot relations) and the friction on the spool and bush walls. This solution results in an increase of impulse hydrodynamic force compensation and is usually only used to reduce the impulse hydrodynamic forces for the input edge.

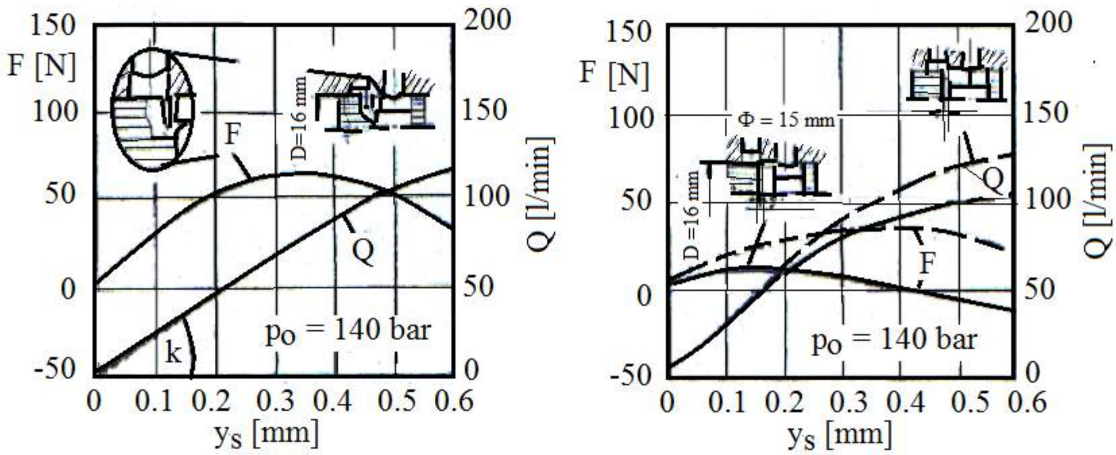

a) b)

Fig. 10. Influence of jet angle and resistance force
a) methods of compensating the impulse hydrodynamic forces
b) fluid recirculation on the spool shoulders.

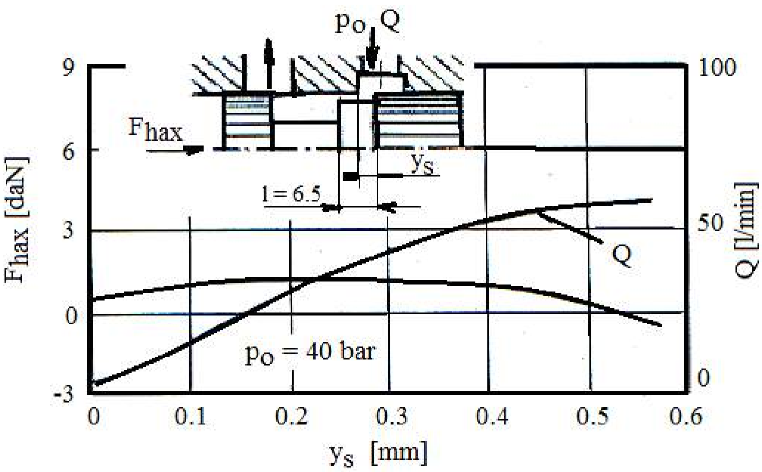

Fig. 11

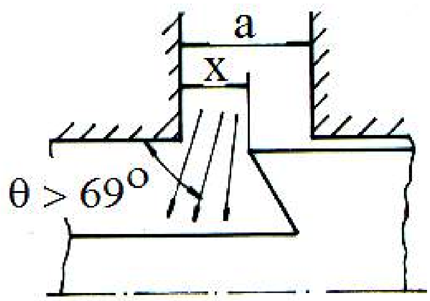

Fig. 12

Another component of the hydrodynamic forces is the transient one, caused by the instability of the stationary flow regime, the transient regime or the resonance phenomenon. Flow instability occurs when passing from one flow regime to another, accompanied by transient phenomena.
In hydraulic installations, although changes in flow conditions occur rapidly, the instability is manifested at a low intensity, except when overlapping other causes. The phenomenon becomes important if the frequency of the transient phenomena is equal to that of the spool, in which case the resonance phenomenon appears. Flow instability may occur when the fluid jet flows directly into a larger chamber, the transient regime being given by the transient components of the hydrodynamic forces.
The transient component $\mathbf{F_{haxtr}}$ of the impulse hydrodynamic force is associated with the fluid inertia in the annular space of the control volume, due to fluid acceleration in the spool chamber and is given by:

$$\mathbf{F_{haxtr}} = \rho\,\mathbf{L_{ie}}\,\frac{\mathbf{dQ}}{\mathbf{dt}} = \rho\,\mathbf{L_{ie}}\,\mathbf{C_d}\,\pi\,\mathbf{D_s}\left\{\sqrt{2\,\rho\,\Delta p}\,\frac{\mathbf{dY_S}}{\mathbf{dt}} + \sqrt{\frac{\rho}{2\Delta p}}\left(\frac{\mathbf{d\Delta p}}{\mathbf{dt}}\right)\right\} \tag{18}$$

This component is oriented opposite to the flow direction of the fluid. The term representing the travel speed of the spool is important because it influences the speed of the movement, decreasing it in the case of "**a**", and increasing it in case "**b**". Under conditions of constant pressure, the second term can be neglected. Where from:

$$\mathbf{F_{haxtr}} = \rho\mathbf{L_{ie}}\,\mathbf{C_d}\,\pi\,\mathbf{C_d}\sqrt{2\,\rho\,\Delta p}\,\dot{\mathbf{Y}}_\mathbf{s} = \mathbf{K_{htr}}\,\dot{\mathbf{Y}}_\mathbf{s} \tag{19}$$

We can express the hydrodynamic force in the form:

$$F_{hax} = (K_{hst} \pm K_{htr})\dot{Y}_S \tag{20}$$

the sign (+) being for the case of the active edge set at the exit, and the sign (-) corresponds to the **inlet** location of the control edge.
From the above, it results that the static component of the hydrodynamic force is independent of the flow direction of the fluid through the adjustment section, and the transient component is dependent on the direction of the resistance flow through the fluid. If the $\mathbf{K_{htr}}$ coefficient is positive (Fig.13.a), the damping is positive, the spool is in static equilibrium, and if it is negative (Fig.13.b), the damping is negative and the spool enters a static imbalance. To improve the static balance condition of the spool, it is necessary to have the positive damping lengths greater than the negative lengths.

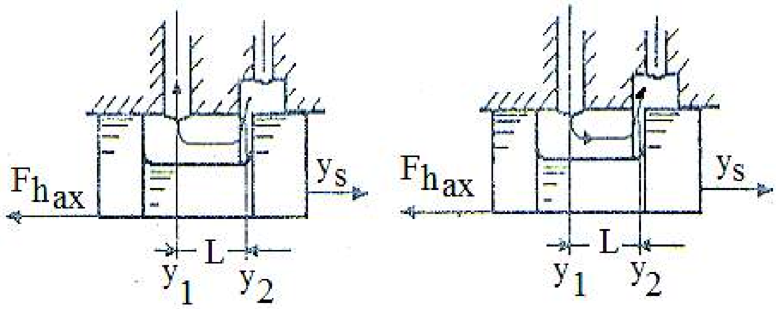

a) b)

Fig. 13

As the component $\mathbf{F_{haxtr}} \cong \dfrac{\mathbf{F_{haxs}}}{\mathbf{30}}$ is negligible in relation to the stationary hydrodynamic force, it can be approximated $\mathbf{F_{hax}} \cong \mathbf{F_{haxs}}$. However, for high pressure ($\mathbf{p_o} > 10\,\mathrm{MPa}$), hydrodynamic forces

can become important in both stationary and transient modes, and therefore it is necessary to compensate them.
If the hydraulic spool has several active edges, the hydrodynamic forces result from summing the forces associated with all the active edges. At the same time, when calculating the final hydrodynamic force at the hydraulic spool, all the forces associated with the control edges, components that tend to close the respective throttle slots, will be considered.

3. Conclusions

Hydrodynamic forces play an important role in the optimal operation of directional spool valves. An important role is played by the stationary component, which depends on the geometry of the edges of the spool and of the valve body bush, influencing the inlet and outlet flow of the liquid jet.
When the flowing passes from one regime to another, the transient component of the hydrodynamic force becomes important.
Hydrodynamic forces become important for a pressure greater than 10 MPa, in both stationary and transient mode, when compensation is required.

References

[1]. Bălășoiu, V., Cristian, I., Bordeașu, I., „Echipamente și sisteme hidraulice de acționare și Automatizare, Aparatura hidraulică”, Editura Orizonturi universitare, Timișoara, 2008.
[2] Bălăşoiu, V., „Cercetări teoretice și experimentale asupra sistemelor electrohidraulice tip servovalvă-cilindru-sarcină, pentru module de roboți industriali”, Teza de doctorat, Institutul Politehnic Timișoara, 1987.
[3] Bălăşoiu V., „Echipamente hidraulice de acționare, fundamente teoretice, echipamente și sisteme, fiabilitate”, Editura Eurostampa, Timișoara, 2001.
[4] Bălăşoiu V., Popoviciu M., Bordeașu I., ”Experimental research upon static and dynamic behaviour of electrohydraulic servovalves”, The 6th International Conference on Hydraulic Machinery and Hydrodinamics, Timisoara, Oct. 2004.
[5] Bălăşoiu V., Popoviciu M., Bordeașu I., ”Theoretical simulation of static and dynamic behavior of electrohydraulic servovalves”, The 6th International Conference on Hydraulic Machinery and Hydrodinamics, Timisoara, 0ct. 2004.
[6] Cristian I., „Servosisteme electrohidraulice incrementale”, Editura Universității Transilvania, Brașov, 2003.
[7] Merritt Herbert E., ”Hydraulic Control Systems”, John Wiley and Sons New York, Inc. Edition, 1967.
[8] Vasiliu N., Vasiliu D., „Acționări hidraulice și pneumatice”, Vol. 1, Editura Tehnică, București, 2005.
[9] ***, ”Industrial Servoventile”, Der Hydraulik, Band V, MANNESMANN REXROTH, Lohr am Main, 1981.
[10] http://www.boschrexroth.de; www.boschrexroth.com, Rexroth Bosch Group, Industrial Hydraulics, Control and Closed loop technology, Industrial Hydraulics, Electric Drives and Control, Service Automation, etc.
[11] ***, ”Moog product information”, http://www.moog.com.
[12] http://www.moog.de, MOOG. Components Group.
[13] Backe W., ”Steuerung - und Schaltungstechnik”, II. Institut fur hydraulische und Pneumatische antriebe und Steuerung der RWTH. Aachen, 1986.
[14] Backe W., ”Servohydaraulik”, Umdruck zur vorlesung, Institut fur hydraulische und Pneumatische Antriebe und Steuerung der RWTH, Aachen., 5.Auflage,1986.
[15] Deacu L., Pop I., „Hidraulica mașinilor unelte”, Litografia Institutului Politehnic Cluj - Napoca, 1983.
[16] Deacu L., „Acționări hidraulice proporționale”, TCMM, Editura Tehnică , București, 1987.
[17] Oprean A. și alții, „Hidraulica mașinilor unelte”, Editura Didactică și Pedagogică București, 1977.
[18] Oprean. A. și alții, „Acționări hidraulice. Elemente și sisteme”, Editura Tehnică București, 1982.

TEMPERATURE CONTROLLERS

Marian BLEJAN[1], Ioana ILIE[1]

[1] INOE 2000 – IHP, Bucharest, blejan.ihp@fluidas.ro

Abstract: *To accurately control process temperature without extensive operator involvement, a temperature control system relies upon a controller, which accepts a temperature sensor such as a thermocouple or RTD as input. It compares the actual temperature to the desired control temperature, or setpoint, and provides an output to a control element. The controller is one part of the entire control system, and the whole system should be analyzed in selecting the proper controller.*

Keywords*: Temperature, controller*

1. Introduction

The following items should be considered when selecting a controller:

1. Type of input sensor (thermocouple, RTD) and temperature range

2. Type of output required (electromechanical relay, SSR, analog output)

3. Control algorithm needed (on/off, proportional, PID)

4. Number and type of outputs (heat, cool, alarm, limit)

There are three basic types of controllers: on-off, proportional and PID. Depending upon the system to be controlled, the operator will be able to use one type or another to control the process.[1][2]

2. On/Off Controllers

An on-off controller is the simplest form of temperature control device. The output from the device is either on or off, with no middle state. An on-off controller will switch the output only when the temperature crosses the setpoint. For heating control, the output is on when the temperature is below the setpoint, and off above setpoint. Since the temperature crosses the setpoint to change the output state, the process temperature will be cycling continually, going from below setpoint to above, and back below. In cases where this cycling occurs rapidly, and to prevent damage to contactors and valves, an on-off differential, or "hysteresis" is added to the controller operations. This differential requires that the temperature exceed setpoint by a certain amount before the output will turn off or on again. On-off differential prevents the output from "chattering" (that is, engaging in fast, continual switching if the temperature's cycling above and below the setpoint occurs very rapidly). On-off control is usually used where a precise control is not necessary, in systems which cannot handle the energy's being turned on and off frequently, where the mass of the system is so great that temperatures change extremely slowly, or for a temperature alarm. One special type of on-off control used for alarm is a limit controller. This controller uses a latching relay, which must be manually reset, and is used to shut down a process when a certain temperature is reached.

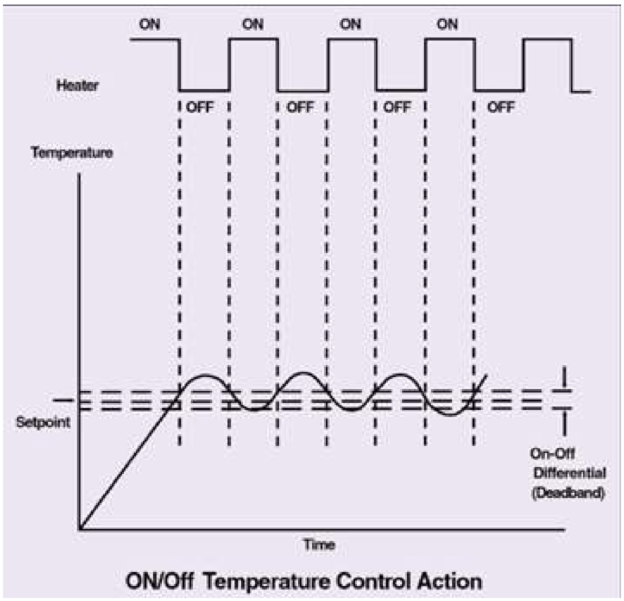

Fig. 1. On/off temperature control action

3. Proportional Controllers

Proportional controls are designed to eliminate the cycling associated with on-off control. A proportional controller decreases the average power being supplied to the heater as the temperature approaches setpoint. This has the effect of slowing down the heater, so that it will not overshoot the setpoint but will approach the setpoint and maintain a stable temperature. This proportioning action can be accomplished by turning the output on and off for short intervals. This “time proportioning” varies the ratio of ‘on’ time to ‘off’ time to control the temperature. The proportioning action occurs within a “proportional band” around the setpoint temperature. Outside this band, the controller functions as an on-off unit, with the output either fully on (below the band) or fully off (above the band). However, within the band, the output is turned on and off in the ratio of the measurement difference from the setpoint. At the setpoint (the midpoint of the proportional band), the output on:off ratio is 1:1; that is, the on-time and off-time are equal. If the temperature is further from the setpoint, the on- and off-times vary in proportion to the temperature difference. If the temperature is below setpoint, the output will be on longer; if the temperature is too high, the output will be off longer. The proportional band is usually expressed as a percent of full scale, or degrees. It may also be referred to as gain, which is the reciprocal of the band. Note, that in time proportioning control, full power is applied to the heater, but is cycled on and off, so the average time is varied. In most units, the cycle time and/or proportional band are adjustable, so that the controller may better match a particular process. In addition to electromechanical and solid state relay outputs, proportional controllers are also available with proportional analog outputs, such as 4 to 20 mA or 0 to 5 V DC. With these outputs, the actual output level is varied, rather than the on and off times, as with a relay output controller. One of the advantages of proportional control is simplicity of operation. It may require an operator to make a small adjustment (manual reset) to bring the temperature to setpoint on initial startup, or if the process conditions change significantly.
Systems that are subject to wide temperature cycling will also need proportional controllers. Depending upon the process and the precision required, either a simple proportional control or one with PID may be required. Processes with long time lags and large maximum rate of rise (e.g., a heat exchanger), require wide proportional bands to eliminate oscillation. The wide band can result in large offsets with changes in the load. To eliminate these offsets, automatic reset (integral) can be used. Derivative (rate) action can be used on processes with long time delays, to speed recovery after a process disturbance.

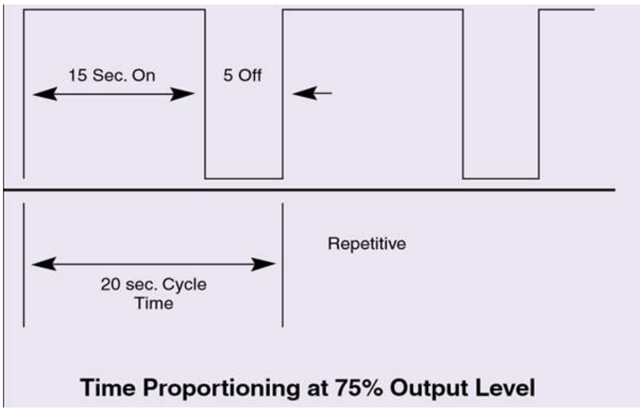

Fig. 2. Time proportioning at 75% output level

There are also other features to consider when selecting a controller. These include auto- or self tuning, where the instrument will automatically calculate the proper proportional band, rate and reset values for precise control; serial communications, where the unit can "talk" to a host computer for data storage, analysis, and tuning; alarms, that can be latching (manual reset) or non-latching (automatic reset), set to trigger on high or low process temperatures or if a deviation from setpoint is observed; timers/event indicators which can mark elapsed time or the end/beginning of an event. In addition, relay or triac output units can be used with external switches, such as SSR solid state relays or magnetic contactors, in order to switch large loads up to 75 A.

4. PID Controllers

The third controller type provides proportional with integral and derivative control, or PID. This controller combines proportional control with two additional adjustments, which helps the unit automatically compensate for changes in the system. These adjustments, integral and derivative, are expresse in time-based units; they are also referred to by their reciprocals, RESET and RATE, respectively. The proportional, integral and derivative terms must be individually adjusted or "tuned" to a particular system, using a "trial and error" method. It provides the most accurate and stable control of the three controller types, and is best used in systems which have a relatively small mass, those which react quickly to changes in energy added to the process. It is recommended in systems where the load changes often, and the controller is expected to compensate automatically due to frequent changes in setpoint, the amount of energy available, or the mass to be controlled.

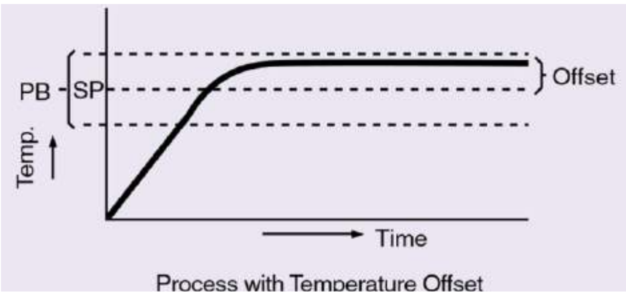

Fig. 3. Process with temperature offset

Rate and reset are methods used by controllers to compensate for offsets and shifts in temperature. When using a proportional controller, it is very rare that the heat input to maintain the setpoint temperature will be 50%; the temperature will either increase or decrease from the setpoint, until a stable temperature is obtained. The difference between this stable temperature and the setpoint is called offset. This offset can be compensated for manually or automatically.

Using manual reset, the user will shift the proportional band so that the process will stabilize at the setpoint temperature. Automatic reset, also known as integral, will integrate the deviation signal with respect to time, and the integral is summed with the deviation signal to shift the proportional band. The output power is thus automatically increased or decreased to bring the process temperature back to setpoint, The rate or derivative function provides the controller with the ability to shift the proportional band, to compensate for rapidly changing temperature. The amount of shift is proportional to the rate of temperature change. A PID, or three-mode controller, combines the proportional, integral (reset) and derivative (rate) actions, and is usually required to control difficult processes. These controllers can also be made with two proportional outputs, one for heating and another for cooling. This type of controller is required for processes which may require heat to start up, but then generate excess heat at some time during operation.

5. Controller output hardware

The output from the controller may take one of several forms. The most common forms are time proportional and analog proportional. A time proportional output applies power to the load for a percentage of a fixed cycle time. For example, with a 10 second cycle time, if the controller output were set for 60%, the relay would be energized (closed, power applied) for 6 seconds, and de-energized (open, no power applied) for 4 seconds. Time proportional outputs are available in three different forms: electromechanical relay, triac or ac solid state relay, or a dc voltage pulse (to drive an external solid state relay). The electromechanical relay is generally the most economical type, and is usually chosen on systems with cycle times greater than 10 seconds, and relatively small loads. An ac solid state relay or dc voltage pulse are chosen for reliability, since they contain no moving parts. Recommended for processes requiring short cycle times, they need an additional relay, external to the controller, to handle the typical load required by a heating element. These external solid state relays are usually used with an ac control signal for ac solid state relay output controllers, or with a dc control signal for dc voltage pulse output controllers. An analog proportional output is usually an analog voltage (0 to 5 Vdc) or current (4 to 20 mA). The output level from this output type is also set by the controller; if the output were set at 60%, the output level would be 60% of 5 V, or 3 V. With a 4 to 20 mA output (a 16 mA span), 60% is equal to (0.6 x 16) + 4, or 13.6 mA. These controllers are usually used with proportioning valves or power controllers.

6. Conclusions

When you choose a controller, the main considerations include the precision of control that is necessary, and how difficult the process is to control. For easiest tuning and lowest initial cost, the simplest controller which will produce the desired results should be selected. Simple processes with a well matched heater (not over- or undersized) and without rapid cycling can possibly use on-off controllers. For those systems subject to cycling, or with an unmatched heater (either over- or undersized), a proportional controller is needed.

Acknowledgments

This paper has been developed in INOE 2000-IHP, with the financial support of the Executive Agency for Higher Education, Research, Development and Innovation Funding (UEFISCDI), under PN III, Programme 2-Increasing the competitiveness of the Romanian economy through research, development and innovation, Subprogramme 2.1- Competitiveness through Research, Development and Innovation - Innovation Cheques, project title: *Computerizing the technological process of heat treatment of metallic materials*, Financial Agreement no. 126CI/2017.

References

[1] www.omega.com
[2] controlengeurope.com

ISSN 1454 - 8003
Proceedings of 2017 International Conference on Hydraulics and Pneumatics - HERVEX
November 8-10, Băile Govora, Romania

STORAGE OF THERMAL ENERGY IN PHASE CHANGE MATERIALS USING HYBRID HEATING SYSTEMS

Daniel Vasile BANYAI[1]

[1]Technical University of Cluj-Napoca, Romania, email: daniel.banyai@termo.utcluj.ro

Abstract: *Thermal energy storage using phase change materials is an important step in solving the frequent problems of heat supply only at times when it is necessary. The paper presents the importance, advantages and applicability areas of latent heat storage units using phase change materials and also information to design heat storage units with this type of substances, consisting of a mixture of saturated hydrocarbons, such as paraffin. Using such a heat storage unit is very profitable because the dimensions are much smaller than a classic one (water) and the heat is stored for a longer period of time, the temperature maintains constant until the whole process of phase change is totally finished.*

Keywords*: Thermal energy accumulator, phase change material, hybrid heating.*

1. Introduction

Transforming solar energy into heat is the most environmentally friendly and economical solution of renewable energy sources (the potential is 60,106 GJ annually). Although, solar thermal installations, have a high energy conversion rate, due to intermittent (periodic) operation, geographic and weather conditions, are generally integrated with other sources of heat (natural gas, liquid or solid fuels, biomass or geothermal) in hybrid systems. The energy that can be obtained on a collector surface of 1 m^2 varies greatly, in Romania, on a sunny day, the average sunshine can reach approx. 1000 W/m^2. (source: ANM, ICEMERG)
There is a constant mismatch between supply and demand for thermal energy produced from renewable energy sources; the problem is not the lack of energy, but finding solutions to supply a sufficient amount of energy, in a usable form, when and where it is needed.

2. Thermal accumulator

Thermal energy storage is an important step in solving the frequent heat supply problems regardless the heat load variation to consumers (heating or domestic hot water preparation). The thermal energy, received from the solar collectors, is currently stored in systems with hot water tank supplied also by other heating systems. The operating principle of a thermal accumulator is the same of a heat exchanger. The storage agent takes the thermal energy from the heating system (solid fuel boilers, gas boilers, heat pumps, solar panels, etc.) through thermal agent, when the heating system supplies a higher amount of energy than is necessary at that time. The heat accumulator stores the heat in the mass of the storage agent and then delivers it as needed, providing users extra comfort. [1], [2], [3]
In the case of domestic hot water obtained from thermal solar panels, the storage capacity is between 13 and 15 liters of water per 1 m^2 of radiant surface. If solar energy is also used as contributor to rooms heating, the storage tanks are cylindrical without an internal heat exchanger (tank in tank) with a larger volume than domestic hot water boilers (about 1000-3000 liters), called puffer tanks for heating. [3], [4]

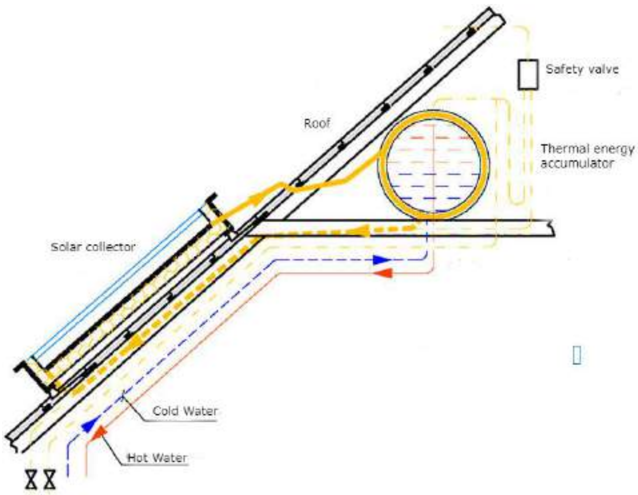

Fig. 1. Scheme of a thermal solar collector with accumulator

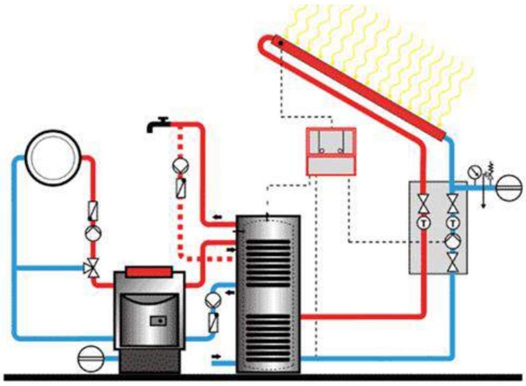

Fig. 2. Hybrid heating system

Taking into account the data obtained from the literature, the thermal solar installations can cover the needs of Domestic Hot Water, considering that a solar thermal panel with the area of 2 sqm provides the necessary for 2 persons, under medium comfort (50 liters of DHW / person / day). The correct sizing of a combined storage facility can fully cover the need for DHW, at least in the warm season (April to September). [3], [4]

The most common heat storage medium is water, due to high specific heat and high density. In order to reduce the volume occupied by the thermal accumulators and to increase the amount of stored heat, two-phase substances can be used. Phase change materials, change their aggregate state when they receive or dissipate heat, but without changing the temperature throughout the phase change process, they can store up to 5-14 times more heat per unit volume than conventional ones. Thus, for 1 m^2 of energy storage area, a volume of 1-3 l of storage agent would be needed compared to 13-15 l for water. [1], [2], [3], [4]

To accumulate and release the required amount of energy, these systems depend basically on the temperature, the latent heat of phase change, of the storage agent.

Phase change substances may be organic (paraffins, esters, glycols) or anorganic salts (salt hydrates and metals class) and, depending on their chemical composition, have different energy storage properties.

The operating principle of paraffin accumulators is similar to the classical ones, so the thermal storage medium, the paraffin, being in solid state, takes the heat from the heating system (solid fuel boilers, gas boilers, heat pumps, systems with solar panels etc.) through heating agent, and starts to melt (phase change). Throughout the melting process, the wax takes heat from the heating agent, but the temperature remains constant (approx. 60^oC – paraffin melting point). After the melting process has ended, i.e., when the total amount of paraffin in the solid state has completely turned into liquid state, it is overheated to the temperature at which the heat exchange of these agents is greatest. The thermal agent circulating in the heating or/and domestic hot water system, takes over this heat and distributes it to consumers as needed. Thus the process will reverse (from liquid to solid state), but the heat transfer and phase exchanges will be the same. [2]

3. Comparative analysis of water and phase change accumulators

Considering that the useful temperature of 50°C of the heating agent is sufficient for domestic hot water and for rooms heating, it was made a calculation for the energy demand, so that water yields the same energy value as if paraffin was used and cooled by at 80°C to 50°C, (see equation 1. - The calculation of the amount of energy required to heat the accumulator media from 20 to 80^{o}C.)

$$Q_{accum} = m_{media} \cdot c_{p\text{-}media} \cdot \Delta T \text{ [kJ]} \qquad (1)$$

where: m_{media} – the mass of accumulator media; $c_{p\text{-}media}$ – specific heat, 4180 [J/kg·K] for water and 4324 [J/kg·K] for paraffin at 20 [^{o}C]; ΔT – temperature difference.
The graph below shows a comparison of thermal energy storage properties for water (green) and technical paraffin (blue).

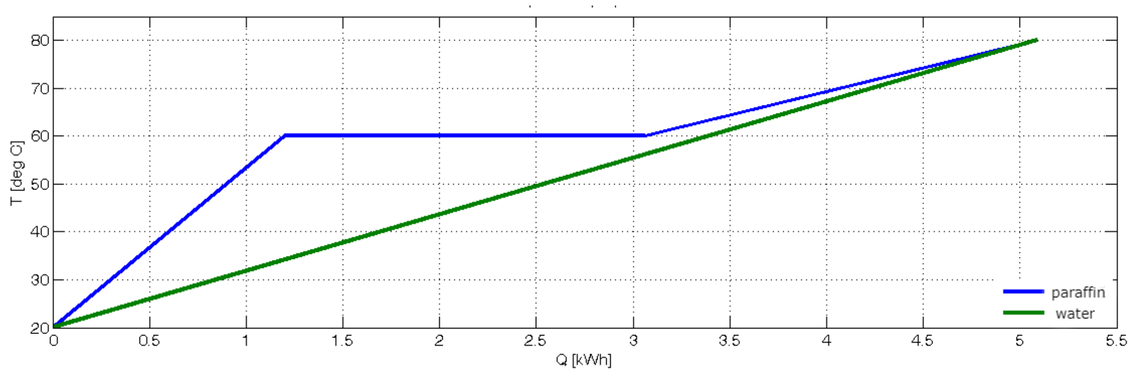

Fig. 3. Comparison of thermal energy storage for water and paraffin

In the graph bellow, the blue curve represents the energy requirements to heat the paraffin from ambient temperature of 20 ºC to a temperature of 80 ºC. The green curve shows that if water is used as a storage medium for the same temperature difference (20 °C to 80 °C), receiving the same amount of heat (5.1 kWh), the mass of the storage medium is higher with about 100%. Comparing the two curves (blue and green) in the situation where the storage agent gives up the heat to the primary agent (from the heating installation) it is found that in the case of the phase change accumulator the temperature is higher for the same amount of energy consumed as compared to a conventional thermal accumulator. The red curve was drawn to highlight that to cool the storage medium from 80 ºC to 50 ºC, using the same amount of energy, the mass in the case of water is about 100% higher. (see equation 1). This also results in the fact that for the previously obtained storage tank (water), a double amount of energy is needed to heat it from 20 °C to 80 °C. In order to develop such products, it is recommended, to perform CFD numerical analysis, which facilitates proper sizing of the thermal accumulator for concrete applications and after the numerical models have to be validated through practical experiments [5], [6]. Regarding the flow of thermal agents, modern solutions described in [7], [8], [9], as well as monitoring the functional parameters.

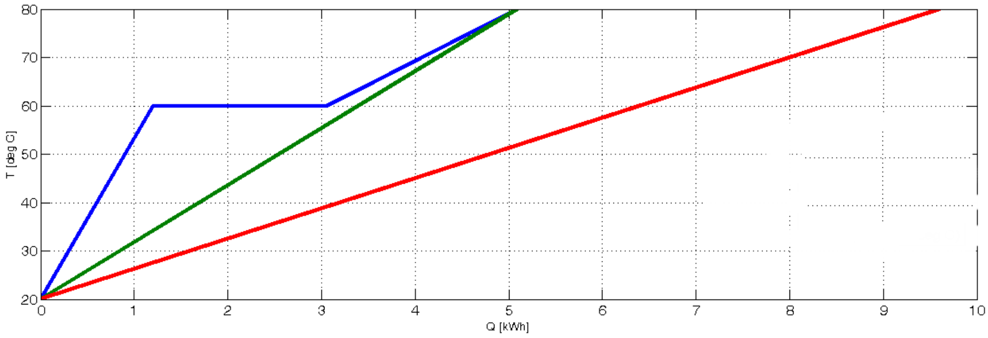

Fig. 4. Comparison of energy requirements to heat 60 ºC for water and paraffin

4. Conclusions and discussions

The volume of national and international researches in the field of renewable energies is increasing, and penetration with new ideas can create important collaboration opportunities.
The accumulators analyzed within the paper, have significant market potential, contributing to the exploitation of renewable energies, a field in which Romania has a very high potential, but with few exceptions, untapped. The lack of exploitation is also due to the lack of products tailored to the purchasing power of the beneficiaries.
The analyzed accumulators are addressed to small users, individual households; the solutions in principle allow them to be adapted for the design of various size installations, thus covering a wide range of demands. Apart from the individual users, the facilities are also useful for various institutions, commercial spaces, offices. The contribution, of this type of products, to increase the quality of users' lives is significant, as products contribute to lowering the costs of heating.
This type of products can be manufactured by many well-equipped national enterprises, which are currently struggling to create a main or secondary development.

References

[1] S. Kakac, E. Paykoc, Y. Yener, "Storage of Solar Thermal Energy", *Energy Storage Systems*, Vol. 167, Springer, Dordrecht, ISBN 978-94-010-7558-9, 1989;
[2] S. Kakac, H. Liu, "Heat Exchangers: Selection, Rating and Thermal Design", second edition, CRC Press, ISBN 0-8493-0902-6, 2002;
[3] S. Esakkimuthu, A.H. Hassabou, C. Palaniappan, M. Spinnle, "Experimental investigation on phase change material based thermal storage system for solar air heating applications", *Solar Energy*, Vol. 88, pp. 144-153, Pergamon, 2013;
[4] L. Socaciu, O. Giurgiu, D. Banyai, M. Simion, "PCM selection using AHP method to maintain thermal comfort of the vehicle occupants", *Sustainable Solutions for Energy and Environment, EENVIRO - YRC 2015, Energy Procedia*, Vol. 85, pp. 489-497, 2016;
[5] A. Plesa, F. Bode, D. Opruta, "The flow simulation through a heat exchanger channel", *Annals of DAAAM for 2008 & Proceedings of the 19th International DAAAM Symposium*, Oct. 2008, Trnava, Slovakia, pp. 1085-1086, ISSN 1726-9679, 2008;
[6] A. Plesa, D. Opruta, P. Unguresan, "Some practical aspects regarding the flow in a plate and fins heat exchanger", *Leonardo Electronic Journal of Practices and Technologies*, Issue 25, pp. 254-263, 2014;
[7] I.L. Marcu, "Functional parameters monitoring for an alternating flow driven hydraulic system", in *AQTR 2008, IEEE International Conference on Automation, Quality and Testing, Robotics*, vol.3, no., pp. 239-242, 2008;
[8] I.L. Marcu, I. Pop, "Interconnection possibilities for the working volumes of the alternating hydraulic motors", *The 6th International Conference on Hydraulic Machinery and Hydrodynamics*, Timisoara, Romania, October 21 - 22, 2004, *Scientific Bulletin of the Politehnica University of Timisoara, Transactions on Mechanics*, Special issue, pp. 365-370, ISSN 1224-6077, 2004;
[9] I.L. Marcu, D. Banyai, "Analytical model of the connection pipes of the alternating flow driven hydraulic systems", "*HIDRAULICA" No. 3/2013, Magazine of Hydraulics, Pneumatics, Tribology, Ecology, Sensorics, Mechatronics*, pp. 80-85, ISSN 1453 – 7303, 2013.

ISSN 1454 - 8003
Proceedings of 2017 International Conference on Hydraulics and Pneumatics - HERVEX
November 8-10, Băile Govora, Romania

HOLLOW PISTONS IN HYDRAULICS – POSSIBILITIES OF INCREASING VOLUMETRIC EFFICIENCIES

Marcel RÜCKERT[1], Hubertus MURRENHOFF[2], Katharina SCHMITZ[3]

[1] Institute for Fluid Power Drives and Controls (IFAS), RWTH Aachen University, Marcel.Rueckert@ifas.rwth-aachen.de

[2] Institute for Fluid Power Drives and Controls (IFAS), RWTH Aachen University, post@ifas.rwth-aachen.de

[3] post@ifas.rwth-aachen.de

Abstract: *The cluster of excellence "Tailor-Made Fuels from Biomass" at RWTH Aachen University is identifying and investigating new potential biofuel candidates. Fuel candidates developed in this process greatly vary in rheological and hydrodynamic properties. One of the most important properties is the fluid viscosity. Low viscosities increase volumetric losses, friction and wear in the fuel pump, therefore lowering the overall efficiency. An optimization of the tribological contacts inside the pump is essential to ensure a sufficient performance. One of the most important tribological pairings is the piston-bushing contact which has a crucial impact on the leakage. A possibility to decrease this leakage is the hollow piston design developed for common-rail pumps. In common-rail injection pumps a reduced gap height can increase the volumetric efficiency by approximately 40% at 120 MPa injection pressure. In this paper, a first attempt is performed to transfer this specific hollow piston into hydraulic pumps. Thereby a possible application preferably operates at low viscosity and high bulk moduli. Relatively low volumetric efficiencies indicate hidden potential. Both of these cases can be found in water hydraulics. With a maximum pressure of 32 MPa radial piston units commonly operate at 25 % of the common rail system´s pressure level. Investigating possible applications of the hollow piston principle for water hydraulics, various potential piston geometries of a radial piston unit are simulated using FEM analysis. In order to ensure an optimal geometry, geometrical approaches are discussed and applied to the hollow piston as well as simulated with a Matlab model using the Reynolds equation regarding the resulting leakage and potential increase in volumetric efficiency.*

Keywords*: Pump, Piston, Common-Rail, Water Hydraulics*

1. Introduction

Within the cluster Tailor-Made Fuels from Biomass, new potential biofuel candidates are investigated and identified for a more sustainable fuel economy and lower global emissions. The primary goal is to find alternatives to current gasoline and diesel fuels. Therefore, the research focuses on two main areas of interest: Production and propulsion. The production side concentrates on finding new potential molecules as well as synthesis-processes for industry scale production, whereas the propulsion group focusses on the performance of the fuel candidates inside the combustion system with the main attention towards fuel compatibility with the current diesel and gasoline system.

In order to reduce emissions, the spray behaviour of the fuel during the injection phase plays a vital role. Here, a fast primary breakup of the fuel jet is highly important for a good atomization and homogeneous spray distribution, resulting in a combustion with lower soot emissions. One of the defining fuel characteristics for primary breakup is viscosity. Lower viscosity values tend to have a positive effect on the spray behaviour.

A promising molecule to act as a replacement fuel to diesel is di-n-butyl-ether (DnBE). Fig. 1a) shows the kinematic viscosity of DnBE in comparison to the standard hydraulic oil HLP46 and water over temperature [1]. With a viscosity value close to water, DnBE performs well in engine - tests. In order to provide the engine with enough fuel, the injection pump needs to deliver fuel at elevated pressures of up to 300 MPa when looking at compression ignition (CI). Here, the low viscosity of DnBE causes high leakage rates and low volumetric efficiencies, see Fig. 1b) [2]. Lower volumetric efficiencies and higher leakage rates would cause the need to use a bigger pump in order to supply enough fuel. Especially in the automotive sector, an increase in size is hardly possible. Therefore, alternative ways to reduce leakage have to be investigated.

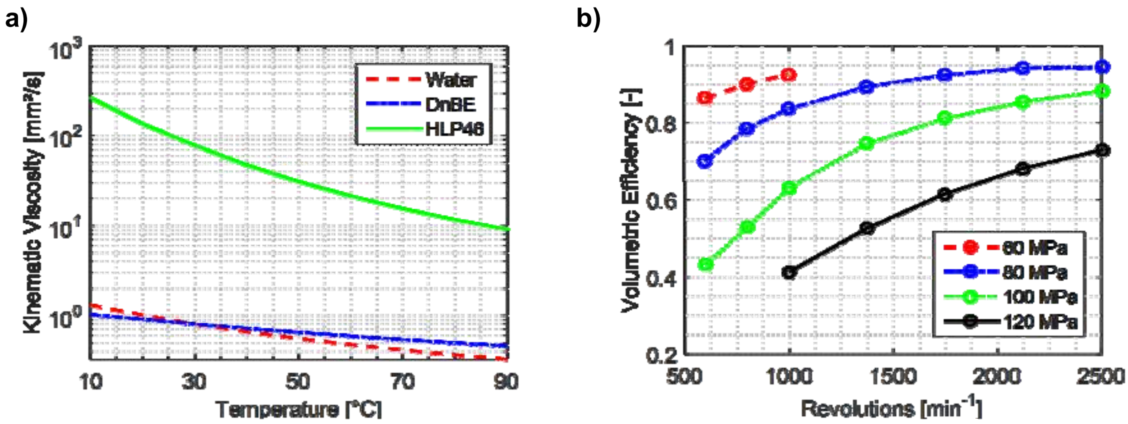

Fig. 1. a) Kinemtatic viscosity over temperature for Water, DnBE and HLP46; b) Volumetric efficiency of the BOSCH CP1 common-rail pump using DnBE

1.1 Hollow pistons in CI injection pumps

In todays common-rail injection systems, the components are developed and optimized for diesel fuel. This ensures an optimal overall system efficiency. Using different molecules with the same components can lead to reduced engine performance. In order to minimize necessary changes to the current engine design, every system component was investigated separately regarding its´ performance. High volumetric losses inside the injection pump made an adaption of the pump towards new fuel candidates essential. Due to high injection pressures of up to 300 MPa, material deformations play a major role for pump performance. Fig. 2 shows the deformation of a standard piston of a Bosch CP1 radial piston common-rail pump during operation at 135 MPa. At initial state, the gap height of the sealing gap is approximately 3 µm. On the left, the gap height between the piston and the bushing over the crankshaft-angle is shown. During the compression stroke, the pressure level rises, causing the piston to shrink, increasing the sealing gap between piston and bushing, ultimately resulting in a high leakage-rate.

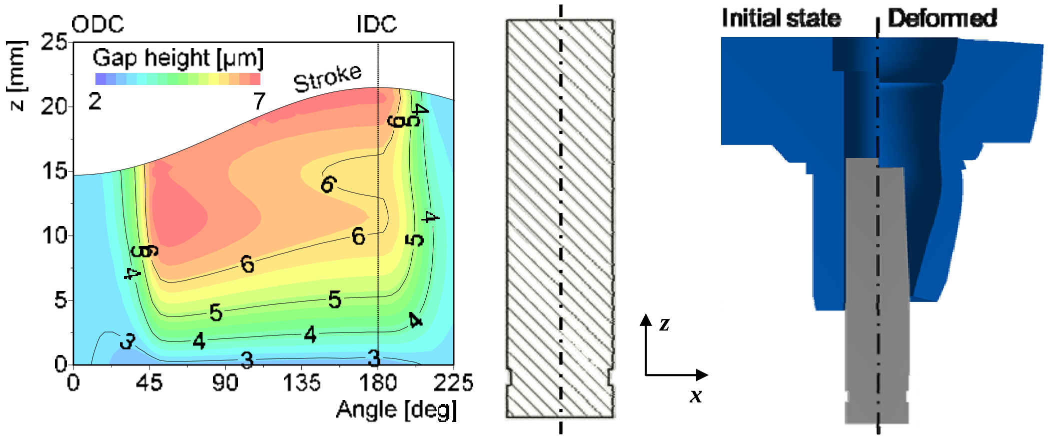

Fig. 2. Deformation of a standard piston inside a common-rail pump at 135 MPa

To reduce high volumetric losses of the injection pump, the hollow piston concept was proposed [3]. Here, the piston is hollow in the middle, see Fig. 3. The pressure within the piston equals the rail-pressure, causing a pressure difference between the piston inside and the sealing gap. The resulting deformation leads to an expansion of the piston diameter towards the bushing, see Fig. 3 right. The expansion results in a reduced gap height and therefore reduced leakage rate during the compression stroke, see Fig. 3 left in comparison with Fig. 2 left.

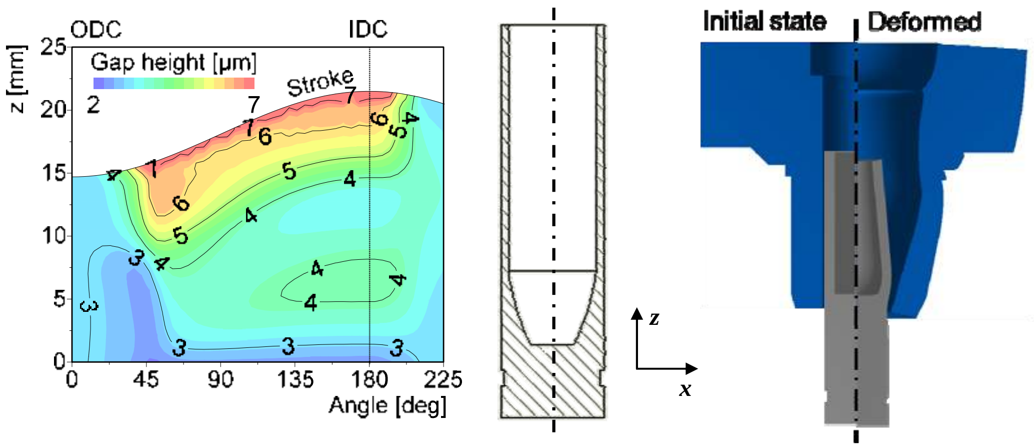

Fig. 3. Deformation of the hollow piston inside a common-rail pump at 135 MPa

The improvement of pump performance with hollow pistons of an exemplary design compared to standard pistons can be seen in Fig. 4. At 120 MPa, an increase in volumetric efficiency of up to 40 % compared to the standard piston was measured using DnBE [4].

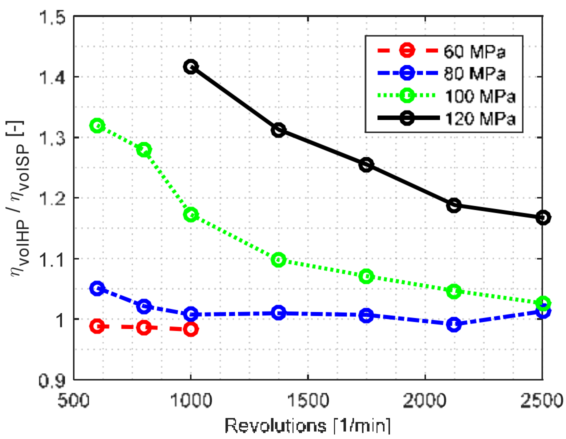

Fig. 4. Comparison of volumetric efficiencies of the standard piston (SP) and the hollow piston (HP)

1.2 Radial piston pumps in water hydraulics

The principle of radial piston pumps can also be found in water hydraulics. One advantage of radial piston pumps compared to axial piston pumps are the reduced lateral forces on the pistons. Therefore, the tendency towards an eccentricity between piston and bushing is reduced, increasing overall efficiency by reducing friction and leakage. Fig. 5 shows a cross-section of a Hauhinco RKP radial piston pump on the left [5]. The RKP pump series is check valve controlled with five or seven pistons. An eccentric drive-shaft rotates, causing the pistons to move up and down, compressing the fluid. Using high-grade steel, a separate lubrication system is avoided, with water being the lubricant. The sealing between piston and bushing is ensured through a sealing gap with no additional sealing elements. As a result, the geometric parameters of the piston-bushing contact are highly relevant, especially for volumetric losses. The right side of Fig. 5 shows a static performance diagram of a radial piston unit with a piston diameter of 30 mm. Volumetric losses cause a decrease of effective flowrate of up to 25 l/min translating into 13.3 kW additional power needed. Leakage between piston and bushing does account for parts of these losses as well as leakage through valves and housing.

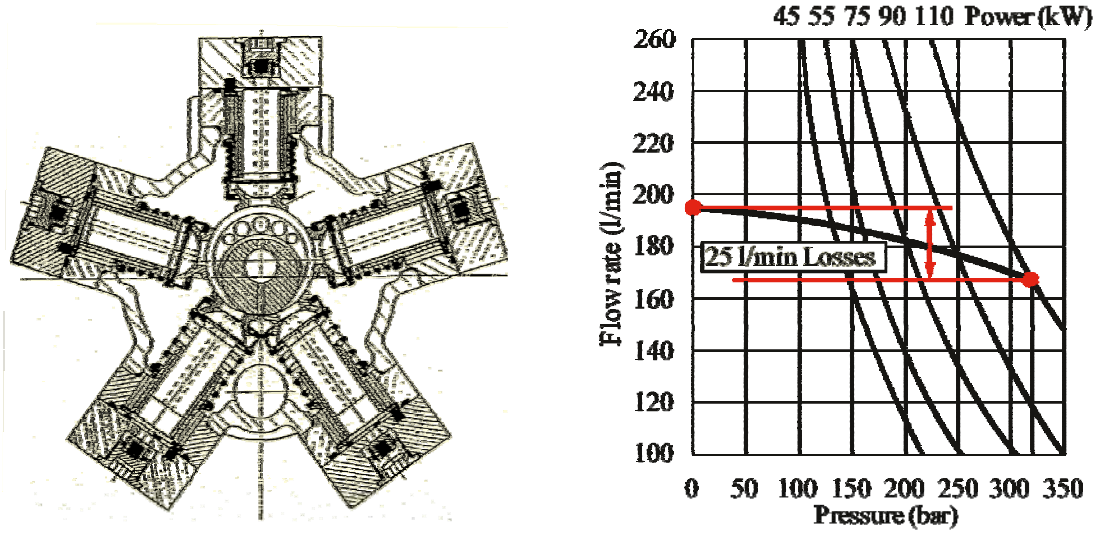

Fig. 5. Cross-section of a Hauhinco radial piston pump (left) and static performance diagram for a piston diameter of 30 mm (right) [5]

Another prominent pump principle used in water hydraulics is the axial piston pump, shown in Fig. 6 [5]. Here, hollow pistons are already in use, see enlargement of Fig. 6. The purpose of these pistons is a different one, though. With water being a relatively stiff fluid, hollow pistons increase the compression volume inside the piston chamber, therefore enhancing the controllability of the pump. Additionally, hollow pistons reduce the inertia, ensuring a more agile pump performance.

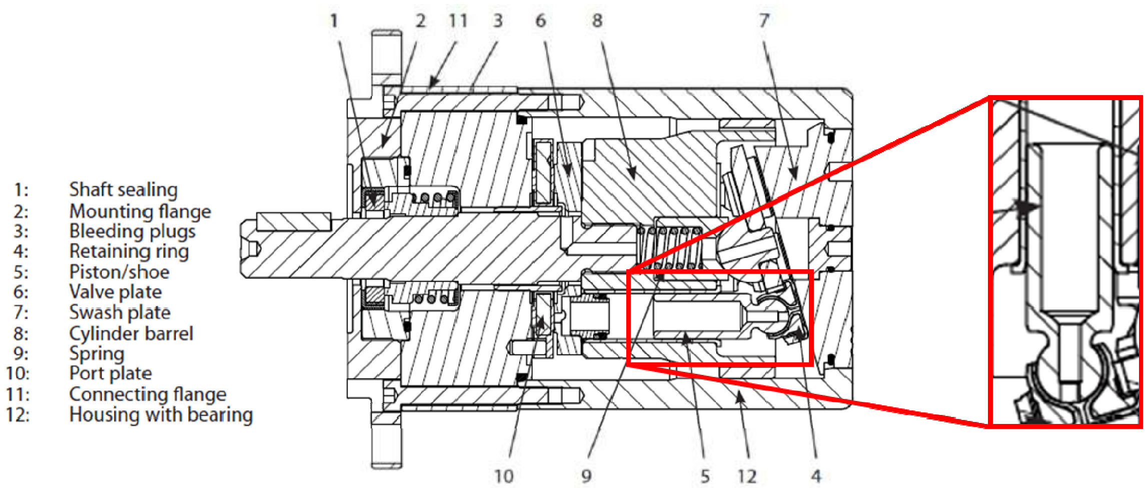

Fig. 6. Cross-section of Danfoss´s axial piston pump Nessie [5]

2. Application in water hydraulics

Looking at common-rail systems, the injection pressures go up to almost 300 MPa. Here, pressure induced deformation plays a significant role regarding the sealing gap between piston and bushing. In water hydraulics, however, pressure levels are usually in the range of up to 25 MPa. This poses the question whether the resulting forces on the piston are sufficient to cause relevant deformations. In water hydraulics, higher flow rates are needed than in fuel pumps. Therefore, the piston diameters are larger, e.g., 28 mm, see Fig. 7. It depicts the simplified piston geometry used in this work, with a stainless steel piston running inside a PEEK bushing. Piston and bushing are arranged concentrically to each other. Investigations on the performance are done at the outer dead center (ODC) where pressure and stress are at a maximum.

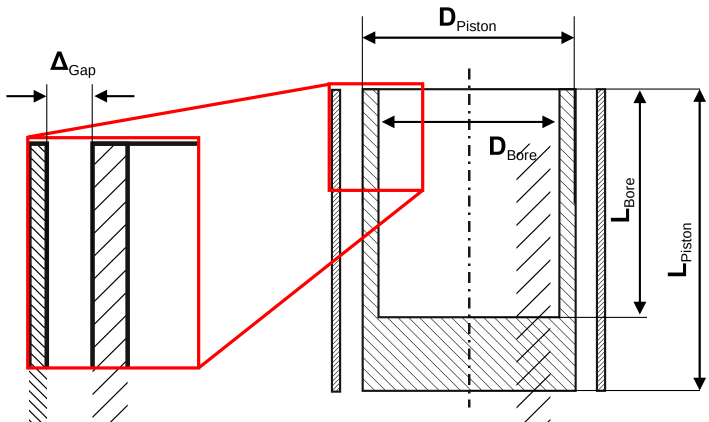

Parameter	Value
D_{Piston} [mm]	28
L_{Piston} [mm]	40
D_{Bore} [mm]	24
L_{Bore} [mm]	30
Δ_{Gap} [µm]	10

Fig. 7. Relevant geometric parameters for the hollow piston investigation

To evaluate the potential performance of hollow pistons in water hydraulics, two different design approaches were chosen, see Fig. 8. The first one being a bore inside the piston. This geometry can easily be manufactured by drilling. A possible downside to this design is the high mechanical stress at the bottom of the piston in the corners of the bore. This might lead to a material malfunction. As a second approach, the corners were adjusted by using splines. Manufacturing of such a geometry can also be done by drilling using an adapted drill. With the adjusted corners, stress is reduced significantly. This might lead to reduced deformations and therefore higher gap heights. In the following both design variations are investigated to compare the aforementioned advantages as well as the constraints.

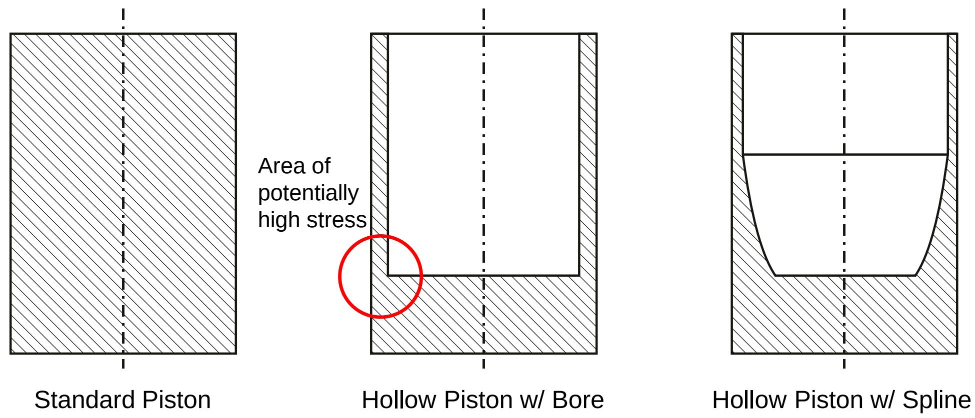

Fig. 8. Design approaches for hollow piston design

3. Simulation Approach

After the design process was done, an elasto-hydrodynamic (EHD) simulation was set up. Deformation and stress are calculated depending on the pressure (*f(p(x),σ*) using FEM. Afterwards, a hydraulic reynolds-simulation determines the resulting flow and pressure profile (*Q,p(x)*). Fig. 9 shows the general simulation approach. Boundary conditions are defined for the initial design. Here, material data, pressure profile for the initial load and other parameters are set. A FEM-simulation is conducted using Ansys mechanical. Piston as well as bushing are simulated at a temperature of 293 K. Afterwards the axial deformation is evaluated and the resulting gap between piston and bushing is calculated. The gap geometry is then transferred to a Reynolds-gap-simulation. With a known pressure at the start and the end of the gap, the pressure dependend flow and the resulting pressure profile are calculated. The new pressure profile then is put into the FEM-simulation as a new boundary condition and new deformations can be calculatet. This iteration process continues until there is no change in deformation, therefore converges to a constant value.

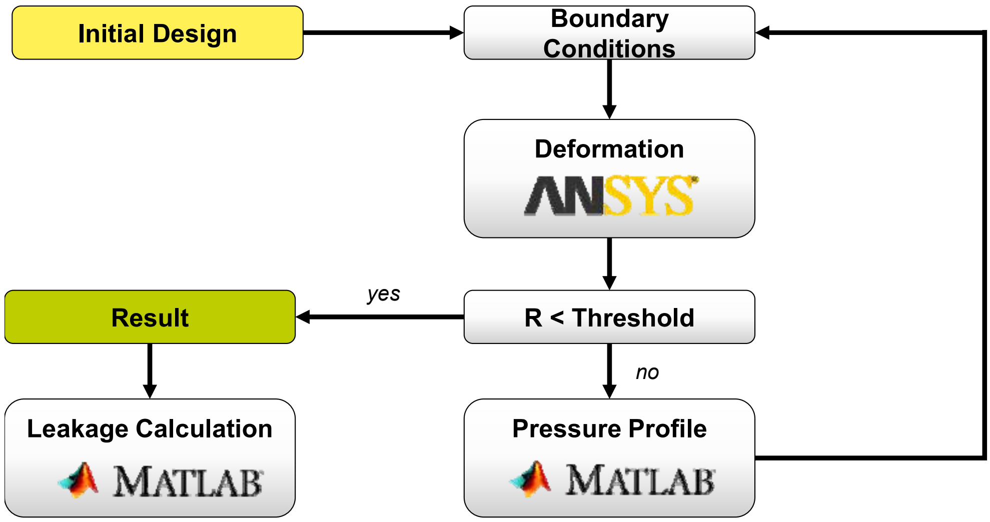

Fig. 9. Sequence diagram of the simulation process

The simulations were done using the simplified model of the piston-bushing contact shown in Fig. 7 for a static operation point at the outer dead center. Lateral forces on the piston were neglected and a concentric postion of the piston inside the bushing was asumed. This was done to get a first estimate on the achieveable improvements for comparable modes of operation. Real pump operation introduces lateral forces on the piston, causing increased wear on the one hand, and tilting and eccentricity of the piston, possibly leading to a significant increase in leakage flow between piston and bushing [6] on the other.
The convergence for the hollow piston simulation is shown in Fig. 10. Here, the maximum deformation is plotted over the position of the peak along the piston length represented in the node number. The graph shows that it takes approximately eleven iterations to reach a converged solution. For all the simulations, an investigation on the convergence was done to ensure reliable results.

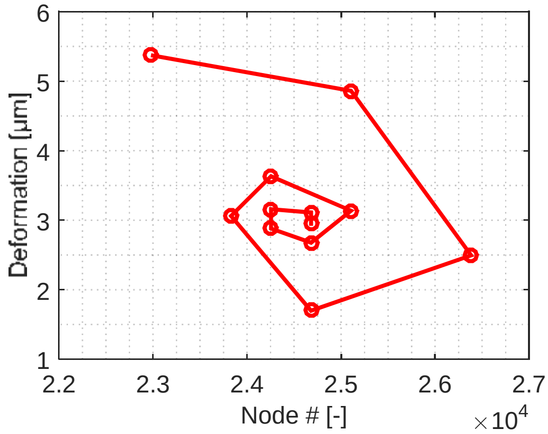

Fig. 10. Convergence graph for the hollow piston: Maximum deformation over the location on the piston

4. Results

After achieving convergence for all simulation models, the different piston designs were evaluated regarding the deformation, the resulting gap height, leakage flow and resulting mechanical stress. Fig. 11 shows the deformation of the hollow piston with bore on the left. Even though the pressure level was set to 25 MPa, significant deformations can be observed with values up to almost 3 µm towards the bushing. The sealing gap between piston and bushing is shown on the right of Fig. 11 with the pressure displayed at the top and the bottom of the gap. The mean gap width is 8.78 µm compared to 10 µm at the initial state (p=0 MPa) at inner dead center (IDC). This results in a leakage rate of 0.1401 l/min.

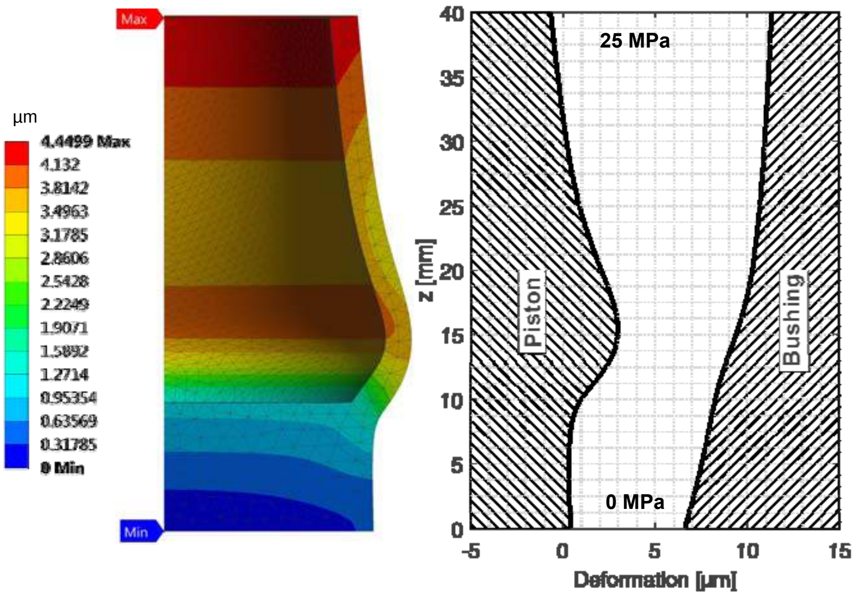

Fig. 11. Deformation and resulting gap geometry of the hollow piston with bore

The sealing gaps for the standard piston and the hollow piston with spline are shown in Fig. 12. For the standard piston, the mean gap height is 9.93 µm and 8.90 µm for the hollow piston with spline. This results in leakage flows of 0.2244 l/min and 0.1626 l/min respectively.

ISSN 1454 - 8003
Proceedings of 2017 International Conference on Hydraulics and Pneumatics - HERVEX
November 8-10, Băile Govora, Romania

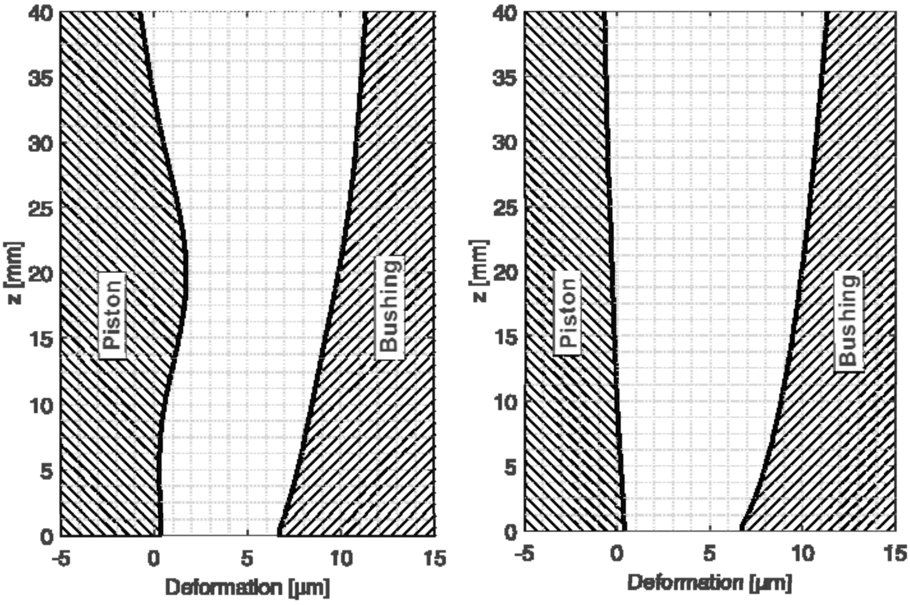

Fig. 12. Deformation and gap geometry of the standard piston (left) and the hollow piston with spline (right)

Table 1: Simulation results for different piston geometries

Pairing	$\Delta Piston_{max}$ [µm]	ΔGap_{mean} [µm]	ΔLeakage [l/min]	Mises stress [MPa]
Standard Piston – Bushing (SP)	-0.71	9.93	0.2244	-
Hollow piston with bore – Bushing (HP_B)	2.95	8.78	0.1401	76
Hollow piston with spline – Bushing (HP_S)	1.73	8.90	0.1626	48

With the simulated leakage rates at 25 MPa, the power loss can be calculated for all three piston designs. Fig. 13 shows the power loss in kW per piston caused by leakage at the outer dead center. The standard piston has a power loss of almost 1 kW compared to 0.68 kW for the hollow piston with spline and 0.58 kW for the hollow piston with bore. This leads to potential savings of 27.5% and 37.6% respectively at the static point investigated.

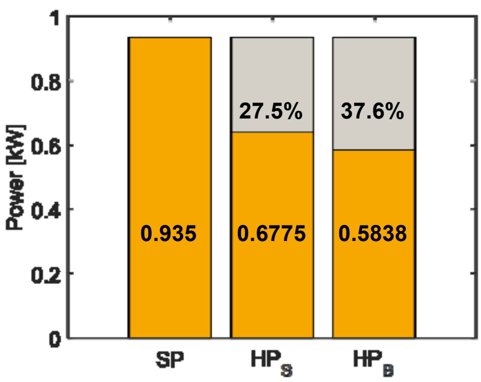

Fig. 13. Comparison of power losses caused by leakage (from left to right): Standard piston (SP), hollow piston w/ spline (HP_S), hollow piston w/ bore (HP_B)

In order to evaluate the mechanical stress on both hollow piston designs the von Mises yield criterion was applied using Ansys mechanical data, see Table 1. As expected, the hollow piston with bore shows the highest stress level at the bottom of the bore with 76 MPa. With the introduction of a spline, the maximum stress is located at the position of maximum deformation with 48 MPa. A stress reduction of almost 40% can be achieved by adding a spline to the bottom of the bore.
Fig. 14 shows a Wöhler-graph for type 316L stainless steel. In order to exceed the fatigue-limit, a specimen has to last 10^7 load-cycles. The stress at which the specimen reaches the limit indicates the stress level fit for durability. For a stress ratio of -0.2, representing alternating strain, the value is approximately 265 MPa [7]. Both of the hollow piston designs are well below that limit with a safety factor of at least 3.

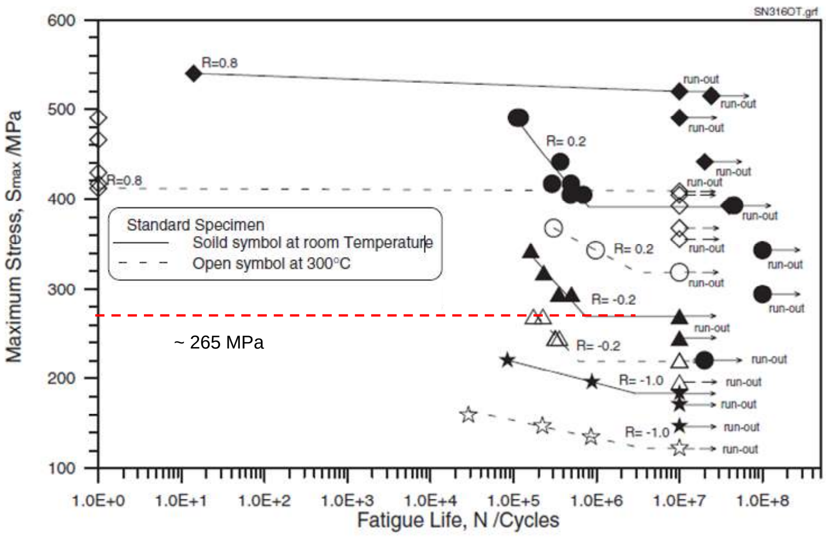

Fig. 14. Wöhler-graph for type 316L steel [7]

5. Conclusion and Outlook

In this paper, a first simulative investigation is done for the use of hollow pistons in water hydraulics to reduce the volumetric losses inside a radial piston pump. First, the knowledge of this principle is transferred from measurements on common-rail injection pumps to water hydraulics. Based on the results, two design concepts for hollow pistons in water hydraulics are derived. The concepts are simulated using Ansys and Matlab to calculate deformation and the resulting leakage flow. Afterwards the results are compared regarding the potential savings in power losses and the mechanical stress on the hollow pistons.
The results indicate a significant saving potential for both the hollow piston with bore and the hollow piston with spline with savings of up to 37.6% and 27.5% for the simulated static operation point. Additionally, the resulting stress through deformation for both designs is below the durability limit. Thus, both variants are suited for pump operation.
Hollow pistons for increasing volumetric efficiencies do show great potential. To evaluate the full potential, a transient investigation on the saving potentials has to be performed. Afterwards, a first test can provide proof of concept. In the end, an analysis on the manufacturing cost compared to the saving potential has to be carried out to ensure added value.

Acknowledgments

This work was performed as part of the Cluster of Excellence "Tailor-Made Fuels from Biomass", which is funded by the Excellence Initiative by the German federal and state governments to promote science and research at German universities.

References

[1] Weinebeck, A., et al., 2014. "Tribological Investigations of new biofuel blends", 19th International Colloquium Tribology, Technische Akademie Esslingen, Tribology - industrial and automotive lubrication, Stuttgart/Ostfildern, Germany;

[2] Rückert, M., et al., 2017. "Holistic investigation of a 50/50 DnBE - 1-octanol blend regarding the complete injection system", 5th International Conference Tailor-Made Fuels - From Production to Propulsion , Aachen , Germany;

[3] Heitzig, S., et al., 2015. "Efficiency Improvement of Common-Rail Pumps by Gap Compensation based on Hollow Pistons", Proceedings of the ASME/BATH 2015 Symposium on Fluid Power and Motion Control, FPMC2015-9528, Chicago, USA;

[4] Rückert, M., et al., 2017. "Influence of a new hollow piston design on volumetric losses of a common-rail pump", Proceedings of the ASME/BATH 2017 Symposium on Fluid Power and Motion Control, FPMC2017-4231, Chicago, USA – SUBMITTED as of 31.07.2017;

[5] Trostmann, E., 1996. "Water Hydraulics Control Technology", 1st Edition, Marcel Dekker, Inc., New York, USA;

[6] Irving, J. B., 1972. "The effect of nonvertical alignment on the performance of a falling-cylinder viscometer", Journal of Physics D: Applied Physics, Vol.5;

[7] Huang, J.Y., 2006. "High-Cycle Fatigue Behaviour of Type 316L Stainless Steel", Materials Transactions, Vol. 47, pp. 409-417.

ISSN 1454 - 8003
Proceedings of 2017 International Conference on Hydraulics and Pneumatics - HERVEX
November 8-10, Băile Govora, Romania

INVESTIGATIONS ON THE RHEOLOGY OF ADDITIVATED HYDRAULIC OILS

Alexandru Valentin RADULESCU[1], Irina RADULESCU[1]

[1]University POLITEHNICA of Bucharest, e-mail address: varrav2000@yahoo.com

Abstract: *The purpose of this paper is to characterize the rheological behavior of the hydraulic oils additivated with viscosity index improvers. This type of lubricants exhibits typical non-Newtonian properties, depending on the concentration of additives. The samples have been tested on a Brookfield rheometer, with a cone and plate geometry, by measuring the variation shear stress versus shear rate. Finally, the rheological parameters of the lubricant have been determined, according to different rheological models.*

Keywords: *Rheology, hydraulic oil, experiment*

1. Introduction

The primary purpose of hydraulic oils is to transfer the potential or kinetic energy, to create volume flow between pump and hydrostatic motor and to reduce the friction and wear between moving parts. In addition, they protect the system from corrosion and help carry away the heat produced during energy transformation [1, 2].
Generally, the rheological properties of hydraulic oils depend on many factors that include temperature, shear rate, concentration, time, pressure, chemical properties and additives [3, 4]. Most of the researches focusing on the effects of temperature, shear rate, concentration and pressure. However, it is normally found that the effect of temperature is much more apparent on the fluid viscosity.
It is known that additives of different types are added to improve the properties of lubricants in almost all types of oils. In the case of hydraulic oils with viscosity index enhancers (long chain polymers and high molecular weight polymers), the resulting fluid exhibit non - Newtonian properties [5, 6].
The aim of this paper is to characterize the rheological behavior of the hydraulic oils additivated with viscosity index improvers. The lubricant being tested is a general purpose hydraulic oil suitable for lubrication of lightly loaded units in machines and installations with flow and circulation systems [7]. This type of oil is produced from specially selected high-grade selective and hydro-refined naphthenic, paraffin-naphthenic base fractions.
The additive used as a viscosity index enhancer is based on polybutene, which is a synthetic transparent liquid polymer obtained by the selective polymerization process of isobutylene containing in the butane-butane stream. The main properties of the additive are: solubility in oils, nontoxicity, thermal stability and high anticorrosion properties [8]. The physical and chemical properties of the base hydraulic oil and additive are presented in Table 1 [7, 8].

Table 1: Physical and chemical properties of the hydraulic oil and additive

Characteristic parameter	Hydraulic oil	Additive
Density at 15°C	900 kg/m^3	887 kg/m^3
Viscosity at 40°C	41.4 – 50.6 cSt	-
Viscosity at 100°C	24.2 – 31.4 cSt	580 – 660 cSt
Viscosity Index	92	-
Viscosity CCS at 30°C	5500 cP	-
Pour point	-25° C	-67° C

Characteristic parameter	Hydraulic oil	Additive
Flash point COC	200° C	170° C
TBN	9.4 mg KOH/g	-
Water (ppm)	-	70
Volatile factions	10 %	-
Viscosity HTHS (150°C)	3.3 cP	-
Molecular weight (g/mol)	-	1300
Colour (ASTM)	L 3.5	15

2. Experimental stand and methodology

The measurements were carried out on a Brookfield rotating viscometer CAP 2000+. Brookfield Viscometers (Amettek, USA) are included in a large number of international standards. All their laboratory viscometers have an accuracy of not less than the entire scale of ± 1,0% and a reproducibility of not less than 0,2% [9]. CAP 2000+ viscometer series (Figure 1) are medium to high deformation tools and operate according to the scheme cone - plate. With this apparatus, the cone angle provides a constant speed of deformation of the fluid placed between the two elements of the device: the rotating element (cone) and the fixed one (stationary plate).

Fig. 1. Brookfield cone-plate viscometer

The measurement range the viscosity depends on the angular velocity and the shape and size of the cone used. The minimum range is from 0.02 Pa.s and reaches 1500 Pa.s, the rotation speed is in range from 5 to 1000 rpm and the shear rate of 10 to 13000 s^{-1}, respectively. The necessary sample volume is in the range of 0.5 to 2 ml. The viscometer has ports for turning on a computer and a printer.
The advantages of the viscometer include built-in temperature control (from 5 ^{0}C to 75 ^{0}C) of the sample, easy adjustment and cleaning, small sample volume, automatically computer controlled software. The Capcalc 32 software allows automated testing, recording and storage of experimental data (up to 1000 data points for test). The data can be visualized graphically, allowing the software to be built several comparative graphs simultaneously. Several mathematical features are embedded in the software models for rapid and easy analysis of rheological fluid behavior.
The hydraulic oil was tested in pure state (0% of additive) and in modified state (five different concentrations of additive: 1%, 2%, 3%, 4% and 5%). To determine the lubricant rheological model in pure and modified state (with additive), it was used an “imposed velocity gradient” test, with the variation limits 1333 ... 13333 s^{-1} and 20^{0}C reference temperature. The tests were carried out with a load up to 13333 s^{-1} and unloading up to 1333 s^{-1}, in order to highlight the effects of lubricant thixotropy.

There were calculated the lubricant rheological parameters, using the regression analysis method with MathCAD software, according to three different rheological model:

- Newtonian model: $$\tau = \eta \frac{du}{dy} \quad (1),$$

  where: τ - shear stress

  $\frac{du}{dy}$ - shear rate

  η - viscosity

- Power law model: $$\tau = m\left(\frac{du}{dy}\right)^n \quad (2),$$

  where: τ - shear stress

  $\frac{du}{dy}$ - shear rate

  m - consistency index (which is equivalent to the Newtonian fluid viscosity)

  n - flow index (equal to 1 if the fluid is Newtonian).

- Rabinowitsch model: $$\tau + k\tau^3 = \eta \frac{du}{dy} \quad (3),$$

  where: τ - shear stress

  $\frac{du}{dy}$ - shear rate

  k – coefficient of pseudo-plasticity (equal to 0 if the fluid is Newtonian)

  η - viscosity

3. Results and discussions

The results refer to experimentally obtained dependencies for the influence of the shear rate on the shear stress and viscosity of the investigated hydraulic oil with additive. Part of the results relate to the impact of the concentration of the additive on the investigated physical properties of the lubricants, as well as the influence of time factor. The work does not take into account thermal effects on the rheological characteristics of the hydraulic oil, the results presented referring to the isothermal mode at 20 ^{0}C.

Figure 2 a and b present rheograms that provide a relationship between the shear rate and shear stress for hydraulic oil in pure state (0% of additive) and in modified state (five different concentrations of additive: 1%, 2%, 3%, 4% and 5%). From these diagrams, it can be seen that when loaded to maximum shear rate and unloading to the initial one, are observed non-matching ascending and descending parts of the rheogram. This shows that the hydraulic oil with different concentration of additives have typical thixotropic properties.

Figure 2 gives also information about the hysteresis of the hydraulic fluid with additive. It can observe that the hysteresis disappears at approx. 7000 s^{-1}, representing about 55% of the total range of shear rate.

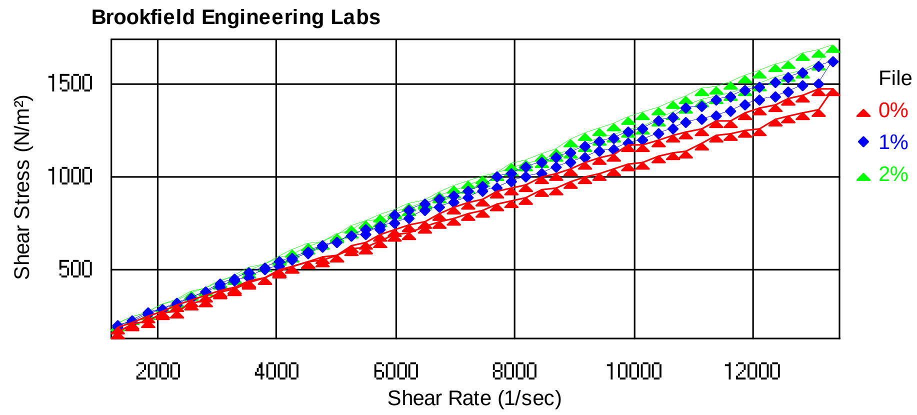

a) Additive: 0%, 1% and 2%

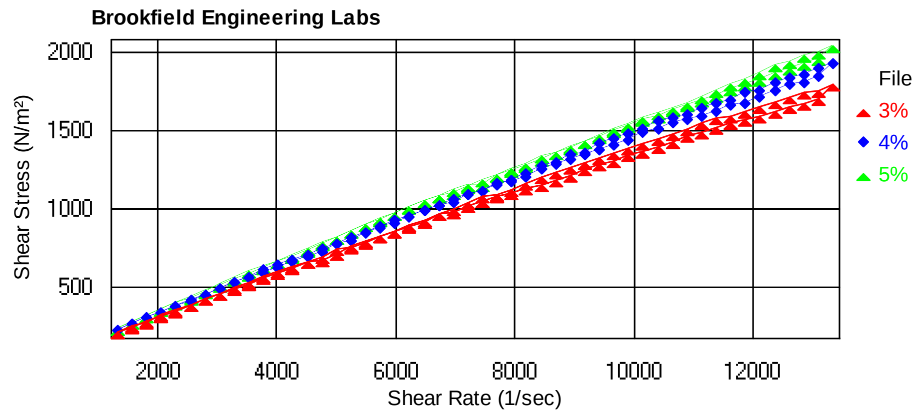

b) Additive: 3%, 4% and 5%

Fig. 2. Rheograms for hydraulic oil in pure and modified state

Table 2 presents the rheological parameters obtained by regression analysis method, corresponding to rheological models Newtonian, power law and Rabinowitsch.

Table 2: Rheological parameters of the investigated fluid

Additive, %	Newtonian model		Power law model			Rabinowitsch model		
	η, Pa·s	Corr. coeff.	m, Pa·s^{-n}	n	Corr. coeff.	k, Pa^{-2}	η, Pa·s	Corr. coeff.
0	0.112	98.6%	0.279	0.900	97%	$4.60 \cdot 10^{-8}$	0.119	99.6%
1	0.123	99%	0,276	0.911	98%	$4.38 \cdot 10^{-8}$	0.131	99.8%
2	0.129	99.2%	0.289	0.912	98.4%	$3.83 \cdot 10^{-8}$	0.139	99.8%
3	0.138	99.3%	0.295	0.917	98.7%	$3.69 \cdot 10^{-8}$	0.148	99.9%
4	0.147	99.5%	0.300	0.922	99.1%	$2.83 \cdot 10^{-8}$	0.157	99.9%
5	0.156	99.6%	0.304	0.927	99.3%	$2.37 \cdot 10^{-8}$	0.165	100%

Analyzing the values presented in Table 2, it can observe that the greatest values of the correlation coefficient are obtained in the case of Rabinowitsch model. In this way, it results that the rheological model that best approximates the behavior of the analyzed hydraulic fluid is the Rabinowitsch model.

Therefore, the variation of the rheological parameters versus concentration of the additive is presented only for the Rabinowitsch model: viscosity in Figure 3 and pseudoplastic coefficient in Figure 4.

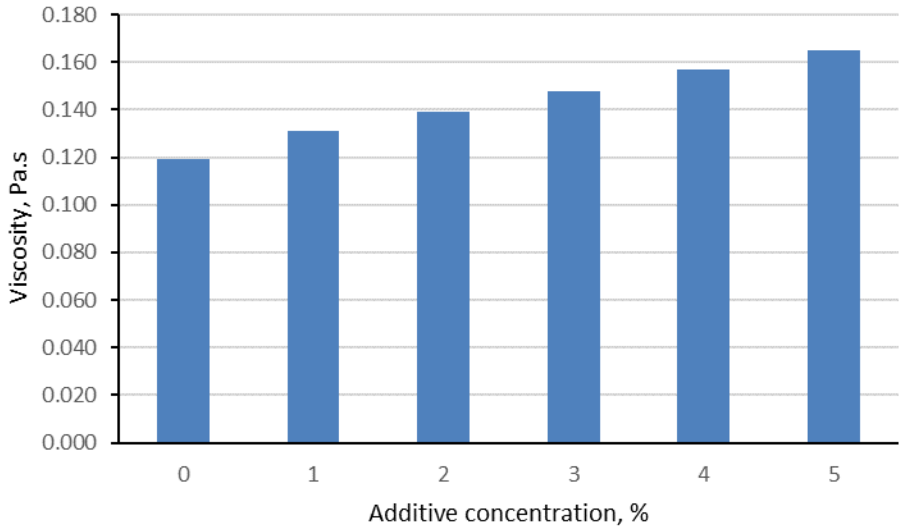

Fig. 3. Variation of the viscosity of hydraulic fluid with the additive concentration

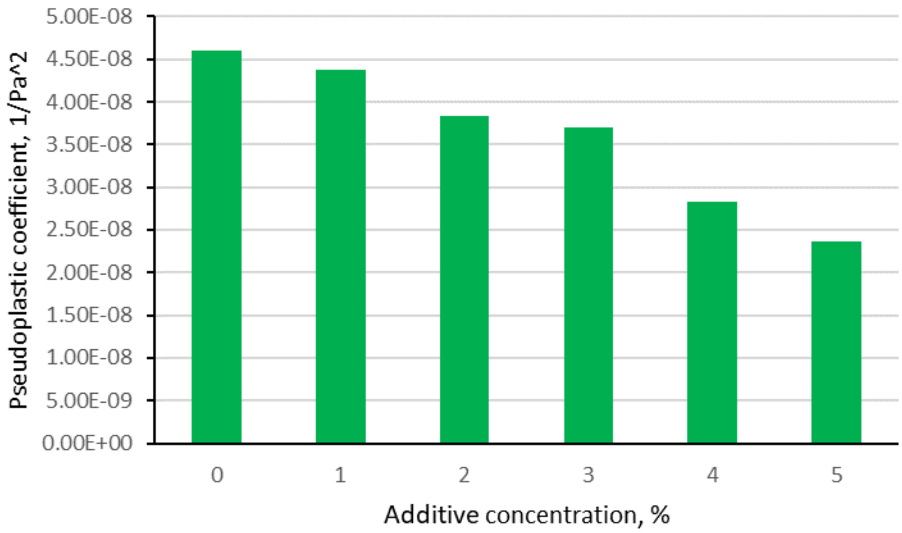

Fig. 4. Variation of the pseudoplastic coefficient with the additive concentration

Analyzing Figures 3 and 4, it is clearly observed that the viscosity increases with the increase of additive concentration, while the pseudoplastic coefficient decrease with the same concentration of additive.

4. Conclusions

An experimental study was performed in order to characterize the rheological behavior of the hydraulic oils additivated with viscosity index improvers.
The graphical dependencies for the shear stress versus shear rate as well as the viscosity and pseudoplastic coefficient function of the additive concentration are presented.
Experimental tests showed the lubricant thixotropy, at high shear rates, which is present for the hydraulic oil in pure and modified state.
The investigated hydraulic oil with additive has pseudoplastic fluid behavior and it is described with high accuracy by the Rabinowitsch model.
The increasing of the concentration of the incorporated additive results in an increase in viscosity and a decrease of the pseudoplastic coefficient.

References

[1] W. D. Philips, J. W. G. Staniewski, “The origin, measurement and control of fine particles in non-aqueous hydraulic fluids and their effect on fluid and system performance”, Lubrication Science, Vol. 28, pp. 43-64, 2016;
[2] J. Rensselar, “Hydraulic fluid efficiency in construction equipment”, Tribology and Lubrication Technology, June, pp. 59-66, 2015;
[3] V. J. Fernandes, I. M. Santos, “Thermoanalytical and Rheological Characterization of Automotive Mineral Lubricants After Thermal Degradation”, Fuel, Vol. 3, pp. 2393-2399, 2004;
[4] S. Bair, M. Khonsari, W. O. Winer, “High-pressure Rheology of Lubricants and Limitations of the Reynolds Equation”, Tribology International, Vol. 31, No. 10, pp. 573-586, 1998;
[5] H. A. Barnes, J. F. Hutton, K. Walters, “An introduction to rheology”, Elsevier, Amsterdam, 1997;
[6] G. W. Stachowiak, A. W. Batchelor, “Engineering tribology”, 2 Ed., Butterworth-Heinemann, USA, 2001;
[7] http://www.icerp.ro/fise/Lubricerp/Uleiuri%20industriale/H_15-100A.pdf ;
[8] https://www.kematbelgium.com/PDFs/KEMAT_Polybut_30_DataSheet_EN.pdf ;
[9] http://www.brookfieldengineering.com/-/media/ametekbrookfield/manuals/lab%20viscometers/cap2000%20instructions.pdf?la=en.

ISSN 1454 - 8003
Proceedings of 2017 International Conference on Hydraulics and Pneumatics - HERVEX
November 8-10, Băile Govora, Romania

INVESTIGATION OF A DIGITAL VALVE SYSTEM EFFICIENCY FOR METERING-IN SPEED CONTROL USING MATLAB/SIMULINK

Essam ELSAED[1], Mohamed ABDELAZIZ[1], Nabil A. MAHMOUD[1]

[1] Faculty of Engineering - Ain Shams University, Egypt;

essam.elsaed@eng.asu.edu.eg, mohamed_abdelaziz@eng.asu.edu.eg, nabil_mahmoud@eng.asu.edu.eg

Abstract: *For a long time, servo and proportional valves have ruled in the flow control field. Since the nearly past decade a new method titled "Digital Valve System" has strived in this area, and has proven some advantages over the elderly valves. The importance of this technique rises because of the inability of analog valves to fulfill fault tolerance, energy efficiency, and manufacture standardization. Also, Digital hydraulics concept has the possibility to be extended to replace traditional pumps, accumulators, transformers, motors and many various valves. Moreover, it manages to raid not only the hydraulic field but also water and pneumatic power systems with acceptable results, when compared to the analog valves.*
The digital valve system utilizes a pack of simple 2/2 on/off valves to compete versus the analog valves. The Digital Valve Unit (DVU) is composed of parallel connected on/off valves with a common input and common output ports; and the output flow has discrete values. To determine the flow rate of each valve in the Digital Valve Unit (DVU), a Pulse Code Modulation (PCM) scheme was chosen, in which the valves flow rates have discrete values and can be presented as a geometric sequence with common ratio two. This paper studies the Feasibility of metering-in speed control using digital valve system. Through the paper, four cases modeled to describe and evaluate DVS: an ideal case with four and five valves, a near real case with four valves and a particular comparative case of an analog valve. A simple open-loop controller is used for the speed control in case of DVU using Simulink and Stateflow, while with the proportional valve a closed-loop controller is used.
The results indicated the possibility to regulate the flow rate in the hydraulic circuit using Digital Unit instead of an analog proportional valve, with a dropping of 93% in energy consumption when compared against a two-way proportional valve. The high efficiency is owing to the lower differential pressure in DVU than with the two-way proportional valve. On the other side, the results show high-pressure peaks with DVU which needs further study.
The theory has advantages of high linearity, low hysteresis, less pressure drop at small flow rates, and fault tolerance. The biggest challenges related to DVU can be summarized to a great package size and valve states uncertainty.

Keywords*: Digital valve system, MATLAB Simscape, tracking control, digital hydraulics, pulse code modulation*

1. Introduction

The traditional way of controlling actuator operational speed can be abridged in two primary methods. First: a fixed displacement fixed speed pump controls many actuators. Unemployed fluid flows to the tank through a relief valve. The required flow by any single actuator is lower than the pump outlet; therefore, a restriction device is needed to bind the flow for every single actuator [1]. In fact, this method contributes to a considerable energy loss. Another issue is when an actuator requires varying speeds during operation; these pumps need to be sized to supply the highest flow needed. But unfortunately, when low speed is required, the excess flow delivered from these pumps must be leaking via the exhaust valve at maximum system pressure. This process results in converting the unwanted energy into heat; So, fixed displacement pumps should only be employed in constant speed applications, or in circuits where speed control is of very short duration [2].
Second: another flow control method is by using pump control; where the flow is controlled either by changing the pump drive speed, or by modifying the pump displacement, or both. Its main advantage is dropping hydraulic throttling losses via operating the pump at lower pressure, which can lower the overall power consumption; However, pump control decreases the system

responsiveness and bandwidths needed for critical applications —for example closed-loop position control circuits— because pumps do not ensure the requisite frequency response. While valves can reach into the 150 to 200 Hz frequency responses [3]. Moreover, servo valves can reach to 400Hz [4], whereas the fastest pump frequency response is a small fraction of that.
A new parallel way has proposed and started by Linjama to solve the previously mentioned problems, the concept called Digital Fluid Power (DFP), it replaces the traditional analog devices of the fluid circuit by digital ones [5]. The roots of Digital Fluid Control go back to 1961, which invented by BOWER [6].
A digital system can comprise a digital accumulator, digital supply units, digital cylinder, and digital control valves [7]. Taking a traditional variable flow control valve for demonstrating; in the digital world, the analog valve is replaced by a group of on/off valves, which have several flow rates at similar pressure drop relative to the coding method. These valves have two states either on or off; therefore, the flow output has discrete steps. So, for low desired speeds operate the valve with small flow rate, and for high speeds open more valves.
Digital valves could also refer to Switching valves in which a variable rate capability can be attained by varying the duty cycle [8-10]. The clearest distinction between Digital valves and switching valves is the former needs many parallel valves, but the latter requires only one valve for flow control. The drawbacks of using these switching valves are the necessity of a robust valve owing to the tremendous frequency switching, and the need for a damping device [11, 12].
To determine the flow rate of each valve in the Digital Valve Unit (DVU) various schematic coding can be chosen, for example, Pulse Code Modulation (PCM) (1Q, 2Q, 4Q…) and Pulse Number Modulation (PNM) (1Q, 1Q, 1Q…). PCM is superior over PNM in the capability of having higher resolution with less number of valves; unfortunately, the former suffers from transient uncertainty. An in-depth evaluation is presented in [12]. The designers should select the code suitable for their application. PCM of three parallel flow lines is described through Figure 1. The equivalent proportional control valve is shown in Figure 2.

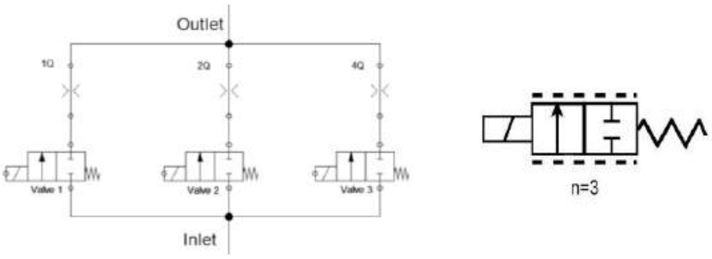

0: closed valve, 1: open valve			Outlet Flow
V 1 (1Q)	V 2 (2Q)	V 3 (4Q)	(ΣQ)
0	0	0	0
1	0	0	1
0	1	0	2
1	1	0	3
0	0	1	4
1	0	1	5
0	1	1	6
1	1	1	7

(a) **(b)** **(c)**

Fig. 1. (a) DVU of three on/off valves. (b) DVU simplified symbol. (c) Corresponding flow rates

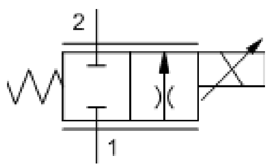

Fig. 2. Two-way electro-proportional flow control valve.

It should be mentioned that DVU is not only limited to replacing the traditional 2-way proportional valves, but it extends to cover many types of valves. Various applications were performed using DVU are shown in [13-15].
Although DFP extends back to 1960's era, it's considered a recent study; as serious researches have been carrying out since the past decade. On the other hand, electrohydraulic servo valves were invented at the end of 1930 as high technology, although the high cost, a solution to accurate motion control was needed. In 1980 proportional valves were presented as a practical and

reasonably priced alternative to servo valves [16]. Till now these valves have dominated over the field of flow control although their faults.
Another aspect considering the future of fluid power in Industry Revolution 4.0 —shorted to I4.0— was studied by Brandstetter et al. [17], via classifying the industrial revolutions into four sections, starting from mechanization (I1.0), electrification (I2.0), and digitalization (I3.0) till connection/Internet revolution (I4.0). Unfortunately, the fluid power currently is still struggling in the I3.0 Industry. This paper takes the path to put a step in the I4.0. Which characterizes by I) Reduction in unit cost by standardization of the components. II) Connecting fluid components to cyber-physical systems, so alive remote access to all system data enables much easier technical support. III) Finally running the valve group by only editing a few commands in the valve software, with no need for replacing a valve when requiring a different task —which decreases resource waste [18].
Continuing on the research studied by Linjama in the field of Digital Valve System (DVS). This paper will review the strength and weaknesses points of using DVU over proportional valve. A selected case of low flow rates and relatively small loads was chosen for investigation.
The paper is divided into three main parts: 1) Modeling and simulation of DVU using MATLAB Simscape Fluids. 2) Velocity control of a hydraulic cylinder using DVU. 3) Performance Comparison between DVU and 2/2 electro-proportional valve.

2. Modeling and Simulation of DVU

2.1 System Overview

The existing below components are founded on real ones, in which experimental validation will be investigated in a future research work. The system comprises a supply unit with DVU of 4 on/off solenoid operated valves against a maximum load of 1000 N. The used code is PCM as a result of its compact size and acceptable flow steps. The velocity output has 15 steps starting from 1 to 15 l/min. Note that in the case of PNM coding, 15 valves are needed with 1 l/min output flow from each valve, to achieve the same purpose.

2.2 System components

The used software is Simscape Fluids, which provides components library for simulating fluid circuits. To solve the Differential Equations in the model, MATLAB recommends ode15s and ode23t for Simscape hydraulic models [19]. In this model, ode15s was selected for higher accuracy [20]. The hydraulic circuit model is shown in Figure 3. The system components are:

- Induction motor and variable displacement pump blocks were selected. The Pump performance curve provides data at 1800; however, the available motor has a rated speed of 1410 rpm, without the need to use affinity laws. Coupling the motor and pump using Simscape provides the value of pump max delivery 19.3 l/min when limiting the pump differential pressure to 20 bar and loading the cylinder with 1000 N. As only the desired flow goes through the DVU is a fraction of this value, so the excess flow is dumped into the tank.
- Electric Motor. A single-phase induction motor with a rated speed of 1410 rpm and 1.5 KW rated power.
- Pump. A variable displacement pump (HYDURA PVQ-06); the pump swash plate angle is stationary at a max delivery of 0.0139 l/rev, the rated speed of the pump is 1800 rpm.
- DVU. Digital valve system can consist of more than one DVU, here one DVU of four valves (Sun Hydraulics-DTDB-XCN) is used [21]. DVU is shown in Figure 4.
- Orifices. Over each 2/2 valve, an orifice is positioned, the orifices used were selected from Hydra Force company have diameters (0.85, 1.3, 1.8, and 2.5) mm, with output flow rates (0.9, 2.2, 4.3 and 8) l/min at the operational pressure [22]. The flow was supposed to be perfectly binary formulated (1, 2, 4, and 8) l/min, but due to the requirements of a high precision diameters values, the mentioned diameters were accepted.

- 4/3 valve. A PONAR (4WE6 E-12/G24 N Z4) spool valve with tandem center [23]. The valve has a small pressure drop of 2 bar at 15 l/min. A better choice is to select a closed center valve with a variable pressure compensated pump, then vary the swash plate angle according to the pressure. But valve and pump bandwidth should be considered when designing this circuit. [24]. Also, the valve response time was disregarded. Here the paper focuses only on flow control using valve digitalized method, and the valve is mainly needed to retract the actuator.
- Actuator. (ϕ32/22—250) mm Cylinder, with a maximum pressure of 100 bar.
- Relief valve. A (VMDR40) relief valve with max pressure set to 20 bar, at this pressure the relief valve can handle 40 l/min flow rate [25].
- Sensors. LVT position sensor is used for circuit operation. A pressure transducer and flow meter sensors are used only for setting up the circuit.

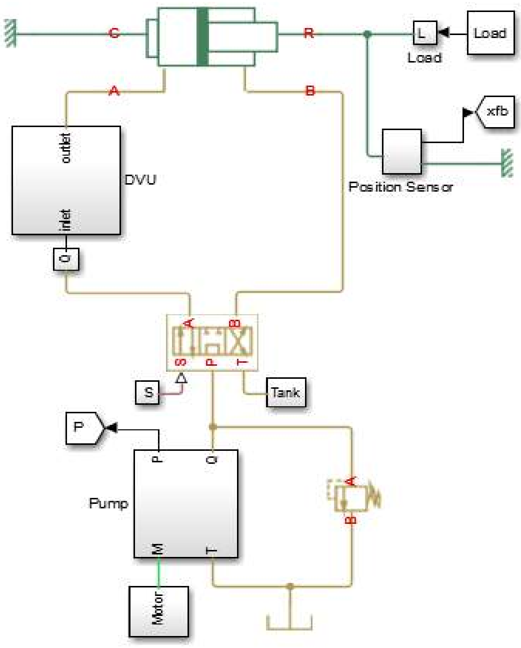

Fig. 3. System Model.

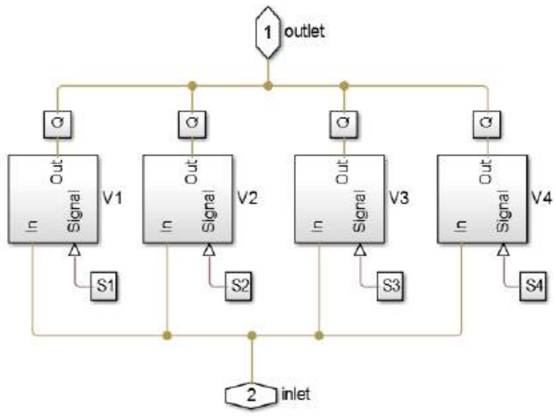

Fig. 4. Digital Valve Unit Model.

2.3 Modeling an Ideal Isolated Case

To fairly judge DVU concept; an optimum case is modeled (Figure 5), this model has a perfect binary PCM code, constant supply pressure, no relief valve bypasses flow, no pressure drop over the 4-way directional valve, and immediate valve response. At constant 20 bar supply pressure, the new precise orifices diameters allow for accurate flow rates (1, 2, 4 and 8) l/min.

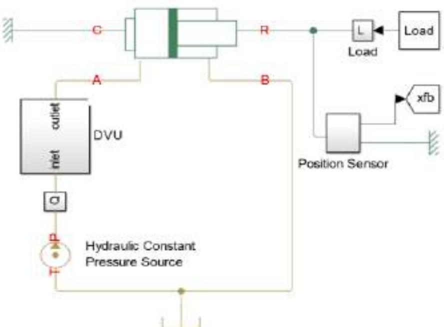

Fig. 5. Ideal Hydraulic Circuit Model.

3. Control and Operation Methodology

Controlling actuator speed can be achieved by using a hydraulic block contains needle valve and return check valve, which is called "metering-in." In the metering-in circuit, cylinder speed is controlled as fluid enter the cylinder; this block is connected to the piston side.
Metering-in circuits are much preferred as long there is no runaway load —runaway load can be prevented by using a counterbalance valve (V2) as shown in Figure 6 consequently preventing cavitation— its best application is for extending an opposing vertical load against gravity force. Another advantage when controlling the feeding in the extension direction; is a precise cylinder speed can be achieved as more fluid entering the piston side than leaving the rod side [1, 26].

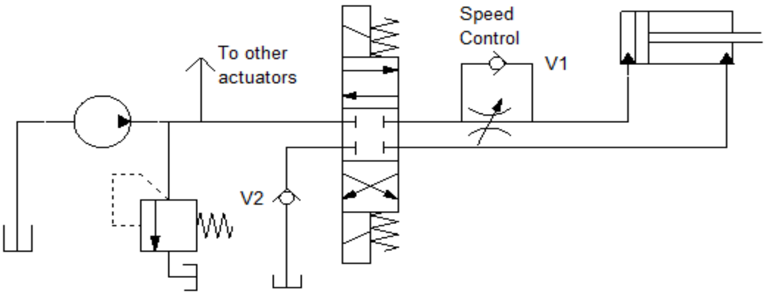

Fig. 6. Meter-in speed control. [1]

The model presented in this paper is based on the meter-in flow control concept, except instead of using conventional analog flow control valve as in Figure 6, a DVU is used.

3.1 Controller Design

An open-loop controller was utilized for the speed control; consequently, there isn't any sensor noise problem, but the system has two issues left, which are Disturbances and Variations in process dynamics. If they are well known, the open-loop controller is an excellent choice, which happened in our case, as the primary purpose of the paper is concentrating on the methodology of speed control using DVU [24].
A simple controller was constructed using MATLAB Stateflow viewed in Figure.7. The controller inputs are the desired flow rate and the position. Also, Position control isn't the paper interest.

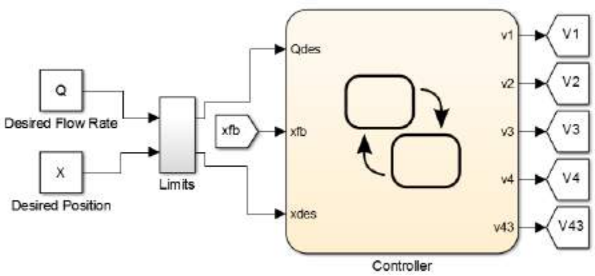

Fig. 7. Velocity Controller.

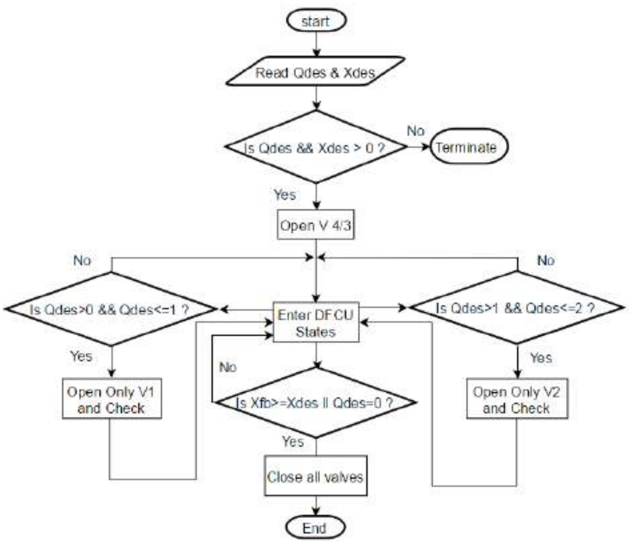

Fig. 8. Controller Flowchart.

As regards to the inputs, the Stateflow control logic selects the suitable “scenario” and opens the combination of valves corresponding to the desired flow rate.
Hence if the desired flow is 7 l//min, with knowing the step size and the valves flow rates values, the corresponding opening valves combination is V1, V2, and V3. The available output flow rate is divided into ranges, thus for 6.8 l/min, the same opening combination will be selected since the minimum step size is 1 —due to the system (DVU n=4) smallest valve has 1 l/min at the rated pressure.

3.2. System Operation

The Flowchart in Figure 8 represents the process steps of the ideal case. Only two valves were selected for presentation, with two valves there are three states: V1 open, V2 open, and both are opened. The third state isn't represented in the flowchart for simplification reason.
The symbols Xdes, Xfb, and Qdes, represent desired output position, feedback position reading from the sensor and desired output speed respectively.

4. Model and Control of Two-Way Electro-Proportional Flow Control Valve

A Sun Hydraulics-FPCCXAN proportional valve is selected for comparison with the modeled DVU [27]. They both are cartridge poppet valves and have an equal maximum flow rate. The maximum valve flow is 15 l/min at 215 bar pressure drop, while the proposed DVU requires only 6.7 bar.
Proportional valves refer to controlling valve output flow proportional to the commanded signal [24]. Proportional valve circuits can be abridged in four paths: I) Open-loop proportional valve system. II) Closed-loop proportional valve system by a mean of an LVDT transducer mounted on the valve. III) A closed-loop proportional valve system, with LVDT linked to the actuator. IV) A closed-loop proportional valve system, with LVDT connected to both the valve and the actuator. More information can be found in [28]. In this model, the third configuration was chosen for comparison with the DVU.
Proportional valve performance curve was uploaded to the model, and I-controller was used as depicted in Figure 9. The controller transfer function is (3.644/s). All the remaining parameters of proportional valve circuit model are the same as the "Near Real DVU Model."
Knowing that the proportional valve hysteresis, linearity, repeatability and dead-band are: <4%, <8%, <2%, <2% and 25% respectively [27]. The valve hysteresis, repeatability, resolution and step response were neglected. These previous issues will be much reduced in the case of using DVU.
Figure 10. shows the tracking performance of output flow of the 2/2 proportional valve to the reference sinusoidal reference with amplitude 15, and 1 rad/sec frequency. It can be seen that the result is nearly consistent with the reference signal after 0.2 seconds —when passes the dead-band zone.

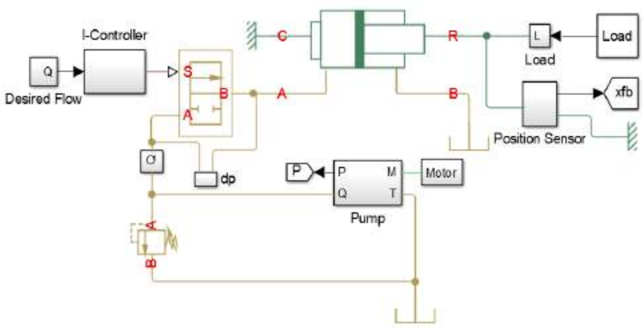

Fig. 9. Proportional Valve Circuit

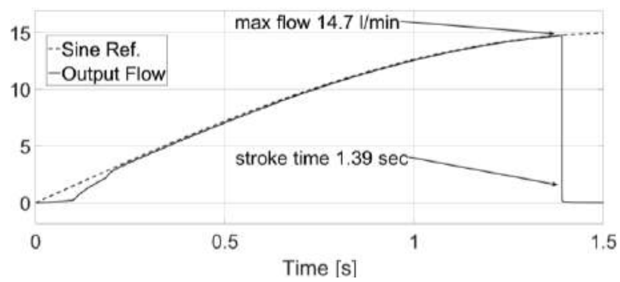

Fig. 10. Proportional Valve. Sine input reference and the response output.

5. Results and Discussion

5.1 Ideal Case

The system's valves have two states, either be operated by 1 input signal or be closed by 0 signal. The controller signals are sent to 24V DC solenoids to activate the valves. In Figure 11, the maximum flow rate 15 l/min is achieved when a ramp input signal of slope 12 is selected. Therefore, all the four valves (n=4) needed to be opened as described in Figure 12.

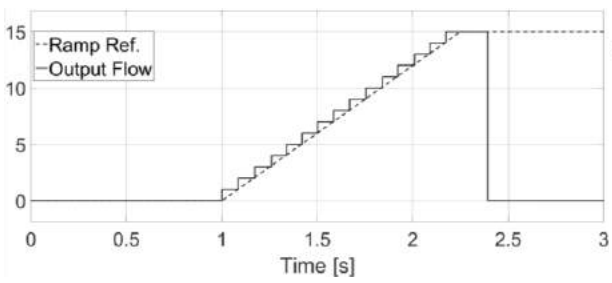

Fig. 11. Ideal DVU (n=4). Ramp input reference.

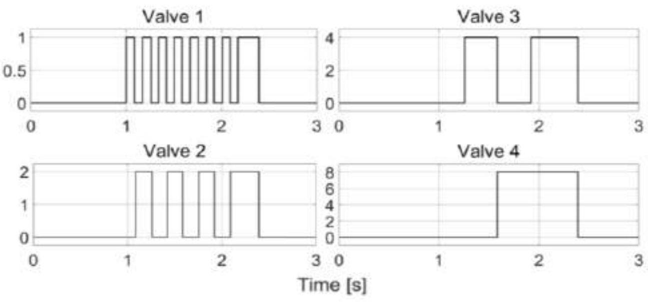

Fig. 12. Ideal DVU (n=4). Output flow from each valve for a Ramp input.

As the number of valves increments by one, the valves' states output increase according to the relation: N_states=2^(n-1), where n is the number of valves in DVU, and N_states is the total number of the states a DVU can possess. Therefore, a DVU output resolution is clearer as the number of valves increases. A comparison demonstrates this point shown in Figures 13 and 14 when a sinusoidal input with 1 rad/sec frequency and xdes = 250mm is used. Also, the output flow rate for the DVU (n=5) is 15.5 l/min which is more than DVU (n=4) by 0.5 l/min.

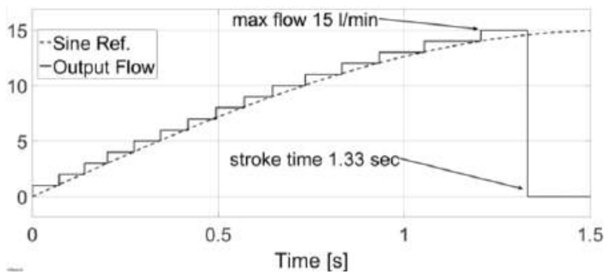

Fig. 13. Ideal DVU (n=4). Sine input reference and the response output.

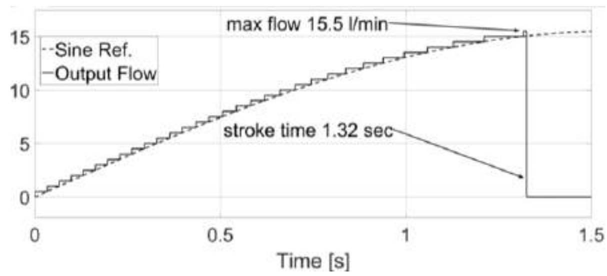

Fig. 14. Ideal DVU (n=5). Sine input reference and the response output.

5.2 Near Real Case

In Figure 15, a trapezoidal input of amplitude 15 for 0.5 sec is used, the corresponding output flow is 14.7 l/min, due to the low precision orifice diameters used.
In Figure 16. When tracking a sinusoidal signal with amplitude 15, and 1 rad/sec frequency, flow peaks were seen, this is caused by the switching on and off delay time of the valves.
More explanation of the flow peaks is as follows: consider the first desired output is 7 l/min this will require a state (V1: on, V2: on, V3: on, V4: off). Secondly, a transition value of 8 l/min is required, this will need an opposite state which is (V1: off, V2: off, V3: off, V4: on). Due to the delay in opening and closing the valves; a transient state appears in which all the valves are opened altogether for a variable period. This issue can be resolved either by using a high response valves, or another suitable coding scheme such as PNM coding, or both. In paper [29], delay problem is solved by delaying the valve closing time based on the measuring values of the inherent

characteristics of valve switching time. The valve opening uncertainty can also cause pressure peaks, which can be resolved by using accumulators, relief valves, and suitable controllers [30].

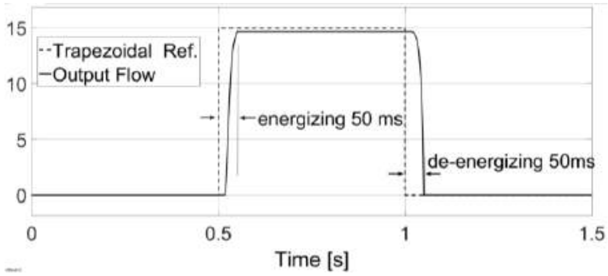

Fig. 15. Near Real DVU. Trapezoidal input reference and the response output flow.

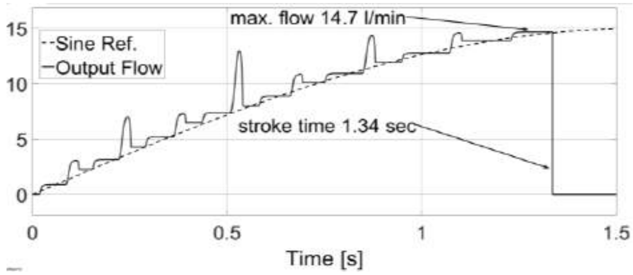

Fig. 16. Near Real DVU. Sine input reference and the response output flow.

5.3 Two-Way Electro-Proportional Flow Control Valve and DVU Comparison Points

In Table 1, data extracted from simulations through Figures 10, 13, 14 and 16 are listed. Here the hydraulic energy consumption is taken for evaluation —of course the prime mover needed to operate the pump will consume higher energy— the energy is calculated as formula (1):

$$Energy_{Hydraulic} = \int_{t=0}^{T} Power_{pump}\,(t)\;dt \tag{1}$$

The cumulative root mean square (CRMS) error was integrated over the cylinder stroke time as shown in formula (2): [31]. U(t) is the variation between the output flow and the reference signal.

$$CRMS = \sqrt{\frac{1}{T}\int_{t=0}^{T} \|u(t)\|^{2}\;dt} \tag{2}$$

Table 1: Comparison layout

system configuration	energy consumed (kJ)	CRMS error	stroke time (sec.)
Proportional valve	11.85	0.31	1.39
Near Real/DVU (n=4)	0.82	0.89	1.34
Ideal/DVU (n=4)	0.40	0.54	1.33
Ideal/DVU (n=5)	0.40	0.28	1.32

It's obvious in Table 1 that the proportional valve consumed greater energy than DVU; this is because the proportional valve operates at much higher pressure drop than DVU to achieve similar flow rates. Also, the energy consumption for Ideal/DVU (n=5) and Ideal/DVU (n=4) is equal due to both operate at fixed pressure source of 20 bar, and the only difference is an excess flow of 0.5 l/min (0.5+1+2+4+8) of the former over the latter (1+2+4+8).
Another important remark, is here the primary cause of CRMS in proportional valve arises from the valve dead-band, and no compensations were made to reduce this error. In fact, both CRMS error and response time in Near Real/DVU and Proportional valve can be decreased with the aid of a more advanced controller. The comment on achieving maximum stroke with Ideal/DVU (n=5) in a shorter time than Ideal/DVU (n=4) is due to a higher maximum flow rate of Ideal/DVU (n=5) by 0.5 l/min. The energy consumption reduction ratio when calculated from equation (3), is 93%.

$$R_{e.c} = \frac{E_{\text{Proportional valve}} - E_{Near\ Real\ DVU}}{E_{Proportional\ valve}} \tag{3}$$

6. Conclusion

In this research, a proposed Digital Valve Unit (DVU) was presented, which showed the possibility to control the flow using DVU instead of the traditional proportional valve. Comparison between the proposed system and the analog 2/2 proportional valve was carried out. The results showed a reduction in energy consumption with the aid of DVU. The system has advantages such as I) Low hysteresis. II) High linearity. III) The possibility of programming valves by many functions. IV) Less pressure drop with small flow rates. V) Fault tolerance, as the system could still operate with less performance when a working valve is malfunctioned. V) Standardization, by substituting different valves for a group of semi-similar programmable ones. It's clear that the concept difficulties are large package size, valve states uncertainty, and pressure peaks. The studied model in this paper can be considered an initial step for digital hydraulic separate meter-in and separate meter-out (SMISMO) control which is a major competitor to load sensing circuits. The present study suggests that DVU can provide a significant improvement in flow control field, especially concerning energy saving.

References

[1] Parr, Andrew. Hydraulics and pneumatics: a technician's and engineer's guide. Elsevier, 2011.
[2] Arora, Www.indiamart.com Designed by Mukesh. "Fixed Displacement Vs Variable Displacement Pumps." Santec Exim Pvt. Ltd. Accessed June 20, 2017. http://www.santecindia.com/variable-displacement-pumps.html.
[3] Jack Johnson | Mar 19, 2007. "Pump control vs valve control: Efficiency or performance?" Hydraulics & Pneumatics. December 09, 2011. Accessed June 20, 2017. http://www.hydraulicspneumatics.com/200/TechZone/HydraulicPumpsM/Article/False/46094/TechZone-HydraulicPumpsM.
[4] Cundiff, John S. Fluid power circuits, and controls: fundamentals and applications. CRC Press, 2001.
[5] Linjama, Matti. "Digital fluid power: State of the art." In 12th Scandinavian International Conference on Fluid Power, Tampere, Finland, May, pp. 18-20. 2011.
[6] Bower, John L. "Digital fluid control system." U.S. Patent 2,999,482, issued September 12, 1961.
[7] Matti, Karvonen. "Energy Efficient Digital Hydraulic Power Management of a Multi-Actuator System." Ph.D. diss., Tampere University of Technology, 2016, Publication; Vol. 1384.
[8] Yamada, Hironao, Guy Wennmacher, Takayoshi Muto, and Yoshikazu Suematsu. "Development of a high-speed on/off digital valve for hydraulic control systems using a multilayered PZT actuator." International Journal of Fluid Power 1, no. 2 (2000): 5-10.
[9] Pipan, Miha, and Niko Herakovič. "Volume Flow Characterization of PWM-Controlled Fast-Switching Pneumatic Valves." Strojniški vestnik-Journal of Mechanical Engineering 62, no. 9 (2016): 543-550.
[10] Brorsen, Anette. “Feasibility Study of a Novel ON/OFF Valve Solution for Velocity Servo Systems.” master’s thesis, Aalborg University, 2014, http://projekter.aau.dk/projekter/files/198466718/Brorsen2014_Feasibility_Study_of_a_Novel_ON_OFF_Valve_Solution_for_Velocity_Servo_Systems.pdf
[11] Kogler, Helmut, Rudolf Scheidl, Michael Ehrentraut, Emanuele Guglielmino, Claudio Semini, and Darwin G. Caldwell. "A compact hydraulic switching converter for robotic applications." *Fluid Power and Motion Control (FPMC 2010)/Bath, UK* (2010): 55-68.
[12] Linjama, Matti, and Matti Vilenius. "Digital hydraulics-Towards perfect valve technology." In: Vilenius, J. & Koskinen, KT (eds.) The Tenth Scandinavian International Conference on Fluid Power, May 21-23, 2007, Tampere, Finland, SICFP'07. 2007.
[13] Hänninen, Henri, and Matti Pietola. "Analysis on the adaptability of two different hydraulic energy recovery circuits on various machine types and work cycles." In ASME/BATH 2013 Symposium on Fluid Power and Motion Control, pp. V001T01A043-V001T01A043. American Society of Mechanical Engineers, 2013. RECOVERY CIRCUITS ON VARIOUS MACHINE TYPES AND WORK CYCLES
[14] Linjama, Matti, Juho Seppälä, Jouni Mattila, and Matti Vilenius. "Comparison of digital hydraulic and traditional servo system in demanding water hydraulic tracking control." In: Johnston, DN & Plummer, AR (eds.). Fluid Power and Motion Control FPMC 2008, 10-12 September 2008, Bath, UK (2008).
[15] Gan, Zhenyu, Katelyn Fry, R. Brent Gillespie, and C. David Remy. "A novel variable transmission with digital hydraulics." In Intelligent Robots and Systems (IROS), 2015 IEEE/RSJ International Conference on, pp. 5838-5843. IEEE, 2015.

[16] DeRose, Don. "Proportional and servo valve technology." Fluid Power Journal 4 (2003): 8-12.
[17] Brandstetter, Reinhard, Till Deubel, Rudolf Scheidl, Bernd Winkler, and Klaus Zeman. "Digital hydraulics and “Industrie 4.0”." Proceedings of the Institution of Mechanical Engineers, Part I: Journal of Systems and Control Engineering (2015): 0959651816636734.
[18] Linjama, M., and M. Vilenius. "Digital hydraulic control of a mobile machine joint actuator mockup." In Bath Workshop on Power Transmission and Motion Control, vol. 2004, p. 145. PROFESSIONAL ENGINEERING PUBLISHING, 2004.
[19] MATLAB. "Documentation." Simulating Hydraulic Models - MATLAB & Simulink. Accessed June 20, 2017. https://www.mathworks.com/help/physmod/hydro/ug/running-hydraulic-models.html.
[20] MATLAB. "Odeset." Choose an ODE Solver - MATLAB & Simulink. Accessed June 20, 2017. https://www.mathworks.com/help/matlab/math/choose-an-ode-solver.html.
[21] Sunhydraulics. "Value Series, 2-way, solenoid-operated directional poppet - valve 3600 psi (250 bar)." Accessed June 20, 2017. http://www.sunhydraulics.com/model/DTDB/XCN212N.
[22] HydraForce. "Orifice Disc Installation & Sizing Guide." Orifice Discs for HydraForce Hydraulic Valves. Accessed June 20, 2017. http://www.hydraforce.com/Acc-hous/Acc_html/8-460-1_Orifice_Discs/8-460-1_Orifice%20Discs.htm.
[23] Ponar Wadowice. "Directional control valves." Directional control valves - Ponar Wadowice. Accessed June 20, 2017. http://www.ponar-wadowice.com/directional-control-valves.
[24] Cetinkunt, Sabri. Mechatronics with experiments. Chichester: Wiley, 2015.
[25] Oleoweb. "Search results for 'vmdr40'" Search results for: 'vmdr40' Accessed June 20, 2017. https://www.oleoweb.com/en/catalogsearch/result/?q=vmdr40.
[26] "Designing Slow Feed Circuits - Part 1, Hydraulic Cylinders." Womack Machine Supply Company. Accessed June 20, 2017. http://www.womackmachine.com/engineering-toolbox/design-data-sheets/designing-slow-feed-circuits-part-1,-hydraulic-cylinders.aspx.
[27] Sunhydraulics. "Electro-proportional flow control valve - normally closed." Accessed June 20, 2017. http://www.sunhydraulics.com/model/FPCC/XAN214N.
[28] P, Written By joji. "Understanding the Concepts of Proportional Electro-hydraulic Valves in Ten Minutes." Industrial Hydraulic Systems - Theory and Practice. January 06, 2017. Accessed June 20, 2017. https://industrialhydraulicsystemsbook.com/2017/01/06/understand-the-concepts-of-proportional-hydraulic-valves-in-ten-minutes/.
[29] Laamanen, A., L. Siivonen, Ml Linjama, and M. Vilenius. "Digital flow control unit-an alternative for a proportional valve?" In BATH WORKSHOP ON POWER TRANSMISSION AND MOTION CONTROL, vol. 2004, p. 297. PROFESSIONAL ENGINEERING PUBLISHING, 2004.
[30] Laamanen, A., M. Linjama, and M. Vilenius. "Pressure peak phenomenon in digital hydraulic systems-a theoretical study." In: Johnston, DN, Burrows, CR & Edge, KA (eds.). Bath Workshop on Power Transmission and Motion Control (PTMC 2005), 7-9 S eptember 2005. 2005.
[31] MATLAB. "Documentation." Compute continuous-time, cumulative root mean square (CRMS) of signal - Simulink. Accessed September 13, 2017. https://www.mathworks.com/help/sldo/ref/crms.html.

ISSN 1454 - 8003
Proceedings of 2017 International Conference on Hydraulics and Pneumatics - HERVEX
November 8-10, Băile Govora, Romania

AUTOMATED HYDRAULIC OIL COOLING SYSTEM DRIVEN BY A VARIABLE SPEED HYDRAULIC MOTOR

Iulian-Claudiu DUȚU[1], Radu-Iulian RĂDOI[2]

[1] University Politehnica of Bucharest, Romania, iulian_claudiu.dutu@upb.ro

[2] Hydraulics and Pneumatics Research Institute, Bucharest, Romania, radoi.ihp@fluidas.ro

Abstract: *Oil cooling systems are used widely in hydraulic systems, mainly to maintain working fluid's (oil) temperature within a given range, where its flowing parameters have small variations. It is a well-known fact that hydraulic oil parameters, such as viscosity and pressure drop, are dependent to current oil temperature therefore in many cases it must be controlled using automated cooling systems. The authors propose an automated hydraulic oil air cooling system having as main actuator a variable speed rotary hydraulic motor. Cooling capacity must be calculated, using standardized formulae that are to be found in scientific literature, under-sizing always lead to poor temperature balance. Overheating can create favorable conditions for the occurrence of cavitation phenomenon, leading to premature wear or damage of hydraulic equipment. The testing stand that the authors propose is made of an operator console placed on a hydraulic oil tank, a battery of oil filters, hydraulic directional valves, safety valve, electronic temperature to current transducers and the electronic controller module.*

Keywords: *automated system, testing stand, transducers, simulation*

1. Introduction

Hydraulic fluids, also known as hydraulic oil or hydraulic liquid, can be defined as the medium used to transfer power in hydraulic installations or systems. Its physical and chemical characteristics can be measured and give the extent to which system's overall efficiency is appreciated. In energy terms, an automated cooling system is working with the energy that the hydraulic installation / system does not consume when working – also known as lost energy:

$$W_{cooler} = W_{input} - W_{used} \tag{1}$$

Trying to maintain the oil at ideal working temperature is highly desired, having direct positive benefits both on hydraulic system's working life and oil life, reduced maintenance and repair costs, lower system downtime and higher efficiency when oil temperature is somewhere around the ideal working temperature (in practice the oil's temperature is varying in a range of values).
The automated hydraulic oil cooling system, was tested on an general purpose electro-hydraulic testing stand, made of an operator console, an oil tank having an approximate volume of 800 liters, a battery of oil filters, several hydraulic directional valves, a safety valve, electronic temperature to current transducers and the electronic controller module. All will be detailed in the following. The operator console is a rectangular metallic plate, having T-shaped channels on which is mounted, mainly, tested equipment and auxiliary hydraulic valves or electro-mechanical devices.
The paper is presenting the electro-hydraulic diagram of the automated cooling system that the authors propose, several key technical parameters of main components. The system is using an air cooler with a variable speed hydraulic motor.

2. Current state of the art

Hydraulic driven cooling system, with an air fan, are using a variable speed motor is considered to offer significant advantages over classic electric or belt-driven solutions, such as energy savings,

ISSN 1454 - 8003
Proceedings of 2017 International Conference on Hydraulics and Pneumatics - HERVEX
November 8-10, Băile Govora, Romania

accurate and variable speed control of the fan, extended working life and the possibility to find integrated cooling systems on the market.

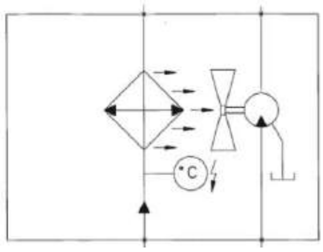

Fig. 1. General connection for an air hydraulic oil cooler with hydraulic rotary motor

Mainly, there are known three technical solutions for hydraulic oil cooling using:

a. *fixed ratio* hydraulic rotary motor, the case which the cooling system's fan has only one rotational speed, proportional with the drive motor's (electric, hydraulic) speed,

Fig. 2. Fixed ratio hydraulic motor

The hydraulic motor can be provided with auxiliary hydraulic equipment, such as pressure relief valves or anti-cavitation valves, but it also can operate in stand-alone configuration, without using these equipment.

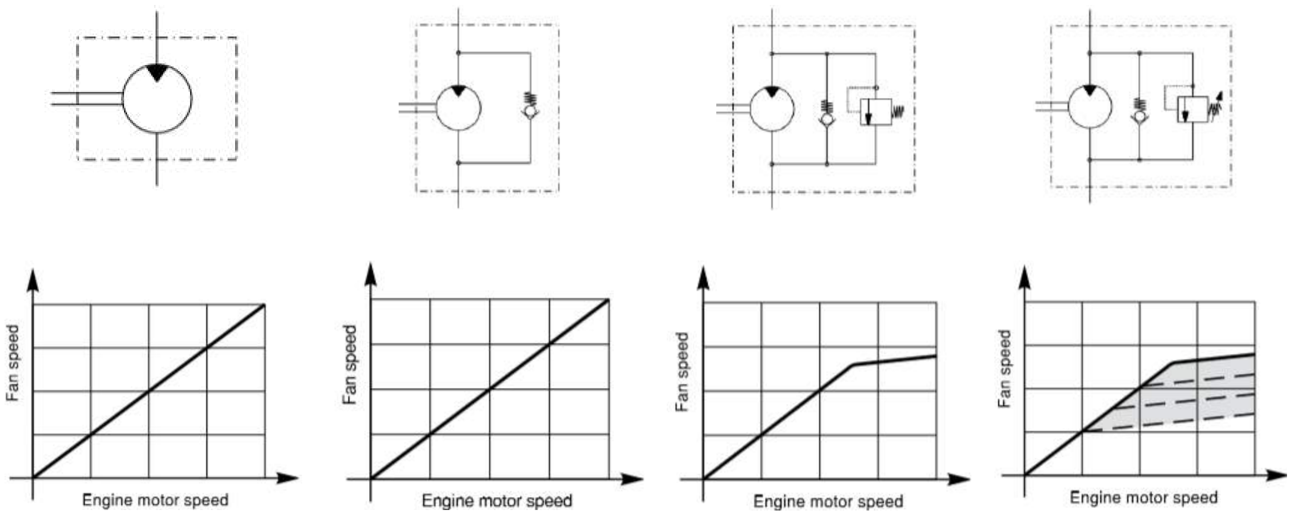

a. stand-alone

b. with anti-cavitation valve

c. with pressure relief valve (fixed) and anti-cavitation

d. with pressure relief valve (adjustable) and anti-cavitation

Fig. 3. Different operating modes for fixed ratio hydraulic motors

Basically, in every one of the four operation modes given above, the hydraulic motor performs the same function, but there are few disparities: in Fig. 3.a, the construction is simple and robust, therefore is expected to be a cost effective solution; in Fig. 3.b, the hydraulic motor is protected, but in the same time it can attain higher rotary speeds then the case before; in Fig. 3.c, the motor has the same benefits as in Fig. 3.b, but a long-life operation if expected than the cases before. The recommended configuration when using a fixed ratio hydraulic motor is the one given in Fig. 3.d, where besides higher rotary speeds, motor protection and larger fan size, the system can be optimized due to its adjustability. Analyzing the associated functional curves, *fan speed vs. engine motor speed*, it can be easily differentiate the functional characteristics in each one of the four connection modes. Best operation case is given in Fig. 3.d, but it is also the most expensive one.

b. *two speed* hydraulic rotary motor, when the cooling system's fan can rotate at two different speeds, therefore the cooling system can operate in two modes: normal cooling mode and turbo cooling mode,

Fig. 4. Two speed hydraulic motor

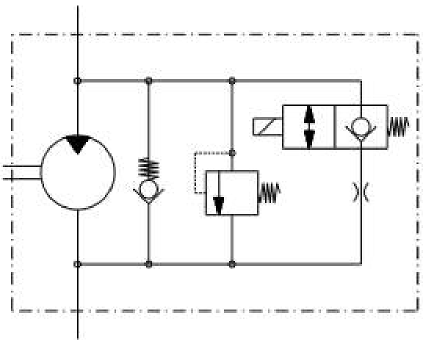

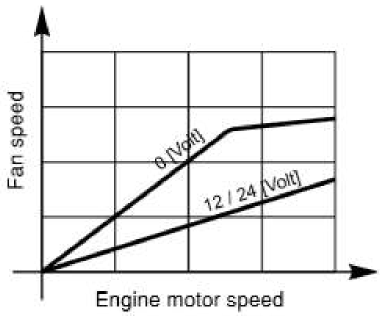

Fig. 5. Two speed hydraulic motor with piloted bypass valve, pressure relief valve (fixed) and anti-cavitation

Technical advantages of using such a configuration are: high operation speeds, hydraulic motor protection against pressure peaks, large fan sizes and the electronic command for two operating cooling speeds. Usually, the electromagnet of the piloted bypass valve operates on 12VDC for normal cooling and 24VDC for turbo cooling. It must be noted that any other intermediate rotary fan speeds are not possible in this configuration, as seen in the characteristic curve in Fig. 5.

c. *variable speed* hydraulic rotary motor, having the benefit of that the operator can change the direction of rotation when needed. In this case, the rotational speed of the fan driving axle is independent of the driving engine speed, but needs, at least, an electronic module to control the speed variation and direction change.

Fig. 6. Variable speed hydraulic motor

In the case of using a variable speed hydraulic motor, the fan speed is independent of drive engine speed. It is the most expensive solution of all presented above, but acquisition costs are not always the only choosing criteria.

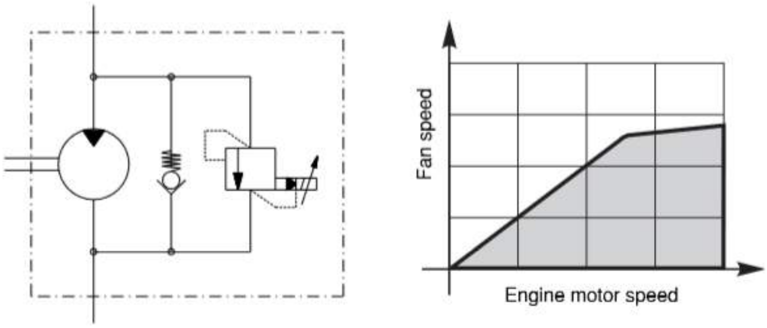

Fig. 7. Variable speed hydraulic motor with proportional relief and anti-cavitation valves

Besides the high speed operation, long operating life and motor protection, there is attained a proportionally precise control of coolant temperature, while in a case of a control module failure, the fan will be rotating at its maximum speed.

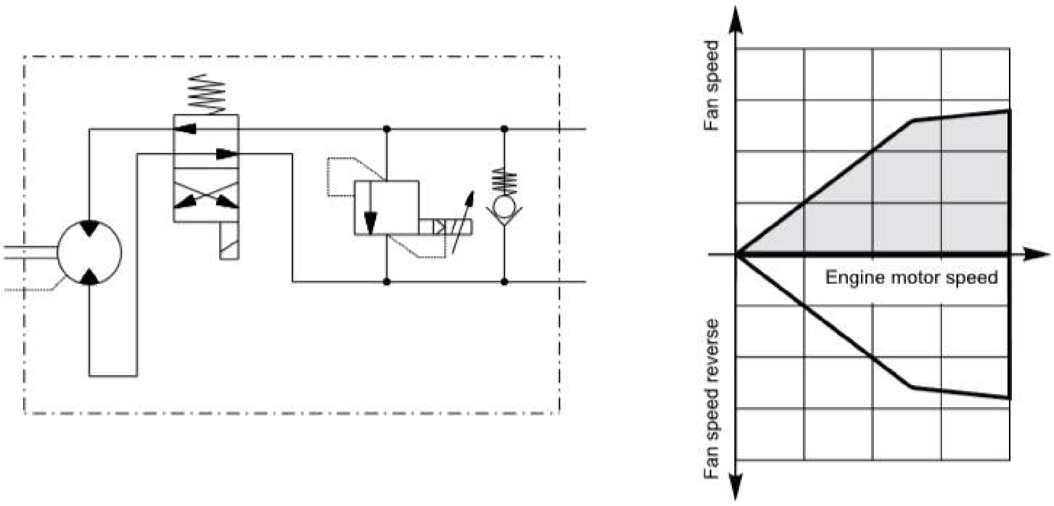

Fig. 8. Variable speed hydraulic motor with
4/2 reverse valve, proportional relief valve and anti-cavitation valve

The most efficient operating mode of an air oil cooler is to use a variable speed hydraulic motor connected using the diagram given in Fig. 8, which is also provided with the possibility to change the direction of rotation - it is used a 4/2 electric valve. In addition to the features presented in the previous case, reversible operation of the cooling fan, allow the system to perform an “auto-cleaning” of the radiator element. The speed variation is current controlled using a specialized electronic module, which generates a PWM signal of which frequency is proportional to hydraulic motor speed, with an adjustable dither signal. The electronic module controls the hydraulic motor rotational speed by simply regulating the current that flows through the electromagnet of the proportional relief valve.

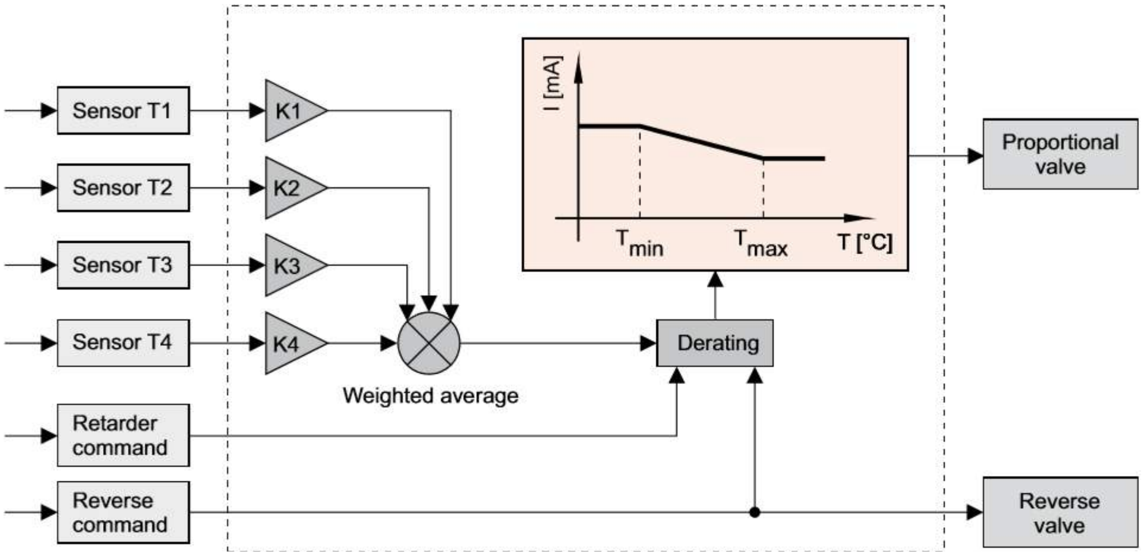

Fig. 9. Schematic of an electronic control module used in a variable speed fan drive system with variable speed hydraulic rotary motor

The schematic given in Fig.9 has a number of four temperature sensor inputs, for each one it can be set the minimum and maximum working (control) temperatures and a weight coefficient in accordance with so-called “thermal importance” in the control loop. Depending on the proportional valve type, the minimum and maximum control currents can be set. From Fig. 9 it can be seen that the electronic control module calculates the proportional valve drive current using a weighted average of temperatures measured in different point of the hydraulic installation. The electronic control module has a retarder function allowing the operator to increase or decrease the hydraulic motor speed by simply changing the control current of the hydraulic proportional valve. There is also available a reverse function used only for reversible hydraulic motors in the reverse valve configuration, thus allowing changing the direction of rotation used for cleaning cycles of radiators.

Fig. 10. Air hydraulic oil cooler using a hydraulic rotary motor (LHC, OA-Technik GmbH)

3. System description

Given the above, the authors propose an electro-hydraulic diagram of the automated oil cooling system, using a variable speed hydraulic motor.

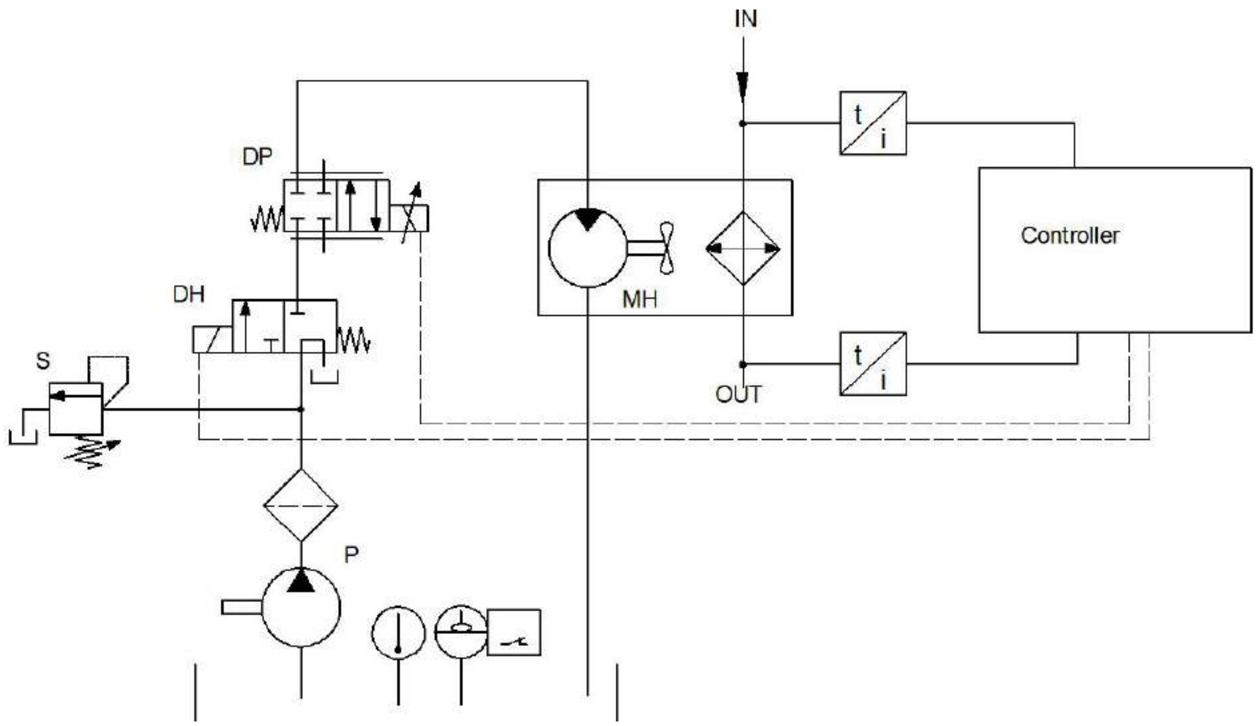

Fig. 11. Schematic diagram of the automated cooling system

The diagram of the automated hydraulic oil cooling system that the authors propose is using: a proportional 4/2 directional valve *DP*, a 3/2 directional valve *DH*, a pressure relief (adjustable) valve *S*, a hydraulic pumping module with electronic level display and mechanical temperature indicator, the air oil cooling with variable speed hydraulic motor *MH*, a hydraulic filter battery, two electronic fluid (hydraulic oil) temperature-to-current transducers and the electronic control module. The electronic fluid temperature transducers are using Pt100 thermocouples, having the operating temperature range of [-50°C … +150°C] and an output voltage of 0…10V, with signal converter. When the cooling function is not needed, the 3/2 directional valve *DH* is acting as a hydraulic switch, decoupling the hydraulic cooling system from the main installation.

3.1. Main components

Referring to the electronic control module, it can be materialized using a dedicated controller based on a RISC microcontroller, a programmable logic controller (PLC) or a personal computer with a data acquisition board. In any case, the control module must be programmed using proper software environment. The controller described in this paper was made using the third option from the above: PC and DAQ board. Presented configuration is using a 16-bit FESTO EasyPort DAQ, as seen in Fig. 12.a, with analog and digital connection boards, Fig. 12.b. This DAQ board is interfacing the cooling system's temperature transducers on two analog inputs and two DC electromagnets, one connected on a digital output (0/24VDC) for directional valve *DH*, while the other one, for *DP* proportional directional valve, is connected on an analog output, generating proportional command. The DAQ board communicates with the PC using a USB connection standard. Also, the DAQ board can supply regulated 24VDC power to the temperature transducers and other electric consumers, max. 1A. When choosing the data acquisition card, the authors have considered the following criteria:

- maximum *sampling rate*, which is the measure of the speed at which an analog input of the acquisition board is scanned and updated, in order to acquire a numerical value of the

analog signal present on the input. If the sampling rate is incorrectly selected, the acquired signal will not be the same as the original signal;
- the *resolution* is represented by the number of divisions in which the input signal variation range is divided;
- number of *analog inputs*, closely related to the number of signals that can be purchased simultaneously;
- number of *analog outputs* used by the PC to generate analog signals send to the testing stand.

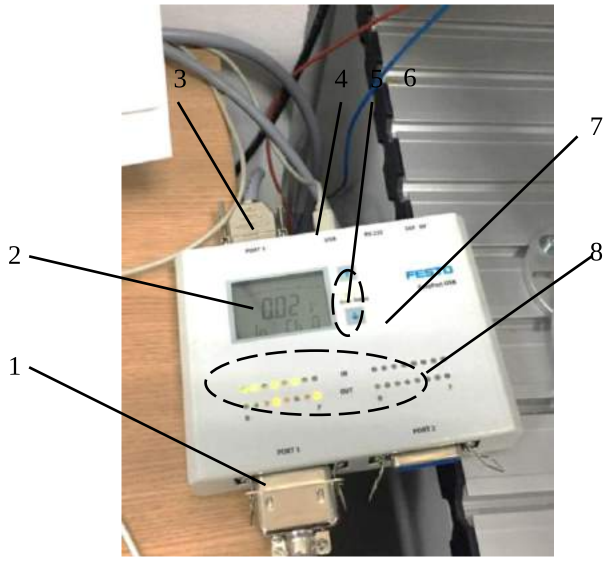

a. DAQ board

b. analog and digital connectors

Fig. 12. DAQ board and its connectors

In Fig. 12.a, are given: 1. digital signal cable; 2. data acquisition board display; 3. analog signal cable; 4. USB data cable; 5. configuration buttons and status LEDs; 6. power supply (24 VDC).

The EasyPort USB DAQ board is equipped with two configuration buttons and two LEDs (green and red) that optically signal the state of the board as follows:
- red LED flashes when a short circuit is detected at one of its outputs. In this case, EasyPort USB outputs are disabled as a protective measure. This LED illuminates briefly when the DAQ board is electrically powered;
- green LED can indicate optically the following states of the DAQ board:
    - an intermittent illumination with a frequency of approximately 1 Hz immediately after the electric powering, meaning that the acquisition card has not started communicating with the computer to which it is connected;
    - a fast flashing, meaning that the acquisition card was recognized and connected to the computer without any errors.

The LCD display of the DAQ board is used to inform the operator about voltage levels from a selected analogue input / output, in numerical form and in the form of a bar-graph, the length of which is proportional to the value of the input. The LCD display also shows the number of input / output displayed and the type of signal: input or output. Two groups of 16 LEDs, Fig. 12, are used on the DAQ board indicating the current state of the digital inputs and outputs. The green LEDs indicate the status of the digital inputs as: LED off – zero (low) input value; LED illuminated – high input value. The yellow LEDs indicate the state of the digital outputs, having the same optical significance as the inputs. The two buttons on the front panel of the DAQ board are used to select

the input or output number and the unit of measure (V, bar, PSI, MPa, l / min, °C) in which the value on the LCD display is displayed.
The transducers of the experimental stand perform the conversion of a physical measure (temperature) into a proportional electrical signal (voltage).

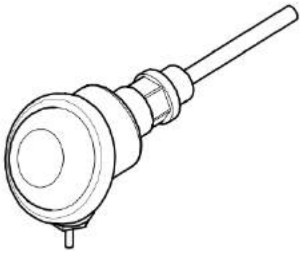

a. schematic drawing

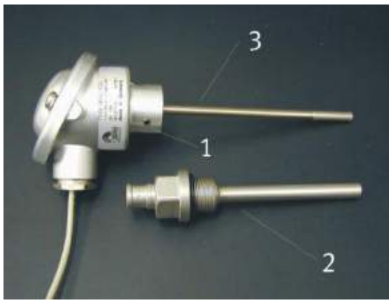

b. physical model

Fig. 13. Temperature transducer, Pt100

Another main component of the automated oil cooling system is the variable speed hydraulic motor, OMM8 type, manufactured by Danfoss, shown in Fig. 14. Few important technical characteristics of the motor are: operating pressure 60 bar, maximum permissible pressure 120 bar, maximum permissible pressure in the return line 50 bar, displacement 8,2cm^3/ rot, 0…10 l/min, 0…1220 rpm, low leakage.

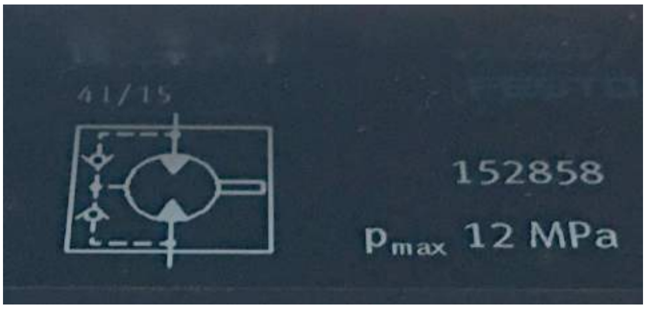

a. motor schematic

b. motor mounted on testing stand

Fig. 14. Variable speed hydraulic motor

The hydraulic motor speed is controlled by the *DP* proportional directional valve, which is driven by the electronic controller.

3.2. Virtual instrument - controller

The electronic controller module, as stated before, is based on a PC – DAQ board system, using a VI, virtual instrument, developed in LabView software environment. Instrument (user) panel of the VI is shown in Fig. 15, where can be seen several displays and control instruments. The VI has an activation switch (ON/OFF) which starts or stops temperature control. There is placed on the instrument panel a display for the rotational speed of the hydraulic motor, a green LED indicator that is lighted in light or dark green according to the ON or OFF state of the *DH* directional valve (bypass valve), two displays calibrated from 0 to 100ºC that display in real time the current temperature value at the in and out connectors of the air hydraulic oil cooler. The most important two controls on the instrument panel are the *PID output [%]* and *PID gains*, the VI uses a standard software proportional-integrative-derivative controller (PID) to calculate the command for the electromagnet of the proportional hydraulic directional valve *DP* and displays it. PID controller output is shown in percent, physically corresponding to electric current values applied to the proportional electromagnet of *DP*, in range from 200 to 800mA.

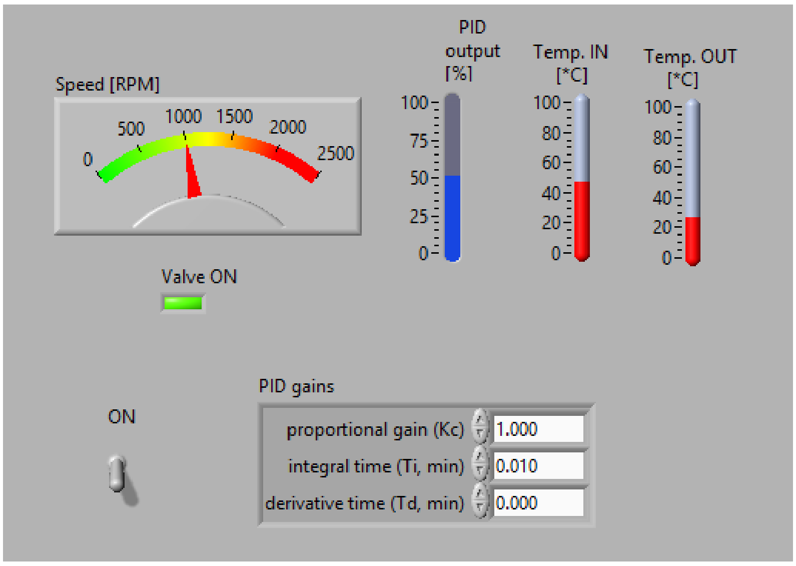

Fig. 15. Virtual instrument for automated control of the oil cooler

4. Conclusions

Automated hydraulic oil cooling systems are necessary extensions of any modern hydraulic testing stand, especially when performing endurance tests on classic or proportional hydraulic equipment. Proper fluid (hydraulic oil) temperature control is a key factor for obtaining accurate results when acquiring data for plotting characteristic curves of hydraulic equipment. Another important aspect of using an automated oil cooling system is reducing premature wear of the hydraulic equipment, implying – on long term – lower maintenance and service costs. Automated systems reduce the percent of human operator intervention on tasks that have a low level of importance in hydraulic systems and installations, taking over monitoring and control task but notifying the operator only in potential dangerous situations.

Acknowledgment

This work has been funded by Executive Unit for Financing Higher Education, Research, Development and Innovation - UEFISCDI, under PNCDI III - Programme 2, Subprogramme 2.1 – Transfer project to the economic operator (PTE-2016), Submission code PN-III-P2-2.1-PTE-2016-0077, Financial agreement no. 11PTE/2016, project title: High energy efficiency (HEE) electro hydraulic equipment (EHE) for multifunction vehicles (MFV), project acronym ECHIPEFEN, Project main domain: 3. Energy, Environment and Climate Change, Subdomain: 3.1. Energy.

References

[1] L. Szabo, “Modelarea sistemelor electromecanice”, U.T.Cluj;
[2] T.Tudorache, “Medii de calcul în inginerie electrică – MATLAB”;
[3] C. Ionete, D. Selişteanu, A. Petrişor, “Proiectarea sistemică asistată de calculator în MATLAB, Reprografia Universităţii din Craiova, 1995;
[4] N.E. Leonard, W.S. Levine, “Using MATLAB to analyze and design Control Systems”, Addison-Wesley Publ., SUA, 1995;
[5] P. Marchand, “Graphics and GUIs with MATLAB”, CRC Press, SUA, 1999;

[6] Fl. Grofu, “Sistem numeric pentru monitorizarea nivelului, Universitatea „Constantin Brâncuşi” din Târgu-Jiu Asist.ing. Cercel Constantin, Universitatea „Constantin Brâncuşi” din Târgu-Jiu, Analele Universităţii „Constantin Brâncuşi” din Târgu Jiu, Seria Inginerie, No. 3/2012, pp. 125-135;
[7] C. Oprea, Cr. Barz, “Tehnica reglării automate”, Tipografia Universităţii de Nord, Baia Mare, 2000;
[8] A.M. Duinea, “Informatica de proces – notițe de curs”, Universitatea din Craiova, 2006;
[9] A.S. Băieșu, “Tehnica reglării automate”, Editura MatrixRom, ISBN:978-973-755-815-2, 2012;
[10] N.E. Leonard, W.S. Levine , “Using MATLAB to analyze and design Control Systems”, Addison-Wesley Publ., SUA, 1995;
[11] *** CASAPPA-Fluid Power Design, “Electro-hydraulic fan drive system”, document ID: FD 04 T A, 04 February, 2014, pp.1–38, http://www.casappa.com;
[12] Pius Emmenegger, “LHC, Air Oil Coolers with Hydraulic Motor for Mobile and Industrial Use”, 01 March, 2015, pp. 1–7, http://www.olaer.ch;
[13] ***, http://www.festo.ro;
[14] ***, DVD-ROM,”FluidLab PA closed loop, Documentation”, Festo Didactic, 07/2015.

ISSN 1454 - 8003
Proceedings of 2017 International Conference on Hydraulics and Pneumatics - HERVEX
November 8-10, Băile Govora, Romania

FOUR-WHEEL DRIVE HIGH EFFICIENCY HYBRID TRANSMISSION FOR MULTIPURPOSE MOTOR VEHICLES

Ioan LEPĂDATU[1], Corneliu CRISTESCU[1], Polifron-Alexandru CHIRIȚĂ[1], Cristian MĂRCULESCU[2]

[1] INOE2000 - IHP, lepadatu.ihp@fluidas.ro

[2] GRADINARIU IMPORT EXPORT SRL, cristian.marculescu@gradinariu.ro

Abstract: *Multipurpose motor vehicles are trucks on which various equipment has been implemented in order to achieve works related to the road that they travel on, such as snow removal, sweeping and spraying the streets, roadside mowing, trimming trees, etc.*
Multipurpose vehicles have two operating modes. ●Marching mode. The vehicles move rapidly from one location to another. Torque at the drive wheels is small and the speed is high. ●Technological mode. The vehicle is traveling at a low speed (max. 8 km/h) imposed by the working technology of multifunctional equipment. Torque at the drive wheels is high and the speed is low. In this sense, the request came from a company in the field of road maintenance to achieve a special transmission that allows achieving low speeds during working operations. The product is made in a research project between the company and a research institute specialized in hydraulic drives.
The article analyzes the solution of increasing efficiency of multifunctional vehicles in the technological mode by using a hybrid (mechanical-hydraulic) four-wheel drive transmission achieved through the implementation of a hydrostatic transmission in the kinematic chain of the mechanical transmission. The following are presented: hybrid transmission components and functioning, hydrostatic transmission schematic diagram and structure, energy efficiency as a result of the hydraulic transmission implementation and numerical simulation of the main functional parameters of the transmission.

Keywords*: Hybrid transmission, four-wheel drive, energy efficiency, multifunctional motor vehicles*

1. Introduction

Multifunctional motor vehicles are trucks on which technological equipment is implemented, with which works generally related to roads are done such as: removing snow from the road, spreading anti-slip materials, sweeping and sprinkling streets, mowing public roads, or trimming trees etc.
These vehicles have two modes of travel: fast and slow.
In the fast-moving mode, vehicles move at high speed on the road from one location to another. The torque on the drive wheels is small and the speed is high.
In slow travel, the vehicle moves at a low speed (max. 5 km/ h) imposed by the multifunctional equipment technology. The engine torque is high and the speed is low. In this regard, a request has come from a road maintenance company for a special transmission that allows for low speeds during the work operations. The product is being developed as part of a research project between the company and an institute specialized in hydraulic drives.
Traditional mechanical transmission (gearbox, drive shaft, differential) is effective in rapid travel mode (high speed) but it is both energy and operating inefficient in the "technological speed" mode.
The mechano-hydraulic transmission [1], which is the subject of the article, adds the benefits of the two types of transmissions. Practically, the vehicle has two types of independent transmission: mechanical and hydraulic. Switching from one transmission to the other is done by a simple switching. Mechanical transmission [2] is used in marching mode, i.e. travel on high-speed road, and the hydrostatic transmission - in "technological mode". Electronic control of the hydrostatic transmission ensures smooth start, continuous speed control and safe braking.

2. Components and functioning of hybrid transmission

The constructive and functional schematic diagram of the hybrid transmission is shown in fig. 1.
In the case of mechanical transmission, the torque supplied by the MT motor is transmitted to the engine wheels (RMF and RMS) via the CV gearbox, the AC drive shaft, the CD distribution box and the front and rear axle (ACF and ACS) - see fig. 1a.

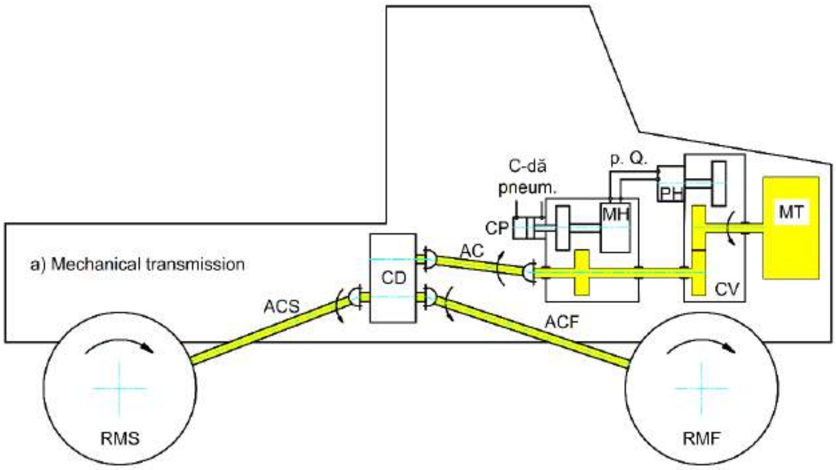

Fig. 1a. Mechanical transmission

The hydrostatic transmission is achieved by introducing the MH hydraulic motor into the kinematic chain of the mechanical transmission - see fig. 1b.

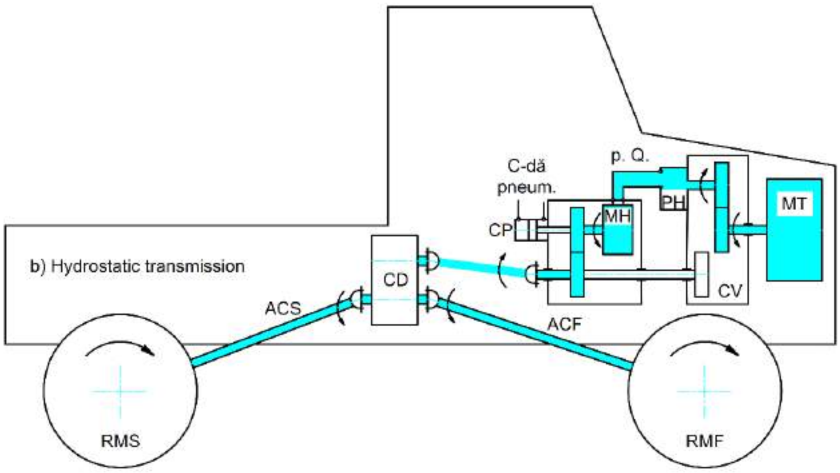

Fig. 1b. Hydrostatic transmission

MT - thermal motor; PH - hydrostatic pump; CP - pneumatic cylinder; DF - differential; CV - gearbox;
MH - hydraulic motor; AC, ACS and ACF - cardan shafts; RMS and RMF - engine wheels; CD - transfer box.

Connecting or disconnecting the MH hydraulic motor from the AC shaft is done with the CP pneumatic cylinder supplied from the compressed air network of the truck.
The hydraulic PH pump is driven from the power outlet of the truck directly or via a cardan shaft.
Activation of the hydraulic transmission [3] is as follows: (see fig. 1b)
- shift the CV gearbox to neutral to deactivate the mechanical transmission.

ISSN 1454 - 8003
Proceedings of 2017 International Conference on Hydraulics and Pneumatics - HERVEX
November 8-10, Băile Govora, Romania

- connect the power take-off to PH pump;
- engage the hydraulic motor MH with the AC shaft with the CP pneumatic cylinder;

The kinematic chain of the hydrostatic transmission has two branches:

- the kinematic chain of the pump composed of: MT - CV - PH;
- engine kinematic chain consisting of: MH - AC - CD - (ACS - ACF) - (RMF - RMS).

The energy flow of the hydrostatic transmission [4] undergoes two transformations:

- hydraulic pump PH converts the mechanical power (torque x speed) received from the MT motor via the CV transmission in hydraulic power (pressure x flow) which it transfers to the hydraulic motor MH;
- Hydraulic engine MH converts the hydraulic power received from the PH pump into mechanical power (Torque x speed), which it transfers to the drive wheels via AC, ACS and ACF shafts and the distribution box.

3. Schematic diagram and structure of hydrostatic transmission

The hydrostatic transmission is part of the hybrid transmission and consists mainly of: hydraulic pump 1, hydraulic motor 2 and refreshment valve 3 (see figure 2). These components together form a closed hydraulic circuit. [5]

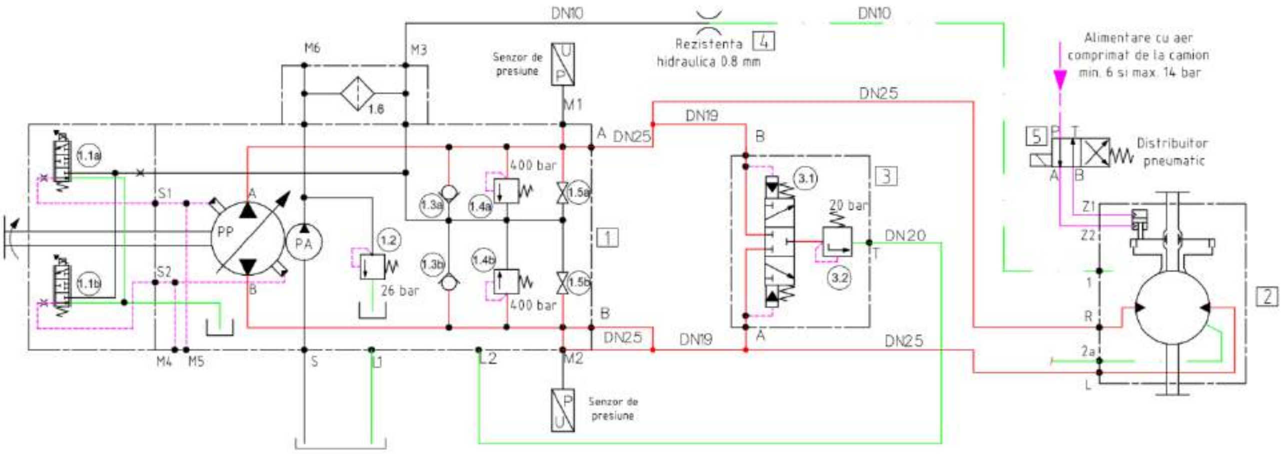

Fig. 2. Hydraulic schematic diagram of a hydrostatic transmission

Main pump PP supplies hydraulic power to the engine 2.

The PA auxiliary pump compensates for the internal losses of the two hydraulic machines and introduces cooled and filtered oil into the closed hydraulic circuit.

Reversing the discharge direction and changing the flow rate of the PP pump is done by proportional electrical valves 1.1.a and 1.1.b.

Safety valve 2 protects the PA overpressure pump.

The sensing valves 1.3.a and 1.3.b lead the flow rate of the PA pump into the low pressure branch of the closed circuit. [6]

The pressure valves 1.4.a and 1.4.b protect the two branches A and B of the closed circuit against overpressure. The valves 1.5.a and 1.5.b open when the truck is towed, and the hydro-motor 2 becomes a pump. Filter 1.6 ensures filtering of oil pumped into the system. The valve 3.1 removes from the low pressure branch of the closed circuit a quantity of oil (about 10% of the flow rate of the PP pump) coming from the hydro-motor. The extracted oil is replaced with "fresh" oil supplied by the PA pump through the filter 1.6 and the sensing valves 1.3.a or 1.3.b.

Pressure valve 3.2 maintains a pressure of approx. 20 bar on the closed circuit low pressure branch.

Part of the flow rate of the PA pump is routed through the resistor 4 to the hydromotor 2 in order to lubricate and cool it in the fast displacement phase. The pressure sensors transmit information to the electronic controller of the transmission. The pneumatic valve 5 engages / disengages the hydro-motor 2 from the shaft.

4. Energy and functional efficiency of transmission

The thermal motors fitted to multifunctional vehicles operate at maximum efficiency in the speed range of 1200 to 1800 rpm, as shown in fig. 3.

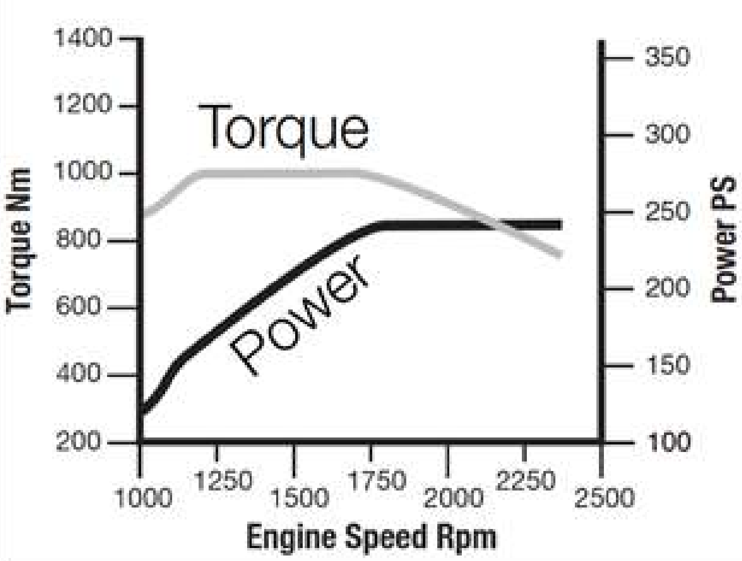

Fig. 3. Torque, power and engine speed characteristic [7]

In the maximum efficiency range, the torque developed by the engine is constant and maximum. Also, the ratio of the power / torque supplied and the fuel consumption is maximum, i.e. its energy efficiency is maximum.
Using the thermal engine at speeds below 1200 rpm: In order to achieve the very low travel speeds required by the technological needs of multifunctional equipment, one should remove the thermal engine from the working range with maximum efficiency.
Hydrostatic transmission offers what the mechanical transmission can not accomplish: low travel speeds with the thermal engine operating in the maximum efficiency range. This can be seen from the shematic diagrams shown in fig. 4.

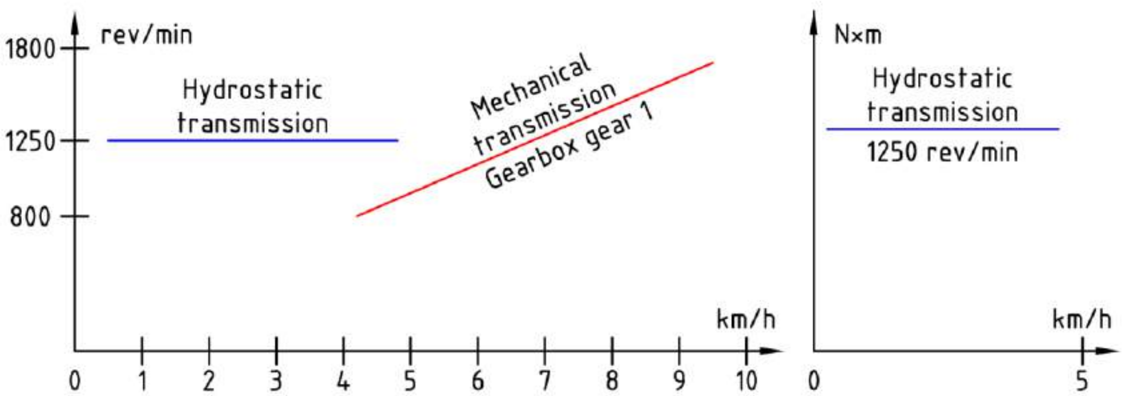

a) velocity - speed diagram
b) speed - torque diagram

Fig. 4. Comparative diagrams: mechanical vs. hydraulic transmission

It results from this figure that the hydrostatic transmission ensures that the vehicle is driven at very low speeds (0.5 ÷ 5 km / h) at an engine speed of 1250 rpm, located in the maximum efficiency range. The mechanical transmission can not achieve low travel speeds in the efficient running range of the thermal engine.

5. Numerical simulation of the multipurpose motor vehicles

The numerical simulation of the main parameters of the hydrostatic transmission has been performed using the AMESIM simulation environment [8] [9]. The simulation schematic diagram is shown in Figure 5.

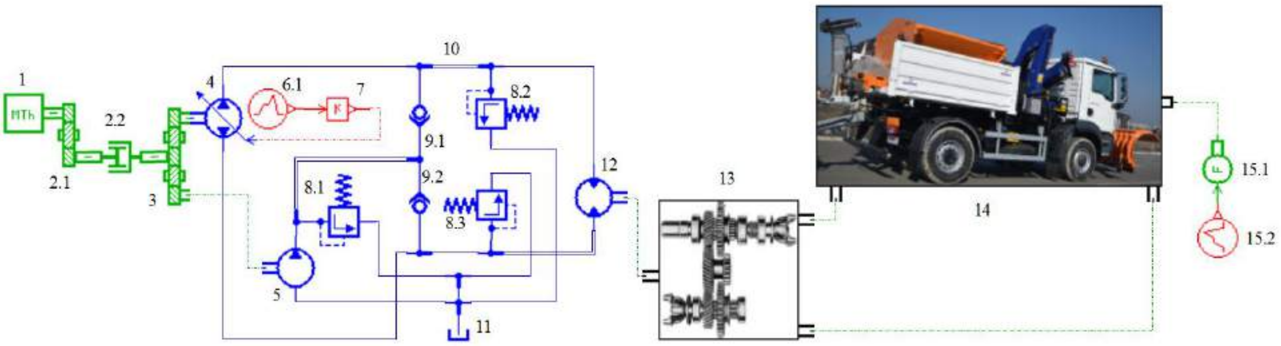

Fig. 5. Simulation schematic diagram

Table 1: Components included in the simulation schematic diagram

1 Thermal engine	8 Relief valve
2.1 Mechanical speed reducer	9 Check valve
2.2 Elastic couplings	11 Hydraulic tank
3 Mechanical node	12 Hydraulic motor
4 Variable flow pump	13 Transfer box
5 Compensation pump	14 Multifunctional motor vehicle
6.1 User-defined signal source	15.1 Conversion of signal input into a force [N]
7 Gain	15.2 User-defined signal source

The charts resulting from numerical simulation are shown in Figure 6a and Figure 6b.

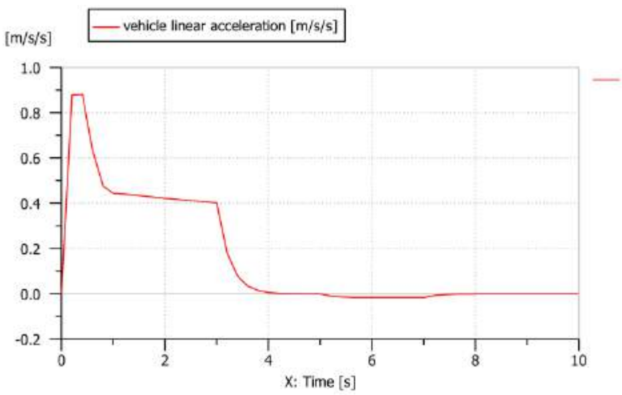

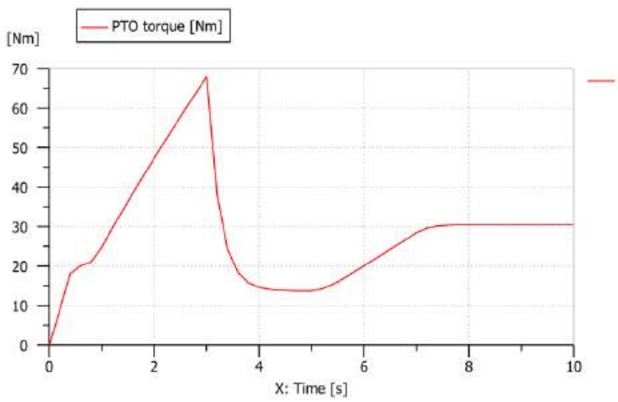

Fig. 6a. Variation of the main parameters of the simulated system

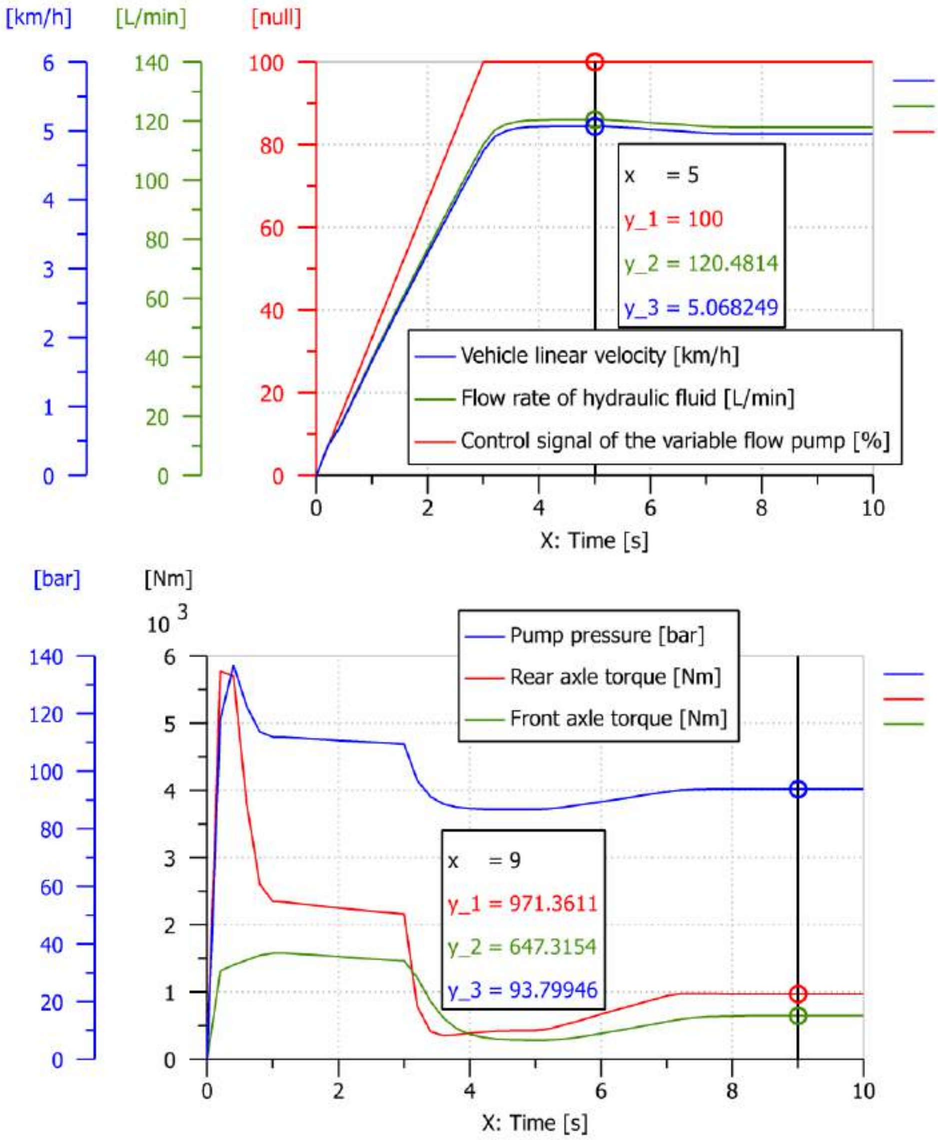

Fig. 6b. Variation of the main parameters of the simulated system

After achieving the physical model and testing it, the results obtained by simulation will be compared with the experimental ones.

6. Conclusions

For the energy efficiency of multifunctional vehicles in the very low speed technological operation mode, the article proposes the solution of the implementation of a hydraulic transmission in the kinematic chain of the truck's mechanical transmission.
Following the analysis of the proposed solution it can be concluded that the use of hydraulic transmission in the technological travel regime has the following advantages:
A) The truck can achieve lower travel speeds than those it can achieve with mechanical transmission;
B) The thermal engine operates in the maximum efficiency range even at these very low speeds.
The hydrostatic transmission ensures for the multifunctional vehicle operation performances that the mechanical transmission can not achieve: very low travel speeds at the maximum energy efficiency of the thermal motor.

Confirmation of these conclusions and the results obtained by numerical simulation will be done after the physical development and testing of the hydro-mechanical transmission model.

Acknowledgments

This paper has been developed in INOE 2000-IHP, with financial support of Executive Agency for Higher Education, Research, Development and Innovation Funding - UEFISCDI, under PNCDI III - Programme 2, Subprogramme 2.1 – Transfer project to the economic operator (PTE-2016), Submission code PN-III-P2-2.1-PTE-2016-0077, Financial agreement no. 11PTE/2016, project title: *High energy efficiency (HEE) electro hydraulic equipment (EHE) for multifunction vehicles (MFV)*, project acronym ECHIPEFEN, Project main domain: 3. Energy, Environment and Climate Change, Subdomain: 3.1. Energy.

References

[1] V. Bălășoiu, I. Cristian, Il. Bordeașu, "Hydraulic drive and automation equipment and systems" ("Echipamente și sisteme hidraulice de acționare și automatizare"), Vol. I and II, Orizonturi Universitare Publishing House, Timișoara, 2007;
[2] I.M. Oprean, C. Andreescu, "Automatic transmissions for motor vehicles", "Vol.1 – Hydraulic transmissions" ("Transmisii automate pentru autovehicule", "Vol.1 - Transmisii hidraulice"), Politehnica University of Bucharest, Romania, 1997;
[3] N. Vasiliu, D. Vasiliu, "Hydraulic and pneumatic drives" ("Acţionări hidraulice şi pneumatice"), Vol. I, Technical Publishing House, Bucharest, ISBN 973-31-2248-3, (820 p.), 2005;
[4] P. Drumea, C. Dumitrescu, Al. Hristea, A.-M. Popescu, "Energy use in hydraulic drive systems equipped with fixed displacement pumps", *Hidraulica Magazine*, Romania, issue 2, pp. 48 – 57, 2016;
[5] T.C. Popescu, D.D. Ion Guta, Al. Marin, "Adjustment of hydrostatic transmission through virtual instrumentation technique", ENERG_02, *Proceedings of ISC 2010*, June 7-9, 2010, Budapest, Hungary, ISBN: 978-90-77381-5-57, pp. 248-253;
[6] P. Drumea, C. Dumitrescu, et al., "Energy loss reduction in hydraulic systems with fixed pump in agricultural machinery", *Proceeding of the 5th International Conference of Thermal Equipment, Renewable Energy and Rural Development TE-RE-RD 2016*, Golden Sands – Bulgaria, 2-4 June 2016, ISSN 2359-7941, ISSN-L 2359-7941, pp. 221-226;
[7] ***, MAN TGM BL15R250/06 Issue Date: April 2011;
[8] ***, LMS Imagine.Lab AMESim Help;
[9] ***, MAN guide to fitting body TGL/TGM Edition 2017 v 0.1.

ISSN 1454 - 8003
Proceedings of 2017 International Conference on Hydraulics and Pneumatics - HERVEX
November 8-10, Băile Govora, Romania

CHARACTERIZATION OF AN EFFICIENT DIGITAL HYDRAULIC SYSTEM

Mohab GADOU[1], Mohamed ABDELAZIZ[1], Nabil A. MAHMOUD[1]

[1] Faculty of Engineering, Ain Shams University, Cairo, Egypt,

mohab.gadou@gmail.com, mohamed_abdelaziz@eng.asu.edu.eg , nabil_mahmoud@eng.asu.edu.eg

Abstract: *The characterization of a digital valve system is discussed in this paper. Four flow paths are used to control a double acting cylinder independently by using parallel on/off valves, a path to control each side of actuator, tank and pressure sides, each digital flow control unit (DFCU) consisting of five 2/2 on/off valves. The aim of this paper is to discuss the energy efficiency of this system by combining the digital and IMV systems. Flow capacities of valves are set according to binary coding which is to powers of two. The pros of IMV and digital systems are combined to improve the hydraulic systems' performance and to reduce power consumption and losses. Moreover, a control system is implemented to best get advantage of IMV and digital systems. Traditional proportional flow control valve has a spool to meter flow between the two sides of cylinder, pump and tank, valve is only suitable for one application. In this system many applications are suitable with different control techniques. An additional energy saving method which is the energy efficiency using a variable displacement pump. The main points to be discussed, 1) IMV and digital hydraulic advantages over traditional proportional system, 2) feasibility of combining all these energy saving methods together. The aim is to implement an efficient system with the minimum power consumption and to select the best control (won't be discussed in this paper) to achieve it.*

Keywords: *Digital hydraulic, Independent Metering Valves, Energy saving, on/off valves*

1. Introduction

The key idea is to use simple binary components and intelligent control algorithms to produce a digital equivalent to the analogue proportional- or servo valve as discussed by Arto Laamanen et al. [1].
The DVS (Digital Valve System) discussed in this paper consist of 4x5 on/off-valves which results in 220 state combinations. Five valves give good enough controllability for most applications and thus the total number of valves is typically 20. Independent metering valve realized by digital control edges consisting of parallel connected on/off-valves. Flow areas of the control edges are completely independent in the digital valve system and the valve system can implement different control modes together with simultaneous velocity and pressure control [3]. In proportional valves the spool geometry is normally in hardware and cannot be changed during operation, in digital valve this can be done when all of the four control notches are independently controllable, the valve is capable of changing the operation mode from inflow/outflow to differential mode, or vice versa. Some of these modes are regenerative. Serial Connection, Kato and Oshima [5] introduced the concept of the digital small stepping method and studied the effect pressure difference, volume size, oil temperature and cycle frequency on the step size. Parallel connection, valves in parallel give stepwise controllable velocity that yields higher maximum velocity, smaller pressure transients and better accuracy [1].
Coding determines flow rates of valves of DFCUs expressed relative to the smallest valve. Some coding schemes are binary coding (1, 2, 4, 8,16, … , 2N−1), Fibonacci coding (1, 1, 2, 3, 5, 8, … , PN−2+ PN−1) and Pulse Number Modulation (PNM) coding (1, 1, 1, 1, … , 1). The system in this paper uses binary coding, the inary-coded DFCU is similar to DA converter and output has 2N discrete values depending on which valves are open. On/off valves are not expensive, reliable, and not affected by contamination and possibly zero leak. Independent metering reduces metering losses and thus, energy consumption. Servo or proportional valves have good controllability but they give many problems, such as cavitation (To avoid cavitation and good efficiency call SMISMO control that is impossible with standard spool type valves), high power losses, sensitive to

contamination and high price. The on/off control is associated with many negativities such as noise, pressure rise, jerky motion and poor controllability motion control with slow-response valves, improved idleness and reduced durability necessity, when compared to PWM way. The response time is not critical in these applications and slow response is many times advantageous in order to reduce pressure peaks, energy efficient motion control is possible with slow-response on/off, valves Matti LINJAMA and Matti VILENIUS [2]. Plurality of similar components makes digital systems redundant, for example, failure in single valve causes only a reduction in performance not the system to fail or stop[4].

Digital components are also easier to optimize for performance because there are no requirements for linearity or hysteresis. Digital component is either ON or OFF but nothing between. Challenges of digital technology are large number of components and/or risk for jerky control. The control problem of the digital valve system is: “Select the best possible control combination of the valves at each sampling instant”. Two basic problems are how to define integrity of a control combination and how to find the best one. Good controllability requires proper design together with sufficient number of components or extremely fast components. Digital systems have always been more expensive at the beginning but mass production has made them cheaper than analogue counterparts. The control of traditional valves is simple because the control signal and spool position are closely related. The drawback is that only predefined control modes are possible and that pressure level cannot be adjusted because of the fixed ratio between flow areas [9].

In fixed displacement pumps the quantity of displaced flow by each pump shaft rotation cannot be altered. The pump's displacement is changed by varying pump’s speed. Since industrial hydraulic systems usually use invariable speed electric motors as main movers, fixed displacement pumps do not find many applications. In case of fixed displacement pump, the actuators need changing flow rates during operation so these pumps must be sized to deliver the maximum flow required. But unfortunately, when less flow is required, the extra flow from these pumps must be dumped over the system relief valve at maximum system pressure. This process converts the unnecessary energy into heat. For this reason fixed displacement pumps should only be used in constant speed applications or in systems where speed control is of short durations. Important issue is the best use of available energy resources. Using energy-saving, variable displacement pumps has contributed to overcoming that hydraulic systems are by structure not efficient. These variable displacement pumps only give flow when needed and as required. Variable displacement pumps cancel the need for flow control and pressure reducing valves.

It is necessary to use a separate control of the two fluid streams to minimize the throttling losses. The independent metering valve (IMV) concept has lately attracted interest since IMV uses a mix of multiple electro-hydraulic poppet valves (EHPV) and thus enables flow regeneration by switching among several metering modes. Another feature of IMV that EHPVs constituting IMV are electronically controlled contributes to energy efficiency through precise flow control and fast response. Load-sensing hydraulics used in mobile machinery have very low efficiency could reach low as 4% [6]. Successfully the energy losses of a wheel loader were reduced by using a digital hydraulic valve system (DVS) as an alternative for traditional Load Sensing system [7]. More efficient system could be attained by using pressurized tank line [8]. High performance digital hydraulic force, velocity and position tracking control solution has been experimentally validated [10].

2. Modeling and simulation

The system that will be discussed is depicted by the schematic diagram of fig.1

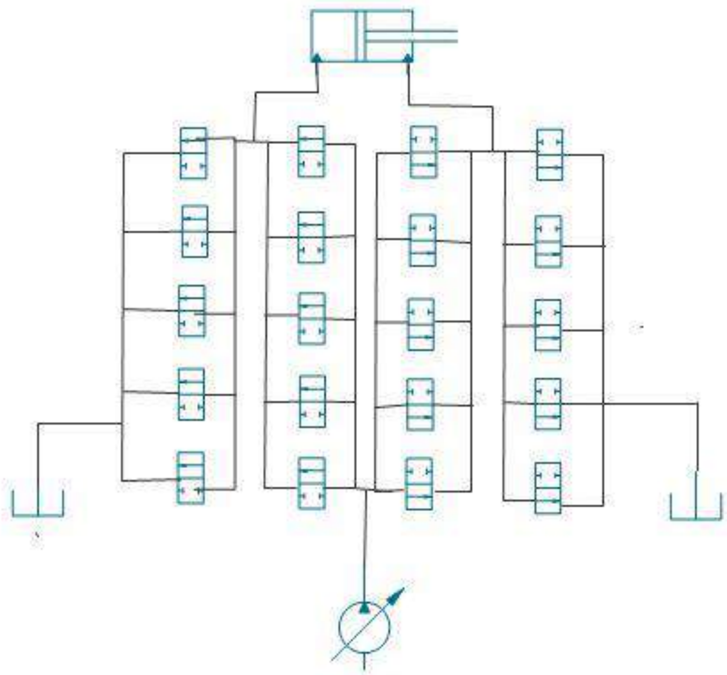

Fig. 1 system schematic diagram

The model consists of four control paths; each includes five parallel connected on/off valves. A variable displacement pump is used to help achieve the target high efficiency system, the metering modes that are discrete metering modes where valves provide a flow path and switching to another mode involves closing a valve and opening another to provide for a different flow path.

At constant load and fixed pump displacement, Low pump revolutions, velocity maximum actuator and lowest energy when PA fully opened & BT fully opened, velocity minimum actuator with highest energy at PA 2 opened & BT fully opened. Increasing pump revolutions, maximum velocity actuator increases with same findings as highest energy at minimum velocity actuator at PA 2 opened & BT fully opened and lowest energy at PA fully opened & BT fully opened. At pump max revs., maximum velocity actuator and lowest energy when PA fully opened & BT fully opened, minimum velocity actuator with highest energy at PA 2 opened & BT fully opened. Minimum velocity actuator not affected by pump revolutions as it remains constant regardless of pump rpm, lowest energy at any state except lowest pump revs. as energy slightly lower. At low pump rpm, maximum velocity of actuator could be achieved with three different states at same pump speed but with higher power consumption when increasing throttling, all by valves' switching.

Same actuator velocity could be achieved with different techniques at same pump speed as well as different pump speeds using different valves' switching. At same pump speed, highest actuator velocity is achieved when all valves in upstream side are open and downstream side also opened which mean highest pump flow rate, as long as upstream side DFCU's valves are all opened pump flow rate is max. at that pump speed but power consumption differs depending on downstream side DFCU's valves states. When pump speed increases, Vmax actuator increases and also pump flow rate with less actuator stroke time.

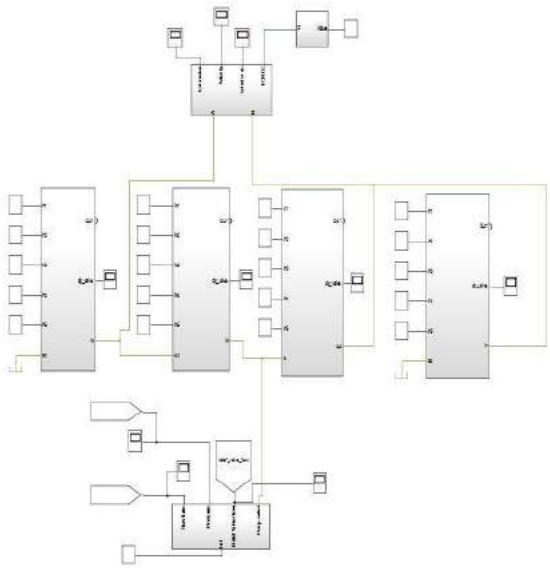

Fig. 2 Full system Matlab model

3. Discussion and results

Three cases are discussed in this paper. First case digital valve system with four DFCUs, second case digital valve system same as first system but largest orifices have been removed to decrease pressure drop over DFCUs, hence, power consumption decreased as a result, third system is a common proportional valve system. The idea behind using separate meter-in separate meter-out system (SMISMO) is achieving both pressure and velocity control. Velocity control by switching outflow side DFCU's valves and pressure compensation by inflow side DFCU's valves switching.
All three following cases achieve same velocity and extension results to be able to compare between them from different point of views.
The following figures show the power consumption (Y-axis) as function of time (X-axis) in different states depicted by the following figures. The first figure, the digital valve system where all valves are set according to binary coding as discussed before, shows highest power consumption of all three states where the pressure drop is the highest as well. Second figure, depict same digital valve system but with a modification that is, excluding the orifices in the fourth and fifth valves' lines to decreases pressure drop, hence power consumption decreased as a consequence. Third figure shows proportional valve system with lowest power consumption between the three states, only small difference in comparing with no orifice digital valve system (system depicted by figure 2). Working on the efficient digital valve system which mentioned by second case, to get the most out of SMISMO technique by first switching upstream valves pressure compensation is achieved but power consumption slightly increased.
The digital valve system with separate metering shows a great potential of further lowering power consumption even better than proportional valve system, by increasing number of parallel connected on/off valves and selecting the best control to achieve optimum result and to get the most advantages of this power saving digital valves system over the proportional valve system.

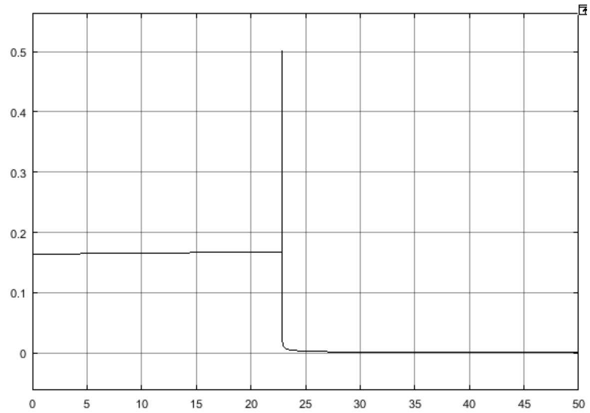

Fig. 3 With orifices

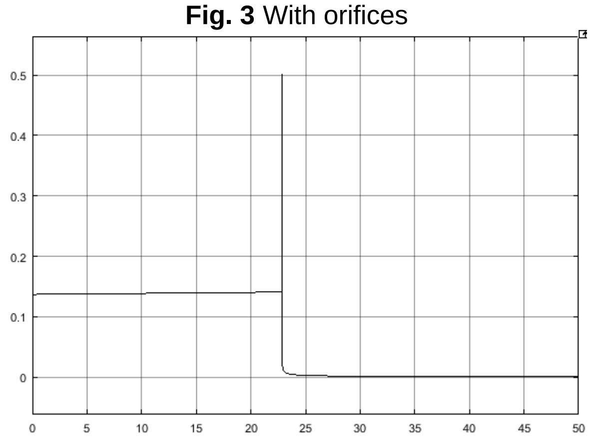

Fig. 4 Without orifices

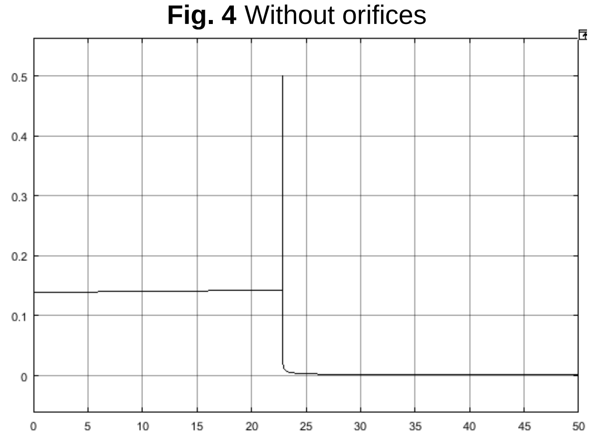

Fig. 5 Proportional Valve

A comparison table 1 is best to decide whether the digital valve system a potential power saving method or not. All three systems achieve same stroke time with same load, which means same target to select best system by least energy consuming. The table compares between the three systems discussed previously from three points of view which are pressure difference over pump, pressure difference over upstream DFCU or upstream side in case of proportional valve system, and energy consumed.

Table 1 : Comparison Table

System	dp_Pump (bar)	dp_Valve (bar)	Energy consumed (KJ)
Digital Valve_1	20	3.6	3.8
Digital Valve_2	16.5	0.59	3.2
Proportional Valve	17	0.85	3.3

By observing the comparison table, it is clear that at same conditions digital valve system_2 showed a great power saving potential and even better than proportional valve system, especially by applying new control solutions will increase power saving greatly, which will be discussed in next paper. This paper was mainly intended to study only mechanical behavior without any control solution.

References

[1] M. Linjama, A. Laamanen, M. Vilenius, Tampere University of Technology, Institute of Hydraulics and Automation, *The Eighth Scandinavian International Conference on Fluid Power, SICFP'03*, May 7-9, 2003, Tampere, Finland;

[2] M. Linjama, M. Vilenius, Institute of Hydraulics and Automation Tampere University of Technology, *proceedings of the 6th JFPS International Symposium on Fluid Power, TSUKUBA 2005* November 7-10, 2005;

[3] M. Linjama, M. Huova, M. Vilenius 2008, Online minimization of power losses in distributed digital hydraulic valve system, *Proceedings of the 6th International Fluid Power Conference*, April 1–2, Dresden, Germany, pp. 157–171 (Vol. 1);

[4] L. Siivonen, M. Linjama, M. Vilenius, 2005, Analysis of fault tolerance of digital hydraulic valve system. In: Johnston, D. N., Burrows, C. R. & Edge, K. A. (eds.) Power Transmission and Motion Control, PTMC2005, pp. 133–146 (John Wiley & Sons, Ltd., 2005);

[5] N. Kato, S. Oshima, 1999, A Method of Digital Small Stepping Drive of Hydraulic Cylinder,*48th annual symposium by Tokai branch of JSME*, No.993-1, pp. 183–184 (in Japanese);

[6] T. Virvalo, M. Vilenius, The influence of pumps and valves on the efficiency of a hydraulic boom. Cracow, Poland: *Development in Fluid Power Control of Machinery and Manipulators*, 2000;

[7] M. Huova, M. Karvonen, V. Ahola, M. Linjama, M. Vilenius, Energy efficient control of multiactuator digital hydraulic mobile machine. In: *The 7th international fluid power conference (IFK),* Aachen, Germany; 2010;

[8] M. Huova, M. Linjama, Energy efficient digital hydraulic valve control utilizing pressurized tank Line. In: *The 8th international fluid power conference (IFK),* Dresden, Germany, 2012;

[9] M. Linjama, On the numerical solution of steady-state equations of digital hydraulic valve-actuator system, *The Eight Workshop on Digital Fluid Power*, May 24-25, 2016, Tampere, Finland;

[10] M. Linjama, M. Huova, O. Karhu, K. Huhtala, High-Performance Digital Hydraulic Tracking Control of a Mobile Boom Mockup, *10th International Fluid Power Conference, Dresden 2016*.

ISSN 1454 - 8003
Proceedings of 2017 International Conference on Hydraulics and Pneumatics - HERVEX
November 8-10, Băile Govora, Romania

DIGITAL LINEAR HYDRAULIC MOTORS

Petrin DRUMEA[1], Ioan PAVEL[1], Gabriela MATACHE[1], Ioan BALAN[1]

[1]Hydraulics and Pneumatics Research Institute INOE 2000-IHP; ihp@fluidas.ro

Abstract: *This paper presents a different approach to variation in force and speed of linear hydraulic motors by using multiple-area digital linear hydraulic motors. The article presents multiple-area digital hydraulic cylinder solutions, a stand solution for functional testing, schematic diagram and testing methodology for multiple-area digital hydraulic cylinders.*

***Keywords**: Multiple-area cylinders, digital cylinders, digital hydraulics, digital cylinder test stand, multiple-area cylinder testing methodology*

1. Introduction

Hydrostatic drive is a basic element of complex technologies that are used in the manufacturing, servicing and maintenance industries, but also in many other industries. This technology, according to ISO 5598, refers to the methods and equipment through which signals and energy are conveyed, controlled and distributed by means of a pressurized fluid.
The general structure of a hydraulic drive system, in which energy types can be highlighted, is shown in Figure 1. The thermal or electric energy is converted into hydraulic energy, transmitted to a hydraulic motor, which converts it into mechanical work.

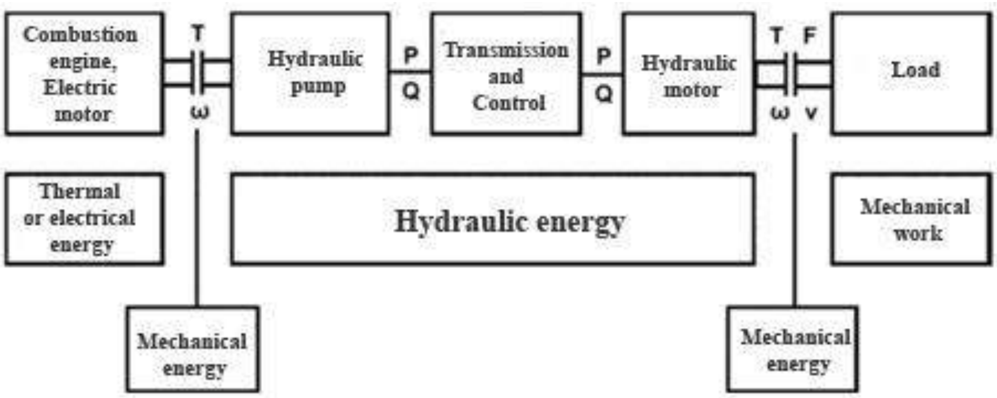

T= Rotative speed, Ω= Torque, P= Pressure, Q= Flow, F= Force, V= Speed

Fig. 1. The general structure of a hydraulic drive system [1]

The final element acting as actuator in a system is the hydraulic motor, which converts hydraulic energy into mechanical energy, type rotative speed and torque (rotary motors) or force and speed (linear motors). The task of performing a translation-rectilinear movement simultaneously with the transmission of force is accomplished by a cylinder with a minimum of structural elements and high power density.
The hydraulic cylinder is the most known equipment in the field of hydraulic drives, as it is also the most widespread execution element of a drive installation and in most cases it is the starting point for the design of the entire hydraulic installation.
The possibilities to vary force and speed along the stroke, as well as the possibilities of using different gripping modes, combined with various levers and joints, make the hydraulic cylinder an indispensable element in most machines and equipment involving hydraulic drives.
In terms of the way in which the drive is performed, namely the way in which the fluid acts on the sides of the piston, power cylinders may be single or double acting.

In terms of the ratio of rod diameter and piston diameter, they can be:
- cylinders with the diameter of the piston greater than the diameter of the rod;
- cylinders with piston diameter equal to that of the rod, that is cylinders with plunger pistons.

More recently, a branch of the Hydraulics studies new solutions for multiple-area digital hydraulic cylinders.

2. Multiple-area digital hydraulic cylinders

Digital Hydraulics refers to systems that use binary components connected in parallel or switching control elements which have certain discrete input values and can actively control the system. A system is considered to be digital if it has at least one digitally controlled item.

A digital version for the active control of speed and force in a hydraulic system with constant pressure and flow is the multiple-area digital hydraulic cylinder. The constructive solution is studied in a large number of papers and it involves dividing the active surface of the piston into multiple surfaces with equal areas or with values multiplied following well established rules (Fig. 3 c,d or e), which are powered separately but also cumulatively, to achieve combinations of powered areas with which an active speed or force control on the cylinder stem is obtained. Selecting combinations of supplied areas ensures a relatively linear movement with variable speeds or loads, with possibilities for active control but also secondary control (with energy recovery), thus meeting the energy requirements of a hydraulic system.

The literature offers several examples of theoretical solutions for multiple-area cylinders:

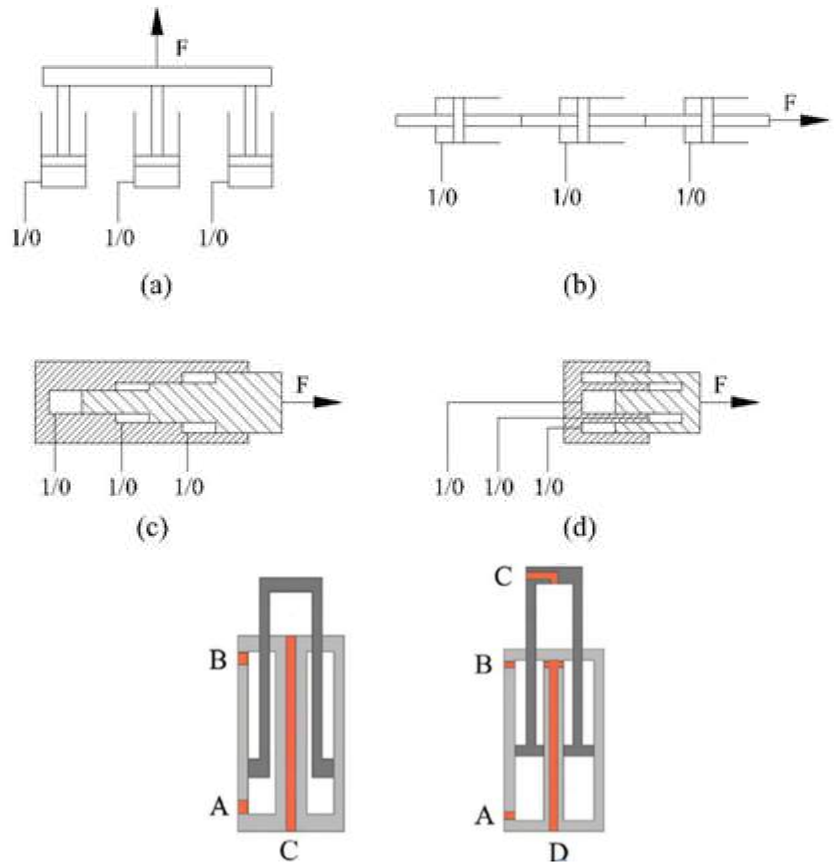

(e)

Fig. 2. Examples of solutions for multiple-area cylinders
serial cylinders; b) inline cylinders; c),d),e) concentric area cylinders [3], [4]

Driving of multiple-area cylinders can be done by using pairs of on / off devices, Fig. 3, or by means of classic equipment, Fig. 4, depending on the system requirements.

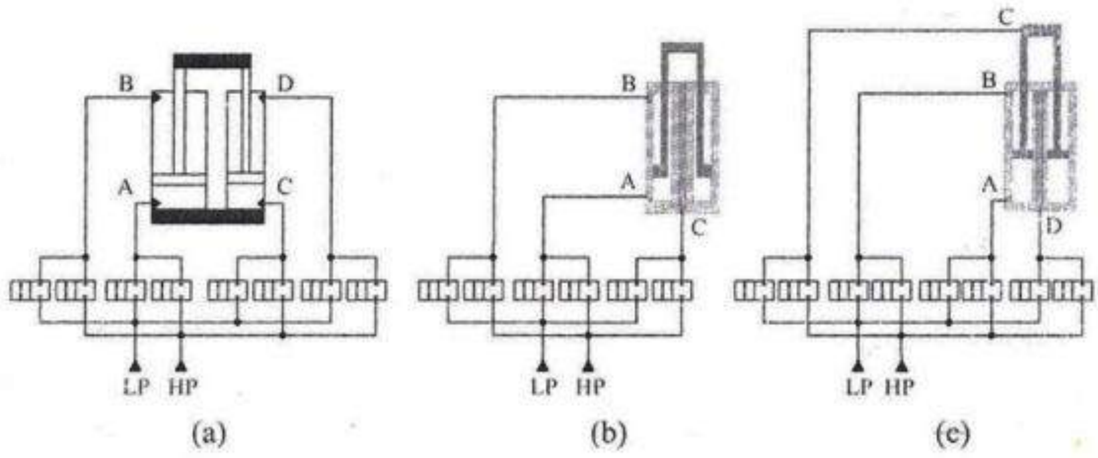

Fig. 3. Driving of multiple-area cylinders by means of on / off devices [2]
LP= low pressure line, HP= high pressure line

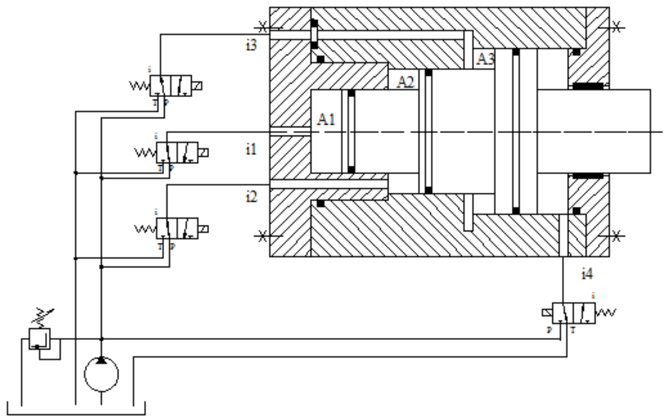

Fig. 4. Driving of multiple-area cylinders by means of classic equipment [2]

A fundamental characteristic of parallel connected digital hydraulic systems is that the output is quantified. The actual number of output values depends on the number of components and coding method. There are several methods for coding the surfaces of a digital cylinder, but the most important are:

- Surface is divided into surfaces of the same value - Modulation Number Pulse (PNM coding)
- The divided areas are in a ratio according to the binary series, 1: 2: 4: 8, etc.
- The divided areas are in a ratio according to the Fibonacci method, 1: 1: 2: 3: 5: 8: 13, etc.

All methods result in a step flow curve (graph), where step size is constant and inversely proportional to the number of items used.
Of the three solutions, the lowest number of output values is obtained by using the method of components of the same size, and the number of output values is N^{+1}. This method is known as Modulation Pulse Number (PNM coding).
Another coding method is following a binary code (divided surfaces with area ratios 1: 2: 4: 8, etc.), where each status combination gives a different output value. If the cylinder has "n" divided surfaces, each having two statuses (to pressure or to the tank), the total number of status combinations is 2^{n-1}. Each of the status combinations can give a different output in the system

and thus the maximum number of output values is equal to the number of status combinations. Fibonacci coding is a method between the PNM and the binary coding.[5]

The team of specialists within INOE 2000-IHP has filed two patent applications for two digital hydraulic cylinder solutions: one solution (Fig. 5) which involves dividing the piston area into three concentric areas multiplied binary [6], technically and technologically feasible, and the other solution (Fig. 9), compact, which involves dividing the piston area into nine equal areas [8], symmetrically arranged around the axis of the main piston. Also, there have been developed within the "Nucleu" project [7] several technical solutions for digital hydraulic cylinders with concentric areas multiplied binary.

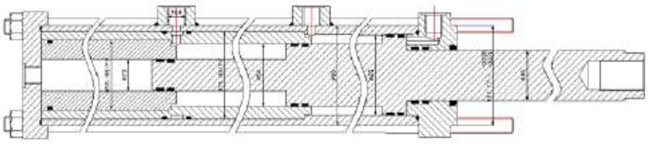

Fig. 5. Patented solution for a digital hydraulic cylinder with three binary coded areas [6]

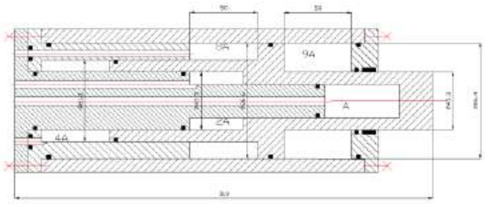

Fig. 6. Solution for a digital hydraulic cylinder with four binary coded areas [7]

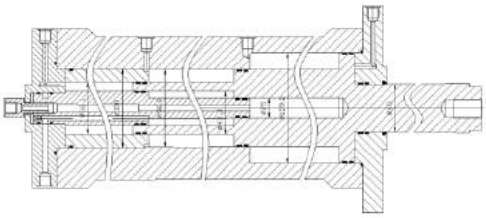

Fig. 7. Solution for a digital hydraulic cylinder with five binary coded areas [7]

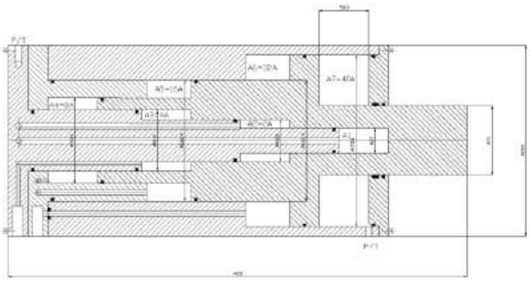

Fig. 8. Solution for a digital hydraulic cylinder with six binary coded areas [7]

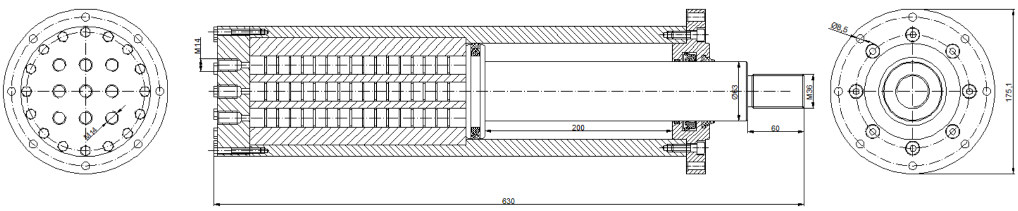

Fig. 9. Patented solution for a digital hydraulic cylinder with nine equal areas, PNM coding [7], [8]

3. Hydraulic digital cylinder test diagram and procedure

As a technical means of measuring the quality of digital hydraulic cylinders there is used the hydraulic stand shown in Fig. 10, which is able to provide the test conditions required for subjecting the digital hydraulic cylinders to functional tests and determination of the technical designed characteristics.

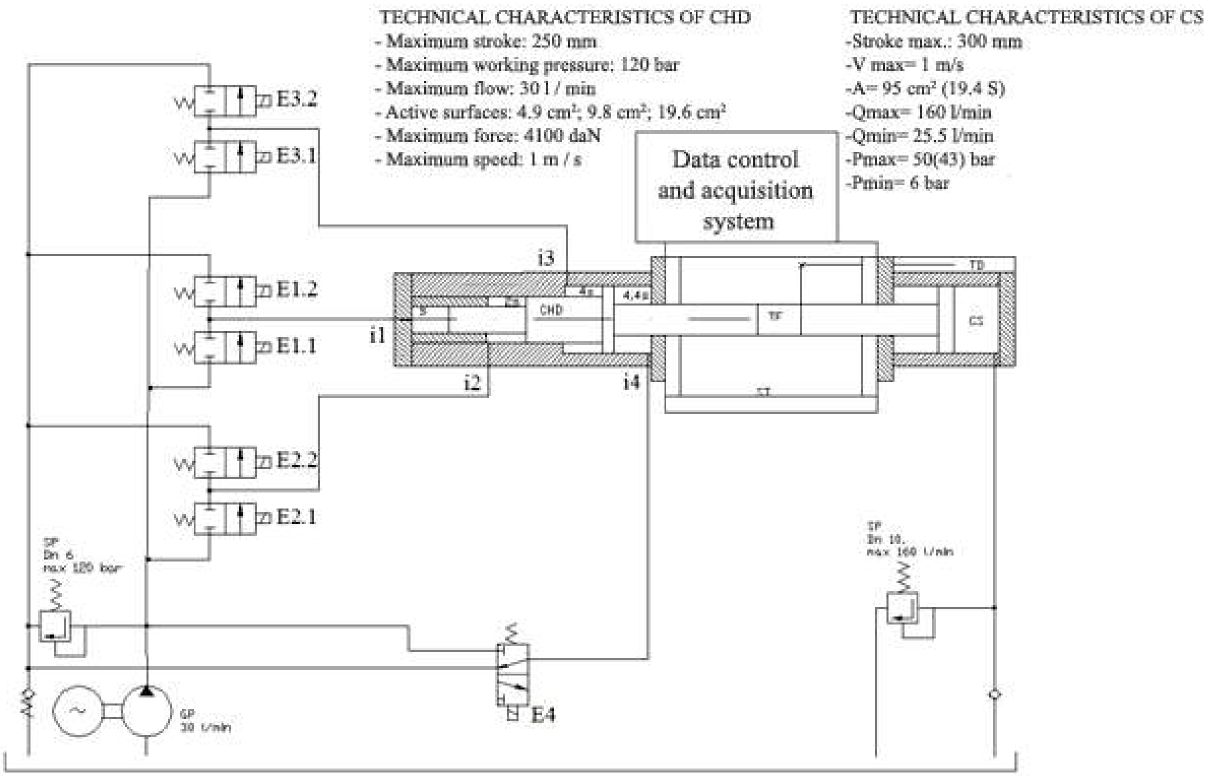

Fig. 10. Diagram of digital hydraulic cylinder test stand

Caption:
CHD- Digital Hydraulic Cylinder
CS- Load Cylinder
TF- Force Transducer
TD- Displacement Transducer
SP- Pressure Valves
GP- Pumping Unit
ST- Test Stand
E1-4 – Electromagnets

Because of dividing of their active area, multiple-area cylinders cannot be tested according to standard methodology; that is why it is necessary to conceive a set of tests inspired from the mentioned methodology, through which to verify the technical characteristics designed and demonstrate the basic idea that at constant pressure and flow supply there are achieved (by selecting combinations of areas), at the digital hydraulic cylinder rod, actively controlled force and speed values, repeatable according to specified graphs.
Testing is conducted on a specialized device, as depicted in Fig. 11, composed of:
- load cylinder (1) which creates the simulated load;
- force transducer (2), for active control of the force adjusted to the cylinder under testing;
- displacement transducer (3) for active control of the speed adjusted to the cylinder under testing;
- frame (4).
The two transducers also enable data acquisition.

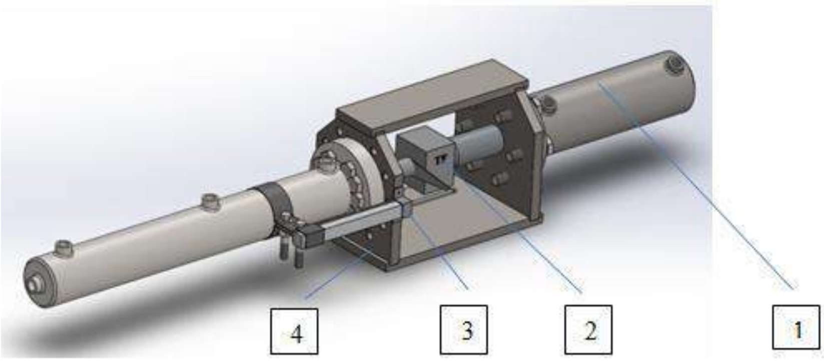

Fig. 11. Multiple-area cylinder test device [7]

The stand consists of a frame (4) which allows direct grip or attachment through an adaptive flange of a wider range of digital hydraulic cylinder.

Between the rods of the two cylinders there is positioned the force transducer (2), and the position transducer (3) is fixed on the side. The data control and acquisition system is located next to it. Configuration of the connection of the control components and configuration of hydraulic connections will vary depending on the type of cylinders under tests and the test to be performed, according to the testing methodology presented below.

Testing of multiple-area digital cylinders at variable forces and speeds with constant pressure and flow is done by selecting combinations of surfaces.

The successive sequences of the tests are as follows [9]:

- re-check that the stand and the equipment mounted on it correspond to the mounting diagram;
- check exterior tightness;
- check interior tightness;
- check starting pressure and minimum idling pressure;
- force tests are carried out; F=f(Ai) at constant pressure;
- speed tests are carried out; V=f(Ai) at constant flow.

The tests on digital hydraulic cylinders are performed as follows:

Checking of the exterior tightness is performed to the test pressure of:

- p_{min}
- 0.5 $p_{n,}$ but no more than 50 bar
- 1.25-1.5 $p_{n,}$ but no more than 1.1 $p_{max.}$

after performing five double strokes at the minimum speed (all areas are active).

During the tests, to the outside of the cylinder behind the sealing and scraping system no visible oil traces shall occur which increase over time. It is admissible an oil film under the condition of not agglomerating in the form of drops on the piston rod. The result of the measurements is listed on the test data sheet.

Checking of the interior tightness is usually done in the extreme positions of the piston and in three to five intermediate points located equidistant along the entire stroke of the piston at the test pressure p_i= 1.25-1.5 p_n but no more than 1.1 p_{max},, for 1 minute for each area of the multiple-area cylinder. For the 3-area cylinder commands corresponding to the control code 1,2 and 4 are executed, and for the 5-area cylinder commands corresponding to the control code 1,2,4,8 and 16 are executed; the control codes are listed in the command cyclogram of each of the cylinders.

For each position the internal losses are estimated by reading the indications of the stroke transducer (or comparator) for 1 min. Displacement of the rod is not admissible. The measurement result is added to the test sheet.

Checking of the minimum pressure for uniform and shock-free movement of the piston and checking of the starting pressure are done in idling. The working chambers are filled with oil at the ambient temperature at which the test is carried out and kinematic viscosity ν=35 cSt. All surfaces of the multiple-area cylinder are connected to a source of oil under pressure according to the test diagram. There is recorded the lowest pressure at which the piston displacement with minimum speed occurs and also the pressure for which the piston has a smooth motion without shocks for each surface of the multiple-area cylinder but also on all the summed surfaces, over the entire length of the stroke. For the 3-area cylinder commands corresponding to the control code 1,2,4 and 7 are executed, and for the 5-area cylinder commands corresponding to the control code 1,2,4,8,16 and 31 are executed; the control codes are listed in the command cyclogram of each of the two cylinders. Uniformity of the piston displacement speed is checked by means of a recorder. The measurement result is added to the test sheet.

Checking of the thrust force is made at constant pressure by selecting combinations of sections of the multiple-area digital cylinder, over the entire length of the stroke. Force is measured by means of force transducers with precision class of at least 1 on a stroke sector corresponding to pressure and force stabilization. The resistance-type load is created by means of a hydraulic cylinder powered by a separate hydraulic installation, low pressure, and it can be continuously varied through the adjustable pressure valve. Measurement is made to determine the force variation depending on the combination of selected areas, F=f(Ai) at constant pressure. Check commands are made according to the command cyclogram, successively for all combinations along the advance rod stroke. The measurement result is listed on the test sheet and compared to the expected result.

Checking of the piston speed is made at constant flow; the displacement must be carried out under load, smoothly and without shocks over the entire length of the stroke. Verification is done for each combination of surfaces of the multiple-area cylinder but also on all the summed surfaces, along the advance rod stroke. Measurement is made to determine the speed variation depending on the combination of selected areas, V=f(Ai) at constant flow. Check commands are made according to the command cyclogram. The measurement result is listed on the test sheet and compared to the expected result.

The command cyclogram to plot the graph of F=f(Ai), at p=ct and V=f(Ai), at q=ct for a three-area CHD: F corresponds to the force obtained with the smallest area at constant pressure, and V corresponds to the speed achieved with constant flow for the smallest section.

Control code	Input commands							Output values	
	s		3 s		3.76 s		4.2 s	Force	Speed
	E1.1	E1.2	E2.1	E2.2	E3.1	E3.2	E4		
0	0	0	0	0	0	0	0	0	0
1	1	0	0	1	0	1	0	1F	1V
2	1	0	1	0	0	1	0	3F	0.33V
3	1	0	1	0	0	1	0	4F	0.25V
4	1	0	0	1	1	0	0	4.76F	0.2V
5	0	1	1	0	1	0	0	6.76F	0.16V
6	1	0	1	0	1	0	0	7.76F	0.14V
Retraction	0	1	0	1	0	1	1	4.4F	0.227V
Energy recovery (retraction with external load; secondary control)									
-1	1	0	1	0	0	1	1	0.2F	0.227V
-2	0	1	0	1	1	0	1	0.44F	0.227V
-3	0	1	1	0	0	1	1	1.2F	0.227V
-4	1	0	0	1	0	1	1	3.4F	0.227V

Fig. 12. The command cyclogram [7]

1. Expected results for rod advance:

a) For: F=f(Ai)

F=P x S

Where: F- Force; P-Pressure (constant); S-Surface (variable)
We obtain the proportional force corresponding to the command code.

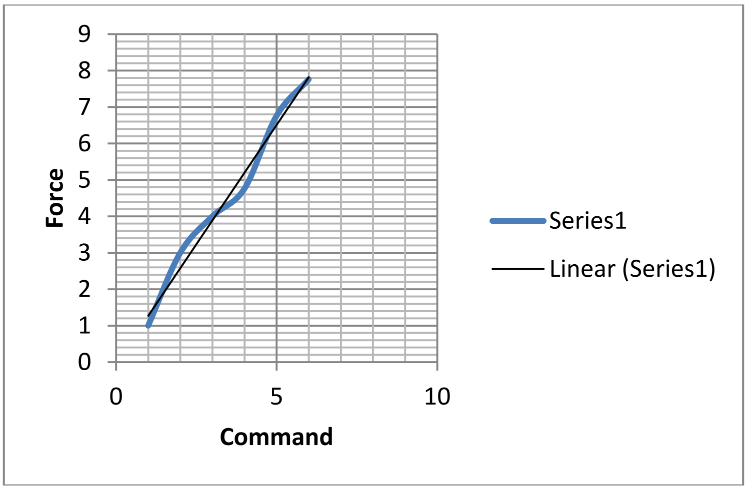

Fig. 13. Expected results for rod advance (1) [7]

b) For: V=f(Ai)

V= $\frac{Q}{S}$

Where: V- Speed; Q- Flow (constant); S-Surface (variable)
We obtain the proportional speed corresponding to the command code.

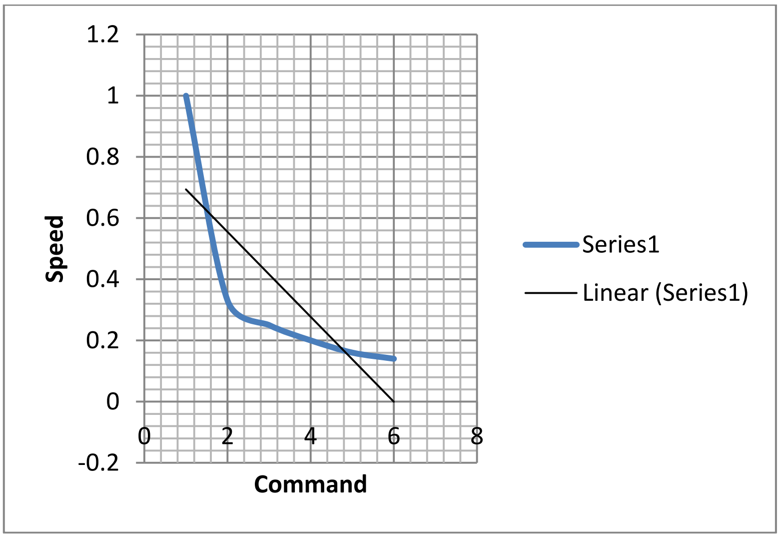

Fig. 14. Expected results for rod advance (2) [7]

2. Expected results for energy recovery in the case of retraction with external load (secondary adjustment):

a) For force

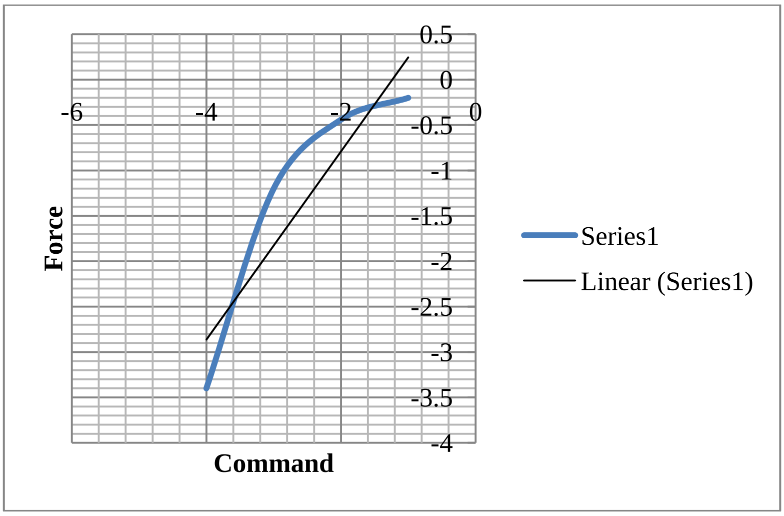

Fig. 15. Expected results for rod retraction (1) [7]

b) For speed

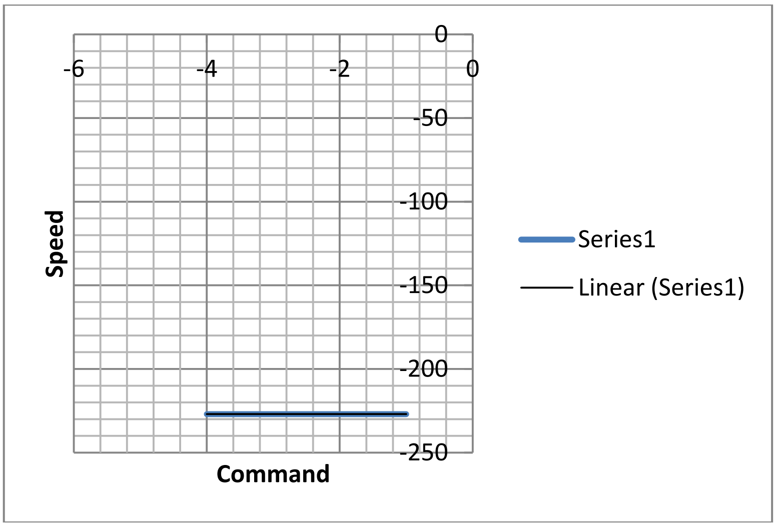

Fig. 16. Expected results for rod retraction (2) [7]

The tests will be performed according to the testing methodology for multiple-area digital cylinders, using the stand, testing diagrams, and control system codes. The data will be acquired and a test report for the tests performed will be elaborated. The aim will be to demonstrate the idea that the digital hydraulic cylinder is supplied with constant pressure and flow and there are obtained variable forces and speeds, controllable by selecting surface combinations according to the command cyclogram for tracing the graphs of F=f(Ai), at p=ct and V=f(Ai), at q=ct.

4. Conclusions

The basic idea in promoting and implementing digital hydraulic cylinders is to replace the expensive and sensitive servo cylinders by multiple-area cylinders with an assembly of multiple on/off directional control valves, which are cheap and reliable. Digital technology has the potential

to create cheaper, more energy-efficient and more reliable hydraulic systems, but a decisive role will be played by research and technological development in the field. For the digital hydraulic cylinder segment the challenge lies in developing simple, technologically achievable, more compact and cheaper technical solutions. The emergence of experimental models of multiple-area digital hydraulic cylinders required the establishment of a functional testing methodology and their testing diagrams and this paper tries to meet this requirement.
Over the next period, cost reductions and increased energy efficiency will be dominant as success factors for any industry. Currently, the hydraulics industry is not fit to meet these requirements: classic hydraulic systems and components are rather expensive and energy-inefficient. Correct dimensioning and choosing the best technical and economic solutions could make the hydraulic systems the fastest and most efficient form of power transmission. Energy savings resulting from the implementation of digital hydraulic solutions can improve the technical and economic performance of the technology lines in which they are used, reflecting ultimately in the execution price of the products put on the market. At the same time, through energy savings and efficient use of resources, they contribute to the foundations of sustainable development [10].

References

[1] Assofluid, "Hydraulics in industrial and mobile applications", Publisher: Grafiche Parole Nuove – Brugherio (Milano), 2007;
[2] P. Drumea, I. Pavel, G. Matache, "Digital hydraulic motors", *Proceedings of 2016 International Conference on Hydraulics and Pneumatics – HERVEX*, November 9-11, Baile Govora, Romania, ISSN 1454 – 8003, pp. 50-55;
[3] P. Drumea, R. Rădoi, B. Tudor, I. Bordeașu, "Digital hydraulics solutions", *Proceedings of 2016 International Conference on Hydraulics and Pneumatics – HERVEX*, November 9-11, Baile Govora, Romania, ISSN 1454 – 8003, pp. 73-79;
[4] M. Linjama, H.-P. Vihtanen, A. Sipola, M. Vilenius, "Secondary controlled multi-chamber hydraulic cylinder", *The 11th Scandinavian International Conference on Fluid Power, SICFP'09*, June 2-4, 2009, Linköping, Sweden, vol. 1, 15 p.;
[5] M. Linjama, "Digital fluid power – State of the art", *Proc. of The Twelfth Scandinavian International Conference on Fluid Power*, Volume 2(4), SICFP'11, May 18-20, 2011, Tampere, Finland; pp.331-354;
[6] P. Drumea, I. Pavel, G. Matache, Patent application no. A/00779 on 01.11.2016;
[7] Project of INOE 2000 IHP, PN 16-40-03-01, 'Physics of processes for reducing energy losses and developing renewable energy resources by use of high-performance equipment", phase no.3.1.1, phase name "Theoretical and experimental research on models of linear hydraulic motors as a digital concept*"*;
[8] I. Balan, R. Radoi, Al. Hristea, I. Pavel, Patent application no. A/00648 on 14.09.2017;
[9] I. Pavel, R. I. Rădoi, Al.-P. Chiriță, M.-Al. Hristea, B. Al. Tudor , "Technical Solutions for Digital Hydraulic Cylinders and Test Methods", "HIDRAULICA" (No. 3/2017) Magazine *of Hydraulics, Pneumatics, Tribology, Ecology, Sensorics, Mechatronics,* ISSN 1453 – 7303, pp. 41-49;
[10] I. Pavel, B. Tudor, M. Al. Hristea, A.-M. Popescu, "Maintaining Position of Servo Cylinders by Means of Digital Hydraulics", "HIDRAULICA" (No. 2/2017), Magazine of Hydraulics, Pneumatics, Tribology, Ecology, Sensorics, Mechatronics, ISSN 1453 – 7303, pp. 62-67.

ISSN 1454 - 8003
Proceedings of 2017 International Conference on Hydraulics and Pneumatics - HERVEX
November 8-10, Băile Govora, Romania

DETERMINATION OF THE INDUCED STRESS STATE IN AN ALUMINIUM ALLOY COUPLING BAR FOR ROAD VEHICLES BY USING FEM

Liviu Daniel PIRVULESCU[1], Liviu MARSAVINA[2]

[1] Polytechnic University of Timisoara, Mihai Viteazul No.1, 300222, Timisoara, Romania, e-mail: liviu-daniel.pirvulescu@upt.ro

[2] Polytechnic University of Timisoara, Mihai Viteazul No.1, 300222, Timisoara, Romania, e-mail: liviu.marsavina@upt.ro

Abstract: *The work present the stress state analyzes in an aluminum coupling bar for the rear axle of the Mercedes Benz S320 model W140 car, with mass of 2500 kg, by using the finite element method and the program ANSYS. The results obtained by ruling the program lead to the conclusion that at the inferior part of the coupling bar curvature, the tension does not overcome 80 MPa which corresponds from the point of view of the car safety, because the value is smaller than the yield point of the material.*

Keywords*: aluminium alloy, coupling bar, stress*

1. Introduction

The use of light alloys, such as those based on aluminum, gain more and more ground in modern technology because their advantages, such as: small unit weight, good cast ability and easy to be work out [1], [2]. The essential characteristics of a rear axle are the compactness and the ability to maintain the vehicle stability. The role to maintain the wheels in permanent contact with the ground remain for the suspension and the axle [3]. To meet the above requirements, for luxury cars were adopted independent axles, allowing for each wheel to oscillate independent from the other ones. By the number of coupling rods (in our case 4) and their disposal, it was assured the desired comfort and stability as well as the reduction of the undesired liberty degrees for the wheels. By eliminating the mentioned negative effects, the movement of the car runs without perturbations, and the passengers have the sensation of “floating” over the road.

2. Researched material

The analyzed rod is a component of the Mercedes Benz S320 rear axle which, together with the steering knuckle sustains the car body fig. 1, position 92.

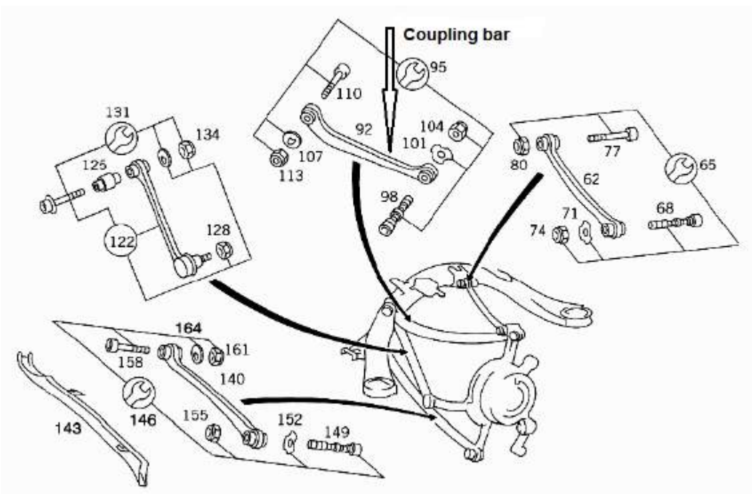

Fig. 1. The scheme of rear axle ensemble

The material from which the rod is manufactured is an aluminum alloy AlZn5.5MnCu with the following mecanical characteristics, determined in the Timisoara Polytechnic University Laboratory for Material Strength:

- Elastic module: $E = 71500\ MPa$
- Coefficient of transverse contraction: $\nu = 0{,}33$
- Yield limit: $R_{p\ 0{,}2} = 495\ MPa$
- Fracture strength: $R_m = 574\ MPa$
- Breaking tenacity: $K_{I_c} = 13{,}27\ MPa\sqrt{m} = 419{,}63\ MPa\sqrt{mm}$

3. Tension state analyze with FEM

The stress state analysis can be done by one of the following methods: analytical, numerical, and experimental [4, 5, 6, 7]. On a large scale is used the Finite Element Method (FEM) which, even providing approximate numeric solutions, is very accurate and the results are close to the real ones. The shape and dimensions of the aluminum rod is presented in fig. 2.

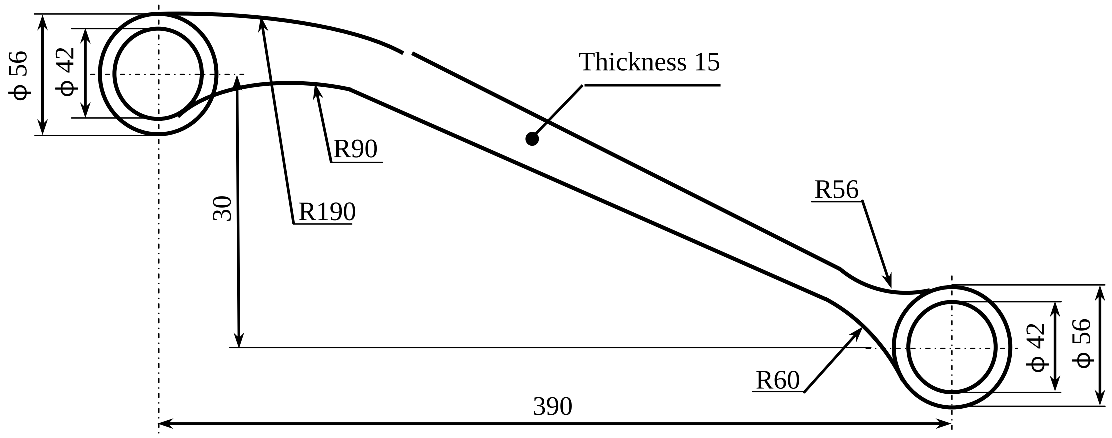

Fig. 2. The rod constructive solution

The rod numeric analyze was realized with the ANSYS FEM program [8]. For an accurate modeling of the load transmitted to the rod, we consider that it is realized through a bolt with distributed load. In conformity with [4] the load definition was done on the half of the orifice surface, being 0 (zero) for the extremities and p_{max} for the middle, fig. 3, and the maximum value is obtained with the relation (1).

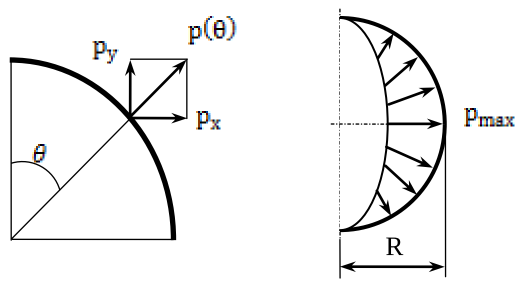

Fig. 3. Scheme of the load distribution

$$p_{max} = \frac{F \cdot \pi^2}{16 \cdot R \cdot t} = \frac{1000 \cdot \pi^2}{16 \cdot 21 \cdot 15} = 1{,}96\ MPa \qquad (1)$$

where:
F = the transmited force
R = radius of rod
t = rod thickness
The finite element meshing, fig. 4 was realized with 1872 SOLID elements, having 107703 finite elements nodes.

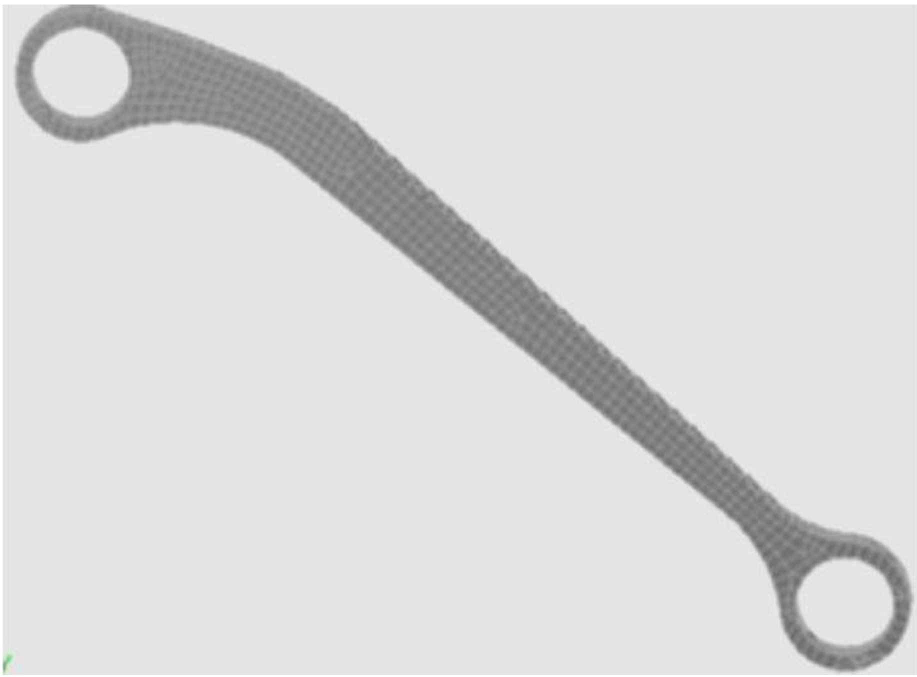

Fig. 4. Finite element meshing

The rod is mounted on the rear axle by two pins introduced in the fixing holes and the bearing conditions are presented in fig. 5.

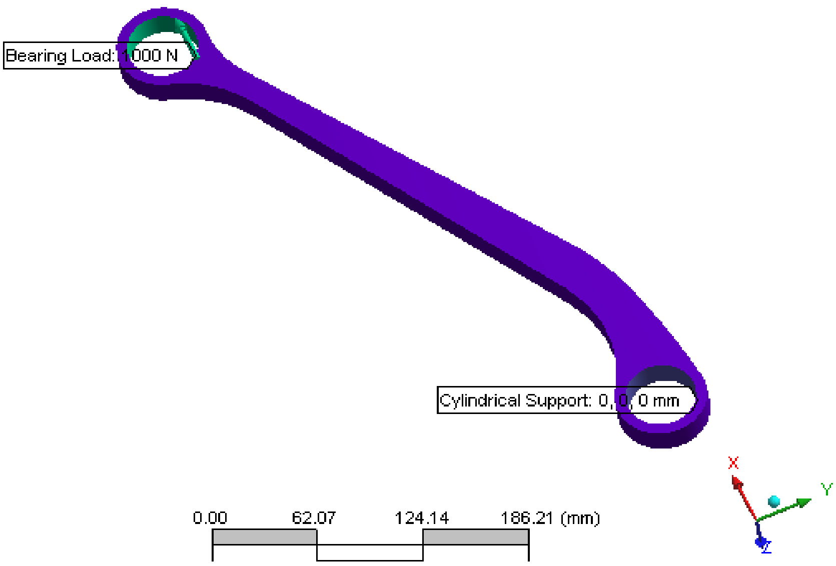

Fig. 5. Bearing conditions

Running the computation program there were obtained the normal stresses after the three orthogonal directions $\sigma_x, \sigma_y, \sigma_z$ *and* $\sigma_{ech\,VM}$, which are presented in fig. 6.

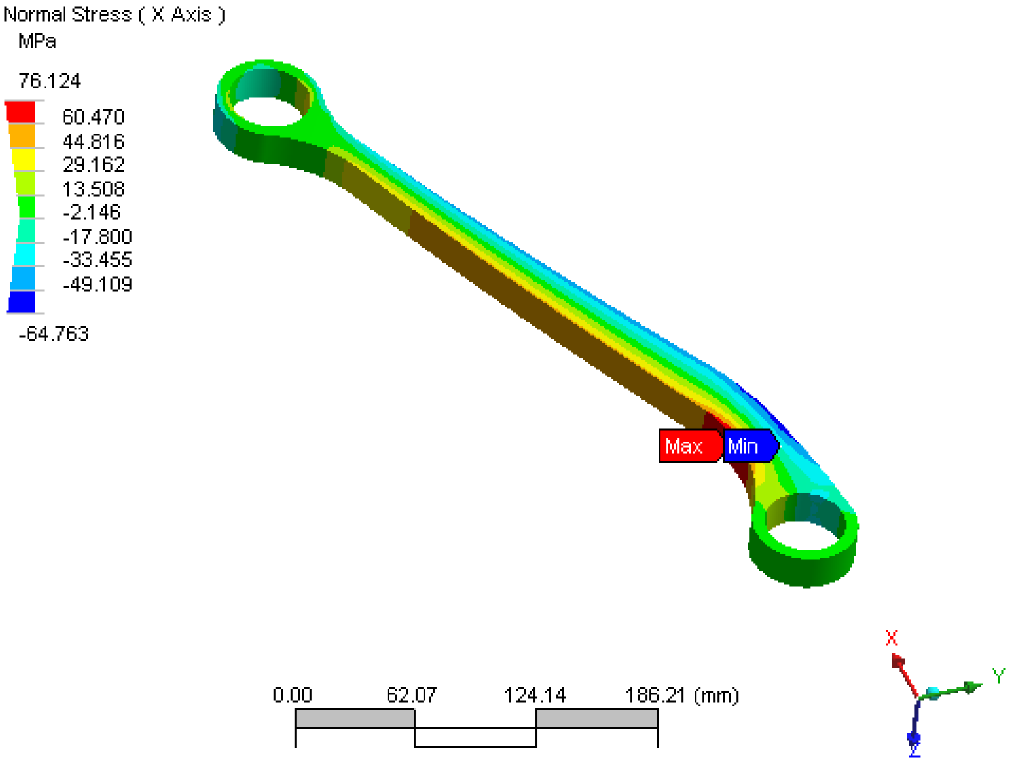

6a) Ox axes normal stresses

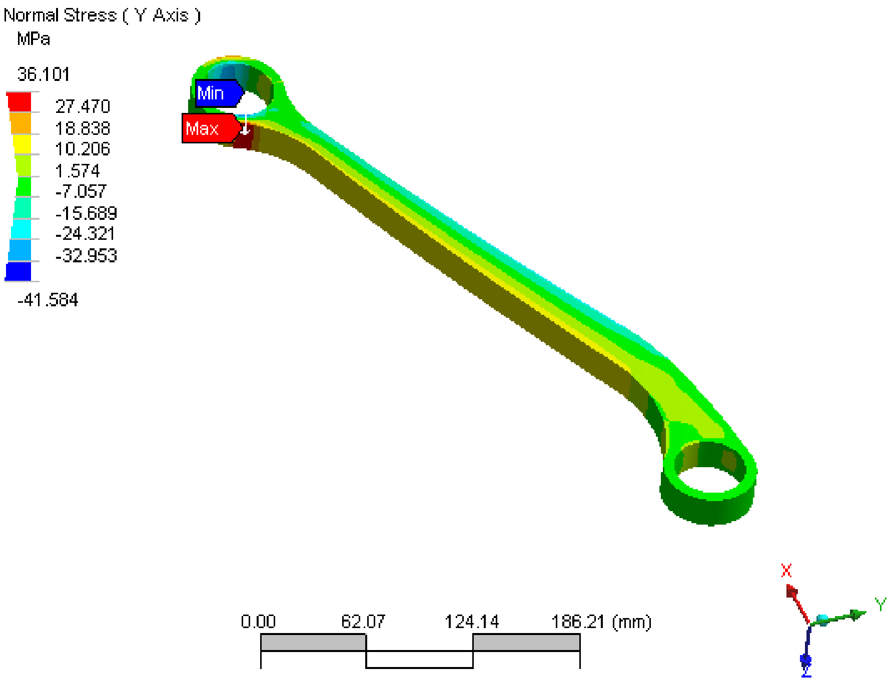

6b) Oy axes normal stresses

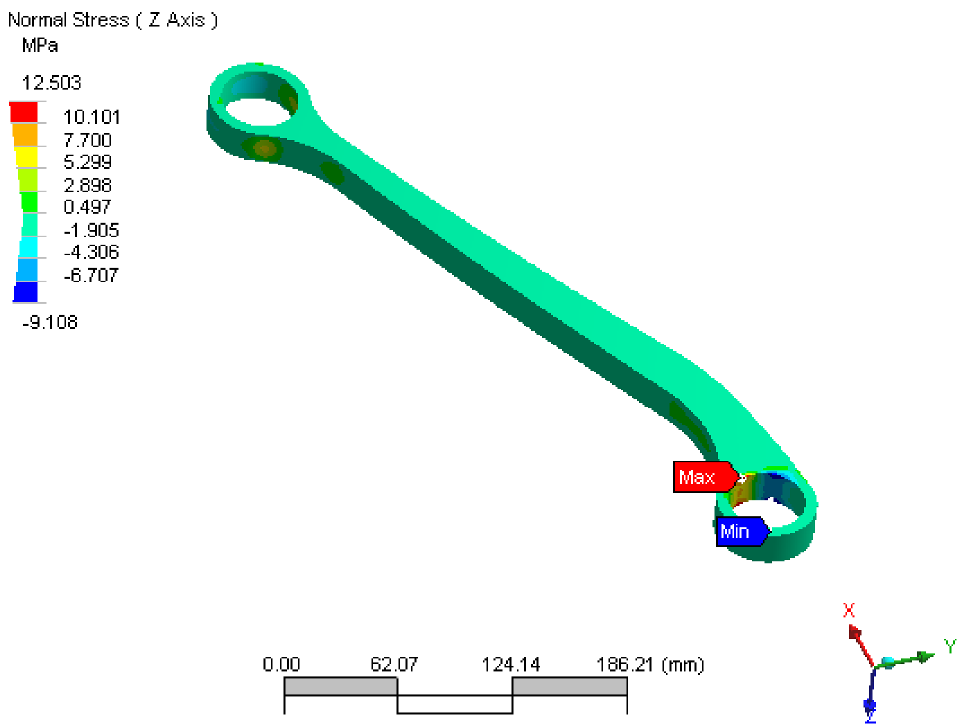

6c) Oz normal stresses

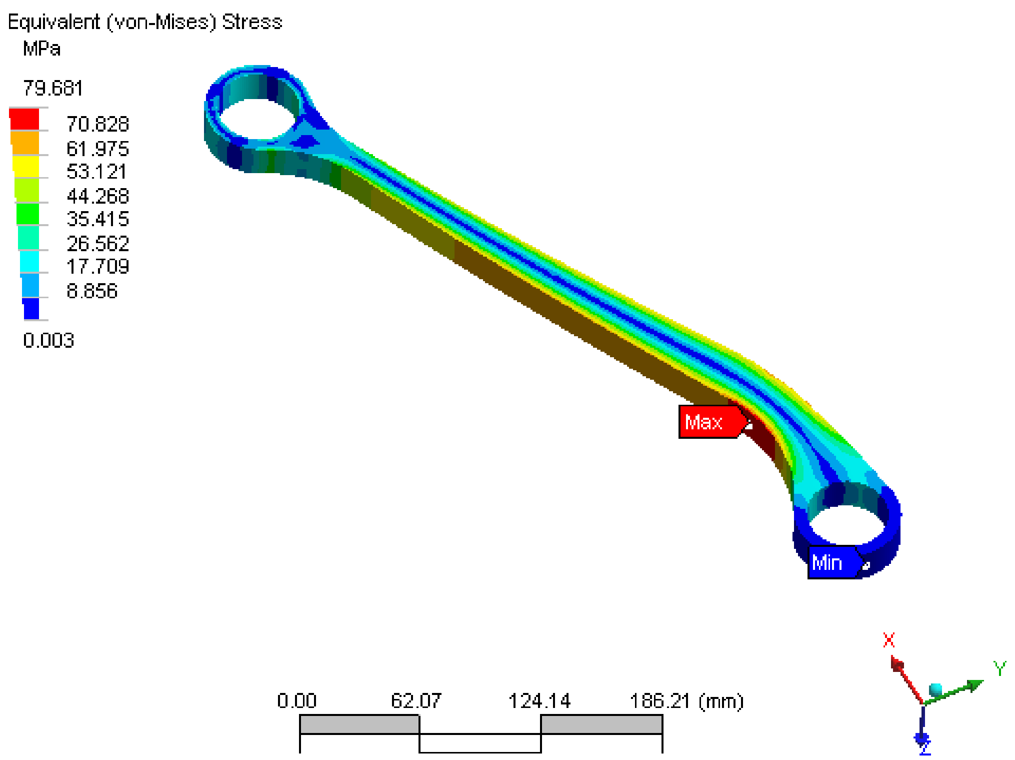

6d) Von Misses stresses

Fig. 6. Normal stresses and Equivalent (von-Mises) stress

The FEM analyze of the stress by using the ANSIS program, for the rear axle coupling bar of the Merced Benz S320 car, model WDB 140, gave the values presented Tab. 1.

Table 1: Numerical values of the stresses induced in the rod

Stress type	Measurement unit	Value
Normal σ_x	[MPa]	**76,12**
Normal σ_y	[MPa]	36,10
Normal σ_z	[MPa]	12,50
Normal $\sigma_{ech\ VM}$	[MPa]	**79,68**

From the data presented in Table 1 we can see that all the values are below the material characteristics, for both the flow limit ($R_{p\ 0.2}$ = 495 MPa) and, of course the fracture strength (R_m = 574 MPa).

4. Conclusions

- The finite element method permit the determination of the stresses $\sigma_x, \sigma_y, \sigma_z\ and\ \sigma_{ech\,VM}$ which allow to compute the principal tensions $\sigma_1\ and\ \sigma_2$ for the plan state of stresses and the displacements $u\ and\ v$ for the plan state of deformations.
- The application of the program for the analyze, using the ANSYS finite element method, in the study of the stress state for the rod of the car vehicles allow to determine both the critical points and also other values of the stresses occurring during the running.
- The FEM analyze of the model rod, used in the rear axle of Mercedes Benz S320 model W140 car show that theoretically there are fulfilled all the running condition as well as the running safety
- However, the coupling bar degradation is sometimes possible as the result of either fatigue or when important shocks occur during the car running.

References

[1] E. Cadoni, M. Dotta, D. Forni, H. Kaufmann, „Effects of strain rate on mechanical properties in tension of a commercial aluminum alloy used in armor applications", 21st European Conference on Fracture, ECF21, Procedia Structural Integrity, 20-24 June 2016, Catania, Italy, Volume 2, ISSN: 2452-3216, pp. 986-993;
[2] V. Paradiso, F. Rubino, P. Carlone, G. S. Palazzo, „Magnesium and Aluminium alloys Dissimilar Joining by Friction Stir Welding", 17th International Conference on Sheet Metal, SHEMET17, Procedia Engineering, Volume 183, 2017, ISSN: 1877-7058, pp. 239-244;
[3] L. D. Pîrvulescu, „Fracture Mechanics studies for light alloys", Teza de doctorat, Timișoara, 2006;
[4] L. Marșavina, „Numerical methods in Fracture Mechanics", Editura Mirton, Timișoara, 1998;
[5] N. Faur, „Finite elements-fundamentals", Editura Politehnica, Timișoara, 2002;
[6] D. Garbea, „Finite Element Analysis", Editura Tehnica, București, 1990;
[7] D. U. Shanyi, „Finite Element Analysis of Slow Crack Growth", Engineering Fracture Mechanics, vol. 16, No. 2, 1982;
[8] *** http://www.ansys.com., ANSYS FLUENT 12.0, User's Guide, ANSYS, Inc. is certified to ISO 9001:200

ISSN 1454 - 8003
Proceedings of 2017 International Conference on Hydraulics and Pneumatics - HERVEX
November 8-10, Băile Govora, Romania

EXPERIMENTAL DETERMINATION OF FRICTIONAL FORCES OCCURRING WHEN SWITCHING HYDRAULIC DIRECTIONAL VALVES

Corneliu CRISTESCU[1], Cătălin DUMITRESCU[1], Radu RĂDOI[1], Liliana DUMITRESCU[1]

[1] Hydraulics and Pneumatics Research Institute INOE 2000-IHP, Bucharest; cristescu.ihp@fluidas.ro

Abstract: *The article presents some research conducted in the Hydraulics and Pneumatics Research Institute INOE 2000-IHP, Romania, regarding the experimental determination of the frictional forces that occur when switching hydraulic distributors used in hydrostatic drives. In the first part of the paper, there are presented some theoretical considerations on the possibility of assessing the frictional forces that needed to be known, to be overcome in switching process by the actuating mechanism, in order to change the direction of fluid flow. In the second part, the paper presents some experimental results obtained in the laboratory, which emphasize not only the value of these frictional forces, but also the dynamics of switching process of the hydraulic distributors.*

Keywords*: Tribology, dynamic seals, frictional forces, viscous frictional forces, hydrostatic drive, testing bench, working fluid.*

1. Introduction

In the structure of hydrostatic drive systems, in addition to the hydrostatic pumps and motors, an important role is played by elements directing the flow of pressurized fluid, currently known as the directional control valves. For carrying out the process of directing fluid under pressure or to stop it, it is required a certain way to generate the switching force of the spool valve, force that can be generated: in a manual, hydraulic, pneumatic, electric way etc.
The force required for switching / moving the spool of directional valve includes several types of forces and it depends on several factors, namely: working pressure, flow conveying through, speed of the fluid through the directional valve, fluid viscosity (viscous friction), dry friction (Coulomb) coefficient etc. Generally, a directional valve, Figure 1, comprises the following major components: body of the directional valve (1), spool (2), compression springs (3), and depending on the drive various subparts are attached, for example two electromagnets (4) or a drive mechanism (5) [1]. The spool (or distributor) is the mobile element that connects the inlet port (P) to the outlet ports (A, B); the outlets, and in some versions also P, are also connected to the tank (outlet port T).
There are directional valves with 2, 3 or 4 ports or ways, and 2 or 3 working positions (e.g. 4/2, 4/3). During the switching operation, which is performed by the movement of spool, the drive mechanism (actuating mechanism) must develop the force necessary to overcome the resistance forces. That's why, it is very important to determine the resistance forces in both theoretical and the experimental way, especially when a drive electromagnet must be designed.
It is known that single stage directional valves are preferred because they are cheaper and most reliable, but increasing the rated size of coils / solenoids, electric actuators, they no longer cope, no longer develop the force required to switch spool, so for large sizes, i.e. high flow rates, there are preferred multistage directional valves [2].
The article presents theoretical considerations concerning the determination of resistance friction forces, and in the second part we present an experimental research that led to the determination of resistance forces when switching the directional control valve from a working position to another.

2. Some aspects regarding the determining of the frictional forces

Switching the hydraulic directional control valve from one position to another, for example, to achieve the flowing of the fluid *Q* under the pressure *p* transmitted by the pump through the port P to the hydraulic consumer connected to the port A of the directional valve where the flow rate Q_1

reaches, as a low flow rate q_a drains through metal-to-metal seal of spool, as shown in Figure 2, the actuator must develop an axial force F_{ax} at least equal to or greater than the sum of forces opposing the movement of spool [3].

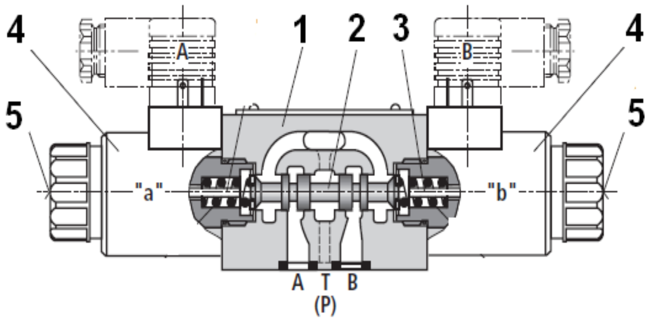

Fig. 1. Components of one hydraulic distributor [1]

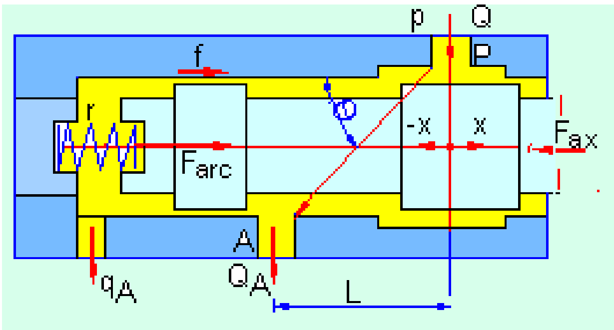

Fig. 2. The fluid flow when switching spool

From Figure 2, it can be noted that, in addition to the dynamic forces related to the spool movement, of mass m, it entrains a quantity of fluid that is on the length, L between the ports P and A, which varies over time, and a frictional viscous force which depends on the speed of movement *v* and the viscous friction coefficient *f*. In addition to these dynamic forces that vary over time, there also occur static forces represented by the force in the spring which varies with spool stroke *x* an spring constant *r*, and also the hydrodynamic force of the flow of fluid stream through the distributor.
In addition to the forces considered, in spool switching there also occur others; more significant is the bonding force, commonly called stick-slip, which is important to the long stay of the spool on a certain position. Stick-slip is the spontaneous jerking motion that can occur while two objects are sliding over each other, with a corresponding change in the force of friction.
If the directional valve is left to stand under pressure for a few moments, in the next switching the stick-slip phenomenon occurs, which results in a higher than the normal operating resistance.
This additional resistive force disappears after several successive switching operations of the directional valve. This force can create discontinuity of the spool movement, respectively of the supplied flow, and finally discontinuity of the hydraulically driven working velocity of machine.
But these bonding forces are difficult to assess, so it is necessary to experimentally determine total resistance forces that occur when switching the spool of hydraulic distributors.
Such an experimental determination is shown in the following.

3. Experimental research infrastructure presentation

In order to determine the total resistance forces occurring during operation of directional valves, there has been designed and developed an experimental device, able to simulate, in the laboratory, the real operating conditions of a directional valve.
This device has been installed on a test bench arranged with help of some components existing in the laboratory, capable of generating the working fluid on the pressure and, also, a working device to assure the working load.

3.1. Constructive principle of the experimental device

The principle at the basis of developing the experimental device has consisted in using a manual directional control valve, being in the current manufacturing of company REXROTH BOSCH GROUP, from its market documents [4], shown in Figure 3.
The basic idea used is that, in order to measure the resistant forces in switching of hydraulic directional valves, there should be used for switching the original actuating mechanism, and between the actuating mechanism and the directional valve spool there should be interposed a force transducer.

3.2. Presentation of the experimental device

For the physical development of the experimental device for measuring the forces of total resistance, which occur in switching of hydraulic directional control valves there has been designed a constructive solution which was based on the use of a hydraulic directional control valve with manual control, of the size 10, existing in the Laboratory of Tribology of INOE 2000-IHP, shown in Figure 4. In order to achieve the device there has been detached body of the directional control valve (1a) from the mechanism for manual control (1b), for placing a force transducer FT on the axis of the directional valve spool, on the one hand, and, on the other hand, for performing actuation of directional control valve during tests precisely with the original control mechanism of the directional valve.

Fig. 3. Manual directional control valves [4].

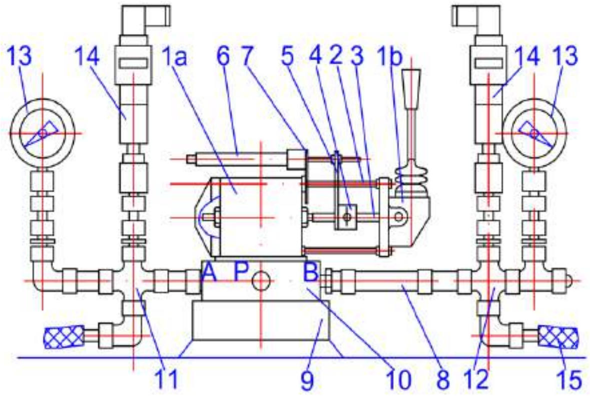

Fig. 4. Layout of experimental device for measuring switching forces

For connecting / coupling the two parts of the main directional control valve, 1a and 1b, there were used four threaded rods (2) which replaced the original screws, thus achieving a space between the two parts of the main directional control valve. In this way, the possibility is created to insert, by means of threaded sleeves (3), a force transducer (4), between the control rods of the directional valve spool. To measure the stroke achieved by the spool, a rigid blade (5) is attached to the force transducer (4), which drives the rod of a potentiometric stroke transducer (6) which is fixed to the body of the directional valve by a supporting plate (7). The directional control valve is mounted by means of screws, on a compatible distribution plate (8) which is placed on another supporting plate (9). From the ports A and B of the distribution plate (8), pressurized fluid passes via two manifolds (11) and (12), to the gauges (13) allowing direct reading of the pressure, and also to the pressure transducers (14), by which pressure variations are acquired by the computer system, and through the flexible hoses /piping (15), the fluid reaches the hydraulic motor actuated by the directional valve drive.
Physical development of the test device is shown in Figure 5, where one can see the actual technical solutions for developing it.

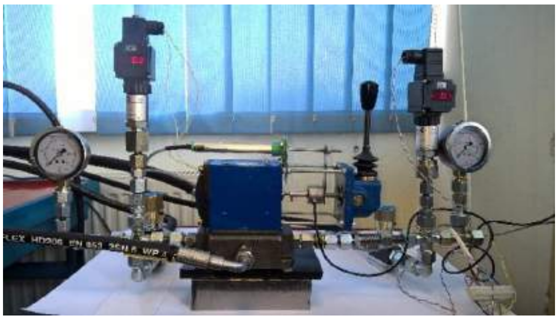

Fig. 5. Physical development of the test device

3.3. Presentation of the experimental stand

To conduct the experimental research in order to determine the hydraulic resistance forces when switching directional valves, in the Laboratory of Tribology of INOE 2000-IHP there was arranged a test stand, in accordance with the diagram shown in Figure 6.

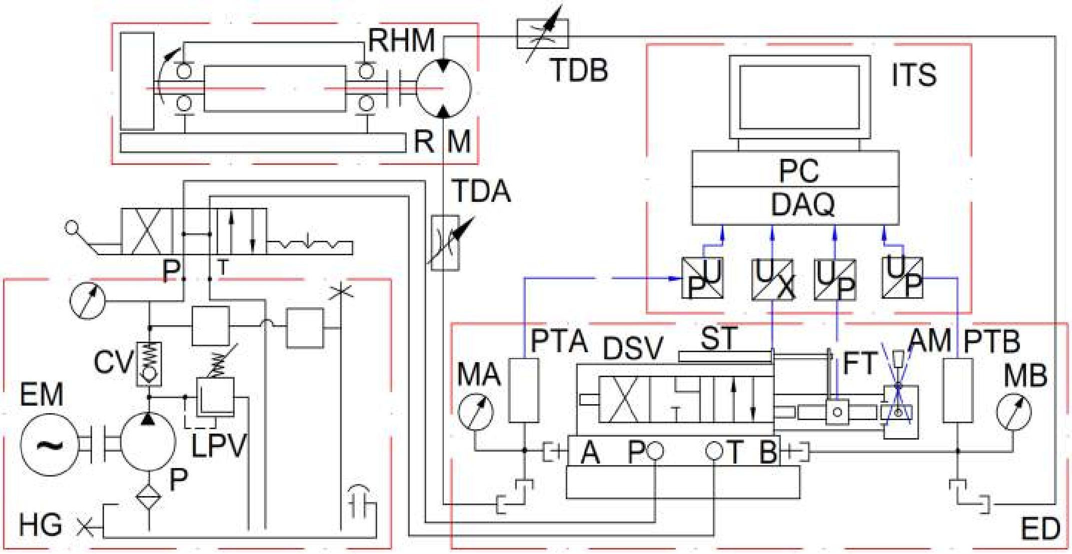

Fig. 6. Concept diagram for arranging the experimental stand

Besides the experimental device ED which contains a force transducer FT, a stroke /displacement transducer ST, two pressure transducers PTA and PTB, and two manometers MA and MB, the stand also includes a hydraulic mini-station for generating pressurized fluid HG, a rotating mechanism RM driven by a rotating hydraulic motor RHM and a system for data acquisition and processing ITS, consisting of a data acquisition board DAQ, National Instruments type, and a PC type computer. The hydraulic generator GD is composed of a gear pump P driven by an electric motor EM, and assisted by a pressure limiting valve LPV, a check valve CV and a manual directional valve MDV through which pressurized fluid is sent to the ports A or B of the test device, and from here, through the throttles TDA and TDV, it reaches the rotating hydraulic motor RHM. Figure 7 presents an overview of the experimental stand, and in Figure 8 one can see in detail the data acquisition and IT system.

Fig. 7. Overview of the experimental stand

Fig. 8. View of the IT system

By means of special electric cables all signals provided by transducers reach the acquisition board installed on the computer, and this one, based on specialized software, allows capturing, storage and processing of the measured data.

4. Some experimental results presentation

In order to measure and record the variation of total resistance forces which occur on the spool of the directional spool valves, there has been conducted experimental research which led to obtaining a lot of graphical experimental results; some of them are presented bellow.
The object subjected to an experimental research was a hydraulic directional spool valve, directly operated, with manual actuation, size 10, manufactured by Rexroth Bosch Group, code 4 WMM 10 J 31/, which is a four-way distributor, with three operating positions, the central position providing communication of ports A and B to the tank T and the pump port P, closed, [5].
To this end, there has been necessary to set the parameters of interest and define a testing methodology.
Regarding the switching process in hydraulic directional spool valves, parameters of interest are:
- spool stroke x, measured by the stroke transducer ST in Figure 6, item 6 in Figure 4;
- resistive force Fax that opposes the spool movement, which is measured by the force transducer FT in Figure 6, item 4 in Figure 4;
- pressure at the port A, p_A, which occurs when opening the port A, measured by the pressure transducer PTA in Figure 6, item 14 in Figure 4;
- pressure at the port B, p_B, which occurs when opening the port B, measured by the pressure transducer PTB in Figure 6, item 14 in Figure 4.

4.1 The test methodology

The test methodology consists of the following sequence:
- Start the PC computer systems and launch the data acquisition and processing software;
- Adjust, at the pressure limiting valve LPV in Figure 6, the desired pressure;
- Manually control the directional valve MDV in Figure 6, which opens the way for the pressurized fluid to the port P of the experimental device ED;
- Activate the data acquisition software;
- Manually control the tested directional valve DSV to open ways / ports, A and / or B for supplying the rotating hydraulic motor RHM, which begins to rotate the mechanism in one direction or the other. The command is for a specified duration of tens of seconds, about a minute to a full cycle of control, which requires opening one at a time, both ports A and B;
- Stop data acquisition at the end of the control stroke of the directional control valve;
- Save the data acquired in the computer memory;
- Display and analyze the graphs of variation of parameters of interest;
- Repeat the sequences to get 2-3 records in the same case for a certain level of pressure;
- Repeat the sequences for other pressure levels;
- Stop PC computer system and end the testing session.

Following the developed experimental research, there have been obtained a lot of complete sets of experimental results, for 4 steps of pressure: 25 bar, 50 bar, 75 bar and 100 bar. For each pressure step, each measurement having 3 complete working cycles, for each half of cycle 3 determination, which means 6 determination and, also, for each quarter of cycle 3 determination, which means 12 determination. In total, there were 21 experimental determinations for each pressure step. For 4 pressure steps there were obtained 4x21 = 84 determinations.
One example of one complex graphic obtained is presented in Figure 9.

4.2 Analysis of the graphs obtained

After analyzing complex graphs obtained there were drawn some important conclusions, namely:
- graphs of variation of each parameter of interest have a logical progression, normal and repeatable;
- pressure values correspond to those directly read on the gauges MA and MB. They are slightly lower than the pressure values set at pressure limiting valve LPV because of pressure losses / drops along rotating hydraulic motor RHM circuits;

- the overall shape of the graph of spool stroke corresponds to a full work cycle in the drive / control mechanism with positive or negative values corresponding to the direction of movement of the control handle. Imperfections, small variations on the graph are due solely to the uneven manual drive by the human operator;
- the graph of resistance forces at spool is variable from one quarter of cycle of work to another, and also along individual quarter of cycle of work, but the differences between the maximum and minimum values are not very high, being in the range of (0-50) N, where it is admissible;

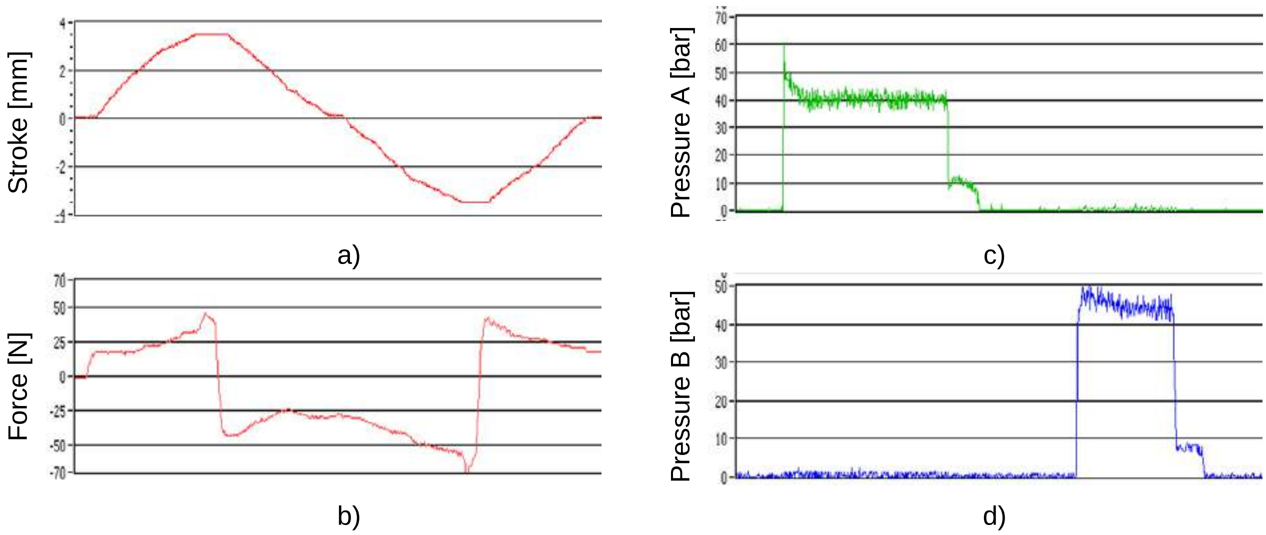

Fig. 9. Complex graphs for pressure step of 50 bar

- with the exception of the peaks, mean values of the resistance forces over a quarter of a stroke, are within the range (20 - 30) N [5], when extending the spool, and within the range (30 - 40) N, when compressing the spool, respectively the force transducer, which seems logical and corresponds to the recommendations in the literature [6];
- from a comparative analysis of graphs of variation of the resistant forces for the four pressure levels, no significant differences appear in proportion to the increase of pressure value. This may be due to internal balances based on special profiles of surfaces of elements in relative motion.

5. Conclusion

In the paper there are presented the research infrastructure and the results obtained following the development of an experimental research, on assessment of total resistance forces occurring in switching process of a directional spool valve.
Following the design and development of an experimental device and a testing stand, there have been obtained several complex numerical data and variation graphs for the parameters of interest, which enabled assessment of resistance forces, which occur during the switching process of the directional spool valves.
After analyzing numerical data and graphs obtained, it was concluded that the graphs of variation of parameters of interest, especially resistive force, have a normal form, and the mean values of them fall in a range of values close to the values mentioned in technical literature of reference [5].
Another important conclusion is that we cannot talk about a significant variation in the resisting forces with increasing working pressure, the pressure having a reduced influence on the switching force.
Through the numerical results and graphics, and especially through the conclusions reached following comparative analysis, this paper has special scientific and technical value and further research is required.

Acknowledgments

This paper has been developed in INOE 2000-IHP, with financial support of ANCSI, under the national research *Programme NUCLEU-2016,* project title: *Physics of processes for reducing energy losses and developing renewable energy resources by use of high-performance equipment,* project code PN 16 40.03.01, financial agreement no. 5N/2016, Additional act no. 1/2017.

References

[1] Rexroth Bosch Group, "Spool hydraulic directional control valve direct-operated / 4/3-way WExx73xxA12", available at: http://www.directindustry.com/prod/bosch-rexroth-industrial-hydraulics/product-9143-1268489.html, accessed: 29.03.1017;

[2] Y. Qinghui, Y. Li. Perry, "Using Steady Flow Force for Unstable Valve Design: Modelling and Experiments", *Journal of Dynamic Systems, Measurement and Control*, available at: http://dynamicsystems.asmedigitalcollection.asme.org/article.aspx?articleid=1410901, accessed: 27.03.2017;

[3] V. Marin, R. Moscovici, D. Teneslav, "Hydraulic Systems for Automatic Drive and Control", Technical Publishing House, Bucharest, pp. 46-61, 1981;

[4] Rexroth Bosch Group, "Directional spool valves, directly operated, with manual actuation", available at: https://www.boschrexroth.com/en/us/products/product-groups/goto-products/goto-hydraulics/directional-valves/4wmm-and-4wmr/index, accessed: 30.03.2017;

[5] Rexroth Bosch Group, "Directional spool valves, directly operated, with manual and fluid logics actuation (size 6)", available at: https://dcus.resource.bosch.com/media/us/products_13/product_groups_1/industrial_hydraulics 5/pdfs_4/re22280.pdf, accessed: 30.03.2017;

[6] Rexroth Bosch Group, "Directional spool valves, directly operated, with manual and fluid logics actuation (size 10)", available at: https://dc-us.resource.bosch.com/media/us/ products_13/product_groups_1/industrial_hydraulics 5/ pdfs_4/ re22334.pdf, accessed: 30.03.2017.

ISSN 1454 - 8003
Proceedings of 2017 International Conference on Hydraulics and Pneumatics - HERVEX
November 8-10, Băile Govora, Romania

DESIGNING A PID CONTROLLER FOR WATER HYDRAULIC SERVO MOTOR SYSTEMS WITH ZIEGLER-NICHOLS METHOD

Oğuz EROL[1], Yusuf ALTUN[2], Melih AKTAŞ[3]

[1]Duzce University, Engineering Faculty, Mechatronics Engineering, oguzerol@duzce.edu.tr

[2]Duzce University, Engineering Faculty, Computer Engineering, altunyusf@hotmail.com

[3]Duzce University, Engineering Faculty, Electrical and Electronics Engineering, melihaktas@ duzce.edu.tr

Abstract: *This paper presents a PID controller for water hydraulic servo motor systems. Ziegler-Nichols method estimates the control parameters of the controller. Even though the highly nonlinear nature of water hydraulic servo motor systems makes the implementation of this controller a challenge with the help of linearization techniques it is been successful in controlling the system. Ease of use and simplicity are two big advantages of this control method in hydraulic servo motor systems.*

Keywords*: PID, Ziegler-Nichols, hydraulic servo motor systems.*

1. Introduction

Water hydraulic servo motor systems are getting increasingly common in industrial use every day mostly thanks to their eco-friendly nature. Since the system uses water as the fluid it's clean, easily available and safe since water is a non-combustible liquid. Another advantage of water based hydraulic systems over their oil based counterparts is better responsiveness of the hydraulic system. But that does not mean that it has no disadvantages. Firstly, the system is highly nonlinear also higher friction at lower motor speeds is a disadvantage. These advantages limit the viability of water based hydraulic systems. To overcome these disadvantages different control techniques are used on these systems. For example a gain scheduling PID controller is proposed in [1]. Sliding mode control with disturbance observer is used in [2]. PID funnel control with future distance estimation is used in [3]. An adaptive pressure controller for hydraulic servo motor systems is designed in [4]. A simple adaptive control application is proposed in [5]. A PID controller, whose parameters are determined by genetic algorithm could be seen in [6]. In [7], an adaptive neural controller is designed for the velocity of the system via feedback linearization.

2. System Model

The system model of the water hydraulic servo motor system is shown in figure 1.

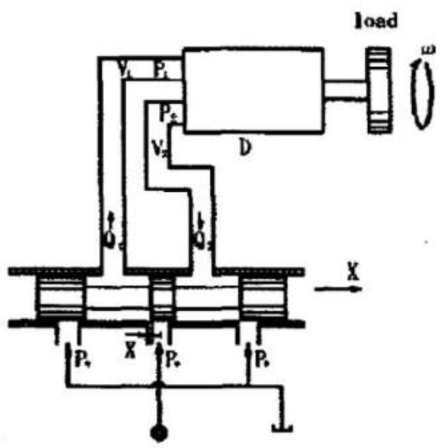

Fig. 1. Water hydraulic servo motor system [1]

The system has basic elements. There is a flywheel which is attached to a servo motor that generates the outputs. The outputs of the system are rotational θ(t) angle and spool displacement of xv(t) servo valve. The goal of this paper is to control these outputs by using a PID controller.
The mathematical model of the system is obtained by making few assumptions first. There are no external leakage from the servo valve and the motor, there are no overlap between the valve body and the spool, spool displacement is linear to the input voltage applied to the servo amplifier, The density and the viscosity of the medium are assumed constant. Also the motor displacement and supply pressure are assumed as constant too [1]. Only after these assumptions the following equations could be obtained. As seen in the figure 1 our outputs are $\theta(t)$ angle and $x_v(t)$ servo valve displacement. By controlling the $\theta(t)$ angle or $\dot{\theta}(t)/\omega(t)$ *speed with control signal* $u(t)$ we can control the spool displacement of servo valve.
The $x_v(t)$ is regarded to u(t) as follows where k_v and τ_v are gain and time constants.

$$\tau_v \dot{x}_v(t) = x_v(t) + k_v u(t) \tag{1}$$

In order to obtain load discharge flow, equations at below is used.

$$P_L = P_1 - P_2 \tag{2}$$

$$Q_L = \frac{Q_1 + Q_2}{2} = \frac{k_q x_{ve}}{\sqrt{2}} \sqrt{P_s - P_r - sign(x_{ve}) P_L} \tag{3}$$

By using these equations, the system is linearized so a PID controller can be used. Where (P_L) is load pressure and flow-gain coefficients related to the servo valves are assumed to be $k_q = k_{q1} = k_{q2}$. After determining k_x, k_p values the load discharge flow equation is as follows:

$$Q_L = k_x x_{ve} - k_p P_L \tag{4}$$

$$Q_L = \frac{V_0}{2E} \dot{P}_L + \frac{D_M}{2\pi} \dot{\theta} \tag{5}$$

Because of the previous assumptions for linearization of the system now the system output x_{ve} is now directly related to the control signal u(t) as shown in $x_{ve}(t) = k_v u(t)$ equation. By using these equations, we can obtain the transfer function as below:

$$K_d = (0.6 * K_{cr} * T_{cr}) / 8 = 0.00462 \tag{6}$$

$$\frac{\theta(t)}{u(t)} = \frac{\left(E D_M k_v k_x / \pi V_0 I_{fw}\right)}{s^3 + \left(E D_M^2 / 2\pi^2 V_0 I_{fw}\right) s^2 + \left(2 E k_p / V_0\right) s} \tag{7}$$

The values of the system is as shown below in the table:

Table 1: The values of parameters for the tank system

Parameter	Symbol	Value
Valve time-constant	τ_v	0.02 s
Servo gain	k_v	1.153×10^{-4} m/V

Table 1: The values of parameters for the tank system (continued)

Parameter	Symbol	Value
Right valve dead zone	b_r	$0.3\text{x}10^{-4}$ m
Left valv deead zone	b_l	$0.4\text{x}10^{-4}$ m
Discharge coefficient	C_d	0.61
Bulk modulus	E	$2.2\text{x}10^{9}$ Pa
Displacement volume of motor	D_M	$15\text{x}10^{-6}$ m^3
Leakage coefficient	C_{Li}	10^{-12} m^3/s Pa
The moment of inertia for flywheel	I_{fw}	4.5 kgm^2
Volume of pipe	V_0	$5\text{x}10^{-2}$ m3
Flow gain coefficients	$k_{q1} = k_{q2}$	$0.858\text{X}10^{-3}$ $m^2/\sqrt{Pa}$s

3. Controller Design

PID control method will be used as the controller for this plant. PID controller is a simple yet effective control method. In order to control a system with PID controller first control constants shall be determined. There are many methods for determining these constant, the method that is used in this paper is Ziegler-Nichols method. This method follows four step to determine these parameters, these steps are as follows:
1 Turn off the I-term and the D-term in the controller. This can be done by setting the reset time to "infinite" and the derivative time to 0.
2 Turn $K_p = K_{p\text{-}0}$, and the increase it slowly, while you are looking at the controllable variable (y) or - some times better - the output of the controller, u. Increase KP until the output exhibits sustained oscillations.
3 At this "quasi steady-state" point you have the critical gain, called $K_{P,crit}$, and a given period of time, T_{crit}

4 Then you should turn on the I- and D-term by using the following values, see the table below:

Ziegler-Nichols Method

Control Type	Kp	Ki	Kd
P	*0.5Kcr*	-	-
PI	*0.45Kcr*	*KpTcr/1.2*	-
PID	*0.6Kcr*	*KpPcr/2*	*KpPcr/8*

The first value that must be obtained is K_{cr} in order to obtain this value the system is driven by only the P controller, the controller constant of this controller gets increased slowly until the system reaches persistent oscillation. After obtaining the K_{cr} value the period between oscillations is also calculated than the PID constants are obtained by using the chart above. For the system that is modeled in this paper the obtained values are:

$$K_{cr} = 0.28$$

$$T_{cr} = 0.22$$

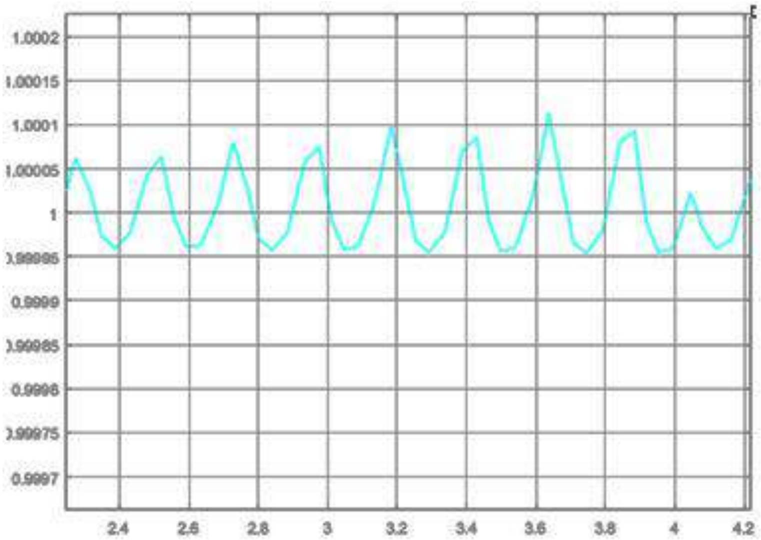

Fig. 2. Step response for K_{cr}

$$K_p = 0.6 * K_{cr} = 0.168$$

$$K_i = 1.2 * (K_{cr} / T_{cr}) = 1.527$$

$$K_d = (0.6 * K_{cr} * T_{cr}) / 8 = 0.00462$$

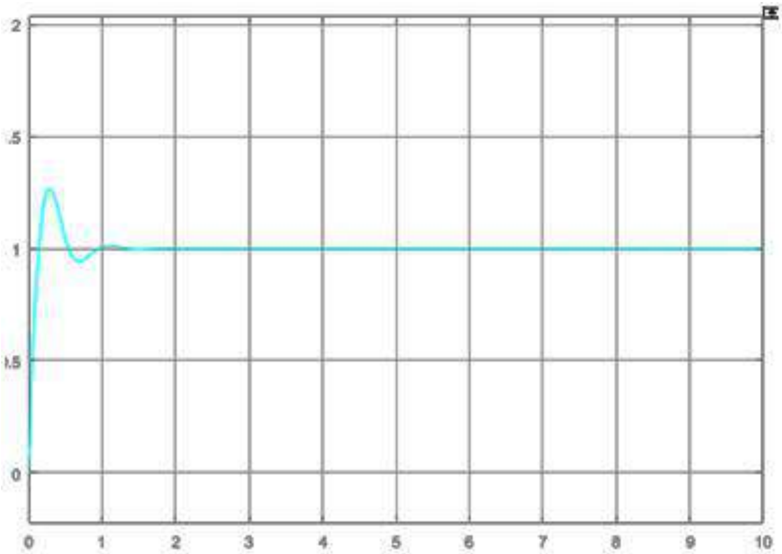

Fig. 3. Constant response after PID tuning.

4. Conclusions

This paper presents a PID controller for water hydraulic servo motor systems. The controller parameters were determined with Ziegler-Nichols method. This easy and basic controller could be used in water hydraulic servo motor systems in future with ease of use and hopefully increase usage in industry.

References

[1] K. Ito and S. Ikeo, "PID control performance of a water hydraulic servomotor system," in *Proceedings of the 41st SICE Annual Conference. SICE 2002.*, 2002, vol. 3, pp. 1732–1735.

[2] Kazuhisa Ito; Hidekazu Takahashi; Shigeru Ikeo; Koji Takahashi, "Robust Control of Water Hydraulic Servo Motor System Using Sliding Mode Control with Disturbance Observer," SICE-ICASE, 2006. International Joint Conference

[3] Chanyut KHAJORNTRAIDET, Kazuhisa ITO, "Water Hydraulic Servo Motor Velocity Control Using PID Funnel Control with Future Distance Estimation," JFPS International Journal of Fluid Power System Vol. 10 (2017) No. 1 p. 1-8

[4] Kazuhisa ITO, "AN ADAPTIVE PRESSURE CONTROLLER DESIGN OF HYDRAULIC SERVO SYSTEM WITH DEAD ZONE," in *Proceedings of the 6th JFPS International Symposium on fluid Power, TSUKABA 2005*

[5] K. Ito and S. Ikeo, "Application of Simple Adaptive Control to Water Hydraulic Servo Cylinder System," TRANSACTIONS OF THE JAPAN FLUID POWER SYSTEM SOCIETY Vol. 43 (2012) No. 2 p. 23-29

[6] A. A. Aly, "PID Parameters Optimization Using Genetic Algorithm Technique for Electrohydraulic Servo Control System," *Intelligent Control and Automation*, vol. 2, no. 2, pp. 69–76, 2011..

[7] Z. Alzahra, S. Dashti, M. Gholami, and M. A. Shoorehdeli, "Neural – Adaptive Control Based on Feedback Linearization for Electro Hydraulic Servo System," IOSR Journal of Electrical and Electronics Engineering, vol. 8, no. 1, pp. 2278–1676.

ISSN 1454 - 8003
Proceedings of 2017 International Conference on Hydraulics and Pneumatics - HERVEX
November 8-10, Băile Govora, Romania

MOBILE AND STATIONARY EQUIPMENT FOR MELTING SNOW FROM THE URBAN PUBLIC SPACE

Corneliu CRISTESCU[1], Liliana DUMITRESCU[1], Ioan LEPĂDATU[1], Radu SAUCIUC[1]

[1] National Institute for Optoelectronics, INOE 2000-IHP Bucharest, cristescu.ihp@fluidas.ro

Abstract: *The article presents a new category of technological equipments used to remove the fallen snow on the public urban spaces such as parking, airport runways, public roads and private spaces. It shows the principle of operation, structure and performance of such equipments, currently called snow melters, which actually are an alternative to the classic snow removal solution by transporting it to predestined locations, usually at long distances, which offers certain advantages, especially in terms of speed of decongestion of traffic, but also the interface with the environment, the removal of snow beeing an ecological process.*

Keywords*: Snow melters, mobile snow melters, stationary snow melters, urban snow melters, self-propelled snow melters, trailed snow melters*

1. Introduction

Snow melters are machines equipped with either electric heating systems or diesel, or gas burners that melt snow for the purpose of removing it from crowded urban areas, airports, parking malls and hypermarkets, parking facilities for hospitals, public institutions, business or exhibition centers, private spaces etc.
They represent an alternative to the classic snow removal solution by the transport with trucks outside of the localities and have a number of advantages such as: quick unlocking of the carriageway and the parking spaces, decongesting car traffic and deploying it safely, ecological snow removal by controlled discharge water. The water from snow melting is coarsely filtered and then discharged into the public sewer /rainwater collection system and from there to the treatment plant where it is decanted and then filtered.
Snow melting equipments may be self-propelled or semi-mobile. The semi-mobiles can be transported to various work points by fitting them on a trailed platform, and these are the usually of large capacity (18 ... 300 t /hour); are used to decongest large areas of urban agglomerations (roads, car parks etc.) or to airport runways when rapid release of functional spaces is required. The self-propelled ones are truck type and have lower capacities (3 ... 15 t /hour); are used in specific objectives of local units (parking of public institutions, hospitals, etc.).
The most famous manufacturing companies come from the USA and Canada: Snow Removal Systems [1], Snow Dragon [2], Trecan Combustion Limited [3], [4], Michigan Melters [5], and Aero Snow Removal Corp [6] and they have numerous models with snow melting capacities ranging from a few tons and up to 300 t /h and even more.

2. Technical solutions applied by construction companies

Generally, snow melting requires a heat source and a hot water tank and, of course, the other components for operating control.
Although all companies follow this general conception, the concrete technical solutions differ from manufacturer to manufacturer, solutions that differ according to the performance.
In principle, depending on the mobility of the equipments, there are two basic categories:

2.1 Stationary snow melting equipments

Figure 1 shows an example of stationary snow melting equipment, made by ***Trecan Combustion Limited*** [3], type **Trecan 20-SG**, 20-Ton stationary snow melter, with a capacity of 20 tons per hour, its burner 4.5 million BTU /hr can melt 50 to 100 cubic meters of snow with an average snow density of 15 to 30 lb./ft. /hour, ie 200 to 500 kg /m^3. The machine from Figure 2 is also a stationary snowmelter, type **Trecan 40-SG**, 40-Ton stationary snow melter, manufactured by the same company [3] with a capacity of 40 tonnes per hour, its 9 million BTU /hour can melt 100 to 200 cubic meters of snow with the same density.

Fig. 1. Trecan 20-SG, stationary snow melter [3]

Fig. 2. Trecan 40-SG, stationary snow melter [3]

2.2 Mobile snow melting equipments

Mobile snow melting machines are brought to the place where snow removal is needed, when is needed, and they are also of two kinds, namely:

- mobile self-propelled snow melting equipments, which have a towing vehicle dedicated to the machine, thus enabling it to move independently where it is needed.

An example of such equipment is given in Figure 3, which shows a self-propelled mobile equipment achieved by ***Snow Removal Systems*** [1], type **SRS M150**, which melts 150 tons of snow per hour with a BTU 35,000,000 burner.

Other self-propelled snow melting equipment is shown in Figure 4 and is produced by canadian company ***Trecan Combustion Limited*** [3]. The **500-PD** has a melting capacity of 500 tons of snow per hour, the six burners each of 14 million BTUs, with 84 million BTU / hr and is capable of melting 1.234 to 2.469 cubic meters of snow. The model 500-PD is a dual side loading snow melter and is designed for use at large airports and large city snow dumps.

Fig. 3. Self-propelled snow melter SRS M150 [1]

Fig. 4. Self-propelled snow melting type 500-PD [3]

Aero Snow Removal Corp. [6] achieves direct removal and collection snow equipments, Figure 5, but especially self-propelled snow melting equipments, both small size and large size, Figure 6, for large airports.

Fig. 5. Direct snow removal equipment [6]

Fig. 6. Self-propelled snow melting equipment for airports [6]

Aero Snow Removal Corp. has been clearing snow in airports, cities, municipalities, shopping malls, sports complexes, seaports and at commercial sites for more than 30 years. We are innovators in the snow removal and snow melting industry. Aero provides numerous snow removal services at major airports throughout the United States [6].
- trailed mobile equipment that can be driven by another vehicle. These in turn, depending on size and performance, can be with an axis, figure 7, two axes, figure 8, three axes, figure 9 and even four axes, figure 10.

Fig. 7. Model Michigan Melters with one axis [5]

Fig. 8. Two-Axis Trecan Model [4]

Fig. 9. Snow Dragon Three-Axis Model [2]

Fig. 10. Model Michigan 4-Axis Melters [5]

Snow Removal Systems [1] also has outstanding achievements in snow traction equipment. Thus, in Figure 11, there is shown a snow melting equipment type **SRS-P70** which, due to a burner of $17\cdot10^6$ BTU, has a melting capacity of 70 t / hour, and in figure 12, is shown a device snow melting type **SRS-P100**, which, having a $30\cdot10^6$ BTU burner, has a melting capacity of 100 tons per hour.

Fig. 11. Snow Removal Systems typ SRS-P70 [1]

Fig. 12. Snow Renoval Systems typ SRS-P100 [1]

Deltamed Company, in collaboration with ***Energo-Term***. achieved un prototype of snow melting equipment, presented in Figure 13.

Fig. 13. Snow melting equipment Energo-Term [7]

The equipment currently in the testing phase is called "**Urban Snow Melter**" and effectively melts the snow, and the resulting water is sent directly to the city's sewerage system, after a rough filtering, the equipment beeing thus environment-friendly [7].

3. Structure and functioning of snow melting equipments

To present structure and functioning of snow melting equipments, is used the data presented in [1], referring to the **SRS-P70** models shown in Figure 11 and the **SRS-P100** model shown in Figure 12. The components of the snow melting plant are mounted on the platform of a triple axle trailer, which has all the necessary accessories for public roads (electric brakes, signaling, towing hook etc.).
The melting plant is made up of three large subassemblies, shown in Figure 14: generator module and heat exchanger; the technical module; the snow melting tank.
The generator module and heat exchanger (1) is also composed of:
● the tank of heat exchanger that contains water for melting snow;
● the ignitubular heat exchanger that transfers heat from the hot gases to the hot water bath for snow melting;
● standard fuel burner (diesel) that produces the heat needed to melt the snow.

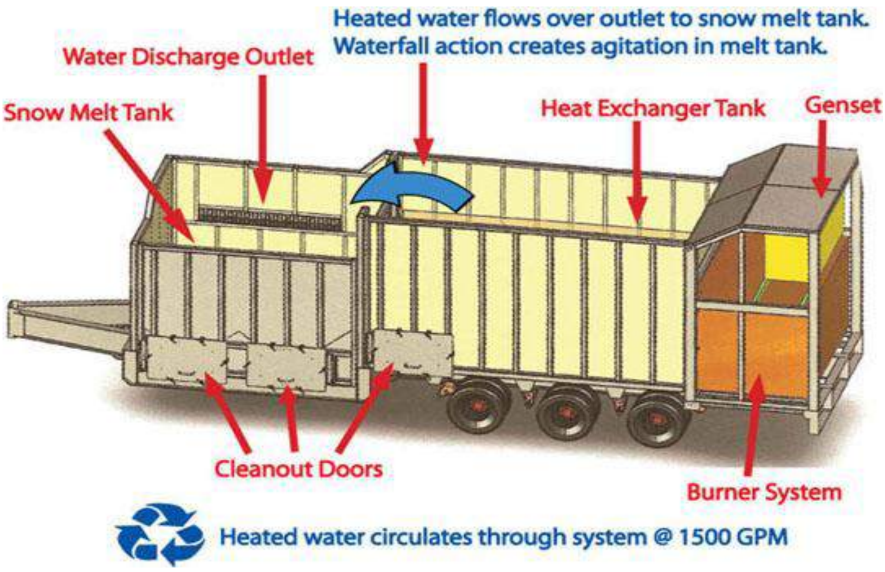

Fig. 14. The composition and flow circulation of water at the snow melting equipment SRS-P100 [1]

The technical module of the equipments (2) comprises:
● an electric generator with a thermal motor for producing the electric current needed for the plant equipment: burner, combustion fan, electric pump, electric panel etc.;
● a combustion fan that ensures forced circulation of hot gases inside the heat exchanger pipes;
● a water circulation pump that sends hot water from the heat exchanger to the snow melting unit;
● an electric control panel, control and automation;
● a fuel tank that provides a minimum operating time of 4 hours.
The snow melting tank contains water in which snow is downloaded and melting. The melting tank is supplied with hot water from the tank of heat exchanger.
The equipment is mounted on a three-axle trailer. It has two distinct tanks, a tank for heating water and a tank for snow melting. The snow is loaded into the melting tank through the back or the side of it using a milling cutter or excavator. Here the warm water from tank transfers the heat to the snow or the ice blocks. Additionally, some melters are equipped with a snow-mixing /shaking system and a spray system located at the top of the tank that throws hot water over the snow in the tank, Figure 15. The thermal energy needed to melt the snow is provided by a burner with liquid fuel (diesel fuel) and has an operating autonomy that depends on the capacity of the fuel tank. The burner together with a fan provides the hot air flow to transfer its heat through an ignitubular heat exchanger to the water in the tank. An electro-pump delivers warm water from the changer tank into the melting tank and into the spraying system. The volume of snow introduced into the tank

coupled with snow melting leads to increased levels and the discharge of the melted water through the holes too. From the melting tank, the water is discharged either through the overflow or through the drainage connections to the sewer after a preliminary rough filtration. The tank has on the bottom some slurry outlet doors. A hydraulic system, shown in Figure 16, inclines the melting tank so that deposits on its bottom (sand, anti-slip material, etc.) can be removed and washed gently.

Fig. 15. Hot water spraying system in the melting tank [2]

Fig. 16. Melting tank inclining system [1]

The location of the component subassemblies and the principle of operation of the snow melting plant is shown in Figure 17, below.

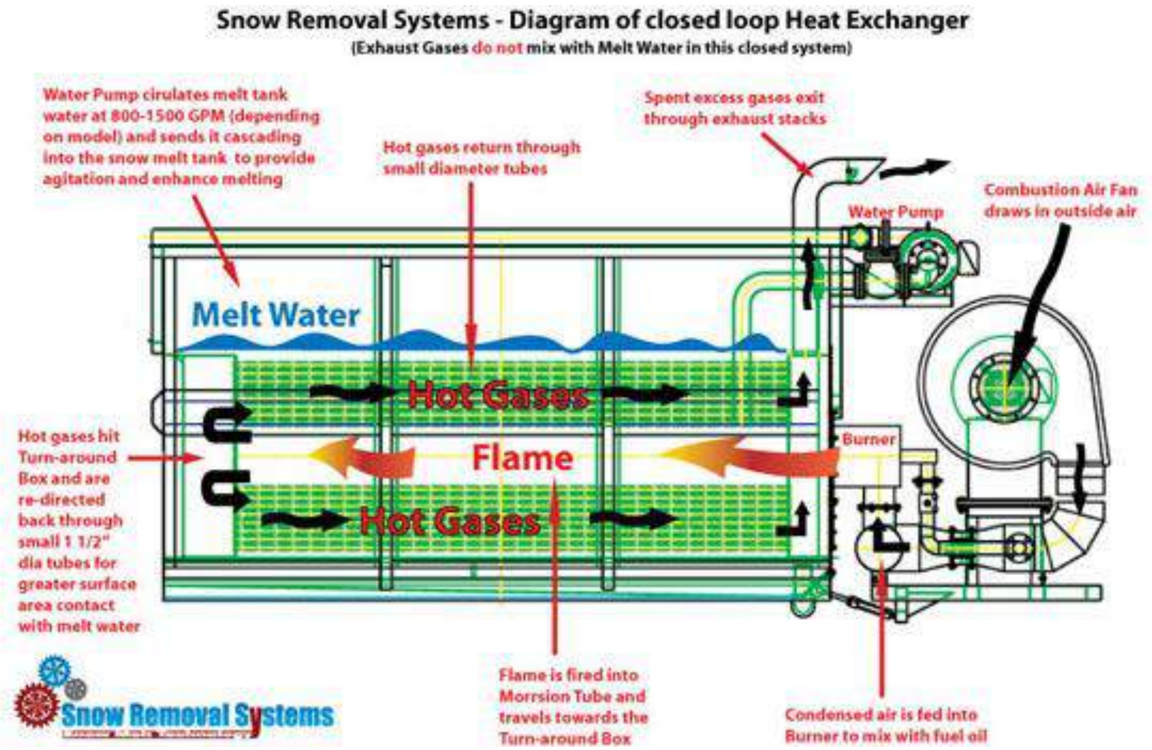

Fig. 17. Layout diagram of components and heat transfer system [1]

Based on the data presented above, as well as on their detailed analysis, it can be concluded that on the market there is a very wide range of technical solutions for the production of snow melting equipments, solutions that can meet all the requirements of potential customers.
As for the principle of achievement, the equipments are generally like, but differs from the concrete technical solutions. It can be said that such equipments can be designed and built in the country, with both design potential and companies /companies for effective physical realization, as well as potential clients, both private companies as well as companies and public institutions.

4. Conclusions

The article presents a new category of technology equipment made by foreign firms and used to remove snow fallen on the urban public spaces such as public roads, parking, airport runways, private spaces etc.
It also presents the working principle, the structure and the performance of such machines, currently called snow melters, which, through the technology and through performances, perform the ecological removal of snow.
From the analysis of the melters presented above, results that there is a wide range of snow melter equipments that can satisfy all customer requirements.
From the analysis of the principle of realization and of the technical solutions in detail, it can be said that such equipments can be designed and realized also in ROMANIA, having the potential for physical design and realization (firms /companies), but also potential users (private companies, companies and public institutions in the local government etc.).

Acknowledgments

This paper has been developed in INOE 2000-IHP, with the financial support of the Executive Agency for Higher Education, Research, Development and Innovation Funding (UEFISCDI), Programme 2- Increasing the competitiveness of the Romanian economy through research, development and innovation, Subprogramme 2.1- Competitiveness through Research, Development and Innovation - Innovation Cheques, project title: "Eco-friendly snow melting machine", Financial Agreement no. 22 CI/2017.

References

[1] *** Snow Removal Systems, Inc. Products. In: http://www.snowremovalsystems.com/<, 2017;
[2] *** Snow Dragon. Products. In:http://www.snowdragonmelters.com/default.asp?ID=3, 2017;
[3] *** Trecan Combustion Limited. Canadian designer and built snowmelter used in worldwidw. In: www.trecan.com, 2017;
[4] *** Snowmelters.Presented by comercial boiler systems inc. In: http://www.snowmelters.com/, 2017;
[5] *** Michigan Melters. Snow Melting Machines and Equipment: Commercial Snow Melters. In: http://www.michiganmelters.com/, 2017;
[6] *** Aero Snow Removal Corp. In: https://www.linkedin.com/company/aero-snow-removal-corp, 2017;
[7] *** Deltamed. Urban Snow Melter - Prototip de echipament de topire a zăpezii. In: http://www.deltamed.ro/product/urban-snow-melter/, 2017.

ISSN 1454 - 8003
Proceedings of 2017 International Conference on Hydraulics and Pneumatics - HERVEX
November 8-10, Băile Govora, Romania

PNEUMATICALLY ACTUATED STEPPING ROBOT

Mihai AVRAM[1], Adrian CARTAL[1], Constantin BUCŞAN[1]

[1] POLITEHNICA University of Bucharest, mavram02@yahoo.com

Abstract: *The paper presents the control system of a stepping robot pneumatically actuated, consisting of the electric scheme, the control algorithm and the control program.*

Keywords*: Stepping robot, pneumatic actuation, control system*

1. Introduction

A mobile robot is an autonomous or remotely operated programmable mobile machine that is capable of moving in a specific environment. Mobile robots use sensors to perceive their environment and make decisions based on the information gained from the sensors [1].
There are many types of mobile robots: terrestrial (stepping robots, wheeled robots, track robots), aquatic, aerial and space robots [2].
Mobile robots are used in a large number of fields: military, geology, archeology, nuclear applications, various services as pipes and tanks inspecting and cleaning, fire extinguish, maintenance of high buildings fronts etc.
Stepping robots have a higher mobility and cause less damage to the terrain then the track robots.
The paper presents the control system of a stepping robot pneumatically actuated, developed in the Mechatronics and Precision Mechanics Department within POLITEHNICA University of Bucharest [3].

2. The structure of the stepping robot

A view of the stepping robot is shown in figure 1.

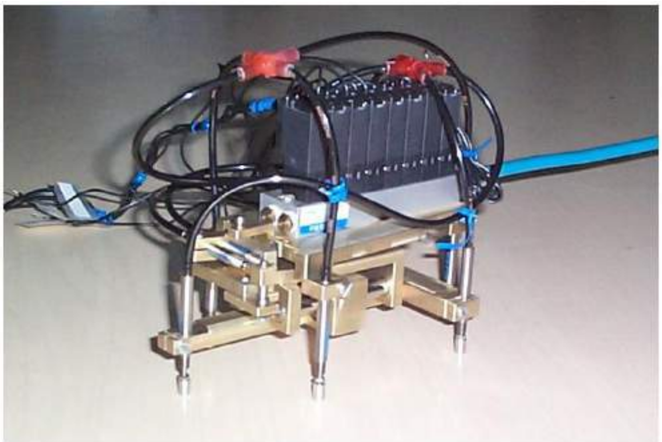

Fig. 1. A view of the stepping robot

The principle scheme of the robot is shown in figure 2 and the structure of the stepping robot is shown in figure 3.

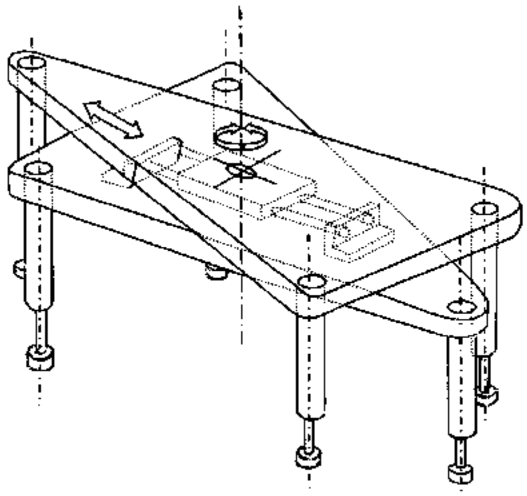

Fig. 2. The principle scheme of the robot

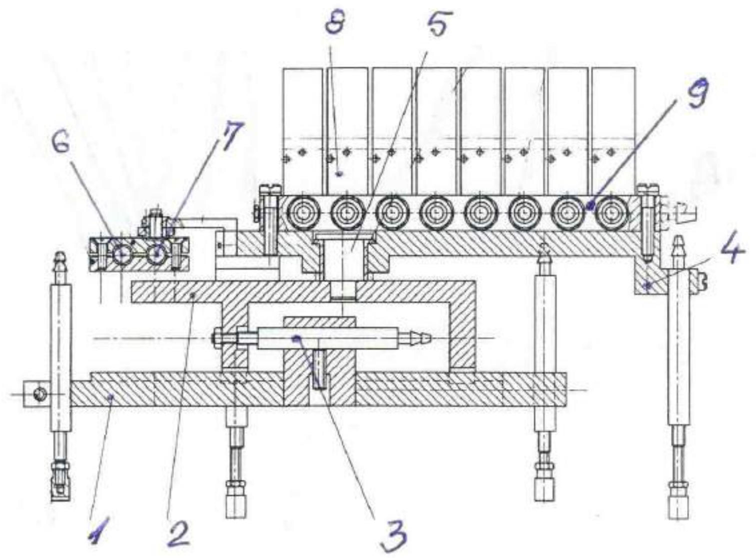

Fig. 3. The structure of the stepping robot

The lower platform 1 has three “legs” attached, consisting in three pneumatic cylinders. The intermediate part 2 is guided on ball bearings and is actuated by the pneumatic cylinder 3. The upper platform 4 is connected to the intermediate part 2 by the bolt 5, allowing the platform to rotate relative to the part 2. The upper platform has also three “legs”. The relative rotation of the platforms is performed by the pneumatic cylinders 6 and 7. The pneumatic cylinders are controlled by 3/2 valves, one for the three cylinders of the lower platform, one for the three cylinders of the upper platform, two for the cylinders used to rotate a platform relative to the other, and one valve for the cylinder used to obtain the translation movement of one platform relative to the other. The valves are mounted on a plate in order to optimize the supply and command circuits.

3. The control of the stepping robot

Figure 4 shows the electric scheme of the control system.

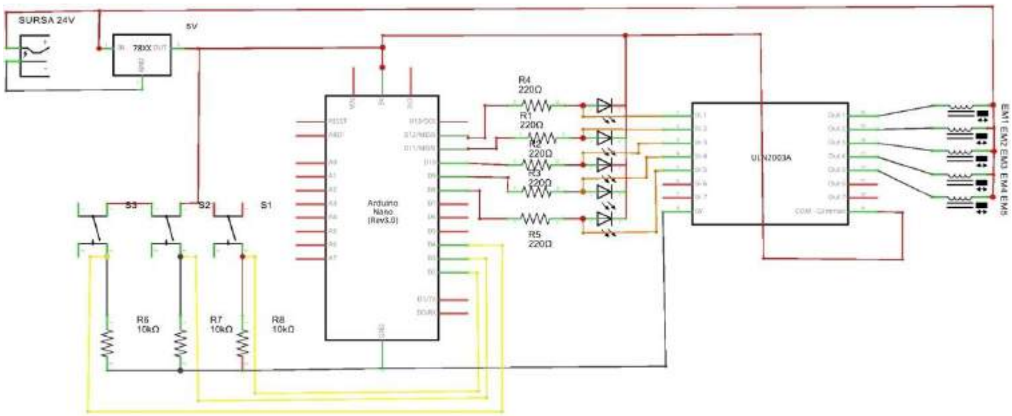

Fig. 4. The electric scheme of the control system

The control of the pneumatic stepping robot is performed using an Arduino Nano V3 microcontroller. In order to command the electromagnets of the valves a power amplifier using ULN2003A transistors is used. Three push-buttons are connected to three digital inputs of the microcontroller to allow manually selection of different control sequences.
Figure 5 shows the logical diagram of the control algorithm.

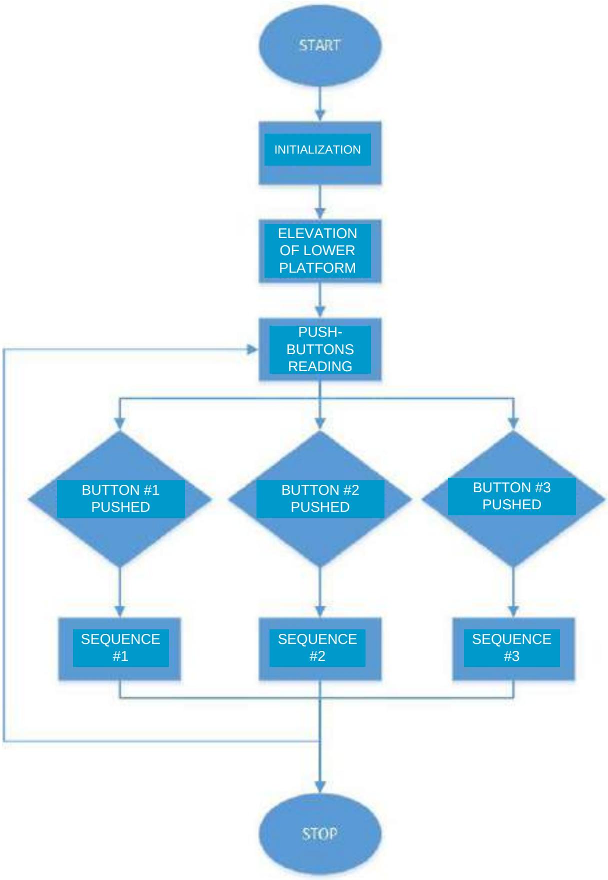

Fig. 5. The logical diagram of the control algorithm

The control algorithm reads the push-buttons state and the chosen step sequence is executed, as shown in figure 6, where LPV is the lower platform valve, UPV is the upper platform valve, FMV is the forward movement valve, LRV is the left rotation valve and RRV is the right rotation valve.

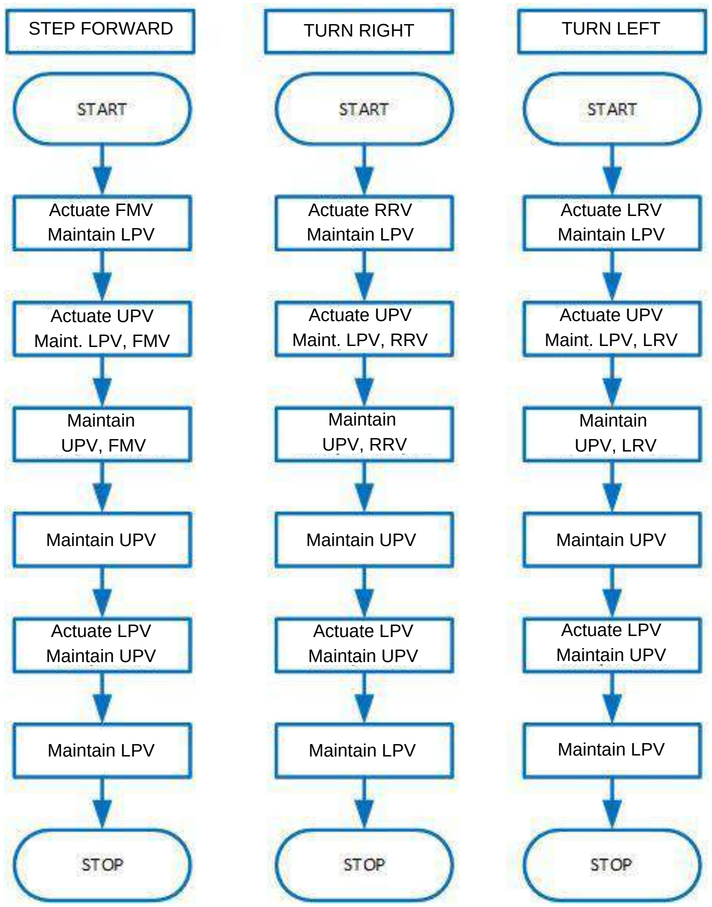

Fig. 6. The moving sequences

A control program was developed on the basis of the control algorithm described.

4. Conclusions

The stepping robot is an experimental model with the following characteristics: stepping on terrains with variable configuration, actuation with pneumatic micro-cylinders (p=4 bar), moving speed: 1.8 m/min; weight: 0.7 kg, maximum load: 0.8 kg, size: 160 x 75 x105 mm.
Further development: implementation of various sensors in order for the robot to become autonomous, using pneumatic suckers attached to the “legs” in order to allow moving on vertical surfaces etc.

References

[1] Z. Gacovski, ”Mobile Robots - Current Trends”, ISBN 978-953-307-716-1, published under CC BY 3.0 license, 2011;
[2] S. Hirose, “Biologically Inspired Robots”, Oxford University Press 1993;
[3] H. Panaitopol, L. Bogatu, M. Avram, “Minirobot păşitor cu actuatori pneumatici”, *Hidraulica* no. 3-4, 2000, ISSN 1453-7303, pp. 70-72.

ISSN 1454 - 8003
Proceedings of 2017 International Conference on Hydraulics and Pneumatics - HERVEX
November 8-10, Băile Govora, Romania

PORTABLE TEST EQUIPMENT FOR AUTOMOTIVE POWER-STEERING WITH DATA TRANSMISSION

Alexandru HRISTEA[1], Radu RĂDOI[1], Bogdan TUDOR[1], Ioan BĂLAN[1]

[1] INOE 2000-IHP, hristea.ihp@fluidas.ro

Abstract: *The steering system is one of the components that ensure safe movement of vehicles; besides this, keeping it in optimum condition leads to a minimum fuel consumption but also the lack of pollution associated with the loss of hydraulic fluid. Power steering is one of the most requested options in a car of small and medium size, for the vehicles weighing over 1200 kg entirely common. In figure 1 is represented the percent's according to the type of assistance steering boxes; from this graph, in conjunction with the average age of the fleet in Romania (13 years in the year 2017), it is deduced that most power-steering's mounted on cars have hydraulic power steering or electro-hydraulic, so the need for a portable test equipment is needed to discover and resolve the problem regarding faults of the system without disassembling the vehicle. Advantage of the device lies in its capability to transmit data that is collected by flow and pressure transducers and sent to a mobile device (smartphone or tablet) or fixed (PC) using Wireless technology. Also data can be transmitted to an operator who is specializes in repairing hydraulic steering boxes to confirm their state of function.*
This article presents the state of the art portable test equipment with data transmission for hydraulic power boxes and pumps from cars, this test device will have reduced dimensions and will be formed of a flow transducer and pressure transducer and a 2 way distributor with and a wireless module, all of which are connected to an electronic unit with an display located on the device panel.
This data is then transmitted to a device that has software installed on it, capable of play back information that receives from the transducers.

Keywords*: Fault test, power steering, public safety, automotive*

1. Introduction

The basic functionality of the hydraulic power box and components are represented in figure 2. Hydraulic power steering main purpose is that it can provide the driver less effort to steer the wheels of the car when driving at typical speeds, and reduce considerably the physical effort necessary to turn the wheels when a vehicle is stopped or moving slowly , is achieved by applying pressure to the sides of a piston rod mounted on a bilateral body (Fig.2); fluid access is made thru an opening after rotary valve(1) mounted on the steering column, receives a response from the pinion (2) always engaging the steering rack rigidly connected to the piston (4). The fluid flows through ducts (3) and position (5) represent the body of hydraulic cylinder.

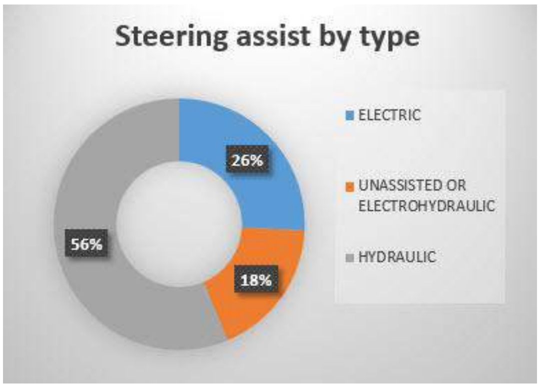

Fig. 1. Steering assist by type of the vehicles manufactured today in the world

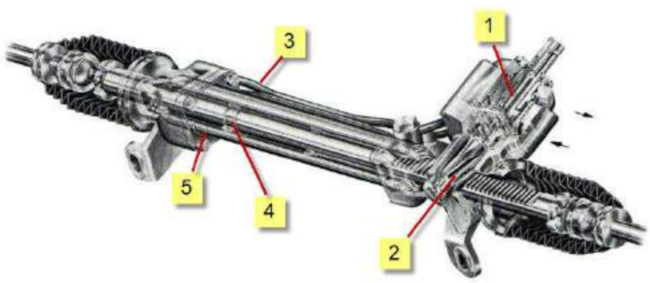

Fig. 2. Main components of the hydraulic steering box

Hydraulic power steering (pump directly driven by the vehicle engine with its rpm) is responsible for fuel consumption of approx. 0.3 l / 100 km; For drive pump by a separate electric motor (electro-hydraulic power steering), that consumption is reduced by half.
However, regardless of version, malfunction is accompanied by an increase in consumption and the loss of power steering fluid, both with negative effects on the environment and road safety [1].

2. Product description

The **portable test equipment with data transmission,** fig. 3, is a new invention which by allowing to test the hydraulic power steering system of vehicles without having to dismantle the subassemblies, thus reducing the immobilization time of the vehicle and possible hydraulic fluid drainage on the road, endangering the safety of the others involved in traffic. The device is also capable of transmitting data from pressure and flow sensors to a smartphone, tablet, or to desktop PC via a wireless module. It can also be produced with an integrated display for rendering the measured values as well as with the possibility of storing this information.

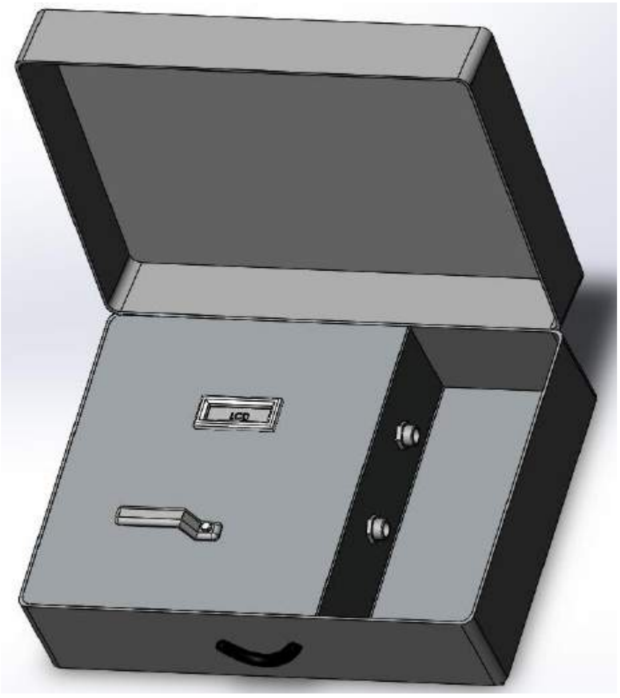

Fig. 3. 3D drawing of the portable equipment

The usefulness of this equipment is due to the poor quality of roads in Romania that puts the power steering's under a lot of wear and tear, whey over the operating limit designed by the manufacturer. This new device it also reduces the time with the defects repair due to the flexibility offered by the data transmission system, which sends to a repair specialist of the hydraulic power steering boxes, very much needed by the industry. The device is also capable of generating a test report, which it can then be passed on to a specialist who can accurately determine the cause of the fault and the solution needed to repair the servo-hydraulic system. This portable test device is been produced in Romania being only one of its kind. In fig.4 it can be seen a block diagram with the components of the portable test equipment and the informatic data transmission system and local display.

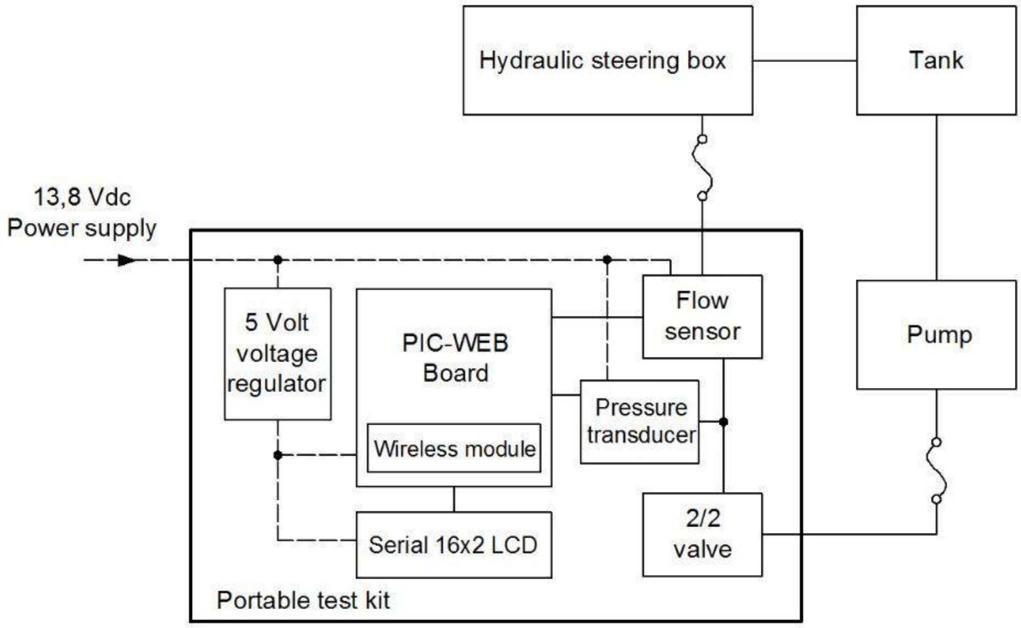

Fig. 4. Block diagram of portable test equipment with data transmission

The portable test equipment is composed of several sensors needed to record the parameters which are critical to determine the condition of the steering box. The sensors used in the hydraulic scheme are: pressure sensor with a domain of 0-160 bar, flow sensor 0,1-12 l/min [2]. All the sensors are connected to the input ports from Pic Web Board. The equipment is supplied with electricity from the cigarette lighter socket on the vehicle. The electrical connection of the electronic components can be seen in figure 5. The pressure and flow transducer are powered by a voltage of 13.8 V, and the PIC-Web and the liquid-crystal electronic module are powered by 5 V via a voltage regulator integrated circuit. The pic-web module is provided with an optional wireless transmission module connected via the UEXT connector. The display receives the data to be displayed through the serial port from the pic-web module to the RX pin.

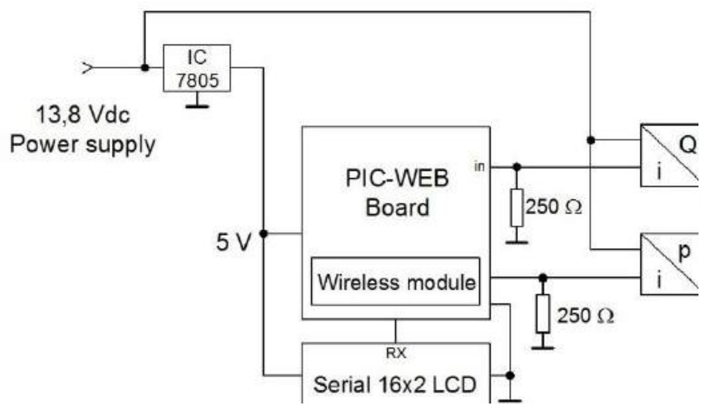

Fig. 5. The electric connection of electronic components of portable equipment

Fig. 6. The Pic-Web electronic development board from Olimex

Figure 6 shows the Pic-Web electronic development board from Olimex [3]. The Pic-Web board is designed to have Web page of no more than 128 kB. If necessary a lot of images in the application they can be stored on other server visible on the network where you have the PIC-WEB connected. The potential of the board is to generate a fluid communication between some specific sensors or actuators across a TCP/IP net including the controls of it.

Pic-Web board features:

- PIC18F67J60 microcontroller
- 1Mbit on board serial flash for web pages storage
- ICSP/ICD mini connector for programming and debugging with PIC-ICD2, PIC-ICD2-POCKET and PIC-ICD2-TINY.
- Reset button
- User event button
- Analogue trimmer potentiometer
- Thermistor for temperature monitoring
- RS232 driver and connector
- Complete web server and TCP-IP stack support as per Microchip's open source TCP-IP stack
- Power plug-in jack for DC power supply
- Voltage regulator +3.3V and filtering capacitors
- Status LED
- UEXT connector
- Extension header to connect to other boards
- Dimensions 60×65 mm (2.36×2.55")

3. Operating mode

The test kit connects to the car's hydraulic assisted steering system with two hoses. Unscrew the hose that comes from the pump to the hydraulically assisted steering box and insert the equipment between the pump and the steering box. The built-in transducers will read the system pressure and flow. By closing the valve for a short time, the maximum pressure delivered by the steering pump can be determined. At the end of the stroke hydraulic cylinder piston, the steering box leakage can be determined.
All the tests are performed with the help of the software developed by Hydraulics and pneumatics research Institute with the aid of an internet protocol Web page program. Test data is displayed locally on the device panel and transmitted wirelessly by the web application stored in the Pic-Web module. Viewing test data and recording data is done by accessing the application through a web browser on any mobile device (phone or tablet). Connection of the mobile device to the web application is done wirelessly by accessing the IP address of the web application. Connecting to the web application can also be done with a desktop PC via an Ethernet cable, the Pic-Web module being equipped with an RJ45 Ethernet connector.
All the data recorded it will be compared with those in the database and the system will decide whether the data recorded for the hydraulic steering box comply with the standards accepted by its manufacturer. On the software page (fig. 7) the parameters obtained from the test can be seen and it is possible to record the data such as: name of the operator that perform testing, beneficiary of the test report, date and registration number of the test report. With this portable test device can be determined the rate of oil leakages at the stroke ends of steering box or in the middle of the stroke of hydraulic cylinder (car wheels in the center position). The leakage rate is determined by the wear of the piston and rotary valve seals. In figure 7the panel of the software application displays data obtained from testing. If the flow of loss at the end of stroke is above 1.5 l / min is recommended to replace or repair the steering box. A steering box worn, with large internal losses, will lead to disturbance in handling the power steering [4].

Fig. 7. Panel of the software application for test report issue

In order to issue the test report, in the software application the information for the beneficiary, the test operator and the test date must be noted. Once the data has been filled in, it will be possible to save a file containing the test parameters and identification data (report number, date, beneficiary, etc.). This report is stored and can be printed or sent by e-mail [5].

4. Conclusions

The test portable equipment with data transmission allows quick testing of the hydraulically assisted steering system without the need to dismantle the parts from the car.
Advantages of the device lie in its capability to transmit data that is collected by flow and pressure transducers and sent to a mobile device (smartphone or tablet) or fixed (PC) using Wireless technology.
Through the web application can issue test reports with data transmitted wirelessly from the test equipment, which can then be archived.
The amount of sensors and the domain of them, determine how accurate is the report for increase the road safety and human loses due to malfunction of hydraulic power steering [6].

Acknowledgments

This work has been funded by Executive Agency for Higher Education, Research, Development and Innovation Funding - UEFISCDI, under PNCDI III - Programme 2, Subprogram 2.1 – Cheques of Innovation (CI-2017), Submission code PN-III-P2-2.1-CI-2017-0229, Financial agreement no. 3CI/2017, project title: Portable test equipment for the power steering of vehicles with data transmission, project acronym ETSAD, Project main domain: 2. Information of technology and communications space and security, Subdomain: 2.3. Security.

References

[1] P.A. Adegbuyi, I.L. Marcu, "Hydraulic and pneumatic cylinder failures, the effect of fluid cleanliness on component life", *Hidraulica Magazine*, ISSN 1453-7303, Romania, no.1, pp. 27-30, 2013;
[2] I. Dutu, G. Matache, "Computer assisted electro-hydraulic stand for testing servovalves", *Hidraulica Magazine*, ISSN 1453-7303, Romania, no.3-4, pp. 73-77, 2012;
[3] https://www.olimex.com/Products/PIC/Development/PIC-WEB/resources/PIC-WEB-manual.pdf;
[4] G. Matache, St. Alexandrescu, Gh. Sovaiala, I. Pavel, I.C. Girleanu, "Testing of linear pneumatic actuators with hydraulic load", *Hidraulica Magazine*, ISSN 1453-7303, Romania, no.3, pp. 53-56, 2013;
[5] G. Matache, St. Alexandrescu, A. Pantiru, Gh. Sovaiala, M. Petrache, "The analysis of flow losses through dynamic seals of hydraulic cylinders", *Hidraulica Magazine*, ISSN 1453-7303, Romania, no.1, pp. 52-60, 2013;
[6] C. Cristescu, C. Dumitrescu, G. Vranceanu, L. Dumitrescu, "Considerations on energy losses in hydraulic drive systems", *Hidraulica Magazine*, ISSN 1453-7303, Romania, no.1, pp. 36-46, 2016.

ISSN 1454 - 8003
Proceedings of 2017 International Conference on Hydraulics and Pneumatics - HERVEX
November 8-10, Băile Govora, Romania

PIPELINE LEAKAGE DETECTION BY MEANS OF ACOUSTIC EMISSION TECHNIQUE

Claudiu-Ionel NICOLA[1], Marcel NICOLA[1], Iulian HUREZEANU[1], Adrian VINTILĂ[1], Ancuța-Mihaela ACIU[1], Dumitru SACERDOȚIANU[1]

[1]National Institute for Research, Development and Testing in Electrical Engineering – ICMET Craiova

nicolaclaudiu@icmet.ro, marcel_nicola@yahoo.com, iulian_hurezeanu@yahoo.com, adrian_vintila@icmet.ro, ancutu13@yahoo.com, dumitru_sacerdotianu@yahoo.com

Abstract: *The inspection and maintenance of underground technological pipes are marked by difficulties and restraints. Accidental leakage is inevitable and may pose a serious problem for the environment and the economy. Also, stricter legal rules implemented in developed countries require reliable and secure systems for detecting leaks during the last decade, the acoustic emission (AE) technique was widely used as a non-destructive testing (NDT) technique for detecting leaking pipes, heat exchangers or pressure vessel structures. Although these structures are relatively large, the EA can be used for their inspection. The paper presents a system for leak detection based on the principle of leak location by means of the cross-correlation method using a data acquisition system, acoustic sensors and software application developed in LabVIEW programming environment.*

Keywords*: cross-correlation, acoustic emission, leakage detection, LabVIEW environment*

1. Introduction

With increasing public awareness and concern for the environment, occurrences of pipeline leakage showed that financial losses incurred by a company can be much higher than the downtime and cleaning costs. Also, stricter legal rules implemented in developed countries require reliable and secure systems for leakage detection [1].
The inspection and maintenance of underground technological pipes are marked by difficulties and restraints. Accidental leakage is inevitable and may pose a serious problem for the environment and the economy.
The timely detection of leakage also offers other advantages beside the economic ones: safety of water supplies, environment protection, water quality protection, avoiding subsequent pipe cracks which may cause damage [2].
Due to the limit of detection, it is usually necessary to install several sensors along the line. These sensors detect the acoustic signals in the pipe and discriminates leakage acoustic emission from other sounds generated by normal operating changes [3].
The rapid development of electronics industry allowed the development of electroacoustic equipment, acoustic sensors, amplifiers, digital filters, data acquisition, storage, processing and transmission systems, which help to increase fault detection efficiency.
The greatest intensity of sound is in the proximity of the noise source and decreases proportionally in all directions with the distance to the source. The sound propagation speed is influenced to the greatest extent by the pipeline material. For example: for steel and cast iron, the intensity is also present at longer distances from the fault, while in the case of PVC and HDPE the sound can only intercepted near the source.
The acoustic correlation allows determining the exact location of the fault based on the sound propagation speed in the fluid or the pipe wall. The sensors (surface microphones, or hydrophones) placed on both ends of the section of pipe where the fault is assumed to occur will detect the sound produced by an offset except for the situation when the fault is halfway between those two sensors. The basic unit of the correlator will analyze the signals transmitted by the two sensors based on the time of incidence. By knowing the sound propagation speed, the correlator

will specify the exact location of the fault.
The fault location procedure can include a stage of “listening” to the noise caused by cracks from using equipment which includes special microphones. This type of location depends very much on user experience, which will assess the location of the crack by means of headphones. The next stage consists in the “precise location” by using a noise and vibration correlator [4].
The flow of fluid out of the pipeline, through cracks, generates noise which propagates through the fluid inside the pipe, to the material of the pipe and the soil around the pipe. This kind of signals is known in the literature as “cracking noises” or “leakage noises”.
During the last decade, the acoustic emission technique was widely used as non-destructive testing (NDT) technique for detecting leaking pipes, heat exchangers or pressure vessel structures. Although these structures are relatively large, the AE technique can be used for their inspection [5].

2. The description of the leakage location principle by using the acoustic emission technique

In the case of noise and vibration correlators, the sensors come into contact with the pipe material. They will retrieve the cracking noises and transmit them to a noise and vibration correlator, and due to the fact that the noise propagates with same speed, the sensor which is located closer to the fault will retrieve the signal faster. The propagation speed depends primarily on the material of the pipe. If this speed is known or determined by experiments, the difference between the time it takes for the cracking noise to reach the two sensors will indicate the crack location [6].
The correlator operation principle is shown in Figure 1.

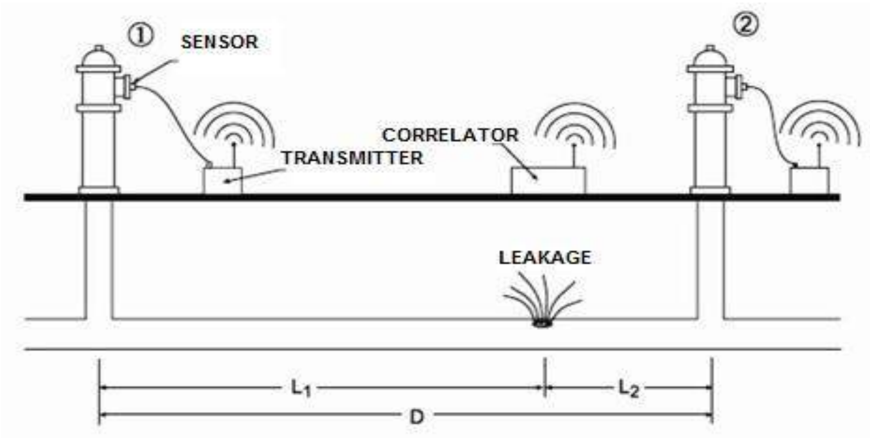

Fig. 1. The principle of noise source location by mean of correlation

The fault location, if the origin of the axis is by the sensor on the left is given by the formula (1).

$$L_1 = \frac{1}{2}(D - \Delta T \cdot C) \quad (1)$$

where:

- *D* – the distance between the sensors;
- *C* – acoustic signal propagation speed in the pipe (constant);
- ΔT – sample frequency^{-1} * time lag.

The transmission of the signals picked up by the sensors, to the correlators is achieved by mean of radio waves or wires. The operation of signal processing algorithms for the identification of noise sources is based on the cross-correlation method.
The cross-correlation function identifies the degree of similarity between two data sets, and is an important tool for the statistical analysis of signals.
The cross-correlation method makes reference to the relation between a signal and its lagged version; the cross-correlation method allows determining the difference in propagation time by the

position of its peak value [7, 8].
If we consider the signals *x(n)* and *y(n)* as signals which propagate from the noise source to the two piezoelectric sensors (the signals contain N samples and are considered stationary with zero mean value), we can define the cross-correlation function as follows:

$$r_{xy}(l) = \frac{1}{N} \cdot \sum_{n=-\infty}^{\infty} x(n) \cdot y(n+l), \quad l = 0, \pm 1, \pm 2 \ldots N-1 \tag{2}$$

The index *l* is considered to be the time lag. The order of the indices show that signal *x(n)* remains unchanged while *y(n)* is lagged by *l* time units, practically *y(n)* represents a lagged version of signal *x(n)* by *l* time units.
In order to obtain a normalized cross-correlation (with peak values in the range -1 ÷ 1) the following formula can be applied (3):

$$\rho_{xy}(l) = \frac{r_{xy}(l)}{\sqrt{r_{xx}(0) \cdot r_{yy}(0)}} \tag{3}$$

In special cases when the crack is located midway between the sensors, the peak value is negative concentration value. For example, if the index of peak value of FIC is r samples, then the lag value expressed in units of time $D_{time} = r^*T_e$ can be calculated, where T_e represents the value of the sampling period (see Figure 2).

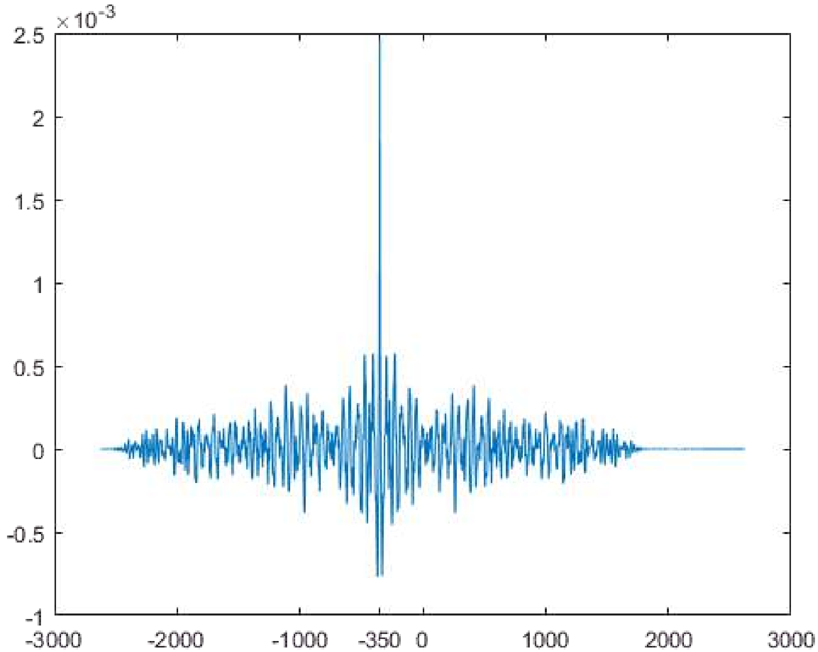

Fig. 2. Non-normalized FIC calculated for signals x, y

3. Hardware and software description of the system

The rapid adoption of the PC in the last 20 years catalyzed a revolution in instrumentation for test, measurement, and automation. One major development resulting from the ubiquity of the PC is the concept of virtual instrumentation, which offers several benefits to engineers and scientists aiming for increased productivity, accuracy, and performance [9].
A virtual instrument consists of an industry-standard computer or workstation equipped with powerful application software, cost-effective hardware such as plug-in boards, and driver software, which together perform the functions of traditional instruments. Virtual instruments represent a

fundamental shift from traditional hardware-centered instrumentation systems to software-centered systems that exploit the computing power, productivity, display, and connectivity capabilities of popular desktop computers and workstations. Although the PC and integrated circuit technology have experienced significant advances in the last two decades, it is software that truly provides the leverage to build on this powerful hardware foundation to create virtual instruments, providing better ways to innovate and significantly reduce cost. With virtual instruments, engineers and scientists build measurement and automation systems that suit their needs exactly (user-defined) instead of being limited by traditional fixed-function instruments (vendor-defined) [10].
The hardware and software architecture of the pipeline leak detection system is achieved for implementation of the cross-correlation method.

3.1. Hardware description

For method validation a hardware structure is presented where the connection between the two sensors and the data acquisition and processing system is achieved by wire.
The designed structure is shown in Figure 3 and has the following components:

- S1, S2 – acoustic sensors - VS30-SIC-46dB;
- Data acquisition card (DAQ) NI-USB 6003;
- PC host.

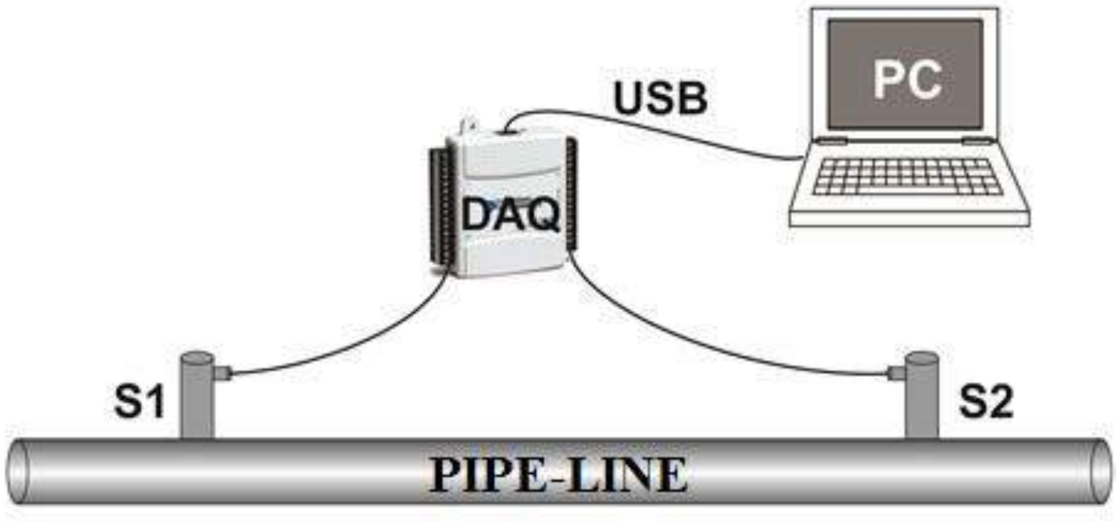

Fig. 3. Hardware architecture of the leakage detection system

The VS30-SIC-46dB is a piezoelectric AE-sensor with integrated preamplifier. The low frequency response makes it especially suited for monitoring large objects or objects made of highly attenuating material. The VS30-SIC-46dB can be used for tank floor corrosion and leak detection, leak detection in pipelines, partial discharge detection and integrity testing of concrete structures. The integrated preamplifier has a 46 dB gain and supports pulse through for automatic sensor testing [11].
The NI-USB‑6003 is a low-cost, multifunction DAQ device. It offers analog I/O, digital I/O, and a 32‑bit counter. Some specification of the NI-USB 6003 are 8 AI (16-Bit, 100 kS/s), 2 AO (5 kS/s/ch), 13 DIO USB Multifunction I/O Device [12]. The USB‑6003 provides basic functionality for applications such as simple data logging, portable measurements, and academic lab experiments. The included NI‑DAQmx driver and configuration utility simplify the configuration and the measurements.
A schematic diagram for the module of power supply and decoupling AC component from the signal is presented in figure 4.

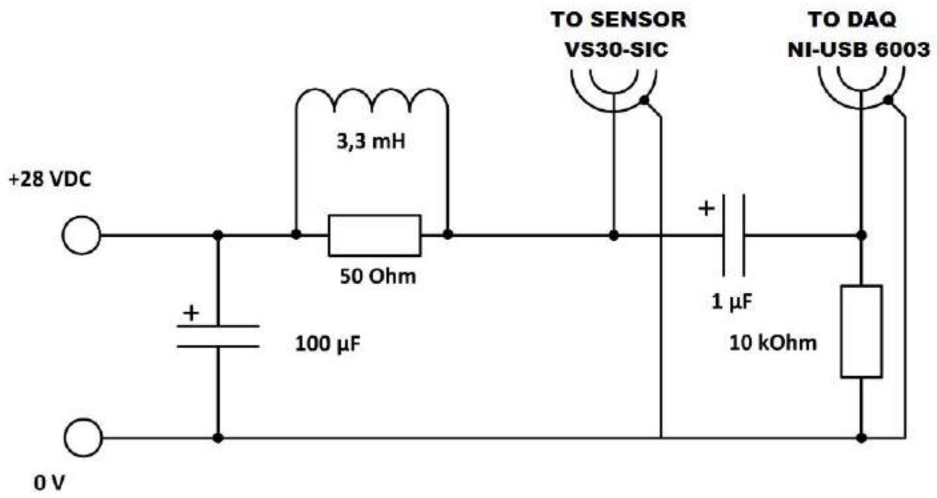

Fig. 4. Module to supply power to the preamplifier and decoupling AC component from the signal

3.2. Software description

LabVIEW is a graphical programming language that uses icons instead of lines of text to create applications. In contrast to text-based programming languages, where instructions determine program execution, LabVIEW uses dataflow programming, where the flow of data determines execution [13].

The programming language used in LabVIEW, also referred to as G, is a dataflow programming language. Execution is determined by the structure of a graphical block diagram (the LV-source code) on which the programmer connects different function-nodes by drawing wires. These wires propagate variables and any node can execute as soon as all its input data become available. Since this might be the case for multiple nodes simultaneously, G is inherently capable of parallel execution. Multi-processing and multi-threading hardware is automatically exploited by the built-in scheduler, which multiplexes multiple OS threads over the nodes ready for execution [14].

Figure 5 presents the software interface of the proposed pipeline leakage detection system.

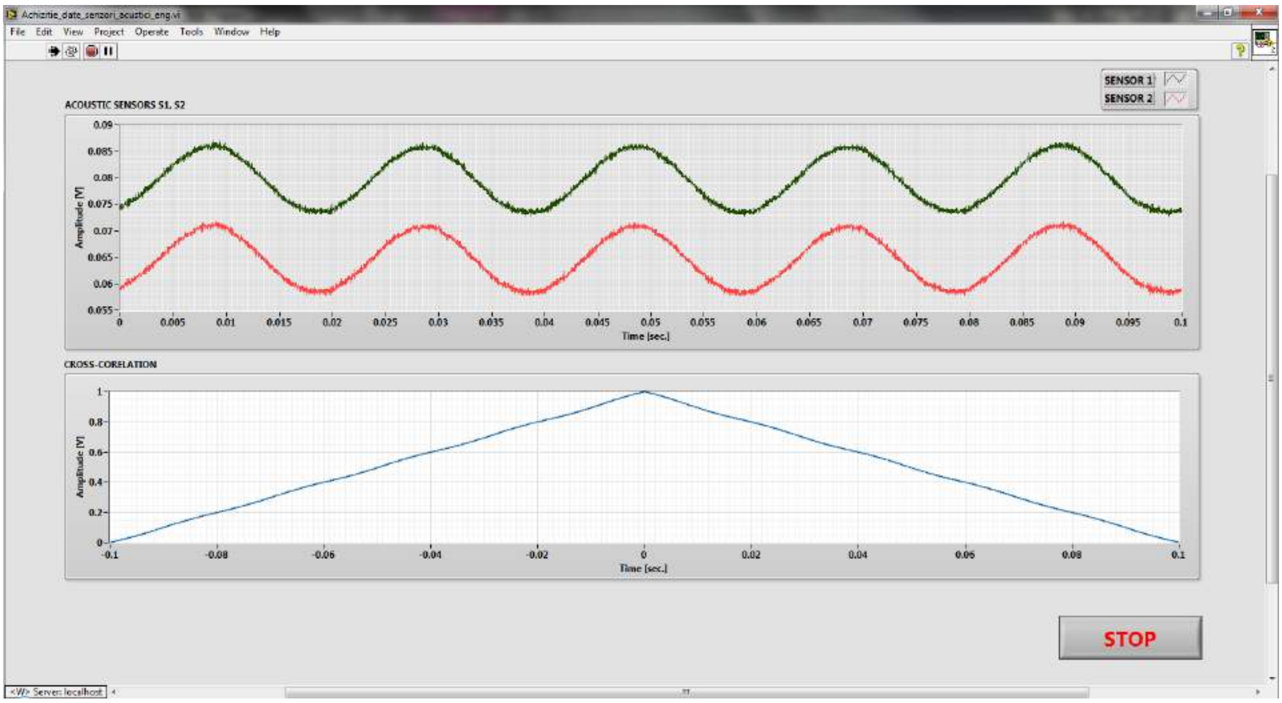

Fig. 5. Software interface of the application

Figure 6 presents the block diagram of the software application.

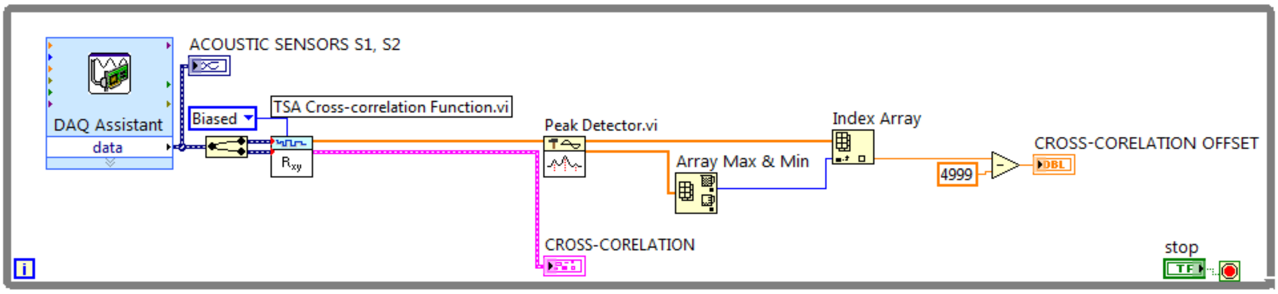

Fig. 6. Block diagram of the application software

The following block diagram shows one way to index the Cross-Correlation function by a virtual instrument (VI) [15].

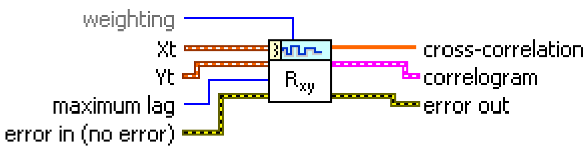

Fig. 7. Cross-Correlation VI

The elements of VI are:

- *weighting* specifies the use of biased or unbiased weighting in the cross-correlation calculation. The default weighting is Biased. Refer to the Details section for information about this parameter;
- *Xt* specifies the univariate time series;
- *Yt* specifies another univariate time series and is used to perform cross-correlation with Xt;
- *maximum lag* specifies the maximum value of the lag used by this VI to compute the cross-correlation. The default is –1, which means the maximum lag equals max(M, N)–1, where M and N are the lengths of Xt and Yt, respectively;
- *cross-correlation* returns the cross-correlation values between the two time series Xt and Yt;
- *correlogram returns*, on an XY graph, the cross-correlation values against the lag.

The cross-correlation $R_{xy}(t)$ of the sequences x(t) and y(t) is defined by the following equation [15]:

$$R_{xy}(t) = x(t) \otimes y(t) = \int_{-\infty}^{\infty} x(\tau) \cdot y(t+\tau) d\tau \tag{4}$$

where the symbol $\otimes$ denotes correlation.

The discrete implementation of the Cross-Correlation VI is as follows [15]. Let h represent a sequence whose indexing can be negative, let N be the number of elements in the input sequence X, let M be the number of elements in the sequence Y, and assume that the indexed elements of X and Y that lie outside their range are equal to zero, as shown by the following equations:

$$x_j = 0, j < 0 \quad \textit{or} \quad j \geq N \tag{5}$$

and

$$\mathrm{y_j = 0, j < 0 \quad or \quad j \geq M} \tag{6}$$

Then the Cross-Correlation VI obtains the elements of h by using the following equation:

$$h_j = \sum_{k=0}^{N-1} \overset{\bullet}{x_k} \cdot y_{j+k} \tag{7}$$

for j = –(N–1), –(N–2), … , –1, 0, 1, … , (M–2), (M–1)
The elements of the output sequence R_{xy} are related to the elements in the sequence h by

$$R_{xyi} = h_{i-(N-i)} \tag{8}$$

for i = 0, 1, 2, … , N+M–2.
LabVIEW arrays cannot be indexed with negative numbers, the corresponding cross-correlation value at t = 0 is the Nth element of the output sequence Rxy. Therefore, Rxy represents the correlation values that the Cross-Correlation VI shifts N times in indexing.
The normalization biased in LabVIEW is used as follows:

$$R_{xy(biased)} = \frac{1}{max(M,N)} \cdot R_{xy} \tag{9}$$

for j = 0, 1, 2, … , M+N–2, where R_{xy} is the cross-correlation between x and y with no normalization.

4. Experiments

Figure 8 presents an experimental model which will follow the steps described in the previous sections for pipe leak location. The origin point of the axis system is fixed in sensor S1 and the axis is oriented towards sensor S2. The length of the studied pipe section is of 3 m and the sound propagation speed in the pipe is of 5500 m/s.

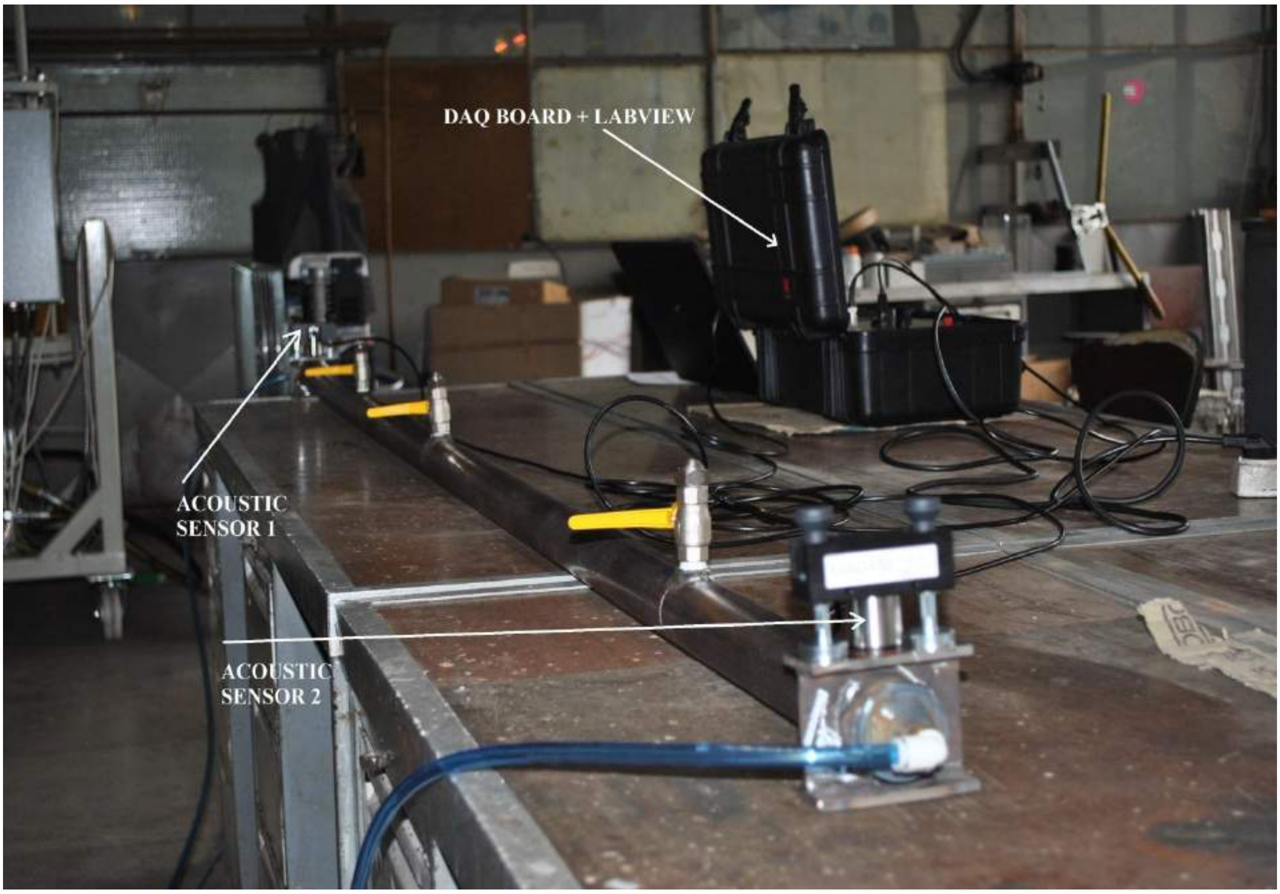

Fig. 8. Experimental image

As a result of the experiments carried out in order to simulate leaking in the middle of the pipeline (by opening the middle valve) the cross-correlation function in Figure 9 is obtained. By applying the formula (1) the fault location in the mid pipe is obtained with an error under 0.01 m.
In order to simulate a pipeline leak at 0.235 m (by opening the valve on the left) the cross-correlation function in Figure 10 is obtained. The number of samples for which we obtain the peak cross-correlation function is 22, and the lag it indicates is of 0.00044 seconds.
The fault location is determined at 0.25 m from the sensor S1 by applying the formula (1).
Generally after a series of experiments, a relatively satisfactory location error (for a practical system) of less than 2% is obtained.

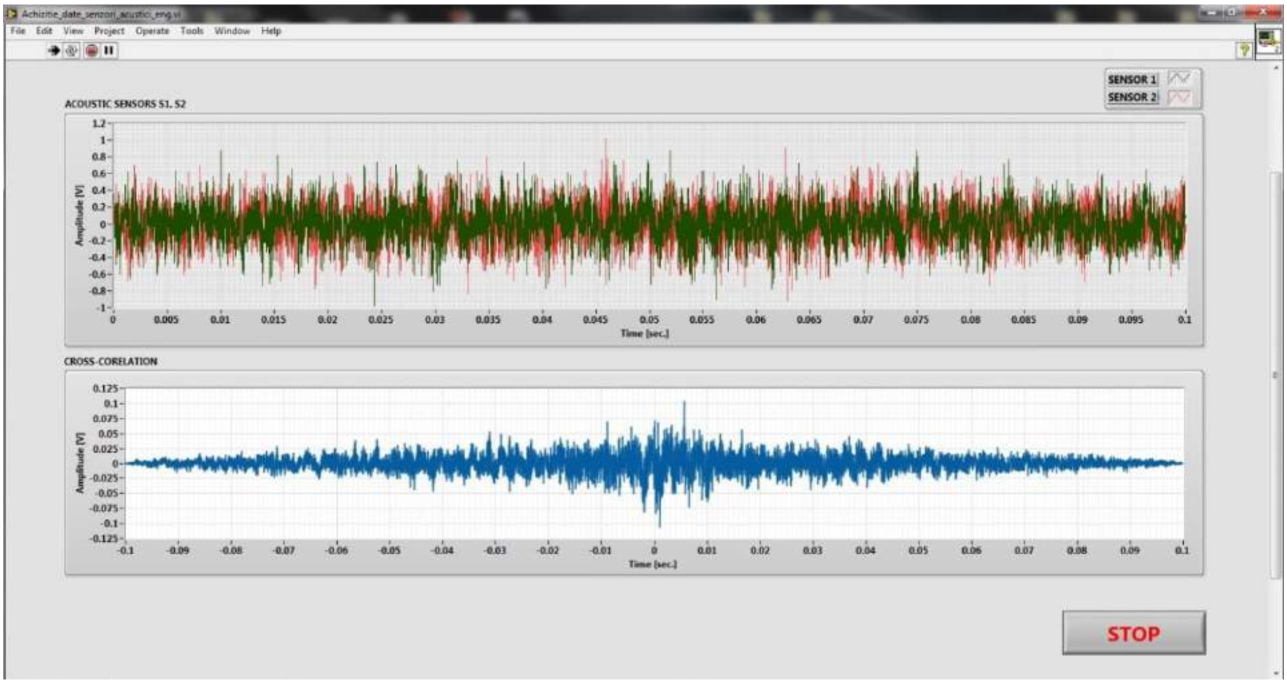

Fig. 9. Software interface for simulation of the leakage in the middle of the sensors

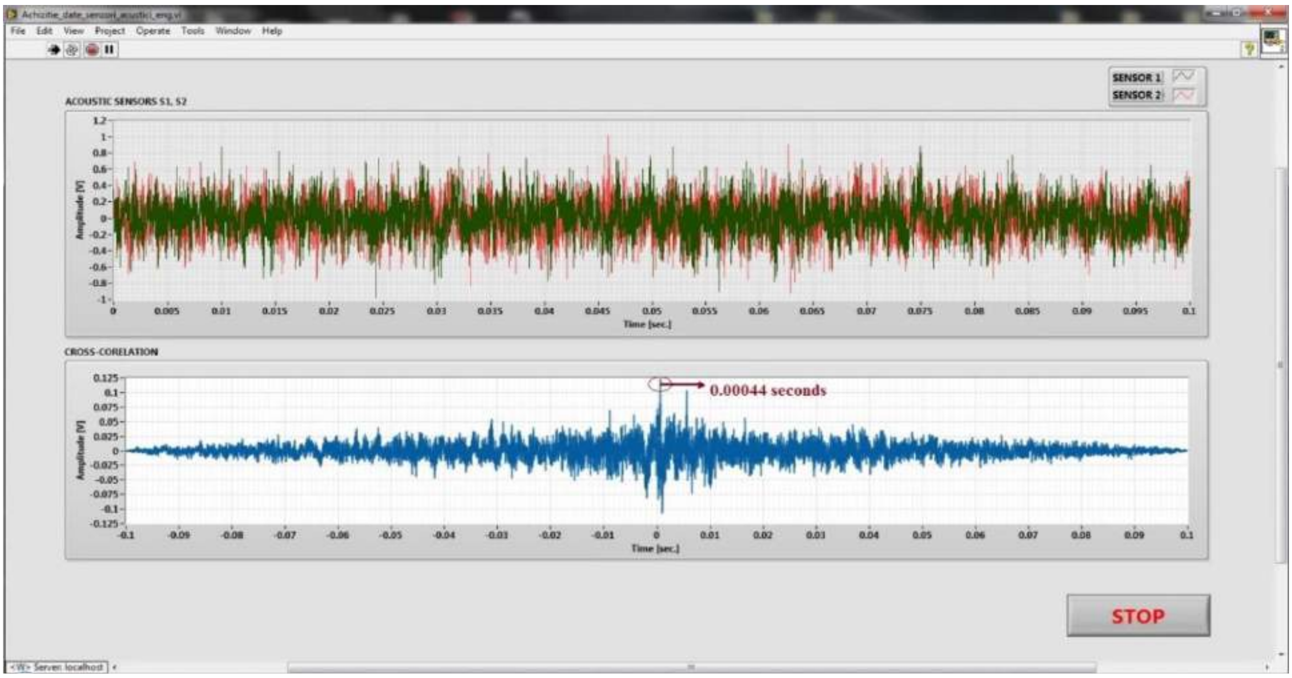

Fig. 10. Software interface for simulation of the leakage at 0,25 m from S1

5. Conclusions

The use of acoustic emission technique for leak-off location is the top method, made possible due to the development of electronics (high-performance sensors, data acquisition systems) as well as the development of high-performance software with computing power and precise pipe fault location.
By following the steps specified by the EA technique, a pipeline leak-off detection system was developed and presented based on the cross-correlation method. As a result of experiments it was found that the system has a relatively good accuracy, subsequent developments will focus on expanding the system to a wireless multi-sensor network for leak-off detection in intertwined pipeline sections.

References

[*] T.C. Popescu, A. Drumea, I. Dutu, "Numerical simulation and experimental identification of the laser controlled modular system purposefully created for equipping the terrace leveling installations", ISSE-2008, Budapest, Hungary; 7-11 May, 2008, *Proc. Reliability and Life-time Prediction*, ISBN: 978-963-06-4915-5; pp.336-341
[1] G. Geiger, "Principles of Leak Detection. 1st Edition", Krohne Oil & Gas, Breda, 2008;
[2] L. Boaz, S. Kaijage, R. Sinde, "An overview of pipeline leak detection and location systems", *Pan African International Conference on Information Science, Computing and Telecommunications* (2014), DOI: 10.13140/2.1.4328.8327
[3] I.G. Scott, "Basic Acoustic Emission", Gordon and Breach, New York, 1991;
[4] M. Wevers, "Listening to the Sound of Materials: Acoustic Emission for the Analysis of Materials Behaviour", NDT&E International, 1997, 30(2), pp. 99-106, doi.org/10.1016/S0963-8695(96)00051-5;
[5] R. K. Miller, P. McIntire, "Nondestructive Testing Handbook. Vol. 5 : Acoustic Emission Testing", American Society for Non-Destructive Testing, New York, 1987;
[6] L. Min-RaE, L. Joon-Hyun, "A Study on Characteristics of Leak Signals of Pipeline Using Acoustic Emission Technique", Solid State Phenomena Vol. 110 (2006) pp. 79-88, Online available since 2006/Mar/15 at www.scientific.net, Trans Tech Publications, Switzerland doi: 10.4028/www.scientific.net/SSP.110.79;
[7] M. M. Hafezi, M. Mirhosseini, "Application of Cross-Correlation in Pipe Condition Assessment and Leak Detection; Using Transient Pressure and Acoustic Waves", Resources and Environment 2015, 5(5): 159-166, DOI: 10.5923/j.re.20150505.04;
[8] J. Li, S. Chen, Y. Zhang, S. Jin, L. Wang, "Cross-Correlation Method for Online Pipeline Leakage Monitoring System", Published in: Image and Signal Processing, 2009. CISP '09. 2nd International Congress, DOI: 10.1109/CISP.2009.5302839;
[9] J. Jovitha, "Virtual Instrumentation Using Labview", PHI Learning, New Delhi, 2011;
[10] R. Bitter, T. Mohiuddin, M. Nawrocki, "LabVIEW: advanced programming techniques, Second Edition", CRC Press, 2006;
[11] http://www.vallen.de/?id=87
[12] http://www.ni.com/pdf/manuals/374372a.pdf
[13] http://www.ni.com/getting-started/labview-basics/environment;
[14] LabviewTM – Development Guidelines. [Online]. Available: http://www.ni.com/pdf/manuals/321393d.pdf
[15] http://zone.ni.com/reference/en-XX/help/371361J-01/lvanls/crosscorrelation/

ISSN 1454 - 8003
Proceedings of 2017 International Conference on Hydraulics and Pneumatics - HERVEX
November 8-10, Băile Govora, Romania

DETERMINATION OF THE FATIGUE LIFE OF AN ELECTRIC VEHICLE CHASSIS

Yunus MARAL[1], Yusuf ALTUN[2], Fikret POLAT[3]

[1] Bursa Technical University, Mechanical Engineering, Bursa, Turkey.

[2] Duzce University, Engineering Faculty, Computer Engineering, Duzce, Turkey.

[3] Duzce University, Engineering Faculty, Mechanical Engineering, Duzce, Turkey.

Abstract: *In recent years, electric vehicles have tremendous potential due to their low maintenance costs and environmental friendliness. The purpose of this study is to provide fatigue analyses on the vehicle chassis to determine the parts to be fatigued and to find the critical life of these parts. Within the scope of this plan, first of all static analysis was carried out with 600 kg load on the chassis model. According to the results of the static analysis, it was observed that the system was within the safety limits, and then fatigue analysis was started. Fatigue analysis were carried out with 5 different road data collected during road tests. As a result of the analysis, the fatigue lives of the parts on the model were determined and It has been seen that the vehicle chassis is far below critical values in terms of fatigue life.*

Keywords*: Fatigue analysis, electrical vehicle chassis, finite element analysis.*

1. Introduction

Our current technology is largely dependent on fossil fuels as essential energy source for almost all activities needed to sustain daily life. It is envisaged that the use of fossil-based fuels will pose two threats to humanity in the long run. The first threat is the increased costs associated with reduced reserves, particularly the reduction of fuels such as oil and natural gas, and hence the size of the social and economic impacts. The second threat is the harmful emissions resulting from the burning of fossil fuels and the environmental impacts of greenhouse gases [1-3].

In recent years, advances in electric vehicle technology, along with advances in electric machines, batteries and power electronics technologies, promise promising solutions in the near-term to prevent these threats. And also in the long run promises solutions that will completely eliminate it [2-4].

The first electric vehicle model was made in the Netherlands in 1835 by Professor Stratingh. It was reported by Thomas Davenport between 1834 and 1836 that an electric road vehicle was developed and put into practice in the United States. This vehicle is driven by non-rechargeable batteries with three wheels. Four years later, Robert Davidson developed an electric locomotive driven by a non-rechargeable battery. After 1859, lead-acid batteries were developed and started to be used. In 1882, Professor William Ayrton and John Perry in England implemented the application of three electric vehicles. There are 10 lead-acid batteries in each of these vehicles. The range of vehicles is 16-20 km depending on the conditions of the land and the maximum speed is 14 km / h. Three years later, Carl Benz developed three-wheeled vehicles with internal combustion engines. Towards the end of the 19th century, many companies in America, England and France started to produce electric vehicles. The most important of these producers is Morris and Salomon who owns Electric Carriage and Wagon Company [3-6].

One of the most important points to consider when designing a vehicle is that the elements of the vehicle must be safe in terms of strength. Therefore, the strength analysis of the vehicle chassis needs to be done very well [7-9]. Using the solution of the balance equations under the forces and moments acting is not so easy. In this case it is necessary to use different methods. Finite element analysis of these methods is due to be integrated with computer-aided design system especially easy to use and is very heavily used in the automotive industry [10-13].

With using the finite element methods in fatigue analysis, fatigue behaviours of elements can be examined without being subjected to test. Therefore, the fatigue behavior of many parts of the machine is determined before production. There are three important steps in fatigue analysis: Selection of Fatigue Method, Selection of Loading Method, Selection of Fatigue Curve. In this study we will use Variable Amplitude Loading Conditions Methods cause of collected data in different road conditions [14-16].

2. Materials and Methods

2.1 Static Analysis

The prepared solid model has been transferred to the Ansys Static Structural Programmer in .stp format for finite element models with some arangements. Static analysis will be done by applying the necessary boundary conditions. The mesh structure is created to chassis as shown in Fig.1. Mesh structure consists of a total of 119401 hekzahedron and tetrahedron elements and 502966 nodes.

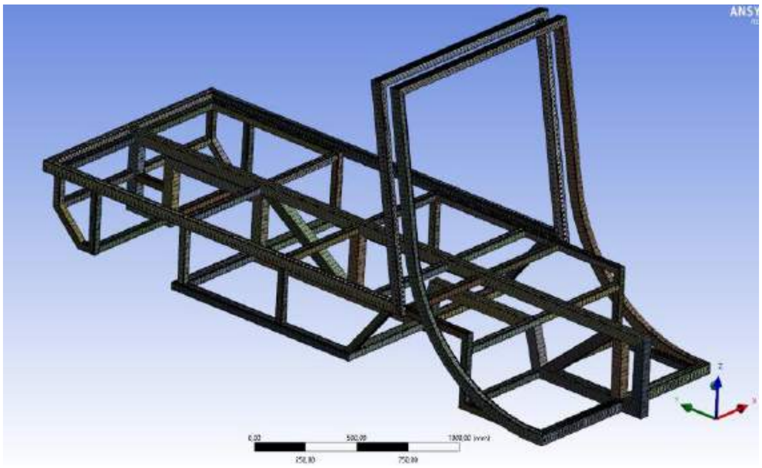

Fig. 1. Mesh structure of chassis model

The mechanical properties of St 37 steel were used for material information in the chassis model. The mechanical properties of St 37 steel are as follows.
Modulus of Elasticity : 210 GPa
Density : 7850 kg/m^3
Yield Stress: 250 MPa
Tensile Stress: 460 MPa
Poisson's Ratio: 0.3
When the loads acting on the cab area and the rear cab area were measured with the 600-kg load on the car, it was seen that the load of the cab area is 650 kg and the load of the rear cab area is 730 kg. These load values found were applied to the contact areas on the chassis from the centre of gravity calculated on the cabinet and the rear cab as shown in Fig. 2.

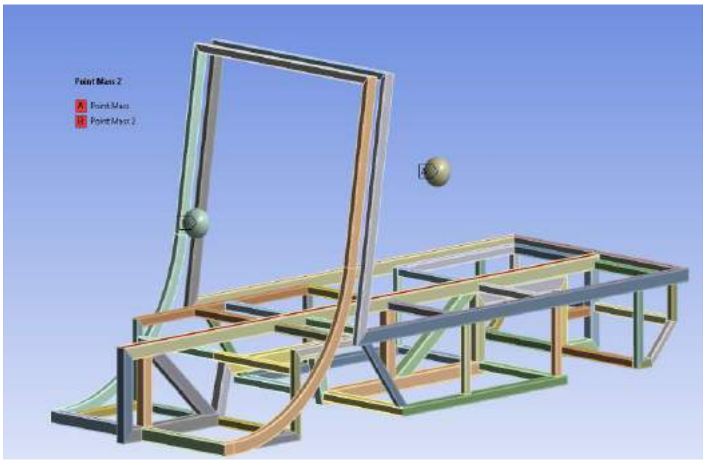

Fig. 2. Effective loads to cabinet and rear cab area

After all the data required for static analysis has been entered, the model of finite element created was runned. As a result of static analysis, the equivalent stress distribution is obtained as shown in Fig.3.

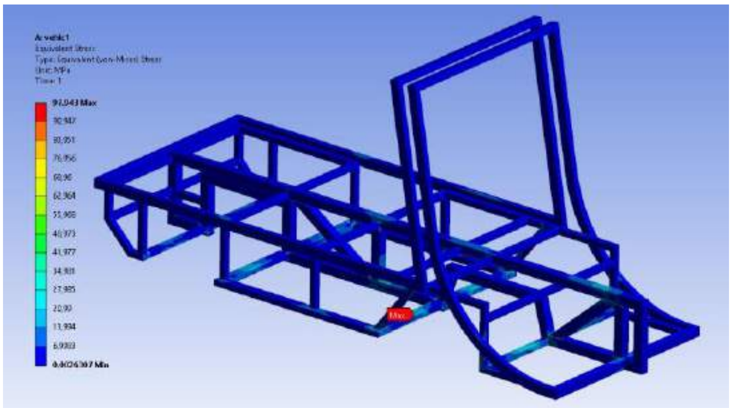

Fig. 3. Equivalent stress distribution

And as a result of static analysis, the elastic deformation on model is obtained as shown in Fig.4. The maximum stress on the model here is 97.9 MPa, and it occurs in the connection area of the suspension system. As can be understood from this stress value on the model, there is no problem in terms of static loading on the chassis and the safety coefficient is approximately 2.5.

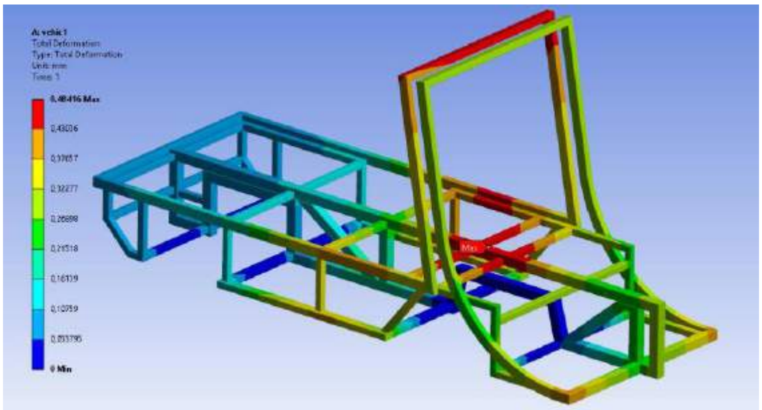

Fig. 4. Elastic deformation on the model

Fatigue analyzes were followed after observing that no permanent damage would occur on the model in the static analysis performed on the chassis.

2.2 Fatigue Analysis

After the selection criteria and the method steps, fatigue analysis solution diagram was formed in nCode DesignLife programme as shown in Fig.5.

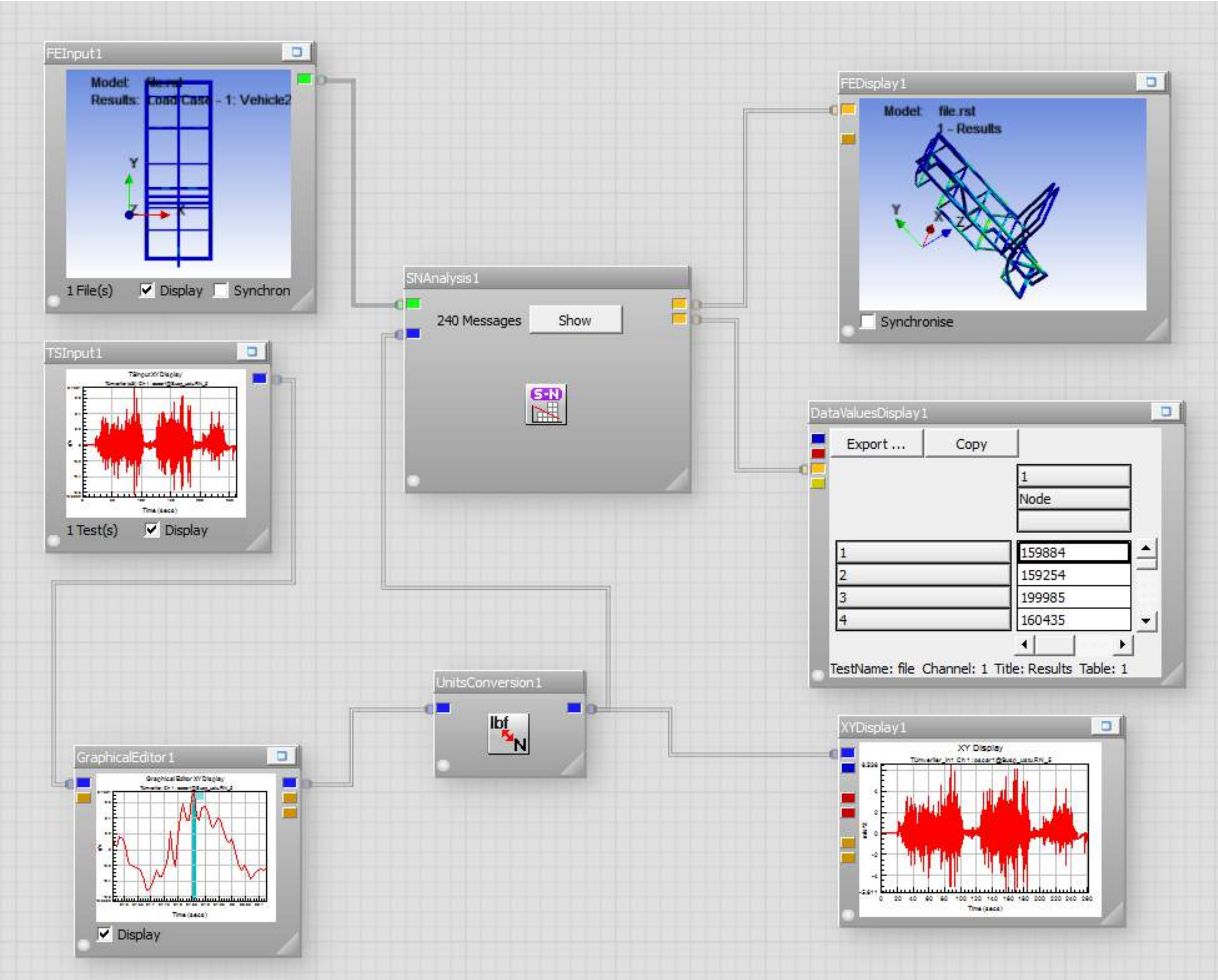

Fig. 5. Design life fatigue analysis flowchart

3. Results

By entering 3 basic parameters required for fatigue analysis, the analysis models prepared for each of the 5 different path data were solved. As a result of analysis, the life and damage values on the chassis model were obtained for four different tracks as shown in Table 1.

Table 1: Fatigue life and damage results for five different test tracks

	Asphalt Road	Downgrade	Rugged Road	Parker road	Unpaved Road
Life	$1{,}082 \times 10^{3}$	$1{,}155 \times 10^{5}$	3,303	$4{,}081 \times 10^{3}$	8,686
Damage	$4{,}607 \times 10^{-4}$	$7{,}022 \times 10^{-6}$	$8{,}571 \times 10^{-2}$	$1{,}420 \times 10^{-4}$	$1{,}135 \times 10^{-3}$

As can be seen from Table 1, the most critical result for fatigue life and damage was found in the analysis with test data from rugged area. As a result of the analysis in the rough road data, the life distribution on the chassis model is as shown in Fig.6. The connection profiles of the suspension system are locally shown because this is the part that gives the minimum value in terms of life on the vehicle.

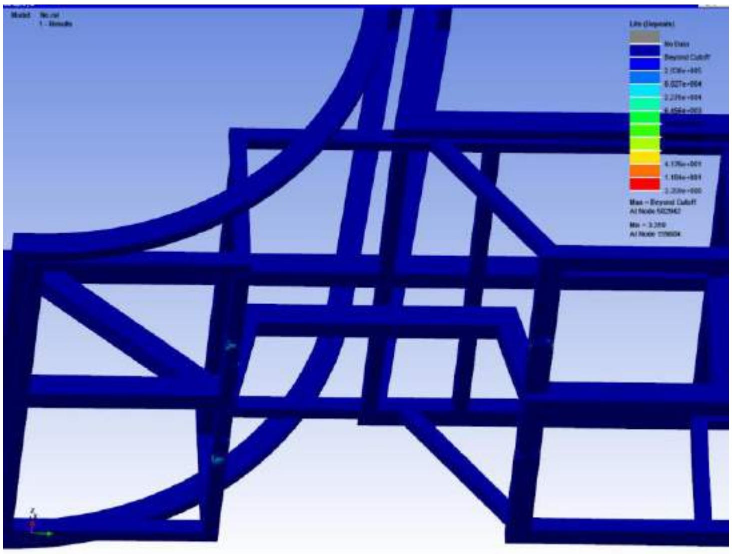

Fig. 6. Lifetime distribution on chassis with rugged road

4. Conclusions

The length of the data used in the analysis; 200,000 km * 3,303 = 660,600 km. The meaning of the damage value obtained as a result of the analysis is how many percent damage is caused by the fatigue analysis on the part. In the analysis made from rugged road data, life and damage amounts were obtained at the most critical values according to fatigue results from the other test tracks. However, when these values are examined, the minimum lifetime of the chassis is around 600,000 km. This value does not mean risk. As a result of these analyzes, it has been seen that the critical value of the existing vehicle chassis is far below the fatigue life.

5. Acknowledgement

This work was supported by Duzce University Scientific Research Project, No. 2016.06.01.433. We thank Duzce University Scientific Research Project Coordinatorship for their support.

References

[1] D.C. Han, 19-23 Ekim, 2002, "Electric Vehicle Symposium 19 proceedings", EVAAP, Busan, Korea.
[2] M.H. Westbrook, 2001, "The electric and Hybrid Electric Car.", SAE, London
[3] I. Husain, 2003, "Electric and Hybrid Vehicles Design Fundamentals", CRC Presss, New York.
[4] C.M. Jefferson, R.H. Barnard, 2002, "Hybrid Vehicle Propulsion", WIT Press, Boston.
[5] C. C. Chan, K. T. Chau, 2001, "Modern Electric Vehicle Technology", Oxford University Press, New York.
[6] C.C. Chan, 2002. "The State of the Art of Electric and Hybrid Vehicles", Proceedings of the IEEE, 90, 247-275.
[7] R. Talreja, "Fatigue of Composite Materials: Damage Mechanisms and Fatigue-Life Diagrams," Proc. R. Soc. A Math. Phys. Eng. Sci., vol. 378, pp. 461–475, 1981.
[8] C. Wang, H. Zhang, C. Castorena, J. Zhang, Y. R. Kim, "Identifying fatigue failure in asphalt binder time sweep tests," Constr. Build. Mater., vol. 121, pp. 535–546, 2016.
[9] W. Wang, L. Deng, X. Shao, "Number of stress cycles for fatigue design of simply-supported steel I-girder bridges considering the dynamic effect of vehicle loading," Eng. Struct., vol. 110, pp. 70–78,

2016.
[10] D.J. Whıte, J. Lewszuk, “Cumulative damage ın fretting fatıgue of pınned joınts subjected to narrow band random loadıng,” Aeron Quart, vol. 21, no. 4. pp. 400–408, 1970.
[11] W. Zhang, C. S. Cai, F. Pan, Y. Zhang, “Fatigue life estimation of existing bridges under vehicle and non-stationary hurricane wind,” J. Wind Eng. Ind. Aerodyn., vol. 133, pp. 135–145, 2014.
[12] E. Masoumi, K. Abad, S. Arabnejad Khanoki, D. Pasini, “Fatigue design of lattice materials via computational mechanics: Application to lattices with smooth transitions in cell geometry,” Int. J. Fatigue, vol. 47, pp. 126–136, 2013.
[13] S. H. Jeong, D.-H. Choi, G. H. Yoon, “Fatigue and static failure considerations using a topology optimization method,” Appl. Math. Model., vol. 39, no. 3–4, pp. 1137–1162, 2015.
[14] G. Saracoglu, A. Yapici, “Fatigue analysis of girth gear of a rotary dryer,” Eng. Fail. Anal., vol. 68, pp. 187–196, 2016.
[15] C. A. Sciammarella, R. J. S. Chen, P. Gallo, F. Berto, and L. Lamberti, “Experimental evaluation of rolling contact fatigue in railroad wheels,” Int. J. Fatigue, vol. 91, pp. 158–170, 2016
[16] D.-Y. Song, N. Otani, “Fatigue life prediction of cross-ply composite laminates,” Mater. Sci. Eng. A, vol. 238, no. 2, pp. 329–335, 1997.

ISSN 1454 - 8003
Proceedings of 2017 International Conference on Hydraulics and Pneumatics - HERVEX
November 8-10, Băile Govora, Romania

RESULTS ON THE RESEARCH OF THE INFRARED THERMOGRAPHY METHOD APPLIED TO THE HYDRAULIC SYSTEMS DIAGNOSIS

Alexandru-Daniel MARINESCU[1], Corneliu CRISTESCU[1]
Teodor Costinel POPESCU[1], Carmen-Anca SAFTA[2]

[1] Hydraulics and Pneumatics Research Institute INOE 2000-IHP, marinescu.ihp@fluidas.ro

[2] University "Politehnica" of Bucharest, Power Engineering Faculty, safta.carmenanca@gmail.com

Abstract: *The maintenance is an important activity, absolutely necessary for the proper operation of any kind of technical system, even for the hydraulic drive systems. Condition-based preventive maintenace (or predictive maintenance) is more than to prevent maintenance because it continuoslly evaluates the state of technical performances of a system. One of the most well-known predictive methods is the infrared thermography. This paper presents the results of an experimental research on a gear pump, in order to demonstrate the advantages of using the infrared thermography method in predictive maintenance of the pump. There are simulated different operation modes of the gear pump by changing the work conditions in the hydraulic drive test system. Specific thermograms are obtained for each operation mode. Observations regarding the measurement errors and the application limits of infrared thermography are made, too.*

Keywords*: Maintenance, predictive maintenance, infrared thermography, hydrostatic pumps, hydraulic drive systems*

1. Introduction

Maintenance is regarded as an important factor in product and service quality and it can be considered a system "viewed as an integrated input-output model" which can be planned, organized, monitored and controlled, [1]. In Figure 1 the input-output maintenance system is shown. In the scientific literature regarding on he maintenance and maintenance management three maintenance strategies are underlined: the corrective (or breakdown) maintenance, time-based (or use-based) preventive maintenance and condition-based preventive maintenance. Other maintenance strategies are: opportunity maintenance, fault finding, design modification, overhaul, replacement, reliability-centred maintenance, total productive maintenance. All these strategies or policies depend on the relationships between maintenance system and organization objectives, [1].
Corrective maintenance (noticed as CM) is focused on performing repair after the system or component failure occurred.
Time-based preventive maintenance, or simple preventive maintenance and noticed as PM, is a planned maintenance performed to prevent and fix problems before failure occurs.
Condition-based preventive maintenance (CBM) is based on monitoring and collecting information concerning the condition of the equipment to prevent unexpected failures and determine optimal maintenance schedules, [2]. Condition-based maintenance is a form of predictive maintenance strategy and is more than a simple PM because the system's reliability indicators are improved and the cost of maintenance is less. The time between two stops is shorter in CBM than in PM. Condition-based maintenance is applied to a sub-assembly, a component or a machine system. Over time, all data obtained from the monitoring parameters according to predictive maintenance program (or CBM) are studied, processed, and compared to the existing data. The statistical analyse will allowed to predict the periodicity of the future maintenance program and to optimize it, too. The most common predictive maintenance methods used in hydraulic systems, are: vibration analysis, oil analysis, infrared thermography and ultrasound control, Fig. 2.
It is not necessary to use all methods in the monitoring the parameters of the hydraulic system within predictive maintenance program. In the references literature, oil analysis, infrared thermography and vibration analysis (or ultrasound control) are recommended, [2].

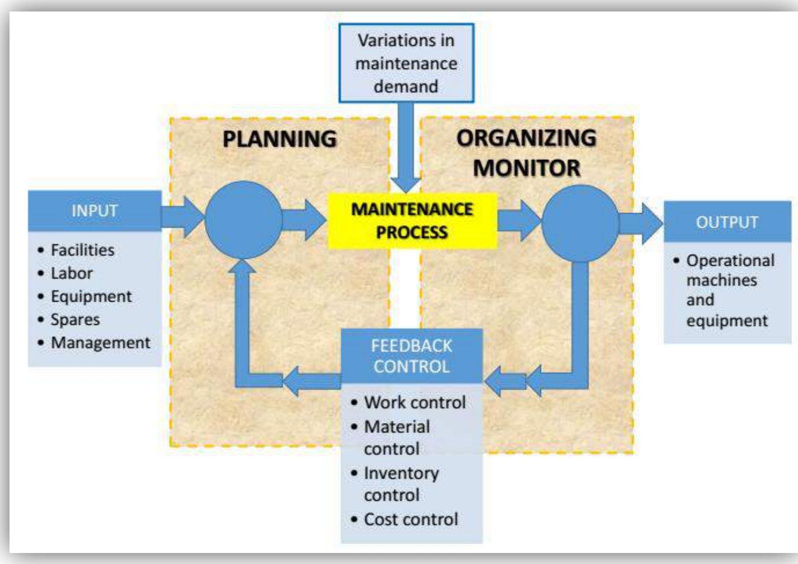

Fig. 1. Maintenance system as input-output model, [1]

Fig. 2. Condition-based maintenance monitoring methods

Starting from these considerations, the authors of the paper present new experimental researches, in continuation of those started at INOE 2000-IHP in 2016, demonstrating the utility and efficiency of using the infrared thermography method in the predictive study of the hydraulic actuation systems operating behaviour, [3].

2. Experimental test rig

In order to achieve the research objective, a testing rig was conceived, designed and physically realized at INOE 2000-IHP Bucharest, to allow the demonstration of the usefulness and the efficiency of the infrared thermography method, using in the behavioral prediction of hydrostatic drive systems. The hydraulic diagram of the test bench is shown in Figure 3.
The test rig is used to test a Vivoil hydraulic gear pump, model XV-2P D / C, having a geometric volume of 9 cm^3/rev (see Fig. 4) used in hydraulic drive systems. The test consists in the simulation of various operating modes, i.e. the operation at different pressure stages, as well as the gradual change of the pump suction conditions, after a suitable procedure.

The hydraulic components of the test rig are: a hydraulic oil tank (T) fitted with a filling and ventilation filter (FAF) and a return filter (RF). A three-phase electric motor (EM) is mounted on the oil tank cover, which, via a coupling (C), drives the hydrostatic pump (HP) to be tested. The pump (HP) sucks the oil out of the tank, a valve (V), a non-return valve (NRV) being mounted on the suction pipe to maintain full-oil the suction circuit, and a throttle (ST) by can modify by throttling the suction circuit of the pump, to change the suction conditions. Throttling of the suction pipe section will lead to increased operating temperature, a phenomenon that will be sensed, measured and recorded by a FLIR infrared thermal imaging camera. The hydrostatic pump (HP) discharge the oil under the pressure indicated by the pressure gauge (G) and is adjusted to the pressure return valve (PRV) by means of a throttle (RT) mounted on the pump discharge, which allows the required pressure steps to be achieved, the oil being returned to the tank through a return filter (RF).

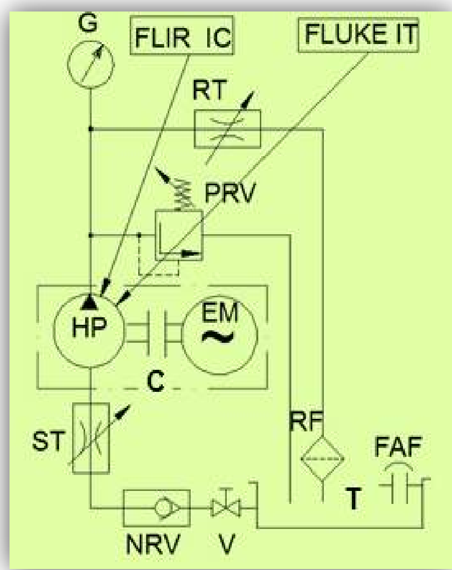

Fig. 3. Hydraulic scheme

Fig. 4. Hydraulic gear pump, Vivoil brand– Italy, [4]

The hydraulic components of the test rig are: a hydraulic oil tank (T) fitted with a filling and ventilation filter (FAF) and a return filter (RF). A three-phase electric motor (EM) is mounted on the oil tank cover, which, via a coupling (C), drives the hydrostatic pump (HP) to be tested. The pump (HP) sucks the oil out of the tank, a valve (V), a non-return valve (NRV) being mounted on the suction pipe to maintain full-oil the suction circuit, and a throttle (ST) by can modify by throttling the suction circuit of the pump, to change the suction conditions. Throttling of the suction pipe section will lead to increased operating temperature, a phenomenon that will be sensed, measured and recorded by a FLIR infrared thermal imaging camera. The hydrostatic pump (HP) discharge the oil under the pressure indicated by the pressure gauge (G) and is adjusted to the pressure return valve (PRV) by means of a throttle (RT) mounted on the pump discharge, which allows the required pressure steps to be achieved, the oil being returned to the tank through a return filter (RF).

During the experiments, the measured and monitored parameters were: ambient temperature, oil temperature, working pressure read on the pressure gauge (G), noise in installation read with Smart-Sensor (SSM), but particularly, the pump temperature, measured with 3 devices, namely: with a contact thermometer (CT), placed directly on the pump, with a FLUKE IT infrared thermometer, and with a FLIR IC infrared thermal imaging camera. To measure the temperature at the interest points (pump, tank, oil), the stand was provided with:

- contact thermometer (CT), Checktemp 4 by Hanna brand, to measure the temperature directly on the pump housing (see Fig. 5);

- infrared thermometer (FLUKE IT) for non-contact temperature measurement at the three points of interest (see Fig. 6);
- infrared thermal imaging camera (FLIR IC), required for temperature measuring and recording, at interest points (see Fig. 7);
- Soundmeter (SSM) for noise measurement, Smart Sensor AR 814 brand, (see Fig. 8)

Fig. 5. Contact thermometer Checktemp 4 by Hanna

Fig. 6.FLUKE infrared thermometer

Fig. 7. FLIR infrared thermal imaging camera

Fig. 8. Smart Sensor AR 814 Soundmeter

To highlight the possibility of using the infrared thermography method, to the behavioral prediction of hydrostatic drive systems, some working scenarios were imagined. Thus, under laboratory conditions, different pump operating modes are simulated, leading in an increase of the pump temperature. This is like as the pump is operating with major failures, which lead to the temperature increase, seized through periodic measurements, which allow the early detection of possible failures in the future. In this way major major malfunctions in pumps operation mode can be prevented and important technical and economical decissions regarding the gear pump manufacturing process can be done.
The experiments procedure consists into applying various pressure steps to the hydrostatic pump and for each pressure step, the temperature is measured after regular periodes of time (i.e. 10 min.). Two situation of working are considered: pump operating with the throttle valve (named SITUATION I) and pump opearting without throttle valve (named SITUATION II). The first scenario

is as like the pump is on going to fail because the throttle valve (ST) is on the pump input (Fig. 3.) and cavitation phenomenon can appear when the suction conditions are changed.
The temperature of the pump is measured with three measuring devices: an infrared FLIR thermal imaging camera (FLIR IC, see Fig. 3), an infrared FLUKE thermometer (FLUKE IT, see Fig. 3) and a contact thermometer (CT), placed directly on the pump.
During the experiments were measured the temperatures (with all three types of devices), and the noise for each pressure step in each operating mode.
The main phases of the experiments are as follows:

- setting of the time interval for the measurements, respectively for reading values;
- reading the temperature of the environment, T_{env};
- reading the background noise, A_{env};
- starting the electric motor (EM) to drive the pump;
- adjusting the desired pressure step by actuating the pressure circuit throttle (RT);
- changing the suction conditions of the pump by actuating the throttle mounted on the suction pump circuit (ST);
- monitoring the pump operation temperature and the noise for each setting time interval;
- stopping the pump when the temperature reaches about 80 °C;
- the resumption of the measurement cycle for another pressure stage and for another section area of the suction throttle valve (RT).

The procedure is the same in each working situations with suction throttle valve (SITUATION I) and without suction throttle valve (SITUATION II). If the pump is working in SITUATION II the suction throttle valve is widely opened.

3. Experimental measurements

The experiments were carried out on three steps of pressure, namely: 50 bar, 75 bar and 100 bar. Following experimental procedure described above, the results of the experimental measurements of temperatures and noise are shown in Table 1 and Table 2. for the case of 75bar pressure step. For the pressure of 50bar and 100bar the results were reported in paper [5].
In Table 1 are presented the results of SITUATION I of working, with suction throttle valve and in Table 2, SITUATION II without the suction throttle valve.
During the experiments were monitoring not only the pump temperature measured on the pump housing (T_{pp}) but also the oil temperature (T_{oil}) and the reservoir temperature (T_{rez}), too.
The temperature measurements were made with all three devices mentioned above: infrared FLIR thermal imaging camera, infrared FLUKE thermometer and a contact thermometer (CT), placed directly on the pump.
The temperature measured with contact thermometer can be considered as a standard temperature.

Table 1: Experimental results in SITUATION I, with suction throttle valve ST

Time [min]	FLUKE IT [°C]			FLIR IC [°]			CONTACT THERMOMETER CT [°]	Noise [dB]
	T_{pp}	T_{rez}	T_{oil}	T_{pp}	T_{rez}	T_{oil}	T_{CT_pp}	A
0	25	24,7	24,5	25	24,4	25,4	25	44,5
10	51	31	32	57,2	31,4	33,9	56,8	77,9
20	72	42	33	**78,4**	45,5	49,8	76,7	67
30	77	46	65	84,1	47	58,9	81,7	75,7
40	83	50	60	**86,3**	51,8	60,2	84,4	67
50	80	50	63	88,3	54	-	87	

Table 2: Experimental results in SITUATION II, without suction throttle valve ST

Time [min]	FLUKE IT [°C]			FLIR IC [°]			CONTACT THERMOMETER CT [°]	Noise [dB]
	T_{pp}	T_{rez}	T_{oil}	T_{pp}	T_{rez}	T_{oil}	T_{CT_pp}	A
0	29	28	28	29	28	28,4	29	44,5
10	47,2	33,3	38,7	48,2	34,4	37,6	42	75,7
20	58,2	43,9	48,2	**58,5**	45,2	47,2	50,8	75,7
30	70,1	55,2	55,4	69,3	57,1	54,7	65,5	72,5
40	78,6	65,1	63,9	**78**	66,1	63,5	71,7	75,7
50	86,1	73	70,1	86,3	74,1	68	84	75,7
60	92,8	79,2	88,5	93,7	80,2	74,9	89,8	75,7

All temperatures measured in the experiment are plotted, Figure 9. Some snapshot with FLIR IC infrared imaging camera are presented in Figure 10 and Figure 11.

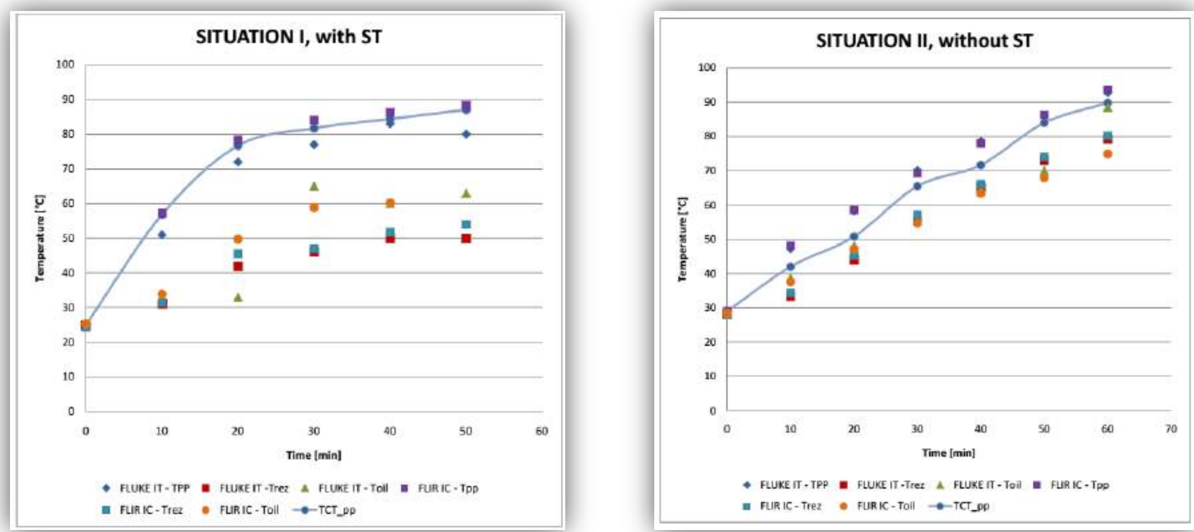

a) b)

Fig. 9. Temperatures measured in the case of 75bar pressure step: a) SITUATION I with suction throttle valve; b) SITUATION II without suction throttle valve.

Fig. 10. Pump FLIR IC snapshots in the case of SITUATION I, see Table 1 the bold numbers

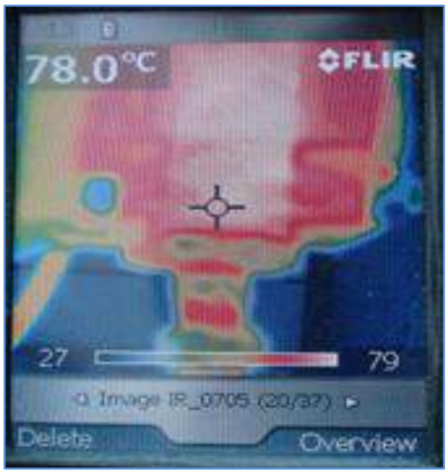

Fig. 11. Pump FLIR IC snapshots in the case of SITUATION II, see Table 2 the bold numbers

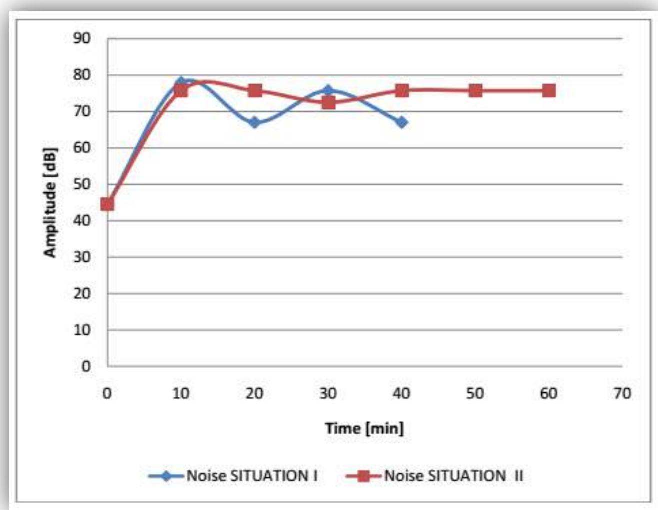

Fig. 12. Noise variation for 75bar pressure step

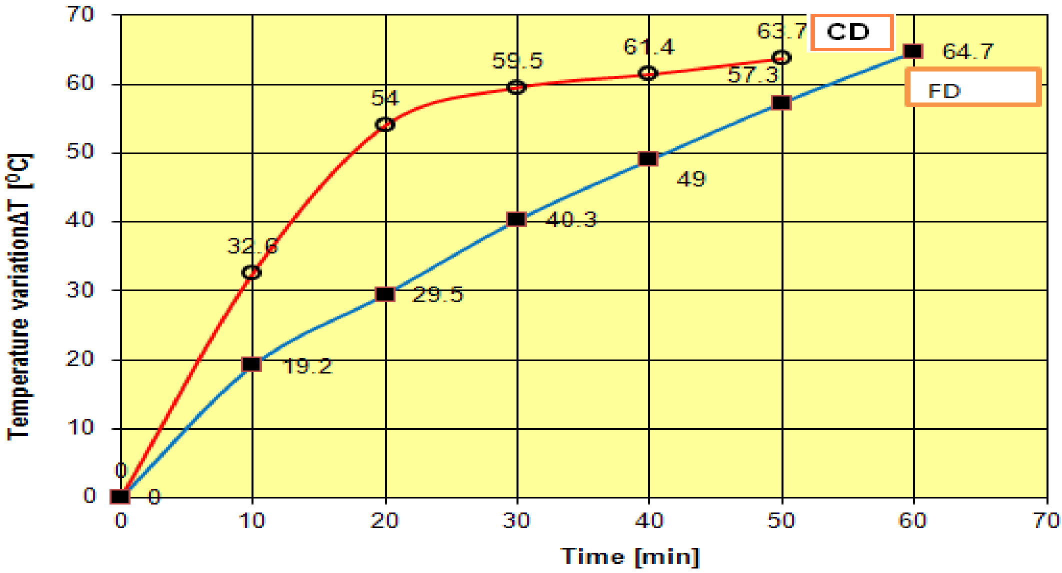

Fig. 13. Relative temperatures variation, for p= 75bar, with throttling (CD) and without throttling (FD)

Noise variation is plotted in Figure 12 for all period of the experiments in the two cases mentioned before.
Considering that the environment tempretaure is at the zero moment of time, according with the tables, at 25 °C (Table 1) and 29 °C (Table 2) the increased temperetaure on the pump measured with FLIR IC is plotted in Figure 13.

4. Discussions

Experimental results show that the pump measuring temperatures using contact thermometer are in accordance with the non-contact temperature measured with the FLIR thermal imaging camera, see Figure 9 and Figure 13. Also, it can be observed that the pump temperature, T_{pp}, measured with FLIR infrared camera keeps close enought for the considered standard temperature measured with contact thermometer, T_{CT_pp}, Fig. 9. It can be observed that the curve of temperature variation has the same trendline as the temperature curve plotted with full line in Figure 9. Even the temperatures measured with FLIR IC and infrared thermometer FLUKE IT have close values in the case of the reservoir temperature, T_{rez}, Fig. 9. Only the temperatures of the hydraulic oil cannot be compared, Fig. 9.a.
Considering the fact that the pump operating mode with different openings of the suction throttle valve is a simulation procedure of the pump in the case of a failure (i.e. cavitation), and comparing the pump temperatures in SITUATION II (without suction throttle valve) with the failure mode of operation (SITUATION I) it is observed the difference in the plotted temperatures, Fig. 9.
In Figure 9.b all the temperatures are "stick together" closer to the standard temperature line (T_{CT_pp}), in contrast with SITUATION I, Fig. 9.a. More than that, even the noise measurements warn us that the pump is in a failure mode of operation, Fig. 12.
In the discussion of experimental results we must be objective and recognize that the infrared thermography method has some limitations and method errors, calibration errors, signal errors can appear [6 ÷ 12]. For example the errors giving by the method occur because of an incorrect evaluation of the infrared thermography parameters. Commonlly, object emissivity, ε, atmospheric temperature, T_{atm} [K or ° C], ambient temperature T_0 [K or °C], humidity, ω [%], the distance between the infrared thermal imaging camera and the measured object, d [m] are some of them.
The influence of ambient radiation, directly or indirectly reflected by the object and detected by the camera is another thermography parameter not easy to evaluate and essentially in infrared image camera calibration.

5. Conclusions

The results of experimental research regarding the using of infrared thermography as method of condition-based maintenance were presented in the paper. The experimental simulations of a failure pump and the temperature monitoring with three different temperature devices help us to compare the behavior of the malfunction pump with the good one. The monitoring of noise was tested, too, as method in the maintenance of the hydraulic drives and the results confirm the connection between noise and the pump failure state.
In the paper is presented the test bench rig designed as a simple hydraulic circuit with a gear pump and a suction throttle valve mounted on the input of the pump to simulate the cavitation operating mode (named SITUATION I).
The normal operation mode was named SITUATION II.
Three steps of pressures were considered but only for 75bar the results were commented.
Analysing the temperature results we conclude that infrared thermography method can be used to monitor the behavior of a hydraulic drive system in the case of indoor hydraulic systems to avoid the influence of the environment in the calibration of infrared imaging camera.
The authors are intending to develop the procedure of infrared thermography maintenance method applied to hydraulic drives but the errors analyse of the measurements is necessary. Only with

more temperatures data the experimental simulation can improve the infrared thermography method.

Acknowledgments

This paper has been developed in INOE 2000-IHP, with the financial support of the Executive Agency for Higher Education, Research, Development and Innovation Funding (UEFISCDI), under PN III, Programme 2- Increasing the competitiveness of the Romanian economy through research, development and innovation, Subprogramme 2.1- Competitiveness through Research, Development and Innovation - Innovation Cheques, project title: “Method for assessing the wear and the functionality degree at pumps and hydraulic cylinders through infrared termography”, Financial Agreement no. 8 CI/2017.

References

[1] S.O. Duffuaa, A. Raoul, ”Planning and control of maintenance systems. Modelling and analysis”, Ed. Springer, 2nd Edition, 2015;
[2] R.K. Mobley, ”Maintenance Engineering Handbook”, 7th Edition, McGraw-Hill, Section 7. Instruments and Reliability Tools, 2008;
[3] A.D. Marinescu, T.C. Popescu, L. Enache, C.A. Safta, ”Researches on specific malfunctions diagnosis of hydraulic drive systems equipments using the infrared thermography method”, Proceedings of International Conference on Hydraulics and Pneumatics HERVEX – 22nd edition, Băile Govora (9-11) Nov. 2016, pp. 218-224;
[4] https://www.vivoil.com/it/prodotto/xp210/;
[5] A.D. Marinescu, C. Cristescu, T.C. Popescu, C.A. Safta, ”Assessing the opportunity to use the infrared thermography method for predictive maintenance of hydrostatic pumps”, 8 th International Conference of Energy and Environment -CIEM, Bucharest,Romania, 19 -20 October, 2017;
[6] A. Mihai, ”Thermography in infrared- Fundamentals” („Termografia în infraroșu- Fundamente”), Technical Publishing House, Bucharest, 2005;
[7] W. Minkina, S. Dudzik, ”Infrared Thermography, Errors and Uncertainties”, Wiley & Sons Publishing House, 2009;
[8] K. Chrzanowski, ”Non - contact thermometry – measurement errors”, SPIE, Vol. 7, Warsaw, 2000;
[9] R. Babka Robert, W. Minkina, ”Influence of calibration of an infrared camera on accuracy of sub-pixel edge detection of thermal objects, Measurement, Automation and Monitoring”, Vol. 48, No.4, pp.11-13, 2000;
[10] R.P. Madding, ”Emissivity measurement and temperature correction accuracy considerations”, Proceedings of the SPIE, Vol. 3700, 1999, pp. 393-401;
[11] A.D. Marinescu, C.A. Safta, T.C. Popescu, ”Advantages, errors and limitations of infrared thermography used to mantain hydraulic drive systems” („Avantajele, erorile și limitele termografierii în infraroșu utilizată la mentenanța sistemelor de acționare hidraulică”) – 17th Multidisciplinary International Conference ”Professor Dorin Pavel – the founder of Romanian hydropower” – Sebeş, Romania, (1-3) June 2017, published in ”Science and Engineering” („Știință și Inginerie”), ISSN 2067-7138, Year XVII, vol. 32/2017, pp. 65-74;
[12] Childs P.R.N., ”Practical Temperature Measurement”– Butterworth, Heinemann Linacre House, Jordan Hill, Oxford OX2, 8DP 225 Wildwood Avenue, Woburn, MA 01801-2041, First published 2001.

ISSN 1454 - 8003
Proceedings of 2017 International Conference on Hydraulics and Pneumatics - HERVEX
November 8-10, Băile Govora, Romania

SCADA SYSTEMS ARCHITECTURE BASED ON OPC SERVERS AND APPLICATIONS FOR INDUSTRIAL PROCESS CONTROL

Marcel NICOLA[1], Claudiu-Ionel NICOLA[1], Dumitru SACERDOȚIANU[1], Marian DUȚĂ[1]

[1]National Institute for Research, Development and Testing in Electrical Engineering – ICMET Craiova

marcel_nicola@yahoo.com, nicolaclaudiu@icmet.ro, dumitru_sacerdotianu@yahoo.com, marianduta@icmet.ro

Abstract: *SCADA (Supervisory Control and Data Acquisition) is the most modern tool used for the control and monitoring of technological processes. A SCADA system consists of two main components: the Server (one or more) and the Clients (the Viewers). The aim of OPC (OLE-Object linking and embedding for Process Control) is to define a common interface that once conceived can be reused for any other project, SCADA, HMI (Human Machine Interface) or other software packages. An OPC server is an application which acts as application programming interface (API-Application Programming Interface) or protocol converter. The paper presents an example of OPC server based application software which can be integral to a SCADA system. The application focuses on monitoring a quasi-general industrial process defined by a 2nd order transfer function, on identifying the transfer function and managing the client-server communication of the quantities of interest by online viewing and creating a record using TDMS (Technical Data Management Streaming) files and a MySQL database server.*

Keywords*: OPC-UA, database, SCADA, process control, transfer function*

1. Introduction

SCADA is a computer based system designed for the control and monitoring of technological processes.
SCADA is the most modern concept and the tool used for the control and monitoring of technological processes. SCADA systems include both software and hardware components. The hardware collects and transmits data to a PC with installed SCADA software. The PC then processes these data in an acceptable time frame [1, 2].
Substantial progress in this field have allowed the SCADA systems to be used in the most various fields, from the manufacturing of consumer goods, to metallurgy, industrial hydraulics and pneumatics, chemistry and power engineering, and the nuclear field.
A SCADA system consists of two main hardware components:

- The server (one or more) - It is connected to the (process) field elements through various data acquisition systems. Data acquisition systems are generally created based on microcontrollers designed to acquire data from the process and to monitor and control the operation of the process. Data acquisition is also carried out by using intelligent sensors which can connect directly to the computer or through some intermediate devices called stations or communication masters which collect data from multiple intelligent sensors. The data acquisition and process control devices in the industry field are represented mostly by programmable automata - PLC's (Programmable Logic Controller).
- The server manages all the data collected from the process (it achieves the database, provides the communication with the PLC's in the process);
- The Client (the Viewer) - is connected to the network with the server, it uses the data from it and provides communication with the human operator.
- The servers are connected to the controllers through a wide range of communication drivers (hundreds of drivers providing connections with all PLC's from known companies).

A single server can communicate simultaneously across multiple protocols, but new communication drivers can also be developed.

The servers and viewers are connected to the Ethernet network. The web technology used now also allows visualization of a process done via the Internet.
One of the most important functions of the SCADA systems is the monitoring and control function.
The monitoring and control of technological processes is carried out by means of graphical pages which mimic the technological process and are displayed on one or more computer monitors. These graphical pages are also called HMI's (Human Machine Interfaces). The control operation is also called monitoring. We can thus state that the monitoring and control of technological processes is carried out via the HMI's.
Among the main functions of the SCADA system we can mention the following:

- The automatic control of the technological process in order to optimize the output parameters and in order to improve the efficiency;
- The real-time display of the technological process state;
- The graphical display of the process data with a view to creating efficient operating strategies;
- The efficient management of process quantities record, state of equipment, and condition of alarms;
- The periodic generation of operation reports;
- The possibility of direct user intervention in the process depending on his rights of access;
- The possibility of remote process control by using SCADA client stations.

The OPC (OLE for Process Control) standard or the more recent Openness Productivity Connectivity is a series of specifications defined by the OPC Foundation to facilitate connectivity in industrial automation. The OPC uses Microsoft DCOM (Distributed Component Object Model) technology to provide a communication line between the OPC servers and OPC clients. The OPC was designed to enable the safe communication in industrial processes, such as in electric power generation and distribution, industrial hydraulics and pneumatics, petrochemical refining, assembly lines for motor vehicles, etc.
The state-of-the-art control of industrial processes integrated into SCADA systems entails both the use of up-to-date data transmission and management facilities, and also the use of drive and control software facilities starting with the estimation of parameters and identification of the linearized transfer function, proceeding with the control design of the controller and finishing with the validation and testing of the entire chain of the industrial process control [3-5].
LabVIEW is the development software which includes the concepts outlined above and which will be used for the application described in this article.
The rest of the article is organized as follows: section 2 presents the OPC client/server concept, and section 3 presents an application for monitoring a quasi-general industrial process described by a 2nd order transfer function, the identification of the transfer function and management of client-server communication for the quantities of interest by online viewing and creating a record using TDMS files and a MySQL database server. Section 4 presents conclusions and course of action concerning future research.

2. OPC server

The OPC (OLE for Process Control) is an industry standard created by the collaboration of a group of important world suppliers of automation software and hardware with Microsoft company. The standard defines the methods for data communication between real time automation systems and client applications run on computers with Microsoft operating systems [6].
OPC standard was created to enable the access of client applications to automation data in a uniform manner. Widespread conformity in the industry can bring many benefits such as:

- The hardware manufacturers will have to write a single set of software components for their products, which customers will use for their applications;
- The software manufacturers will no longer have to rewrite the drivers as a result of the changes or additions from new hardware versions;

- The customers will have a wider range of options to achieve high quality integrated production systems, in a heterogeneous computer environment.

The OPC standard provides access of production and economic applications to field information in real time and in a consistent manner, facilitating the interoperability between different equipment and the "plug and play" connectivity, but also a greater flexibility, lower integration, development and assembly costs for process automation or control systems.
An OPC server (see Figure 1) is an application which behaves as an API-Application Programming Interface or protocol converter.
OPC servers arose from the imperative necessity of making the production and economic computer systems communicate among themselves. There were often barriers due to incompatibilities between custom communication interfaces and the automation hardware and software from different vendors.
The specifications of the OPC define a standard COM (Component Object Model) interface for use in industrial applications for data acquisition and control.
The specs include a protocol for defining objects, for determining their properties and for standardization of function calls and events. For this purpose, OPC comprises a wide variety of data sources.
The input-output devices include data acquisition devices, actuators, communication bus systems and programmable logic controllers (PLC). The specifications also include protocols for working with data control systems (DCS) and database applications as well as for access to on-line data, alarm and event control and access to data records for all these data sources [7].

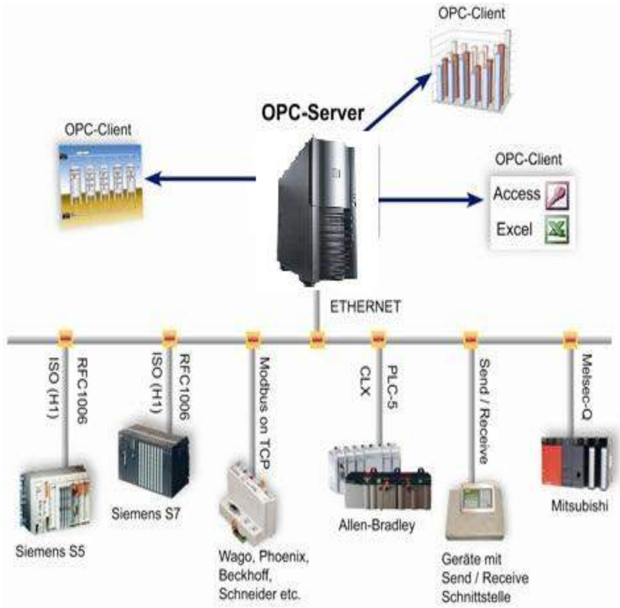

Fig. 1. SCADA system based on OPC server architecture

The OPC architecture benefits by the advantages of COM interfaces, which provide a convenient mechanism for extending OPC functionality.
Their architecture and design facilitates the creation of OPC servers which allow the client applications to access data from multiple OPC servers from different vendors running on different nodes on a single object.
The main advantage of the OPC interface is independence from a particular manufacturer, product or hardware. All commercially available SCADA systems, process control systems and PC-based controllers now provide a free OPC client interface for access to any OPC server.
The technology provides clear distinction between server and client applications, it encapsulates product-specific features and allows easy upgrading to a new version or switching to a different product. The independence to the platform also enables OPC communication between

components running different operating systems and via the Internet.
Considering that the OPC standard is based on the DCOM (Distributed Component Object Model) technology, its use is restricted to Windows operating system, at the same time, the DCOM contributed to the success of OPC.
The rapid acceptance of Windows computers as automation components has enabled the OPC technology to gain worldwide relevance in just a few years, while on the other hand, by the more intense use of the OPC, the emerging new application fields which determine the general trend towards Web technologies entail new requirements for the OPC standard.
OPC UA (Unified Architecture) is the next generation of OPC technology and is the OPC technology used by the application described in section 3. OPC UA is a more secure, open, reliable mechanism for transferring information between servers and clients. It provides more open transports, better security and a more complete information model than the original OPC, “OPC Classic.” OPC UA provides a very flexible and adaptable mechanism for moving data between enterprise-type systems and the kinds of controls, monitoring devices and sensors that interact with real world data [8].
OPC UA is much more complex than previous OPC specifications and is designed to:

- use cross-platform capable communication instead of Windows DCOM;
- combine the OPC DA (Data Access), A&E (Alarm &Events), HDA (Historical Data Access) functionality into a single set of services;
- model complex data structures for collaboration with other standards organizations;
- be implementable on different platforms, from embedded systems to enterprise systems.

An OPC UA server endpoint is the side of an OPC UA communication that initiates a communication session and provides data to an OPC UA client. There is no standard OPC UA server either in functionality, performance or device type. Devices from small sensors to massive chillers may be OPC UA servers. Some servers may host just a couple of data points. Others might have thousands. Some OPC UA servers may use mappings with high security and lower performance XML, while others may communicate without security using high performance OPC UA Binary Encoding. Some servers may be completely configurable and offer the client the option to configure data model views, alarms and events. Others may be completely fixed.
Clients in OPC UA are much more flexible than other network clients. OPC UA Clients have the capability to search out and discover OPC UA servers, discover how to communicate with the OPC UA server, discover what capabilities the OPC UA servers have, and configure the OPC UA server to deliver specific pieces of data when and how they want it. OPC UA clients will generally support many different protocol mappings so that they can communicate with all different types of servers.

3. Example of OPC-UA server based SCADA application for the control of an industrial process

Most industrial processes can be defined around the quiescent operating point by a 2nd order transfer function. The application presented is achieved in the LabVIEW development environment using Mathscript type Matlab scripts, it uses an OPC-UA type server, TDMS type files and a MySQL type database server [9]. The general architecture of the application is shown in Figure 2.
For the identification of the transfer function of the technological process, by using an acquisition board, the step signal applied is acquired and respectively the response (represented in simulated form in Figure 3).
The types of software modules of the experimental model, on the server machine are the following:

- The OPC read-write module; this module will provide intrinsic connection between the data acquired from input modules and the OPC server.
- The MySQL read-write module; this module will achieve MySQL type database query, where obviously data writing and reading are the most used functions.
- The TDMS read-write module; this module will manage data writing and reading in TDMS files, in order to achieve additional cache. These files can be opened in EXCEL, the facilities being thus obvious.

- Interface configuration module for data acquisition channels; this module will achieve the configuration of acquisition channels from various acquisition modules, but in the application presented the process quantities are simulated but maintain a natural similarity to real applications which process data from transducers.

The clients will be programs located on the server computer or on separate computers connected through a router in the same Intranet network.

These programs will be Viewer type programs which will access data from the OPC client, from MySQL database or from TDMS files. Data processing and viewing will be primary, focusing on the data communication itself, in that the data will be acquired by the client uniformly from databases or EXCEL-compatible files, although initially the data sources are heterogeneous (different data acquisition modules, for different protocols) [10-15].

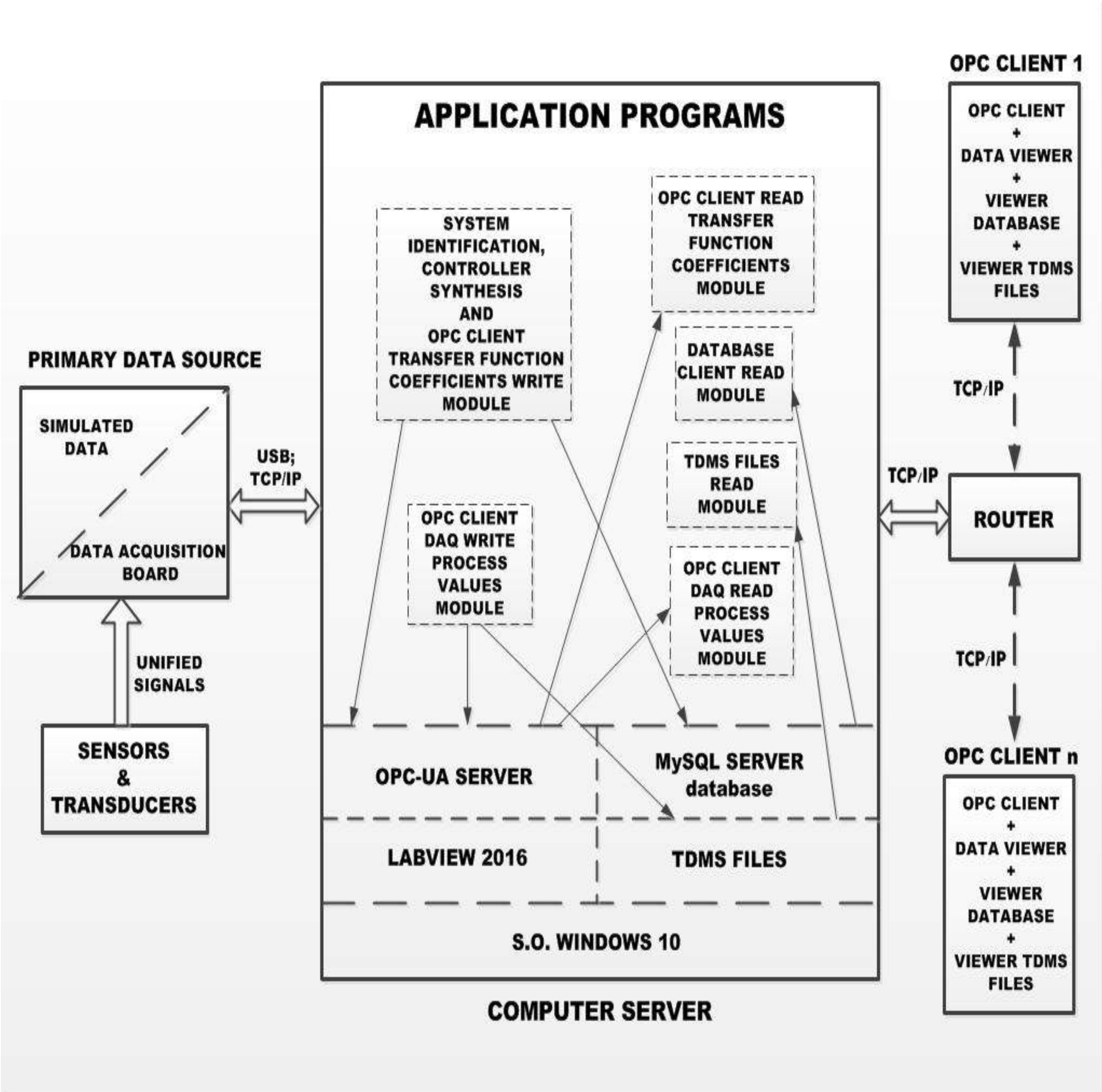

Fig. 2. SCADA application architecture

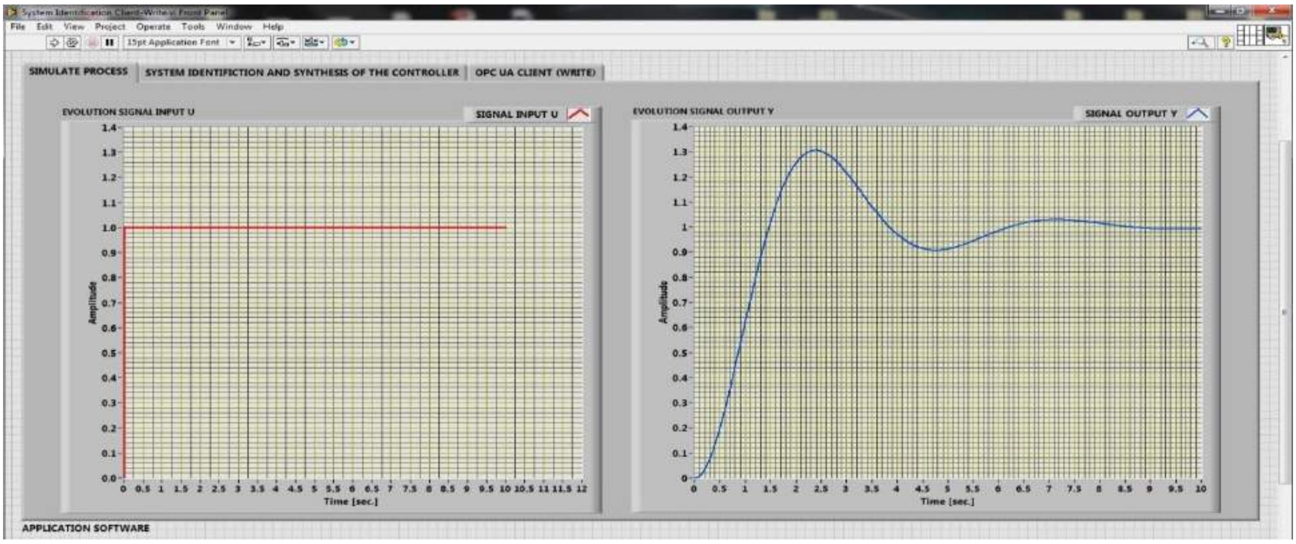

Fig. 3. The step signal applied and the response of the second order system

The use of LabVIEW further allows the transfer function coefficients to be determined, a LQR (Linear Quadratic Regulator) type regulator to be synthesized, a possible state description equations of open circuit, and respectively closed circuit (with regulator) system, as shown in Figure 4. It is obvious that this procedure is asynchronous and is run on operator request when the operating conditions allow it. The validation of the system and regulator identification is also presented in Figure 4. where it’s see that the identified system response is overlaid on the initial response.

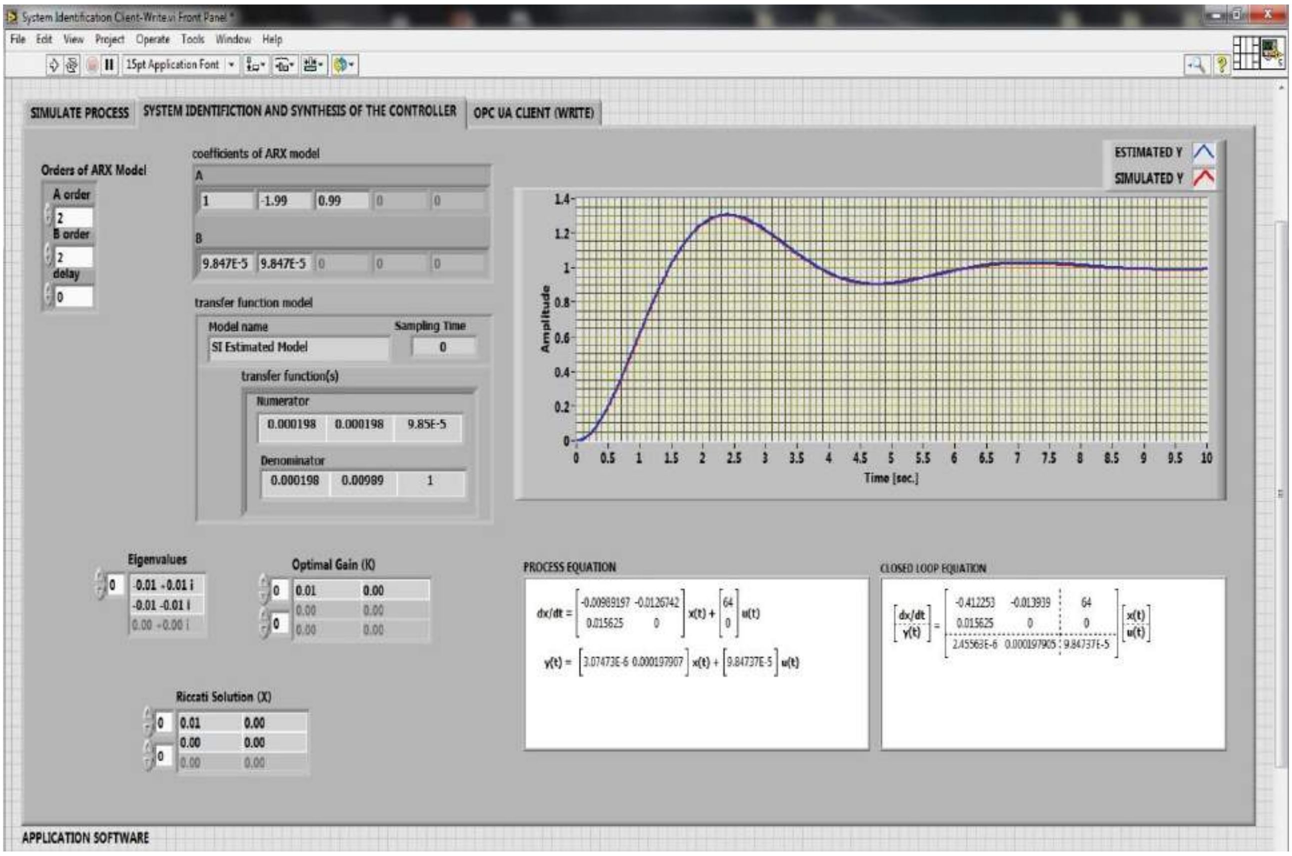

Fig. 4. System identification, LQR controller synthesis, state equations and system validation

The OPC-UA Server which supports communication is defined by the block diagram in Figure 5, and its interface is presented in Figure 6.

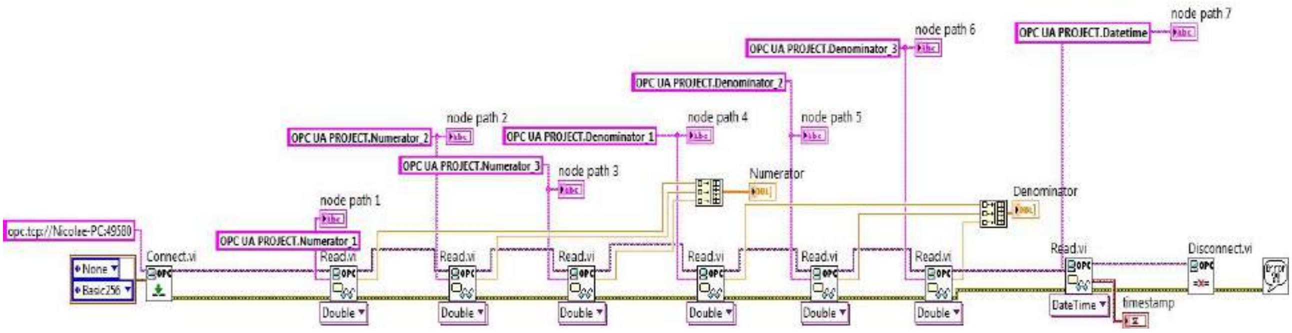

Fig. 5. OPC-UA server block diagram

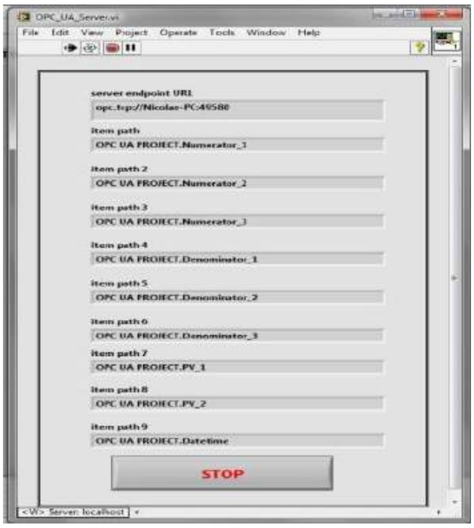

Fig. 6. OPC-UA server interface

There will be 8 quantities which will be transferred via the OPC client-server technology, in the presented application. The first 6 quantities are the transfer function numerator, respectively denominator coefficients (see Figure 7). These quantities will be transferred asynchronously at request and then they will be stored on the MySQL Server (see Figure 8).

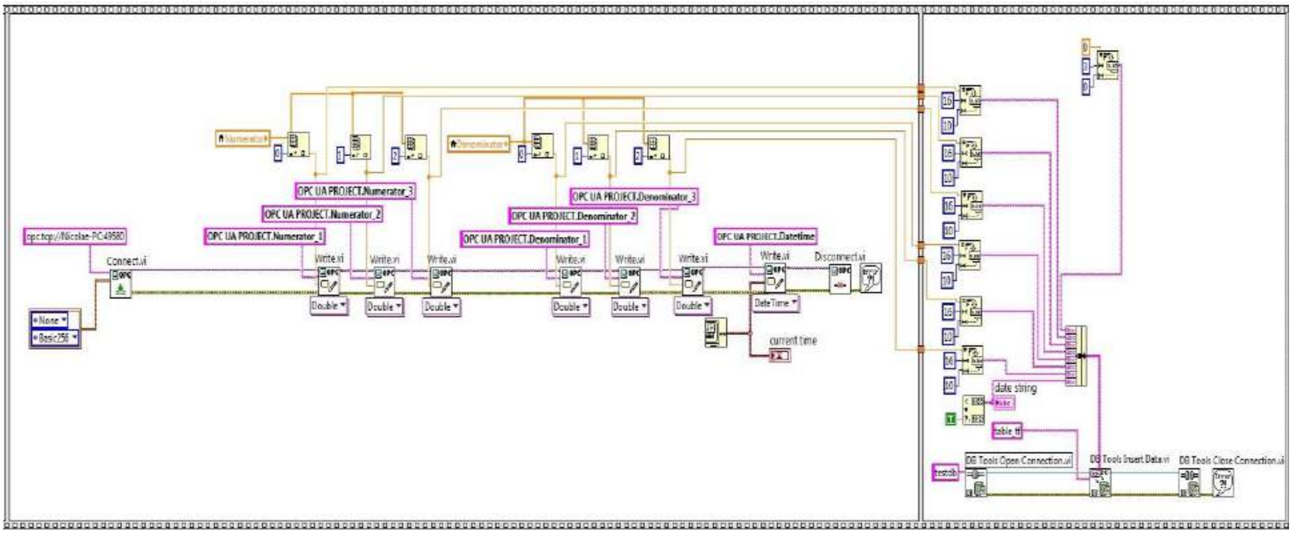

Fig. 7. OPC-UA client block diagram for transfer function coefficients

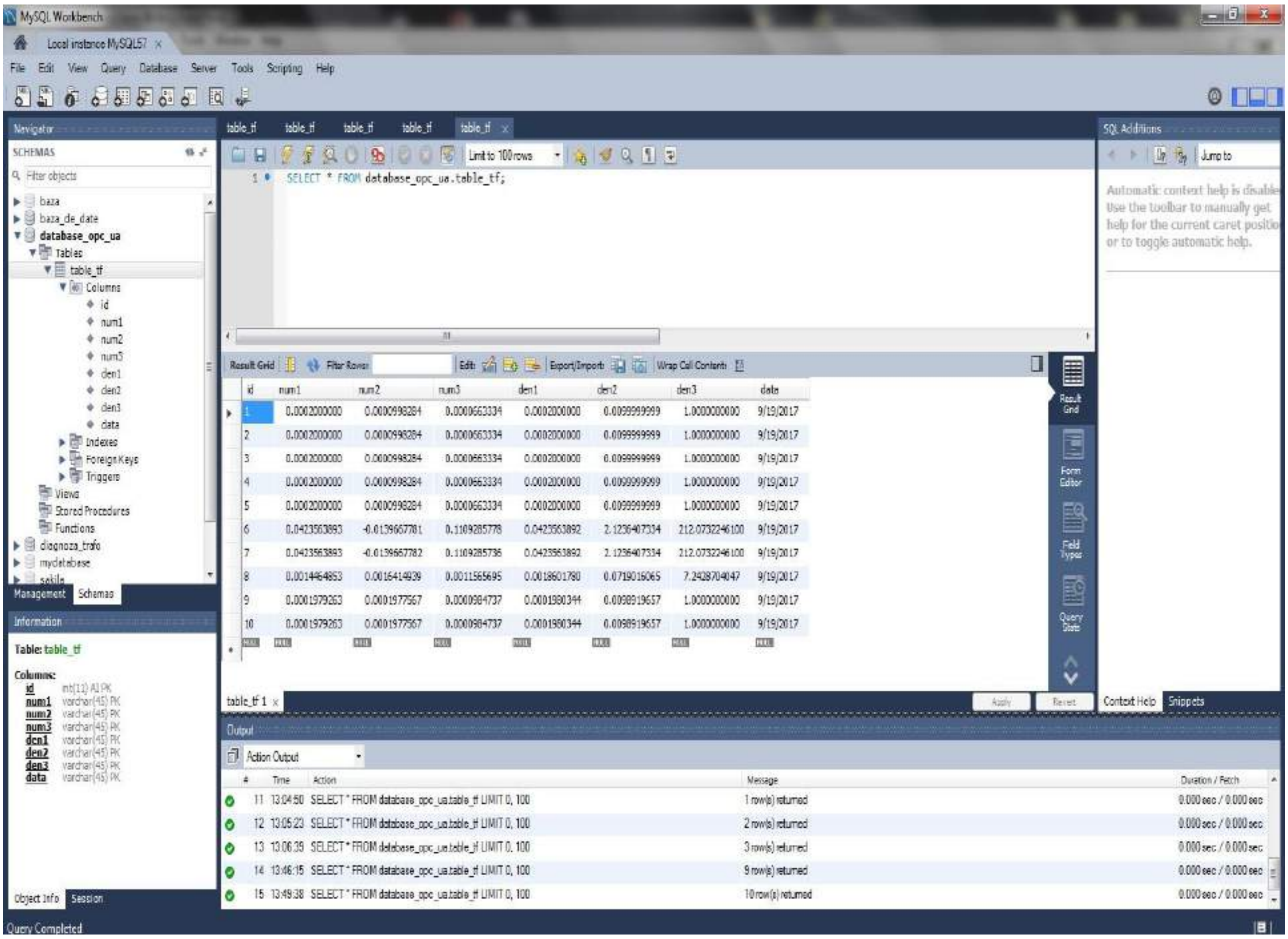

Fig. 8. MySQL server database for transfer function coefficients

In addition, another asynchronous software module can read the history of the transfer functions stored in the MySQL Server (defined as the six coefficients) see figs. 9 and 10.

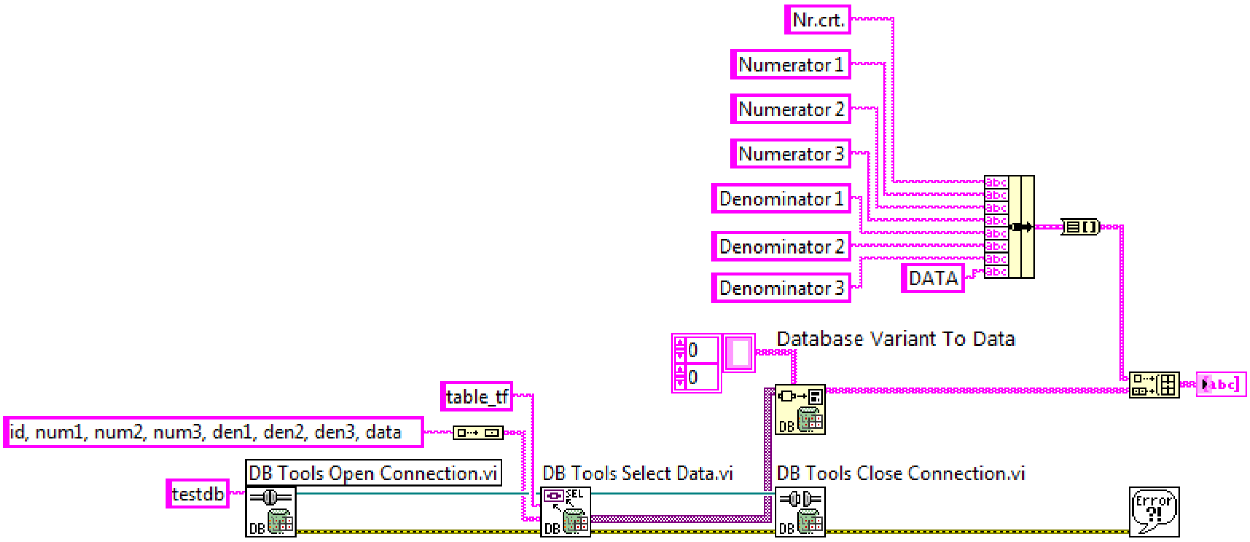

Fig. 9. Client read from MySQL server database transfer function coefficients block diagram

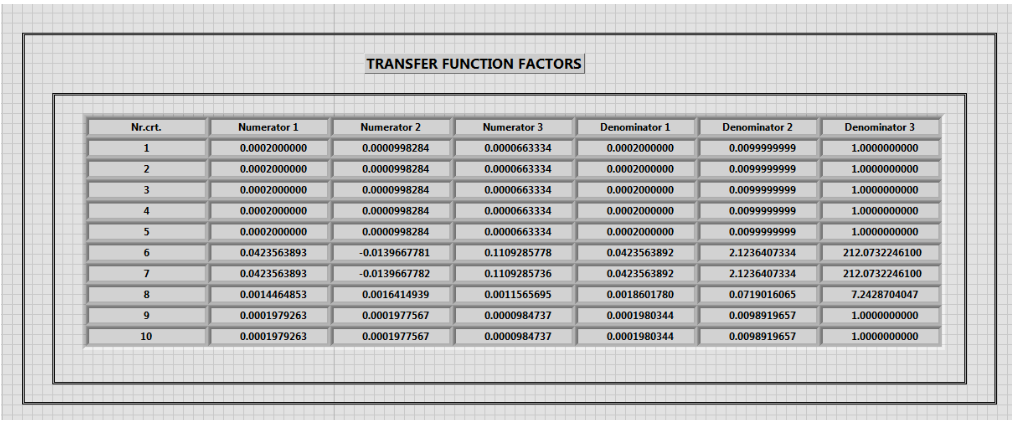

TRANSFER FUNCTION FACTORS

Nr.crt.	Numerator 1	Numerator 2	Numerator 3	Denominator 1	Denominator 2	Denominator 3
1	0.0002000000	0.0000998284	0.0000663334	0.0002000000	0.0099999999	1.0000000000
2	0.0002000000	0.0000998284	0.0000663334	0.0002000000	0.0099999999	1.0000000000
3	0.0002000000	0.0000998284	0.0000663334	0.0002000000	0.0099999999	1.0000000000
4	0.0002000000	0.0000998284	0.0000663334	0.0002000000	0.0099999999	1.0000000000
5	0.0002000000	0.0000998284	0.0000663334	0.0002000000	0.0099999999	1.0000000000
6	0.0423563893	-0.0139667781	0.1109285778	0.0423563892	2.1236407334	212.0732246100
7	0.0423563893	-0.0139667782	0.1109285736	0.0423563892	2.1236407334	212.0732246100
8	0.0014464853	0.0016414939	0.0011565695	0.0018601780	0.0719016065	7.2428704047
9	0.0001979263	0.0001977567	0.0000984737	0.0001980344	0.0098919657	1.0000000000
10	0.0001979263	0.0001977567	0.0000984737	0.0001980344	0.0098919657	1.0000000000

Fig. 10. Client read from MySQL server database transfer function coefficients interface

The process quantities defined in the OPC-UA Server as process value PV_1 and PV_2 are transferred synchronously within 1 second and stored in TDMS files with preset time periods (days, weeks, etc.), see Figures 11 and 12.

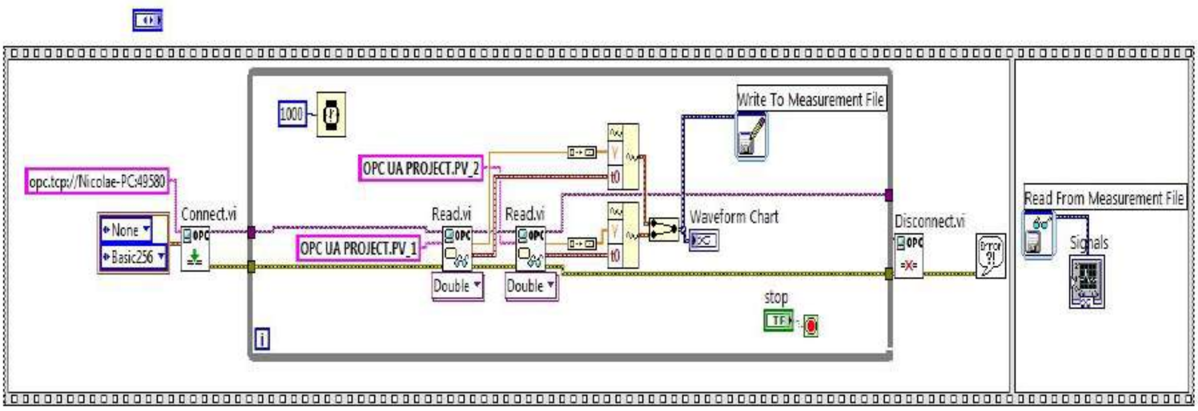

Fig. 11. OPC-UA client write and read TDMS block diagram

Fig. 12. OPC-UA client read TDMS interface

The presented application is modular and can be extended to multiple quantities for an actual industrial process by following the steps implemented in the presentation above. Practically the quantities implemented into SCADA are defined in each software module by groups of interest (quantities accessed synchronously or asynchronously, quantities acquired from the process through acquisition boards from transducers or system description quantities resulting from the process of identification).
The inclusion of several quantities of interest is carried out naturally by following the steps described above.

4. Conclusions

This article summarizes the SCADA systems and the principles of OPC client-server communication. Hence an application was achieved and presented for monitoring a quasi-general industrial process defined by a 2nd order transfer function, for identifying the transfer function and managing the client-server communication of the quantities of interest by online viewing and creating a record using TDMS files and a MySQL database server.
The issue of data communications in industrial environments is not abstract, but arises practically in industrial and monitoring applications, and can become a separate issue, but it can only be studied on condition that minimal software modules are provided for data communication and management from an actual application.
We consider that by achieving such an experimental model like the one described above, but especially by means of the experiments conducted on it, the main benefit will consist in the increase of the amount of knowledge on this topic and a significant facilitation in achieving future complex monitoring applications for systems with a relatively large volume of data and for heterogeneous data acquisition systems.

Acknowledgments

The paper was developed with funds from the Ministry of Education and Scientific Research as part of the NUCLEU Program: PN 16 15 02 06.

References

[1] M. Nicola, D. Sacerdoțianu, M. Duță, D. Popa, „Sisteme SCADA pentru monitorizarea echipamentelor electrice", Ed. Electra (ICPE), 2011;
[2] D. Bailey, E. Wright, „Practical SCADA for Industry", IDC Technologies, 2003;
[3] S. A. Boyer, „SCADA: Supervisory. Control and Data. Acquisition. 3rd Edition", ISA The Instrumentation, Systems, and Automation Society, 2004;
[4] http://www.ni.com/getting-started/labview-basics/environment;
[5] http://www.mathworks.com/products/simpower/model-examples.html.
[6] http://www.opcconnect.com/;
[7] T. V. Bhaskarwar, S. Giri, R. G. Jamakar, „Automation of shell and tube type heat exchanger with PLC and LabVIEW", Industrial Instrumentation and Control (ICIC), pp. 841 - 845, 28-30 May 2015;
[8] https://opcfoundation.org/about/opc-technologies/opc-ua/
[9] https://www.mysql.com/
[10] http://home.hit.no/~hansha/documents/labview/training/Database%20Communication%20 in%20LabVIEW/Database%20Communication%20in%20LabVIEW.pdf
[11] J. Jovitha, "Virtual Instrumentation Using Labview", PHI Learning, New Delhi, 2011;
[12] R. Bitter, T. Mohiuddin, M. Nawrocki, "LabVIEW: advanced programming techniques, Second Edition", CRC Press, 2006;
[13] N. Kehtarnavaz, P. Loizou, M. Rahman, "An Interactive Approach to Signals and Systems Laboratory", Connexions, Huston, 2011;
[14] http://www.ni.com/pdf/manuals/371303n.pdf
[15] D. Selisteanu, C. Ionete, E. Petre, "Virtual Instrumentation. Digital Signal Processing Applications," Ed. Universitaria, Craiova, 2012;

ISSN 1454 - 8003
Proceedings of 2017 International Conference on Hydraulics and Pneumatics - HERVEX
November 8-10, Băile Govora, Romania

OBTAINING OF PI CONTROL PARAMETERS FOR VECTOR CONTROLLED PMSM

Oğuz EROL[1], Melih AKTAŞ[2], Yusuf ALTUN[3]

[1] Duzce University, Engineering Faculty, Mechatronics Engineering, Duzce, Turkey

[2] Duzce University, Engineering Faculty, Electrical and Electronics Engineering, Duzce, Turkey

[3] Duzce University, Engineering Faculty, Computer Engineering, Duzce, Turkey, yusufaltun@duzce.edu.tr

Abstract: *PMSM motor are getting more common each day in industrial applications due to their superiorities such as lacking physical parts such as brushes or commutators, higher reliability and high efficiency and better life expectancy. Another advantage of a pmsm is that it can operate at speeds above 10,000 rpm in bot loaded and unloaded conditions. It is also capable of operating with less noise and electromagnetic interference than a brushed motor. Only disadvantage of a PMSM is that it needs for a control system which is complex. One of the common ways to control a PMSM is the field oriented control method. PMSM is used for the hydraulic servo motor systems. In this study, a PMSM is controlled with FOC method by using Simulink model and the* K_p *and* K_I *coefficients of PI have been determined by using Ziegler-Nichols method.*

Keywords: *PMSM, field oriented control, Ziegler-Nichols method, hydraulic servo motor.*

1. Introduction

The use of PMSM in industrial applications is getting more common each day due to their advantages on other electric motor types. Thanks to rapid development in both power electronics and control systems more and more areas can benefit from the advantages of the PMSM [1]. There are many control methods on PMSM systems for example sliding mode extended state observer (SMESO) technique, an adaptive disturbance compensation finite control set optimal control strategy [2], using linear state feedback controller using the Jacobian linearization [3] or combining Generalized Predictive Control (GPC) with Sliding Mode Disturbance Compensation [4] there are also direct torque control technique which also may include fuzzy logic in the control system [5] but FOC method has significant advantages against the other methods this control method could be applied all kinds of electrical motors by using space vector algorithms [6]. P, PI and PID controllers could be used for speed control in this motor type. Even though PI and PID have simple structures they are widely used in industrial applications. In order to control a system with a PI controller first the controller parameters shall be determined. A good method for determining these parameters is the Ziegler-Nichols method. This method has been used in this paper to speed control a PMSM model in Matlab/Simulink [7].

2. PMSM Model and Control

In order to implement our control system on a PMSM model first we need the mathematical model of the motor by using the equivalent motor circuit. The mathematical equations and equivalent circuit of PMSM has been shown below.

$$V_d = R_s i_d + L_d \frac{di_d}{dt} - N\omega i_q L_q, V_q = R_s i_q + L_q \frac{di_q}{dt} + N\omega(i_d L_d + \psi_m) \quad (1)$$

$$V_0 = R_s i_0 + L_0 \frac{di_0}{dt} \quad (2)$$

$$T = \frac{3}{2} N(i_q(i_d L_d + \psi_m) - i_d i_q L_q) \tag{3}$$

where:

$L_d = L_s + M_s + {}^3\!/_2 L_m$, L_d is the stator d-axis inductance.

$L_q = L_s + M_s - {}^3\!/_2 L_m$, L_q is the stator q-axis inductance.

$L_0 = L_s - 2M_s$, L_0 is the stator zero-sequence inductance.

ω is the rotor mechanical rotational speed.

N is the number of rotor permanent magnet pole pairs.

T is the rotor torque.

dq-abc transform;

$$\begin{bmatrix} a \\ b \\ c \end{bmatrix} = \sqrt{\frac{2}{3}} \begin{bmatrix} \cos\theta & -\sin\theta \\ \cos\theta + 4\frac{\pi}{3} & -\sin\theta + 4\frac{\pi}{3} \\ \cos\theta + 2\frac{\pi}{3} & -\sin\theta + 2\frac{\pi}{3} \end{bmatrix} \begin{bmatrix} d \\ q \end{bmatrix} \tag{4}$$

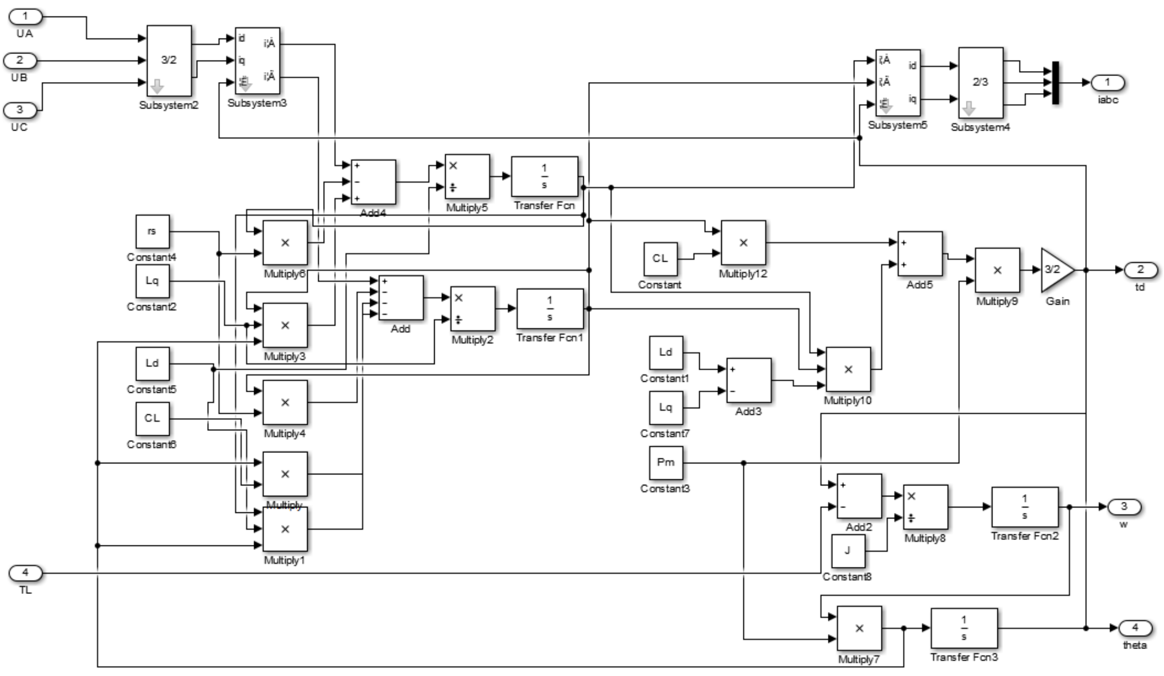

Fig. 1. PMSM Simulink Model Block

The Field Orientated Control (FOC) consists of controlling the stator currents represented by a vector. This control is based on projections which transform a three phase time and speed dependent system into a two co-ordinate (d and q co-ordinates) time invariant system. These projections lead to a structure similar to a DC machine control. Field orientated controlled machines need two constants as input references: the torque component (aligned with the q co-ordinate) and the flux component (aligned with d co-ordinate). As Field Orientated Control is simply based on projections the control structure handles instantaneous electrical quantities [8]. This makes the control accurate in every working operation (steady state and transient) and independent of the limited bandwidth mathematical model. The FOC thus solves the classic scheme problems [9] [10].

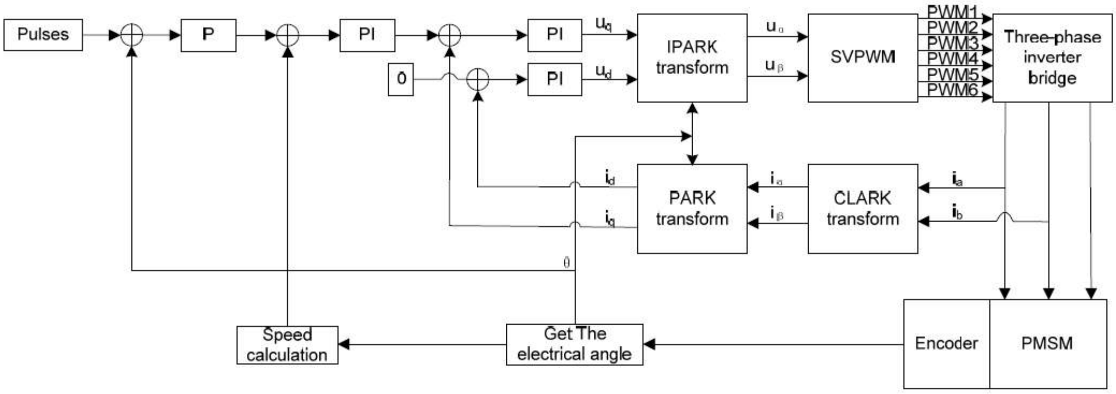

Fig. 2. Vector Control Block Scheme [11]

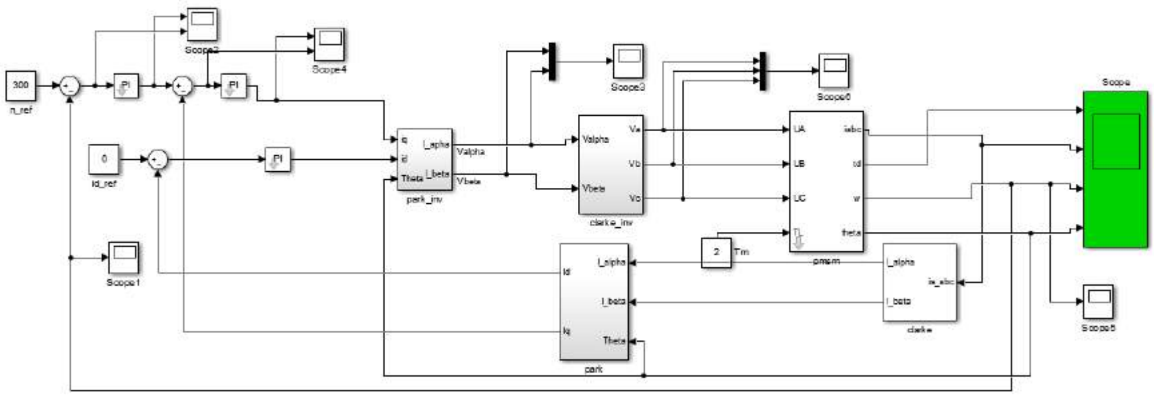

Fig. 3. PMSM FOC Model in Simulink

Figure 3 shows the simulation block diagram. Ziegler–Nichols method is a technique used in PID tuning to find ideal parameters. Method find these parameters by trial and error. The steps to use this method is as follows.

• The I and D gains are first set to zero.

• The "P" gain is increased until it reaches the "critical gain" Kcr at which the output of the loop starts to oscillate.

• Kcr and the oscillation period Pcr are used to set the gains as shown.

Ziegler-Nichols Method			
Control Type	***Kp***	***Ki***	***Kd***
P	***0.5Kcr***	**-**	**-**
PI	***0.45Kcr***	***KpPcr/1.2***	**-**
PID	***0.6Kcr***	***KpPcr/2***	***KpPcr/8***

ISSN 1454 - 8003
Proceedings of 2017 International Conference on Hydraulics and Pneumatics - HERVEX
November 8-10, Băile Govora, Romania

The values are given by

$$K_{cr} = 11.11,$$

$$K_p = 0.45 * 11.11 = 5$$

$$K_p * P_{cr} = \tilde{T} = 12$$

$$K_i = \tilde{T} / 1.2 = 10$$

By using the *P* and *I* parameters that has been calculated above, we ran our simulations and obtained the speed graphic of PMSM as shown below.

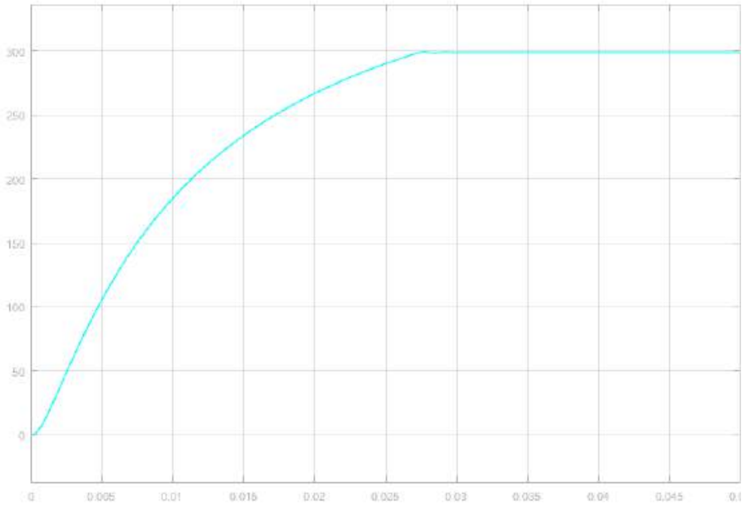

Fig. 4. Motor Mechanical Speed [rad/s]

As seen from the figure, we can control the speed of the PMSM very precisely by using the parameters that we found by using Ziegler-nichols method.

3. Conclusions

In this study, speed control of the PMSM has been performed by using Ziegler-Nichols method on Matlab/Simulink software. Ziegler Nichols method has been successful on designing parameters and controlling PMSM speed according to the simulation results.

References

[1] http://empoweringpumps.com/ac-induction-motors-versus-permanent-magnet-synchronous-motors-fuji/;
[2] Yun-jie Wu, Guo-fei Li, “Adaptive disturbance compensation finite control set optimal control for PMSM systems based on sliding mode extended state observer” Mechanical Systems and Signal Processing Volume 98, 1 January 2018, pp. 402-414;
[3] Aishwarya A. Apte, Vrunda A. Joshi, Rahee A. Walambe, Ashwini A. Godbole, “Speed Control of PMSM Using Disturbance Observer” IFAC-PapersOnLine Volume 49, Issue 1, 2016, pp. 308-313;
[4] Xudong Liu, Chenghui Zhang, Ke Li, Qi Zhang, “Robust current control-based generalized predictive control with sliding mode disturbance compensation for PMSM drives” ISA Transactions;
[5] O. Ouledaliab, A. Meroufelb, P. Wiraab, S. Bentoubaab, “Direct Torque Fuzzy Control of PMSM based on SVM” Energy Procedia Volume 74, August 2015, pp. 1314-1322;
[6] J. Jacoba, A. Chitrab, “Field Oriented Control of Space Vector Modulated Multilevel Inverter fed PMSM Drive” Energy Procedia Volume 117, June 2017, pp. 966-973;
[7] Duarte Valério, José Sá da Costa, “Tuning of fractional PID controllers with Ziegler–Nichols-type rules” Signal Processing, Volume 86, Issue 10, October 2006, pp. 2771-2784;

[8] J. Jacoba, A.Chitrab, ”Field Oriented Control of Space Vector Modulated Multilevel Inverter fed PMSM Drive” Energy Procedia Volume 117, June 2017, pp. 966-973;
[9] W. Lina, X. Kun, L. De Lillo, L. Empringham, P. Wheeler, ”PI controller relay auto-tuning using delay and phase margin in PMSM drives”, Chinese Journal of Aeronautics Volume 27, Issue 6, December 2014, pp. 1527-1537;
[10] Qiang Song, Chao Jia, ” Robust Speed Controller Design for Permanent Magnet Synchronous Motor Drives Based on Sliding Mode Control” Energy Procedia Volume 88, June 2016, pp. 867-873;
[11] http://www.mstarlabs.com/control/znrule.html.

ISSN 1454 - 8003
Proceedings of 2017 International Conference on Hydraulics and Pneumatics - HERVEX
November 8-10, Băile Govora, Romania

THEORETICAL AND EXPERIMENTAL RESEARCH ON GAS DYNAMICS SONIC DISCHARGE PROCESS IN BIG BLASTER TYPE CANNONS

Florin TEIȘANU[1], Constantin CHELAN[1], Marinela BUTOI[1], Claudiu-Ionel NICOLA[1], Marcel NICOLA[1]

[1]National Institute for Research, Development and Testing in Electrical Engineering – ICMET Craiova, tunuri@icmet.ro

Abstract: *In industrial applications, the Big Blaster type air-cannon systems are used for clearing/cleaning bunkers/hoppers and silos of bulk/powder material in cement mills and building material factories, coal thermal power stations, mining industry and ferrous metallurgy, etc. The paper presents some of the research conducted in the field of aerodynamics and the results obtained for these types of mechanical-pneumatic equipment. In terms of the theoretical research, with reference to the law of conservation and transformation of energy of compressible fluids under non-permanent flow state, an analysis was carried out for the gas dynamics phenomenon of blast air stored in a container flowing through an opening, i.e. for the sonic flow rates and time duration of the phenomenon. Also in relation to the theoretical level, the phenomenon is customized for the actual parameters of an air cannon type TP150, featuring a tank capacity of 150 liters, a round discharge opening with DN100 mm and maximum operating pressure of 10 bar. The developed measuring system is based on the data acquisition board which allowed the recording of the dynamic phenomenon of critical discharge and by default the actual pneumatic pulse duration, and the software application for the analysis of the actual pneumatic pulse duration is created in LabVIEW programming environment.*

Keywords*: Big-Blaster cannon, thermal aerodynamics, sonic airwave, data acquisition, LabVIEW*

1. Introduction

Air cannons (TP) presented in simplified form in Figure 1 are mechanical-pneumatic equipment which store potential compressed air energy into a container, and further converts it instantly by external control through a set of special air valves into kinetic energy and implicitly into useful mechanical work.

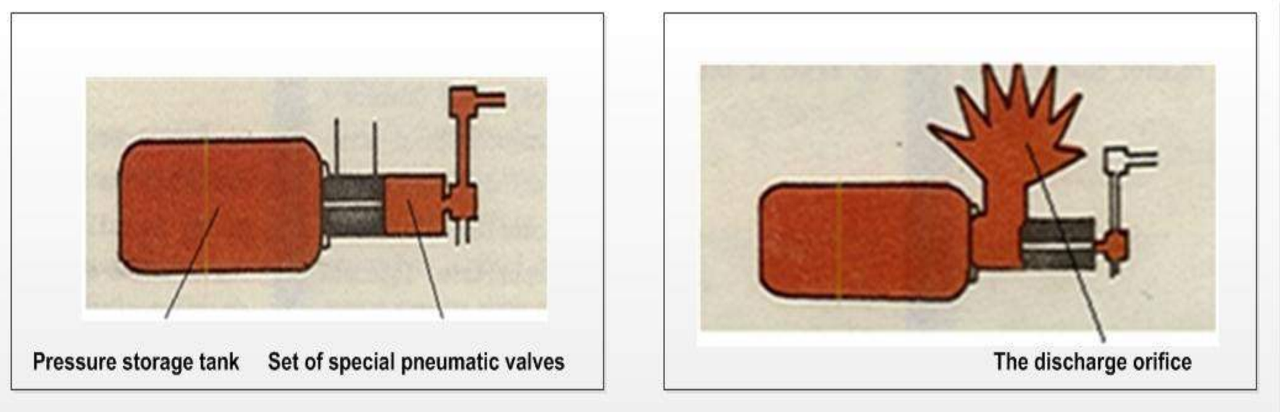

Fig. 1. Air cannons

In industrial technical applications, the Big Blaster type air-cannon systems designed and manufactured by ICMET CRAIOVA [1, 2] presented in Figure 2, are used in cement mills and building material factories, coal thermal power stations, mining industry and ferrous metallurgy, etc. Thus, the pneumatic shock wave generated and guided through pipes and nozzles ensures the unlocking and cleaning of bunkers/hoppers, silos where tens and hundreds of tons of bulk and powder material are stored/decanted, such as: cement, lime, ores, coke, charcoal, etc.

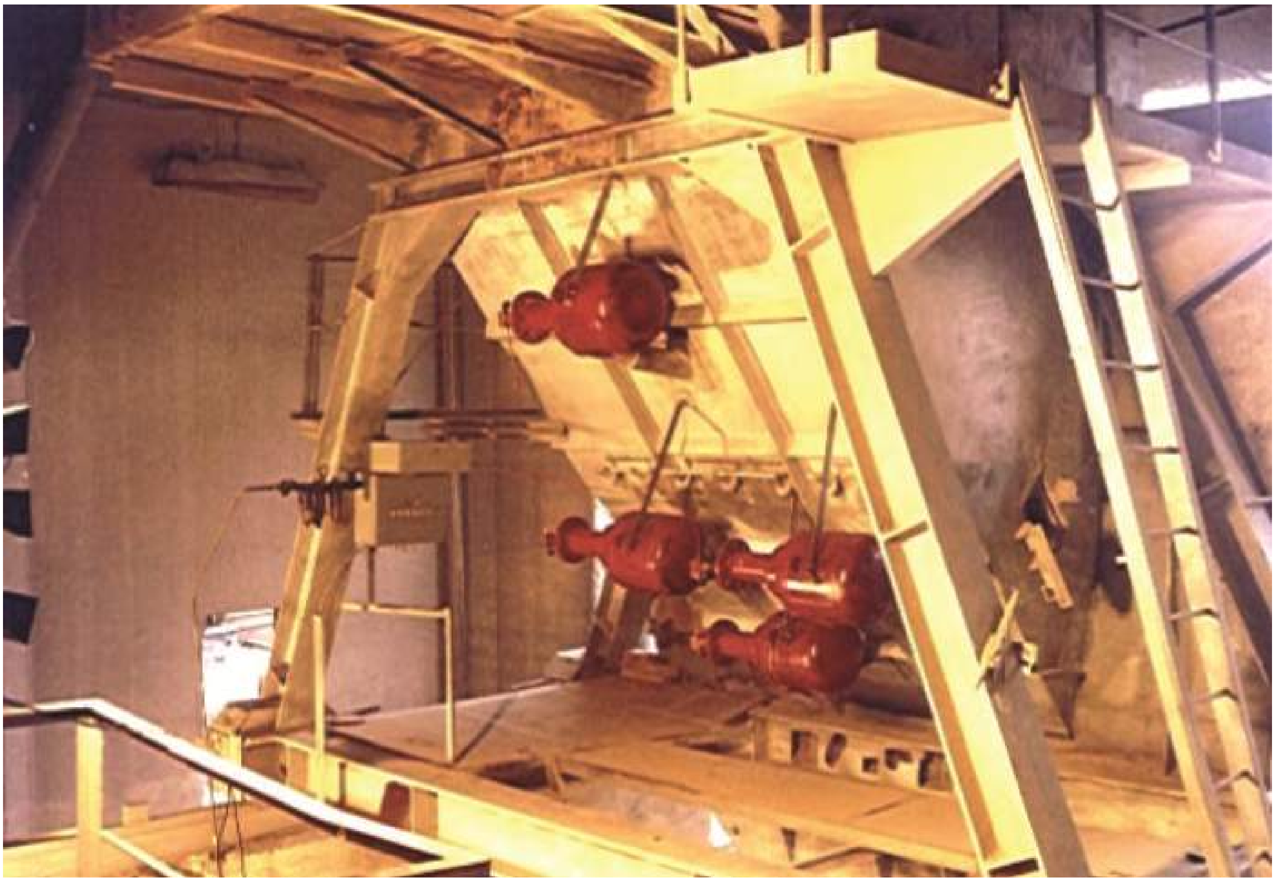

Fig. 2. Big-Blaster type air cannon systems

In general, in order to cover the entire range of applications for the beneficiaries, the air cannons governed by the European directives on pressure equipment are designed in various types and sizes. They are defined by design values (air capacity, loading/working pressure), and the performances are ensured by discharge parameters such as: discharge rate, duration of pneumatic pulse or impact force.

The equipment is designed and sized in order to achieve a sudden/blast release of the potential energy stored in the container through a set of special air valves [3], i.e. sonic discharge rates and pneumatic pulse durations of the order of milliseconds. These features distinguish between the types of air cannons developed by various specialized companies in Germany, France, Poland, Romania etc. [2, 4, 5] from the point of view of efficiency of use.

2. The thermodynamics of the compressed air discharge – a theoretical approach

The thermodynamic condition of compressible fluids with mass m, is defined by energy parameters pressure p, temperature T and volume V, according to the next state equation of perfect gases [6]:

$$p \cdot V = m \cdot R \cdot T \tag{1}$$

where R is the constant specific to each gas (for air pressure R=287 $m^2/s^2 \cdot K$

In the case of compressible fluid dynamics, gas (air) flow is studied at rates comparable to the speed of sound, a process where compressibility and thermal phenomena cannot be neglected. In the case of compressible fluids with adiabatic flow, the law of density variation ρ, depending on pressure p, in two initial and final moments, is indicated by [6]:

$$\frac{p}{\rho^k} = \frac{p_o}{\rho_o^k} \qquad \text{or} \qquad p = \rho \cdot R \cdot T \tag{2}$$

where k- adiabatic coefficient, specific to each type of gas (k=1,4 air)
In the case of adiabatic (constant-entropy) flow, with compressible fluids rate "v", the law of conservation and transformation of energy of compressible fluids under non-permanent flow follows the Bernoulli equation [7]:

$$\frac{v^2}{2} + \frac{k}{k-1} \cdot \frac{p_o}{\rho_o} \cdot \left(\frac{p}{\rho_o}\right)^{\frac{k-1}{k}} = \frac{v_o^2}{2} + \frac{k}{k-1} \cdot \frac{p_o}{\rho_o} \tag{3}$$

In the case of sudden adiabatic expansion of compressed gas stored in the tank (v_o = 0 m/s from the relation (3), the rate of gas flow through a small and free opening becomes [6, 7]:

$$v = \sqrt{\frac{2k}{k-1} \cdot \frac{p_o}{\rho_o} \cdot [1-(\frac{p}{\rho_o})^{\frac{k-1}{k}}]} \tag{4}$$

If the section of gas flow from the tank is Sc, then the theoretical flow rate Q_m is calculated by using the known relation:

$$Q_m = S_c \cdot v \cdot \rho \tag{5}$$

The speed of sound in air "a" is determined by using the known relation [7]:

$$a = \sqrt{\frac{k \cdot p}{\rho}} = \sqrt{k \cdot R \cdot T} \tag{6}$$

In standard atmospheric conditions: $\mathrm{a} = \sqrt{\mathrm{k} \cdot \mathrm{R} \cdot \mathrm{T}} = \sqrt{1.4 \cdot 287 \cdot 288} = 340\ \mathrm{m/s}$
In aerodynamics, local Mach number is defined as $M = v/a$
Under the situation where $M \cong 1$, then $v = a \cong 340\ m/s$, and the flow/discharge is called sonic (critical or Laval state). For M<1 (v<a) there is subsonic discharge, while for M>1 (v>a) we have the supersonic discharge situation.
In the case of our application, i.e. the sonic discharge of the blast air stored in the air cannon tank, the phenomenon corresponds to non-permanent flow which occurs over a very short time period.
The analysis of this dynamic phenomenon will be carried out by using the sampling method, i.e. as if the process occurs through successive decrease in pressure with a rate of 1 bar, starting from the maximum pressure in the container of 10 bar ($10 \cdot 10^5$ N/m^2). Thus, for the 9 successive pressures ranges (10÷9 bar; 9÷8 bar; … 2÷1 bar), the phenomenon is analyzed in terms of the discharge rates, by applying the relation (4) and the blast air dynamic density by applying the relation (2).
The discharge occurs in standard atmosphere, with known parameters: $p = p_{at} = 1 \cdot 10^5$ N/m^2 (1 bar); T=273+15=288°K(15°C) ; ρ=1.2 Kg/m^3.
For the first discharging interval analized, respectively for air discharging from 10 bar pressure to 9 bar pressure, it will result:

$$\mathrm{p_{med}} = \frac{10+9}{2} = 9.5\mathrm{bar} = 9.5 \cdot 10^5 \mathrm{N/m^2}; \rho_0 = \frac{\mathrm{p_{med}}}{\mathrm{R \cdot T}} = \frac{9.5 \cdot 10^5}{287 \cdot 288} = 11.4 \mathrm{Kg/m^3} \tag{7}$$

$$v = \sqrt{\frac{2k}{k-1} \cdot \frac{p_o}{\rho_o} \cdot [1-(\frac{p}{\rho_o})^{\frac{k-1}{k}}]}\ ;\ \mathrm{v} = \sqrt{\frac{2 \cdot 1.4}{1.4-1} \cdot \frac{9.5 \cdot 10^5}{11.4} \cdot [1-(\frac{1 \cdot 10^5}{9.5 \cdot 10^5})^{\frac{1.4-1}{1.4}}]} = 523\ [\mathrm{m/s}] \tag{8}$$

For intermediate ranges the calculations are similar.
For the last discharging interval analized, respectively for air discharging from 2 bar pressure to 1 bar pressure, the speed will be:

$$p_{med} = 1.5bar = 1.5 \cdot 10^5 N/m^2; \rho_0 = \frac{p_{med}}{R \cdot T} = \frac{1.5 \cdot 10^5}{287 \cdot 288} = 1.8 Kg/m^3 \tag{9}$$

$$v = \sqrt{\frac{2 \cdot 1.4}{1.4-1} \cdot \frac{1.5 \cdot 10^5}{11.4} \cdot [1-(\frac{1 \cdot 10^5}{1.5 \cdot 10^5})^{\frac{1.4-1}{1.4}}]} = 253\ [m/s] \tag{10}$$

In the case of blast air discharged from the air cannon tank with volume V=0.150 m^3, charged at the initial pressure p=10 bar, which corresponds to the initial blast air mass m=1.814 Kg, the phenomenon (partial mass flow) can be analyzed in terms of decreasing pressure ranges with rate Δp=1 bar, in relation to the flow output (relation 5) and the duration of each of these pneumatic pulses, as follows:
10 bar→9 bar corresponding to the blast air discharge from 10 bar pressure to 9 bar pressure:

$$\begin{aligned}\Delta m &= m_{10} - m_9 = V \cdot (\rho_{10} - \rho_9) = V \cdot (\frac{p_{10}}{R \cdot T} - \frac{p_9}{R \cdot T}) \\ &= 0.150 \cdot (\frac{10 \cdot 10^5 - 9 \cdot 10^5}{287 \cdot 288}) = 0.150 \cdot \frac{(10-9) \cdot 10^5}{287 \cdot 288} = 0.181\, Kg\end{aligned} \tag{11}$$

The mass flow rate corresponding to the discharge to the atmosphere (p_{at}=1 bar ; ρ_{at}=1.2 Kg/m^3) from 10 bar pressure to 9 bar pressure, i.e. the mass output m=0.181Kg through section S=78.5 cm^2=78.5·10^{-4} m^2, with calculated rate v=523 m/s, is [3]:

$$\dot{m} = v \cdot S \cdot \rho_{at} = 523 \cdot 78.5 \cdot 10^{-4} \cdot 1.2 = 4.92\ \ Kg/s \tag{12}$$

The duration " t_{10-9} " of the discharge to the atmosphere of m=0.181 Kg of blast air from initial 10 bar pressure to 9 bar pressure, with flow rate $\dot{m} = 4.92\ \ Kg/s$ is [3]:

$$t_{10-9} = \frac{\Delta m}{\dot{m}} = \frac{0.181}{4.92} = 0.036\, s \tag{13}$$

The period of time „ t_{2-1}" , for the last discharging interval analized, respectively for air discharging from 2 bar pressure to 1 bar pressure, will result :

$$\Delta m = m_2 - m_1 = V \cdot (\rho_2 - \rho_1) = 0.150 \frac{(2-1) \cdot 10^5}{287 \cdot 288} = 0.181\, kg \tag{14}$$

$$\dot{m} = v \cdot S \cdot \rho_{at} = 253 \cdot 78.5 \cdot 10^{-4} \cdot 1.2 = 2.383\ \ kg/s \tag{15}$$

$$t_{2-1} = \frac{\Delta m}{\dot{m}} = \frac{0.181}{2.383} = 0.075\, s \tag{16}$$

The period of time for full discharge of the tank (air cannon working time) from 10 bar initial pressure to atmospheric pressure p_{at}=1 bar, is obtained by summing the calculated times [8]:

$$\begin{aligned}&t_{10-1} = t_{total} = t_{10-9} + t_{9-8} + ... + t_{2-1} \\ &t_{total} = 0.036 + 0.037 + 0.038 + 0.039 + 0.040 + 0.042 + 0.045 + 0.052 + 0.075 = 0.404\, s\end{aligned} \tag{17}$$

The state of the system for TP150 air cannon, and the thermodynamic quantities are presented in table no.1

Table 1: State of the system (TP150 air cannon) and the calculated aerodynamic quantities

Thermodynamic state	State variables				Aerodynamic parameters		Observations
	Pressure p [bar]	Volume V [m^3]	Temperature T [^oK]	Density ρ [Kg/m^3]	Rate v [m/s]	Duration of phenomenon t [s]	
Adiabatic compression	10	0.150	288	12.1	0	-	Initial steady state
Sonic adiabatic expansion	10→9	0.150	288	11.4	523	0.036	non-permanent sonic flow
Sonic adiabatic expansion	9→8	0.150	288	10.2	512	0.037	non-permanent sonic flow
Sonic adiabatic expansion	8→7	0.150	288	9	500	0.038	non-permanent sonic flow
Sonic adiabatic expansion	7→6	0.150	288	7.8	488	0.039	non-permanent sonic flow
Sonic adiabatic expansion	6→5	0.150	288	6.6	470	0.040	non-permanent sonic flow
Sonic adiabatic expansion	5→4	0.150	288	5.4	451	0.042	non-permanent sonic flow
Sonic adiabatic expansion	4→3	0.150	288	4.2	418	0.045	non-permanent sonic flow
Sonic adiabatic expansion	3→2	0.150	288	3	366	0.052	non-permanent sonic flow
Subsonic diabatic expansion	2→1	0.150	288	1.8	253	0.075	non-permanent subsonic flow
Stationary state	1	0.150	288	1.2	0	-	Final steady state

The state of the system (TP150 air cannon) and the thermodynamic quantities are presented in a centralized form as follows:
Total sonic adiabatic expansion time (10 bar → 2 bar range): t=0.329 s
Total sonic adiabatic expansion time (9 bar → 2 bar range): t=0.293 s
Total subsonic adiabatic expansion time (2 bar → 1 bar range): t=0.075 s
Total air cannon discharge time (10 bar → 1 bar range): t=0.404 s
Total air cannon discharge time (9 bar → 1 bar range): t=0.368 s.

3. Hardware and software description of measurement system

Rapid advances in Personal Computer (PC) hardware and software technologies have resulted in easy and efficient adoption of PCs in various precise measurement and complex control applications [9].
A PC based measurement or control application requires conversion of real world analog signal into digital format and transfer of digitized data into the PC. A data acquisition system that performs conversion of analog signal to digital data and the digital data to analog signal is interfaced to a PC

to implement the functions of measurement and control instrumentation applications [10-12].

3.1 Hardware description

The data acquisition system consists of the following components:

- a process computer running the application software;
- a Data Acquisition Board NI USB-6009;
- an electronic pressure sensor.

The NI USB-6009 data acquisition device is ideal for applications where a low-cost, small form factor and simplicity are essential. With plug-and-play USB connectivity, these devices are simple enough for quick measurements but versatile enough for more complex measurement applications. The NI USB-6009 has 8 analog inputs, 2 analog outputs, 2 digital inputs/outputs and 32-bit counter. Maximum sample speed by each analog input is 48 kS/s. Sample speed on analog outputs is 150 Sample/s and it can't be changed. Analog inputs have 14-bit resolution and analog outputs have 12-bit resolution [13].

A transducer is a device that converts a physical phenomenon into a measurable electrical signal, such as voltage or current. The ability of a DAQ system to measure different phenomena depends on the transducers to convert the physical phenomena into signals measurable by the DAQ hardware. Transducers are synonymous with sensors in DAQ system. There are specific transducers for many different applications, such as measuring temperature, pressure, or fluid flow. Below we see some common phenomena and the transducers used to measure them.

The parameters of the pressure sensor type PN2593 produced by IFM company are:

- Measuring range: -1...25 bar / -14.5...362.5 psi / -0.1...2.5 MPa;
- Function programmable;
- Measuring element: ceramic-capacitive pressure measuring cell;
- Process connection: G ¼ A / M5 I (according to DIN EN ISO 1179-2);
- Output function: 2 x normally open / closed programmable or 1 x normally open / closed programmable + 1 x analog (4...20 mA / 0...10 V; programmable 1:5)
- Shock resistance: DIN EN 60068-2-27 50 g (11 ms);
- Vibration resistance: DIN EN 60068-2-6 20 g (10...2000 Hz);
- Response time analog output: < 3 ms;
- Operating voltage: 19-30 V c.c.;
- Weight: 0.218 kg.

3.2 Software description

The application software for acquisition and analysis of the pressure signal is developed in LabVIEW. The application software transforms the PC and the data acquisition USB 6009 into a complete data acquisition, analysis, and presentation tool.

The software LabVIEW is a programming environment based on G language (graphic language) core intended mainly to develop applications for data control and acquisition, their analysis and results presentation, develop an interface to allow for the data analysis. LabVIEW contains a comprehensive set of tools for acquiring, analyzing, displaying, and storing data, as well as tools to help us troubleshoot the code you write [9].

The application software is based on state machines. A state machine is programming architecture that can be used to implement any algorithm that can be explicitly described by a state diagram or flowchart. The main states of the algorithm are acquisition of the pressure signal, analysis of the pressure signal and the ratio by the waveform graph of the pressure discharge. According to the analysis stages the main structure used to develop the software application is flat sequence structure. Data flow for the flat sequence structure differs from data flow for other structures. Frames in a flat sequence structure execute from left to right and when all data values wired to a frame are available. The data leaves each frame as the frame finishes executing. This means the input of one frame can depend on the output of another frame [10-13].

The interface of the application software is developed in a menu-based system for easy and efficient management of acquisition and analysis of the pressure signal.

Figure 3 shows the time evolution of the pressure signal for the entire period of the 150 liters tank loading process.

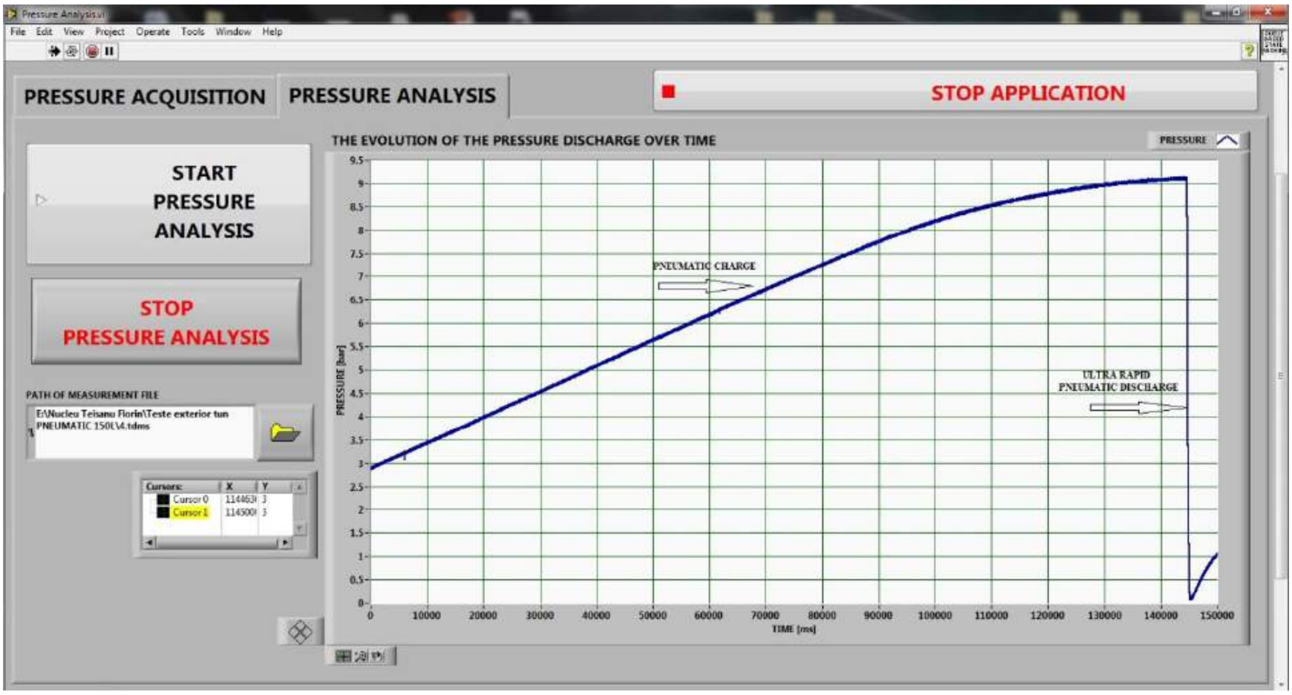

Fig. 3. Software interface of the acquisition and analysis for pressure signal

In general, data acquisition programming with DAQmx involves the following steps: create a Task and Virtual Channels, configure the Timing Parameters, start the Task, perform a Read operation from the DAQ, stop and Clear the Task as presented in Figure 4 [14, 15].
Technical Data Management Streaming (TDMS) file format was used for storing data [9]. This file format is a specific type of binary file created for National Instruments products. It actually consists of two separate files: a XML section contains the data attributes, and a binary file for the waveform.
In order to analyze the pressure discharge area, we use the option of zooming in on an area of the graph along the x-axis (time) as presented in Figure 5.

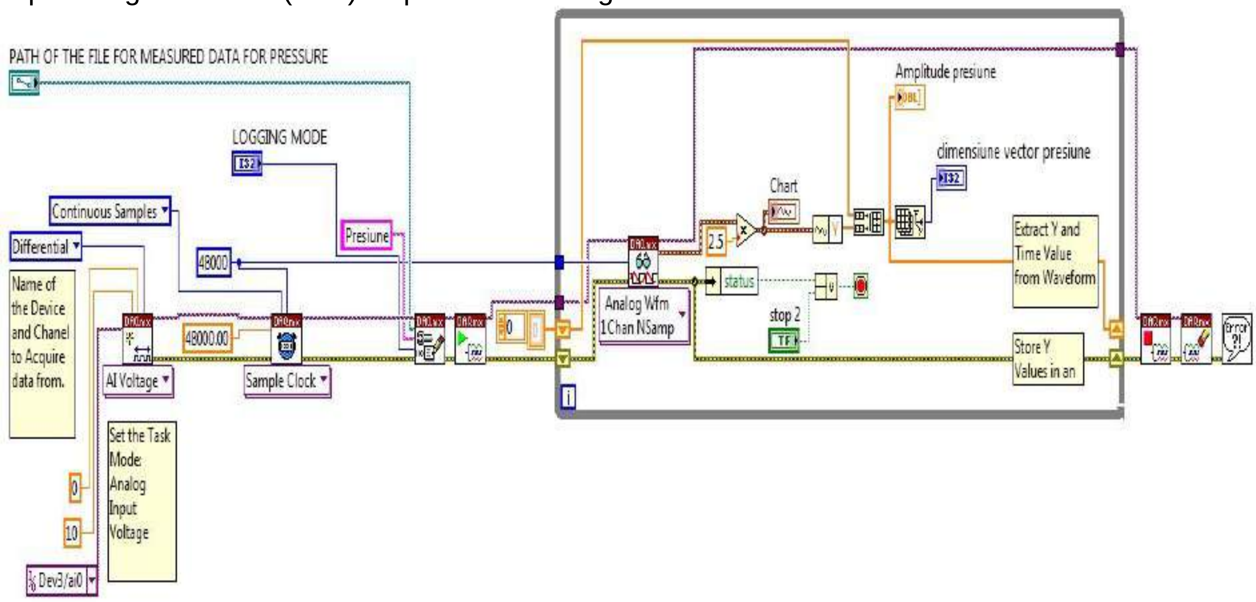

Fig. 4. The block diagram of the pressure acquisition

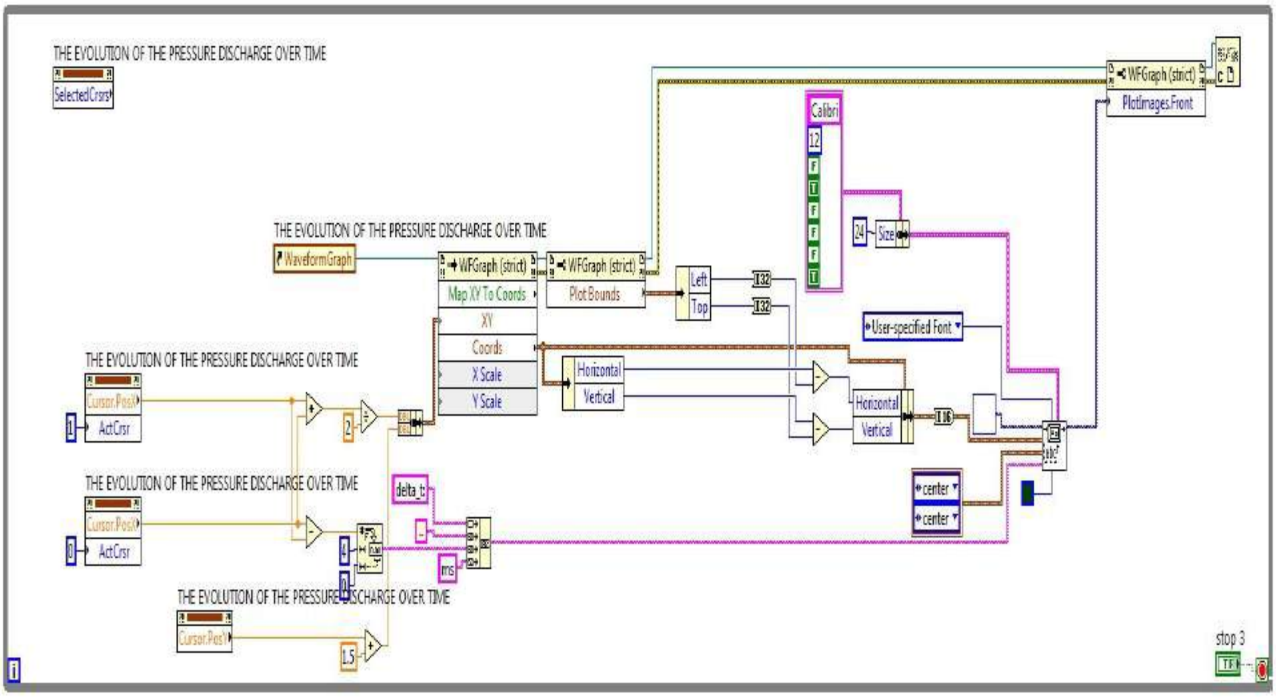

Fig. 5. The block diagram of the pressure analysis

4. Experimental research

The experimental research which performed the on-line recording of the dynamic phenomenon of critical discharge, allowed the determination of the pneumatic pulse duration Δt, for the 8 pressure ranges 9 → 1 bar. The critical discharge of the TP 150 air cannon is presented in Figure 6.
Figures 7 and 8 show the time evolution of the pressure discharge from the pneumatic tank.

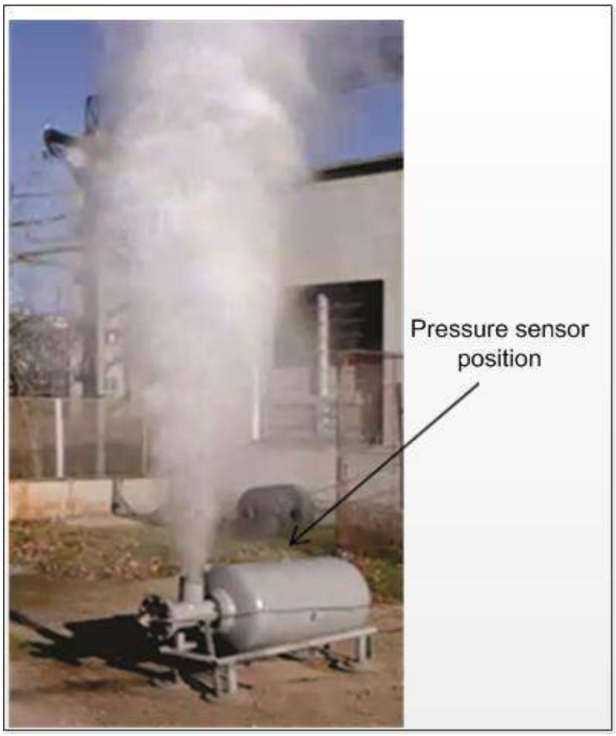

Fig. 6. Critical discharge of TP 150 air cannon

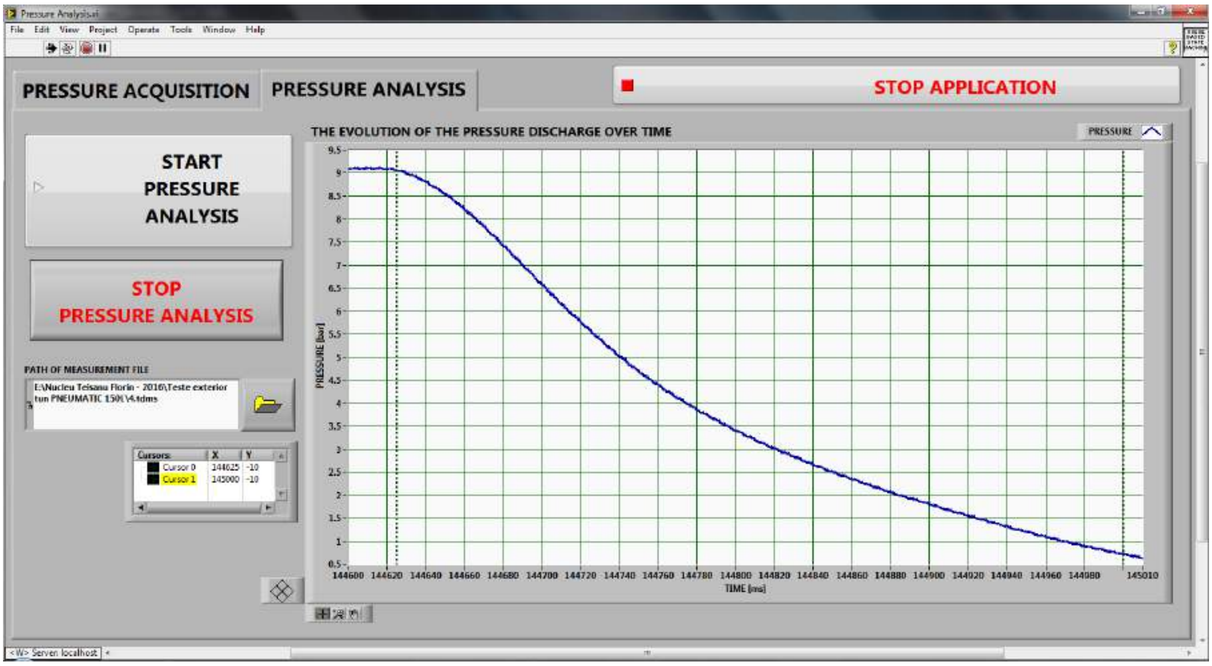

Fig. 7. Time evolution of the pressure discharge - details

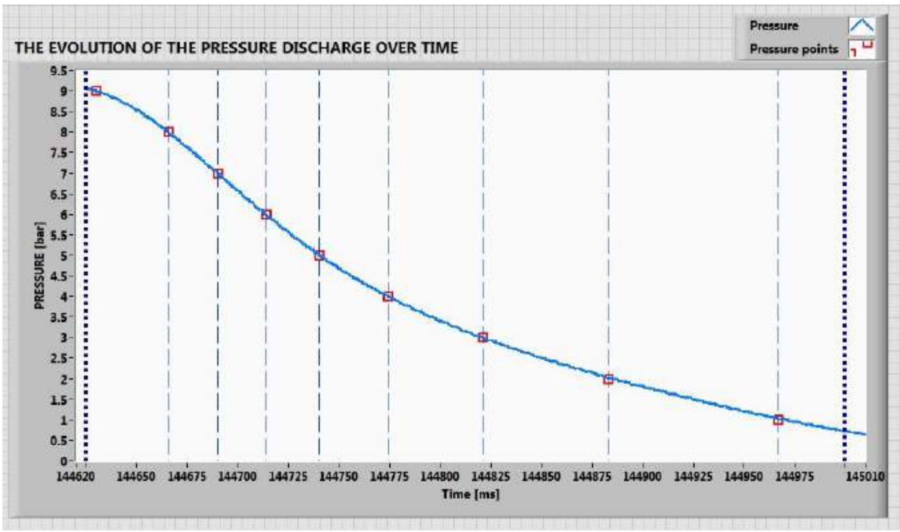

Fig. 8. Time evolution of the pressure highlighting the ranges between 9 to 1 bars

Table 2: The state of the system (TP 150) and the duration of the pneumatic pulse measured and recorded during the air cannon discharge

Pressure range [bar]	Time range [ms]
9÷8	30
8÷7	24
7÷6	25
6÷5	26
5÷4	34
4÷3	47
3÷2	62
2÷1	84

The graphical recording of the pressure decrease p [bar] with time Δt [ms] reads as follows:
Total sonic adiabatic expansion time (9 bar → 2 bar), Δt =0.248 s;
Total subsonic adiabatic expansion time (2 bar → 1 bar), Δt =0.048 s;
Total air cannon discharge time (9 bar → 1 bar), Δt =0.332 s;
These values of the pneumatic pulse duration Δt determined by experiments are close to the values determined and presented in the paper at the theoretical research chapter and can define the dynamics of the sonic discharge phenomenon in type TP 150 air cannons.

5. Results and interpretation

The results of the theoretical research presented under a systematized form in table 1 describe the thermodynamic state of the system (TP150 air cannon) in balanced state (p = 10 bar/charged, p = 1 bar/discharged) as well as the intermediate states - dynamics of transformation for the 9 pressure ranges from 10 bar to 1 bar.
The adiabatic expansion, for the pressure drop range from 10 bar → 2 bar is of sonic type, i.e. the rate is superior to the local speed of sound (v>340 m/s), and at the end of the range, i.e. for the range 2 → 1 bar there is subsonic adiabatic exchange (v≅253 m/s <340 m/s).
The calculated pneumatic pulse duration Δt, through the discharge opening is noted to be shorter for higher pressure values (10 → 4 bar) and increases with the decrease in pressure to the atmospheric pressure value (4 → 1 bar).
The experimental research which performed the on-line recording of the dynamic phenomenon of critical discharge, allowed the determination of the pneumatic pulse duration Δt, for the 8 pressure ranges 9 → 1 bar. The data presented in table 2 show that the pneumatic pulse duration is shorter at higher pressure values (9 → 6 bar) and increases continuously with the decrease in pressure to the atmospheric pressure value (4 → 1 bar).
The long duration Δt = 30 ms, for the pressure range 9 → 8 bar is abnormal and is due to the fact that the construction of the air cannon TP150 includes a compression spring located behind the piston which slows the recoil/release stroke.
In conclusion, in the range of pressure drop 9 → 2 bar, the duration of the air cannon discharge determined theoretically by calculation Δt = 0.293 is close to the value determined by experimental methods Δt = 0.248 s. The two sets of results are comparable and we consider that they can define this complex phenomenon of critical discharge.
The high operating pressures in the range 4 ÷ 10 bar create flow rates superior to the sonic speed (v > 340 m/s), a short duration of the pneumatic pulse and thus generate a superior efficiency of air cannons use.
The impact force developed in the air cannon discharging, i.e. the force which generates the useful work, is another important feature to be studied. This raises particular problems due to the fact that it has a dynamic nature, is generated by the sonic flow of a pressure gas, for a very short period of time, which in turn requires a theoretical approach and an experimental model for validation.
In synthesis we can conclude that:

- The adiabatic expansion, for the pressure drop range from 10 bar → 2 bar is of sonic type.
- The adiabatic expansion, for the pressure drop range from 2 bar → 1 bar is of subsonic type.
- The high operating pressures in the range 4 ÷ 10 bar create flow rates superior to the sonic speed (v > 340 m/s), a short duration of the pneumatic pulse and thus generate a superior efficiency of air cannons use.
- The two sets of times Δt (calculated and experimentally determinated) are comparable and we consider that they can define this complex phenomenon of critical discharge.

6. Conclusions

In this paper was presented at the theoretical level, the phenomenon is customized for the actual parameters of an air cannon type TP150, featuring a tank capacity of 150 liters, a round discharge

opening with DN100 mm and maximum operating pressure of 10 bar. Also was presented a developed measuring system based on the data acquisition board which allowed the recording of the dynamic phenomenon of critical discharge and by default the actual pneumatic pulse duration, and the software application for the analysis of the actual pneumatic pulse duration created in LabVIEW programming environment.
The impact force developed in the air cannon discharging is another important feature which will be studied in future works.

References

[1] ICMET Craiova – Brevet de inventie RO Nr.101147/1988 – Dispozitive pentru descarcarea rapida a aerului comprimat, (Devices for quick discharge of compressed air);
[2] ICMET Craiova – Sisteme cu tunuri si microtunuri pneumatice – tip Big-Blaster, pentru rezolvarea problemelor de curgere a materialelor vrac/pulverunte, (Air cannon and Micro-cannon System Big-Blaster type for solving the problems of bulk/pulverulent material flow), Editia 2015;
[3] V. Cosoroba, Th. Demetrescu, Gh. Georgescu-Azuga, "Pneumatic drive" („Actionari pneumatice"), Ed. Tehnica, Bucuresti, 1971;
[4] http://www.vsr-industrietechnik.de/
[5] http://inwet.eu/en/flow-recovery-systems/air-blasters/
[6] E. Carafoli, V.N. Constantinescu, "Compressible fluid dynamics" („Dinamica fluidelor compresibile"), Ed. RSR, Bucuresti, 1984;
[7] J. Florea, V. Panaitescu, "Fluid Mechanics" („Mecanica Fluidelor"), Ed. Diactica si Pedagogica, Bucharest, 1979;
[8] J. Florea, Gh. Zidaru, V. Panaitescu, "Fluid Mechanics - Problems" („Mecanica Fluidelor - Probleme"), Ed. Diactica si Pedagogica, Bucuresti, 1979;
[9] http://www.ni.com/getting-started/labview-basics/environment.
[10] J. Jovitha, "Virtual Instrumentation Using Labview", PHI Learning, New Delhi, 2011;
[11] R. Bitter, T. Mohiuddin, M. Nawrocki, "LabVIEW: advanced programming techniques, Second Edition", CRC Press, 2006;
[12] N. Kehtarnavaz, P. Loizou, M. Rahman, "An Interactive Approach to Signals and Systems Laboratory", Connexions, Huston, 2011;
[13] http://www.ni.com/pdf/manuals/371303n.pdf
[14] D. Selisteanu, C. Ionete, E. Petre, "Virtual Instrumentation. Digital Signal Processing Applications," Ed. Universitaria, Craiova, 2012;
[15] M. Dobriceanu, "Transducers, interfaces and data acquisition", Ed. MATRIX ROM, București, 2010.

ISSN 1454 - 8003
Proceedings of 2017 International Conference on Hydraulics and Pneumatics - HERVEX
November 8-10, Băile Govora, Romania

REDUCING THE ENERGY CONSUMPTION IN THE HYDRAULIC CYLINDER ENDURANCE TEST

Teodor Costinel POPESCU[1], Radu Iulian RĂDOI[1], Mihai-Alexandru HRISTEA[1]

[1)]INOE 2000-IHP Bucharest; popescu.ihp@fluidas.ro

Abstract: *From inventorizing the tests and verifications to which the hydraulic cylinders are subjected, it is found that the endurance test, which establishes the normal service life, is very energy-consuming. This energy consumption is caused both by the duration of the test and the fact that it is carried out at rated power. Starting from stand diagrams for energy recovery in endurance tests on rotary positive displacement machines, existing in the literature, the authors of this paper develop a similar diagram, intended for endurance tests on hydraulic cylinders.*

Keywords: *Energy consumption, endurance, hydraulic cylinders*

1. Introduction

Tests on general use hydraulic cylinders must contain the following information: name, destination, symbolization and hydraulic diagram; values of the functional parameters listed in the Table 1; conditions for use in hydraulic diagrams; data on braking at the end of stroke (type, adjustment mode, etc.); conditions for mounting (position, fastening mode, etc.), connecting and commissioning; admissible non - coaxiality of the drive force against the geometric axis of the cylinder; content in dust, water and aggressive substances in the environment in which the cylinders can operate normally; maintenance conditions; type of functional characteristics to be determined; reliability indicators.

Table 1: Functional parameters of hydraulic cylinders

Item no.	Parameter name		Symbol	Measurement units	
				SI	Permissible
1.	Rated pressure		p_n	N/m^2	bar
2.	Main dimensions	Rated bore of the cylinder (piston or plunger diameter)	D	mm	
		Rod diameter	d	mm	
		Piston stoke	L	mm	
		Active surface ratio (for differential cylinders)	φ	-	
	Main dimensions of telescopic cylinders	Active diameters of the extension steps 1...n	$D_1...D_n$	mm	
		Active diameters of the retraction steps 1...n	$d_1...d_n$	mm	
		Strokes of the pistons 1...n	$L_1...L_n$	mm	
		Total cylinder stroke	L	mm	
3.	Rated force	thrust		N	
		tensile		N	
4.	Piston speed	minimum	v_{min}	m/s	
		maximum	v_{max}	m/s	
5.	Total efficiency	thrust	η=f(p) η=f(v)	- -	
		tensile	η=f(p) η=f(v)	- -	

Table 1: Functional parameters of hydraulic cylinders (continued)

Item no.	Parameter name		Symbol	Measurement units	
				SI	SI
6.	Working fluid	Fluid type			
		Minimum kinematic viscosity	v_{min}	mm^2/s	cSt
		Optimum kinematic viscosity	v_{opt}	mm^2/s	cSt
		Maximum kinematic viscosity	v_{max}	mm^2/s	cSt
		Minimum temperature	t_{min}	K	^0C
		Maximum temperature	t_{max}	K	^0C
7.	Ambient temperature	minimum	t_{min}	K	^0C
		maximum	t_{max}	K	^0C
8.	Cylinder mass (without working fluid)		m	kg	-

As part of the type, periodic and batch checks on hydraulic cylinders the tests indicated in the Table 2 shall be carried out.

Table 2: Tests and checks on hydraulic cylinders

Item no.	Technical condition to be verified		Checks		
			type	periodic	batch
1.	Appearance		x	x	x
2.	Dimensions of gauge and connection		x	x	x[1)]
3.	Functioning		x	x	x
4.	Quality of materials and dimensional checks on the main parts and subassemblies		x	x	-
5.	Cylinder mass (without working fluid)		x	x	-
6.	Pressure	minimum for piston displacement	x	x	x
		at the start	x	x	x
7.	Force	thrust	x	x	x
		tensile	x	x	x
8.	Piston speed	minimum	x	x	-
		maximum	x	x	-
9.	Tightness	internal	x	x	x
		external	x	x	x
10.	Braking at the end of stroke		x	x	-
11.	Pressure resistance		x	x	x[1)]
12.	Plotting the characteristic curves		x	x	-
13.	Functioning at cut-off temperatures		x	-	-
14.	***Functioning time (endurance)***		***x[2)]***	-	-
15.	Reliability		x	-	-

[1)] The check can be performed by sampling. The size of the sample lot and the acceptance conditions will be determined by the technical documentation.

[2)] 100000 cycles are performed, at rated power, then internal tightness is checked; no external leakage is allowed. The test is very energy-consuming. Stands with energy recovery are recommended.

2. Energy recovery in endurance tests on rotary positive displacement machines

During the endurance tests on rotary positive displacement machines energy consumption shall be reduced by simultaneous testing of two machines, hydraulically connected in a closed circuit, one operating as a pump and the other as a motor. The hydraulic power produced by the pump is re-used to drive the pump through the motor. Thus, the power supplied to the system must cover the difference between the power consumed by the pump and that supplied by the motor; this energy-saving process is called "recirculation of hydromechanical power" and it can be materialized with several types of diagrams, which differ by the power loss compensation mode.

2.1 Mechanical compensation of power losses by using one adjustable machine

In the case of mechanical compensation the energy source is an electromotor. If one of the machines under tests is adjustable, there is used the diagram in the Figure 1, characterized by the coupling of the two machines via the electric motor (np = nm = n).

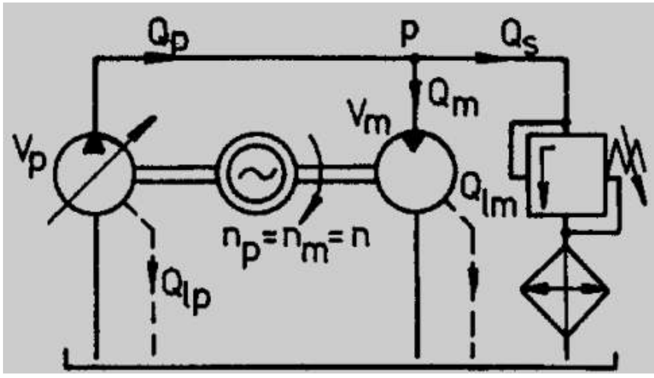

Fig. 1. Stand with mechanical compensation of power losses, an adjustable machine and a fixed machine

If the flow rate provided by pump, Q_p, is equal to the one used by motor, Q_m, pump discharge pressure, p, is practically null; as the pump capacity, V_p, increases relative to the motor capacity V_m, its discharge pressure increases to evacuate the excess flow through clearances and gaps. The normally closed valve limits the pressure p to the rated value specific to the tested machines.
The power supplied by electromotor, N_e, is the difference between the power absorbed by pump, N_p, and the one provided by motor, N_m:

$$N_e = N_p - N_m \tag{1}$$

Where

$$N_p = \frac{p \cdot Q_{tp}}{\eta_{tp}} = \frac{p \cdot n \cdot V_p}{\eta_{tp}} \tag{2}$$

and

$$N_m = p \cdot Q_{tm} \cdot \eta_{tm} = p \cdot V_m \cdot \eta_{tm} \tag{3}$$

It results:

$$N_e = p \cdot n \cdot V_m \left(\frac{V_p}{V_m} \cdot \frac{1}{\eta_{tp}} - \eta_{tm} \right) = N_{tm} \left(\frac{V_p}{V_m} \cdot \frac{1}{\eta_{tp}} - \eta_{tm} \right) \tag{4}$$

This power is minimal if the valve flow is null, so:

$$Q_p = n \cdot V_p \cdot \eta_{vp} = Q_m = \frac{n \cdot V_m}{\eta_{vm}} \tag{5}$$

It results:

$$\left(\frac{V_p}{V_m} \right)_{min} = \frac{1}{\eta_{vp} \cdot \eta_{vm}} \tag{6}$$

and

$$\left(\frac{N_e}{N_{tm}} \right)_{min} = \frac{1}{\eta_{tp} \cdot \eta_{vp} \cdot \eta_{vm}} - \eta_{tm} \tag{7}$$

For instance, for $\eta_{vp} = \eta_{vm} = 0.95$ and $\eta_{tp} \cong \eta_{tm} = 0.9$, it is required that $(V_p/V_m)_{min} \cong 1.1$ and $(N_e/N_{tm})_{min} \cong 0.33$.

$$\left(\frac{V_p}{V_m} \right)_{min} = \frac{1}{\eta_{vp} \cdot \eta_{vm}} = \frac{1}{0.95 \cdot 0.95} = 1.108$$

$$\left(\frac{N_e}{N_{tm}} \right)_{min} = \frac{1}{\eta_{tp} \cdot \eta_{vp} \cdot \eta_{vm}} - \eta_{tm} = \frac{1}{0.9 \cdot 0.95 \cdot 0.95} - 0.9 = 0.331$$

2.2 Mechanical compensation of power losses by using two fixed machines with equal capacities

If the machines have equal and constant capacity, $V_p = V_m = V$, the electromotor and the hydraulic motor must drive the pump through a speed multiplier with the transmission ratio $i = n_p / n_m > 1$ (Figure 2).

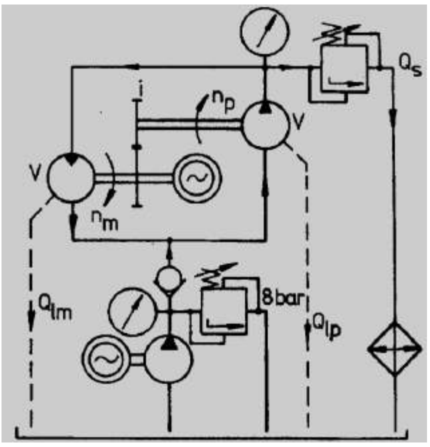

Fig. 2. Stand with mechanical compensation of power losses and two fixed machines

In this case
$$N_p = p \cdot i \cdot n_m \cdot \frac{V}{\eta_{tp}} \tag{8}$$

$$N_m = p \cdot n_m \cdot V \cdot \eta_{tm} \tag{9}$$

$$N_e = N_p - N_m = p \cdot n_m \cdot V \left(\frac{i}{\eta_{tp}} - \eta_{tm}\right) = N_{tm}\left(\frac{i}{\eta_{tp}} - \eta_{tm}\right) \tag{10}$$

So
$$\frac{N_e}{N_{tm}} = \frac{i}{\eta_{tp}} - \eta_{tm} \tag{11}$$

The flow discharged through the testing pressure control valve is calculated from the continuity equation:

$$Q_p = i \cdot n_m \cdot V \cdot \eta_{vp} = Q_m + Q_s = n_m \frac{V}{\eta_{vm}} + Q_s \tag{12}$$

So
$$Q_s = n_m \cdot V \left(i \cdot \eta_{vp} - \frac{1}{\eta_{vm}}\right) \tag{13}$$

Or
$$\frac{Q_s}{Q_{tm}} = i \cdot \eta_{vp} - \frac{1}{\eta_{vm}} \geq 0 \tag{14}$$

The minimum value of the transmission ratio is determined from the condition that the flow through the valve to be null ($Q_s = 0$):

$$i_{min} = \frac{1}{\eta_{vp} \cdot \eta_{vm}} > 1 \tag{15}$$

The minimum power provided by the electromotor is the same as the one in the previous case. If $i = 1.15$, $\eta_{tp} \cong \eta_{tm} = 0.9$ and $\eta_{vp} \cong \eta_{vm} = 0.95$, $Q_s / Q_{tm} = 0.04$ and $N_e / N_{tm} \cong 0.38$.

$$\frac{Q_s}{Q_{tm}} = i \cdot \eta_{vp} - \frac{1}{\eta_{vm}} = 1.15 \cdot 0.95 - \frac{1}{0.95} = 1.0925 - 1.0526 = 0.0399$$

$$\frac{N_e}{N_{tm}} = \frac{i}{\eta_{tp}} - \eta_{tm} = \frac{1.15}{0.9} - 0.9 = 0.377$$

2.3 Mechanical compensation of power losses by using an auxiliary pump

Hydraulic power loss compensation is performed by means of an auxiliary pump according to the diagram in Figure 3.

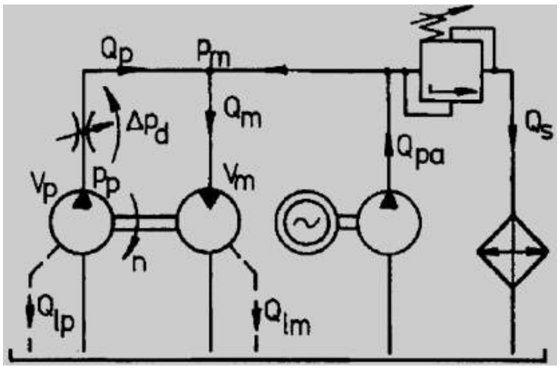

Fig. 3. Stand with hydraulic compensation of power losses

If the valve flow is null, from the continuity equation

$$Q_m = \frac{n_m \cdot V_m}{\eta_{vm}} = Q_p + Q_{pa} = n_m \cdot V_p \cdot \eta_{vp} + Q_{pa} \tag{16}$$

pump and motor speed result:

$$n_m \left(\frac{V_m}{\eta_{vm}} - V_p \cdot \eta_{vp} \right) = Q_{pa} \quad ; \qquad n_m = n_p = \frac{Q_{pa}}{\frac{V_m}{\eta_{vm}} - V_p \cdot \eta_{vp}} \tag{17}$$

Where Q_{pa} is the flow rate of the auxiliary pump.
From the system of equations

$$N_p = \frac{Q_p \cdot p_p}{\eta_{tp}} = N_m = Q_m \cdot p_m \cdot \eta_{tm} \tag{18}$$

$$p_p = p_m + \Delta p_d \tag{19}$$

one can deduce pressure drop on the motor, as a function of pressure drop across the throttle, Δp_d:

$$Q_p(p_m + \Delta p_d) = Q_m \cdot p_m \cdot \eta_{tm} \cdot \eta_{tp} \; ; \; p_m = \frac{\Delta p_d}{\frac{V_m}{V_p} \cdot \frac{\eta_{tp} \cdot \eta_{tm}}{\eta_{vm} \cdot \eta_{vp}} - 1} \tag{20}$$

The capacities of the tested machines are chosen or adjusted, so that

$$\frac{V_m}{V_p} \cdot \frac{\eta_{tp} \cdot \eta_{tm}}{\eta_{vm} \cdot \eta_{vp}} > 1 \tag{21}$$

so the motor capacity must always be higher than the pump capacity:

$$\frac{V_m}{V_p} > \frac{1}{\frac{\eta_{tp} \cdot \eta_{tm}}{\eta_{vm} \cdot \eta_{vp}}} > 1 \tag{22}$$

If the denominator of the equation (20) is very small, a low pressure drop across the throttle generates large test pressures.
The power consumed by the stand is equal to the power of the auxiliary pump:

$$N_{pa} = N_e = p_m \cdot Q_{pa} \cdot \frac{1}{\eta_{tpa}} = \frac{n_m \cdot \Delta p_d \left(\frac{V_m}{\eta_{vm}} - V_p \cdot \eta_{vp} \right)}{\eta_{tpa} \left(\frac{V_m}{V_p} \cdot \frac{\eta_{tp} \cdot \eta_{tm}}{\eta_{vm} \cdot \eta_{vp}} - 1 \right)} \tag{23}$$

For instance, if $V_m \cdot \eta_{tp} \cdot \eta_{tm} / V_p \cdot \eta_{vm} \cdot \eta_{vp} = 1.025$, it results $p_m = 40 \cdot \Delta p_d$.

$$p_m = \frac{\Delta p_d}{\frac{V_m}{V_p} \cdot \frac{\eta_{tp} \cdot \eta_{tm}}{\eta_{vm} \cdot \eta_{vp}} - 1} = \frac{\Delta p_d}{1{,}025 - 1} = \frac{\Delta p_d}{0{,}025} = 40 \Delta p_d$$

A pressure drop of *10bar* across the throttle results in a motor test pressure $p_m = 200\ bar$, and $p_p = 210\ bar$.

$$p_p = p_m + \Delta p_d = 200 + 20 = 220\ bar$$

Admitting that $\eta_{tp} = \eta_{tm} = 0.9$ and neglecting the volumetric efficiencies, it results $V_m / V_p \cong 1.265$.
If $V_p = 125\ cm^3/rev$, $V_m = 158.1\ cm^3/rev$; at $n = 1000\ rev/min$ and $\eta_{vp} \cong \eta_{vm} = 0.95$, the auxiliary pump must supply the flow rate $Q_{pa} = 0.795\ l/s$.

$$Q_{pa} = Q_m - Q_p = n\left(\frac{V_m}{\eta_{vm}} - V_p \cdot \eta_{vp}\right) = 1\,000 \cdot 10^{-3}\left(\frac{158.1}{0.95} - 125 \cdot 0.95\right) = 47.67 \frac{l}{min} = 0.7945 \frac{l}{s}$$

For $\eta_{tpa} \cong 0.9$, the auxiliary pump consumes the power $N_{pa} = 17.65\ kW$, while the theoretical power of the tested motor is $N_{tm} = 47.43\ kW$, so $N_e / N_{tm} = 17.65 / 47.43 = 0.37$.

$$N_{pa} = N_e = p_m \cdot Q_{pa} \cdot \frac{1}{\eta_{tpa}} = 200 \cdot 10^5 \cdot 0.7945 \cdot 10^{-3} \cdot \frac{1}{0.9} = 176.5 \cdot 10^2 W = 17.65\ kW$$

$$N_{tm} = Q_m \cdot p_m \cdot \eta_{tm} = \frac{Q_{pa}}{\frac{V_m}{\eta_{vm}} - V_p \cdot \eta_{vp}} \cdot \frac{V_m \cdot p_m \cdot \eta_{tm}}{\eta_{vm}}$$
$$= \frac{0.7945 \cdot 10^{-3}}{10^{-6}\left(\frac{158.1}{0.95} - 125 \cdot 0.95\right)} \cdot \frac{10^{-6} \cdot 158.1 \cdot 200 \cdot 10^5 \cdot 0.9}{0.95} = 47.43\ kW$$

3. Stand with energy recovery for endurance tests on hydraulic cylinders

As an extension of the stand with mechanical compensation of power losses (Figure 1), used at the simultaneous endurance testing of two rotary positive displacement machines (a pump and a motor), the power recirculation stand shown in Figure 4 is developed, for performing endurance tests, with energy saving, on hydraulic cylinders.

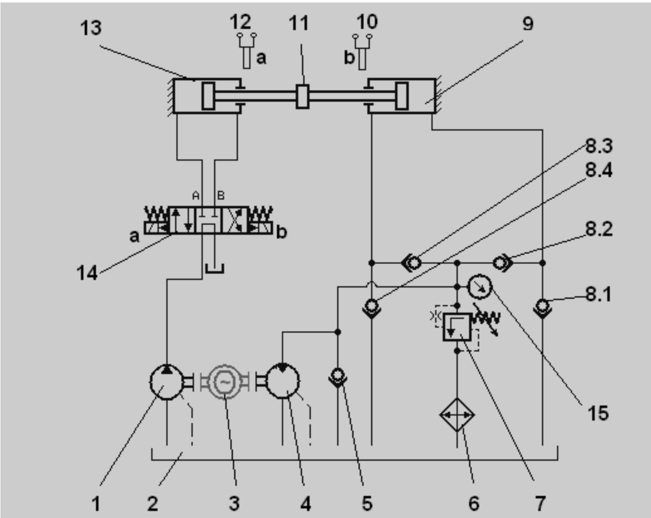

Fig. 4. Power recirculation stand for endurance tests on hydraulic cylinders

The stand in Figure 4 has the following advantages: it has a single pumping group for the test cylinder, and for the load cylinder the hydraulic oil supply is based on its operation in the pump mode; it has a single electrohydraulic directional valve for controlling the displacement of the two cylinders; it operates on the basis of "recirculation of hydromechanical power"; energy dissipation in heat is reduced, due to a much smaller flow discharged to the tank, through a single normally closed pressure valve; it requires small oil coolers.

The electromotor **3** of the stand has two drive heads, to which there are coupled a fixed positive displacement pump **1**, which absorbs from the oil tank **2**, and a fixed hydraulic motor **4**. The two hydraulic cylinders are identical; one of them is for testing **13**, the other is a load cylinder **9**. They have their rods fixed in the coupling **11** and they can move between two stroke limiters, namely towards the limiter **10**, when to electrically driven hydraulic directional valve **14** the electromagnet **a** is switched, and towards the limiter **12**, when to hydraulic directional valve the electromagnet **b** is switched. The check valve **5** allows hydraulic oil supply of the hydraulic motor from the tank in the non-actuated position of the hydraulic directional valve, and the check valves **8.4** and **8.2** allow, when the electromagnet **a** is switched, oil supply to the rod chamber of the load cylinder, and respectively oil discharge from the piston chamber of the load cylinder. The check valves **8.1** and **8.3** allow, when the electromagnet **b** is switched, oil supply to the piston chamber of the load cylinder, and respectively oil discharge from the rod chamber of the load cylinder. The stand is also equipped with a testing pressure control valve **7**, the pressure gauge **15**, which reads the adjusted pressure and the oil-water cooler **6**.

While the electromotor **3** is running and the directional control valve **14** is not actuated, the fixed pump is driven idle, the hydraulic cylinders **13** and **9** do not move, the hydraulic motor **4** is also driven by the electromotor and supplied through the check valve **5,** which opens.

The stand operates in two modes: **manual mode**, through which the hydraulic circuits are aerated / filled with oil and the test pressure is adjusted; **automatic mode**, through which the endurance test is performed at the set pressure.

In manual mode the electromagnets **a** and **b** are manually operated, and the testing pressure is adjusted by means of valve **7** and pressure gauge **15**.

In automatic mode the actuation of electromagnets **a** and **b** is made from the automation panel of the stand, depending on the signals received from the stroke limiters **10** and **12**, and the operation of the stand is as follows:

When the electromagnet **a** is switched on the spool valve of the hydraulic directional valve moves to the left position, the pump **2** sucks out of the tank and discharges in the chamber of the cylinder **13** piston, which expands its volume, and the cylinder **13** rod chamber collapses in volume, the oil being discharged through the directional valve to the tank. The effect of varying the volume of the two chambers is the displacement of the cylinder **13** rod to the right. The coupling **11** in this movement also drives the cylinder **9** rod. By displacement of this rod, the cylinder **9** rod chamber expands in volume and sucks oil out of the tank, through the check valve **8.4**, which opens, the cylinder **9** piston chamber collapses in volume and discharges oil through the check valve **8.2**, which opens, on two circuits: a larger part on the hydraulic motor **4** intake circuit, and a smaller part, equal to the difference between pump flow and motor flow, through the valve **7**.

When the electromagnet **b** is switched on the spool valve of the hydraulic directional valve moves to the right position, the pump **2** sucks out of the tank and discharges in the chamber of the cylinder **13** rod, which expands its volume, and the cylinder **13** piston chamber collapses in volume, the oil being discharged through the directional valve to the tank. The effect of varying the volume of the two chambers is the displacement of the cylinder **13** rod to the left. The coupling **11** in this movement also drives the cylinder **9** rod. By displacement of this rod, the cylinder **9** piston chamber expands in volume and sucks oil out of the tank, through the check valve **8.1**, which opens, the cylinder **9** rod chamber collapses in volume and discharges oil through the check valve **8.3**, which opens, on two circuits: a larger part on the hydraulic motor **4** intake circuit, and a smaller part, equal to the difference between pump flow and motor flow, through the valve **7**.

To avoid cavitational wear of the load cylinder it is recommended either to overfill it or that the oil tank be mounted above the hydraulic cylinders.

Conclusions

Two rotary positive displacement machines, a pump and a motor can be subjected to endurance tests at the same time, in advantageous conditions in terms of power consumption, by using three methods:

a) Mechanical compensation of power losses, based on the coupling of the drive axles of the two positive displacement machines, via a two-axis electromotor or an electromotor with a drive shaft and 1:1 ratio gear transmission. In this case the rotative speeds of the two machines are equal ($n_p = n_m$), and the geometric volume of the pump is higher than that of the hydraulic motor ($V_p>V_m$);

b) Mechanical compensation of power losses, based on the coupling of the drive axles of the two positive displacement machines, via an $i = n_p / n_m>1$ ratio gear transmission. In this case the geometric volumes of the two machines are equal ($V_p=V_m$), and the pump speed is higher than the motor speed $n_p>n_m$;

c) Hydraulic compensation of power losses by using an auxiliary pump. In this case the rotative speeds of the two cars are equal ($n_p = n_m$), and the geometric volume of the hydraulic motor is greater than that of the pump ($V_m>V_p$).

In the *a)* and *b)* cases the power supplied by the electromotor represents the difference between the power absorbed by the pump and that supplied by the hydraulic motor, and in the *c)* case the power supplied by the electromotor is equal to the power consumed by the auxiliary pump.
The *a)* case for conducting endurance tests on rotary positive displacement machines can be extended to endurance tests on hydraulic cylinders, with the stand illustrated in the figure 4.

Acknowledgments

This paper has been developed in INOE 2000-IHP, with the financial support of the Executive Agency for Higher Education, Research, Development and Innovation Funding (UEFISCDI), under PN III, Programme 2-Increasing the competitiveness of the Romanian economy through research, development and innovation, Subprogramme 2.1- Competitiveness through Research, Development and Innovation - Innovation Cheques, project title: “Power recirculation stand for testing hydraulic cylinders”, Financial Agreement no. 50 CI/2017.

References

[1] N. Vasiliu, D. Vasiliu, “Fluid Power Systems“ („Acţionări hidraulice şi pneumatice”), Vol.I,Technical Publishing House, Bucharest, 2005, ISBN: 973-31-2248-3;

[2] T.C. Popescu, P. Drumea, D.D. Ion Guta, I. Balan, “Power recirculation stand for endurance tests on hydraulic cylinders” (“Stand cu recirculare de putere pentru anduranța cilindrilor hidraulici”), Patent No. 127042/30.09.2016.

ISSN 1454 - 8003
Proceedings of 2017 International Conference on Hydraulics and Pneumatics - HERVEX
November 8-10, Băile Govora, Romania

MECHANICAL COMPENSATION OF POWER LOSS IN THE ENDURANCE TESTS ON ROTARY AND LINEAR POSITIVE DISPLACEMENT MACHINES

Teodor Costinel POPESCU[1], Radu Iulian RĂDOI[1], Mihai-Alexandru HRISTEA[1]

1)INOE 2000-IHP Bucharest; popescu.ihp@fluidas.ro

Abstract: *Through experimental tests and numerical simulations the authors of this paper demonstrate a method of reducing energy consumption on the endurance stands of rotary and linear positive displacement machines. The method is based on mechanical compensation of power losses, achieved by coupling the drive shafts of two positive displacement machines, a pump and a rotary motor, with pump capacity greater than motor capacity and equal rotary speeds. The method can be applied in the simultaneous endurance tests on the two rotary positive displacement machines, and by extension, on the endurance test stands designed for hydraulic cylinders.*

Keywords: *Mechanical compensation of power loss, endurance, rotary and linear positive displacement machines*

1. Introduction

Mechanical compensation of power losses [1] can be done on the power recirculation stand in the Figure 1, used for endurance tests on rotary positive displacement machines, and also on the power recirculation stand in the Figure 2, used for endurance tests on linear positive displacement machines.

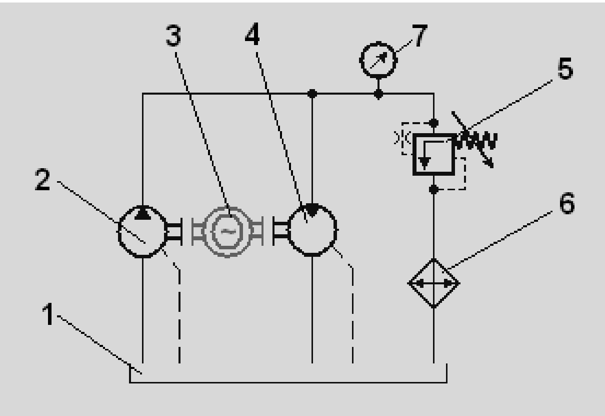

Fig. 1. Power recirculation at endurance tests on rotary positive displacement machines: **1**=tank; **2**=fixed pump; **3**= two-axis electromotor; **4**=hydraulic motor; **5**= pressure control valve; **6**= return filter; **7**=pressure gauge

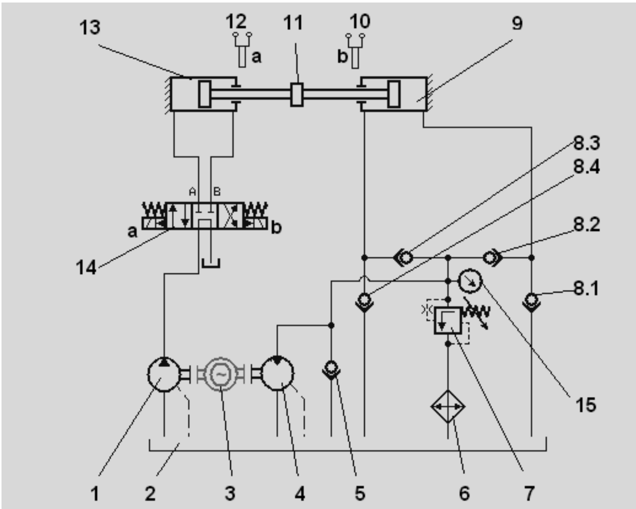

Fig. 2. Power recirculation at endurance tests on linear positive displacement machines

The tank, pump, electromotor, hydraulic motor, control valve, filter and pressure gauge which make up the stand in the Figure 1 can also be found in the structure of the stand in the Figure 2. For both stands the capacity of the pump is higher than the capacity of the hydraulic motor, and the rotary speeds are equal.
In addition, the stand in the Figure 1 also contains the following parts [2]: **5**= non-return valve for supplying the hydraulic motor in the "non-actuated" position of the hydraulic directional valve with electrical control **14**; **8.1**, **8.2**, **8.3**, **8.4**= non-return valves for supplying / discharging the chambers of the load cylinder **9**; **10**, **12**=stroke limiters; **11**=coupling; **13**=test cylinder.

For the stand in the Figure 1 a demonstrative experimental module has been developed in order to promote the method of compensation for power losses at the stands for endurance tests, with low energy consumption, of rotary and linear positive displacement machines.

2. Experimental determinations of recovered energy in endurance tests on positive displacement machines

2.1. The demonstrative experimental module

The hydraulic basic diagram of a small demonstrative stand is shown in the Figure 3 and it comprises: a fixed positive displacement pump with a capacity of 6 cm^3/rev (**2**) and a fixed positive displacement motor (**3**), with a capacity of 4 cm^3/rev, both coupled to an electric motor (**1**), of 0.37 kW, with a constant rotary speed of 1375 rev/min; a pressure control valve (**4**); a 4/3 hydraulic directional valve, with electric control (**5**), a pressure gauge (**6**) and an oil tank (**7**).
Physical development of the experimental demonstrative module, which in order to couple the electromotor to the pump and hydraulic motor axes uses a gear transmission, with 1:1 transmission ratio, is shown in the Figure 4.

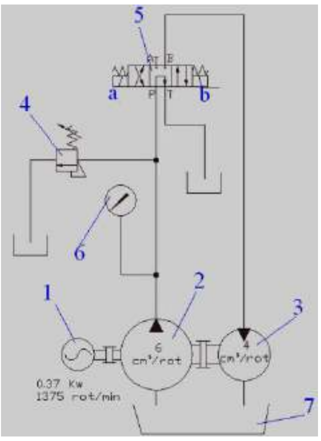

Fig. 3. Hydraulic diagram of the experimental demonstrative module

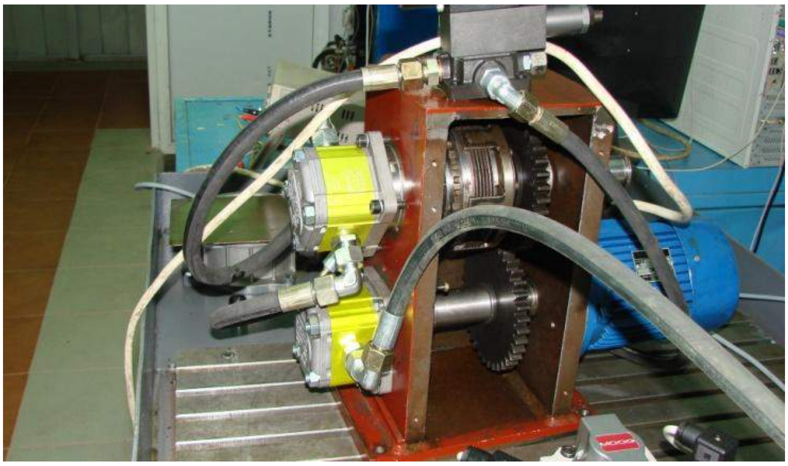

Fig. 4. Physical development of the experimental demonstrative module

In order to test the energy recovery system only the extreme switch positions of the sliding valve of the 4/3 hydraulic directional control valve are used (excluding the center position).
When the electromagnet “b” of the directional control valve is actuated, there is achieved the distribution “P” to “A” (a plug was fitted on “A”) and “B” to “T”, the entire flow of the pump is discharged through the valve to the oil tank, the hydraulic motor feeds from the tank, being driven at the same time with the pump by the electric motor, but it does not generate a mechanical torque and does not “help” the electric motor which drives the two positive displacement machines.
When the electromagnet “a” of the directional control valve is actuated, there is achieved the distribution “P” to “B” and “A” to “T”, (the plug remains fitted on “A”). The discharged flow of the pump is divided into: 5.5l/min, entering the hydraulic motor, and 2.75l/min, conveyed through the pressure control valve. The hydraulic motor is supplied by the pump and it is driven, simultaneously with the pump, by the electromotor. In this situation the hydraulic motor contributes to the production of part of the mechanical torque required to actuate the positive displacement pump.

2.2. Experimental results

By using the test stand shown in the Figure 4 there have been measured: pump discharge pressure - *p (bar)*; single phase electric current absorbed by the motor - *I (A)* and electric motor speed - $n_{me}=n_p=n$ *(rev/min)*.

To plot the experimental characteristics there have been calculated: hydraulic power generated by the pump - P_h *(W)*; power absorbed by the electric motor - P_a *(W)*; power output generated by the electric motor - P_u *(W)* and mechanical power generated by the hydraulic motor - P_{mh} *(W).*

The following equations have been used:

$$P_h = \frac{V_p \cdot n_p \cdot p}{\eta_p \cdot 612} \tag{1}$$

where: P_h – hydraulic power (*W*); V_p - pump capacity (*cm³/rev*); n_p – pump speed, which is equal to hydraulic motor speed n_{mh} (*rev/min*); *p* – pump discharge pressure (*bar*); η_p – total pump efficiency (-); 612 – dimensionless factor (-).

$$P_a = 3U \cdot I \cdot \cos^{\varphi} \tag{2}$$

where: P_a – power absorbed by the electric motor (*W*); *U* – phase voltage (*V*); *I* – electric current intensity (*A*); $\cos^{\varphi} = 0.71$.

$$P_u = P_a \cdot \eta_{me} \tag{3}$$

where: P_u – power output generated by the electric motor (*W*); η_{me}– electric motor efficiency (-).

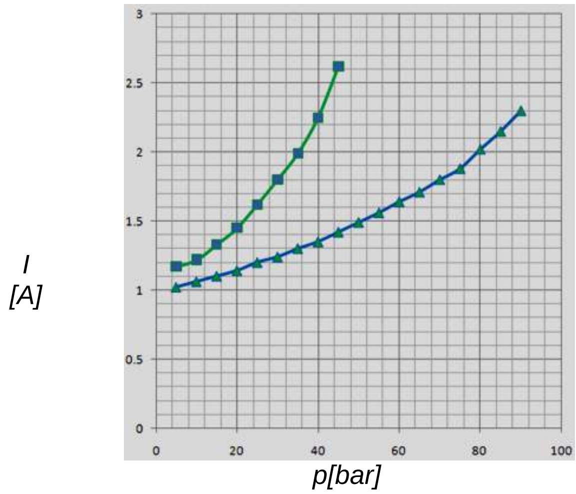

Fig. 5. The I=f(p) characteristic
Series 1: P to A; Series 2: P to B

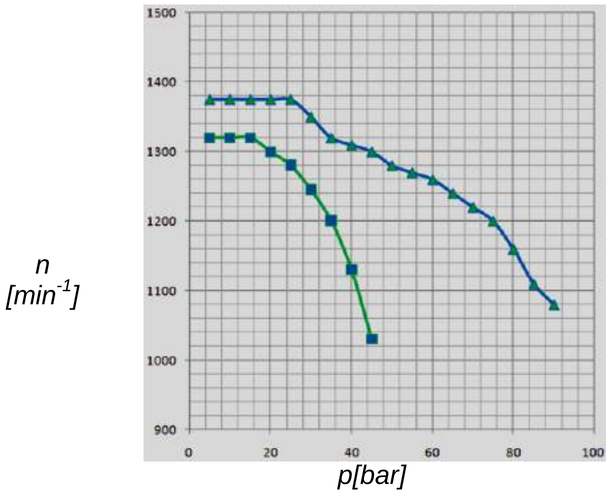

Fig. 6. The n=f(p) characteristic
Series 1: P to A; Series 2: P to B

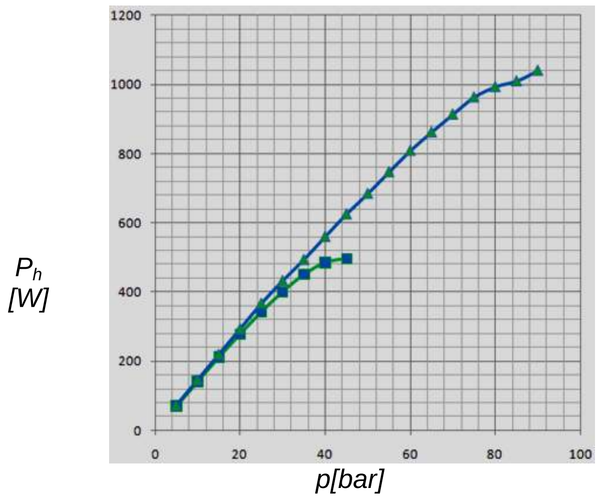

Fig. 7. The P_h=f(p) characteristic
Series 1: P to A; Series 2: P to B

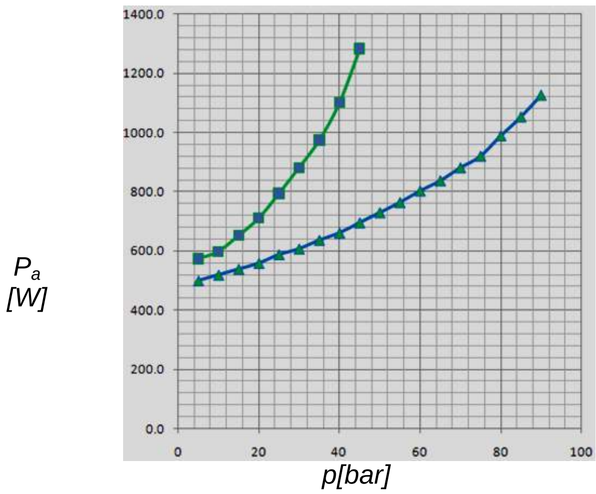

Fig. 8. The P_a=f(p) characteristic
Series 1: P to A; Series 2: P to B

$$P_{mh} = \frac{V_{mh} \cdot n_{mh} \cdot p \cdot \eta_{mh}}{612} \quad (4)$$

where: P_h – hydraulic power (*W*); V_{mh} - hydraulic motor capacity (*cm³/rev*); n_{mh} – hydraulic motor speed n_{mh} (*rev/min*); *p* – hydraulic motor intake pressure (*bar*); η_{mh} – total hydraulic motor efficiency (-); 612 – dimensionless factor (-).

The figures 5...8 depict four characteristics determined experimentally, namely: variation of the current absorbed by the electric motor *I [A]* (Fig. 5), variation of electric motor speed *n[rev/min]* (Fig. 6), variation of hydraulic power generated by the pump P_h *[W]* (Fig. 7), variation of power absorbed by the electric motor P_a *[W]* (Fig. 8), all depending on pump discharge pressure *p[bar]*.

2. Numerical simulations on energy recovery in endurance tests on positive displacement machines

2.1. Simulation model in AMESim

To study the dynamics of the energy recovery experimental demonstrative module the simulation model in AMESim [3] shown in Figure 9 has been used.

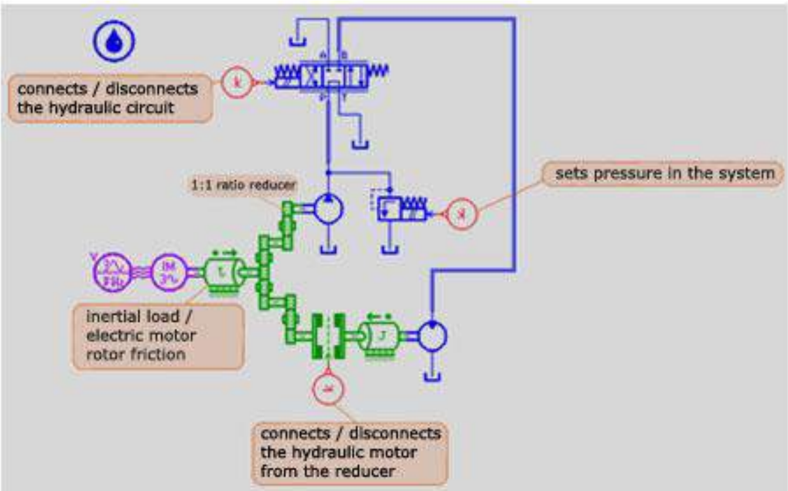

Fig. 9. Simulation model in AMESim

The AMESim model includes an inductive electric motor, to which a load has been introduced to simulate the inertial torque of the rotor and friction in the electric machine. To simulate system operation, in versions with and without energy recovery, a friction coupling has been introduced, which can be opened or closed, depending on the value of the excitation signal (0, and respectively 1).

For the hydraulic motor there is also the possibility of changing the load value, by changing the parameters of the inertial mass attached to its shaft.

Connecting and disconnecting the hydraulic circuit of the rotary positive displacement motor is carried out via the hydraulic directional control valve, and pressure in the system is set through the valve.

The two operating modes of the system are: with the hydraulic motor connected (with energy recovery) and with the hydraulic motor disconnected (without energy recovery).

In "connected" operating mode the signal "1" is sent to the coupling and the normally closed valve is set to the value of *30 bar*.

In "disconnected" operating mode the excitation signal of the coupling is set to the value "0", to interrupt the mechanical connection between the electric motor and the hydraulic motor. The pressure in the system is then increased so that to the hydraulic motor shaft there is obtained the same rotational speed as for the "connected" hydraulic motor. Thus it is possible to compare the torques to the electric motor shaft, in the two operating modes, under the same loading conditions for the consuming positive displacement machines.

2.2. Results of numerical simulations

In the graph depicted by the Figure 10 one can notice that the torque of the electric motor drops after the hydraulic motor speed becomes equal to the electric motor speed (lag of 0.1 s).

Electric motor torque [Nm]

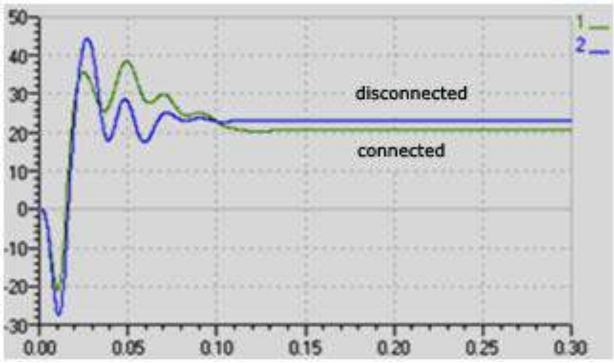

Time [s]

Fig. 10. Variation over time of electric motor (EM) torque, disconnected (1) / connected (2) from / to the hydraulic motor

In the graph depicted by the Figure 11 one can notice that the torque to the shaft attached to the reducer drops after the hydraulic motor speed becomes equal to to the electric motor speed (lag of 0.1 s).

Transmission shaft torque [Nm]

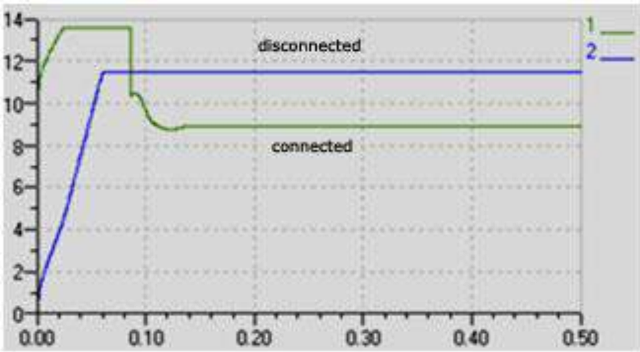

Time [s]

Fig. 11. Variation over time of torque to the reducer shaft; the EM disconnected (1) / connected (2) from / to the HM

In the graph depicted by the Figure 12 one can identify the time after which the hydraulic motor speed is equal to the electric motor speed (0.1 s - "connected", and respectively 0.4 s - "disconnected" from /to the electric motor).

Hydraulic motor speed [x 10^3 rpm]

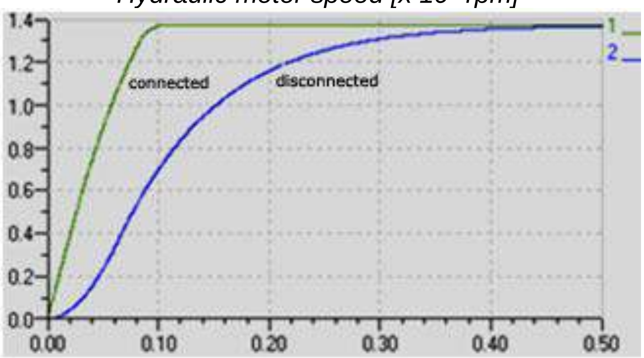

Time [s]

Fig. 12. Variation over time of hydraulic motor (HM) speed; disconnected (1) / connected (2) from / to the HM

In the Figure 13 one can notice the variation in flow through the pump, hydraulic motor and normally closed valve.

Flow in the pump-valve-hydraulic motor node [l/min]

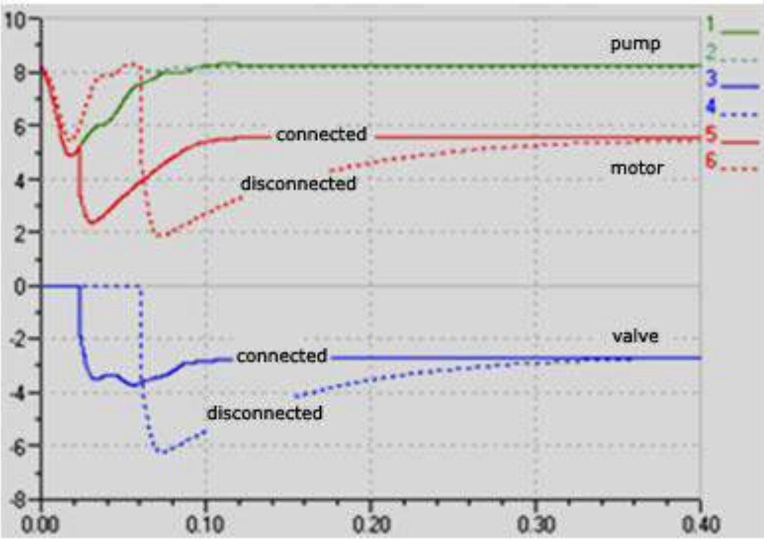

Time [s]

Fig. 13. Flow variation in the pump (1,2)–valve (3,4)-hydraulic motor (5,6) node

In the Figure 14 one can notice pressure variation in the pump-valve-directional control valve node.

Pressure in the pump-valve-directional control valve node [bar]

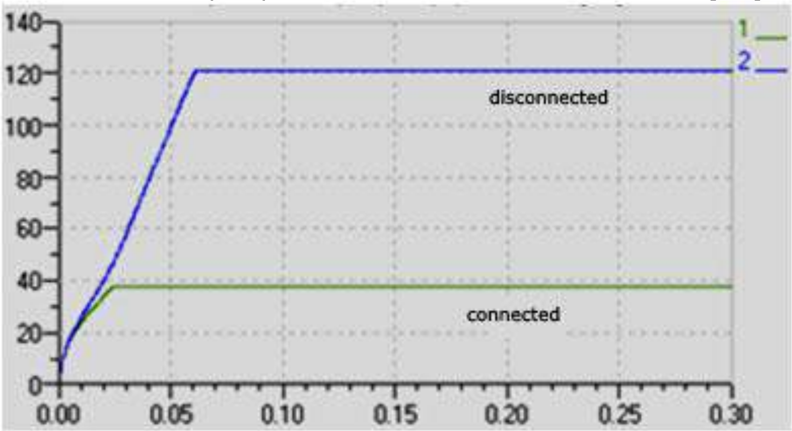

Time [s]

Fig. 14. Pressure variation in the pump-valve-directional control valve node; the EM disconnected (1) / connected (2) from / to the HM

Conclusions

Experimental tests performed on the demonstrative module shown in Fig. 4 have demonstrated the efficiency of energy recovery, based on mechanical compensation of power losses, namely:

- powering of the hydraulic motor coupled to the electric motor results in the doubling of the pressure produced by the demonstrative stand, for the same current absorbed by the electric motor. For instance, for *I=2A,* there results *p=36 bar,* when the hydraulic motor is not powered by the pump, and respectively *p=80 bar,* when the hydraulic motor is powered by the pump (Fig. 5);

- powering of the hydraulic motor coupled to the electric motor results in the doubling of the pressure produced by the demonstrative stand, for the same speed of the electric motor. For instance, for *n=1300 rpm,* there results *p=20 bar,* when the hydraulic motor is not powered by the pump, and respectively *p=40 bar,* when the hydraulic motor is powered by the pump (Fig. 6);
- pump maximum hydraulic power and maximum pressure produced by the stand are: $P_h=480\ W;\ p=48\ bar$, when the hydraulic motor is not powered, and respectively $P_h=1040W;\ p=90\ bar,$ when the hydraulic motor is powered (Fig. 7);
- powering of the hydraulic motor coupled to the electric motor results in the doubling of the pressure produced by the demonstrative stand, for the same power absorbed by the electric motor. For instance, for $P_a=800\ W,$ there results *p=25 bar,* when the hydraulic motor is not powered by the pump, and respectively *p=60 bar,* p when the hydraulic motor is powered by the pump (Fig. 8).

Numerical simulations performed on the AMESim model shown in Fig. 9 have demonstrated the dynamic performance of the energy recovery system based on mechanical compensation of power losses, namely:

- connecting of the hydraulic motor to the shaft of the reducer (with *1:1* transmission ratio) results in lower torque developed by the electric motor, following a lag of *0.1 s* (Fig. 10);
- connecting of the hydraulic motor to the shaft of the reducer results in lower torque developed by the electric motor, after the moment when the speeds of the two motors become equal, with a lag of *0.1s* (Fig. 11);
- the time in which the hydraulic motor speed equals the electric motor speed is of *0.1 s*, when the hydraulic motor is connected to the electric motor, and respectively *0.4 s*, when the hydraulic motor is disconnected from the electric motor (Fig. 12);
- after *0.3 s* from connecting the hydraulic motor to the electric motor pump flow is equal to the sum of flow through the hydraulic motor and flow through the pressure control valve (Fig. 13);
- speed achieved by the hydraulic motor at a pressure of *40 bar* when it is mechanically connected to the electric motor is equal to hydraulic motor speed at a pressure of *120 bar* when it is mechanically disconnected from the electric motor (Fig. 14).

All the conclusions listed, demonstrating the benefits of energy recovery by mechanical compensation for power losses, have applicability to the endurance stands of rotary and linear positive displacement machines (pumps, hydraulic motors, hydraulic cylinders).

Acknowledgments

This paper has been developed in INOE 2000-IHP, with the financial support of the Executive Agency for Higher Education, Research, Development and Innovation Funding (UEFISCDI), under PN III, Programme 2-Increasing the competitiveness of the Romanian economy through research, development and innovation, Subprogramme 2.1- Competitiveness through Research, Development and Innovation - Innovation Cheques, project title: “Power recirculation stand for testing hydraulic cylinders”, Financial Agreement no. 50 CI/2017.

References

[1] N. Vasiliu, D. Vasiliu, “Fluid Power Systems“ („Acţionări hidraulice şi pneumatice”), Vol. I, Technical Publishing House, Bucharest, 2005, ISBN: 973-31-2248-3;
[2] T.C. Popescu, P. Drumea, D.D. Ion Guta, I. Balan, “Power recirculation stand for endurance tests on hydraulic cylinders” (“Stand cu recirculare de putere pentru anduranța cilindrilor hidraulici”), Patent No. 127042/30.09.2016;
[3] *AMESim* Software Suit.

ISSN 1454 - 8003
Proceedings of 2017 International Conference on Hydraulics and Pneumatics - HERVEX
November 8-10, Băile Govora, Romania

APPLICATION SOFTWARE FOR REACTOR SIZING CALCULATION

Claudiu-Ionel NICOLA[1], Marcel NICOLA[1], Ion PĂTRU[1],
Maria Cristina NIȚU[1], Viorica VOICU[1], Sebastian POPESCU[1]

[1]National Institute for Research, Development and Testing in Electrical Engineering – ICMET Craiova
nicolaclaudiu@icmet.ro, marcel_nicola@yahoo.com, ipatru@icmet.ro, cristinanitu@icmet.ro
programe@icmet.ro, tn.popescu@icmet.ro

Abstract: *One of the primary goals of computer science, as interdisciplinary science is to develop methods for solving complicated research and computing problems by means of computational techniques. Currently, however, computer science has become an independent science, with its own methods and objects of research, which are based on mathematical regularities. Computer tools allow the problems to be solved both by analytical methods and simulation methods. Regardless of the method used, the solving of any problem includes several steps such as problem analysis, elaboration of the mathematical model of the problem and elaboration of the algorithm which enables the development of the application software. The paper presents a software application based on the LabVIEW programming environment which implements the mathematical model on calculating the size of reactors. The software is modular with a user friendly interface and presents the general advantages of modern software*.

Keywords*: reactors, mathematical model, sizing, application software, LabVIEW*

1. Introduction

One of the primary goals of computer science, as interdisciplinary science is to develop methods for solving complicated research and computing problems by means of computational techniques. Originally, computer science was developed as a branch of applied mathematics. The first issues addressed in the context of computer science were purely mathematical, and were solved by only carrying out a great amount of complex calculations. Currently, however, computer science has become an independent science, with its own methods and objects of research, which are based on mathematical regularities [1].
There are a considerable amount of software packages, (EPLAN, OrCAD, PSpice, AUTOCAD, CATIA, MathCAD, LabVIEW, MATLAB, SIMULINK), for the various types of CAD/CAM systems. Each package has its own capacity and particularity and is generally intended for certain markets and a specific group of users. For example, there is mechanical, electrical and architectural, CAD/CAM software, for users in the respective fields [2-10].
Computer tools allow the problems to be solved both by analytical methods and simulation methods. Regardless of the method used, the solving of any problem includes several steps, each of them with the same importance [11].

- *Problem analysis*. This is the stage of researching the content of the problem: determining the set of initial data, the result to be achieved, the relations between the original data and the results. Additional restrictions on the data and results are also set during this stage.
- *Elaboration of the mathematical model of the problem*. The initial data are represented by mathematical structures during this stage. The relations allowing the result to be obtained from the original data are defined using the mathematical language. Depending on the problem, these relations can be recurrent (creating a simulation model) or they can allow direct calculation of the result (analytical model). Also during this stage the problem is divided (if necessary) into sub-problems, and the mathematical models are elaborated separately for each of them.
- *Elaboration of the algorithm*. In the case of problem solving by means of computational techniques, the algorithm contains the set of instructions necessary for solving the problem, defined by a default form (pseudocode, flowchart, etc.), as well as the sequence of their

execution (the steps of the algorithm). If the problem was divided into sub-problems, in addition to defining sub-algorithms, the algorithm also determines the method and conditions of their call.

As a result of carrying out these steps the software application is implemented, solving the problems related to the sizing of the reactors. Further on, the article presents in Chapter 2 the general information relating to the mathematical simulation of reactors, and in Chapter 3 the proposed software implementation solution for calculating the size of reactors. Chapter 4 presents a practical example of using the developed software, and the conclusions and ideas for subsequent developments are presented in Chapter 5.

2. Reactors. Mathematical modeling

Reactors are used for: balancing the reactive - capacitive power in electrical networks, limiting short-circuit currents in the power system or limiting the operate current in induction motors, filtering harmonics from AC curves or DC smoothing in rectifier power grids, protection of electrical networks against earth faults, protection of high-voltage lines against surges.

The concept of reactors or inductors is assigned to the elements of an electric circuit or of a power system which under electromagnetic quasi-stationary conditions are considered as having only one inductance, i.e. an inductance reactance.

Their introduction into the power system is aimed at generating a voltage drop when an alternating current or a current varying in time passes through it, i.e. achieving an exchange of reactive power to the system [12].

The AC voltage drop generated by the reactor, assuming that the winding resistance is neglected and under quasi-stationary conditions is denoted by the relation:

$$U_b = 2\pi \cdot f \cdot L \cdot I \tag{1}$$

The voltage drop is proportional to virtual current *I* and frequency *f*, if it is assumed that the inductance L of the coil is constant.

The reactive power of the coil is:

$$Q = \frac{U_b^2}{2\pi \cdot f \cdot L} \tag{2}$$

The stages of the reactor sizing:

- *calculation of reactor pre-sizing*

Determination of the inductance of the solenoid:

$$L = \mu_0 \cdot w^2 \cdot \frac{\pi \cdot d_m^2}{4} \cdot \frac{1}{h} \cdot k_L \, [H] \tag{3}$$

where:

- $\mu_0 = 4\pi \cdot 10^{-7}$ [H / m], the vacuum permeability;
- w – the number of turns which fill the entire space of the winding;
- $d_m = ½ (d_E + d_i)$ [m] – average diameter of the winding;
- d_E [m] – outer diameter of the winding;
- d_i [m] – inner diameter of the winding;
- h [m] – height of the coil (size in the axial direction of the winding);
- k_L - a coefficient which depends on the geometry of the winding and is specified in nomograms from [12, 13] according to ratios: h/d_m and b/d_m;
- $b = ½ (d_E - d_i)$ [m] – is the thickness of the winding (size in radial direction).

Given the horizontal size of the uninsulated conductor *no*, vertical size of the uninsulated conductor *nv* and the thickness of the insulation Δ_{iz} summed for both sides of the conductor, the following parameters can be determined:

- horizontal size of the insulated conductor – ino;

$$\text{ino} = \text{no} + \Delta\text{iz}[\text{mm}] \tag{4}$$

- vertical size of the insulated conductor – inv;

$$\text{inv} = \text{nv} + \Delta\text{iz}[\text{mm}] \tag{5}$$

Determining the number of turns on the flat coil "n" by the formula:

$$\text{n} = \frac{\text{b}}{\text{no} + \Delta_{\text{iz}}}[\text{turns/flat}] \tag{6}$$

Determining the number of flat coils *Ng* by the formula:

$$\text{Ng} = \frac{\Delta\text{R}^2 + \text{kv} \cdot \Delta\text{R}}{\Delta\text{R1} \cdot (\text{inv} + \text{kv})}[\text{flat}] \tag{7}$$

where *ΔR* is the thickness of the reactor and *ΔR1* is the thickness of the winding.
Determining the inductance of the equivalent coil Lc is based on the formula:

$$\text{Lc} = \left(\text{N} \cdot \frac{\text{ino} \cdot \text{inv}}{\text{g}^2}\right)^2 \cdot \left(1 + \frac{\text{ko1} \cdot \text{kv}}{\text{ino} \cdot \text{inv}} + \frac{\text{kv}}{\text{inv}} + \frac{\text{ko1}}{\text{ino}}\right)^2 \cdot \text{Ln}[\text{H}] \tag{8}$$

where:

- N – the number of paralleled conductors;
- kv – distance between vertical flat coils;
- g – section of elementary turns;
- ko – width of cooling ducts;
- ko1 = Δ_{iz} +ko/n;
- L_n – inductance of the coil to which an increase is applied.

➢ *heat exchange*

The heat exchange [14] by radiation plays a greater part in cooling the windings of dry reactors compared to a winding located in an oil tank. The amount of heat radiated per unit time by the unit area is denoted by the relationship [15]:

$$\text{grad} = 5{,}15 \cdot 10^{-12} \cdot (\text{T}^4 - \text{T}_{\text{amb}}^4) \tag{9}$$

where T is the absolute temperature of the winding surface, and T_{amb} is the absolute ambient temperature (both expressed in Kelvin).
In simplified form, the calculation of the quantity of heat transmitted by convection by the unit surface per unit time is denoted by the formula:

$$q_{\text{con}} = \alpha_{\text{con}} \cdot (t - t_{\text{amb}}) \tag{10}$$

where t and t_{amb} are the temperature of the cooled surface and the ambient temperature, in °C and αcon is the convection efficiency.
The following analytical expression of the function α_{con} =f (h_{bob}, Δ, ϑ) will result from the

combination of the previous relations:

$$\alpha_{con} = \sqrt[4]{\frac{4 \cdot \vartheta}{h_{bob}}} \tag{11}$$

where the values of the quantities are expressed as : ϑ [°C], h_{bob}. [m]. and Δ [cm].

- *the permissible current density in the windings*

The permissible current densities, calculated according to the relation (12) combined with (11) with radial thickness b = 0,010; 0,015; 0,020; 0,025 and 0,030 m, for copper cylindrical windings with class insulation A (c_i = 115,7; ϑ = 60°C), F (c_i = 130,5; ϑ = 100°C) and H (c_i = 139,7033; ϑ = 125°C), and for aluminum cylindrical windings with class insulation A (c_i = 183,2; ϑ = 60°C), F (c_i = 205,74; ϑ = 100°C) and H (c_i = 219,834; ϑ = 125°C).

$$j = \sqrt{\frac{\vartheta \cdot \alpha_{con}}{c_i \cdot 10^{-10} \cdot k_S \cdot b}} \tag{12}$$

- *calculation of losses under stationary regime*

The determination of losses under rated load is based on the relation:

$$P = k_S \cdot R_{\Omega\theta} \cdot I^2 = k_S \cdot \rho_{20} \cdot [1 + \alpha \cdot (\theta - 20)] \cdot \frac{M}{\gamma} \cdot j^2 [\text{Watt}] \tag{13}$$

where:

- k_s – coefficient of additional losses;
- ρ_{20} – resistivity of the material at 20°C: for copper $\rho_{20} = 1/58 \cdot 10^{-6}$ [Ω·m] and for aluminum $\rho_{20} = 1 / 36,2 \cdot 10^{-6}$ [Ω·m];
- α – temperature coefficient of electrical resistance for copper $\alpha = 428 \cdot 10^{-5}$ [1/°C], and for aluminum $\alpha = 408 \cdot 10^{-5}$ [1/°C];
- θ – reference temperature: for insulation classes A, E and B: θ = 75°C and for insulation classes F and H: θ = 115°C;
- M – mass of active winding conductor [kg];
- γ – material density $\gamma = 8,9 \cdot 10^3$ [kg/m^3];
- j – current density.

- *short-time rated current operation*

The operation of the reactor under short-time rated current I_{sc} is adequate if the following inequality is met:

$$T1 \leq T2 \tag{14}$$

$$T1 = \theta + a + j_{SC}^2 \cdot t \cdot 10^{-3} [^\circ C] \tag{15}$$

where:

- T1 is the temperature rating determined by calculation;
- T2 is the standard rating of the maximum permissible average temperature [17].
- θ [°C] – maximum admissible initial temperature a rated winding according to insulation class;
- a – coefficient given in the table [12], according to parameter ½ (θ + T_2);
- j_{sc} – the short-term nominal current density;
- t – the duration of the short-term nominal current in seconds according to international standards.

3. Application software for reactor sizing calculation

A development environment is a set of programs allowing the programmer to write programs and combines all the steps necessary for creating a program, such as source code editing, documentation compiling, debugging, testing and generating, in a single application software, which typically provides a user-friendly graphical interface.
The main elements of a development environment are the source code editor and the debugger. The development environments call on compilers or parsers, which can be provided in the same package as the environment itself, or can be installed separately by the programmer. The facilities present in more sophisticated development environments include: source code scanners, version control systems, graphical interface designers, or software engineering tools.
LabVIEW is a graphical programming language that uses icons instead of lines of text to create applications. In contrast to text-based programming languages, where instructions determine the program execution, LabVIEW uses dataflow programming, where the flow of data determines the execution [18].
The programming language used in LabVIEW, also referred to as G, is a dataflow programming language. Execution is determined by the structure of a graphical block diagram on which the programmer connects different function-nodes by drawing wires. These wires propagate variables and any node can execute as soon as all its input data become available. Since this might be the case for multiple nodes simultaneously, G is inherently capable of parallel execution. Multi-processing and multi-threading hardware is automatically exploited by the built-in scheduler, which multiplexes multiple OS threads over the nodes ready for execution [20].
The software automatically creates the report to an excel file with the calculated quantities necessary for calculation of reactor sizing and plots with certain parameters which are inserted automatically by the software from a set of charts whereby they are selected (see Figure 1).
Figure 2 shows the block diagram of the software application. LabVIEW MathScript RT Module adds math-oriented, textual programming to LabVIEW. The MathScript Node offers an intuitive means of combining graphical and textual code within LabVIEW, both of which are currently used in a number of science, engineering and technology programs and industries for simulation and analysis [19].

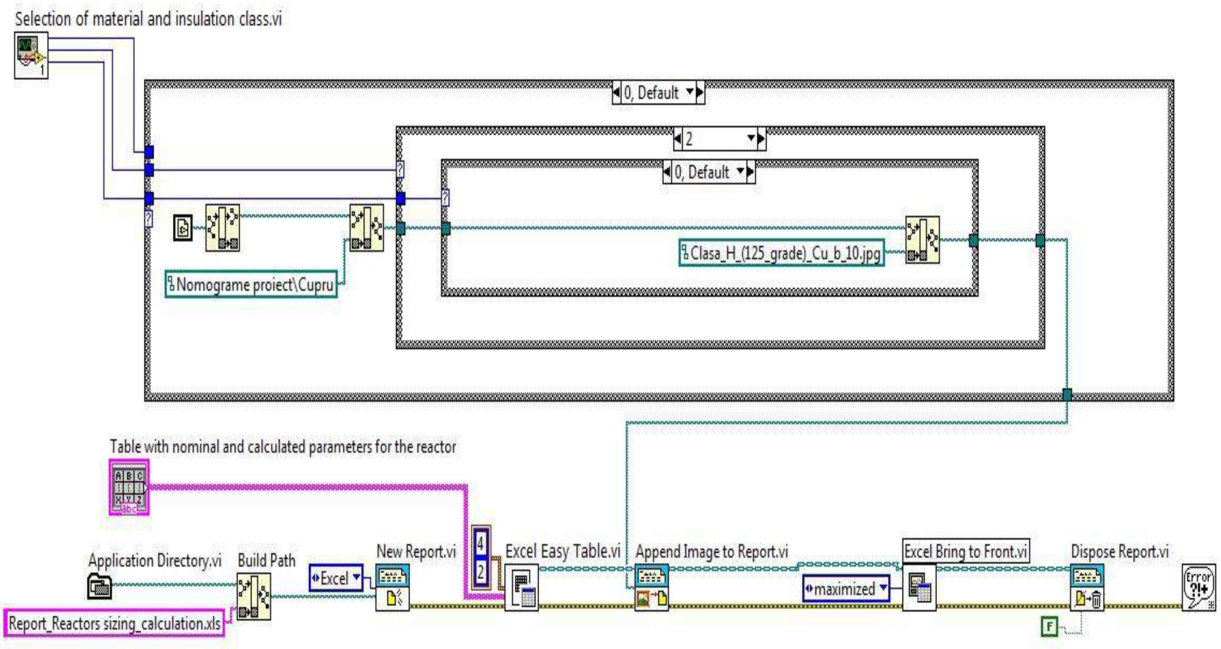

Fig. 1. The block diagram part for the Excel report

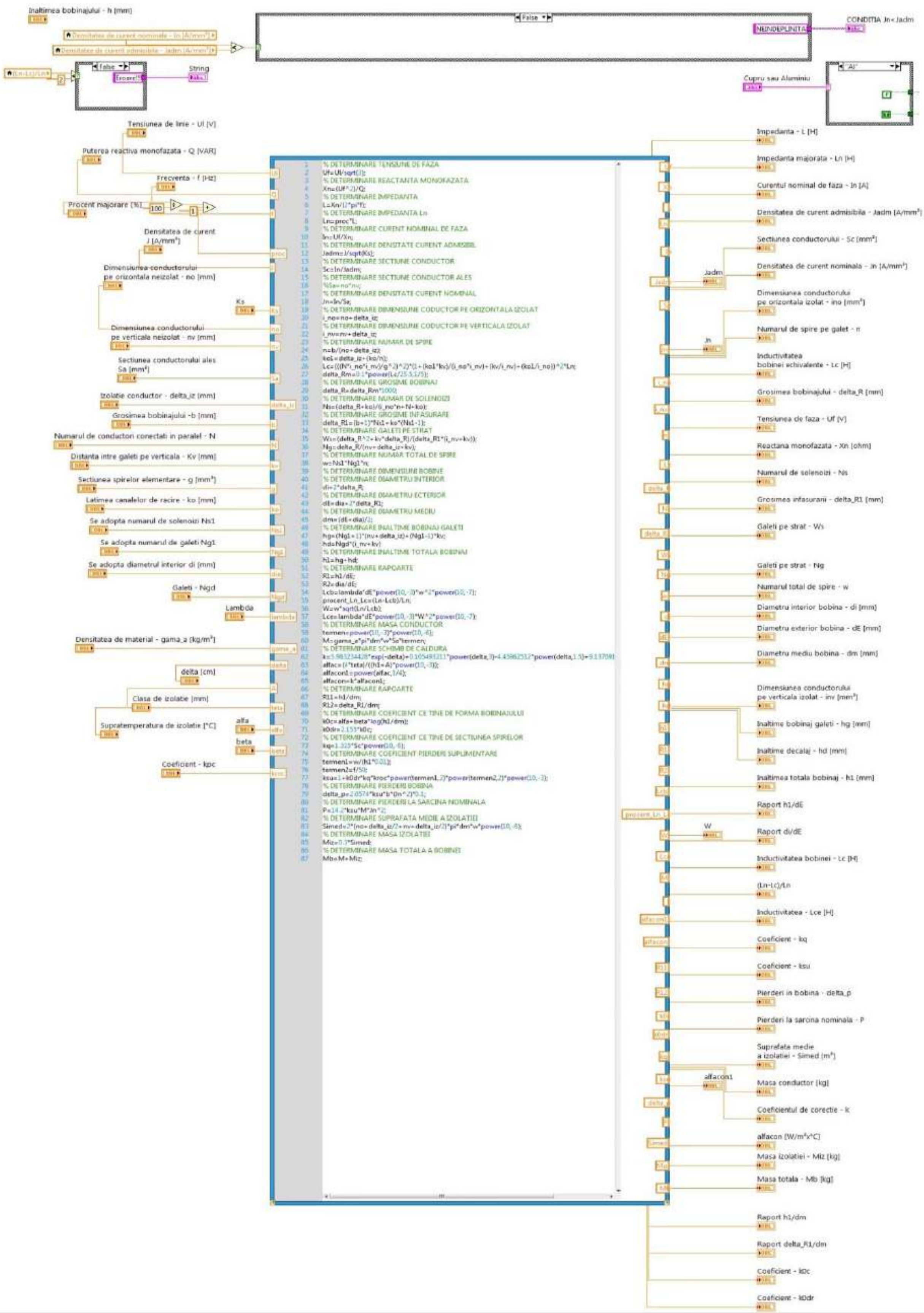

Fig. 2. The block diagram for calculation of reactor sizing of the software application

4. Example of calculation

The reactor with the ratings: line voltage U_l=20 kV, single phase reactive power Q=140 kVAr, phase voltage U_f=11,547 kV, frequency : f=50 Hz, single phase inductance X_n=952 ohm, impedance L=3,03 H, phase rated current I_n=12,1 A.

The figures 3-7 present the interfaces of the software application corresponding to the calculation steps for the reactor sizing according to the mathematical model in section 2.

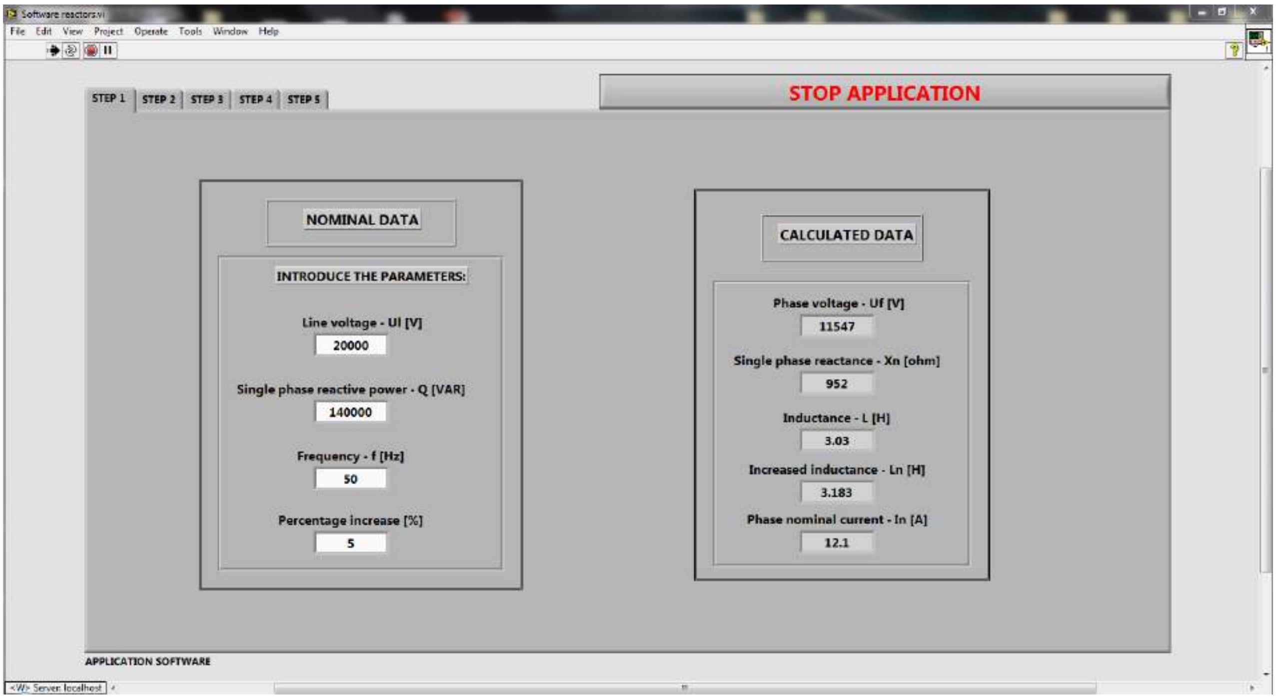

Fig. 3. Software interface – step 1

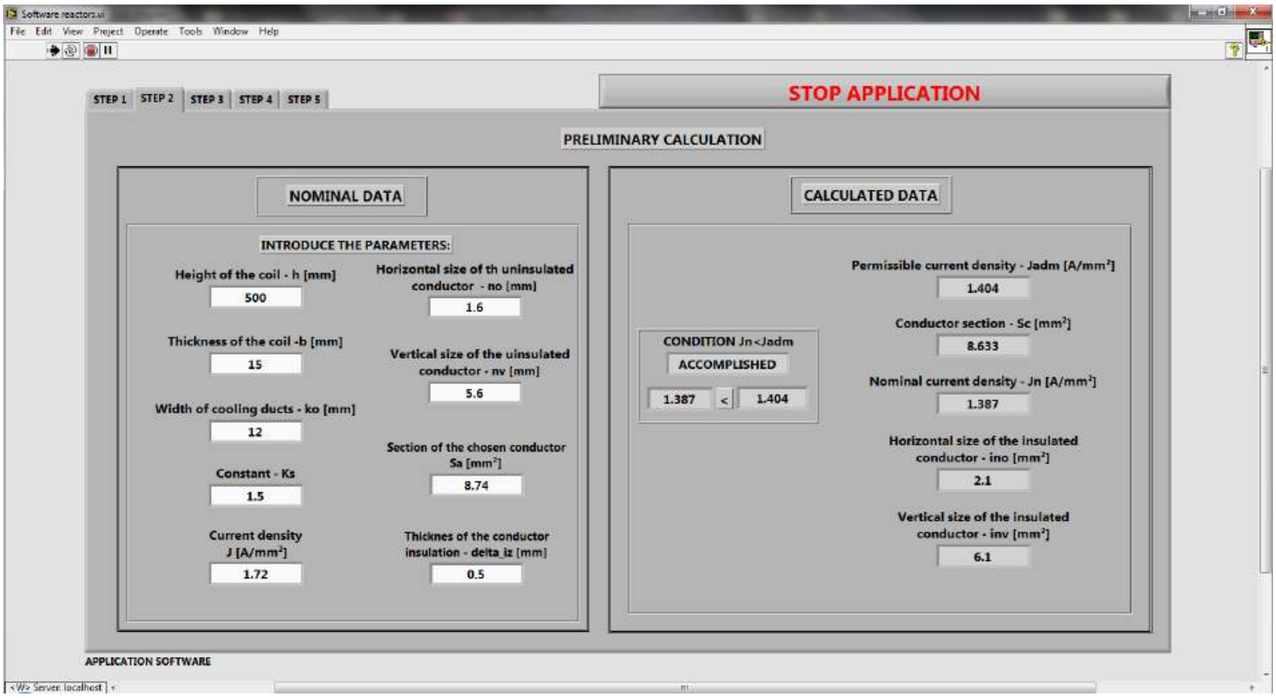

Fig. 4. Software interface – step 2

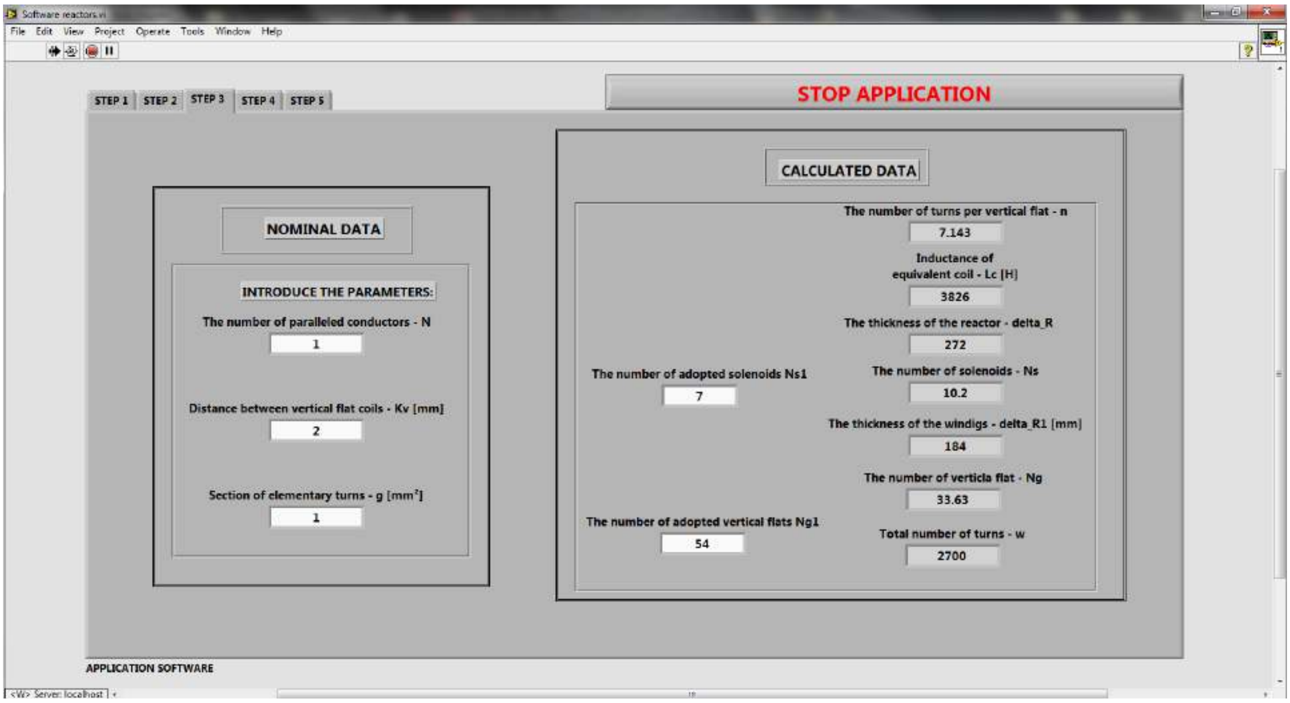

Fig. 5. Software interface – step 3

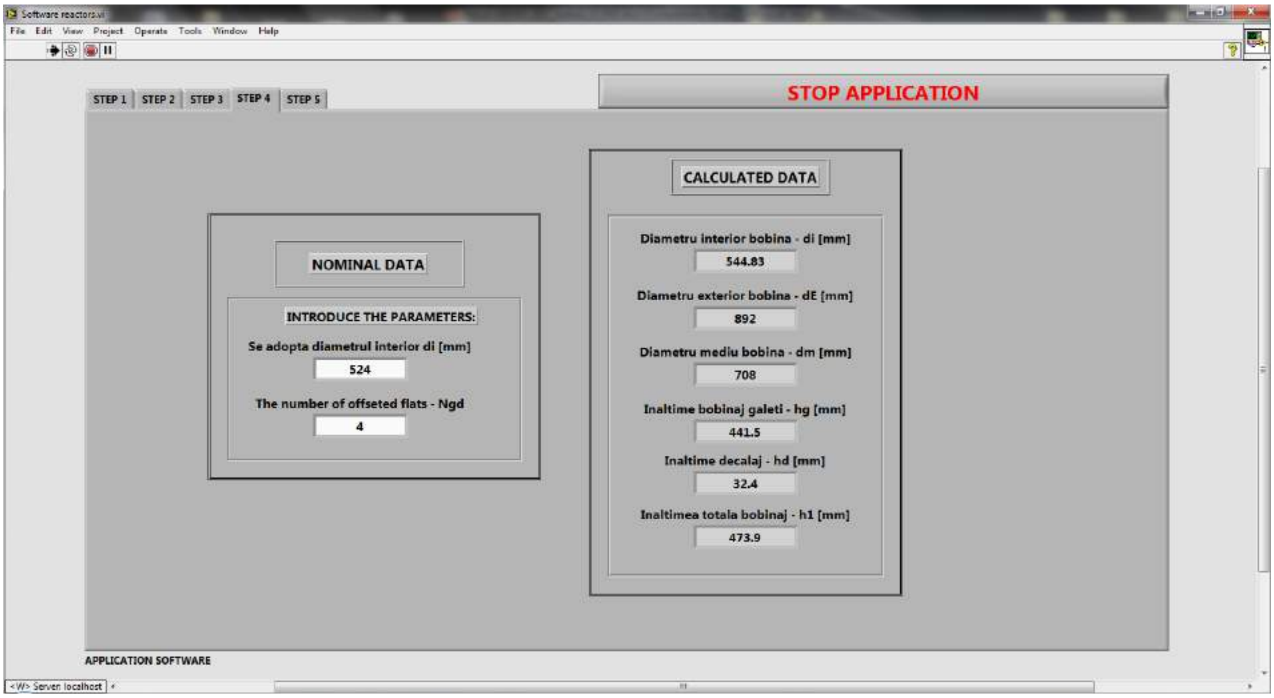

Fig. 6. Software interface – step 4

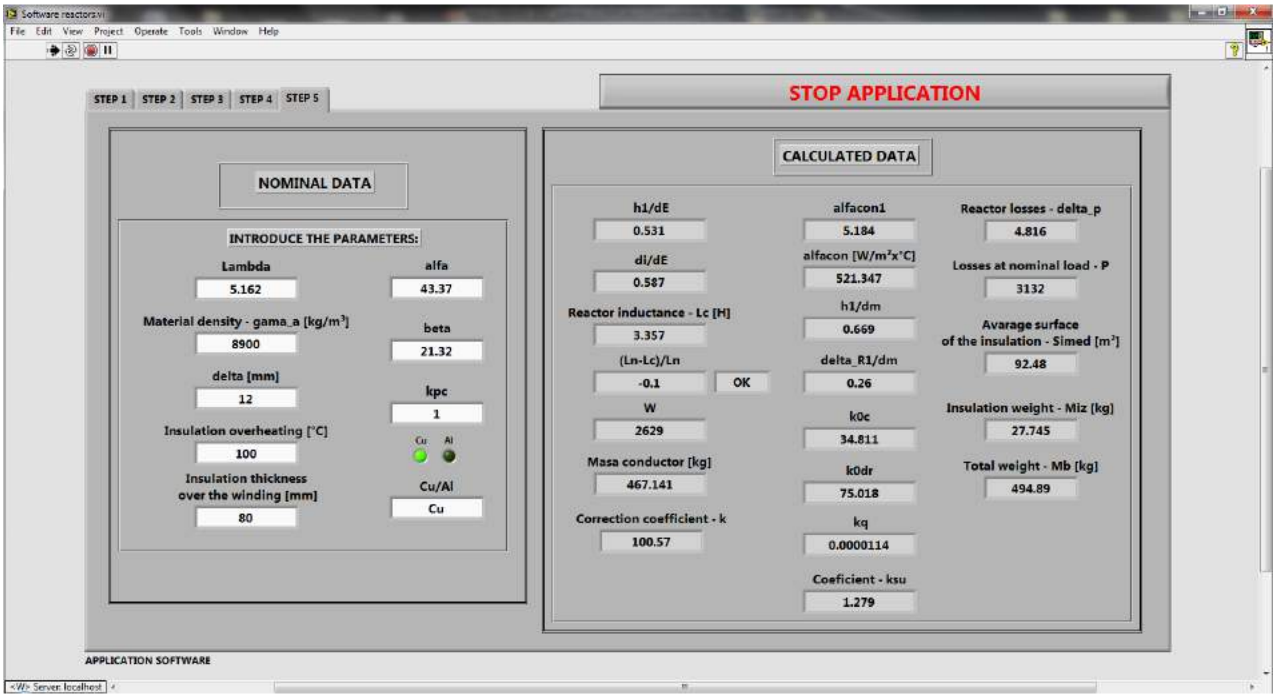

Fig. 7. Software interface – step 5

4. Conclusions

This article presents the application software which implements the mathematical model on reactor sizing calculation. The software is modular with a user friendly interface and presents the general advantages of modern software. Among them it suffices to mention the automatic generation of a report in Excel format and the possibility of creating a record of the calculated models.
The developed software is a useful tool for the designing activity of expert engineers by decreasing the duration of calculation and by excluding altogether miscalculations in mathematical relations. In the future, the research will be broadened in order to achieve complementary modules for other elements and physical processes that are suitable to be modeled.

Acknowledgments

The paper was developed with funds from the Ministry of Education and Scientific Research as part of the NUCLEU Program: PN 16 15 02 07.

References

[1] H. Ciocarlie, „Limbaje de programare. Concepte fundamentale", Ed. de Vest, Timisoara, 2010;
[2] Getting Started - EPLAN efficient engineering [Online]. Available: http://149.237.200.202/fileadmin/dateien-CA/BeginnerGuide_P8_enUS_NorthAmericanStyle_NFPA.pdf
[3] Orcad Capture User's Guide[Online]. Available: http://www.seas.upenn.edu/~jan/spice/PSpice_CaptureGuideOrCAD.pdf
[4] PSpice User's Guide - Penn Engineering [Online]. Available: http://www.seas.upenn.edu/~jan/spice/PSpice_CaptureGuideOrCAD.pdf
[5] Manual CATIA V5 [Online]. Available: http://www.ehu.eus/asignaturasKO/DibujoInd/Manuales/R12_manual_catia_v5.pdf
[6] Mathcad Users Guide. [Online]. Available: http://www2.peq.coppe.ufrj.br/Pessoal/Professores/Arge/Nivelamento/Mathcad/2-Apostilas/Mathcad%20Users%20Guide.pdf
[7] LabVIEW MathScript RT Module [Online]. Available: http://www.ni.com/LabVIEW/mathscript/

[8] Introduction to LabVIEW. [Online]. Available: http://home.hit.no/~hansha/documents/labview/training/Introduction%20to%20LabVIEW/Introduction%20to%20LabVIEW.pdf
[9] Introduction to matlab for engineering students. [Online]. Available: https://www.mccormick.northwestern.edu/documents/students/undergraduate/introduction-to-matlab.pdf
[10] MATLAB numerical computing. [Online]. Available: http://mayankagr.in/images/matlab_tutorial.pdf
[11] Labview^{TM} – Development Guidelines. [Online]. Available: http://www.ni.com/pdf/manuals/321393d.pdf
[12] P.G. Anoaica, "Bobine de reactanţă fără miez ferromagnetic", Ed. Universitatii din Craiova,2009
[13] P.L. Kalantarov, L.A. Teitlin, "Calculul inductanţelor", Bucureşti, Ed. Tehnica, 1958.
[14] I. Gheorghiu, A. Fransua, "Tratat de maşini electrice volumul al II-lea ransformatoare", Bucureşti, Ed. Academiei, 1970.
[15] C. Bala, L. Togui, "Bobine de reactanţa pentru sisteme energetice", Bucureşti, Ed. Tehnică, 1982.
[16] I. Cioc, Transformatorul electric: Construcţie. Teorie. Proiectare. Fabricare. Exploatare", Ed. Scrisul Romanesc, Craiova, 1989,ISBN 973380021X.
[17] R. Rudemberg, "Fenomene tranzitorii în sistemele electromagnetice", Bucureşti, Ed. Tehnica, 1959.
[18] J. Jovitha. (2010, January 30). "Virtual Instrumentation Using Labview", [Online]. Available: https://www.academia.edu/9455052/Virtual_Instruments_using_LabView_by_-_Jovitha_Jerome
[19] Developing Algorithms Using LabVIEW MathScript RT Module: Part 1 – The LabVIEW MathScript Node [Online]. Available: http://leeseshia.org/lab/releases/1.70/documents/
[20] LabVIEW^{TM} - Getting Started with LabVIEW, [Online]. Available: http://www.ni.com/pdf/manuals/373427j.pdf

.

ISSN 1454 - 8003
Proceedings of 2017 International Conference on Hydraulics and Pneumatics - HERVEX
November 8-10, Băile Govora, Romania

UPGRADED STAND FOR TESTING OF HYDRAULICALLY ASSISTED STEERING BOXES FOR CARS

Radu – Iulian RĂDOI[1], Gabriel ANGHELACHE[2], Alexandru HRISTEA[1], Mihai ALEXE[1], Bogdan TUDOR[1]

[1] INOE 2000 – IHP Bucharest, radoi.ihp@fluidas.ro

[2] University Politehnica of Bucharest, gabriel.anghelache@upb.ro

Abstract: *An economic partner wanted to improve a test bench for testing hydraulic assisted power steering and pumps for passenger cars and vans. Modernization of existing technology through computerization will reduce testing time and diminish the consumption of electricity, but also eliminate any human error which may occur in the verification process of repair; in this way there is the certainty of a subassembly that provides full security to the user. For upgrading, a number of subassemblies have been installed on the stand that allow the stand to be interfaced with a computer. The subassemblies consist of a series of transducers, electronic block, a data acquisition board and a drive system for the steering box valve. The paper presents the construction and functioning of the necessary subassemblies for stand upgrading and their characteristics.*

Keywords: *Hydraulic steering box, test stand, transducers, automotive*

1. Introduction

An economic partner which provides maintenance for hydraulic assisted power steering wanted to upgrade his test bench. The technology is made with technical level of the last decade and met the requirements of the company in the initial period; with increased business activity, this technology has reached its limits. The current technology is based on a human operator witch simulate manual steering by turning the steering column, followed by visualizing and writing values read on the test bench analog equipment (Fig. 1). The upgrade was done by installing measurement units, data acquisition system, and testing software.

Fig. 1. View with the steering boxes test stand

1. Force loading device, 2. Flowmeters, 3. 2 way valve, 4. 3 way valve, 5. Manometers, 6. Thermostat adjustment, 7. Pump speed display, 8. Mounting device for steering box, 9.Emergency stop button, 10. Pump speed adjustment

The upgraded test bench can determine the condition of the seals in the hydraulic valve of the steering box and the hydraulic piston by measuring the flow of oil during tests. The installed subassemblies consist of a series of transducers, electronic block, a data acquisition board and a drive system for the steering box valve. The computer system newly installed can issues a report bulletin which contains records such as pressure to each end, handling with predetermined load, oil flow, oil temperature and torque at the hydraulic distributor shaft during handling, series box name operator and company name. The system contains a data acquisition board, pressure transducers, flow, torque, temperature, an actuator and a software application for testing sequences; the system can acquire and store, process and print recorded data. They are compared with a database conducted under modernization process.

2. Subassemblies for modernization

To connect the equipment for measuring the working and control parameters it was necessary to use some adaptation pieces. For example, for the connection of the pressure transducer, a T-connection has to be connected to the circuit. In the following subchapters are presented the solutions adopted for connecting the transducers and the steering box valve actuator

2.1 Pressure measuring subassembly

The pressure measuring assembly (Fig. 2) for the steering box supply circuit consists of the following parts: T connector (1) , a short pipe (2), 1/4”female connector (3) and a pressure transducer (4). The pressure transducer has a range of 0-160 bar and an output signal of 4 ... 20 mA. The signal from the transducer is converted to voltage and connected to an analog input of the data acquisition board. With the pressure transducer, it is possible to measure the system pressure during the action of steering box with load at the rod or at the end of the stroke. It is also possible to determine the maximum pressure that the power steering pump can lift.

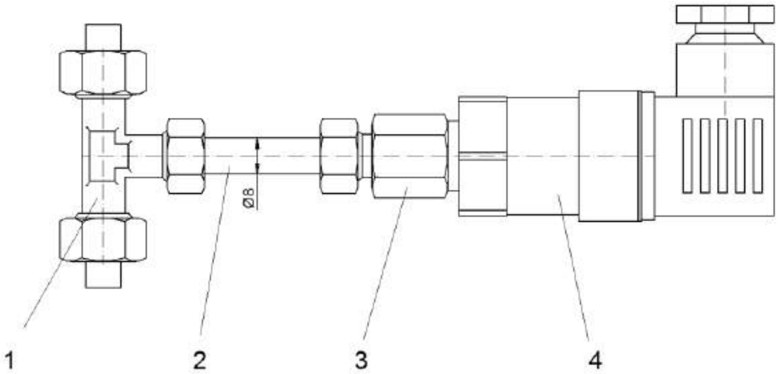

Fig. 2. Pressure measuring subassembly

2.2 Flow measuring subassembly

The subassembly (Fig. 3) consists of two hose connections (1), two gaskets (2) and the flow transducer(3). The flow transducer can measure the maximum flow rate of the power steering pump or the leakage rate of the rotary valve or due to wear of piston seal [1, 2]. The flow meter consists of a spinner which is rotated by the flowing medium. The rotor's rotational speed is proportional to the flow volume per unit time and is read by an inductive sensor. Its measuring range is 0.1 - 12 l/min and the output signal is in pulses per volume unit. The input and output connections of the transducer are female thread G3/8. The signal connects to the counter input of the data acquisition board. The pulse signal is processed and displayed in l/min.

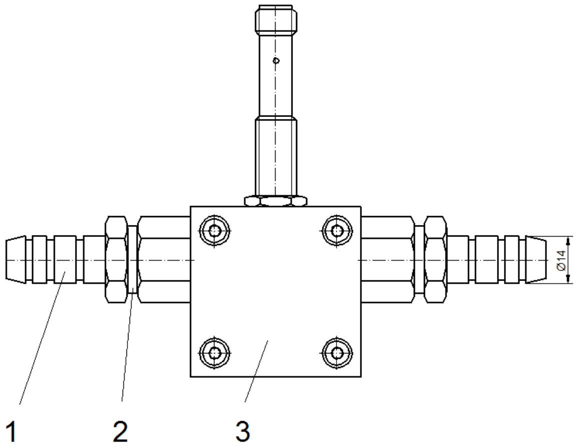

Fig. 3. Flow measuring subassembly

2.3 Force measuring subassembly

The subassembly (Fig. 4) consists of two adapters (1.4) for connecting to the loading device [3] with hydraulic cylinder and to the end of tie rod of steering box. Two locking nuts (2) are provided on the adapter threads. The transducer (3) for determining the force of the steering box rod is a type S load cell. The force transducer is provided with an amplifier with 0 ... 10 V output signal. The force signal from the steering box stem is scaled into daN by the software application. The force transducer has a measuring range of +/- 5000 daN.

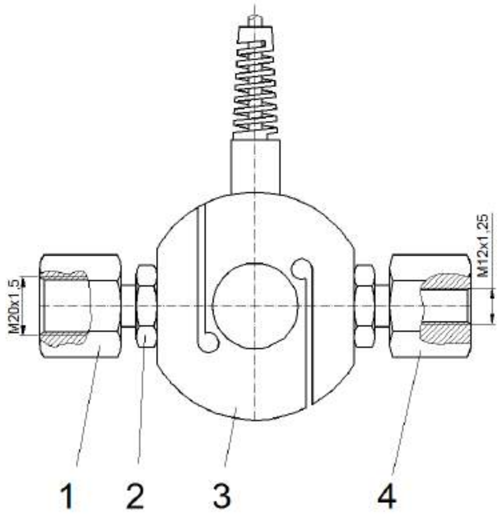

Fig. 4. Force transducer and coupling parts

2.4 Subassembly for measuring the position of steering box rod

The subassembly for measuring the stroke of the power steering rod (Fig. 5) consists of connector (1), position transducer (2), M4 bolt (3), clamping bracket (4), braid clamp for housing of hydraulic cylinder from the force load device (5), two M6 nuts (7) and connecting bridle for the rod of the force load device with hydraulic cylinder. The transducer has a 225 mm stroke and is resistive type with a resistance of 5 kΩ. The signal provided by it is connected to an analog input of the data acquisition board. The supplied voltage signal is proportional to the read position and is converted by the software application in mm The position transducer is useful to determine the positions from middle and from the stroke end of the steering rod, where the pump reaches the maximum pressure.

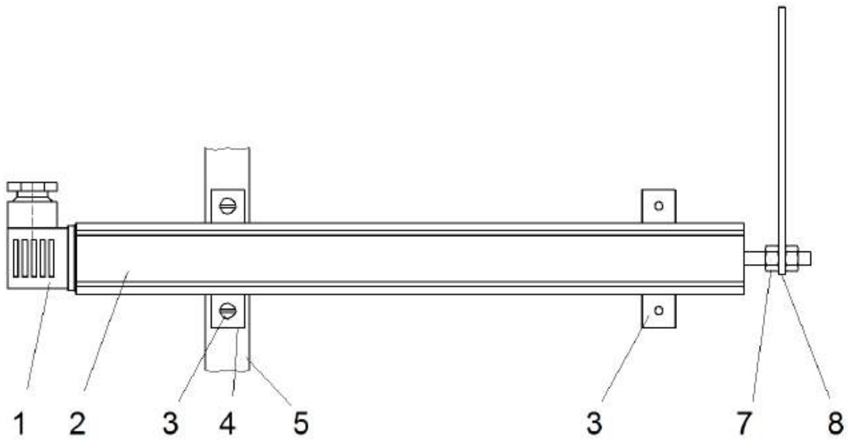

Fig. 5. Transducer for position of steering box rod

2.5 Subassembly for measuring the current of electric motor for driving rotary valve

Measuring the current absorbed by the electric motor can provide information about the torque variation required to drive the input shaft of the power steering box. The current sensor has the ACS711EX (Fig. 6) code and can measure the current in the range of -15.5A to +15.5A [4]. The sensor is produced by the company 'Pololu Robotics and Electronics'. The voltage signal provided by the sensor can be calibrated and scaled in Nm. For this it is necessary to be made an initial measurement of the torque, of the rotating valve shaft. This can be done with a specialized transducer. Torque information is useful to determine the tightening of rotary valve seals.

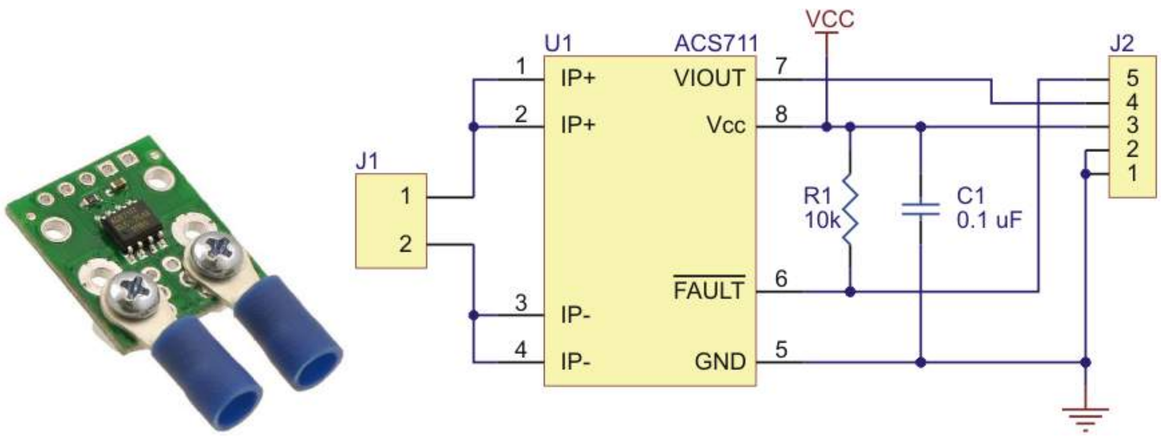

Fig. 6. PCB of current sensor and schematic diagram

2.6 Subassembly for measuring the temperature of hydraulic fluid

Tests of the stand are made with hydraulic oil at a temperature of 40°C. In order to achieve this, the stand is equipped with a heating resistance and a thermostat. It will be used a PT100 sensor in order to acquire the temperature value during the test and to register it in the test report. The sensor is placed in a sheath inserted into the oil tank. The signal is taken over by the data acquisition board via a transmitter (Fig. 7). The signal 4 up to 20 mA is converted to a voltage between 1 and 5 V for one of the analogue inputs of the DAQ board. In the software application, the signal is scaled to the temperature, which is printed in the test report form.

ISSN 1454 - 8003
Proceedings of 2017 International Conference on Hydraulics and Pneumatics - HERVEX
November 8-10, Băile Govora, Romania

Fig. 7. Pt 100 temperature sensor and transmitter

2.7 Subassembly for driving input shaft of steering box rotary valve

The rotary valve actuator (Fig. 8) consists of an adjustable support, an electric windshield wiper motor and a belt drive. The adjustable support allows the electric motor to tilt, so that the output of the drive shaft from the output of the reducer to be parallel to the rotary valve shaft on the steering box. The support also allows stretching of the drive belt after fitting it between the speed reducer and the valve shaft(Fig. 9).

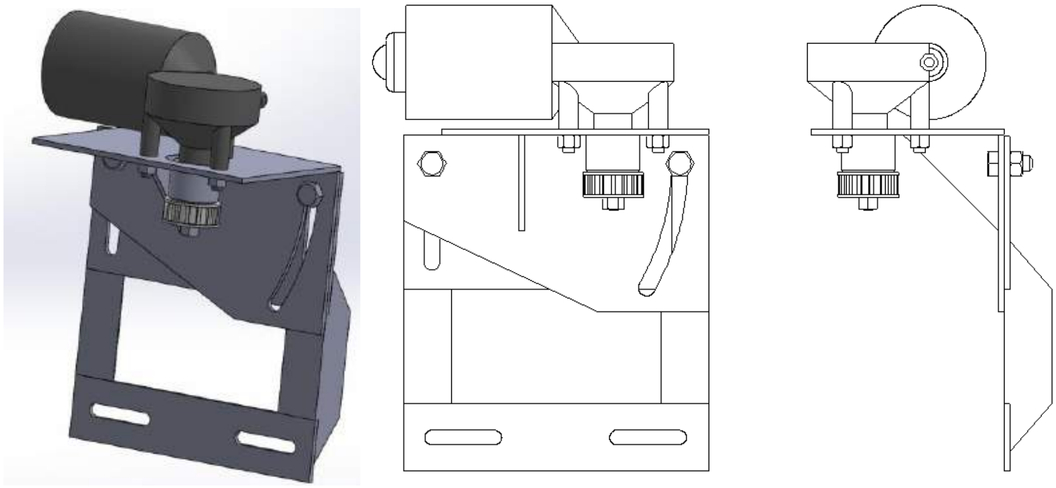

Fig. 8. Device for adjusting the position of the driving electric motor

Fig. 9. Belt pulley and coupling for the shaft of rotary valve

ISSN 1454 - 8003
Proceedings of 2017 International Conference on Hydraulics and Pneumatics - HERVEX
November 8-10, Băile Govora, Romania

The support is attached to the stand frame and the valve shaft pulley is fixed by means of and elastic coupling, (Fig.9) which is tightened by a screw. From the electric motor is used the low speed socket, the speed is reduced moreover (1: 2 ratio) with a belt transmission . With the electronic controller, the speed can be adjusted to a small extent so that it does not fall below the torque required to rotate the shaft of the valve.
The electric motor is controlled by an H-bridge electronic controller (Fig.10). The controller has an input voltage between 0 to 5 V through which it can control the rotational direction and speed. At 2.5 V, the electric motor is switched off and when the control voltage increases above 2.5 V, the motor rotates in a direction with a maximum speed of 5 V. For the other direction of rotation, the control decreases below 2.5 V and the maximum speed being at 0 V. The range between 0 to 5 V has been chosen since the NI USB-6008 data acquisition board has a maximum output signal of 5V. The controller also has two LEDs which indicate the direction of the rotating electric motor.

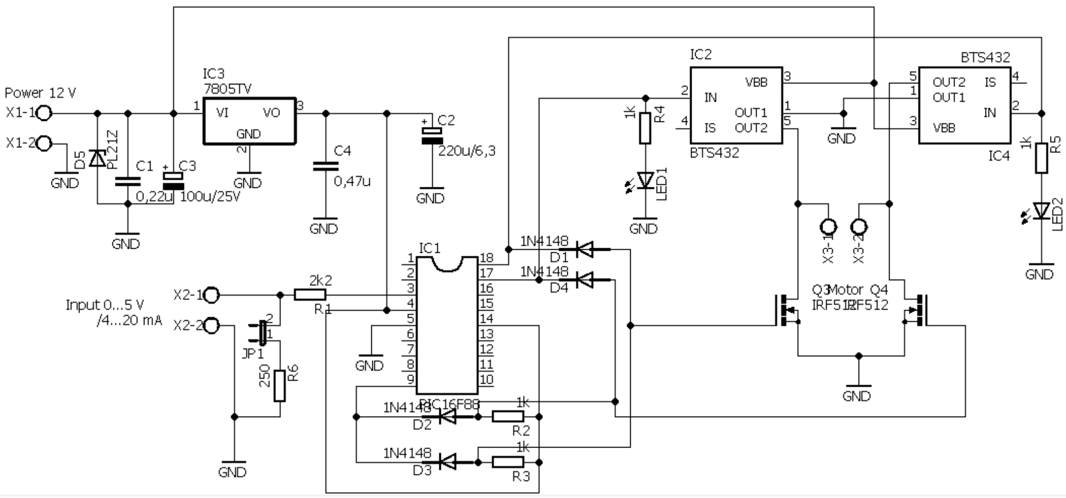

Fig. 10. H-Bridge electric motor speed and direction controller

3. The test software application

The software application is made in LabView and allows to monitor the parameters captured by the stand transducers through a DAQ board (Fig. 11) and to control the steering box via the rotary valve. The application has a panel on which you can view the parameters from the transducers and a series of controls for interacting with the software application. With the help of some buttons, the operator can switch the manual or automatic test mode, enrolling the test product data, the operator name, the name of the recipient and listing the test report. With the help of the application, the operator can manually control the steering box and read the operating parameters on the computer display, and for the test report issue, the program uses a test cycle, the parameters obtained being printed in the test report.

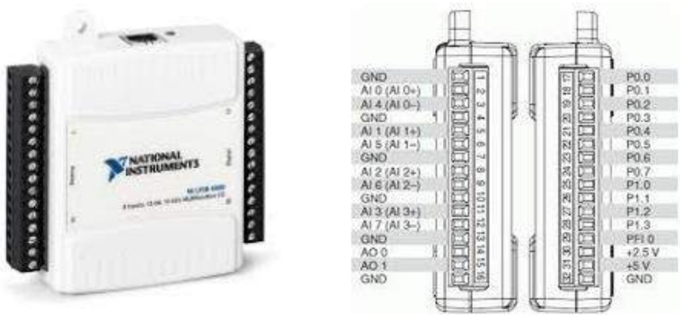

Fig. 11. National Instruments USB – 6008 DAQ

4. Conclusions

New computerized technology reduce testing time and diminish the consumption of electricity, but also eliminate the human error which may occur in the verification process.
The test stand is equipped with transducers and data acquisition system.
The system helps prevent accidents by detecting and contributing to the remedy of non-compliant automotive equipment.
The upgraded installation allows the test bulletin to be issued quickly and without difficulty.

Acknowledgments

This work has been funded by Executive Unit for Financing Higher Education, Research, Development and Innovation - UEFISCDI, under PNCDI III - Programme 2, Subprogramme 2.1 – Transfer of knowledge to economic agent – Bridge Grant, Submission code PN-III-P2-2.1-BG-2016-0111, Financial agreement no. 91BG/2016, project title: Computerized system for testing automotive steering boxes in view of increasing the safety of traffic participants, Acronym SITECH.

References

[1] G. Matache, St. Alexandrescu, A. Pantiru, Gh. Sovaiala, M. Petrache, "The analysis of flow losses through dynamic seals of hydraulic cylinders", *Hidraulica Magazine*, ISSN 1453-7303, Romania, no.1, pp. 52-60, 2013;
[2] C. Cristescu, C. Dumitrescu, G. Vranceanu, L. Dumitrescu, "Considerations on energy losses in hydraulic drive systems", *Hidraulica Magazine*, ISSN 1453-7303, Romania, no.1, pp. 36-46, 2016.
[3] G. Matache, St. Alexandrescu, Gh. Sovaiala, I. Pavel, I.C. Girleanu, "Testing of linear pneumatic actuators with hydraulic load", *Hidraulica Magazine*, ISSN 1453-7303, Romania, no.3, pp. 53-56, 2013;
[4]http://tet.pub.ro/materiale/altele/Documentatie/Senzor%20curent%20ACS711EX/Pololu%20-%20ACS711EX%20Current%20Sensor%20Carrier%20-15.5A%20to%20+15.pdf

ISSN 1454 - 8003
Proceedings of 2017 International Conference on Hydraulics and Pneumatics - HERVEX
November 8-10, Băile Govora, Romania

SIMULATION AND ANALYSIS OF HYDRAULIC-PNEUMATIC QUADRUPLE TANK SYSTEM

Yusuf ALTUN[1], Oğuz EROL[2], Melih AKTAŞ[3]

[1] Duzce University, Engineering Faculty, Mechatronics Engineering, Duzce, Turkey, yusufaltun@duzce.edu.tr

[2] Duzce University, Engineering Faculty, Electrical and Electronics Engineering, Duzce, Turkey

[3] Duzce University, Engineering Faculty, Computer Engineering, Duzce, Turkey

Abstract: *This paper presents the simulation and analysis of hydraulic-pneumatic quadruple tank system, which is generally used in industrial processes. The system is complex and has many variables. So, the program tool brings to examine the effects of the system parameters. In addition, this analysis and simulation program provides to teach graduate and undergraduate students without laboratory for hydraulic-pneumatic quadruple tank system. The linear dynamic model is used for the simulation and analysis under some operating conditions. Eventually, some simulation examples are exhibited for the parameter effects.*

Keywords*: hydraulic-pneumatic, quadruple tank, fluid system, simulation tool.*

1. Introduction

The water tank systems are widely used in industrial applications especially for the chemical process systems. The liquid level or flow control between tanks is a prominent issue for the process industry. So, this issue the liquid level control of the combined tanks is very interesting for a lot of researchers in the literature and they are working on this issue. In addition, it is admitted that this is a significant benchmark problem due to its behaviors. It is generally purposed for many combined tank systems to control some demanded levels of the liquids in the tanks where an outflowing or inflowing of liquid is existent to the tanks. The combined tank systems are multi-input multi-output (MIMO), where inputs are generally pump voltages and the outputs are generally liquid levels. The pumping, storing in tanks of liquids, and then pumping to another tank is orderly needed for the process industry. In critical industries such as petro-chemical and water treatment industries, the tanks have an impact on each other where chemical or mixing processes take up considerable place in process tanks. Therefore, the level control and simulation of liquid systems has a major place in the literature studies. In [1], a new multi-variable laboratory process with four integrated tanks. A sliding mode controller (SMC) based on fractional order (FO) is designed for a level control of coupled tank in [2] whereas SMC is designed for quadruple tank process in [3] and coupled-tank system in [4]. In [5], the control of the liquid levels and temperature for combined three tanks is made via feedback linearization, a decentralized fuzzy logic control is performed by LabVIEW for a coupled-tank process in [6] and [7]. In [8], a FO-PI controller is designed for a liquid level of round tank. In [9], a linear quadratic regulator (LQR) and a type-2 fuzzy logic are designed on the level control of three-tank system. In [10], FO-PI controller is performed for a coupled two-tank system. In [11], fuzzy logic control is fulfilled for a tank system. In [12], an adaptive model reference controller is designed for a hybrid nonlinear tank system. In [13], controller based quadratic programming is proposed for a quadruple tank problem. In [14], a corrected mathematical model is proposed for quadruple tank system.
LabVIEW™ is a sufficient simulation and analysis program for the academic computation, process systems, measurement and industrial implementations due to the fact that it has a flexible program which is together with many tools particularly for the measurements, controls, and tests as in [15]. it is also an sufficient program for learning and teaching because it satisfies several requirements for a lot of applications [16].
Some of laboratory sets are quite expensive. In addition, many of them cannot give the changing their parameters such as chemical process, power systems, robotic systems. So, a virtual

laboratory or analysis tool is sufficient to analyze the changings of parameter. some systems which are not experimental can be difficult to good understand in view of the teaching and learning of students. In addition, to be perceived the influences of the system parameters on the operating are limited by many students. In the literature, the researchers have been investigated on the educational virtual tools for a lot of systems such as [17]–[19]. In this paper, an educational analysis tool is designed with LabVIEW for the hydraulic-pneumatic quadruple tank. They have been used in undergraduate chemical and mechatronics engineering laboratories in a lot of universities.

2. The Hydraulic-Pneumatic Quadruple Tank System Model

A new process is proposed for the four tanks in [20]. Figure 1 shows this process. In this process, pneumatic volume above the water levels is connected. Also, the orifices are replaced into the circuits, so, the cross interactions exist only in transient states so the working area is not reduced [20]. It has an integration of pneumatic and hydraulic parts. The circuits of pneumatic bring about cross coupling between both classical couple tank parts. Four cylindrical tanks are the basic elements. The water is pumped into left upper (LH) and right upper (RH) tanks by two pumps and so, it flows into left lower (LL) and right lower (RL) tanks. Then, it backs into the reservoir. Water flow rates are controlled by u_L, u_R voltages of the pumps between 0 and10 volts, which is amplified into 4-10 volts. Difference pressure sensors indirectly measure the lower tanks. The pressure sensor outputs are between 0 and10 volts.
Air spaces above the tank levels are connected by pneumatic circuits H and L with the changeable valves. The orifices in air gaps work as a coupling between atmosphere and pneumatic volumes. The structure can be changed by the size of orifices and by valves in the pneumatic circuits. There is a atmospheric pressure in pneumatic in the steady-state. The water level changes by the pressure in pneumatic. the air is progressively equilibrated with atmospheric pressure by flowing in the air chambers. Thus, the multi-variable adverse effect has only dynamic property.

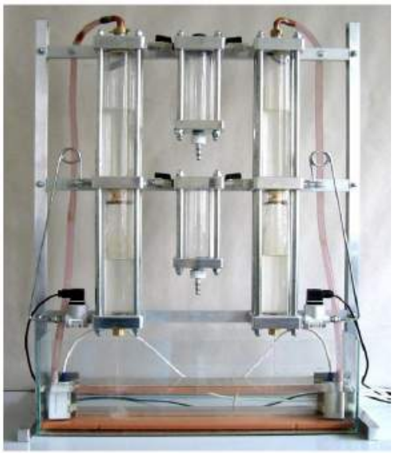

Fig. 1. Hydraulic-Pneumatic Quadruple Tank System [20]

The mathematical model is obtained by the dynamic equations of four tanks, pump static properties, dynamic equations of the bottom pneumatic circuit and static properties of the pressure sensors. The tanks have different diameter. Both orifices are the same. The model is nonlinear but, it can be linearized at some working points. The linearized differential equations are as in (1) from [20] where all of the equations are detailed regarding to (1).

$$
\begin{aligned}
\frac{d\Delta h_{LH}}{dt} &= -\frac{1}{T_L}\Delta h_{LH} + \frac{Z}{T_L}\Delta h_{LL} + \frac{Z_{uL}Z_{QL}}{T_L}\Delta_{uL} \\
\frac{d\Delta h_{RH}}{dt} &= -\frac{1}{T_R}\Delta h_{RH} + \frac{Z}{T_R}\Delta p_L + \frac{Z_{QR}Z_{uR}}{T_R}\Delta_{uR} \\
\frac{d\Delta p_L}{dt} &= -\frac{Z_{hl}}{T_p}\Delta h_{LH} + \frac{Z_{hr}}{T_p}\Delta h_{RH} - \frac{1}{T_p}\Delta p_L - \frac{Z_{hl}}{T_p}\Delta h_{LL} - \frac{Z_{hR}}{T_p}\Delta h_{RL} \\
\frac{d\Delta h_{LL}}{dt} &= \frac{1}{T_L}\Delta h_{LH} - \frac{2Z}{T_L}\Delta p_L - \frac{1}{T_L}\Delta h_{LL} \\
\frac{d\Delta h_{RL}}{dt} &= \frac{1}{T_R}\Delta h_{RH} - \frac{2Z}{T_R}\Delta p_L - \frac{1}{T_R}\Delta h_{RL}
\end{aligned}
\tag{1}
$$

According to the equations, the linear state space model is in (2) where all expressions are detailed in [20].

$$
\dot{x} = A(x) + B(x)u
$$

$$
A = \begin{bmatrix} -\frac{1}{T_L} & 0 & \frac{Z}{T_L} & 0 & 0 \\ 0 & -\frac{1}{T_R} & \frac{Z}{T_R} & 0 & 0 \\ -\frac{Z_{hl}}{T_p} & \frac{Z_{hr}}{T_p} & -\frac{1}{T_p} & -\frac{Z_{hl}}{T_p} & -\frac{Z_{hR}}{T_p} \\ \frac{1}{T_L} & 0 & -\frac{2Z}{T_L} & -\frac{1}{T_L} & 0 \\ 0 & \frac{1}{T_R} & -\frac{2Z}{T_R} & 0 & -\frac{1}{T_R} \end{bmatrix}, B = \begin{bmatrix} \frac{Z_{uL}Z_{QL}}{T_L} & 0 \\ 0 & \frac{Z_{QR}Z_{uR}}{T_R} \\ 0 & 0 \\ 0 & 0 \\ 0 & 0 \end{bmatrix}, x = \begin{pmatrix} \Delta h_{LH} \\ \Delta h_{RH} \\ \Delta p_L \\ \Delta h_{LL} \\ \Delta h_{RL} \end{pmatrix}, u = \begin{pmatrix} \Delta_{uL} \\ \Delta_{uR} \end{pmatrix}
\tag{2}
$$

3. The Simulation and Analysis for the Quadruple Tank System

An analysis tool is designed via LabVIEW™. The tool gives the teachers to prove the system behaviour and all effects of parameters in the system model without any laboratory. Such a laboratory may be costly or the parameter effects are not proved since system parameters are fix. Therefore, all parameter effects on the system are examined owing to the tool. Figure 2 presents LabVIEW control front panel for the designed tool. As in Figure 2, all parameters can be changed with buttons and the tank levels are observed as visually. Thus, by modifying all system parameters with the tool interface, their effects can be observed on the system. Also, a designer can examine the crucial parameters by the tool for the validation or control. The default parameter values of the system are as in [20] for the simulation.
The tool is simulated to examine the parameter effects on the system. For instance, to observe the pump voltage inputs, the changings of liquid levels are in Figure (3). So, the effects of the inputs are examined when Δ_{uL} and Δ_{uR} are 5V at the simulation. For another example, Figure (4a) shows the liquid levels when left pump specific coefficient is changed from 0,00798 to 0,01368 whereas Figure (4b) shows the liquid levels when left pump specific coefficient is changed from 0,00853 to 0,01053. Thus, the effects of pump coefficients are on left and right upper tanks. Similarly, by changing the other parameters, the effects can be observed.

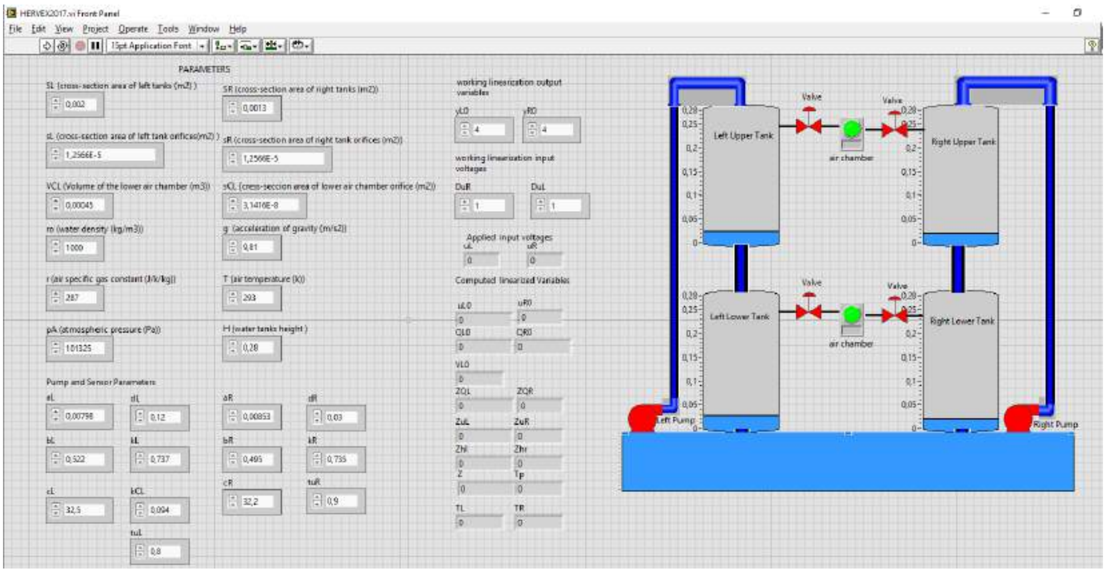

Fig. 2. The designed Labview front panel.

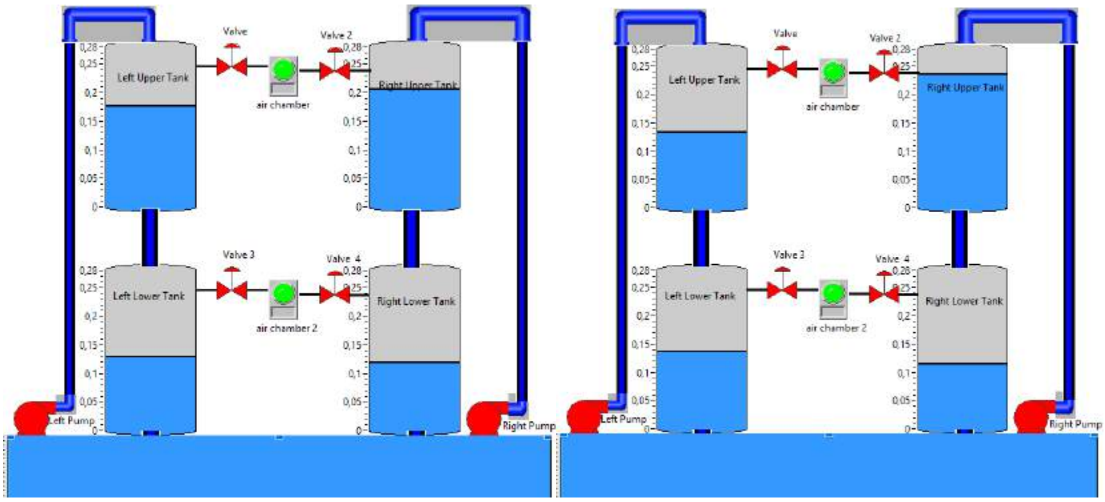

Fig. 3. The liquid levels according to the changes of voltage inputs.

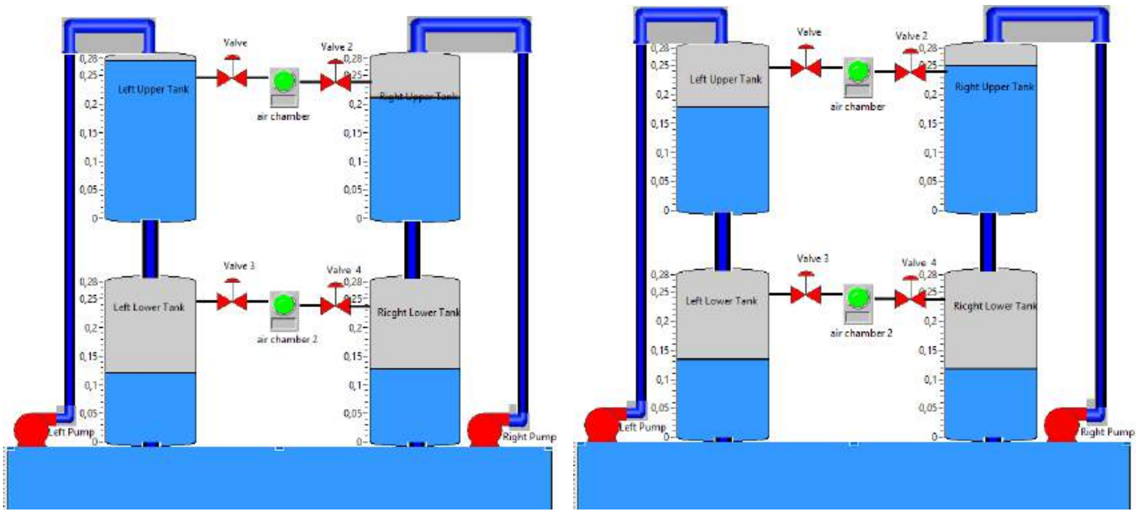

a) b)

Fig. 4. The liquid levels according to the changes of pump coefficients.

According to the simulation results, the whole parameter effects can be analysed by help of the tool. Finally, the designed simulation tool is very beneficial for the learning and teaching. Moreover, the tool is developed by the controller and thus the controller effects can be examined.

5. Conclusions

In this paper, an educational simulation tool is performed for hydraulic-pneumatic quadruple tank model. This tool gives users to modify of system variables, and so they can observe the outputs as visually. It helps students to improve modelling and dynamic system behaviour without any laboratory for the system. In particular, the simulation tool allows either undergraduate or graduate students to compass the parameter influences on the system model. Finally, simulation results show that the students can easily catch the parameter differences and their influences with the analysis tool.

References

[1] K. H. Johansson, “The quadruple-tank process: a multivariable laboratory process with an adjustable zero,” *IEEE Trans. Control Syst. Technol.*, vol. 8, no. 3, pp. 456–465, May 2000.
[2] H. Delavari, A. N. Ranjbar, R. Ghaderi, S. Momani, “Fractional order control of a coupled tank,” *Nonlinear Dyn.*, vol. 61, no. 3, pp. 383–397, 2010.
[3] “Sliding mode control of quadruple tank process,” *Mechatronics*, vol. 19, no. 4, pp. 548–561, Jun. 2009.
[4] H. Abbas, S. Asghar, S. Qamar, “Sliding Mode Control for Coupled-Tank Liquid Level Control,” *10th Int. Conf. Front. Inf. Technol. (Fit 2012)*, pp. 325–330, 2012.
[5] F. Tahir, N. Iqbal, G. Mustafa, “Control of a nonlinear coupled three tank system using feedback linearization,” in *2009 3rd International Conference on Electrical Engineering, ICEE 2009*, 2009.
[6] C. Pornpatkul, T. Suksri, T. C. Process, “Decentralized Fuzzy Logic Controller for TITO Coupled-Tank Process,” in *ICROS-SICE International Joint Conference 2009*, 2009, vol. 2, pp. 2862–2866.
[7] R. Suja, M. Malar, T. Thyagarajan, “Design of Decentralized Fuzzy Controllers for Quadruple tank Process,” *IJCSNS Int. J. Comput. Sci. Netw. Secur.*, vol. 8, no. 11, 2008.
[8] K. Sundaravadivu, V. Jeyakumar, K. Saravanan, “Design of Fractional Order PI controller for liquid level control of spherical tank modeled as Fractional Order System,” in *Proceedings - 2011 IEEE International Conference on Control System, Computing and Engineering, ICCSCE 2011*, 2011, pp. 522–525.
[9] H. Sahu, R. Ayyagari, “Interval fuzzy type-II Controller for the level control of a three tank system,” in *IFAC-PapersOnLine*, 2016, vol. 49, no. 1, pp. 561–566.
[10] P. Roy, B. Krishna Roy, “Fractional order PI control applied to level control in coupled two tank MIMO system with experimental validation,” *Control Engineering Practice*, 2015.
[11] M. Abid, “Fuzzy logic control of coupled liquid tank system,” in *Proceedings of 1st International Conference on Information and Communication Technology, ICICT 2005*, 2005, vol. 2005, pp. 144–147.
[12] K. Asan Mohideen, G. Saravanakumar, K. Valarmathi, D. Devaraj, T. K. Radhakrishnan, “Real-coded Genetic Algorithm for system identification and tuning of a modified Model Reference Adaptive Controller for a hybrid tank system,” *Appl. Math. Model.*, vol. 37, no. 6, pp. 3829–3847, 2013.
[13] “Distributed multiparametric model predictive control design for a quadruple tank process,” *Measurement*, vol. 47, pp. 841–854, Jan. 2014.
[14] “Corrected Mathematical Model of Quadruple Tank Process,” *IFAC Proc. Vol.*, vol. 41, no. 2, pp. 11678–11683, Jan. 2008.
[15] M. Demirtas, Y. Altun, A. Istanbullu, “Virtual laboratory for sliding mode and PID control of rotary inverted pendulum,” *Comput. Appl. Eng. Educ.*, vol. 21, no. 3, pp. 400–409, 2013.
[16] M. Demirtas, Y. Altun, A. Istanbullu, “An educational virtual laboratory for sliding mode and PID control of inverted pendulum,” in *11th International Conference on Optimization of Electrical and Electronic Equipment, OPTIM 2008*, 2008, pp. 149–156.
[17] B. Altrabsheh, “Measurement and classification of heart and lung sounds by using LabView for educational use.,” *J. Med. Eng. Technol.*, vol. 34, no. 5–6, pp. 340–9, 2010.
[18] L. Sevgi and Ç. ¸ Uluişik, “A labview-based virtual instrument for engineering education: A numerical fourier transform tool,” *Turkish J. Electr. Eng. Comput. Sci.*, vol. 14, no. 1, pp. 129–152, 2006.

[19] L. SajoBohus, E. D. Greaves, H. Barros, W. Gonzalez, A. Rangel, "LabView™ Based Nuclear Physics Laboratory experiments as a remote teaching and training tool for Latin American Educational Centers," *Proc. Phys*, vol. 477, no. 101, pp. 498168613–811, 2007.
[20] J. G. R. E. Y. De Pedraza, "Advanced control for a pneumatıc-hydraulıc laboratory plant, proyecto fınal de carrera."

ISSN 1454 - 8003
Proceedings of 2017 International Conference on Hydraulics and Pneumatics - HERVEX
November 8-10, Băile Govora, Romania

WORKING BENCH FOR RECONDITIONING HYDRAULIC CYLINDERS

Liliana DUMITRESCU[1], **Alexandru Polifron CHIRIȚĂ**[1], **Corneliu CRISTESCU**[1]

[1] Hydraulics and Pneumatics Research Institute INOE 2000-IHP; lilianad.ihp@fluidas.ro

Abstract: *Most of the Romanian companies that repair hydraulic cylinders manually perform their dismantling and repair operations after repair. Manual removal and fitting is done with great effort using tools and levers to increase hand strength. The article presents equipment that facilitates the operator's work using hydraulic power instead of arm strength. Hydraulic equipment is carried out under an "innovation check" funded by UEFISCDI through the P2 program to increase the competitiveness of the Romanian economy through research, development and innovation.*

Keywords: *Hydraulic cylinder, piston, rotary flange, unscrew / screw.*

1. Introduction

To repair the hydraulic cylinders, first disassemble them in component parts (washer, piston, guides, seals, etc.) and after reassembling them.

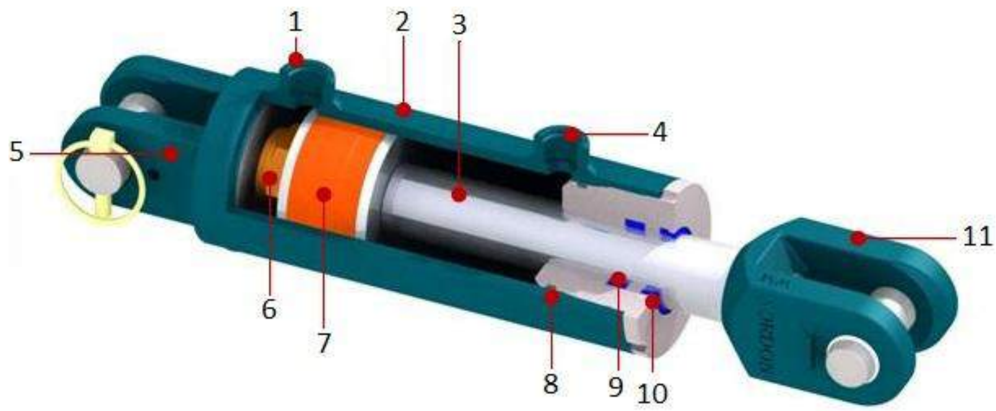

1 – Connection A
2 – Barrel/tube
3 – Piston rod/shaft
4 – Connection B
5 – Base mount
6 – Piston nut
7 – Piston seal
8 – O-ring and backup
9 – Rod seal
10 – Rod wiper
11 – Rod support

Fig. 1. Component parts of hydraulic cylinder [1]

Removing and then replacing the hydraulic cylinders involves a number of operations such as: unlocking the threads, unscrewing / threading the threaded assemblies, extracting / inserting the piston and rod into the cylinder barrel, etc.

For large hydraulic cylinders of heavy series (piston diameter over 200 mm and race over 2000 mm) for these operations, large rotating forces and torques are possible which can be achieved with mechanics driven by linear and rotary hydraulic motors.

2. Description and operation of the equipment

Hydraulic equipment for mounting / dismounting the hydraulic cylinders is shown in Fig. 2.

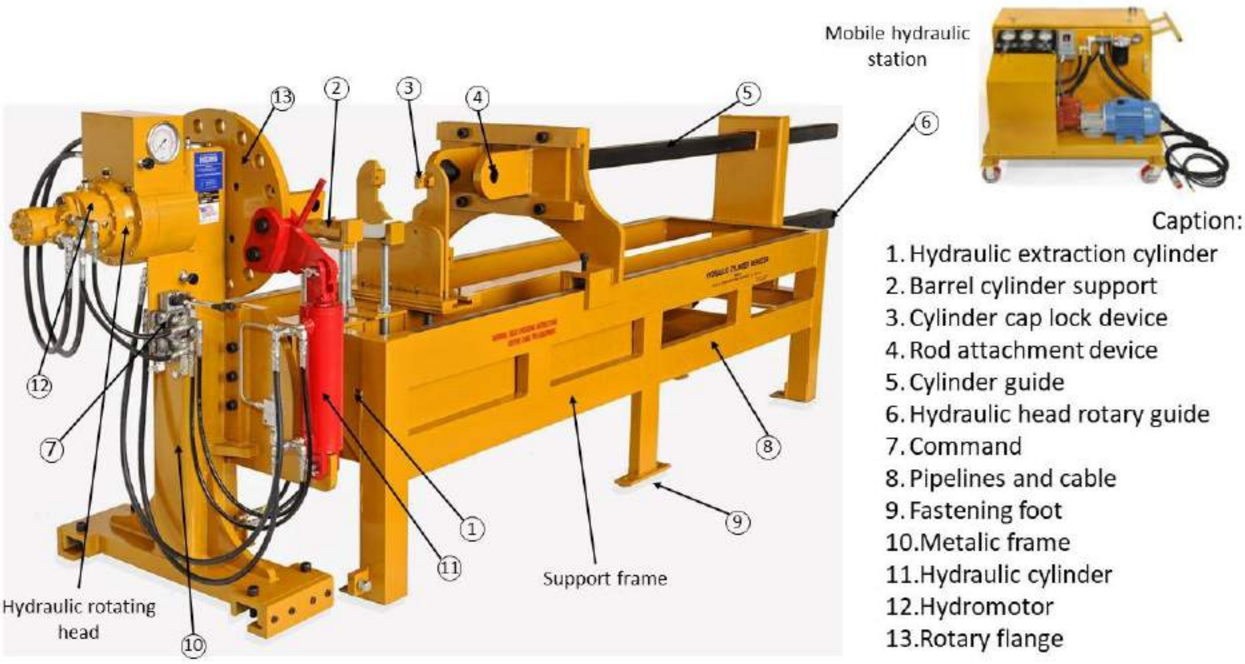

Fig. 2. Working bench for reconditioning hydraulic cylinder [2]

The hydraulic cylinder to be dismantled is fixed to the support frame and rests on the support 2. The roll of the cylinder barrel is fastened to the rotary flange and the cover of the barrel is blocked by the device 3.
The cylinder rod eye is fixed to the device 4. Depending on the length of the hydraulic cylinder, the device 4 moves longitudinally, being guided by the rod 5. The support frame is fixed to the floor by the fixing legs 9. The hydraulic cylinder 1, which is located inside the support frame, longitudinally moves the rotary hydraulic head by pulling the piston together with the rod in the cylinder tube. The longitudinal direction of movement is provided by the guide 6. The connection between the hydraulic station and the rotating head is made with the pipes 8, located inside the support frame. The equipment also has a number of devices that ensure fast fastening on the support frame so that the time for removing / mounting the cylinder is as small as possible.
The metal frame 7 fixes the component parts and hydraulic head. Hydraulic cylinder 1 is used to unlock threaded assemblies as it provides a high torque. The low-speed motor 2 is used to unscrew or screw the components of the cylinder assembled through the thread. The distributor 3 switches the hydraulic energy flow to the cylinder 1 or the hydro motor 2. The connection between hydraulic station and the hydraulic head is made with flexible pipes. The hydraulic station also provides the necessary energy for the pressure samples to which the hydraulic cylinders are repaired. After repair and installation, the cylinder remains attached to the pressure support frame. The repaired cylinder in ‘filled’ with low pressure oil. The high pressure required for the checks is provided by a pneumo-hydraulic accumulator that has been “charged” in the unlocking / locking of the threaded screws. [3]

3. Hydraulic scheme

The hydraulic scheme is presented in Fig. 3.

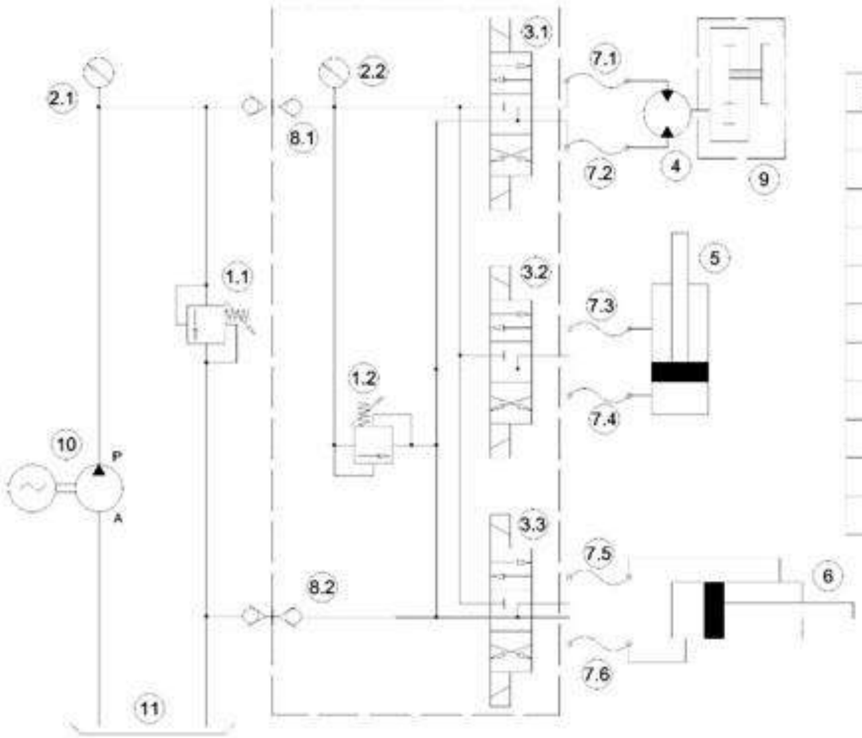

Item	Name
1	Safety valve
2	Manometer
3	Directional control valve
4	Hydraulic orbital engine
5	Hydraulic unlocking cylinder
6	Hydraulic drawing cylinder
7	Flexible connection
8	Quick coupling
9	Speed reducer
10	Electro pump
11	Oil reservoir

Fig. 3. Hydraulic scheme

The electro pump 10, the safety valve 1.1, the pressure gauge 2.1 and the assembled tank 11 are included in the hydraulic station. The hydraulic extraction cylinder 6 belongs to the support frame. The rest of the devices are part of the structure of the hydraulic head.
The hydraulic power required for the equipment is provided by the electropump 10 which sends the fluid under pressure to the distribution block. Hydraulic motor 4 performs screwing / unscrewing the threaded assemblies of the cylinder. The hydraulic motor spindle speed is reduced to 6...10 rpm, as is best for threaded assemblies, by the reducer 9. Reversing the rotating direction corresponding to the direction of thrust / unwinding is done with the directional control valve 3.1.
Unblocking / locking of threaded screws is done with hydraulic cylinder 5 and directional control valve 3.2 reverses the sense of motion corresponding to lock or unlock.
The extraction or insertion of the piston rod together with the piston into the cylinder barrel is accomplished by the hydraulic cylinder 6 and the reversal of the means of the directional control valve 3.3.

4. Technical features

To screw / unscrew the threaded assemblies of the hydraulic cylinder, the equipment mush achieve a torque of up to 6000 Nm at a speed between 6 and 10 rpm. These are made up of an ensemble consisting of an orbital hydraulic motor and a planetary reducer, see Fig. 4.

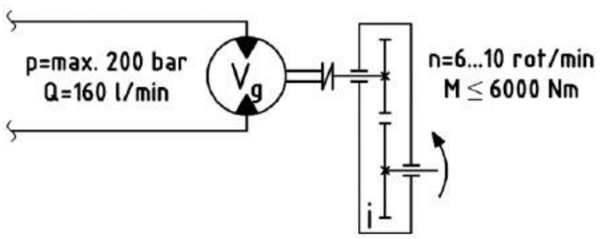

i – gear ratio of reducer
V_g – hydraulic engine capacity
n – screwing / unscrewing speed
M – screwing / unscrewing torque
Q – hydraulic engine flow
p – hydraulic engine pressure

Fig. 4. Assembly of hydro motor and speed reducer

The hydro motor reducer assembly receives a flow rate of 16 l/min at a pressure of maximum 200 bar and must provide a maximum torque of 6000 Nm at a speed of 6 … 10 rpm. Three variants of orbital hydraulic engine with characteristics of V_g = 50, 100 and 150 cm^3/rev and three variants of transmission ratios of the reducer: i = 10, 20 and 30.
The results of the analyses are presented in the diagrams of Fig. 5.

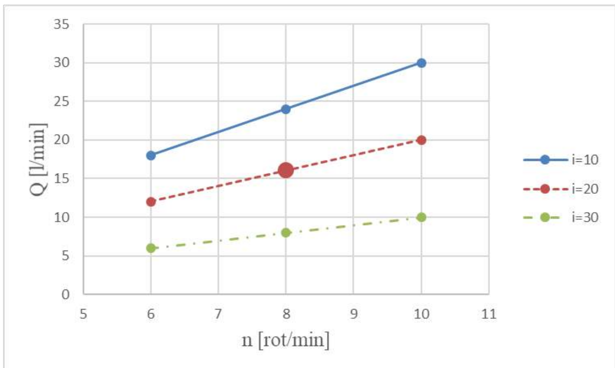

a) Diagram n – Q

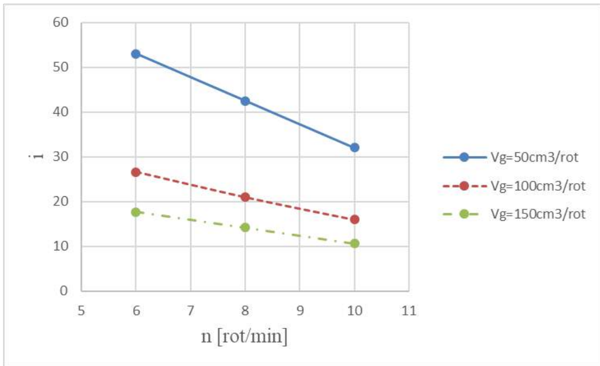

c) Diagram n – i

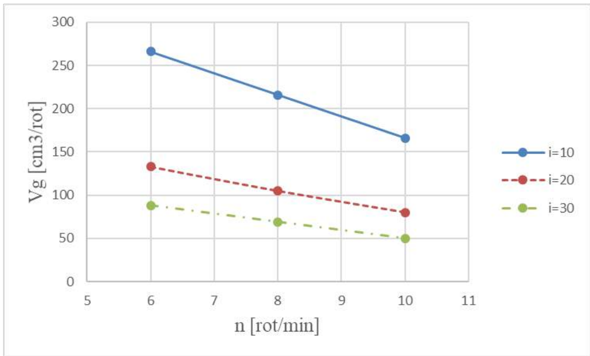

b) Diagram n – V_g

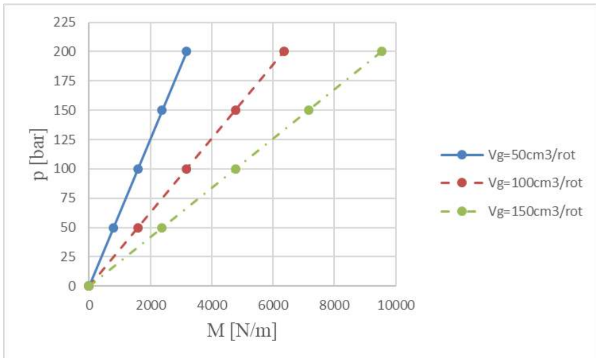

d) Diagram M – p

Fig. 5. Diagrams

It follows from these diagrams that the optimal variant is that of the hydraulic motor with V_g = 100 cm^3/rev and the gear ratio with the transmission ratio i = 20. This combination provides a torque of M = 6000 Nm and a speed of n = 8 rpm, if it receives a flow of 16 l/min at 190 bar. At a pressure of 200 bar the developed torque is M = 6360 Nm.

5. Conclusions

The hydraulic equipment presented is a particularly useful tool for hydraulic cylinders “service” mainly because it facilitates the operator’s work by using hydraulic power instead of the strength of the arms.

The equipment provides the basic operations for the quick dismantling / refitting of hydraulic cylinders:

- unlocking threaded assemblies to loosen the cylinder caps and piston retaining nuts.
- quick screwing and unscrewing of cylinder caps and piston nuts.
- extracting and rapidly inserting piston rods into the cylinder.
- adjusting the position of the parts to ensure their coaxiality so as not to damage the seals during reassembly.

Acknowledgments

This paper has been developed in INOE 2000-IHP, with the financial support of the Executive Agency for Higher Education, Research, Development and Innovation Funding (UEFISCDI), under PN III, Programme 2-Increasing the competitiveness of the Romanian economy through research, development and innovation, Subprogramme 2.1- Competitiveness through Research, Development and Innovation - Innovation Cheques, project title: "Working bench for reconditioning hydraulic cylinders", Financial Agreement no. 53 CI/2017.

References

[1] http://www.shredfast.com/core-charges/ - 2017;
[2] http://www.tuxco.com/products/hydraulic-cylinder-service-equipment.asp – 2017;
[3] V. Bălășoiu, *Echipamente și sisteme hidraulice de acționare și automatizare,* Mașini volumice, 2007.

ISSN 1454 - 8003
Proceedings of 2017 International Conference on Hydraulics and Pneumatics - HERVEX
November 8-10, Băile Govora, Romania

THERMOGRAPHIC INVESTIGATION OF THE HYDRAULIC DRIVE SYSTEMS

Teodor Costinel POPESCU[1], Alexandru-Daniel MARINESCU[1], Alina Iolanda POPESCU[1], Ana-Maria Carla POPESCU[1]

[1] Hydraulics and Pneumatics Research Institute INOE 2000-IHP, popescu.ihp@fluidas.ro

Abstract: *The authors develop a new non-contact diagnostics of hydraulic drive functional plants. It is based on infrared thermography of rotary and linear volumetric machines, as well as two-phases hydraulic equipment: a "no wear" phase, performed at plants commissioning tests, where these components are news or recently repaired, respectively "with possible wears" phase, performed during the periodical technical revisions. By comparing the two sets of thermograms, "standard" and "reals", of the same hydraulic drive plants, we can detect in early the components with wears in incipient or advanced form and we can take precautions to avoid the accidental interruption of the plant operation.*

Keywords: *Thermographic investigation, hydraulic drive systems*

1. Introduction

Thermographic investigation of the industrial machinery and equipments is a component of the maintenance work, that provides the necessary informations on defects and early wears. These informations allows to be taken timely correction necessary measures to reduce the risk of damages.The infrared thermography is a non-destructive control technique, typically used to detect and locate mechanical and electrical defects, which is manifested by overheating components of the machine or its plants.
It is known that the infrared thermography is a latest technology, in the field of the modern diagnostic methods in industry, delivering high precision results, which lead to reduce the faults detection time and performing assessment of the equipments state in operating time, without it may be necessary to stop them, or to perform more complicated operations, such as them dismantling and transporting to a diagnostic center.The method is currently used in multiple technical applications in: the industrial field, the most important branches being energy, electrotechnics, electronics and microelectronics, machine building industry, petroleum industry or metallurgical / steel industry, manufacturing; construction field; the field of technological processes, such as the welding process; the field of medicine and others.
Hydraulic drive systems are characterized by the combined action of the thermal conduction, by the internal energy accumulation and mixing motion, the convection being the most important heat exchange mechanism between the solid surfaces and hydraulic oil, between there is direct contact and relative motion.As a result of the time operation of hydraulic drives plants, some components wear out more or less,having on thermal images, respectivelly on "thermograms", which shows "thermal maps", zones with different "overheating", compared to "standard thermograms", depending on the wear degree.In present, have not developed non-contact diagnostic methods based on infrared thermography at the level of the hydraulic drive system as a whole. However, there are known examples of the use of infrared thermography for diagnosis at the level of a hydraulic component, such as a cylinder, a pump or a hydraulic motor.
The system proposed by the authors represents an extension of the infrared thermography diagnosis from the hydraulic component to the level of the hydraulic drive plant.

2. Examples of hydraulic cylinders diagnosis by infrared thermography

An example of the practical application of infrared thermography for the diagnosis of hydraulic cylinders for terrain equipments is the one made by **SIMCO** in Spain on a Caterpillar charger 993 K

CAT, Z9K series (Fig. 1) provided with six hydraulic cylinders acting the bucket drive: two for lifting, two for lower tilting and two for upper tilting(Fig. 2).

Fig. 1. Caterpillar charger

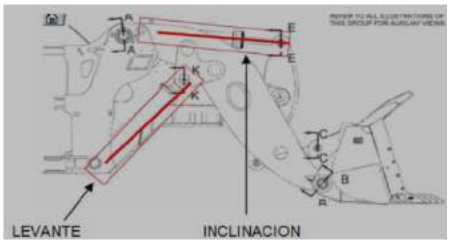

Fig. 2. Hydraulic cylinders for lifting and tiltingof the machine bucket

The machine task book provides 8000 operating hours under normal conditions for the hydraulic drive plant of the bucket. After a normal operating time, the machine beneficiary finds that the bucket lifting is slower and, therefore, is addresses to **SIMCO** for diagnosis.
Prior to thermography diagnosis, check the functional parameters of the bucket machine driving cylinders (table 1 and table 2).

Table 1: Lifting / down bucket times

Measuredpa rameter	**Manufacturer's standard**	**M1**	**M2**
Bucket lifting time (s)	9,4	11	11
Bucket down time (s)	3,7	4	4,1
Pump pressure (psi)	2900	2850	2850

Table 2: Higher / Lowerbucket tilting times

Measured parameter	**Manufacturer's standard**	**M1**	**M2**
Higher tilting time bucket (s)	2,4	3	3
Lower tilting time. bucket (s)	2,1	3	3
Working temperature (°C)	65	64	66

It was noticed that the machine was not working properly due to the internal pressure loss at the lifting cylinders, which worked slowly. It was decided making thermal images to all the drive bucket hydraulic cylinders, after the machine commissioning, the drive bucket and the hydraulic oil temperature raising to 75 ºC.

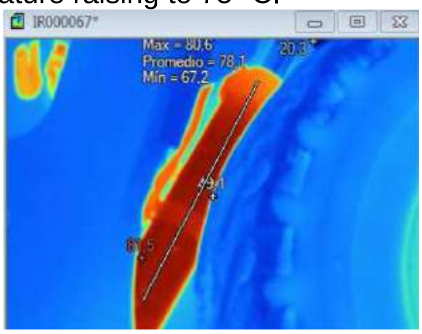

a. Right lifting cylinder

Temp.	Max	Average	Min
[°C]	80,6	78,1	67,2

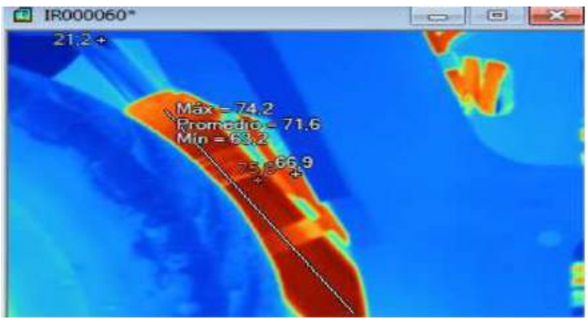

b. Left lifting cylinder

Temp	Max	Δ	Average	Δ	Min	Δ
[°C]	74,2	6,4	71,6	6,5	66,9	0,3

Fig. 3. Thermal images of bucket lifting cylinders

The thermal images of the bucket lifting cylinders (Figure 3) were analyzed and the maximum, minimum and average operating temperatures were compared, measured on two equal lines (one

on each cylinder) parallel to the axes of the cylinders, with the same number of measuring points, identically positioned. It is noted that the maximum, average and minimum temperatures of the right cylinder (Fig. 3a) are higher by 6.4 °C; 6.5 ° C and 0.3 ° C respectively than those of the left cylinder (Figure 3.b), so the lifting cylinders are not work at the same load. The explanation is the damage of the left cylinder piston seal, due to internal pressure loss occurs, respectively oil leaks from the active chamber in the passive chamber of the cylinder.
Further, the thermal images of the left / right cylinder pairs for the higher tilting (Figure 4.a) and for the lower tilting (Figure 4.b) of the bucket were analyzed.

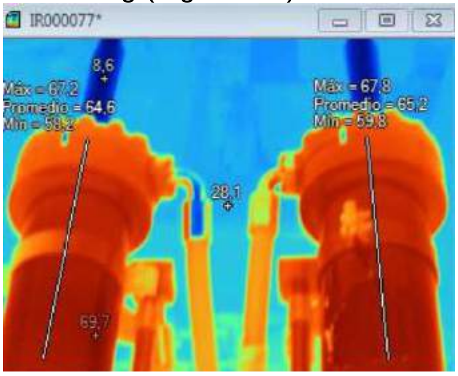

a. Higher tilting left / right cylinders

Left cylinder

Temp.	Max	Average	Min
[^{o}C]	67.2	64.6	58.2

Right cylinder

Temp	Max	Δ	Ave.	Δ	Min	Δ
[^{o}C]	67.8	0.6	65.2	0.6	59.8	1.6

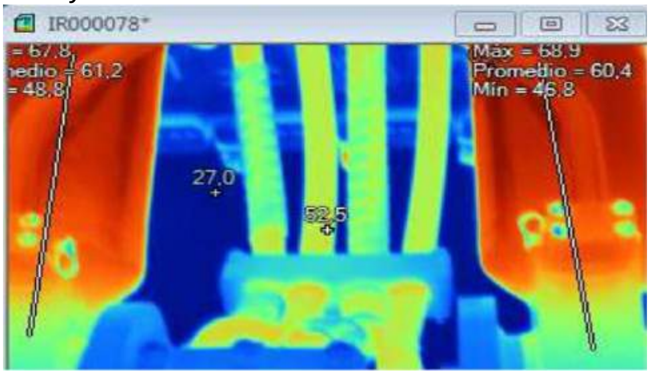

b. Lower tilting left / right cylinders

Left cylinder

Temp.	Max	Average	Min
[^{o}C]	67.8	61.2	48.8

Right cylinder

Temp	Max	Δ	Ave.	Δ	Min	Δ
[^{o}C]	68.9	1.1	60.4	-0.8	46.8	-2

Fig. 4. Thermal images of bucket tilting cylinders

The thermal images of the higher bucket tilting cylinders (Figure 4.a) were analyzed and the maximum, minimum and average working temperatures measured on two equal lines (one for each cylinder), parallel to the axes of the cylinders, with the same number of measured points, identically positioned. It is found that the maximum, average and minimum temperatures of the right cylinder are greater by 0.6 °C; 0.6 °C and 1.6 °C respectively than those of the left cylinder.
The thermal images of the lower tilting bucket cylinder (Figure 4.b) were analyzed and maximum, minimum and average temperatures were compared, measured on two equal lines (one on each cylinder) parallel to the cylindrical axes, with the same number of measuring points, identically positioned. It is noted that the differences between the maximum, average and minimum right cylinder temperatures relative to the left cylinder are of 1.1 °C; -0.8 °C or -2 °C above those of the left cylinder.
Due to the fact that the temperatures differences (especially average temperatures) between the left / right cylinders for the higher / lower tilting of the bucket are under 1 ° C, it is concluded that the left / right cylinders work at the same load for the higher and lower tilting of the bucket.

The final conclusion *of the thermographic diagnosis of the six actuating cylinders of the Caterpillar charger's bucket is the replacement of the internal sealing system of the lifting left cylinder.*

3. Method and system of thermographic investigation of the hydraulic drive systems

The hydraulic drive systems are characterized by the combined action of the thermal conduction, of the internal energy accumulation and of the mixing motion, convection being the most important heat exchange mechanism between solid surfaces and hydraulic oil, between them being direct contact and relative motion. As a result of the time operation of the hydraulic drives plants, some

components wear out more or less, having on thermal images, respectively on the "thermograms", which shows "thermal maps", different "overheating" zones compared to "standard thermal images", depending on the degree of wear.
The authors proposed method comes to support the corrective, predictive and preventive maintenance of hydraulic drive plants, characterized by a high degree of complexity and a large number of components. Without contact and early detection of the used components, from an on-board hydraulic drive plant, being in operation, reduces the cost of its maintenance system.
As a rule, for the detection of a defective or worn component from a hydraulic drive plant, all the components in a plant are dismantled and individually tested on specialized stands.
A method and an investigation system are proposed which have the advantage of removing of this impediment, by finding without contact of the the unused components and respectively dismantling only them from the plant (Fig. 5).

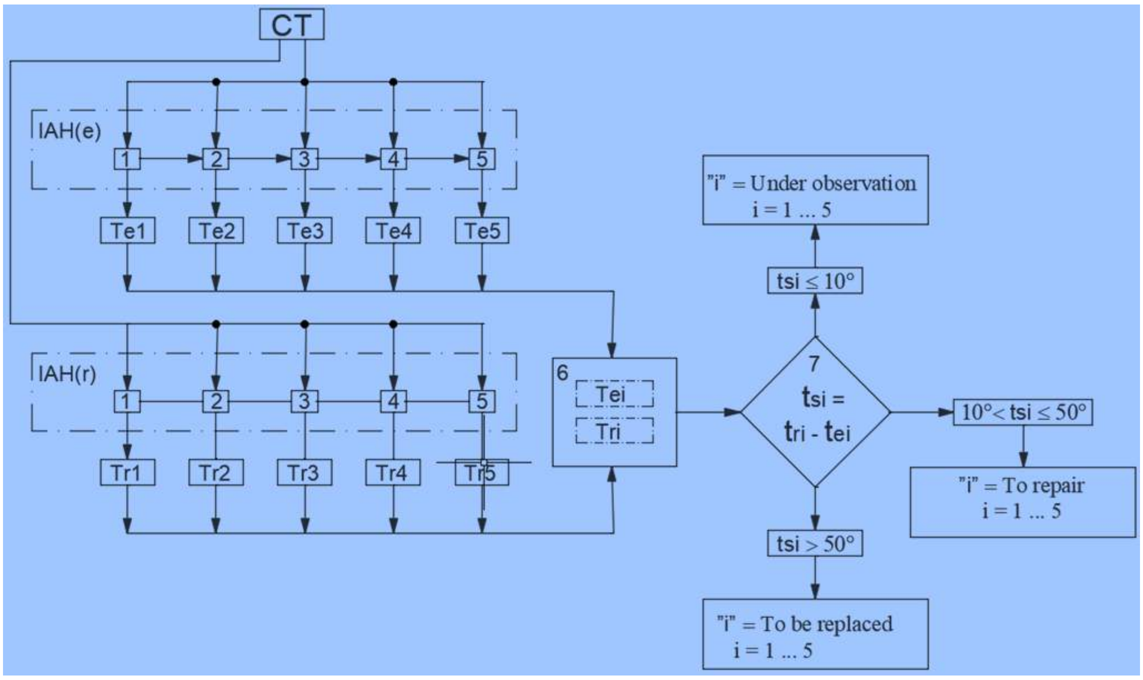

Fig. 5. Method and systemof thermographic investigation of the hydraulic drive systems

The invention also has other advantages in terms of reducing the cost of maintenance of the hydraulic drive systems, serving fixed machinery and equipments, from the manufacturing or mobile flows.The authors proposed method and diagnostic system, presuppose the use of a **CT** thermal imaging camera with which it scaned in thermal images, during the commissioning tests, all the parts of a new hydraulic drive plant , called the standard equipment, **IAH (e),** and all the components of the same installation, called technically revised plant**, IAH (r),** during the periodical technical inspection, namely: oil tank, filters, the hydraulic oil temperature control system **1**; their pumps and their drive motors **2**; pipes, hoses, fittings, hydraulic bindings **3;** valves, hydraulic distributors, throttles, regulators **4**; linear hydraulic motors, rotary hydraulic motors **5**.After the first thermal images scanning, a database of five sets of **Te1** ... **Te5** standard thermal images results, and after the second thermal images scanning, another database with five sets of revision thermal images**Tr1 ... Tr5** results. . The both databases are stored in a module **6**, from where they are taken over by the programmable machine **7**, which, based on a specialized software, compares the thermal images, calculates the overheating of each component of the technically revised plant, then inserts it into one of the three files, namely "**under observation**", "**repaired**", "**to be replaced**".
The "**under observation**" file contains all components of the plant where overheating, ie the difference between the temperature of the standard component and the temperature of the

technically revised component, is incipient (ts ≤ 10°C). These components will be first thermally scanned at the next scheduled technical revision.
The "**repaired**" file contains all the plant components with the overheating in the range of 10°C < ts ≤ 50oC. These components have an advanced overheating, are worn out and no longer achieve functional parameters, but can still be repaired.
The "**to be replaced**" file contains all plant components with the ts > 50 ° C overheating. These components have a serious overheating, very high wear, no longer achieve functional parameters and, as a rule, can not be repaired.
The use of the method and diagnostic system of hydraulic drive plants proposed by the authors, requires that the two thermal images scans of the new and revised hydraulic drive plant components, be carried out under the **same conditions as**:
- **the ambient temperature** in which the plant operates;
- **the temperature of the working fluid** respectively the hydraulic oil flowing through the plant;
- **nominal loads of 50% ... 100%,** ie resistant torques and speeds for rotary hydraulic motors, respectively, resistant forces and speeds for the linear hydraulic motors.

If, during the periodic revision inspection tests of the hydraulic drive plant, the nominal loads can only be achieved in less than 50% of nominal values, a correction must be applied to the temperature values calculated as superheating of the components.

4. Conclusions

-The method and system of investigation proposed by the authors is in support of the corrective, predictive and preventive maintenance of hydraulic drive plants.
-The success of the thermographic investigation of the hydraulic drive systems requires a close collaboration on the maintenance subject of these systems between designer, manufacturer and the beneficiary, namely.
-It is recommended to the components and hydraulic drive designers to determine a set of basic principles for reading, interpreting and comparing of the "real thermal images" with the domain-specific "thermal images".
-It is recommended to manufacturers of pumps, hydraulic motors / hydraulic cylinders, regulating and controlling the flow and pressure equipments to be included in the technical catalogs of the products together with the functional characteristics / parameters and of the "standard thermal images" for which the respective functional parameters are achieved.
-It is recommended to the users of hydraulic drive machines and equipments to make their own bases of "standard thermal images" done on the components of the functionally hydraulic drive plants, during commissioning of the new plants or after capital repairs.

Acknowledgments

This paper has been developed in INOE 2000-IHP, with the financial support of the Executive Agency for Higher Education, Research, Development and Innovation Funding (UEFISCDI), under PN III, Programme 2-Increasing the competitiveness of the Romanian economy through research, development and innovation, Subprogramme 2.1- Competitiveness through Research, Development and Innovation - Innovation Cheques, project title: “Power recirculation stand for hydraulic cylinders testing”, Financial Agreement no. 50 CI/2017.

References

[1] Caterpillar- New Wheel Loaders 993 K https://www.cat.com/en_AU/products/new/equipment/wheel-loaders/large-wheel-loaders/18366798.html;
[2] Caso 3 – Termografia Hidraulica Cilindros - Simco Sistema de Monitoreo Condiciones https://www.yumpu.com/es/document/view/15180136/caso-3-termografia-hidraulica-cilindros;
[3] T.C. Popescu, A.-D. Marinescu, A.I. Popescu, ”Method and system for diagnosing of functionally hydraulic drive plants using infrared thermography”, Patent application No. A/00748/27.09.2017 („Metodă și sistem de diagnosticare a instalațiilor funcționale de acționare hidraulică, utilizând termografia în infraroșu”, Cerere brevet de invenție Nr. A/00748/27.09.2017).

ISSN 1454 - 8003
Proceedings of 2017 International Conference on Hydraulics and Pneumatics - HERVEX
November 8-10, Băile Govora, Romania

ELABORATION OF AUTONOMOUS IRRIGATION SYSTEMS INTEGRATED WITH PHOTOVOLTAIC

Ion BOSTAN[1], Viorel BOSTAN[1], Valeriu DULGHERU[1], Ion SOBOR[1], Nicolae SECRIERU[1], Oleg CIOBANU[1], Radu CIOBANU[1], Valeriu ODAINÂI[1], Sergiu CANDRAMAN[1], Andrei MARGARINT[1]

[1]Technical University of Moldova; valeriudulgheru@yahoo.com

Abstract: *The autonomous irrigation systems integrated with PV, a method of PV pump system calculation for small irrigation and control of agricultural processes are presented. The solar radiation calculation was performed with PVGIS software. The numerical example contains pump flow rates, pumped water volumes (daily, monthly and for all irrigation period)*

Keywords*: Photovoltaic installation, water, solar radiation, solar pump*

1. Introduction

According to the long-term meteorological data during the active vegetation period, the average precipitation amounts of 235 mm in the southern region and of 330 mm in the northern region [1]. Natural moisture is insufficient to obtain expected crops, especially vegetables, even in the years with average climatological characteristics. Often the territories of Moldova, Romania and Ukraine are subject to long-term droughts. Long-term observations indicate that this region is under the influence of a relatively dry 12-year climate cycle and the drought rate is increasing. Figure 1 shows the dynamics of the dry years of the X-XX centuries. The analysis of the drought development data of the 20th century reveals that in the following years the drought will repeat every 2-nd, 3-rd or 4-th year [2]. At the same time, there is a drastic decrease of the irrigated land, figure 1 [1]. The difficulty of this problem varies from country to country, being more striking in those countries that lack fossil energy sources and sufficient sources of potable water for irrigation. RM is a part of this category of countries, which covers from the import about 86% of the needed energy resources and produces only 18,4 % of the electricity consumption.
The main causes of the decrease of irrigated surfaces after 2010 are:

1. Because of privatization, about one million farmers possessing agricultural land with an area not exceeding 2,5 ha have appeared.

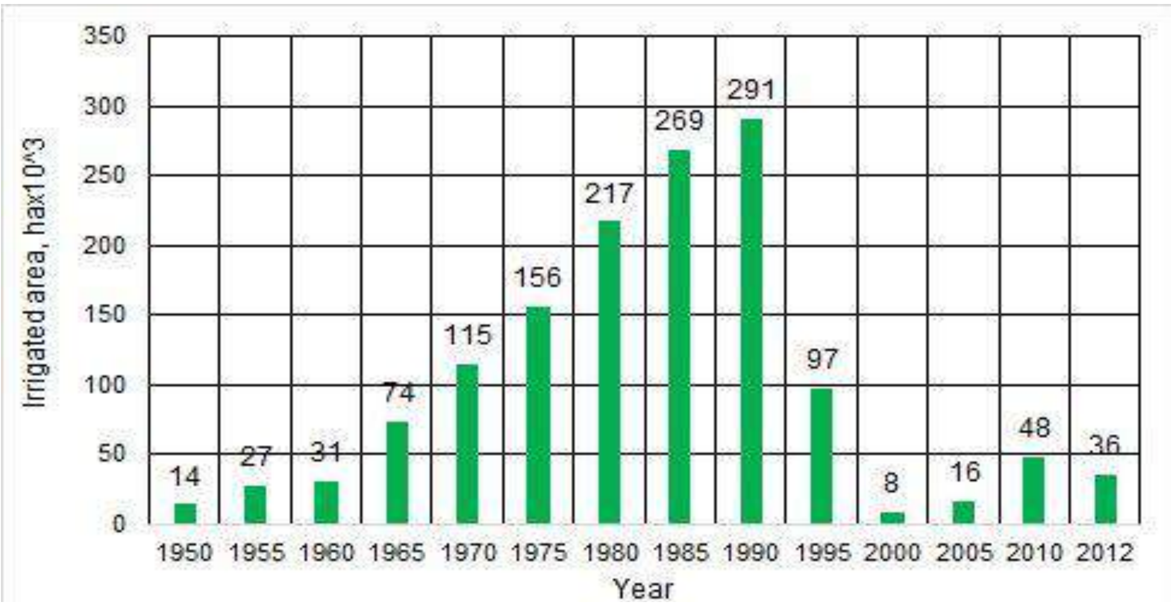

Fig. 1. Variation of irrigated surfaces during 1950-2012

2. Increasing the cost of electricity tenfold.

Existing systems designed to irrigate large areas and with excessive energy consumption have become uncompetitive.

Therefore, taking into account the provisions of the strategy, the development of automation tools in the agri-food sector is an activity meant to facilitate these provisions. In the following compartments we will present the automation facilities for irrigation installations, realized within the UNDP project "*Autonomous integrated irrigation systems based on wind turbines, small hydro and photovoltaic installations*".

2. The photovoltaic pumping

A modern and energy-efficient solution that meets new market conditions is the photovoltaic pumping system, known since 1980s of the last century. In the last five years the cost of solar modules has significantly decreased and photovoltaic irrigation becomes competitive within traditional systems. A growing number of countries launch programs to accelerate the solar technology development. Republic of Moldova is taking the first steps in this field, only a few experimental photovoltaic pumps have been implemented and there is no program to support this technology. The paper presents a PV pump system sizing method for farmers intending to implement low-power photovoltaic systems for small irrigation.

Regardless of the irrigated land particularities the sizing procedure of the PV pumping system comprises several necessary steps to be taken.

2.1 Water requirement

The first step in designing a solar-powered water pump system is to determine the overall water requirement for the operation. In other words, we need to know the required water volume or irrigation norm, the water volume distribution during irrigation, and the daily water requirement etc. These data are available in the literature [1,3] or by consulting agricultural specialists.

2.2. Determining the solar radiation for your location

Appropriate data should be used to determine the amount of solar radiation available at the site. These data are available in the archive of the State Hydro Meteorological Service (SHMS) or in [2,3]. With them, the global solar radiation, G_β in W/m^2, on tilted surface or PV pane can be calculated l. The used formula is the following [3]

$$G_\beta = R_b B + \frac{1}{2}(1+Cos\beta)D + \frac{1}{2}(1-Cos\beta)\rho G, \qquad (1)$$

where R_β is the ratio of total radiation on the tilted surface at angle β to that on the horizontal surface; B – direct or beam radiation; D - diffuse radiation; G – global radiation on the horizontal surface; ρ – reflectance coefficient. The *B, D* and *G* values can be found in [4]. All data are for a horizontal surface as a possessing result of SHMS measurements for the period of 1954-1980.

In [4] are presented numerical values of the ratio R_b for the difference of latitude ϕ and inclination angle β (every 5^0) and the latitude of the place (every 5^0). Based on these data the values of the report R_b for Moldova were interpolated. The territory was divided into three areas - south (latitude 46^0), center - (47^0 latitude) and north - (latitude 48^0). Linear interpolation was used, the difference ϕ - β ranges from 0 to ± 20^0 with a step of 5^0. Numerical data of R_b can be found in [5,6].

Using (1) we can calculate the daily global solar radiation, G_β for a different month for each 3 hour: 6^{30}, 9^{30}, 12^{30}, 15^{30} and 18^{30}. In this case we should use data about *B, D* and *G* published in [4].

EU countries have developed a free online software for calculation of diurnal and monthly solar radiation. The diurnal radiation is calculated every 15 minutes. For the calculation a new database Climate-SAF PVGIS [7] is used. These data are based on satellite images performed by CM-SAF (Geostationary Meteosat and Polar EUMetSat). The database represents a total of 12 years of data. From the first generation of Meteosat satellites, known as MFG, there are data from 1998 to

2005 and from the second-generation Meteosat satellites, known as MSG, there are data from June 2006 to May 2010. The coverage extends from 0° N (equator) to 58° N and from 15° W to 35° E. These data are more representative of the last climate years, and show often higher irradiations than the classic PVGIS data.
Using this software [7], we calculated the diurnal radiation at Chisinau meteorological station on horizontal surface and we compared them with the ones from the 1954-1980 period. The results are included in Table 1.

Table 1: Diurnal radiation, kW/m^2

Month / hour	April			May			June			July			August			September		
	[4]	PVGIS	Diff., %	[4]	PVGIS	Diff., %	[4]	PVGIS	Diff., %	[4]	PVGIS	Diff., %	[4]	PVGIS	Diff., %	[4]	PVGIS	Diff., %
6^{30}	0.10	0.14	+40	0.19	0.23	+15	0.24	0.26	+8.3	0.21	0.25	+19	0.14	0.19	+36	0.07	0.08	+14
9^{30}	0.44	0.46	+4.5	0.55	0.57	+3.6	0.62	0.59	-4.8	0.60	0.60	+0.0	0.55	0.55	+0.0	0.45	0.41	-8.9
12^{30}	0.53	0.55	+2.8	0.62	0.67	+8	0.72	0.68	-5.5	0.70	0.70	+0.0	0.66	0.66	+0.0	0.55	0.49	-11
15^{30}	0.31	0.37	+19	0.39	0.48	+23	0.46	0.50	+8.7	0.47	0.50	+6.4	0.41	0.45	+9.8	0,29	0.31	+6.9
18^{30}	0.01	0.03	+200	0.05	0.11	+120	0.09	0.14	+55.5	0.09	0.12	+33	0.04	0.06	+50	n/a	n/a	n/a

We note the following:
1. The average error from April to September in the period 9^{30} - 15^{30} does not exceed + 3.0%.
2. Early in the morning (6^{30}) and evening (18^{30}) the errors are high and may exceed 100 %. But this does not affect the calculations because at the respective hours the PV pump does not work.
3. The calculated diurnal radiation values based on the new Climate-SAF PVGIS database are higher compared to those from 1954-1980. In our view, these are the consequences of global climate change.

In the present paper, we used the new Climate-SAF PVGIS database and free online software for calculation of diurnal radiation [7].

2.3. Total dynamic head

The total dynamic head (H) for a pump is the sum of the vertical lift, pressure head, and friction loss. The friction losses apply only to the piping and appurtenances between the point of inlet and the point of water distribution in the irrigation pipeline. Therefore, friction losses between the water basin or storage tank and the point of use are independent from the pump and do not need to be accounted for when sizing the pump. So, the H is equal:

$$H = H_G + H_L + H_P, \tag{2}$$

where H_G – is vertical lift or the geodetic height measured from the water level and the highest point of water lifting; H_L - friction losses; H_P – pressure head or the pressure required for the proper functioning of sprinklers or drippers expressed in m.

2.4. Selecting the pump and solar array

Depending on the water source we can select a surface pump or a submersible pump. For PV systems, special pumps, called solar pumps, are also produced. It is characterized by higher efficiency and stable operation under conditions of variation of solar radiation [8,9]. As an example, in fig. 2 are presented the variations of solar pump flow over the course of days for different months.
Depending on the required flow Q and TDH, we can find the power and then select the PV panel with adequate peak power.

2.5. PV panel mounting

As a rule, the PV panel is mounted on special frames and directed to the south. To increase efficiency, we recommend adjusting the inclination angle to the horizon. As the irrigation period in

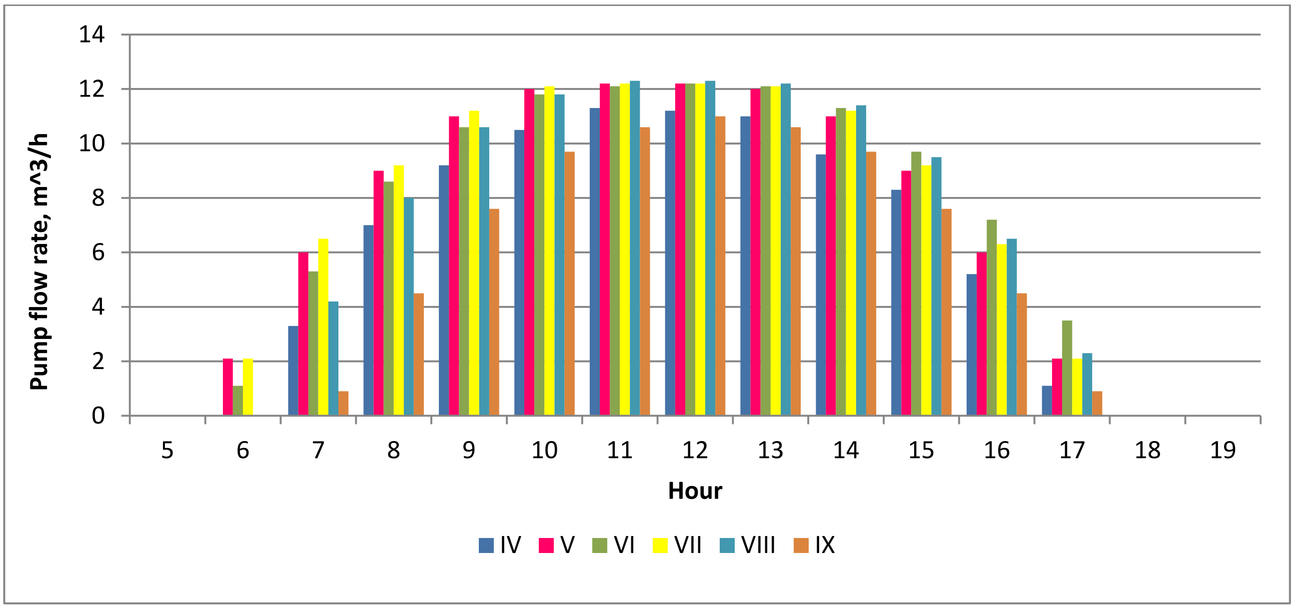

Fig. 2. Variation of solar pump flow over the course of days for different months

the Republic of Moldova is about 6 months (April - September), it is rational to change this angle once in a month. In the table 2 are included the optimal inclination angle for April – September, valid for the central region (latitude $\phi = 47^0$).
If a panel is to be mounted on an existing structure, that structure must first be analyzed to ensure that it has the necessary structural integrity to withstand all local wind, snow, and ice conditions.

Table 2: Optimal inclination angle

Month	April	May	June	July	August	Sept.
Angle, grade	33	20	13	17	28	43

Daly, monthly and total delivery rates. For this purpose, we calculate daily solar radiation using PVGIS software, the power generated by the PV panel and the effective operating time of the pump per day. From the *Q (P, H)* characteristics the pump flow rate and daily water volume are determined.

3. The automatization, informatization and monitoring of the irrigation processes

3.1. Design of the control system

The design of the automated control system for monitoring and optimization to ensure the irrigation processes will be carried out taking into account the following factors: acquisition of climatic data from plantations, application of nutrients and pesticides, herbicides, information processing and automatic control of the irrigation system, such as the monitoring of renewable energy sources. On the other hand, the design of the automated system must take into account the location of renewable plants and resources. In other words, the system has to be territorially distributed and it is reasonable to be hierarchized, considering the various issues that need to be solved.
Taking into account the experience of the most advanced companies in this field as well as their own experience, a three- layer hierarchical system has been proposed. The bottom layer is the most sophisticated, inhomogeneous and dependent and specific of agricultural enterprises. At this level are placed the means of acquiring the climatic data on the plantation field, the means of controlling the valves and pumps with remote control, the means of accelerating the fertilization equipment, as well as the means of monitoring and control of the renewable resources.
The second layer of the system has preponderant communication functions with minimal computing capabilities, decision-making, in other words, a kind of gateway between the lower level and the upper level. The mission of this level is to provide communication coverage with all subsystems at the bottom level and to provide communications to the top level server (server).

Finally, the superior layer of the automation, monitoring and control system for irrigation systems is seen as a typical Internet solution, which will store all information on irrigated plantations as well as the state of the equipment and auxiliary subsystems. On the other hand, it must provide authorized access to users of this system. At the third level (server) will be first remote monitoring of several irrigation systems, groups of stations, including homing. If server monitoring and control node is connected to the Internet, then monitoring stations can be done from any point on the earth.
For any control and monitoring system, including for irrigation installations, data acquisition plays a primary role. For these reasons, it has been decided to build an acquisition subsystem based on an integrated sensor network. It was decided, taking into account the relief and climatic conditions of Rep. Moldova, that the control must be performed by an average performance microcontroller, which will operate autonomously and is monitored and guided by the two most powerful controllers by radio communication at short distances (up to 4-5 km). It was designed and realized the functional schema and real equipment of integrated sensors and valve control modules for irrigation system. The most important sides both of this modules are the autonomous electrical power subsystem with 20W photovoltaic panel and accumulator and remote data acquisition and control by means of radio communication. The integrated sensor includes a set of sensors: air humidity and temperature, soil humidity and temperature at 2 levels; rain sensor, luminosity; photovoltaic panel and accumulator voltage.
As the main goal represents creating architecture of the control unit with the greatest possible reliability (for a duration of 5-7 years of activity) based on small processors it is necessary to analyze all families of microcontrollers from Atmel, Motorola, Renesas, Texas Instruments to select the proper microcontroller for this task. Making a comparative analysis, we outline that three different solutions are required by several parameters simultaneously such as productivity, memory capacity, energy consumption, cost, accessibility and reliability:

a) uC MSP430F155 part of the MSP430 from Texas Instruments;
b) uC MC68HC912DT128A part of the Motorola HC12 family;
c) uC ATMega part of the Atmel family.

Given the specialization of microcontroller core functions of low layer for controlling data acquisition, control, regulation and distribution of electricity, telemetry control the thermal station control and a microcontroller auxiliary functions of quality analysis of electricity generated, it is necessary to analyze low consumption devices, which typically are designed for wind generators and irrigation systems. For the integrated sensor module, it has been decided to use the uC ATMega controller, with performance comparable to other controllers, a very low consumption and a lower price.
In the similar mode the valve control module can open/close 2 valve with DC electro-motors and communicate the states of the valves. One important performance is high velocity of data acquisition (all data may be received by 1-2 sec) and the low cost – about 150 dollars per unit.
The territorial location of the integrated sensors and the control modules with the valves is done depending on the specifics of the plantation land and the configuration of the irrigation installations. For this project it was performed the maps of integrated sensors and valve control modules for irrigation system for the concrete destinations: the farm Tri Dienal (from Criuleni) (fig. 3) and real view emplacement (fig. 4).

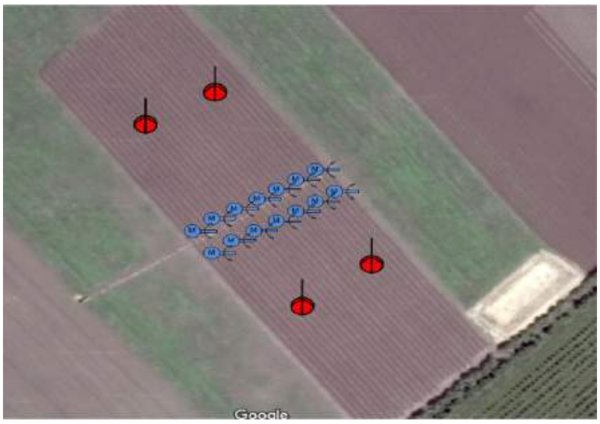

Fig. 3. Emplacement map of the integrated sensors module and the valve control module for irrigation system on Tri Denal (Criuleni) farm

It was decided to use one valve control module and one integrated sensor for 2 parcels (total 6 integrated sensor and 12 valve control modules) on the Fortuna Lapis farm and (total 4 integrated sensor and 14 valve control modules) for the Tri Dienal farm with the goal to minimize the cost of these equipment.

Fig. 4. Irrigation system for the farm Tri Dienal (from Criuleni): real view emplacement

3.2. The medium layer of irrigation control system

It is proposed a farm plantation medium layer control module for irrigation system, that coordinate all the processes for irrigation installation and for communication with high level (servers). For this case it is proposed the Rasberry controller with a higher computing performance and low cost. It was developed the software for this controller, which include more components for the coordinating the communication between low level modules and the servers.
Interaction between the turbine station controllers, integrated sensors and the monitoring system was proposed to be performed according to a model, for example, as shown in fig. 5, which implies the access of the users of the stations practically from an unlimited distance, which is reasonable by the use of communications and computers, including the Internet. The problem is simplified if the station controller connects to the network through units with a range greater than the previous one, sufficient to intercept the communications network. For such a case, high- speed and medium-to-high-speed radio communications, there is at the moment a whole range of possibilities and means. These means must meet the following requirements for this channel type: relatively low emission power, but high sensitivity; the possibility to modify the emission frequencies in a scheduled manner; GSM/GPRS communication modes; possibilities to maintain various communication protocols.

Applying this model, the medium-level controller architecture is proposed, which includes two different communication channels: one for low level interaction in the 435-450 MHz frequency band - the low-band radio amateur band and the second channel based on GSM / GPRS mode for connection to the Internet server. This is a farm plantation control module for irrigation system, that coordinate all the processes for irrigation installation and for communication with high level.

3.3. Monitoring and reports of the plantations irrigation process

Any system for monitoring various processes, including plantation irrigation, requires totalizing means / tools, reporting on current and cumulative outcomes. Therefore, a series of applications have been developed for the irrigation monitoring system, which allows the final user to make the necessary sums and conclusions. We present a series of such reports: the user can visualize the irrigation water consumption on the selected parcel during certain stages of planting development or throughout the season as compared to the irrigation rules and the precipitations (fig. 5), report about portions of irrigation norms about portions of irrigation norms, precipitations and irrigation volumes for the some phase of plant development (fig. 6).

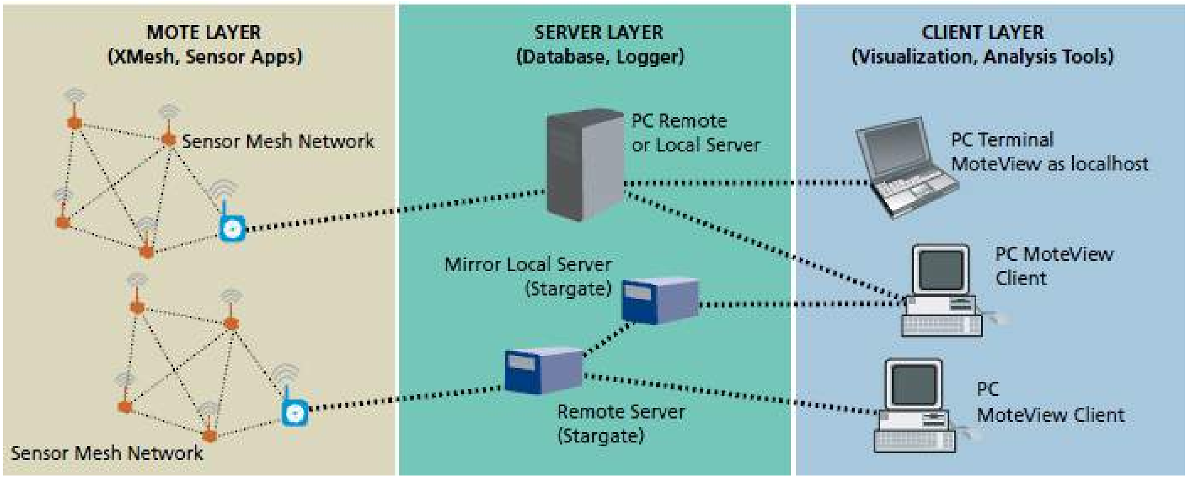

Fig. 5. The model of interaction between components of the irrigation system through various networks, including the Internet

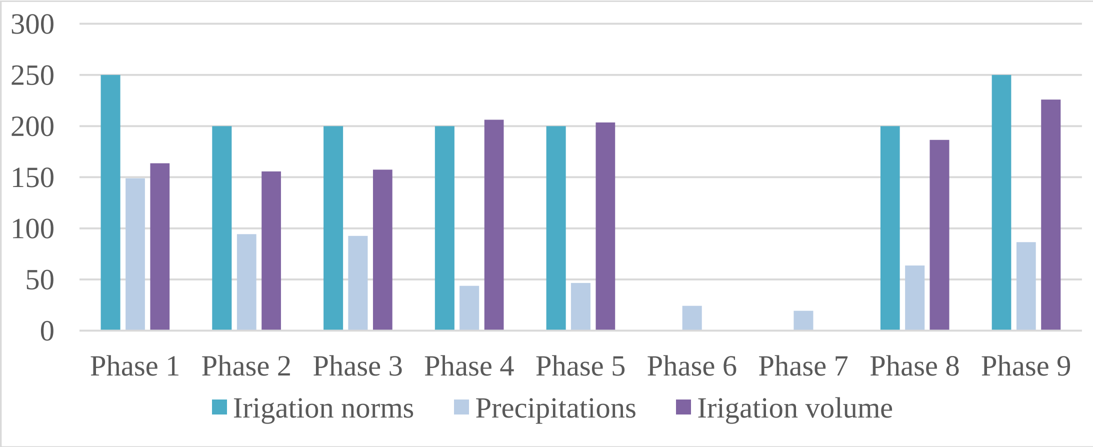

Fig. 6. Example of report diagram about irrigation norms, precipitations and irrigation volumes for the each phase of plant development

3. Results

The proposed land for irrigation presents a superintensive cherry orchard with a 7-ha area and is located in the west of the Criuleni town (central region), figure 3. The water for irrigation is pumped from a 9000 m^3 basin. The basin is part of a large irrigation system that uses water from the Dniester River. Thus, the basin is permanently filled. The solar pump drives water from the basin to the existing irrigation system.

The existing irrigation system is equipped with the SUPERNET™ UD Micro Sprinkler, the operating pressure of which must be 1,5-4,0 Bar [10].

Water Requirement. According to [11] the required irrigation water volume for superintensive orchard is about 5000 m^3/ ha. So, for the April - September irrigation period the required water volume is equal to V_R = 5000 ·7 = 35 000 m^3. For pump selection, we calculate the flow by dividing the required water volume to the number of pump operating hours during the irrigation period

$$Q = V_R /(N_D \cdot N_{hd}) = 35\,000/(170 \cdot 8) = 25{,}7 \text{ m}^3/\text{h}, \quad (3)$$

where N_D – number of days; N_{hd} - pump operating hours per day.

The total dynamic head. H_G = 5 m, H_L = 1,4 m (according to [12] for PVC pipe length-200 m, diameter-100 mm), H_P = 39 m (according to [11] the sprinkler operating pressure that will not exceed 4 Bar or 39 m of the water column). Thus, H = 45 m.

Pump selection. The most suitable pump for the calculated flow rate Q=26 m^3/h and H= 45 m is the Solar Surface Pump System PS7k2 CS-F20-5 [10], rated flow 27 m^3/h at H = 45 m The flow characteristics as a function of input power, $Q(P, H)$ are shown in fig. 7.

As shown in fig. 7, based on a calculated flow rate of 26 m^3/h (rounded) and a H of 45 m a minimum input of 5,8 kW of peak power is required. With daytime variation of solar radiation, the pump's operating point will slip on the $Q (P, H)$ characteristic.

PV panel selection. The PV panel selected for this system must be able to provide the minimum energy requirement to run the pump. In our case about 5,8 kW. However, the panels must have additional capacity to account for any potential reduction in power due to radiation data incertitude, high module temperature, dust, etc. Many PV manufacturers recommend increasing the minimum peak power value by 25 - 30 % to account for these environmental factors. To increase the pump's running diurnal time with a maximum flow, it is rational to increase power by another 50%. Therefore, the PV panel will be sized to provide a minimum output of 1,8·5,8 = 10,44 kW. We accept 11 kW.

Daly, monthly and total delivery rates. First, we calculate diurnal solar radiation using PVGIS software. The selected point coordinate Latitude: 47,200768, Longitude: 29,128662, the optimal tilted angle is 13^0, the panel is facing the south – Orientation: 0^0. The results are displayed every 15 minutes. In the same way, we did for all 6 months of the irrigation period. Diurnal radiation over each hour is shown in fig. 4 on the left. With hour solar radiation, the power generated by the PV panel is calculated using formula

$$P_{PV} = (R_{Daily}/1000)\cdot P_p\,, \tag{4}$$

where R_{Daily} – average hourly solar radiation as result of PVGIS calculation; P_p–PV panel peak power, 11 kW.

Using the pump characteristic $Q\ (P,H)$ for H = 45 m (fig. 7, red color) we determine the pump average hourly flow. The calculations are repeated for all pump operating hours. As a result, we get the daily pump flow variation, the daily and monthly volume of pumped water, fig.8, on the right.

During the irrigation period, the volume of pumped water is equal to the sum of the months volumes from April till September: V_{Total} = 40300 m^3 and is higher than the required by 15 %. We find a relative constancy of maximum solar radiation on the PV panel and the maximum flow rate of the pump, thus:

1. The maximum solar radiation on the PV panel is equal to 784 W/m^2 and corresponds to July. In April, the maximum radiation is lower by 15,3% and in September - by 21,2%.

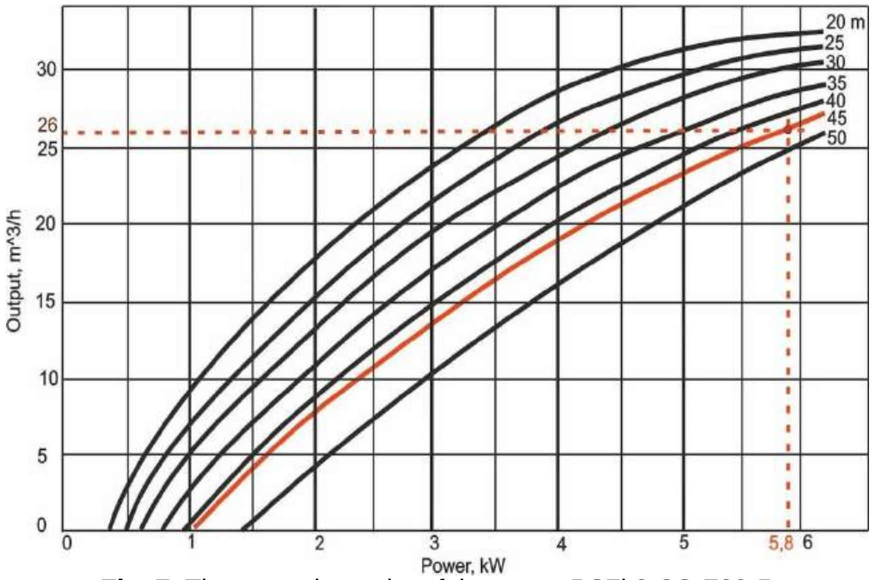

Fig. 7. The operating point of the pump PS7k2 CS-F20-5

2. In May-August over 4 hours a day, the system ensures a maximum flow rate of 27 m^3/h. In April, the maximum flow rate is lower only by 3,7 % and in September - by 4,4 %.

This relative solar radiation and pump flow constancy is due to the selection of a PV panel with higher power and the optimum inclination angle in April – September period.

5. Conclusions

During the irrigation period, the volume of pumped water is equal to the sum of the months volumes from April till September: V_{Total} = 40 300 m^3 and is higher than the required by 15 %. We find a relative constancy of maximum solar radiation on the PV panel and the maximum flow rate of the pump, thus:

- The maximum solar radiation on the PV panel is equal to 784 W/m^2 and corresponds to July. In April, the maximum radiation is lower by 15,3% and in September - by 21,2%.
- In May-August over 4 hours a day, the system ensures a maximum flow rate of 27 m^3/h. In April, the maximum flow rate is lower only by 3,7 % and in September - by 4,4 %.

The developed the hardware of acquisition, processing and communication for the remote control and management of irrigation installation and the realized software of the low and medium layers provide the remote control. The proposed architecture, software structure for the background and public servers can store all the data about irrigation processes.

It have been carried out on the automation of plantation's irrigation process: three irrigation planning and control modalities have been proposed and software testing has been carried out to ensure the high reliability of the information and command system and efficiency.

ISSN 1454 - 8003
Proceedings of 2017 International Conference on Hydraulics and Pneumatics - HERVEX
November 8-10, Băile Govora, Romania

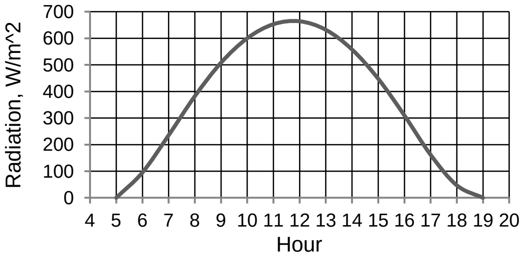

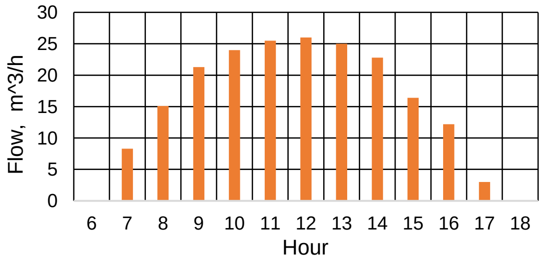

April, V_{IV} = 5268 m^3

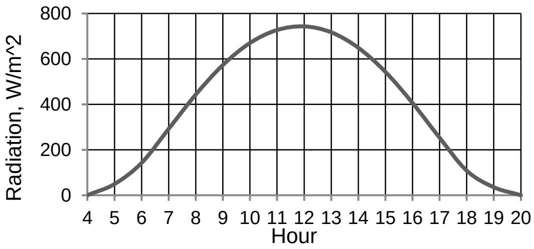

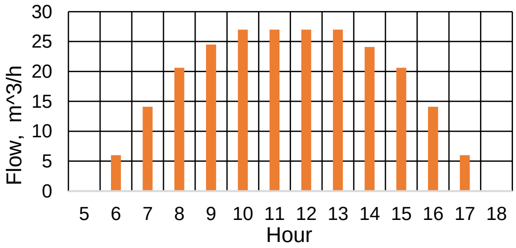

May, V_V = 7378 m^3

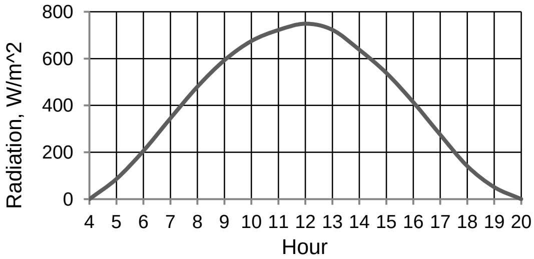

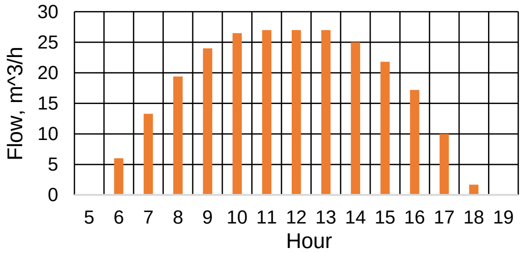

June, V_{VI} = 7377 m^3

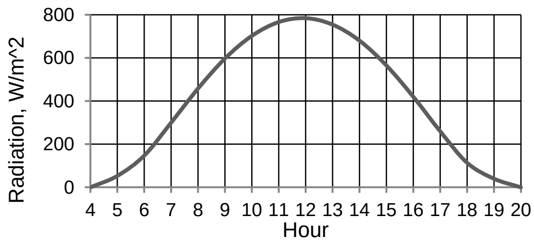

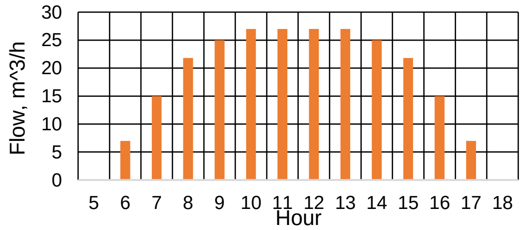

July, V_{VI} = 7614 m^3

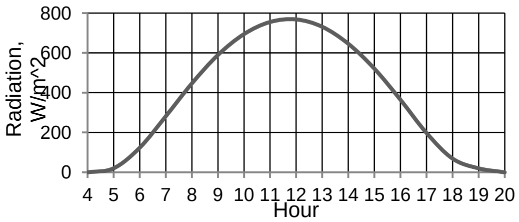

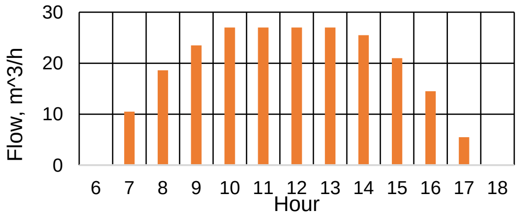

August, V_{VIII} = 7040 m^3

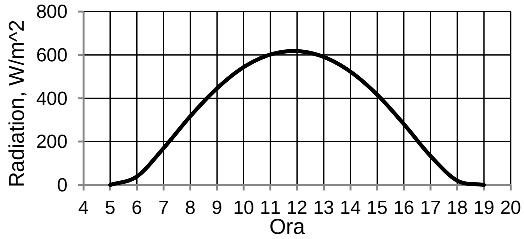

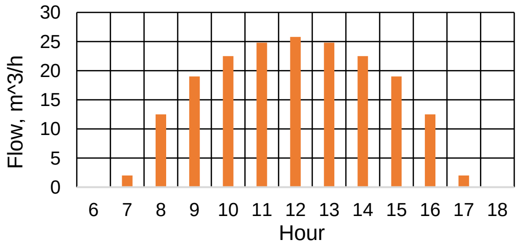

September, V_{IX} = 5622 m^3

Fig. 8. Hourly radiation (on left) and pump flow (on right)

Acknowledgments

This paper has been developed as part of a project co-financed by the Romanian government, project title: nr. 00055003. Autonomous integrated irrigation systems based on wind turbines, small hydro and photovoltaic installations.

References

[1] A. Gavrilița, “Modern problems of irrigation” (“Sovremennye problemy dozhdevaniya”). Ministry of Agriculture and Food of the Republic of Moldova. Kishinev. 388 s. 1993;
[2] S. Andrieş, V. Filipciuc, “Efficiency of irrigation under the conditions of the Republic of Moldova” (“Eficacitatea irigaţiei în condiţiile Republicii Moldova”). *Academos,* no.3, pp. 96-102. Ed. Ştiința, Chișinău. 2014;
[3] J.A. Duffee, W.A. Beckman, “Solar engineering of thermalprocesses”, 2nd ed. *A Wiley-Intersciance publication,* 919 p. 1991. ISBN 0-471-51056-4;
[4] Scientifically-referenced guidebook Climate USSR. Series 3: Multiplayer data (Nauchno-prikladnoj spravochnik po klimatu SSSR. Seriya 3: Mnogoletnie dannye). Chasti 1-6, Vyp.11, MSSR. Ed. Gidrometeoizdat, Leningrad. 1990;
[5] I. Bostan, V. Dulgheru, I. Sobor, V. Bostan, A. Sochireanu, “Renewable Energy Conversion Systems” (“Sisteme de conversie a energiilor regenerabile”). Ed. ”Tehnica Info, Chișinău, 592 p. (2007). ISBN 978-995-63-076-4;
[6] I. Bostan**,** A. Gheorghe**,** V. Dulgheru**,** I. Sobor**,** V. Bostan**,** A. Sochirean, “Resilient Energy Systems. Renewables: Wind, Solar, Hydro”. Ed. Springer, VIII, 507 p. 2013. ISBN 978-94-007-4188-1;
[7] http://re.jrc.ec.europa.eu/pvgis/apps4/pvest.php;
[8] https://www.lorentz.de;
[9] https://net.grundfos.com;
[10] www.netafim.com Micro sprinklers. Product catalog. – 2014;
[11] http://agrari s.ro/vegetal/irigarea-plantatiilor-de-mar;
[12] http://www.engineeringtoolbox.com/pvc-pipes-friction-loss.

ISSN 1454 - 8003
Proceedings of 2017 International Conference on Hydraulics and Pneumatics - HERVEX
November 8-10, Băile Govora, Romania

SPECIALIZED COMPUTING SOFTWARE FOR THE ASSESSMENT OF ENERGY EFFICIENCY AT THE LEVEL OF A STEAM BOILER

Silviu ANDREESCU[1], Claudiu-Ionel NICOLA[1], Marcel NICOLA[1], Sebastian POPESCU[1], Viorica VOICU[1], Marian DUȚĂ[1]

[1]National Institute for Research, Development and Testing in Electrical Engineering – ICMET Craiova
andreescu11@yahoo.com, nicolaclaudiu@icmet.ro, marcel_nicola@yahoo.com, tn.spopescu@icmet.ro, programe@icmet.ro, marianduta@icmet.ro

Abstract: *The assessment of energy efficiency at the level of a steam boiler, inside which an organized activity is carried out is a complex process whose outcome typically has a synthetic character. The performance indicators, either energy efficiency, or specific consumption, etc. were determined based on an algorithm for unit calculation, thus creating a consistent database for fast elaboration of optimal thermo-energetic audits, considering the measured and the determined thermal parameters. These calculation algorithms, specific to balance equations are included in the specialized computing software proposed for the analysis and processing of thermal quantities. The elaboration of such a specialized computing software for the analysis and processing of thermal quantities which are part of balance equations, for major industrial consumers commonly met in the practice of thermo-energetic audits, namely steam boilers, leads to the optimization of the activity from the point of view of thermal energy*.

Keywords*: Thermo-energetic balance, thermo-energetic parameters, computing software, LabVIEW*

1. Introduction

Energy resources represent an important part of material resources, the feedback of developed countries and others being materialized with reference to these resources through the development of the concepts of alternative energy, renewable energy, energy management and energy efficiency. Together, energy efficiency and protection of the environment constitute one of the major strategic objectives undertaken by the European Commission in the first European Energy Charter, signed at the Hague in 1991. The general directions for action recommended in the most recent documents include energy conservation, energy management, and the furtherance of new and renewable sources of energy. One of the most frequent thermo-energetic consumers on the market of energy audits is the steam boiler [1].

The assessment of energy efficiency at the level of a steam boiler, inside which an organized activity is carried out is a complex process whose outcome typically has a synthetic character.

Energy efficiency and inefficiency respectively cannot be measured directly, they can be expressed based on one or more energy efficiency indicators, whose values determined on the basis of the monitoring results are compared with a reference value. The performance indicators, either energy efficiency, or specific consumption, etc. were determined based on an algorithm for unit calculation, thus creating a consistent database for fast elaboration of optimal thermo-energetic audits, considering the measured and the determined thermal parameters. These calculation algorithms, specific to balance equations are included in the specialized computing software proposed for the analysis and processing of thermal quantities.

The elaboration of this computing software leads to the speed-up of the stages of implementation of a thermo-energetic balance, with a possibility to perform several combinations between the thermal parameters which concur for the achievement of an optimal balance.

The elaboration of such a specialized computing software for the analysis and processing of thermal quantities which are part of balance equations, for major industrial consumers commonly met in the practice of thermo-energetic audits, namely steam boilers, leads to the optimization of the activity from the point of view of thermal energy.

The use of specialized computing software allows the thermo-energetic audit and balance activities to be improved in the field of generation and quality of thermal energy, in accordance with the requirements of the current European standards, the rules in force and the energy requirements approved by ANRE (Regulatory Authority for Energy). Due to the multitude of thermo-energetic parameters required for the balance equations, such specialized programs were not developed until now, except for preparing electrical energy balance sheets [2].

2. The calculation algorithm

Consider the Block-Steam type boiler fueled by heating oil, a fuel with low heating value H_l [kJ/kg] and ultimate composition C^l [%]; H^l [%]; S^l [%]; O^l [%]; W [%].
A BA type boiler is a boiler with a fire tube and three burnt gases tubes [3, 4]. The main functional parameters, according to the instruction book are the following:

- Nominal output;
- Nominal pressure;
- Steam temperature: according to the saturation pressure;
- Supply water temperature;
- Chimney gas temperature: [^oC];
- Fuel consumption: [kg/h];
- Efficiency: [%].

The contour of the balance includes the physical limits of the boiler. The thermo-energetic balance sheet was developed for the time unit [5].
The equation of the thermal balance of the boiler is:

$$Q_{c,ch} + Q_{c,f} + Q_a + Q_L + Q_W = Q_u + Q_{ga,f} + Q_{ga,ch} + Q_p + Q_{rc} \, [kW] \quad (1)$$

where:

- $Q_{c,ch}$ – chemical heat of fuel;
- $Q_{c,f}$ – sensible heat;
- Q_a – the sensible heat of the supply water and of the water injected in the steam governor;
- Q_W- heat generated by the electricity supplied to the contour; (to be measured)
- Q_L – sensible heat of air (including infiltrated air) fed into the boiler;
- Q_u – absorbed heat consisting of the heat of the steam generated by the boiler and the heat yielded to the steam reheater;
- $Q_{ga,f}$ – heat loss from sensible heat of burnt gases, including the heat loss from the injection steam of liquid fuels;
- $Q_{ga,ch}$ – heat loss from incomplete chemical combustion;
- Q_p – heat loss from purge water;
- Q_{rc} – heat loss to the environment due to the heating of the outer surfaces.

$$Q_{c,ch} = BH_i \, [kW] \quad (2)$$

where:

- B – is the fuel consumption, in kg/s;
- H_i – the low heating value of the fuel, in kJ/kg.

$$Q_{c,f} = Bc_{pc}t_c \, [kW] \quad (3)$$

where:

- c_{pc} is the specific heat of the fuel, in kJ/(kg ^oC);
- t_c – fuel temperature, in ^oC.

$$c_{pc} = 3{,}849 - 2{,}34\rho + 2{,}299 * 10^{-3} t_c \, [kJ/(kg\,^oC)] \quad (4)$$

for fuel density $\rho \geq 0{,}9$ kg/dm^3, or tabular choice depending on the density and temperature of the fuel.

$$Q_a = D_a i_a \, [kW] \tag{5}$$

where:

- D_a – the supply water flow rate, in kg/s;
- i_a – the enthalpy of the supply water, corresponding to the supply water temperature,
- t_a- supply water temperature in kJ/kg.

$$Q_L = \alpha_{ev} B V_a^0 i_L \, [kW] \tag{6}$$

where:

- α_{ev} – the excess air equivalent coefficient measured with burnt gases evacuation;
- $V^0{}_a$ – theoretical air volume necessary for liquid fuel unit combustion, in $m^3{}_N$/kg;
- i_L – enthalpy of combustion air, in kJ/$m^3{}_N$ at the balance contour inlet temperature, t_L, where: $i_L = c_L t_L$
- or choose from the tables.

$$V_a^0 = \frac{1}{100}\left[8{,}89C^l + 26{,}7\left(H^l - \frac{O^l}{8}\right) + 3{,}33\right] [m_N^3 / kg] \qquad (7),$$

or it can be chosen from the literature.

$$\alpha_{ev} = \frac{21}{21 - 79\dfrac{O_2 - 0{,}5CO}{N_2 - 0{,}429\dfrac{N^l}{K^l}\left(RO_2 + CO\right)}} \tag{8}$$

- V_a^0 – the theoretical air volume necessary for liquid fuel unit combustion can also be chosen from the literature depending on the ingredients of the liquid fuel.
- α_{ev} – the excess air equivalent coefficient measured with burnt gases evacuation may also be chosen from charts, depending on the oxygen, nitrogen, carbon monoxide and triatomic gases ($RO_2=CO_2+SO_2$) percent in the composition of burnt gasses evacuated through the chimney, in%, and depending on the gravimetric percentage components of carbon, sulphur, hydrogen, and water in the fuel used (or it can be chosen from charts)
- O_2, N_2, CO, RO_2 – represent the oxygen, nitrogen, carbon monoxide and triatomic gases ($RO_2=CO_2+SO_2$) percent in the composition of burnt gasses evacuated through the chimney, in %, while:

$$K^l = C^l + 0{,}375S^l \tag{9}$$

$$Q_u = D_{ab} i_{ab} \, [kW] \tag{10}$$

where:

- D_{ab} is the steam production of the boiler, in kg/s;
- i_{ab} – steam enthalpy, determined according to the saturation pressure, p_{ab}, in kJ/kg.

$$Q_{gaf} = \left[0{,}32\frac{C^l + S^l}{0{,}536\left(RO_2 + CO\right)} + 0{,}46\frac{9H^l + W^l 100 d_{inj}}{100}\right] 4{,}186 C_0 t_{ga} \tag{11}$$

where:

- C^l, S^l, H^l, W^l are the gravimetric percentage components of carbon, sulphur, hydrogen, and water in the fuel used;
- $RO_2=CO_2+SO_2$ are triatomic compounds in burnt gases;
- CO – the content of carbon monoxide (RO_2 and CO_2 are percent by volume in terms of dry burnt gases);
- t_{ga} – temperature of burnt gases at the outlet of the balance contour, in ºC;
- d_{inj} – the flow density of steam required for the injection of the liquid fuel mass unit.

$$C_0 = C\left(1-\frac{Q_m}{100}\right)[kg/s] \tag{12}$$

where:

- C – flow rate of the fuel fed to the furnace, in kg/s;
- Q_m – heat loss through incomplete combustion.
- Clearly, for the liquid and gas fuels $C=C_0$.

or:

$$Q_{ga,f} = D_{ga}c_{ga}t_{ga} \tag{13}$$

where D_{ga}, c_{ga}, t_{ga}, refer to the flow rate, specific heat and temperature of burnt gases at the outlet from the boiler.

$$Q_{ga,ch} = 12680CO\frac{C^l}{0{,}536(CO_2+CO)100}C_0[kW] \tag{14}$$

or $Q_{ga,ch}=D_{ga}H_{iCO}CO$;

where: D_{ga} – flow of burnt gases evacuated from the boiler; $D_{ga}=BV_{ga}$;
B – fuel consumption;
V_{ga} – volume of burnt gases evacuated from the boiler;

$$V_{ga} = V_{ga}^0 + (\alpha_{ev}-1)V_a^0 \tag{15}$$

where:

- V_{ga}^0 – theoretical volume of burnt gases resulting from combustion of 1 m^3 of fuel with the necessary theoretical air ($\alpha_{ev}=1$);
- V^0_a – the theoretical air volume necessary for the combustion of 1 m^3 of fuel;
- H_{iCO} – low heating value of carbon monoxide.

$$Q_{rc} = q_5(Q_c+Q_{inj}+Q_L)[kW] \tag{16}$$

where q_5 is chosen from special charts and represents the percentage loss to the environment in relation to the heat fed to the furnace, or, in the case of recovery boilers, hot gas heat.

$$Q_p = D_p i_p [kW] \tag{17}$$

where:

- D_p – the purging flow rate, in kg/s;
- i_p – enthalpy of purge water, $i_p=i'(p_{ab})$, in kJ/kg.

3. Specialized computing software

In the graphical programming environment provided by LabVIEW, the virtual instrument defines a software module, a program consisting of a user interface, front panel (simulating intuitively the

front side of the classic instrument) and a block diagram type program (a diagram, accessible only to the programmer) [6].
The front panel is the user-wise interface of the virtual instrument and the key element of programmes developed in LabVIEW because the data input or extraction to/from the programming environment is achieved by means of this front panel. On the front panel, the controls requiring user interaction are heavily simplified, with emphasis on graphic display and control elements, known as controls or indicators. The controls represent inputs to the virtual instrument, performing data inputs, while the outputs, which communicate the data resulting from the process to the operator are known as indicators (display elements). The controls have different forms, such as key buttons, switches, sliders, dials, etc., each type matching an element from the classical instrument [7].
LabVIEW can be used to deal with data structures from simple to very complex, numeric values, text strings, graphs, etc. In the case of indicators, these data structures managed by the program determine their own optimal shape for presenting the data they receive.
Data inputs and outputs are dual, intended for both the operator and the programme, and the distinction between controls and indicators is not rigid, although some are exclusively display elements, and others are control elements [8].
The block diagram accompanies the front panel and can be conceived as a source code, as it is known in classic programming languages. Its components represent the nodes of the programme such as logical structures, mathematical operators, logical processing functions, etc. The connection of components is achieved through wires defining the flow of data within the virtual instrument created by the program [9].
The block diagram is actually a chart used by the programmer to describe the algorithm required for the application to perform the necessary computing and reasoning for data retrieval and processing. In most cases, after the programmer has developed an application and delivered it to a user, the latter no longer has access to the chart, the same way users of other programs do not have access to their source code [10].
The software interfaces of the computing software application is shown in figure 1, 2 and 3.

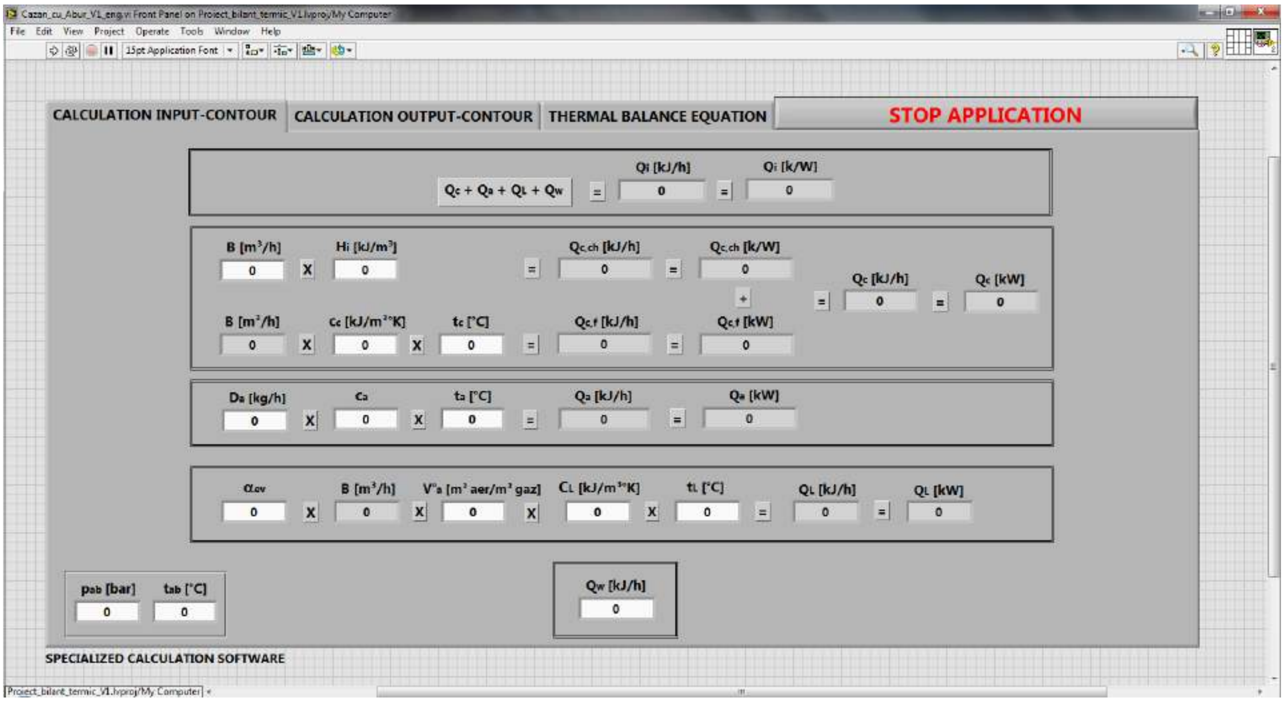

Fig. 1. Software interface of the calculation for input into contour

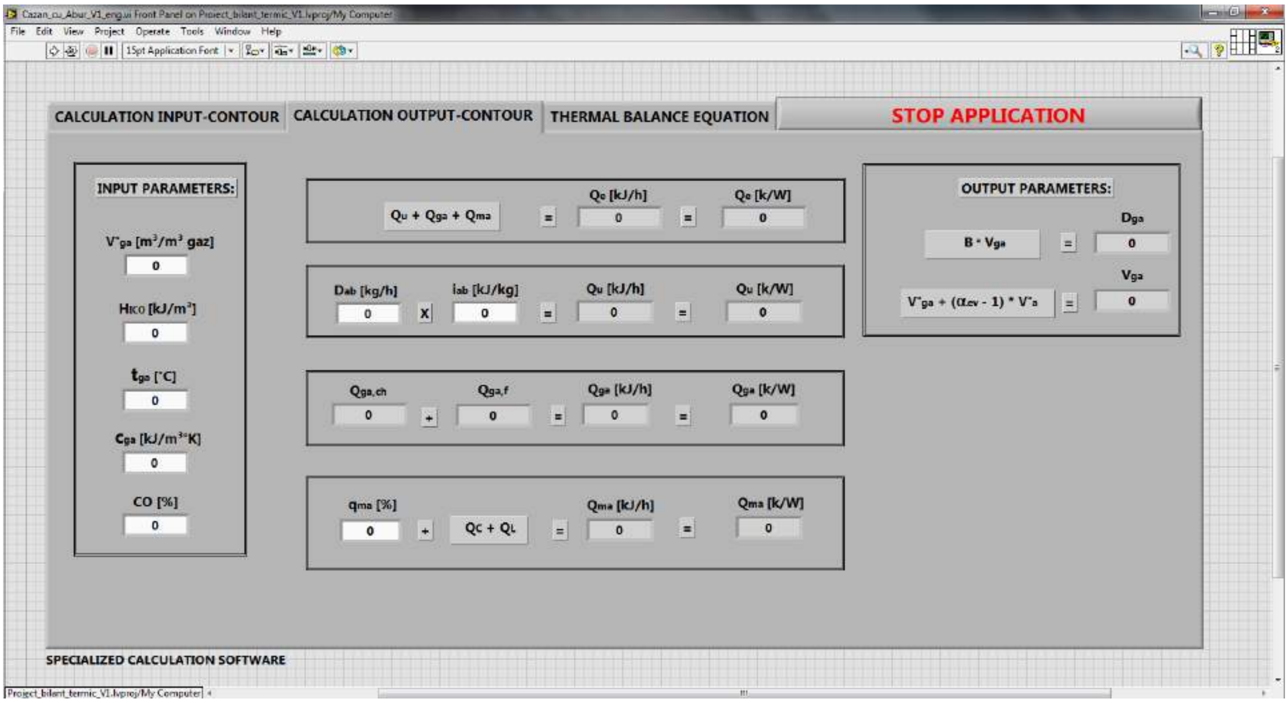

Fig. 2. Software interface of the calculation for output from the contour

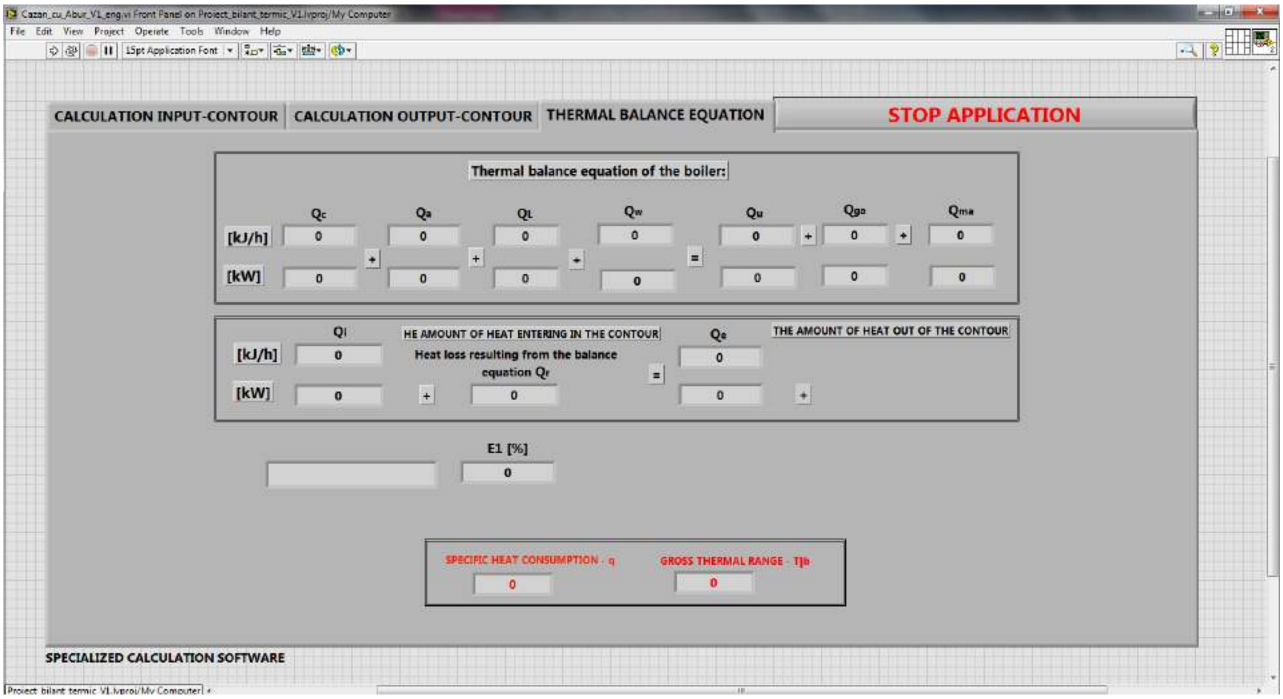

Fig. 3. Software interface of the calculation of the thermal balance equation

Although LabVIEW language consists of all the required elements for writing programs, there is also the possibility of writing source lines in C language, via a special "Formula Node" node structure. Another special structure, the "MathScript Node" allows inputting lines of code similar to MATLAB program. This considerably expands the programming possibilities, enabling the users to write their own code sequences and extending the standard facilities provided by the LabVIEW environment. So we can say that this is an open environment, which increases its performance [11].

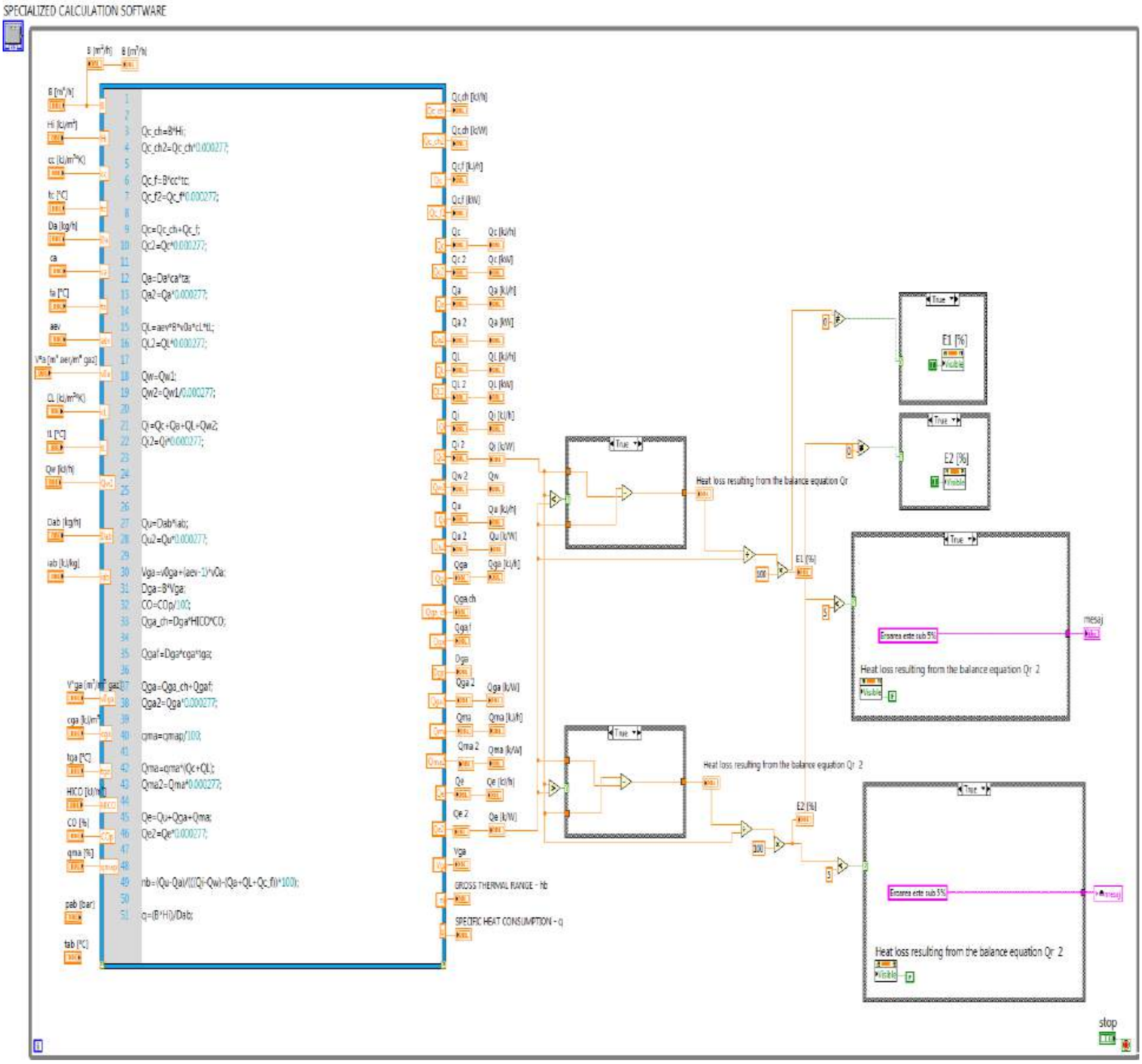

Fig. 4. Block diagram of the specialized computing software

The computing software application also automatically generates reports to Excel files, and the block diagram of the software process is shown in Figure 5:

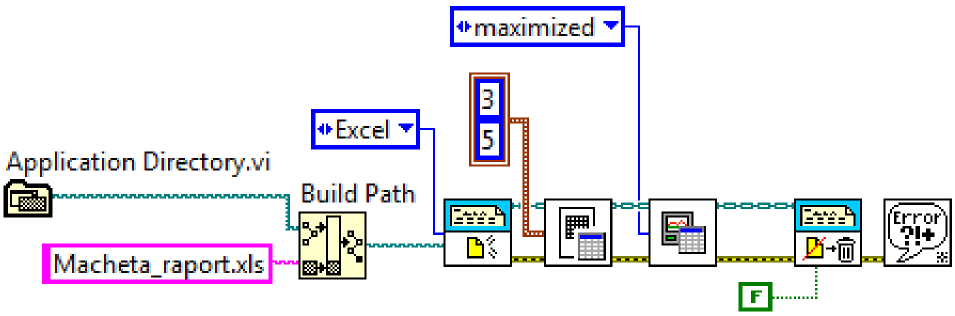

Fig. 5. Generation of Excel type report

4. Example of calculation

The thermo-energetic balance aims to measure the energy quantities input to the contour during the analyzed time span, to determine the energy losses inside the contour and the quantities of useful energy as the difference of two values.

Table 1: The average values of the measurands for a boiler

Measurand	Symbol	Unit	Value
Fuel consumption	B	m^3/h	36
Low heating value of the fuel	H_i	kJ/m^3	33735
Fuel temperature	t_C	°C	20
Temperature of the air inlet in the furnace	t_L	°C	20
Supply water flow rate	D_a	kg/h	500
Supply water temperature	t_a	°C	100
Steam production	D_{ab}	kg/h	425
Steam pressure	p_{ab}	bar	25
Steam temperature	t_{ab}	°C	200
Burnt gases temperature	t_{ga}	°C	110

Starting with the values shown in Table 1, following the application software run, the results obtained in the figures 6, 7, and 8.

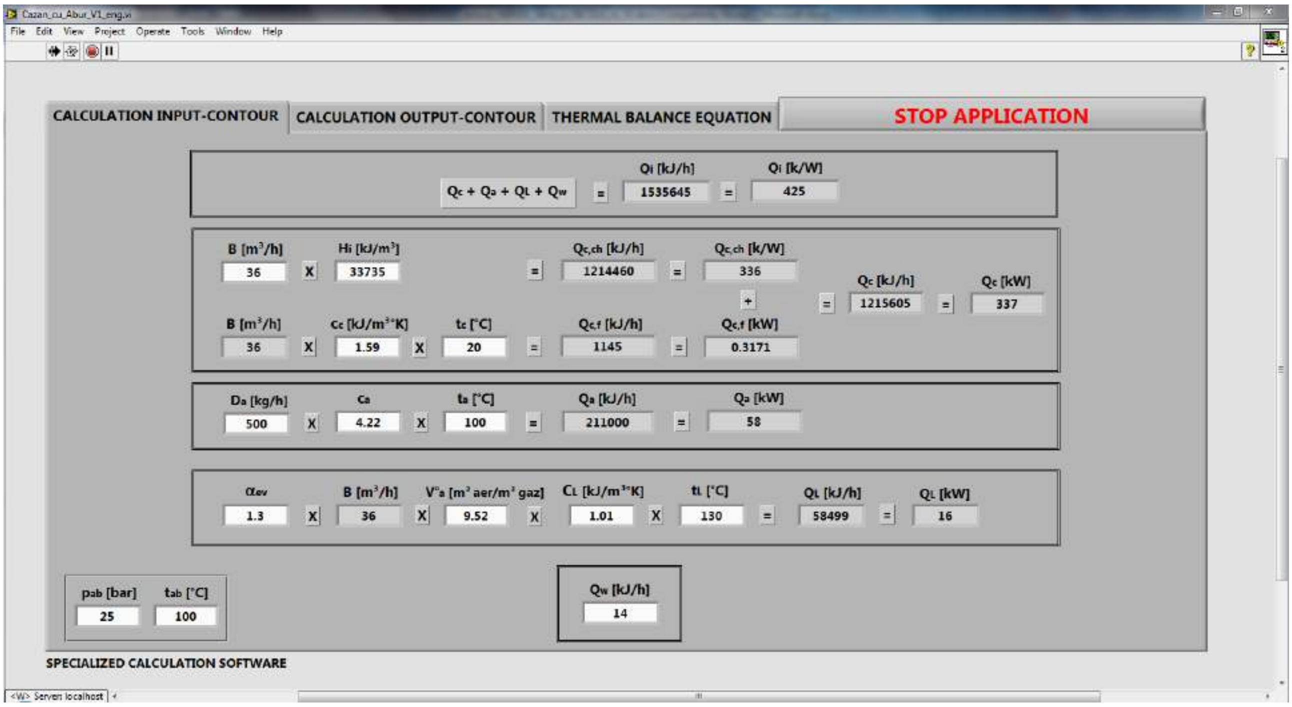

Fig. 6. Software interface of the calculation for input into contour for the steam boiler

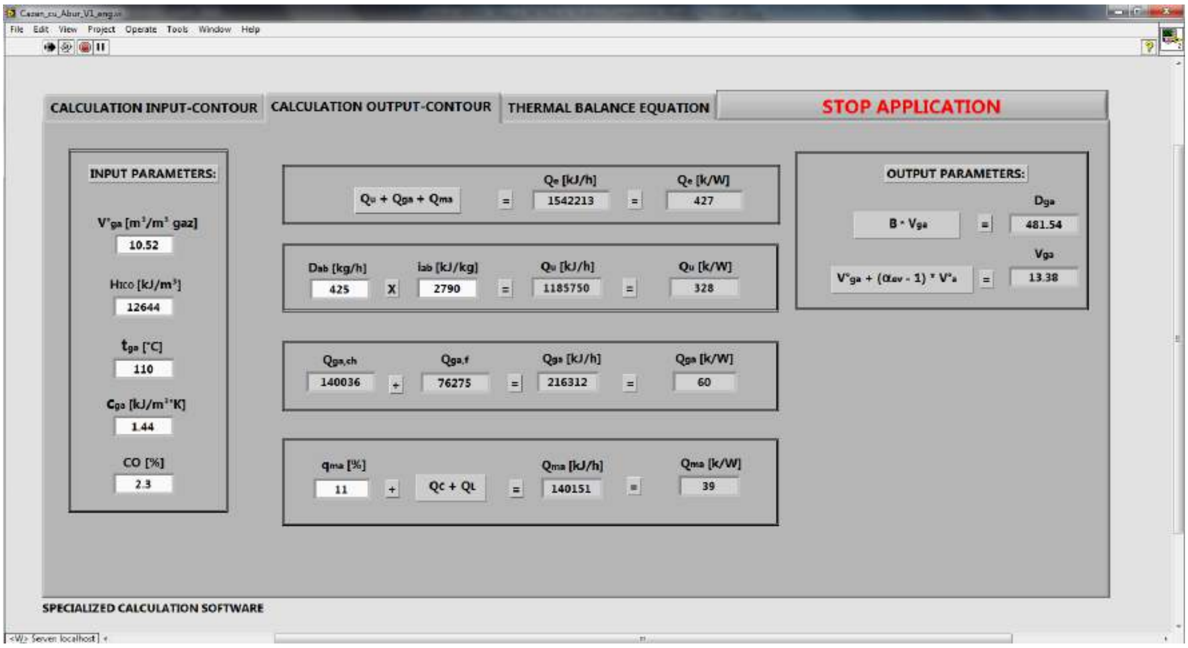

Fig. 7. Software interface of the calculation for output from the contour for the steam boiler

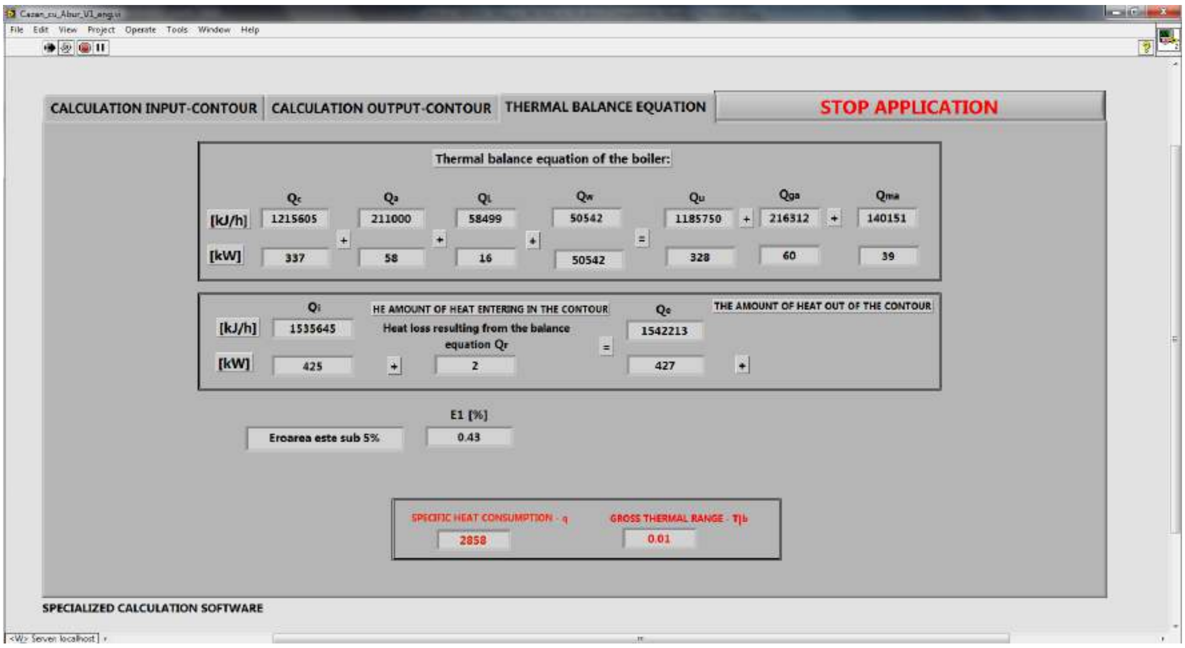

Fig. 8. Software interface of the calculation of the thermal balance equation for the steam boiler

5. Conclusions

The elaboration under a uniform conception of the documentation relating to the algorithms for calculating the thermal parameters associated with steam boilers has promoted the development of software for these types of installations for the production of heat, currently required in the practice of thermo-energetic audits and balances. The calculation algorithms, specific to balance equations, can be found in a specialized computing program for the analysis and processing of thermal quantities.

The analytic expressions for calculating the thermal parameters specific to heat consumers can be found in the LabVIEW graphical programming environment, a programming system which has revolutionized the development of test, measurement and control applications. By mean of this

system, an interface can quickly and efficiently be achieved with the hardware for data acquisition and control, data analysis can be performed, and useful systems can be designed for developing optimized balances.
The parameterized software creates the prerequisites for improving such thermo-energetic audit and balance activities by data management, performance of measurements and analysis, interpretation of phenomena, situations in the field of generation and quality of thermal energy, in accordance with the requirements of the current European standards, the rules in force and the energy requirements approved by ANRE.
The specialized computing software leads to the speed-up of the stages of implementation of a thermo-energetic balance, with a possibility to perform several combinations between the thermal parameters which concur for the achievement of an optimal balance.

Acknowledgments

The paper was developed with funds from the Ministry of Education and Scientific Research as part of the NUCLEU Program: PN 16 15 03 03.

References

[1] A. Badea, M. Stan, R. Patrascu, „Bazele termoenergeticii”, Bucuresti, 2003;
[2] ANRE – Ghid de elaborare a auditurilor energetice. Decizia 2123/23.09.2014;
[3] V. Iliescu Grozavesti, „Cartea fochistului”, Editura tehnica, Bucuresti-1962;
[4] M. C. Dianu, „Aparate termice.Cazane”, Bucureşti, 2009;
[5] C. Raducanu, R. Patrascu, „Bilanturi termoenergetice”, Bucuresti, 2004;
[6] Introduction to LabVIEW”, [Online]. Available: http://home.hit.no/~hansha/documents/labview/training/Introduction%20to%20LabVIEW/Introduction%20to%20LabVIEW.pdf;
[7] LabVIEW™ - Getting Started with LabVIEW, [Online]. Available: http://www.ni.com/pdf/manuals/373427j.pdf;
[8] LabVIEW – User Manual, online:http://www.ni.com/pdf/manuals/320999c.pdf;
[9] J. Jovitha. (2010, January 30). "Virtual Instrumentation Using Labview", [Online]. Available: https://www.academia.edu/9455052/Virtual_Instruments_using_LabView_by_-_Jovitha_Jerome;
[10] H. P. Halvorsen. (2014, Mar. 07). Introduction to LabVIEW. [Online]. Available: http://home.hit.no/~hansha/documents/labview/training/Introduction%20to%20LabVIEW/Introduction%20to%20LabVIEW.pdf;
[11] LabVIEW MathScript RT Module [Online]. Available: http://www.ni.com/LabVIEW/mathscript/.

ISSN 1454 - 8003
Proceedings of 2017 International Conference on Hydraulics and Pneumatics - HERVEX
November 8-10, Băile Govora, Romania

APPLICATIONS OF MICROALGAE IN WASTEWATER TREATMENT. EXPERIMENTAL AND EQUILIBRIUM STUDIES

Emilia NEAG[1], Cecilia ROMAN[1]

[1]INCDO-INOE 2000, Research Institute for Analytical Instrumentation, 67 Donath st., 400293 Cluj-Napoca, Romania, emilia.neag@icia.ro

Abstract: *The aim of this study was to investigate the capacity of Nannochloropsis oculata (microalgae) and Spirulina (cyanobacteria) biomass for Rhodamine B and Methylene blue removal from aqueous solutions. The results reveal that Nannochloropsis oculata was more efficient for Rhodamine B and Methylene blue removal, than Spirulina. The most favourable biosorption of Rhodamine B onto Nannochloropsis oculata and Spirulina was obtained at pH 4 and pH 1, respectively. The optimum pH for Methylene blue removal by Nannochloropsis oculata and Spirulina was 1. The experimental data were analysed using Langmuir, Freundlich, and Dubinin-Radushkevisch isotherm models. The Freundlich model fitted better the experimental results for the removal of Rhodamine B onto Nannochloropsis oculata and Spirulina biomass. Langmuir isotherm model suggested the monolayer coverage of Methylene blue molecules onto Nannochloropsis oculata. Dubinin-Radushkevich isotherm indicated a chemically process involved in Rhodamine B removal onto Nannochloropsis oculata and Spirulina. In case of Methylene blue removal onto Spirulina, Dubinin-Radushkevich isotherm indicated a physically process.*

Keywords*: Nannochloropsis oculata, Spirulina, Methylene blue, Rhodamine B, biosorption*

1. Introduction

The production and usage of synthetic dyes have increased worldwide due to their high stability and cost-effectiveness in synthesis compared with natural dyes [1]. Thus, the discharge of coloured wastes has become one of the main sources of environmental pollution.
The presence of dyes in water can cause significant changes, including a decrease in the photosynthetic activity and dissolved oxygen, an alteration of the pH, an increase in the biochemical oxygen and chemical oxygen demand, in aquatic life. Also, can exhibit chronic effects towards biota, such as mutagenic damage and carcinogenicity [1, 2, 3]. It has been found that above the concentration of 1 mg/L, the dye is visible in the wastewater and typically the concentration of dyes found in textile wastewater is in the range of 10 to 50 mg/L [3].
The Rhodamine dye is a synthetic dye used as a colorant in textile and food industry. Its presence in drinking water could lead to subcutaneous tissue borne sarcoma [4].
Methylene blue (MB) is a cationic dye used in chemistry, biology, medical science and textile industry. Its long term exposure can cause vomiting, nausea, anemia and hypertension affecting human life [5].
Various physical/chemical methods have been investigated for dyes removal from wastewaters [1]. Among these, the adsorption methods appear to be an efficient alternative for the removal of a wide range of compounds [6].
The application of low cost adsorbents has been extensively applied for colour removal but the results showed that they failed to achieve high adsorption capacity.
Microalgae appears to have an advantage due to the use of wastewater as a low cost nutrient source for its production [7].
Several algae were used for dyes removal, such as dead biomass of *Spirogyra*, living biomass of microalgae *Caulerpa lentillifera* and *Caulerpa scalpelliformis*, Chlorella vulgaris, dry and wet biomass of *Chlorella pyrenoidosa* [7].
The aim of the present study was to evaluate the potential application of *Nannochloropsis oculata* microalgae and *Spirulina* (cyanobacteria) biomass for Rhodamine B and Methylene blue removal from aqueous solutions by taking into account the effect of adsorbent dosage and pH.

2. Experimental protocol

The experiments were performed in batch conditions, contacting different quantities of *Nannochloropsis oculata and Spirulina* (1 – 5 g) with 50 mL dye solutions (Rhodamine B and Methylene blue). All the experiments were carried out at the same initial concentration (50 mg/L) and stirring rate (75 rpm) for 240 min. After the equilibrium was reached, the dye solutions were separated from the biomass by centrifugation at 3600 rpm for 10 min. The concentration of Rhodamine B and Methylene blue in solution was determined using Lambda 25 Perkin-Elmer UV/VIS spectrophotometer at 665 nm and 554 nm, respectively.
The dyes amount in the adsorbent phase, q_e (mg/g), was calculated using equation (1), while dyes removal efficiency, E (%) was calculated using equation (2):

$$q_e = \frac{(C_0 - C_e)}{m} \cdot \frac{V}{1000} \tag{1}$$

$$E(\%) = \frac{(C_0 - C_e)}{C_0} \cdot 100 \tag{2}$$

where, q_e is the amount of dye adsorbed per gram of adsorbent at equilibrium (mg/g), V is the volume of solution (mL), m is the weight of the adsorbent (g), C_e is the equilibrium dye concentration (mg/L) and C_0 is the initial dye concentration (mg/L) [7].

2.1 Materials

Nannochloropsis oculata and *Spirulina* as powder were used as received without any further purification.

2.2 Chemicals

Rhodamine B and Methylene blue were purchased from Merck, Germany. The calibration standards (2-10 mg/L) and the initial concentration of 50 mg/L were prepared by diluting a stock solution of 100 mg/L Rhodamine B and Methylene blue. All used chemicals were of analytical purity and used as received without any further purification. The pH adjustments were carried out using dilute 1M NaOH and 1N HCl solutions.

3. Results and discussion

3.1 Influence of adsorbent quantity

To determine the influence of adsorbent doses for Rhodamine B and Methylene blue biosorption, the experiments were performed by contacting different quantities of *Nannochloropsis oculata and Spirulina* (1 – 5g) with 50 mL dye solutions (50 mg/L) at room temperature (22 ± 2°C) for 240 min.
The results obtained for Rhodamine B and Methylene blue biosorption onto *Nannochloropsis oculata and Spirulina* are given in Fig. 1 and Fig. 2, respectively.
The percent removal of Rhodamine B (Fig. 1) onto *Nannochloropsis oculata* and *Spirulina* increased as the adsorbent quantity increased from 1 to 3 g at 50 mg/L dye concentration on equilibrium time. This can be due to the number of available biosorption sites. Thus, the surface area increase by increasing the adsorbent quantity reflecting an increase in the amount of adsorbed dye [7].
It was noted that there was 95.1% removal efficiency for Rhodamine B dye removal at 2 g *Nannochloropsis oculata* and 96.4 at 3 g of *Nannochloropsis oculata* (smaller difference in term of removal efficiency can be seen). Therefore, 2g of microalgae biomass was chosen as optimum quantity for further experiments.
In case of Rhodamine B removal onto cyanobacteria *Spirulina* smaller removal efficiency values were obtained.

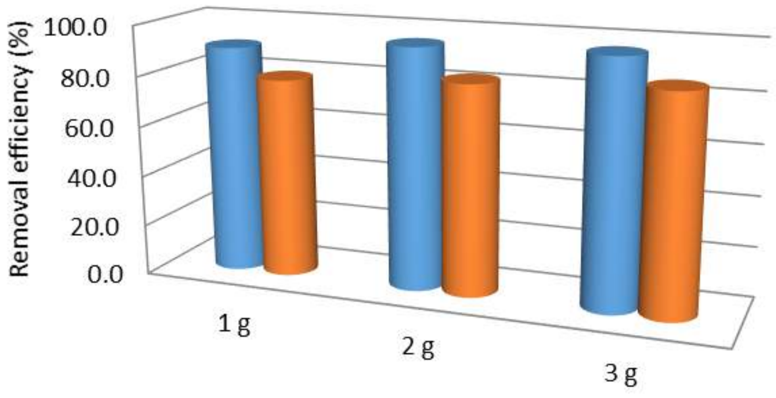

	1 g	2 g	3 g
Nannochloropsis oculata	90.4	95.1	96.4
Spirulina	79.0	82.7	85.4

Fig. 1. Rhodamine B removal onto *Nannochloropsis oculata* and *Spirulina* at different adsorbent quantities. C_0 = 50 mg/L, m = 1 - 5 g, pH = 4, V = 50 mL, t = 240 min

As it can be seen from Fig. 2, the percent removal of Methylene blue onto *Nannochloropsis oculata* and *Spirulina* increased as the adsorbent quantity increased from 1 to 3 g at 50 mg/L dye concentration. The assumption made in case of Rhodamine B removal can be attributed also in this case (the surface area increase by increasing the adsorbent quantity).
It was noted that there was 99.9% removal of Methylene blue dye at 2 g and 3 g of *Nannochloropsis oculata*, respectively.
For Methylene blue removal onto *Spirulina* the removal efficiency values were much smaller than the values obtained for Rhodamine B removal on *Spirulina*.

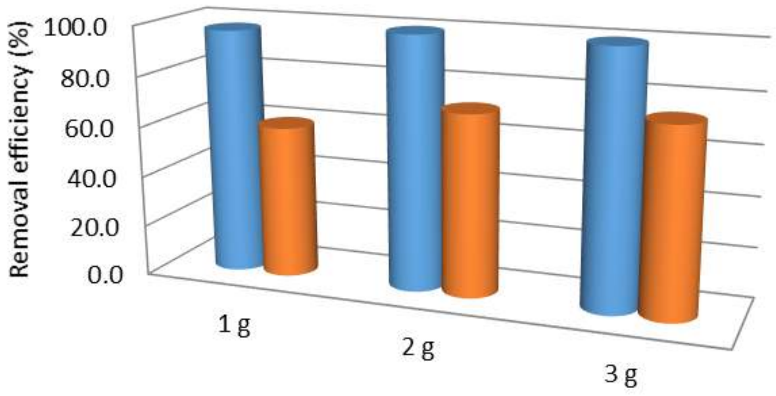

	1 g	2 g	3 g
Nannochloropsis oculata	97.2	99.9	99.9
Spirulina	60.1	71.6	73.6

Fig. 2. Methylene blue removal onto *Nannochloropsis oculata* and *Spirulina* at different adsorbent quantities. C_0 = 50 mg/L, m = 1 - 5 g, pH = 4, V = 50 mL, t = 240 min

ISSN 1454 - 8003
Proceedings of 2017 International Conference on Hydraulics and Pneumatics - HERVEX
November 8-10, Băile Govora, Romania

3.2 Influence of pH

To determine the influence of pH for Rhodamine B and Methylene blue biosorption, the experiments were performed by contacting 2 g of *Nannochloropsis oculata* and *Spirulina* with 50 mL dye solutions (50 mg/L) at different pH values (1 - 13) at room temperature (25 ± 2°C) for 240 min.
The results obtained for Rhodamine B and Methylene blue biosorption onto *Nannochloropsis oculata and Spirulina* are given in Fig. 3 and Fig. 4, respectively.

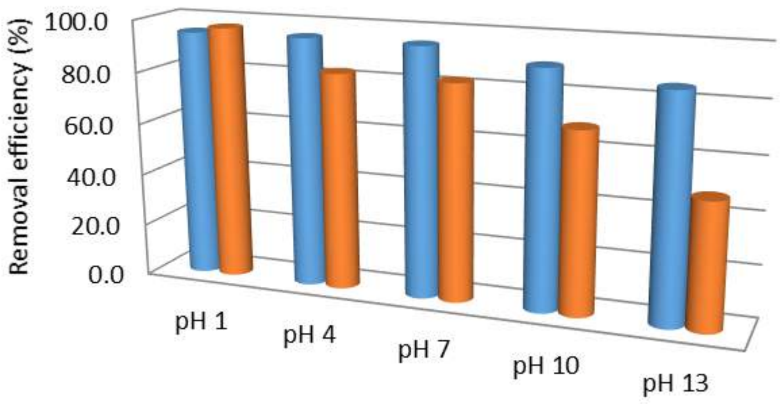

	pH 1	pH 4	pH 7	pH 10	pH 13
Nannochloropsis oculata	94.8	95.1	94.8	89.9	85.3
Spirulina	97.1	82.7	82.3	68.9	48.0

Fig. 3. Rhodamine B removal onto *Nannochloropsis oculata* and *Spirulina* at different pH values. C_0 = 50 mg/L, m = 2 g, pH = 1 - 13, V = 50 mL, t = 240 min

The most favourable biosorption of Rhodamine B onto *Nannochloropsis oculata* and Spirulina was obtained at pH 4 and pH 1 (Fig.3), respectively.

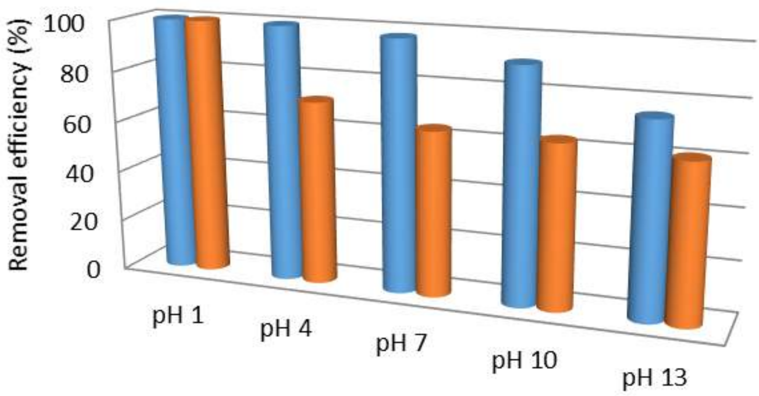

	pH 1	pH 4	pH 7	pH 10	pH 13
Nannochloropsis oculata	100	99.9	97.7	90.9	75.0
Spirulina	100	71.6	64.2	63.7	61.2

Fig. 4. Methylene blue removal onto *Nannochloropsis oculata* and *Spirulina* at diferent pH values. C_0 = 50 mg/L, m = 2 g, pH = 1 - 13, V = 50 mL, t = 240 min

The optimum pH for Methylene blue removal by *Nannochloropsis oculata* and *Spirulina* was 1 (Fig.4). This can be due to the increase of positively charged adsorbent surface sites at the expense of the number of negatively charged surface sites, at lower pH values. Therefore, with an increase of pH a decrease of adsorption capacity was observed (the electrostatic repulsion between the positively charged surface and the positively charged dye molecule increased) [7].

3.3. Equilibrium studies

In order to investigate the Rhodamine B and Methylene blue removal the experimental results were analysed by taken into account the Langmuir, Freundlich and Dubinin-Radushkevich isotherm models.
The Langmuir isotherm was applied in order to determine if the biosorption process occurred onto a monolayer surface [8]. The linear form of the Langmuir isotherm is given in Table 1, where K_L is the Langmuir adsorption constant (L/mg) and q_{max} is maximum amount of dye adsorbed per gram of adsorbent (mg/g) [9].

Table 1: Linear forms of isotherm models

Isotherm model	Linear form	Plot
Langmuir	$\frac{1}{q_e}=\frac{1}{q_{max}K_L C_e}+\frac{1}{q_{max}}$	$\frac{1}{q_e}$ vs. $\frac{1}{C_e}$
Freundlich	$\log q_e=\log K_F+\frac{1}{n}\log C_e$	$\log q_e$ vs. $\log C_e$
Dubinin-Radushkevich	$\ln q_e=\ln q_{max}-\beta\varepsilon^2$ $\varepsilon = RT\ln(1+\frac{1}{C_e})$ $E_L = \frac{1}{\sqrt{-2\beta}}$	$\ln q_e$ vs. ε^2

Langmuir parameters, q_{max} and K_L, obtained from the slope and intercept of the plot $1/q_e$ *vs.* $1/C_e$ are presented in Table 2.
Freundlich isotherm was applied in order to determine if the biosorption process occurs on a heterogeneous surface [10]. Its linear form is given in Table 1, where, K_F is the adsorption capacity (L/mg), $1/n$ is the adsorption intensity [11]. If n value is below 1 it indicates a normal adsorption, > 1 indicates cooperative adsorption and if 1< n < 10 indicates a favourable adsorption process [12].
Freundlich parameters, K_F and n, obtained from the $\log q_e$ *vs*. $\log C_e$ linear plot are presented in Table 2.
The n value obtained for Rhodamine B onto *Nannochloropsis oculata* was found to be lower than 1, indicating a normal biosorption. Also, Freundlich isotherm parameter (n value) indicated a normal biosorption of Methylene blue removal onto *Nannochloropsis oculata* and *Spirulina.* The n value obtained for Rhodamine B onto *Spirulina* was found to be greater than 1, indicating a favourable biosorption of the considered dye.
Based on the correlation coefficient values (R^2), it can be concluded that Freundlich model fitted better the experimental results for the removal of considered dyes except for Methylene blue removal onto *Nannochloropsis oculata* (in this case Langmuir model fitted better the experimental results).
The Dubinin-Radushkevich model was applied to determine the nature of the biosorption process (physically if E_L < 8 kJ/mol or chemically if E_L value lies between 8 kJ/mol and 16 kJ/mol) [13, 14]. Its equations are given in Table 1, where β is Dubinin Radushkevich constant (mol^2/ kJ^2), R is the gas constant (8.314 J/mol·K), T is the absolute temperature (K), ε is the Polanyi potential and E_L is the mean adsorption energy (kJ/mol) (Ayawei et al. 2017).
Dubinin-Radushkevich parameters, q_{max} and β, obtained by plotting $\ln q_e$ *vs.* ε^2 are given in Table 2.

Table 2: Langmuir, Freundlich and Dubinin-Radushkevich isotherm parameters for *Nannochloropsis oculata* and *Spirulina* at different adsorbent quantities.

		Rhodamine B		Methylene blue	
Isotherm model	Parameters	*Nannochloropsis oculata*	*Spirulina*	*Nannochloropsis oculata*	*Spirulina*
Langmuir	q_{max}/(mg/g)	16.23	1.80	142.86	13.87
	K_L/(L/mg)	0.03	0.61	0.13	0.04
	R^2	0.9864	0.9841	0.9483	0.8976
Freundlich	n	0.95	4.65	0.79	0.41
	K_F/(L/mg)	2.26	3.54	21.40	41.73
	R^2	0.9915	0.9961	0.9280	0.9570
Dubinin-Radushkevich	β/(mol^2/ kJ^2)	$7 \cdot 10^{-9}$	$2 \cdot 10^{-9}$	$8 \cdot 10^{-9}$	$2 \cdot 10^{-8}$
	E_L/(kJ/mol)	8.5	15.8	7.90	5.0
	R^2	0.9931	0.9954	0.9233	0.9582

As it can be seen from Table 2 the mean free energy value indicated a chemically process involved in Rhodamine B removal on *Nannochloropsis oculata* and *Spirulina.* In case of Methylene blue removal onto *Nannochloropsis oculata* and *Spirulina,* the mean free energy value indicated a physically process.

4. Conclusions

In this paper, the use of *Nannochloropsis oculata* microalgae and cyanobacteria *Spirulina* was investigated for Rhodamine B and Methylene blue dyes removal from aqueous solutions.
The results revelled that the percent removal of Rhodamine B and Methylene blue onto *Nannochloropsis oculata* and *Spirulina* increased as the adsorbent quantity increased.
By studying the effect of pH the removal efficiency values decreased as the initial pH increased.
The Freundlich parameter suggested that the removal of Rhodamine B onto *Nannochloropsis oculata* and *Spirulina* biomass occurred on a heterogeneous surface.
Langmuir isotherm model suggested the monolayer coverage of Methylene blue onto *Nannochloropsis oculata.*
Also, was found that a physically process was involved in Rhodamine B removal onto *Nannochloropsis oculata* and *Spirulina.* In case of Methylene blue removal onto *Spirulina* a chemically process was involved and a physically one onto *Nannochloropsis oculata.*
Based on the obtained results, *Nannochloropsis oculata* and *Spirulina* biomass have been proven to be potential dye biosorbents for Rhodamine B and Methylene blue removal.

Acknowledgments

This work was funded by Core Program, under the support of ANCS, project OPTRONICA IV (16.40.02.01).

References

[1] H.Y. El-Kassas, L.A. Mohamed, "Bioremediation of the textile waste effluent by Chlorella vulgaris", 2014, *Egyptian Journal of Aquatic Research* 40, 301-308;
[2] *P.M. Dellamatrice, M.E. Silva-Stenico, L.A. Beraldo de Moraes, M.F. Fiore, R.T. Rosim Monteiro,* "Degradation of textile dyes by cyanobacteria", 2017, *Brazilian Journal of Microbiology*, 48(1), 25-31;

[3] N.O.S. Keskin, A. Celebioglu, T. Uyar, T. Tekinay, Microalgae immobilized nanofibrous web for removal of reactive dyes from wastewater, 2015, *Industrial & Engineering Chemistry Research*, DOI: 10.1021/acs.iecr.5b01033;

[4] K. Shen, M.A. Gondal, "Removal of hazardous Rhodamine dye from water by adsorption onto exhausted coffee ground", 2017, *Journal of Saudi Chemical Society*, 21, S120-S127;

[5] D. Pathania, S. Sharma, P. Singh, "Removal of methylene blue by adsorption onto activated carbon developed from Ficus carica bast", 2017, *Arabian Journal of Chemistry,* 10, S1445-S145;

[6] A.S. Sartape, A.M. Mandhare, V.V. Jadhav, P.D. Raut, M.A. Anuse, S.S. Kolekar, "Removal of malachite green dye from aqueous solution with adsorption technique using *Limonia acidissima* (wood apple) shell as low cost adsorbent", 2017, *Arabian Journal of Chemistry* 10, S3229-S3238;

[7] V.V. Pathak, R. Kothari, A.K. Chopra, D.P. Singh, "Experimental and kinetic studies for phycoremediation and dye removal by *Chlorella pyrenoidosa* from textile wastewater", 2015, *Journal of Environmental Management,* 1, 163, 270-7;

[8] I. Langmuir, "The constitution and fundamental properties of solids and liquids", 1916, *Journal of the American Chemical Society*, 38, 2221-2295;

[9] M. Ghaedi, Sh. Heidarpour, S.N. Kokhdan, R. Sahraie, A. Daneshfar, B. Brazesh, "Comparison of silver and palladium nanoparticles loaded on activated carbon for efficient removal of Methylene blue: Kinetic and isotherm study of removal process", 2012, *Powder Technology*, 228, 18-25;

[10] H.M.F. Freundlich, "Over the adsorption in solution", 1906, *Zeitschrift für Physikalische Chemie*, 57A, 385-470;

[11] N. Ayawei, A.N. Ebelegi, D. Wankasi, "Modelling and Interpretation of Adsorption Isotherms", 2017, *Journal of Chemistry*, doi:10.1155/2017/3039817;

[12] A.O. Dada, A.P. Olalekan, A.M. Olatunya, O. Dada, "Langmuir, Freundlich, Temkin and Dubinin–Radushkevich Isotherms Studies of Equilibrium Sorption of Zn^{2+} Unto Phosphoric Acid Modified Rice Husk", 2012, *Journal* of Applied Chemistry, 3, 38-45;

[13] M.M. Dubinin, L.V. Radushkevich, "Equation of the characteristic curve of activated charcoal", 1947, *Proceedings of the Academy of Sciences, Physical Chemistry Section* 55, 331-333;

[14] F. Deniz, "Optimization of Biosorptive Removal of Dye from Aqueous System by Cone Shell of Calabrian Pine", 2014, *Scientific World Journal*, 1-10.

ISSN 1454 - 8003
Proceedings of 2017 International Conference on Hydraulics and Pneumatics - HERVEX
November 8-10, Băile Govora, Romania

PROPERTIES OF CONCRETE CONTAINING PET PLASTIC WASTE FROM POST-CONSUMED BOTTLES

Azad A. MOHAMMED[1]

[1] Civil Engineering, College of Engineering, University of Sulaimani, Sulaimani, Iraq, e-mail: azad.mohammed@univsul.edu.iq

Abstract: *Nowadays, plastic wastes from post-consuming containers or bottles has a serious attack to the environment, because of both land and water resources pollution problems. Civil engineers think that there a good chance to consume a large part of the total mass of plastic wastes via producing a recycled concrete containing this plastic waste, in the form of shredded particles or fibres. Relatively large amount of data on the basic properties of concrete containing different plastic wastes are available in the literature. However, there is a lack of information on the mechanical properties of concrete containing both shredded particles and fibres. This study was arranged to investigate properties of compressive strength and splitting tensile strength of concrete containing 10% of shredded polyethylene terephthalate (PET) waste particles and different volumes of PET waste fibre. Results indicate that the addition of PET fibre to the recycled concrete has some beneficial effect on the losses take place in compression containing shredded particles. The effect of addition PET fibre to the concrete was found more important for the splitting tensile strength property. It is concluded that the addition of both shredded PET particles and fibres to concrete can control the losses take place in strength and accordingly a higher quality of this type of recycled concrete can be produced.*

Keywords: *Compressive strength, PET waste fibre, Splitting tensile strength.*

1. Introduction

Concrete material is known to be weak in tension and cracking resistance. Conventionally, steel reinforcement is provided in concrete in order to carry the tensile forces and prevent any cracking. Adding short dispersed fibers could help in enhancing the flexural and tensile strength of the concrete. The main fibers used as concrete reinforcing materials are steel, glass, and polymeric fiber. The polymeric fibers that can be used in concrete reinforcements are nylon, aramid, polypropylene, polyethylene, polyester, etc. Polyethylene terephthalate (PET) is one of the most widely used plastics in the packaging industry because of high stability, non-reactivity with substances. Therefore, the productions of PET bottles have increased exponentially. The modern technology caused more waste materials productions for which the disposing problem exists. Utilizing these waste bottles in any form is advantageous, not only for the prevention of the environmental pollution but also energy saving in the disposal. Contributions of PET fiber in concrete using a different form of PET fibers have been explored [1-9]. The use of shredded plastics has known a growing interest as recycled materials in civil engineering construction. Shredded PET waste is added to concrete as a sand replacement, and this beneficial in many ways as it produces a lightweight concrete and also consumes less amount of aggregate compared with conventional lightweight concrete. The efficiency of PET waste fibers for reinforcing concrete has been considered in some investigations [1,2,3,9]. Fotti [9] have experimented on PET fiber reinforced concrete. An Important improvement in ductility behavior of concrete subjected to flexure was reported. Other tests [3] were focused on solid waste disposal of non-biodegradable materials used in concrete as a sand replacement. 0.5%, 1%, 2%, 4% and 6% volume of sand was replaced by PET bottle fibers. The waste PET bottles were collected, shredded into flakes or cut to make plastic fibers. The unit weight of concrete was found to be reduced for PET fiber reinforced concrete. It was observed that the compressive, split tensile and flexural strength were increased at 2% addition of fibers, thereafter reduction in strength was resulted.

Test data obtained by Albano et. Al [5] showed a reduction in the properties of compressive strength, tensile strength, and modulus of elasticity as a result of using shredded PET waste particles.

It is observed from past studies that the preparation of plastic waste is important on the residual properties of concrete, shredded particles have no good action in concrete but fibers have some enhancement of the tensile strength of concrete. The present work aimed to study the effect of PET waste fiber addition to concrete containing shredded PET waste particles on the properties of compressive strength and splitting tensile strength. Analysis of data is fairly made and compared with the properties of concrete containing PET waste shredded particles or fiber alone.

2. Experimental Work

2.1 Materials

Basic cconcrete materials used in this study are cement, fine aggregate, coarse aggregate and water.The cement used as ordinary Portland cement (Type I). Both fine and coarse aggregates used were on saturated surface dry (SSD) state with specific gravity equal to 2.64 and 2.65 for coarse and fine aggregates respectively. The maximum size of coarse aggregate was 19 mm.PET polymerwaste from post-consumer plastic containers origin was used in this study. PET particles as shown in Fig.1 shows PET waste shredded particles and fiber used in this investigation. PET waste was used in two different forms, shredded particles of 5mm average dimensions as partial replacement of fine aggregate by 10% and different amounts of fibers(length =30mm, width = 5 mm and thickness = 0.12 mm) as an addition by weight of cement.

2.2 Mix proportion and mixing

Mix proportion for control concrete was 1:2:3 (cement: fine aggregate: coarse aggregate) by weight with water/cement ratio equal to 0.45. No admixture was used in any mix batch. Concrete constituent materials, except water, where fed first to the electrical tilting drum mixer, and left to rotate for three minutes. Later, water was added and left to mix for another two minutes. For those mixes containing shredded PET plastic after the five minute mixing the particles were sprayed on fresh concrete inside the mixer continuously and left to mix for one minute. The same procedure was made for the case of PET fiber addition. For all mixes containing PET was particles 10% of fine aggregate was replaced with shredded PET waste. Fibers were added by weight of cement at percentages of 0.4, 0.8, 1,2 and 1.6. After 24 hours from casting concrete specimens taken from moulds and left in a water tank for 28 days of curing. Casting, mixing and curing were done in the laboratory at the temperature of 25±1^{o}C.

(a) Sredded particl (b) Fiber

Fig. 1. View of PET particles and fibers used in this study

2.3 Test specimens and testing

A total of fifteen 150 mm cube specimens and the same number of 150 x 300 mm cylinder specimens from five mix batches were cast and tested. After curing all specimens were left in the laboratory to dry for 7 days before testing. Measurements were taken for the density of dried concrete. Cubes were tested for compressive strength using the universal testing machine of 3000 kN capacity, at the rate of loading of 0.3 MPa/sec till failure. Splitting tensile strength test was carried out on cylinders using the same testing machine under the rate of loading of 0.2 MPa/sec. Average of three measurements were taken for the two measured strengths.

3. Results and Discussion

3.1 Test results

Table 1 shows test results of concrete density, compressive strength and splitting tensile strength for all concrete mixes. Specimen's designation is as follows, M is a mix, the first number is the ratio of shredded PET particles and the last number is the PET waste fibre ratio. Fig. 2 shows the variation of concrete density ratio with PET waste fiber. Fig. 3 shows the variation of compressive strength ratio with PET waste fiber and Fig. 4 shows the variation of splitting tensile strength ratio with PET waste fiber ratio.
Based on the results of Table 1 and Fig. 2 one can observe that the reduction in concrete density with PET shredded particles and fibre is quite small and not exceeds 0.8%. Therefore, it is concluded that the density is not changed when concrete contained 10% shredded particles and fiber ratio up to 1.6% by weight of cement. Based on the results of Table 1 and Fig. 3 it is observed that there is a moderate compressive strength loss as a result of adding shredded PET particles to concrete reaching 16.44% at 0.8% fiber content, but there is some recovery in the strength with increasing fiber content up to 1.6%. For the latter case, the compressive strength loss is 10.4%. Therefore, there is a moderate effect of PET fiber addition to control the compressive strength loss resulted from PET waste shredded particles added to concrete. Results of splitting tensile strength are somewhat different compared with those of compressive strength, and different from those obtained by other researchers, because there is no splitting tensile loss related to concrete tested in this investigation. This may be due to the fact that the strength of control concrete tested in this study is already small as a result of using a lean mix. The other reason is that the effect of fibre addition, even low, will have a beneficial effect on the splitting tensile strength. It is observed that the tensile strength increased with fibre ratio increase reaching 25% as a maximum value. Therefore, it is concluded that the effect of PET fibre addition is important for increasing splitting tensile strength containing 10% shredded PET waste particles up to 1.6% fiber ratio by cement weight. From the foregoing discussion, one can conclude that the mixture of shredded and fibres is better than using shredded particles alone for producing recycled concrete containing plastic wastes.

Table 1: Test results of dry density and concrete strengths

Specimen designation	Density (Kg/m^3)	Compressive strength (MPa)	Splitting tensile strength (MPa)
M0-0	2358	29.8	2.8
M10-0.4	2341	25.5	3.0
M10-0.8	2340	24.9	3.3
M10-1.2	2343	26.0	3.1
M10-1.6	2339	26.7	3.5

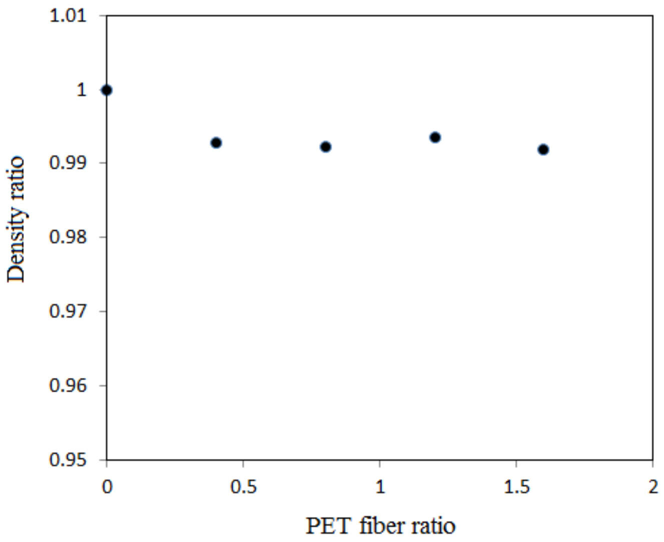

Fig. 2. Variation of concrete density ratio with PET fibre ratio

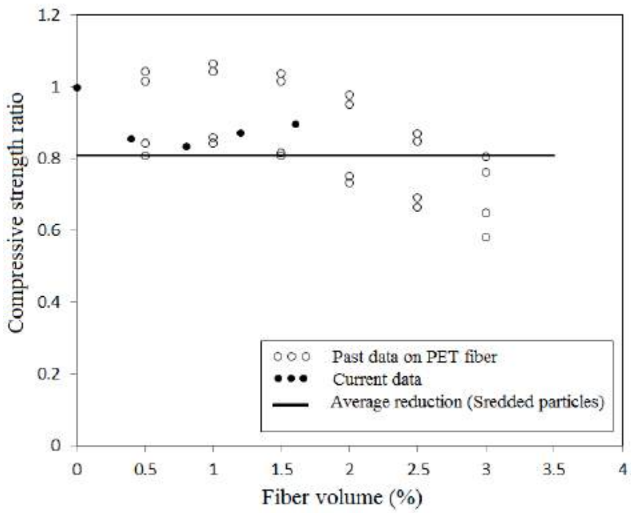

Fig. 3. Variation of compressive strength ratio with PET fibre ratio

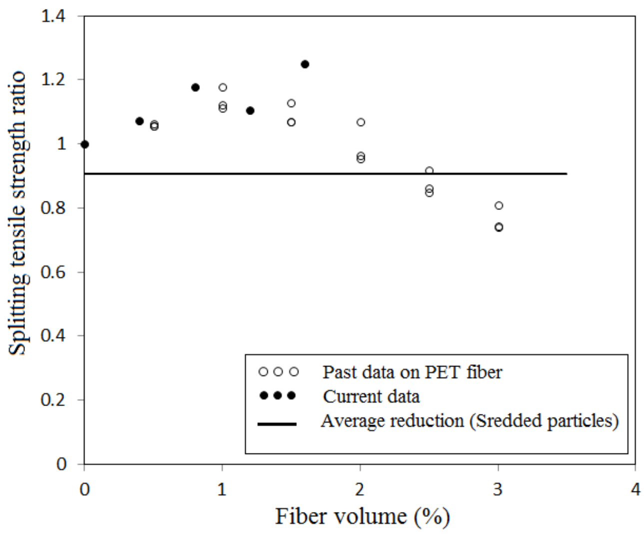

Fig. 4. Variation of splitting tensile strength ratio with PET fibre ratio

3.2 Comparison with the past test data

It is better to compare the obtained test data with those reported by the other researchers related to compressive and splitting tensile strengths of concrete containing PET waste particles or fibres. A total of 32 test data on the compressive strength of concrete containing 10% of PET waste shredded particles were taken from references [5-8] are used here. The compressive strength ratio is varied between 0.581 and 1.026. Average value of the residual compressive strength ratio is 0.808. A total of 18 test data on splitting tensile strength of concrete containing 10% of PET waste shredded particles were taken from references [4-8] are used here. The tensile strength ratio is varied between 0.519 and 1.056. Average value of the residual tensile strength ratio is 0.906. A total of 24 data point tested by Nibudey et al [9] of compressive strength and tensile strength were used for the comparison sake. Fig. 3 shows the variation of compressive strength of concrete with the fibre ratio variation based on the test data obtained in this investigation and those obtained by Nibudey et al [9] in addition to the average percentage reduction related to 10% shredded particles content. It is observed that the maximum strength loss measured in this investigation is smaller than the average strength loss which is 19.2% obtained by the other researchers. The reason of this is because of the existence of fibres. The compressive strength of concrete tested in this investigation is close to those measured by Nibudey et al [9] for concrete contained 30 mm fiber length which is close to that attempted in this investigation, but the optimum fiber content for the minimum loss is somewhat different. One can observe that the strength loss increased with fibre ratio larger than 1% tested by Nibudey et al. The behavior in tension is somewhat different. One can observe that the splitting tensile strength loss as a result of shredded PET waste particles is only 9.4%, smaller than that of compressive strength. The effect of fiber addition is beneficial for fiber content not larger than 2%. The best fiber content is 1% and at this fiber content the increase is splitting tensile strength is 17.8% for the 50 mm length PET fiber and 11.2% for the 30 mm length fiber tested by Nibudey et al [9]. The splitting tensile strength of concrete tested in this investigation is nearly similar to that obtained by Nibudey et al alone as observed from Fig. 4. Therefore, one can conclude that there is no problem related to the tensile strength of concrete contained shredded particles and fibre up to 1.6%.

4. Conclusions

The following conclusions can be drawn from this research study

1. There is a good chance to use a combination of both shredded and PET waste fibre for the production of recycled concrete containing plastic waste. Up to 10% shredded particles and 1.6% fibre ratio can be used for practical applications.
2. Compressive strength loss of the produced concrete is not larger than the average loss obtained by the other researchers which is 19.2%. The splitting tensile strength was found not reduced due to the combination of shredded and fibre wastes.
3. In general, properties of concrete containing both shredded and PET waste fibre is similar to those of concrete containing plastic fibres alone.

References

[1] D. Fotti, “Preliminary analysis of concrete reinforced with waste bottles PET fibers”, *Construction and Building Materials*, Vol. 25, 2011, pp. 1906-1915;
[2] R.N. Nibudey. P.B. Nagarnaik, D.K. Parbat & A.M. Pande, “Strength and Fracture Properties of Post Consumed Waste Plastic Fibre Reinforced concrete”, *International Journal of Civil, Structural, IJCSEIERD*, Vol 3. Issue 2, 2013;
[3] M. K. Ramadevi, Ms R. Manju (2012), “Experimental investigation on the properties of concrete with Plastic PET (bottle) fibers as fine aggregates”, *International Journal of Emerging Technology and Advanced Engineering*, Volume 2 Issue 6, 42-46;
[4] M. R. Frigion, “Recycling of PET bottles as fine aggregate in concrete”, *Waste manage*, Vol. 30, No. 6, 2010, pp. 1101-1106;

[5] C. Albano, N. Camacho, M. Hernandez, A. Matheus, A. Gutierrez, “Influence of content and particle size of waste pet bottles on concrete behavior at different w/c ratios”, *Waste manage*, Vol. 29, 2009, pp. 2707-2716;
[6] E. Rahmani, M. Dehestani, M.H.A. Beygi, H. Allahyari, I.M. Nikbin, “On the mechanical properties of concrete containing waste PET particles”, *Constr. Building Mat*., Vol.47, 2013, pp. 1302–1308;
[7] A. Sadeghifar, M. Sohrabi, “Investigating the properties of mechanical concrete containing waste plastic bottles replaced instead rock material”, *Interdiscip. J. Contem. Res. Bus.*, Vol. 5, No. 10, 2014, pp 131–141;
[8] N. Saikia, J. De Brito, ‘Waste polyethylene terephthalate as an aggregate in concrete”, *Mater. Res.*, Vol. 16, No. 2, 2013, pp. 341–350;
[9] R. N. Nibudey, P.B. Nagarnaik, D.K. Parbat, A.M. Pande, “Strength and fracture properties of post consumed waste plastic fiber reinforced concrete”, *Int. J. Civ. Struct. Environ. Infrastruct. Eng. Res. Dev.* Vol. 3, No. 2, 2013, pp. 9–16.

ISSN 1454 - 8003
Proceedings of 2017 International Conference on Hydraulics and Pneumatics - HERVEX
November 8-10, Băile Govora, Romania

DEVELOPMENTS, TRENDS AND ORIENTATIONS REGARDING THE REALIZATION OF RENEWABLE ENERGY CONVERSION SYSTEMS

Corneliu CRISTESCU[1], Cătălin DUMITRESCU[1], Valeriu DULGHERU[2], Liliana DUMITRESCU[1]

[1] Hydraulics and Pneumatics Research Institute INOE 2000-IHP, Bucharest; cristescu.ihp@fluidas.ro

[2] Technical University of Moldova, Chișinău; dulgheru@mail.utm.md

Abstract: *This article presents some considerations on the generation and use of renewable energies as well as the benefits of using them as an alternative to the current fossil fuel-based power generation system. It is shown the evolution of renewable energies in the last ten years, the trends and new orientations in the development of renewable energy conversion systems, as well as some elements regarding the evolution of the costs and investments in the field.*

Keywords*: Renewable energy, energy efficiency, functional optimization, clean energy, wind energy, hydraulic energy*

1. Introduction

The prospect of exhaustion of fossil energy resources, still dominating global consumption, as well as focusing on environment-friendly technologies, has led to an avalanche of technologies for the superior use of renewable energy sources as an alternative to the future of mankind.
The pace of development and spread of new technologies for all types of renewable sources is explosive, the growth of them being almost exponential.
However, classic / fossil fuels, oil, gas, coal remain the main sources of energy for a long time, Figure 1 [1]. Positive is the fact that the amount of renewable energies in total planetary consumption is continually increasing.

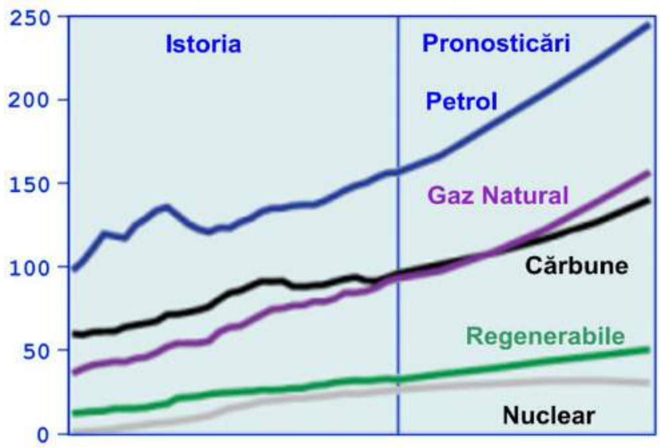

Fig. 1. Global energy consumption, 1970-2025 [1]

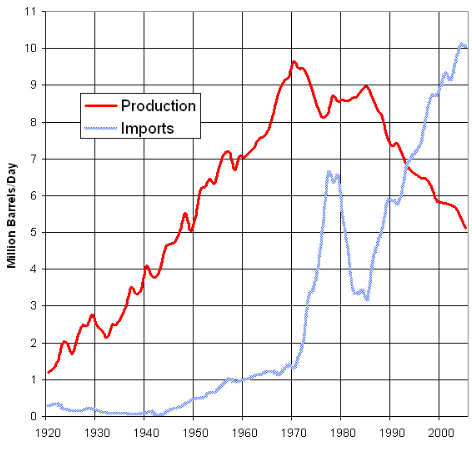

Fig. 2. Production and import of oil in the USA [1]

For example, the same pattern of exponential growth was also the evolution of oil production and import in the USA, with production peaking in 1970, after which import is accentuated, due to a strategic policy of this country, as shown in Figure 2 [1].
A brief analysis of the curve, demonstrates the very similarity to the Hubbert standard curve.
Based on past oil production data, the HUBBERT curve was built, and used to make estimates of future production performance. According to this estimate, in Figure 3, it can be seen that the maximum oil and gas production quota has already been reached around 2007.

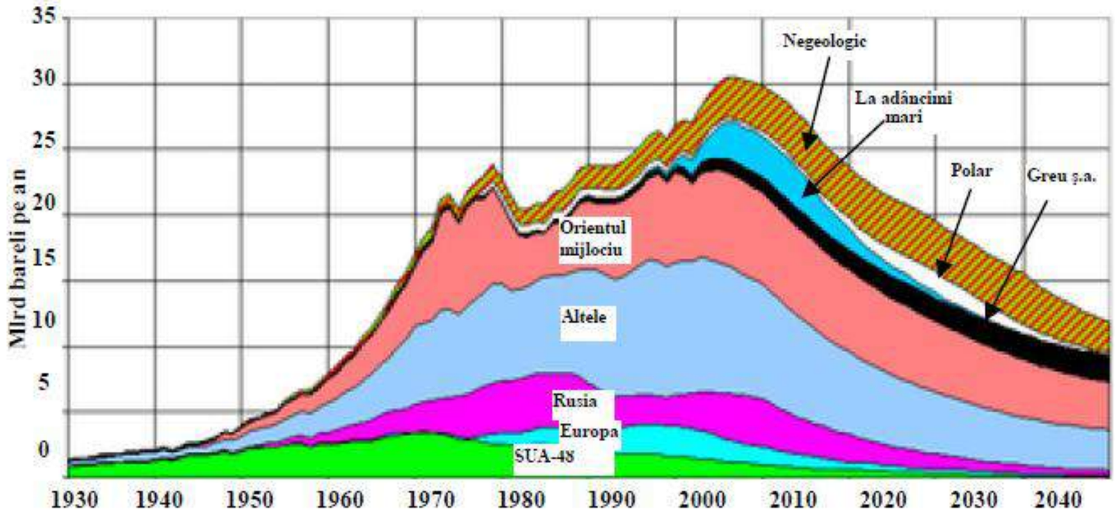

Fig. 3. Estimation of the maximum oil and gas production quota [1]

Interestingly is that, using other estimation methods, the results obtained are similar.
Therefore, in this context, it is important to estimate the energy production in the future, in order to know the moment when the regenerative energies will become the main sources of energy that will ensure the necessity of the development of the human society.
That is why today we can talk about a global energy policy and a concerted strategy to reduce pollutant emissions into the atmosphere, based on concrete technical and economic solutions for rational use of fossil fuel reserves (which still have the main share in the production of energy) and on a growing scale of renewable energy sources, the so-called "clean" energies or unconventional energies, an alternative to the current energy recovery system of the Earth's fossil fuel reserves. However, environmentally friendly renewable (solar, wind, hydraulic and so on) are not able today to meet these ever-increasing needs [1].

2. Overview of the development of renewable energies

Renewable energy comes from natural resources that are constantly renewed over relatively short periods of time. Currently, the functioning of the world economy relies heavily on energy from non-renewable resources (coal, oil, natural gas). Factors such as greenhouse gas emissions that favour global warming (see Figure 1), pollution, acid rain, all caused by the use of these conventional resources, but also the alarm signals that draw attention to the fact that oil - the main fuel source for transport - is about to run out, have triggered a significant global investment process in order to capitalize on renewable energy resources [2].
Worldwide, some renewable energy technologies have reached a certain degree of maturity, but others are in the testing or even applied research phase.
As a result of global population growth and the decline in fossil fuel, oil and natural gas reserves, research and development is increasingly focusing on renewable energy [3].
Renewables are now established around the world as main-stream sources of energy. Rapid growth, particularly in the power sector, is driven by several factors, including the improving cost-competiveness of renewable technologies, dedicated policy initiatives, better access to financing, energy security and environmental concerns, growing demand for energy in developing and emerging economies, and the need for access to modern energy. Consequently, new markets for both centralised and distributed renewable energy are emerging in all regions [4].
Global investment also climbed to a new record level, with further declines in per unit costs of **wind and solar** photovoltaics (PV). For the sixth consecutive year, renewables outpaced fossil fuels for net investment in power capacity additions [4].

In parallel with growth in markets and investments, saw continued advances in renewable energy technologies, ongoing energy efficiency improvements. The year also saw expanded use of **heat pumps**, which can be an energy-efficient solution for heating and cooling [4]. The **power** sector experienced its largest annual increase in capacity ever, **Wind and solar PV** had record additions for the second consecutive year, accounting for about 77% of new installations, and **hydropower** represented most of the remainder [4].
Renewable energy accounted for an estimated **4% of global fuel for road transport** in 2015.
The **solar PV market** was up 25% over 2014 with an annual market in 2015 was nearly **10 times** the world's cumulative solar PV capacity of a decade earlier.
Wind power was the **leading source** of new power generating capacity in Europe and the United States in 2015, and the second largest in China. The **offshore sector** had a strong year.
Global new investment in renewable power and fuels climbed to a record in 2015. This represents a rise of 5% compared to previous year.The global new investment in renewable power and fuels, developed, emerging and developing countries, in peroid of ten years, 2005–2015, is preyented in figure 4.

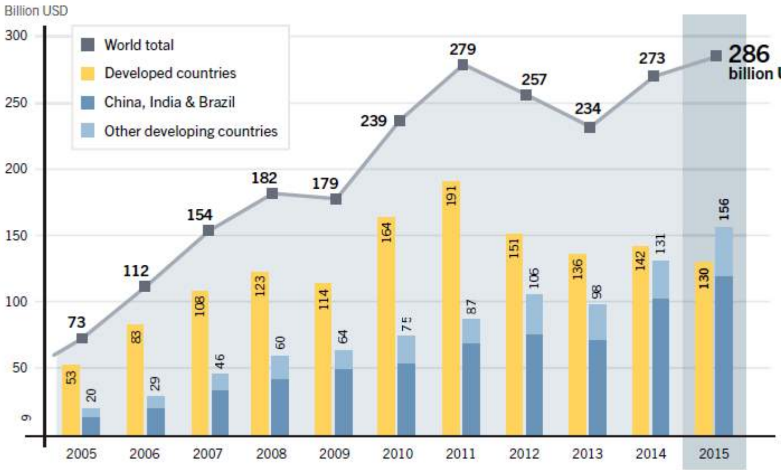

Fig. 4. Global new investment in renewable power and fuels [4]

Energy efficiency improvements reflect, in part, increasing investments. The global primary energy intensity and total primary energy demand, in period 1990–2014, is shown in figure 5.

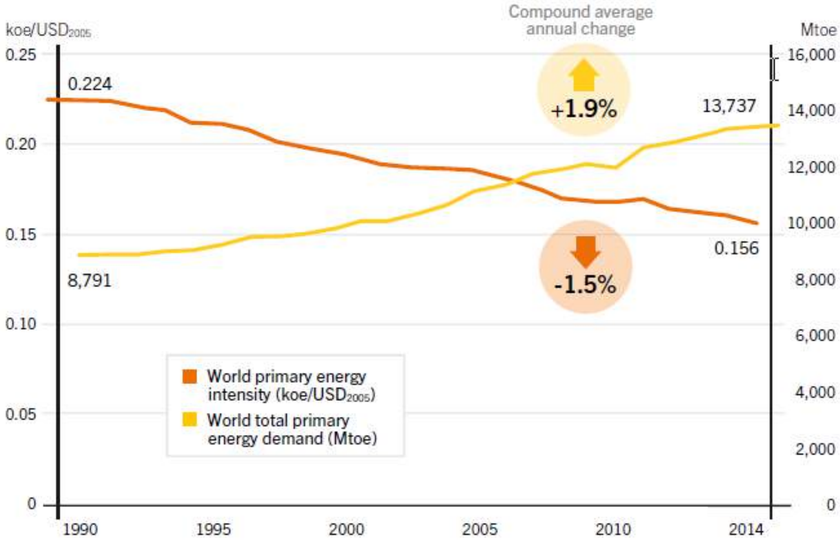

Fig. 5. The global primary energy intensity and total primary energy demand [5]

ISSN 1454 - 8003
Proceedings of 2017 International Conference on Hydraulics and Pneumatics - HERVEX
November 8-10, Băile Govora, Romania

3. Evolution of regenerative energies in the last ten years [5]

3.1. Power

Renewable power generating capacity saw its largest annual increase ever in 2016, Total global renewable power capacity was up almost 9% compared to 2015.
Solar PV saw record additions and, for the first time, accounted for more additional power capacity than any other generating technology. Solar PV represented about **47%** of newly installed renewable power capacity in 2016, and **wind** and **hydropower** accounted for most of the remainder, contributing about 34% and 15.5%, respectively.In 2016, renewables accounted for an estimated nearly 62% of net additions to global power generating capacity. At the 2016 year's end, renewables comprised an estimated 30% of the world's power generating capacity – enough to supply an estimated 24.5% of global electricity, with hydropower providing about 16.6%.
By the end of 2016, the top countries for total installed renewable electric capacity continued to be China, the United States, Brazil, Germany and Canada. China was home to more than one-quarter of the world's renewable power capacity. The ongoing growth and geographical expansion of renewable energy was driven by the continued decline in prices for renewable energy technologies (in particular, for solar PV and wind power), by rising power demand in some countries and by targeted renewable energy support mechanisms. Solar PV and **onshore wind** power are now competitive. Bid prices for offshore wind power also dropped significantly in Europe during 2016.

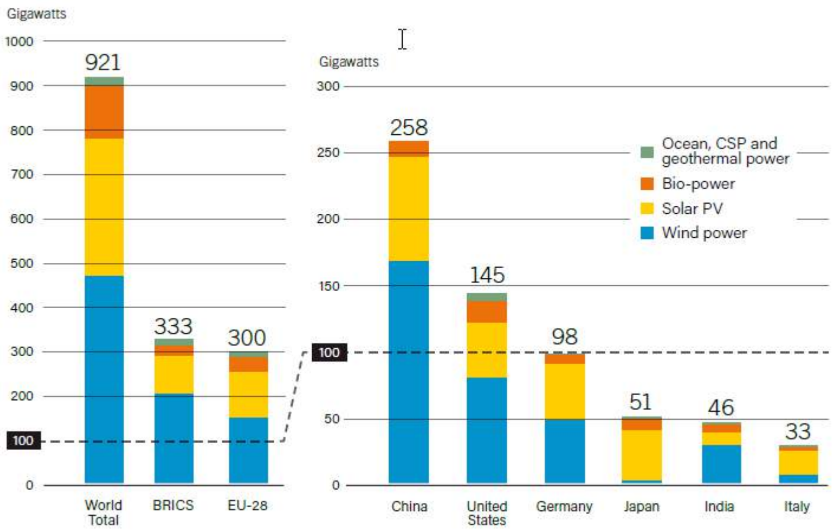

Fig. 8. Renewable power capacities in world, BRICS, EU-28 and Top 6 countries, 2016 [5]

3.2. Biomass Energy

Bioenergy (in traditional and modern uses) is the largest contributor to global renewable energy supply There are many pathways by which biomass feedstocks can be converted into useful renewable energy, figure 9.

Fig. 9. Generating and using energy from biomass [5]

3.3. Hydropower

Global hydropower capacity additions in 2016 are estimated to be in increasing. The top countries for hydropower capacity are China, Brazil, the United States, Canada, the Russian Federation, India and Norway, which together accounted for about 62% of installed capacity at the end of 2016. Global hydropower generation was estimated to be up about 3.2% over 2015. Global **pumped storage** capacity (which is counted separately) also in increasing in 2016, figure 10.

Fig. 10. Hydropower plant [5]

Pumped storage is the dominant source of large-scale energy storage, and new projects are under development. Global pumped storage capacity rose by more than in 2016, with new capacity installed in China, South Africa and Europe. On a smaller scale, pumped storage is being pursued to supplement mini-grids and to help integrate variable renewable energy. For example, a pumped storage facility is being implemented in the Canary Islands as part of a larger programme to improve grid stability and to accommodate variable generation. In Gaildorf, Germany, a **hybrid wind** power and pumped storage pilot project is under way; the upper reservoirs are being integrated into the towers and bases of the wind turbines, creating the added benefit of taller hub heights and thus greater potential wind power generation.

3.4. Solar Photovoltaics (PV)

More solar PV capacity was installed in 2016 (up 48% over 2015) than the cumulative world capacity five years earlier. Figure 11 presents the solar photovoltaics panels.

Fig. 11. Solar photovoltaics panels [5]

By year’s end, global solar PV capacity totalled will be pncreased (see Figure 12). For the fourth consecutive year, ASIA eclipsed all other markets, accounting for about two-thirds of global additions. The top five markets – China, United States, Japan, India and the United Kingdom – accounted for about 85% of additions; others in the top 10 for additions were Germany, the Korea, Australia, the Philippines and Chile. For cumulative capacity, the top countries were China, Japan (which passed Germany) and the United States, with Italy a distant fifth (see Figure 13).

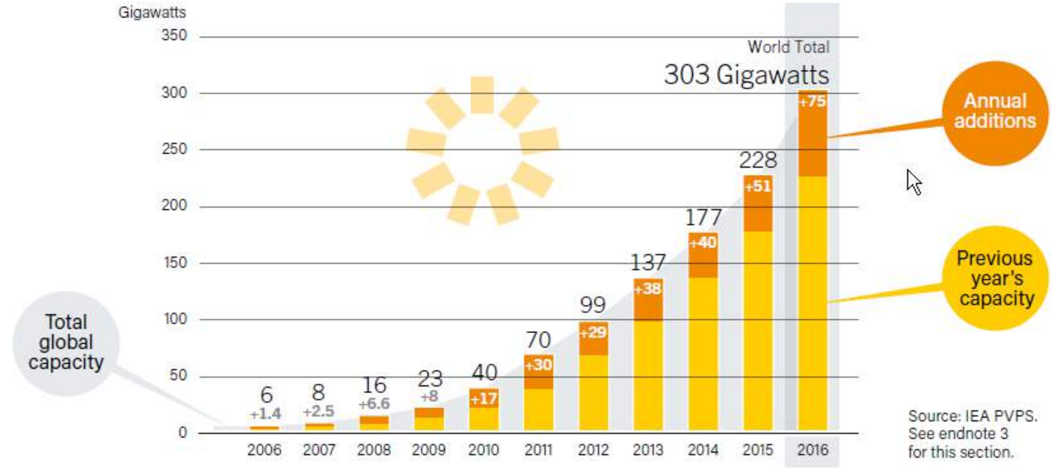

Fig. 12. Solar PV global capacity and annual additions, 2006-2016 [5]

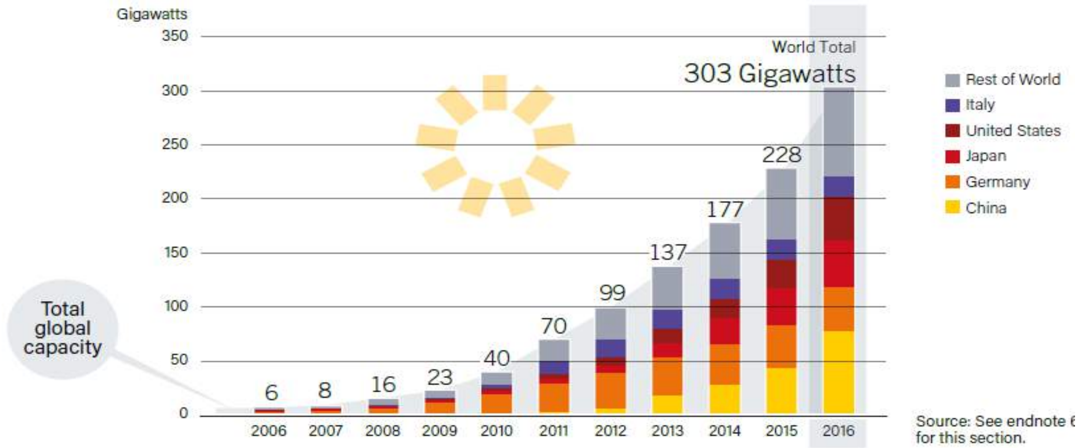

Fig. 13. Solar PV global capacity, by country and region, 2006-2016 [5]

While China continued to dominate both the use and manufacturing of solar PV, emerging markets on all continents have begun to contribute significantly to global growth. In 2016, China added capacity up 126% over 2015, increasing its total solar PV capacity 45% , far more than that of any other country, Figure 14.

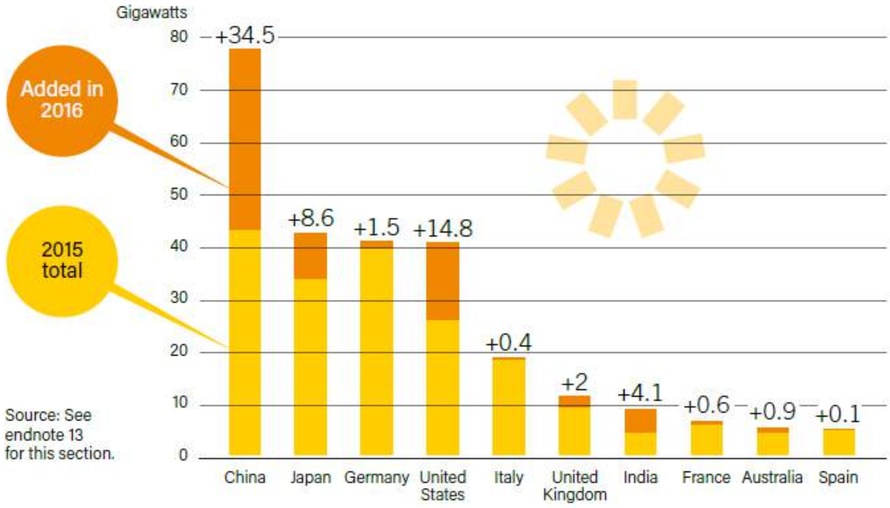

Fig. 14. Solar PV capacity and additions, Top 10 countries, 2016 [5]

Despite tremendous demand growth in 2016, the year brought unprecedented price reductions for modules, inverters and structural balance of systems. Due to even greater increases in production capacity, as well as to lower market expectations, particularly in China, for 2017, **module prices** plummeted. by an estimated 29%, vs the fourth quarter of 2015, dropping to historic lows.
The year 2016 also saw an increased interest in hybrid projects that locally integrate solar PV with other renewables and energy storage technologies, an innovation that can strengthen a plant's generation profile and enable sharing of resources for construction and maintenance.

3.5. Solar thermal heating and cooling

Solar thermal technology is used extensively in all regions of the world to provide hot water, to heat and cool space, to dry products and to provide heat, steam or refrigeration for industrial processes or commercial cooking, figure 15.

Fig. 15. Solar thermal systems [5]

By the end of 2016, solar heating and cooling technologies had been sold in at least 127 countries. The cumulative capacity of glazed (flat plate and vacuum tube technology) and unglazed collectors in operation increased to a year-end total of 456 GWth, up from 435 GWth a year earlier, figure 16.

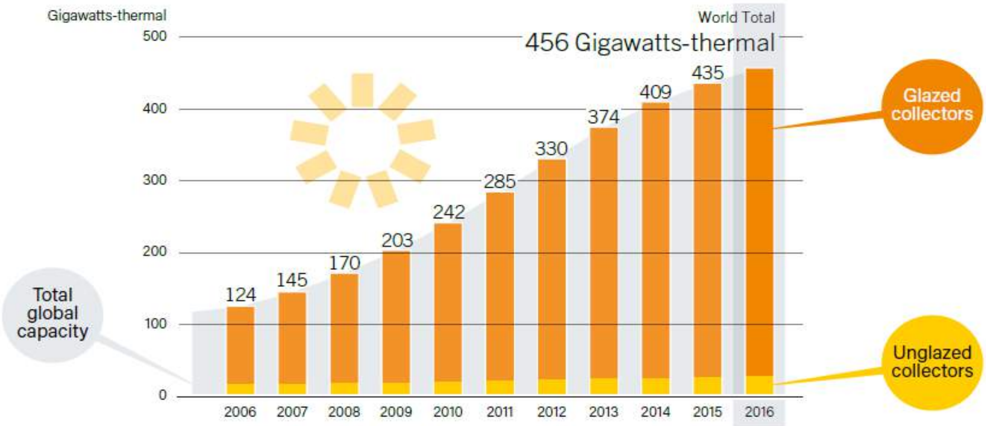

Fig. 16. Solar water heating collectors global capacity, 2006-2016 [5]

The solar water heating collector additions and the Top 20 countries for capacity added in 2016, are presented in figure 17.
Solar PV-thermal technologies capture the waste heat from solar PV modules, which utilise only 12-15% of the incoming sunlight, to provide heat for space and water. Solar thermal cooling continued to face challenges during 2016 in the key markets of Europe and China due to falling solar PV prices, which allow for the cost-effective operation of compression chillers powered by solar electricity during daylight, and to low fossil fuel prices. Even so, significantly hot summer periods in southern Europe, have increased the awareness of solar cooling technologies in the region's construction industry.

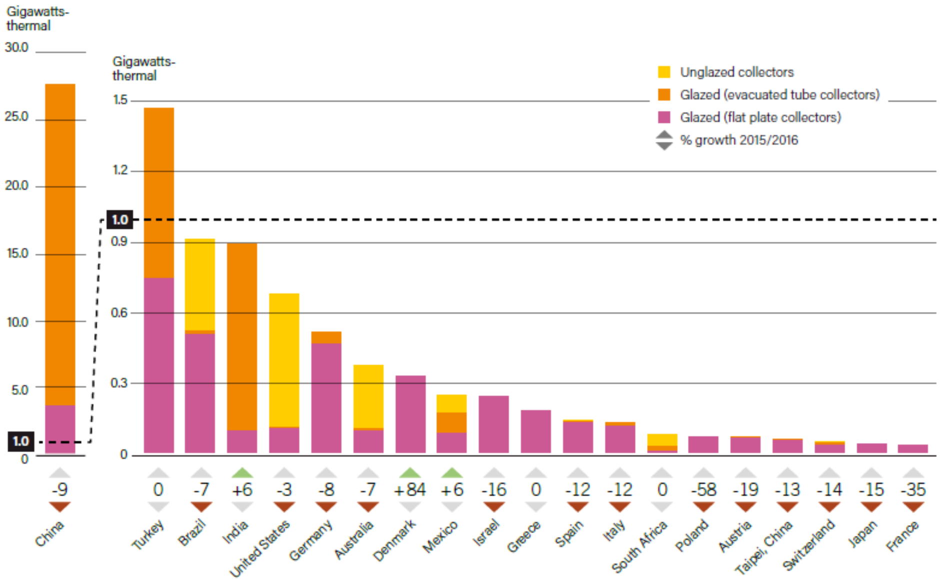

Fig. 17. Solar water heating collector additions, Top 20 countries for capacity added, 2016 [5]

3.6. Wind power

An important quantity of wind power capacity was added during 2016, increasing the global total about 12% vs 2015. Gross additions were 14% below the record high in 2015, but they represented the second largest annual market to date, figure 18

 

Fig. 18. Wind power plants [5]

By the end of 2016, over 90 countries had seen commercial wind power activity, figure 19.

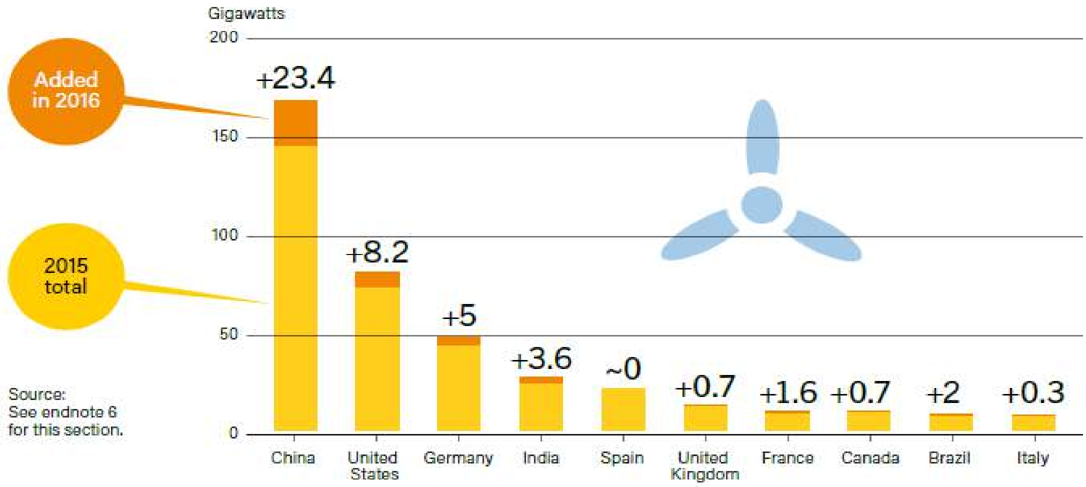

Fig. 19. Wind power capacity and additions, Top 10 countries, 2016 [5]

The wind power global capacity and annual additions are presented in Figure 20.

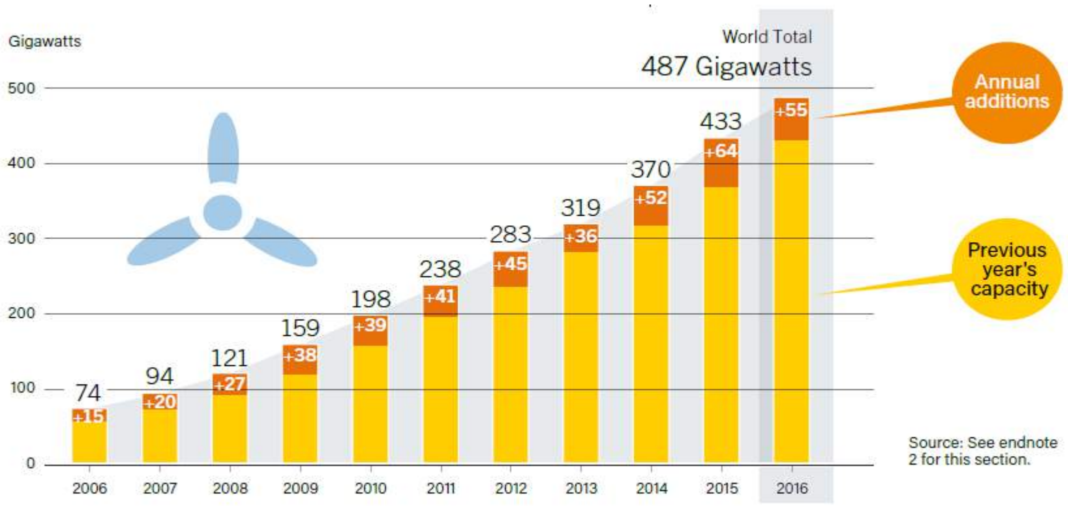

Fig. 20. Wind power global capacity and annual additions, 2006-2016 [5]

A significant decline in the Chinese market, following a very strong 2015, was responsible for most of the market contraction. Even so, China retained its lead for new installations, followed distantly by the United States and Germany, with India passing Brazil to rank fourth. Others in the top 10 for additions were France, Turkey, the Netherlands, the United Kingdom and Canada..
For the eighth consecutive year, Asia was the largest regional market, representing about half of added capacity, with Europe and North America accounting for most of the rest. Wind deployment was driven by cost- ompetitiveness and by environmental and other factors. Wind has become the least-cost option for new power generating capacity in an increasing number of markets.
Offshore wind plants, was connected to grids in 2016, As in previous years, Europe was home to the majority of capacity brought online, 70% of global additions, and total operating offshore, almost 88%, figure 21. Germany, the Netherlands and the United Kingdom were the only European countries to add capacity offshore, although several gigawatts of projects were under construction in European waters at year's end, driven by rapidly falling costs.

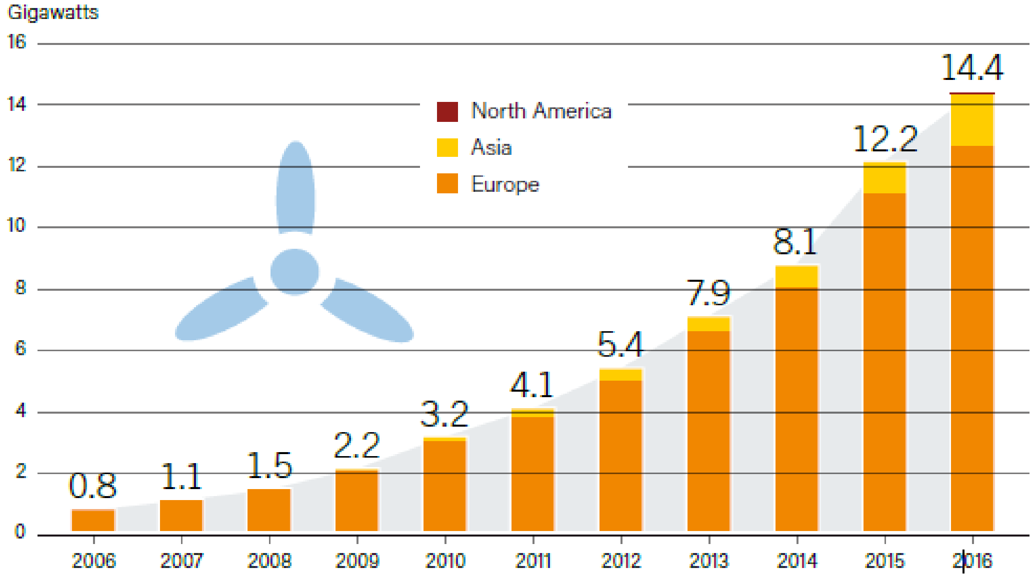

Fig. 21. Wind power offshore global capacity, by region, 2006-2016 [5]

While most countries have some small-scale turbines in use, the majority of units and capacity operating at the end of 2015 was in China, the United States and the United Kingdom. Other leaders included Italy and Germany, with Italy seeing a significant increase in 2016.
Repowering has become a billion-dollar market, particularly in Europe. While most repowering involves the replacement of old turbines with fewer, larger, taller, and more-efficient and reliable machines, some operators are switching even relatively new machines for upgraded turbines (including software improvements). During 2016, at least 721 turbines were decommissioned, representing a significant increase in numbers and capacity over 2015. Germany dismantled 242 turbines, followed by Denmark, the United States, Finland, Canada, the United Kingdom, the Netherlands, Sweden and Japan. In the United States, the extension of federal tax credits has incentivised repowering and retrofitting of existing assets, which enables owners to quality for another decade of credits.
Wind power is playing a greater role in power supply in a growing number of countries. In 2016, wind energy covered an estimated 10.4% of EU demand and equal or higher shares in at least 11 EU member states,
Globally, wind power capacity in place by the end of 2016 was enough to meet an estimated 4% of total electricity consumption.
WIND has become the LEAST-COST option for new power generating capacity in an increasing number of markets. Small-scale wind turbine costs also are trending downwards, while capacity factors are rising. To increase the competitiveness of small-scale wind, several leading US companies begun offering long-term leases to build on of third-party financing for solar PV.

4. Cost trends of the renewable power technology in period of 2010-2016 [5]

Among the most transformative events of the current decade has been the dramatic, and sustained, improvement in the competitiveness of renewable power generation technologies. Around the world, renewables have benefited from a cycle of falling costs spurred on by accelerated deployment, and the competiveness of renewable power generation technologies continues to improve. Bio-power, hydropower, geothermal and onshore wind power all can be competitive with fossil fuel-fired power generation where good resources exist.
Of all renewable energy technologies, utility-scale (larger than 1 MW capacity) **solar PV** has experienced the most rapid decline in the *levelised cost of electricity* (LCOE), driven by reductions in module prices and balance of systems costs.
Onshore wind power has undergone a quiet revolution over the years. During the period 1983 to 2016, and considering the 12 countries that accounted for 87% of deployment, the LCOE dropped by an average of 15% for each doubling of installed capacity. The weighted average investment cost of onshore wind declined by more than two-thirds, from USD 4,880 per kW in 1983 to USD 1,457 per kW in 2016, due to increasing economies of scale and to improvements in manufacturing and technology. Due in large part to technology advances, the global weighted average capacity factor for onshore wind power rose from 20% in 1983 to 29% in 2016.
The global weighted average of *Organization for Economic Co-operation and Development* (LCOE) of onshore wind power fell by 18% between 2010 and 2016 alone, to USD 0.07 per kWh for wind farms commissioned in 2016. China and India have some of the world's lowest total installed costs, resulting in a weighted average LCOE of USD 0.065 per kWh in 2016 (down 7% from 2010); average LCOEs were higher in OECD countries (USD 0.074 per kWh; down 26% from 2010) and in the world (USD 0.083 per kWh; down 29% from 2010).
The global weighted average LCOE of onshore wind power fell by 18% between 2010 and 2016 alone, to USD 0.07 per kWh for wind farms commissioned in 2016. Onshore wind power has seen a significant convergence in average LCOEs across regions, despite differences in regional cost structures, market sizes and technical skills, and varying dynamics in supply chains. China and India have some of the world's lowest total installed costs, resulting in a weighted average LCOE of USD 0.065 per kWh in 2016 (down 7% from 2010); average LCOEs were higher in OECD

countries, Organization for Economic Co-operation and Development, (USD 0.074 per kWh; down 26% from 2010) and in the rest of the world (USD 0.083 per kWh; down 29% from 2010).
Offshore wind power costs, in general, are higher than for other renewable power generation technologies. However, they are falling due to several factors – including technology advances and economies of scale – and good cost reduction opportunities remain. In OECD countries, where most offshore wind capacity is deployed, the average LCOE of projects commissioned in 2016 was estimated at USD 0.15 per kWh.
Concentrating solar thermal power (CSP) costs also remain higher than those for other renewable power generation options on average, but they have good cost-reduction opportunities, and costs are falling. It is estimated that the weighted average LCOE of CSP plants fell by 18% between 2010 and 2016, with an LCOE of USD 0.27 per kWh for plants commissioned in 2016.
LCOEs of the more mature renewable power generation technologies – bio-power, geothermal and hydropower – have been broadly stable, with some short-term exceptions. For example, the global weighted average LCOE of geothermal and hydropower rose between 2010 and 2016. The weighted average total installed cost of hydropower projects reached USD 1,755 per kW (weighted average LCOE of USD 0.05 per kWh) for plants commissioned in 2016, more than offsetting an increase since 2010 in the weighted average capacity factor of new plants.

5. Conclusions

- As a synthetic conclusion, it can be said that the use of renewable energy sources is in full swing and encompasses all existing forms with an explosive evolution;
- The most important renewable energy source is the running water;
- The solar energy has developed greatly, both through photovoltaic collectors and thermal panels;
- Wind power plants also have a very important development;
- The offshore industry moved to deeper waters and continued to grow;
- The interest in storing and storing energy is growing, where many technologies have developed;
- R & D focuses more on renewable sources;
- Some aspects of the economy have also been analyzed, which has shown that the investments made are still expensive, but the cost of a kWh is constantly decreasing.

Acknowledgments

This paper has been developed in INOE 2000-IHP, as part of a project co-financed by the European Union through the European Regional Development Fund, under Competitiveness Operational Programme 2014-2020, Priority Axis 1: Research, technological development and innovation (RD&I) to support economic competitiveness and business development, Action 1.1.4 - Attracting high-level personnel from abroad in order to enhance the RD capacity, project title: *Establishing a high level proficiency nucleus in the field of increasing renewable energy conversion efficiency and energy independence by using combined resources*, project acronym: *CONVENER*, Financial agreement no. 37/02.09.2016.

References

[1] I. Bostan, V. Dulgheru, I. Sobor, V. Bostan, A. Sochireanu, “Renewable Energy Conversion Systems.- Wind, Solar, Hydraulic” („Sisteme de conversie a energiilor regenerabile - eoliană, solară, hidraulică”), Tehnica-Info Publishing House, Chişinău, 2017;
[2] E. Maican, “Renewable energy systems” („Sisteme de energii regenerabile”), Printech Publishing House, Bucharest, 2015;
[3] *** Energii regenerabiile. IMAO. In: http://www.imao.ro/energii-regenerabile
[4] *** Renewables 2016 Global Status Report. REN21 Renewable Energy Policy Network for 21st Century. Paris, 2016; On: http://www.ren21.net/wp-content/uploads/2016/05/GSR_2016_Full_Report_lowres.pdf;
[5] *** Renewables 2017 global status report. REN21 Renewable Energy Policy Network for 21st Century. Paris, 2016.
On: http://www.ren21.net/wp-content/uploads/2017/06/178399_GSR_2017_Full_Report_0621_ Opt .pdf

ISSN 1454 - 8003
Proceedings of 2017 International Conference on Hydraulics and Pneumatics - HERVEX
November 8-10, Băile Govora, Romania

ENERGY CONVERSION UNIT FROM WATER STREAMS FOR USE IN AGRICULTURAL RURAL REGIONS

Fănel ȘCHEAUA[1]

[1] "Dunărea de Jos" University of Galati, MECMET Research Center, fanel.scheaua@ugal.ro

Abstract: *The natural water circuit is of vital importance for maintaining life on our planet. The waters flowing from the mountain heights form important water courses that feed underground aquifers by infiltrations that occur directly from their riverbed but also the oceans that receive the optimum water flow rates initially released by evaporation. In addition to other utilities offered by the rivers, the high potential for obtaining energy from the water flow, which is currently insufficiently exploited, must be shown. A turbine model by means of which energy can be produced based on the water flow is presented in this paper. It is a simple model that can be easily mounted directly into the river bed in order to obtain energy in a particular agricultural rural area that is far away positioned from the centralized electrical network. A complete turbine model has been developed and analyzed in terms of its operation principle in a CFD analysis.*

Keywords*: fluid flow, water stream, impeller, energy conversion, CFD*

1. Introduction

The uninterrupted water flow in nature has ensured the perpetuation of life and offered multiple benefits to flora, fauna and human communities over time.
A continuous water movement in nature has determined man's intervention through constructions designed to capture the moving water energy and transform it into another form of energy, namely electricity, needed to ensure the industry needs but also the optimal comfort in human communities as well.
It has to be remembered that man has used the water power since the earliest times when the first mills located on the course of the fast mountain waters were conceived.
For the power generation, the first power plants were designed at the end of the 19th century, being designed to supply energy to a small number of consumers, but with the passage of time, many hydroelectric power units have been placed on the most important courses of flowing water in the world. Thus the largest hydro-power unit in the world is located in China with a total of 22500 MW installed capacity when working at full capacity.
When energy is needed in a more isolated area adjacent to a flowing stream with a considerable flow rate, it can be considered a solution to generate energy by means of a special construction unit with turbine that can be located directly in the riverbed, meant to take over the potential energy from water flow, converting it into mechanical rotational energy and through a generator into electricity.
This constructive solution is a mobile version of a power plant that uses water to provide electricity, which can be used in specific agricultural applications located in rural areas that do not have an electrical network in the immediate vicinity.

2. Theoretical aspects on water stream flow in nature

The river flow phenomenon in nature can be described using the Navier-Stokes equation system. These equations characterize the movement of the fluids in general and can be considered as a continuation of Newton's fluid movement second law, which for Newtonian compressible fluids can be written: [4]

$$\rho\left(\frac{\partial v}{\partial t}+v\nabla v\right)=-\nabla p+\nabla\left(\mu\left(\nabla v+\left(\nabla v\right)^{n}\right)-\frac{2}{3}\mu\left(\nabla\cdot v\right)I\right) \quad (1)$$

where:
v - fluid velocity;
p - pressure;
ρ - fluid density;
μ - dynamic viscosity.

The equation balances the inertial forces represented by the left-hand term with the fluid pressure and viscosity forces in the right-hand term. These equations representing the mass conservation equations are solved together with the continuity equation constituting the conservation of the moment: [4]

$$\frac{\partial\rho}{\partial t}+\nabla\cdot\left(\rho v\right)=0 \quad (2)$$

The mathematical modelling of a river's water flow can be achieved using a system of equations deduced from the Navier-Stokes equation system called the Saint-Venant system: 0

$$\begin{cases} A_t\frac{\partial v}{\partial x}+v\frac{\partial A_t}{\partial x}+\frac{\partial A_t}{\partial t}=Q_l \\ \frac{\partial v}{\partial t}+v\frac{\partial v}{\partial x}+\frac{g}{A_t}\frac{\partial\left(hA_t\right)}{\partial x}+\frac{vQ_l}{A_t}=g\left(\alpha-\alpha_r\right) \end{cases} \quad (3)$$

where:
A_t - river transversal section area;
v - water velocity;
Q_l - the affluent per length unit;
t- time;
g- gravitational acceleration;
α - river slope;
α_r - hydraulic gradient;
h - the depth between the water section gravity center and the surface.

3. Power unit with turbine assembly model

An overall model of a mobile power unit with turbine has been built. The model is a simplified constructive solution by means of which the water potential energy it can be converted into mechanical rotational energy at the turbine shaft on which electric power can be obtained within a generator. Such simplified solutions can be handy for obtaining energy in areas where there is no electricity network from farms rural areas.
Figure 1 shows the schematically operation principle for the presented constructive solution of power unit with turbine for energy conversion.

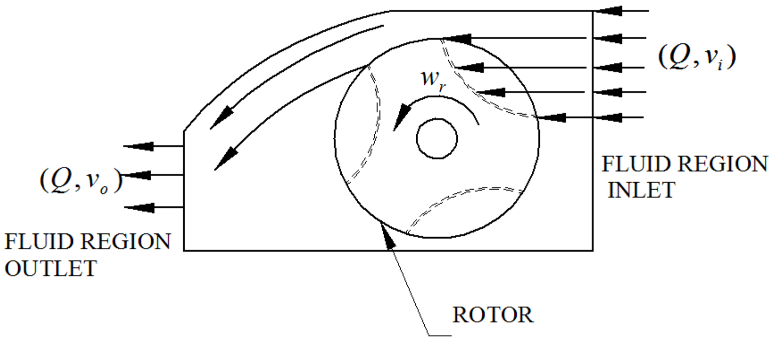

Fig. 1. Schematic representation for the turbine assembly model

The assembly operation consists of introducing into the water so that the water flow rate exerts a force on the propeller blade which causes its rotation movement around the turbine shaft. Due to the continuous water flow, this force is applied sequentially on each blade providing a permanent rotation motion to the turbine shaft.

4. Functional analysis for the turbine model

An analysis describing the turbine virtual model operation was performed using the ANSYS CFX program. Thus, a fluid region having a water working fluid has been defined, inside which the turbine model is placed, being declared as immersed fluid.
A water flow rate of 3 cubic meters per second was declared at the fluid region inlet. The results are presented in terms of fluid velocity and pressure of working fluid inside the analyzed region.
A meshing network having 12774 nodes and 61314 triangular shaped elements was achieved for the analyzed model. Figure 2 shows the analised virtual model and the results obtained.

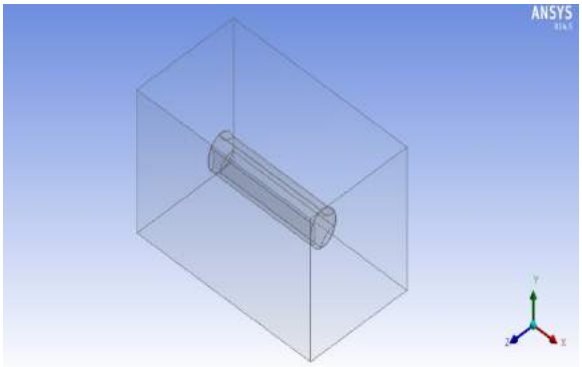

a) The analysed model

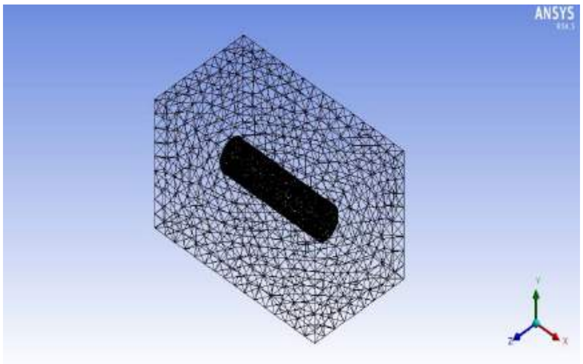

b) Mesh network

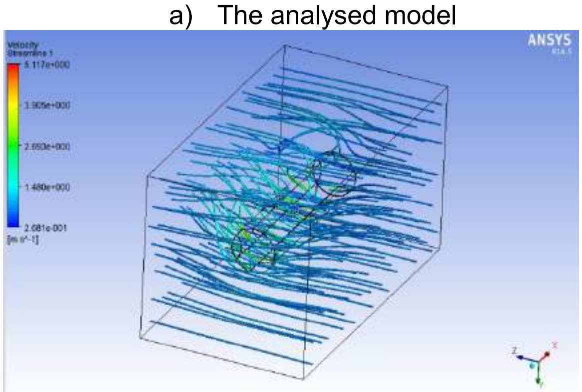

c) Fluid velocity values

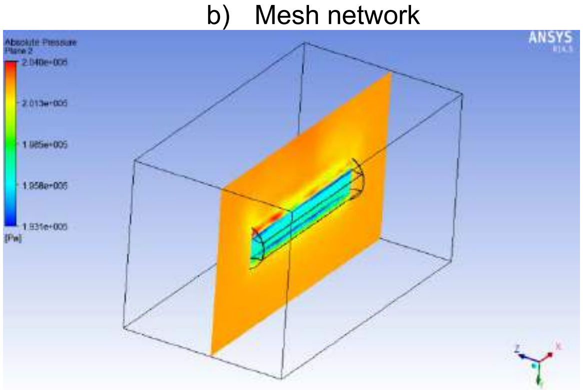

d) Absolute pressure values

Fig. 2. The analyzed virtual model and the results obtained

5. The results obtained from the conducted analysis

Table 1: Fluid velocity and absolute pressure values and diagrams

Fluid velocity values [m/s]	Absolute pressure [bar]
0.09	1.01
1.33	1.07
1.47	1.09
1.58	1.23
1.89	1.44
2.43	1.57
2.85	1.63
3.32	1.72
3.89	1.81
4.07	1.89
4.24	1.95
4.89	1.98
5.37	2.01
5.6	2.03

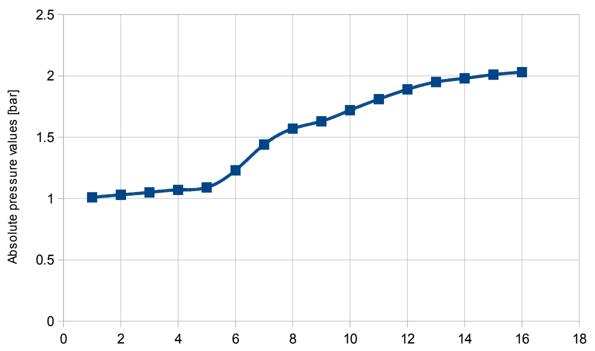

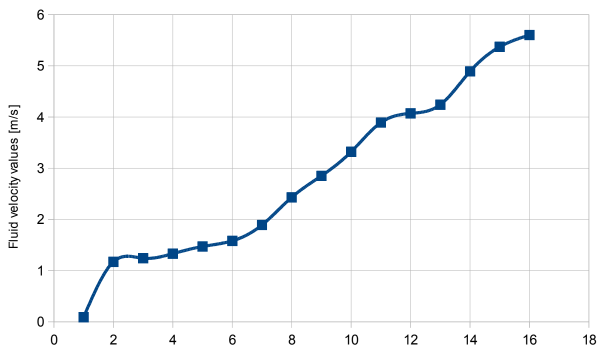

Table 1 shows the values obtained from the analyzed model and corresponding diagrams for the fluid velocity and absolute pressure variation inside the fluid region.
The results obtained show a pressure increase and fluid velocity higher values near the blade region necessary for the blade rotational movement.

6. Conclusions

This paper presents a turbine model that can be used to convert the water flow potential energy into mechanical energy as propeller rotational motion and further into electrical energy by means of a generator.
The model is intended for use on low depth water courses but with a high flow velocity and a relative constant water flow rate.
From the analysis on the virtual model the obtained results reveals that higher values of fluid velocity and pressure are recorded in the fluid region near the blade area. This shows the possibility of achieving rotation movement of the blades around the axis of the turbine.
Such devices can be easily used because they do not require a complex installation solution inside the river bed, but only a mounting by anchorage.

References

[1] G. Axinti, A. S. Axinti, “Acționări hidraulice și pneumatice“, Vol III, Editura Tehnica-Info, Chișinău, 2009;
[2] Al. A. Vasilescu, “Mecanica fluidelor”, Ministerul Educatiei și Învățământului, Universitatea din Galați, Galați, 1979;
[3] F. D. Șcheaua, “Possibilities for Agricultural Farms of Adopting and Applying Optimal Energy Recovery Solutions from Nearby Water Flows”, HIDRAULICA Magazine No. 2/2017, ISSN 1453 –7303, pp. 68-71;
[4] https://www.comsol.com/multiphysics/navier-stokes-equations
http://www.cnaa.md/files/theses/2015/22438/galina_marusic_thesis.pdf.

ISSN 1454 - 8003
Proceedings of 2017 International Conference on Hydraulics and Pneumatics - HERVEX
November 8-10, Băile Govora, Romania

ELEMENTS CONCERNING THE ENERGY CHARACTERISTICS OF BIOMASS AND TECHNOLOGIES FOR CONVERTING IT INTO PELLETS

Gabriela MATACHE[1], Gheorghe SOVAIALA[1], Valentin BARBU[1], Alina Iolanda POPESCU[1], Ana-Maria Carla POPESCU [1], Mihai-Alexandru HRISTEA[1]

[1] Hydraulics and Pneumatics Research Institute – INOE 2000-IHP Bucharest, sovaiala.ihp@fluidas.ro

Abstract: *The European Commission appreciates that the role of biomass used for heat and electricity production in the EU Member States will increase, so that 20% of the produced energy will come from renewable sources by 2020. Biomass is considered to be neutral on greenhouse gas emissions because, while burning biomass generates carbon dioxide as well as burning fossil fuels, at the time of recurrence, it will re-absorb a quantity of carbon dioxide equivalent to that released during burning. Bioenergy is based on a wide range of potential raw materials: forestry and agricultural residues, waste and also materials grown for energy purposes. Raw materials can be converted into heat, electricity or transport fuels. Biomass has the highest degree of flexibility among all forms of renewable energy.*

Keywords*: Biomass, pellets, pelletizing equipment, heat power*

1. Introduction

The Earth's major challenge in the third millennium in the field of energy is the orientation towards renewable energy production systems in conditions of sustainable energy development that will provide the population with the energy they need without altering the planet's major ecosystem.
Renewable energy is one of the alternatives to the replacement of fossil fuels, with great prospects for future development. According to SRE-SEC (2008) estimates, a 34.9 Mtoe (million tons of oil equivalent) energy consumption forecast in Romania is projected by 2020 [1]. Biomass covers more than 60% of total Renewable Energy Sources (RES), namely 190 -200 PJ / year (Gheorghiescu et al. 2007, quoted by [2]). One of the main strategic directions that Romania has to implement is to mobilize all efforts to introduce and implement the RES.
Biomass reserves differ across the European Union and globally. The forest area ranges from 27.6 million hectares in Sweden to 117 ha in Cyprus (Panoutsou, 2011). Worldwide, the forest fund occupies approximately 4 billion ha, with the largest amount being distributed on the territory of the Russian Federation - 809 million ha, Brazil - 478 million ha, Canada - 310 million ha, the US - 303 million ha, China - 197 million Ha.
Of the 27 countries of the European Union, Romania ranks 8th in terms of its forestry fund, and globally Romania owns only 0.15% of the total area of forest land in the world. Biomass resources can also be determined by the degree of usage of the land that each country holds. Thus, approximately 50.1% of the area of 4 303 401 km^2 is used in the European Union, 1 041 423.04 km^2 being used for agricultural purposes and 309 844.87 km^2 for forestry (Eurostat 2012).
Increasing energy efficiency has a major contribution to achieving security in the field of energy and sustainable energy development, competitiveness in saving primary energy resources and reducing greenhouse gas emissions [2].

2. Combustible characteristics and energy potential of the biomass

The combustible characteristics of wood biomass differ from one material to another and of course they differ from those of fossil fuels. Biomass, in addition to the main advantage of being renewable, has a number of disadvantages compared to fossil fuels, which must be taken into consideration: biomass density and calorific value of wood species is lower compared to fossil fuels; some biomass sources are mostly generated only seasonally, requiring material storage in optimum conditions to avoid biodegradation; the thermal systems used for the conversion of

biomass must have high capacities, leading to an acceptable level of energy efficiency; unmanaged biomass usually has a high moisture content, which is the main factor that results in low heat output from combustion processes; the thermo-chemical characteristics of the biomass are inferior to those of fossil fuels because of the high oxygen content, alkaline substances and chlorides.
In industrial practice, manufacturing waste is produced from all the industrialized wood species: Horse chestnut (*Aesculus hipocastanus* L.), Hornbeam (*Carpinus betulus* L.), Turkey oak (*Quercus cerris* L.), Sweet cherry (*Prunus avium* L.), Beech (*Fagus silvatica* L.), Ash (*Fraxinus excelsior* L.), Birch (*Betula pendula* Roth.), Sycamore maple (*Acer pseudoplatanus* L.), Wild pear (*Pyrus pyraster* L.), Acacia (*Robinia pseudacacia* L.), Willow (*Salix alba* L.), Elderberry (*Sambucus nigra* L.), Oak (*Quercus rubur* L.), whose heat power is shown in Figure 1. [2]

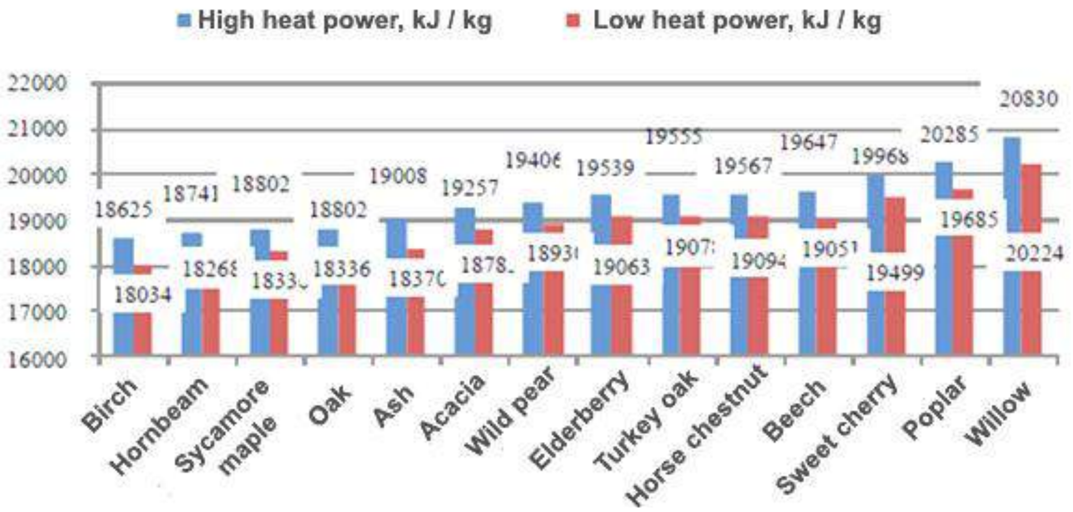

Fig. 1. Heat power of indigenous deciduous species

One of the possibilities of using wood biomass as fuel is in the form of briquettes and pellets. Wood biomass briquettes and pellets are superior products made from shredded wood, by compression and without additional additives.
Figure 2 shows the influence of moisture on calorific value of briquettes and pellets of poplar and beech species [2].

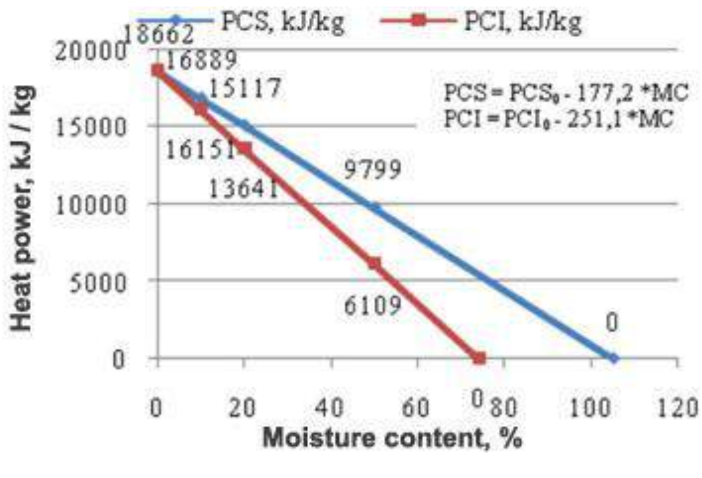

Poplar pellets

a.

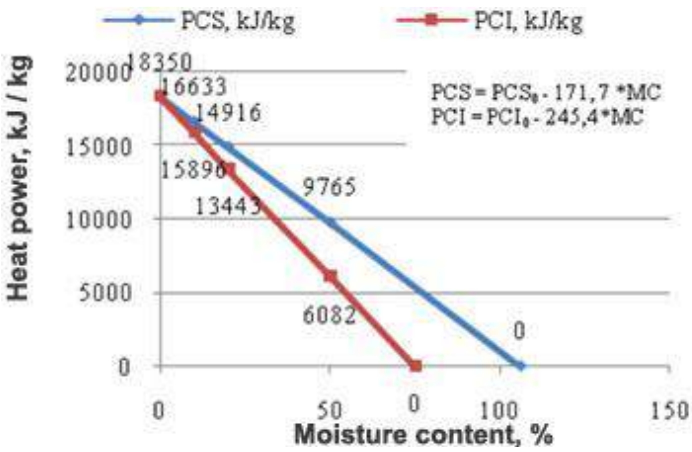

Beech pellets

b.

Fig. 2. Influence of humidity on calorific value of briquettes and pellets made out of poplar (a.) and beech (b.)

The importance of their use compared to massive firewood is due to the fact that the products are dried to 10% moisture content and keep this constant moisture up to the moment of use due to the polyethylene packaging they are stored in.
Figure 3 shows the influence of moisture on the energy density and burning rate of pellets and briquettes made out of poplar and beech species [2].

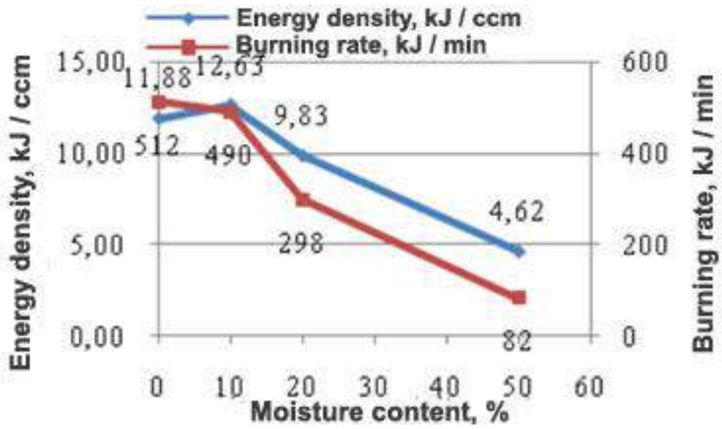

Poplar pellets

a.

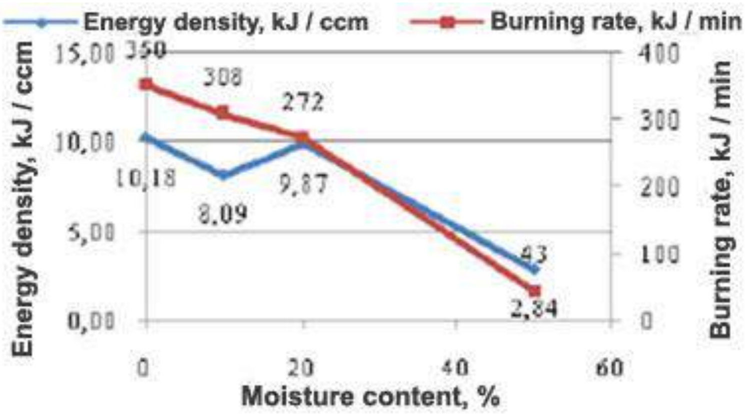

Beech pellets

b.

Fig. 3. Influence of humidity on energy density and burning rate of pellets and briquettes made out of poplar (a.) and beech (b.)

Figure 4 shows the influence of humidity on the energy efficiency of pellets and briquettes made out of spruce and oak tree species [2].

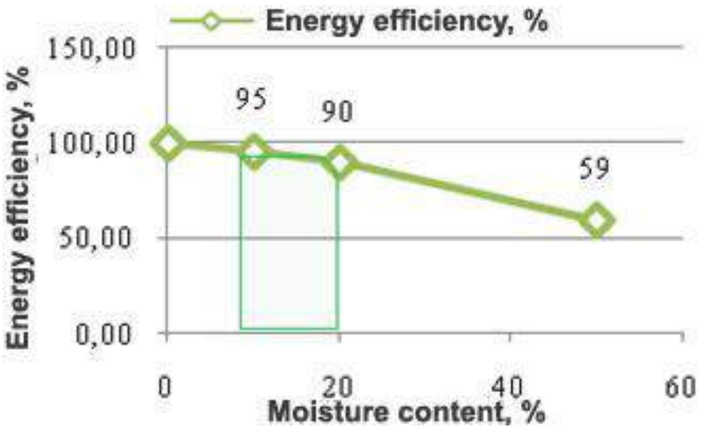

Spruce pellets

a.

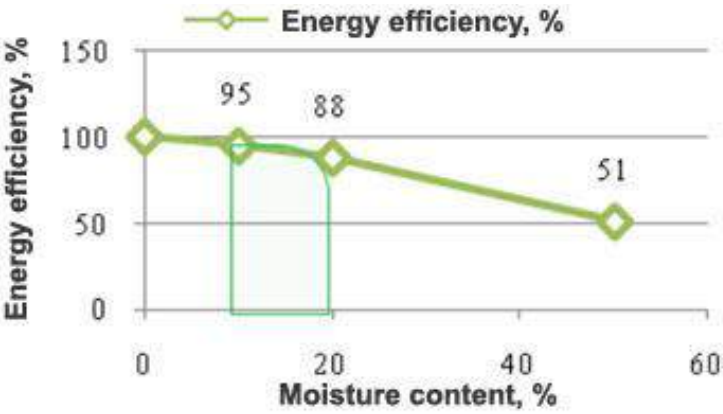

Oak briquettes

b.

Fig. 4. Influence of humidity on energy efficiency of pellets and briquettes made out of spruce (a.) and oak (b.)

3. Increasing calorific value of pellets and briquettes by torrefaction

The calorific density of the pellets and briquettes is better than the wood species actually used as fuel, in that they are used at 10% humidity and have a high compaction degree.

Thermal treatment is increasingly being used in processes for improving the mechanical or physic-chemical characteristics of wood biomass. Changing the structure and properties of biomass is achieved by changing the chemical composition, providing enrichment of carbon content. Biomass thermal treatment or torrefaction is a method by which its energy characteristics approach those of fossil fuels such as coal and pit coal.

Torrefaction is a process similar to pyrolysis, differing by a shorter treatment period which takes place in the low temperature range (200-300^{o}C), (Chen et al., 2010, quoted by [2]).

The torrefaction treatment is carried out at constant parameters: thermal treatment temperature of 200-300°C and treatment time of 3-10 minutes. The fixed values of the duration and temperature of the thermal treatment are top limiting, because by overcoming these values, even if the heat power increases, the cohesion of pellets and briquettes decreases significantly.

The calorific value of wood biomass is directly dependent on the elemental chemical composition (carbon, hydrogen and oxygen), but also on the main chemical compounds of wood (lignin, cellulose and hemicellulose).

By torrefaction, there occur significant mass losses and chromatic changes of process materials, regardless of the studied species - starting from a yellowish colour (the control sample), continuing with light brown (at 240°C) and reaching a dark brown to black (at 300°C). The loss of mass recorded after thermal treatment, Figure 5, is due to the decomposition of the main chemical compounds of wood, namely cellulose, hemicellulose and lignin [2].
Decompositions begin at a temperature of 150^{o}C, at which point water evaporates from the wood; in the range of 150-250^{o}C the volatile substances in the material are eliminated; after 250^{o}C there takes place decomposition of chemical compounds formed such as CO_2 and H_2O (Aghamohammadi et al., 2011; Chen et al., 2012 and 2011, Serrano et al., 2013; Bates et al., 2013 - quoted by [2]).
According to Aghmonammadi's research (2011), one can notice massive mass losses occurring at temperatures above 405^{o}C, and at 570^{o}C there is no mass loss. Mass losses ranged from 0-4% to 8-15%, the results directly depending on the moisture content of the pellets in the treatment process.

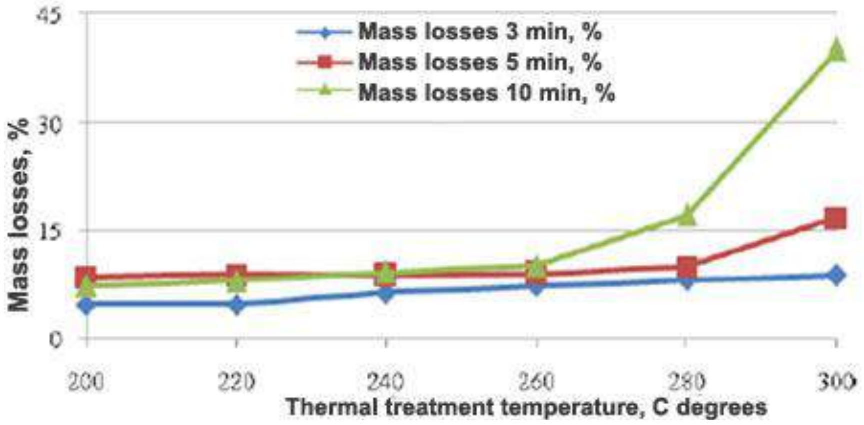

Oak (*Quercus robur* L.)
a.

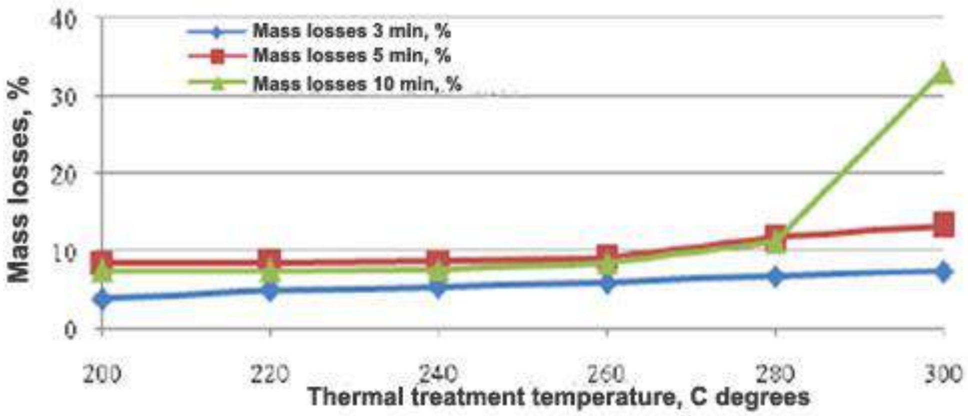

Beech (*Fagus sylvatica* L.)
b.

Fig. 5. Mass loss of oak (a.) and beech (b.) depending on the heat treatment temperature

In the description of Phanphanich et al. (2011) quoted by [2] biomass shows a loss of 10-20% through volatile substances and other chemical elements that are eliminated. Following the heat treatment process, the carbon content is greatly increased compared to the control sample. Mass losses occur in the initial phase on the temperature range of 150 - 220^{o}C, at the time the material is heated and until the ignition takes place (Chen et al., 2011a, Chen et al., 2012, quoted by [2]).

4. Presses for the manufacturing of pellets

The pellets are manufactured by pressing without binders wood waste or secondary agricultural production (straw, sunflower stems, soybeans and rape, corn cobs and corn husks, grains, beans, branches resulting from maintenance works in orchards, leaves, seeds and wheat shells from the food industry).
The pelletised material has to fulfil two essential conditions: the size of chips ranges between 30-50 mm and the maximum moisture is 15%. In this regard, a pellet manufacturing line will comprise equipment for raw material drying, chopping and pelletizing.
Pellet presses, Fig. 6, which will be referred to below, consist of a chassis, drive group (gearmotor or electric motor, coupling and conical reducer), press body, feed basket.

Fig. 6. Pellet making press

The press, which is the main assembly of the pelletizing equipment, consists of a body in which the mold and the presser roller shaft are mounted, Fig. 7a, b.
The pelletizing presses are made in two constructive variants: with rotary mold and fixed axle of the presser rollers, and respectively with fixed mold and rotary axle of the presser rollers.
The fixed mold design [3] offers increased rigidity, allows for more precise and simple tuning; it allows also the use of larger presser rollers, which increase the machine's working capacity and reliability.

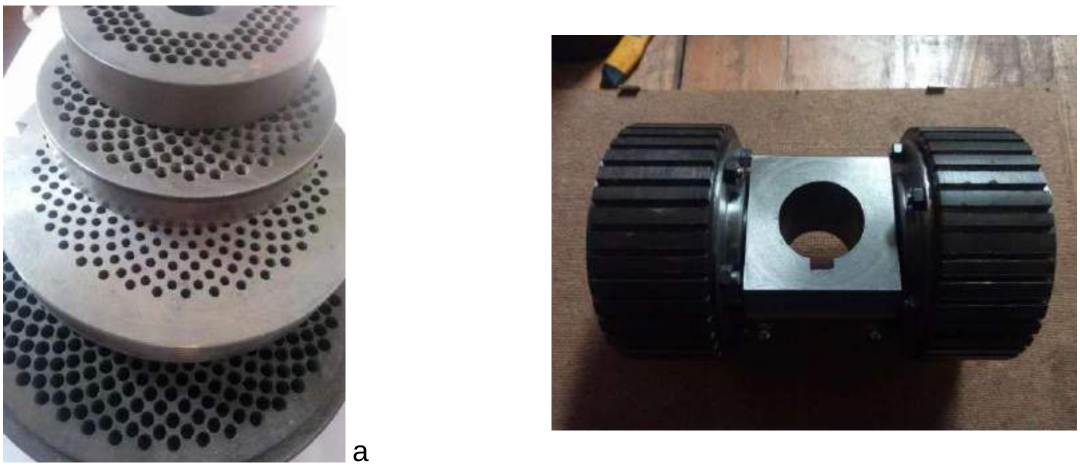
a b

Fig. 7. Pelletizing press: a-mold; b-axle with presser rollers

Of the pelletizing equipment available on the Romanian market, the KRONPELLET brand covers a wide range of powers and working capacities, Table 1.

Table 1: Technical characteristics of the KRONPELLET pelletizing equipment

Pressure Type	Engine power, kW	Diameter of mold, mm	Working capacity, kg / h (wood)
KPP - 120	2.5- monophase	120	30
KPP - 150	4- three phase	150	50
KPP - 200	10-three phase	200	150
KPP - 250	15- three phase	250	250
KPP - 275	18- three phase	275	3oo
KPP -300	30- three phase	320	480

The process of manufacturing the pellets involves extruding the material through the holes in the mold, under the action of the presser rollers (with satellite motion) whose axle is integral with the vertical shaft of the conical gear transmission, Fig. 8.

Fig. 8. Presser chamber of the pelletizing equipment

At IHP Bucharest an original bearing system for the vertical shaft of the press has been designed to allow the use of worm gears capable of transmitting high powers and torques compared to conical gear reducers. The technical solution is the subject of a patent application.

5. Characteristics of pellets, advantages and disadvantages of their use

Diameter: 3-15 mm (the most commonly used are 6 mm diameter pellets)
Length: <60 mm
Bulk weight: ~ 650 kg / m^3
Density:> 1200 kg / m^3
Moisture: <8%
Ash: <1.5%
Heat power: from 3500 to 4500 kcal / kg.
Advantages of wood pellets:
- They are relatively ecological, derived from wood waste;
- They are clean, modern and cheap energy source;
- They have very high autonomy; depending on the built pellet storehouse and the automation of the thermal plant, the autonomy of a pellet boiler can be of 1 month or even 2 months;
- A pellet thermal station, being regarded as ecological, can be purchased through the GREEN HOUSE program;

- The production of pellets is done by using wood waste and thus a cleanup of the natural environment of the soil polluting materials takes place;
- They are carbon neutral because they emit as much as the same amount of CO_2 (carbon dioxide) that was absorbed by the tree during its growth;
- Smoke emission resulting from burning of pellets is very low;
- In the flue gases the dust is alkaline;
- They have a low content of metals and sulphur is almost non-existent;
- The ash resulting from the burning of pellets can be later used as a natural fertilizer because it is rich in minerals;
- The cost of using pellets is lower than in the case of fossil fuels;
- Making a comparison with firewood, it results that pellets are more efficient in terms of combustion efficiency, calorific value, comfort and safety in use;
- In comparison to a conventional gas heating plant, a pellet heating plant will consume about 20-30% less for the same thermal output produced; if a comparison is made with a condensing gas boiler, which has a better efficiency than a conventional one, a pellet boiler will have about the same consumption for the same heat output;
- It requires a relatively low storage space, for a tonne of pellets a volume of approximately 1200 - 1500 liters / 1.2 - 1.5 m^3 is required.

Disadvantages of wood pellets:

- The cost of acquiring a high quality thermal plant on pellets or related equipment (bunker, sink, engine, pumps, safety valves, expansion vessels, etc.) can exceed 2 or 3 times the cost of purchasing a common wood-powered thermal power station, a gas-fired thermal power station, an electric thermal power plant on methane gas or LPG;
- High sensitivity to the pellet feed system of the boiler; the auger engine may clog or burn very quickly, the auger and the burner can be clogged by pellets if there is no periodic cleaning at 2-3 days and if the used pellets are of very poor quality;
- In the case of a pellet thermal plant, a quite large technical space is required for the installation of the boiler, the related equipment and the pellet bunker / pellet storehouse, the chamber which should meet the rules and regulations in force;
- Electric power interruption involves the introduction of safety features in the installation (which leads to an increase in the initial investment), such as a gasoline or diesel automatic generator or a UPS;
- A pellet boiler requires the installation of a chimney;
- Although the pellet boiler is considered to be ecological, however, burning pellets results in noxious matter, even if in a small quantity;
- The choice of pellets is usually done on the basis of the lowest price - the cheapest pellets; in this case there is the risk of buying poor quality pellets that will affect the correct functioning of the pellet boiler, respectively the equipment related to it.

6. Conclusions

At European level, alternative energy sources (RES) will contribute significantly to providing the necessary energy; provisions are made that in 2020 they will represent 20% of total energy used. The high potential for energy production lies with biomass (47%), followed by hydro energy (45%).
The term biomass includes agricultural products, waste and residues resulting from agricultural technological processes (grain straw, residues from the production of sugar, starch, beer, tobacco, canned fruit cans, by-products of the vine and wine industry- cords, grape bunches and grape pits, branches resulting from orchard maintenance works, etc.), wastes from forestry and related industries as well as the biodegradable fraction of urban vegetal and animal wastes.
Thermal treatment or torrefaction is a method by which the energy characteristics of biomass are approaching those of fossil fuels, involving changes in the structure and chemical composition, causing the carbon content to be enriched.

Biomass briquettes and pellets are superior energy products, made from compacted material without compression and without additional additives. The process of manufacturing them involves the existence of complex technological lines, which include equipment for drying, grinding, briquetting / pelletizing and storage of raw material.
Within IHP Bucharest there are concerns about finding innovative, patentable technical solutions in the development of biomass briquetting and pelletizing equipment.

Acknowledgements

This paper has been developed in INOE 2000-IHP, as part of a project co-financed by the European Union through the European Regional Development Fund, under Competitiveness Operational Programme 2014-2020, Priority Axis 1: Research, technological development and innovation (RD&I) to support economic competitiveness and business development, Action 1.2.3 – Partnerships for knowledge transfer, project title: *Eco-innovative technologies for recovery of biomass wastes*, project acronym: ECOVALDES, SMIS code: 105693-594, Financial agreement no. 129/23.09.2016.

References

[1] ***, "State of play on the sustainability of solid and gaseous biomass used for electricity, heating and cooling in the EU", Commission Staff Working Document;
[2] T.B. Grîu (Dobrev), "Assessing and increasing the wooden biomass calorific power" ("Evaluarea şi mărirea puterii calorice a biomasei lemnoase"), PhD thesis - University Transilvania of Braşov, 2014;
[3] ***, https://www.olx.ro/oferta/presa-peleti-ID6DvJO.html - Prejmer pellet press.

ISSN 1454 - 8003
Proceedings of 2017 International Conference on Hydraulics and Pneumatics - HERVEX
November 8-10, Băile Govora, Romania

STUDY OF THE VELOCITY OF THE FLOW IN WASTEWATER TREATMENT PLANT

Adrian CUREU[1], Florin BODE[2]

[1] Technical University of Cluj-Napoca, Romania, email: adriancureu@yahoo.com

[2] florin.bode@termo.utcluj.ro

Abstract: *The paper presents a study that was carried out on the velocity of the wastewater flow through the pumping well in the wastewater treatment plant in the primary stage where the pollutants removal processes such as large particles and solid particles in suspension or sedimentation are carried out. The study of flow rates in the pumping well has been done to obtain results in carrying out works to reconfigure the pumping well invert or to mount a water agitator. There are presented the obtained results, using the Fluent-ANSYS-PC software, at the pumping well, the velocity distribution in a plane parallel to the bottom of the basin at a distance of 10 mm from it. In conclusions, the paper presents the importance of mechanical purging, regarding the results discussed in the paper.*

Keywords*: Waste water, CFD, flow characteristics.*

1. Introduction

Waste water treatment is the set of physical, chemical, biological and bacteriological processes, which reduces the loading of organic and inorganic pollutants and bacteria, in order to protect the environment (air, soil, emissary, etc.). It results obtaining clean water, in different degrees of purification, depending on the technologies and the equipment used, as well as a mixture of bodies and substances which are called, generically, sludges. [1]

The paper presents a study that was carried out on the velocity of the wastewater flow through the pumping well in the wastewater treatment plant in the primary stage where the pollutants removal processes such as large particles and solid particles in suspension or sedimentation are carried out. The concern of conducting this waste water flow study through the pumping well at the treatment plant is to eliminate the deposition of solid particles on the well. The study of flow rates in the pumping well has been done to obtain results in carrying out works to reconfigure the pumping well invert or to mount a water agitator.

Due to the fact that a water treatment system operates continuously, it involves the analysis of its reliability at the conception stage, like pre-condition and to ensure water purification according to the water quality standards. The studies focused mainly on structural investigations of the wastewater treatment plant and the pumping well, where the experimental researches were carried out in order to establish possible effects of the action. [1], [2], [3]

2. Problem identification and approach

The Târgu Lăpuş Treatment Plant is located in Târgu Lăpuş, Maramureş County, 300 m from Târgu Lăpuş-Gâlgău Road, in the river basin Târgu Lăpuş River which is the emissary. It was commissioned in 1975 and was designed for a maximum purge rate of 9 [L/s] with a 82% yield for CBO5 and 74% for suspensions. The new Wastewater Treatment Plant is designed at a rate of 19 [L/s].

The technological flow includes: [1]

1. Mechanical treatment;
2. The biological treatment process;
3. Treatment of sludge.

In the mechanical treatment stage wastewater are removed the large bodies, the impurities that are deposited and the floating ones. Thin and fine suspensions are retained at this stage. For their retention are used the rare grills, screens, grease separator, sand decanter and decanters. [1]

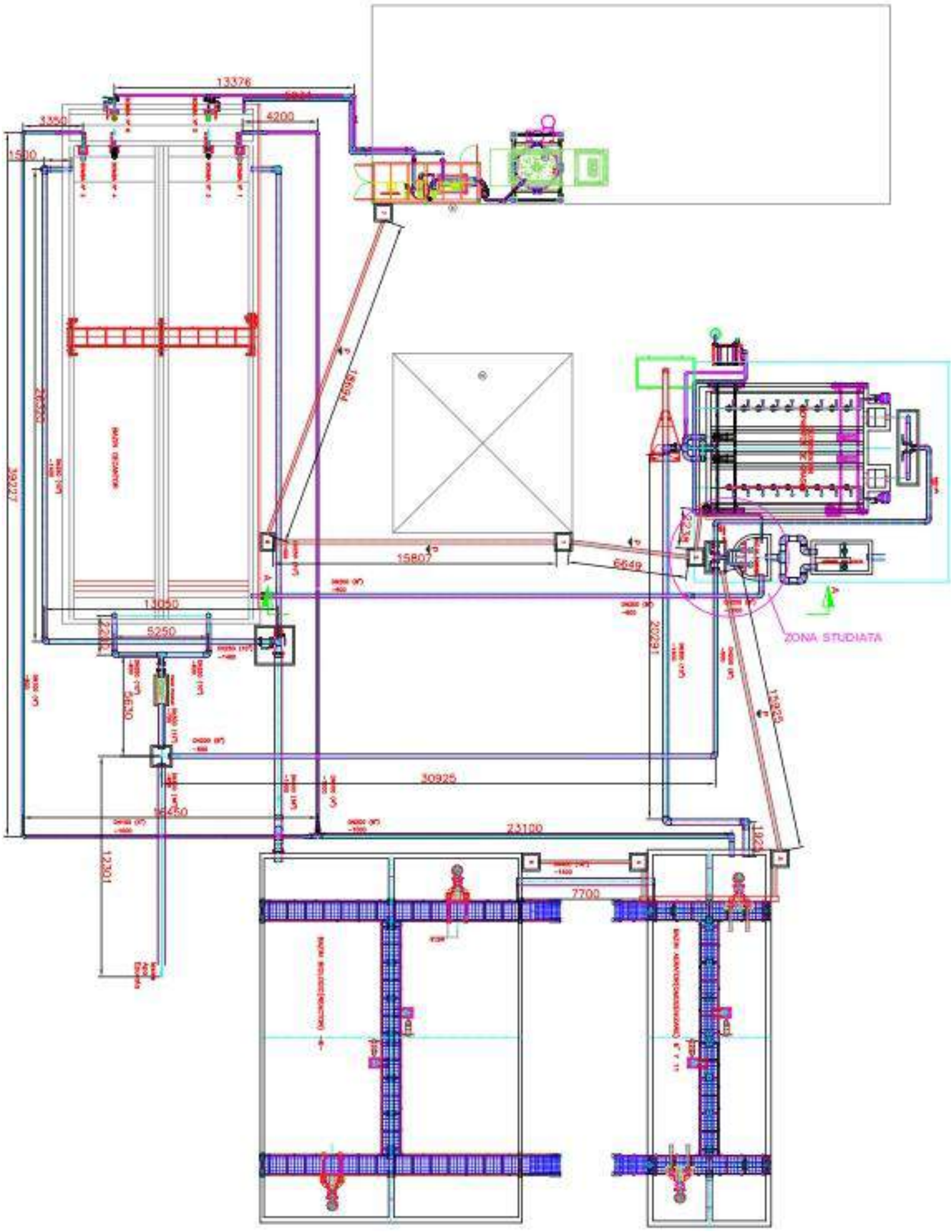

Fig. 1. Scheme of WWTP Targu Lapus

In a sewage treatment plant, water transport and constant flow and homogeneous flow are among the most important steps. Domestic water comes out of the screens basin and enters the pumping

well through two 400 mm diameter pipes and is discharged by means of two sumerable pumps connected to 3" diameter metal pipes in the desiccator and the grease separator.
The submersible pumps carry water and sludge between the technological stages of the treatment plant as well as to and from the treatment plant.

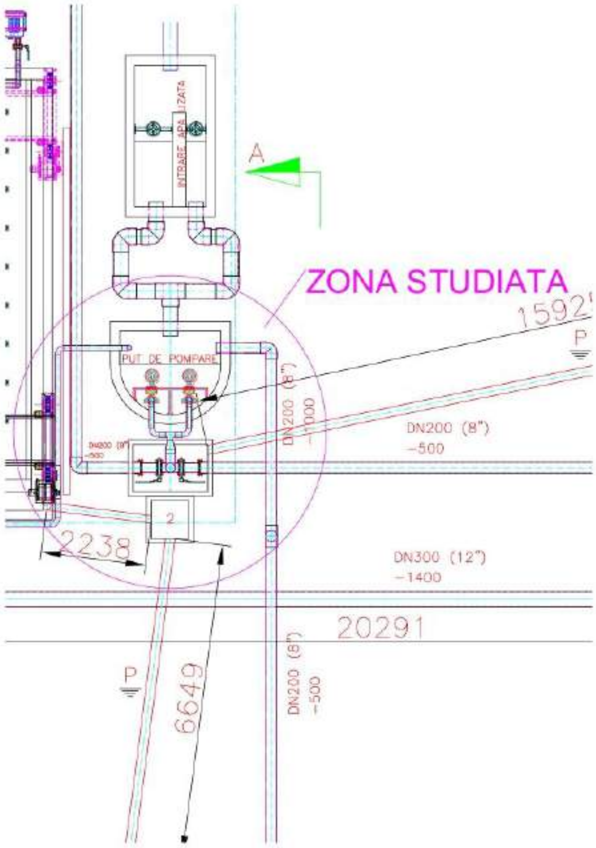

Fig. 2. The well for pumping station

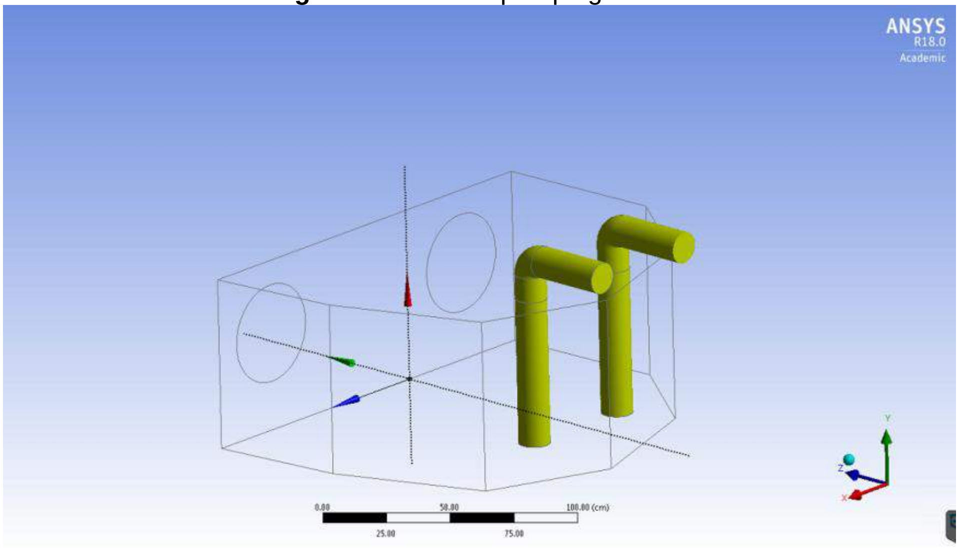

Fig. 3. Axonometry pumping station

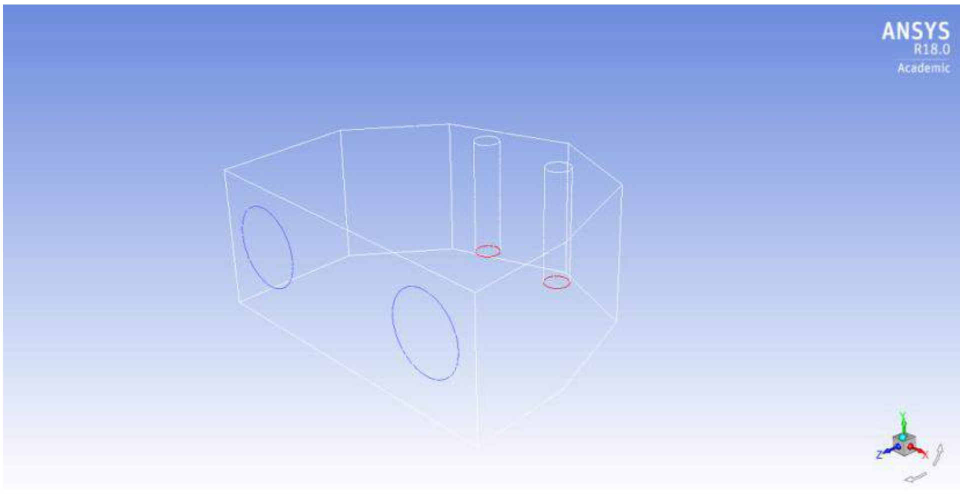

Fig. 4. The well for pumping station - CAD model

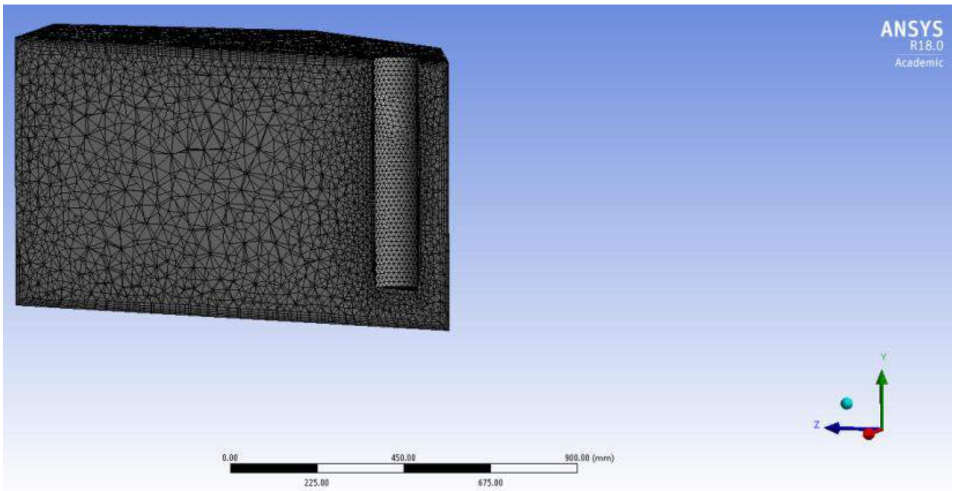

Fig. 5. Section shaft pumping station purification

3. Results

The obtained results using the Fluent @ ANSYS-PC application at the pumping well the velocity distribution in a plane parallel to the bottom of the basin at a distance of 10 mm from it. The mathematical model is based on solving a set of differential conservation equations, supplemented with numerous additional equations, often semicircular models, to handle the turbulence.

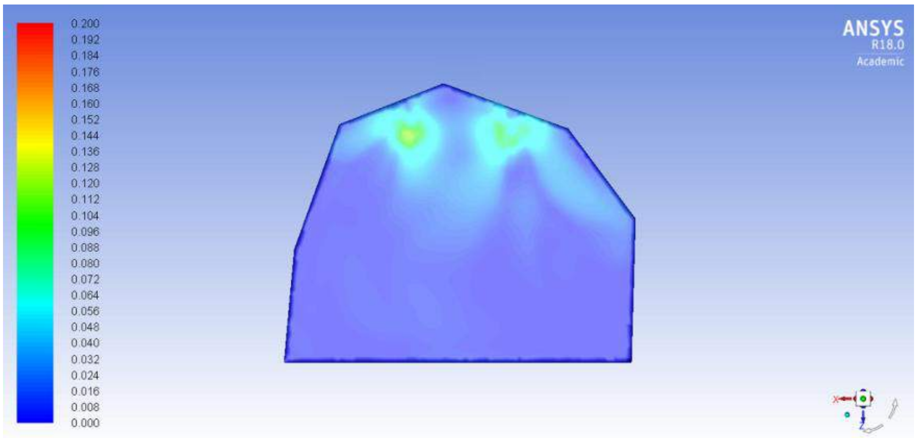

Fig. 6. Pressure-based pumping well

From the above picture we can see that in the pump suction area, the colour is blue and greenish-yellow, making it a scale-grading, the maximum fluid velocity of 0.128 m/s.

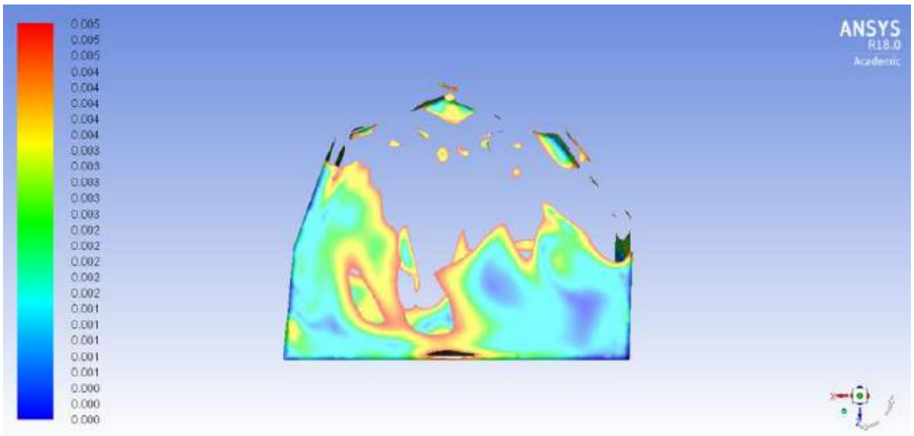

a)

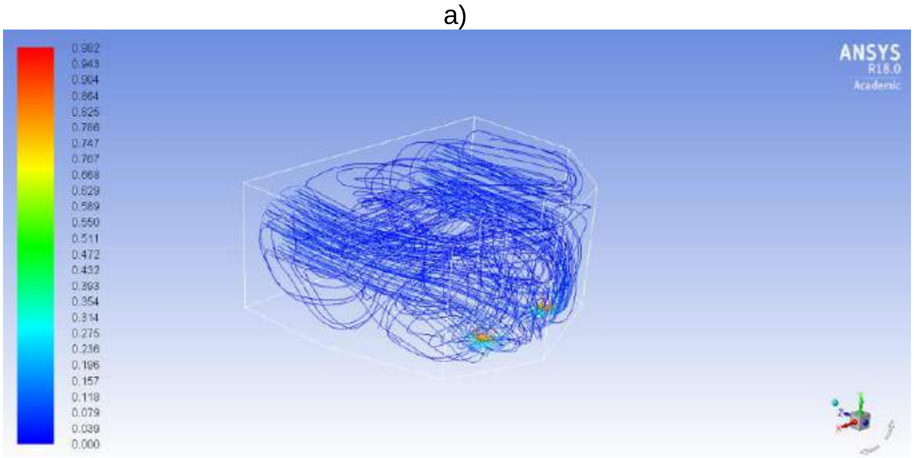

b)

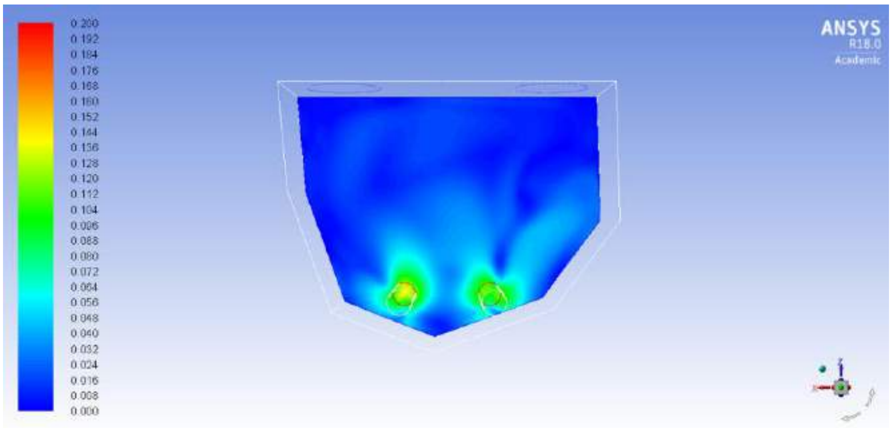

c)

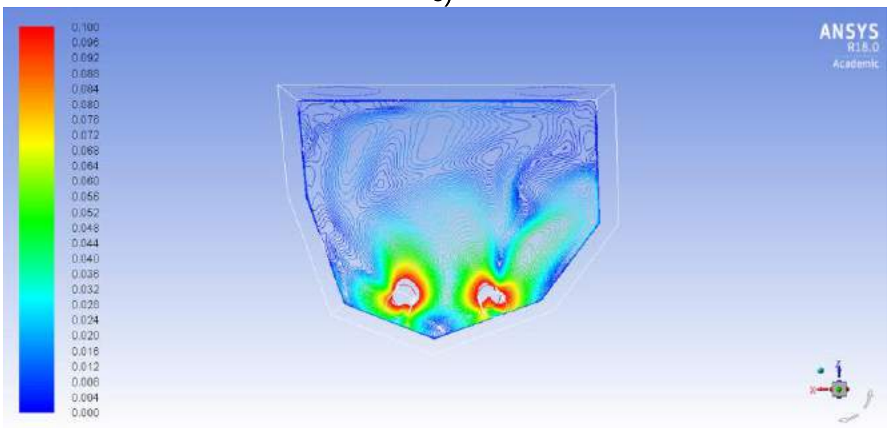

d)

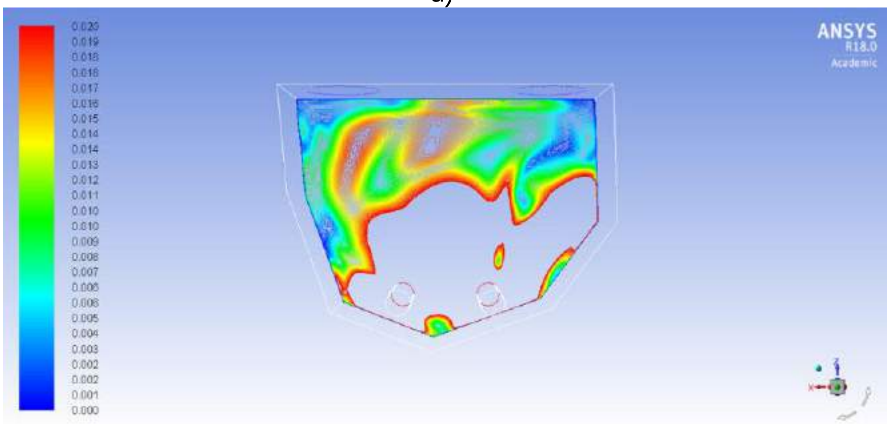

e)

Fig. 7. Pressure distribution in a plane parallel to the bottom of the basin at a distance of 10mm

The K-epsilon (k-e) turbulence model used in this study is the most widely used model used in Dynamics Fluid Computational (CFD) to simulate average flow characteristics for turbulent flow conditions. It is a two-equation model that provides a general description of the turbulence through two transport equations (PDEs). The initial impetus for the K-epsilon model was to improve the mixing length model, as well as to find an alternative to algebraic turbulence balances in moderate-to-high complexity flow. The first variable determines the energy transported in turbulence and is called turbulent kinetic energy (k). The second variable carried is the turbulent dissipation (ε) which determines the rate of dissipation of the turbulent kinetic energy. In fluid mechanics, turbulence or turbulent flow is a flow regime characterized by stochastic fluctuations in properties. These relate

to the diffusion and transport (convection) time, rapid variations of pressure and speed in space and time. [3], [4]
The theoretical studies must be verified by experimental measurements, as in [5] and [6] thus developing useful models for design process.

4. Conclusions

The Târgu Lăpuş Purification Station fails to fully realize the purpose for which it was built, namely the removal of polluting substances from the wastewater and the discharge of relatively clean waters into the emissary, according to the legislation and the agreement with the Apele Romane.
This is due to the following: repetitive failures of various machines that make the process technologically difficult, reduction of deburring due to deposits, loss of station efficiency. It is important that the WWTP discharge the water into the river Târgu Lăpuş a high quality effluent.
The importance of mechanical purging results from the following aspects, discussed in this paper:
• Thick and fine suspensions are retained in the mechanical treatment stage;
• The importance of screens in removing large floating bodies is felt by the entire purification process;
• Fat removal is very important for the mechanical purification of industrial waters and especially for mechano-biological or mechano-chemical treatment to prevent imbalances caused by increased fat content;
• Mechanical cleaning is an effective way of combating pollution by retaining coarse particles and suspended particles from wastewater.

References

[1] E. Baruth, “Water Treatment Plant Design 4th edition”, American Society of Civil Engineers, Reston, VA, McGraw-Hill, ISBN: 0-07-141872-5, pp. 896, 2004;
[2] B. De Clercq, F. Coen, B. Vanderhaegen, P. A. Vanrolleghem, “Calibrating simple models for mixing and flow propagation in waste water treatment plants”, *Water Science and Technology*, Volume 39, Issue 4, pp. 61-69, ISSN 0273-1223, 1999;
[3] Athanasia M. Goula, Margaritis Kostoglou, Thodoris D. Karapantsios, Anastasios I. Zouboulis, “A CFD methodology for the design of sedimentation tanks in potable water treatment: Case study: The influence of a feed flow control baffle”, *Chemical Engineering Journal*, Volume 140, Issues 1–3, Pp 110-121, ISSN 1385-8947, 2008;
[4] D. Opruta, D. Banyai, I. Sfarlea, “Flow rate coefficient and critical Reynolds number for control valves”, *Energy Procedia* 85, pp. 44-51, 2016;
[5] D. Banyai, I. Sfarlea, D. Opruta, “Experimental research on variable hydraulic resistors of servo-hydraulic valves”, *2016 International Conference on Production Research – Africa, Europe and the Middle East 4th International Conference on Quality and Innovation in Engineering and Management*, UT Press Cluj-Napoca, ISBN: 978-606-737-180-3, 2016;
[6] I.L. Marcu, “Functional parameters monitoring for an alternating flow driven hydraulic system", *Automation, Quality and Testing, Robotics, 2008, AQTR 2008*, IEEE International Conference on Automation, Quality and Testing, Robotics, vol.3, no., pp.239-242, 2008.

ISSN 1454 - 8003
Proceedings of 2017 International Conference on Hydraulics and Pneumatics - HERVEX
November 8-10, Băile Govora, Romania

CARBON FOOTPRINT DETERMINATION WHEN USING RESIDUAL AGRICULTURAL BIOMASS FOR ENERGY PRODUCTION

Erol MURAD

EKKO OFFICE AG SRL, erolmurad@yahoo.com

Abstract: *At present, the focus is on distributed energy generation with low or negative carbon emissions as well as high conversion yields. The renewable energy resource that can be used and produced when and wherever necessary is residual agricultural biomass with a potential of 31 million tons, which can produce over 40% of the national energy demand. Residual agricultural biomass is produced with an average energy efficiency of 6 kWh.bm/kWh.input. The CHAB concept produces high yield thermal energy as well as biochar with an average carbon footprint of 140 kg / ton. biomass. If the energy produced is used to produce agricultural output, the negative carbon footprint increases by reducing the consumption of fossil fuels. It increases energy independence, the safety of agricultural production, the number of jobs, and regional economic development.*

Keywords: *Waste biomass, energy, biochar, CHAB, carbon footprint*

1. Introduction

Agriculture has been and remains the main source of raw materials for food and industrialization. The concept of sustainable development and evidence of climate change tends to tackle the issue of adapting efficient and sustainable agricultural production technologies to humanity in order to provide food for an ever-growing population fed by a declining global agricultural area.
Sustainable development of agriculture also involves increasing the energy independence of agricultural farms by reducing fossil fuel consumption, increasing and maintaining productive soil capacity, and reduced use of mineral fertilizers in favor of compost, which is linked to current ecological requirements leads to the need to increase the level of use of residual biomass resulting from agricultural crops. [1,2]
At present, direct biomass burning, chopped, briquetted or pelletized is the majority procedure. As an alternative to current methods of thermal energy production from biomass, it is proposed the **CHAB** concept (**C**ombined **H**eat **A**nd **B**iochar production) which also includes the biochar (**BC**) generation. **BC** is a sterile organic material obtained from biomass pyrolysis in an oxygen-free environment or with a controlled gasification, with a neutral or alkaline pH. It has a carbon content of 75-90% and is characterized by high porosity and adsorption capacity. [2, 3, 4]
BC is used to improve the long-term fertility of agricultural soils, and secondarily as a filtering agent for air, gas and water. Built in soil, it is the most economical and ecological way of sequestering at least 25% of carbon, for extended periods between 100 and 1000 years [18]; it also has many other applications in the most diverse fields of human activity. [3, 5, 6]
In order to evaluate how the waste biomass can be efficiently exploited, an energy balance and carbon mass analysis will be carried out, from which the carbon footprint can be calculated to determine the useful energy produced, and to create a base analysis and optimization of variants and energy conversion regimes.
In nature, spontaneous vegetation uses solar energy, carbon dioxide (CO2) and soil fertility to produce a vegetal mass containing carbon **Cb**, which, through the natural carbon circuit, returns to the atmosphere.
Vegetable crop production has as its main product a biomass destined for human and zootechnical consumption, which we call food biomass, as well as a by-product called waste biomass. (figure 1).
Solar energy, carbon dioxide (CO2) in the atmosphere, soil fertility, as well as **Econs** energy consumed to carry out agricultural works contribute to the achievement of vegetal agricultural

production. This produces an energy accumulation in agricultural products - **Ebal** in the main product and **Ebr** in the wast biomass. [7]

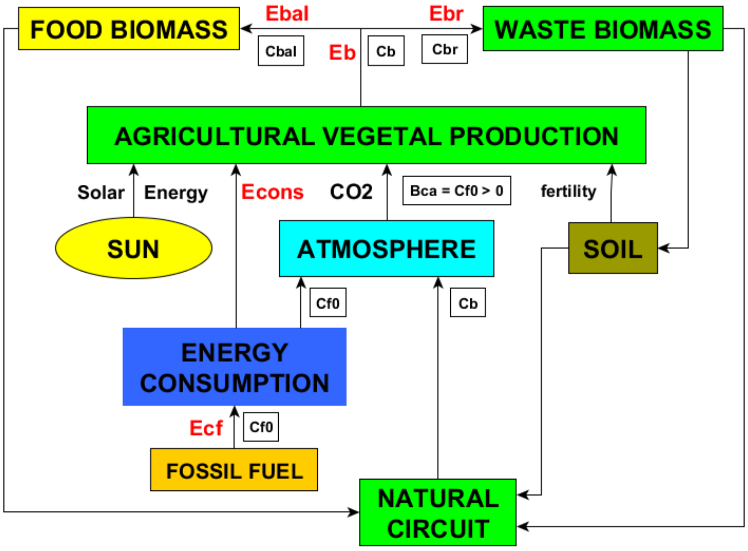

Fig. 1. Agricultural crop production general model

The efficiency of agricultural production is determined by the ratio of energy at exit **Eb** and that of input **Econs.** Therefore energy efficiency is calculated with the relation (1)

$$EFEN = \frac{Eb}{Econs} = \frac{Ebal + Ebr}{Econs} \tag{1}$$

Table 1 presents the energies produced and consumed for the main agricultural crops as well as the total energy efficiency **EFEN**, the main **EFENp** and the secondary **EFENs**. [7]
It is noted that most of the agricultural production has an **EFEN** > 1 overall efficiency and many crops also have an **EFENs** secondary efficiency of more than 3, which confirms the conclusion that the agricultural crop production is also producing renewable energy with low costs and with a reduced carbon footprint (CFPf). [7]
Biomass produced has an **Etotal** energy for which **Econs** was consumed from fossil fuels. It is assumed that the fuel used is diesel fuel having a CFPf = 0.0815 kg / kWh footprint for base energy. The overall diesel fuel efficiency is estimated at η_f = 0.864, which results in a positive footprint in the **CFPatm** atmosphere (kg.C / kWh) for residual biomass:

$$CFPatm = \frac{1}{EFEN}\frac{CFPf}{\eta_f} = 0.0944 \tag{2}$$

Since for the production of **Econs** fossil fuels are consumed in the atmosphere, a quantity of **Cf0** = Econs·CFPf is released.
Table 1 presents the energy efficiency values for the main crops in Romania. It is noticed that the majority of agricultural crops produce residual biomass with an **EFENs** >> 0, so they are economically and ecologically productive renewable energy resources, mainly the corn and wheat crops that offer biomass for pelleting. These aspects regarding the fruit cuttings and of the vines were presented in the works [2, 8]. Further analysis will be developed for corn crop, which has the highest energy efficiency, for pellets produced from corn stalks.
For the energy and carbon balance, Table 2 shows the carbon footprints and the utilization yields for the main fuels entering the energy production processes of the waste biomass: diesel fuel, corn stalk biomass, corn stalk pellets, biochar and syngas [3, 4, 9, 10, 11]

Table 1: Energetic efficiency of agricultural crops

Crops	Energy produced			Energy consumed	Energetic efficiency		
	Etotal	Ebal	Ebr	Econs	EFEN	EFENp	EFENs
	kWh/ha	kWh/ha	kWh/ha	kWh/ha			
Corn	91029	41054	**49975**	**5163**	17.63	**7.95**	**9.68**
Winter wheat	41017	16773	**24244**	**5764**	7.12	**2.91**	**4.21**
Beans	21227	10585	**10642**	**3254**	6.52	**3.25**	**3.27**
Sunflowers	19807	4970	**14837**	**4982**	3.98	**1.00**	**2.98**
Soy	29517	18550	**10967**	**4643**	6.36	**3.99**	**2.36**
Plum	23981	12775	**11206**	**12833**	1.87	**1.00**	**0.87**
Vineyard	17547	8381	**9167**	**16028**	1.09	**0.52**	**0.57**
Apple	22372	14467	**7906**	**17383**	1.29	**0.83**	**0.45**

Table 2: Fuels carbon foot print

Feature	Symbol	UM	Value	Notes
Diesel fuel foot print	CFPdf	kg.C/kWh	**0.0815**	
Corn stalk foot print	CFPbr	kg.C/kWh	**0.0873**	corn stalk
Corn stalk pellets foot print	CFPcp	kg.C/kWh	**0.0873**	corn stalk pellets
Carbon foot print for peleting	CFPcpr	kg.C/kWh	**0.0082**	
Syngas foot print [CFPsg]		kg.C/kWh	**0.1059**	from gasifier
Conversion yeld for diesel burning	Kconv.f	adim	0.864	
Conversion yeld for BM burning	Kconv.bm	adim	0.786	
Conversion yeld for syngas burning	Kconv.g	adim	0.746	
Global BM footprint	CFPbmu	kg.C/kWhu	**0.112**	
Global diesel footprint	CFPfu	kg.C/kWhu	**0.095**	
Global syngas footprint	CFPgu	kg.C/kWhu	**0.142**	

From the calculation of the carbon footprint produced using the primary energy of the residual corn mass, taking into account the part of the carbon footprint due to the energy input at the system entry, it results that for 1 MWh of the residual corn stalk consumed 56.7 kWh at input with a carbon footprint of max. 4.623 kg.C \ MWh.

2. Energy conversion system with burning process

To perform the analysis, a model (figure 2) of a corn stalk pellet energy production system was designed using burning processes. The conversion of the energy biomass into useful energy is achieved with a BIOMASS ENERGY SYSTEMS block, which enters an **Ecs.inp** energy consisting of **Ebre** as a **Kbe** part of the pellet biomass that has been pelletized and a carbon content **Cbre**. To perform the conversion process, an **Ecs**.act power is also introduced with a **CFPcons** footprint.

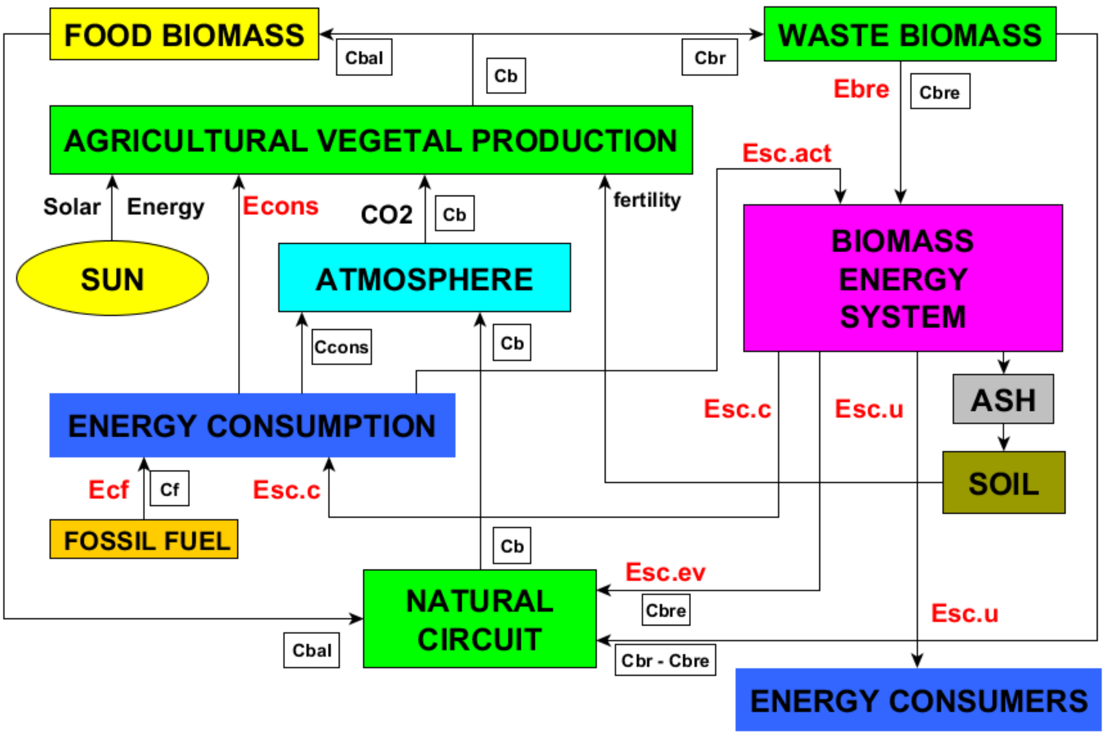

Fig. 2. Model of biomass energy system with burning process

The output energy **Ecs**.out consists of the energy emitted in **Ecs.ev** environment and a useful energy that can be divided: one **Ecs.c** part can be consumed directly for the production of the vegetal agricultural production and another **Ecs.u** that feeds the energy consumers external to the analyzed system. Part of the input energy, which represents the losses of **Ecs.ev**, is evacuated in the case of **Cbre**. Also comes the ASH ash without energy and carbon, which is incorporated into the soil.

The energy balance is:

$$\Delta Ebes = Ecs.inp - Ecs.out = 0 \tag{3}$$

Input energy is:

$$Ecs.inp = Ebre + Ecs.act \tag{4}$$

Energy for system consumption is :

$$Ecs.act = Ecs.pr + Ecs.ard + Ecs.he = Kact \cdot (Kbe \cdot Ebre) \tag{5}$$

Where in the analyzed case, Kact ≈ 0.17, resulting for **Ecs.inp** the relation:

$$Ecs.inp = Kbe \cdot Ebr + Kact(Kbe \cdot Ebr) = (1 + Kact)(Kbe \cdot Ebr) \tag{6}$$

The output energies are: **Ecs.ev** - exhaust gas energy from the heat exchanger; **Ecs.u** - energy usable in external applications to the system; **Ecs.c** - energy consumed for the system by ENERGY CONSUMPTION. The energy relationship at the output is:

$$Ecs.out = Ecs.ev + (Esc.u + Ecs.c) = (1 - \eta_{cs})Ecs.out + (Esc.u + Ecs.c) \tag{7}$$

where
$$\eta_{cs} = \eta_{pr} \cdot \eta_{ard} \cdot \eta_{he} = (1/1.1) \cdot 0.96 \cdot 0.9 = 0.7855 \cong 0.78 \tag{8}$$

The energy **Ecs.c** consumed in the system is determined by the take-off **Kbc** in the useful energy at the exit:

$$Ecs.c = Kbc(Ecs.out - Ecs.ev) = Kbc \cdot \eta_{sc} \cdot Ecs.inp = Kbc \cdot \eta_{sc} \cdot (1 + Kact)Ebre = Kbc \cdot Kconv \cdot (Kbe \cdot Ebr) \quad (9)$$

where
$$Kconv = \eta_{sc} \cdot (1 + Kact) \quad (10)$$

The carbon balance shows that since the carbon footprint for **Ecs.c** + **Ecs.u** is incorporated into the exhaust outlet, it follows that:

$$\Delta Cbes = Cbre - Csc.ev = 0 \quad (11)$$

It is noticed that **Cbre** re-enters the atmosphere through the combustion gases exhausted at the exchanger outlet. It follows that the carbon footprint for **Ecs.u** and **Ecs.c** is zero
Another important block is the ENERGY CONSUMPTION subsystem. In block is the **Ecf** energy produced from fossil fuels with **Cf** carbon content and **Ecs.c** energy from the energy produced by the system with a zero footprint. The exit is **Econs** = cnt. used directly for agricultural crop production and **Ecs.act** for the energy conversion system. The energy balance is:

$$\Delta Eec = (Ecf + Ecs.c) - (Econs + Ecs.act) = 0 \quad (12)$$

Ecf energy from fossil fuels produces a positive carbon footprint.

$$Ecf = (Econs + Ecs.act) - Ecs.c \quad where \quad Econs = \frac{Etotal}{EFEN} \cong \frac{Ebr}{EFENs} \quad (13)$$

The carbon balance is:

$$\Delta Cec = Cf - Ccons = Ecf \cdot CFPf - Ccons = 0 \quad and \quad Ccons = Cf \quad (14)$$

For ATMOSPHERE carbon balance is:

$$\Delta Catm = (Ccons + Cb) - Cb = Ccons \quad (15)$$

Carbon footprint in atmosphere is:

$$CFPatm = \frac{Ccons}{Econs + Ecs.c} = \frac{Cf}{Ebr / EFENs + Ecs.c} = Ecf \frac{CFPf}{Ebr / EFENs + Ecs.c} \quad (16)$$

If we want to get a zero fingerprint, **CFPatm** = 0, then **Ecf** = 0 and require an **Ecs.c** energy in the system with the value:

$$Ecs.c = Econs + Ecs.act = Ebr / EFENs + Kact \cdot (Kbe \cdot Ebr) = Ebr(1 / EFENs + Kact \cdot Kbe) \quad (17)$$

If an **Ecs.u** useful power is required for applications, it is necessary to determine which **Kbe** quota of residual biomass to be harvested should be used.

$$Ecs.u = (1 - Kbc) \cdot Kconv \cdot (Kbe \cdot Ebr) \quad from\ where \quad Kbc = 1 - \frac{Esc.u}{Kconv \cdot (Kbe \cdot Ebr)} \quad (18)$$

$$Ecs.c = (1 - \frac{Esc.u}{Kconv \cdot (Kbe \cdot Ebr)}) \cdot Kconv \cdot (Kbe \cdot Ebr) = Kconv \cdot (Kbe \cdot Ebr) - Esc.u \quad (19)$$

And using the relation (9) results:

$$Ecs.c = Kconv \cdot (Kbe \cdot Ebr) - Esc.u = Ebr(1 / EFENs + Kact \cdot Kbe) \quad (20)$$

It is shared with **Ebr** and it follows:

$$Kconv \cdot Kbe - Esc.u / Ebr = 1 / EFENs + Kact \cdot Kbe \quad (21)$$

In order to ensure the **Ecs.u** value required for the **Kbe** harvested waste biomass, it must be greater than:

$$Kbe \geq \frac{1}{Kconv - Kact}\left(Kbu + \frac{1}{EFENs}\right) \quad where \quad Kbu = \frac{Esc.u}{Ebr} \tag{22}$$

Table 3 shows the values of the **Kbe** coefficient according to the **Kbu** share of the energy demand.

Table 3: Use of residual biomass for zero carbon footprint

Kbu	0.100	0.200	0.300	0.400	0.512
Kbe ≥	0.330	0.493	0.655	0.818	1.000

3. Energy conversion system with CHAB concept

As previously described, the application of the **CHAB** concept leads to the production of energy and biochar. Figure 3 presents a model for a system that produces bio-fuel and energy from pyrolysis or gasification processes from residual biomass. [2, 4, 9, 10, 12]
Tables 4 and 5 show the energies and carbon content of the input and output products.

Table 4: Corn stalks pellets for pyrolysis

Feature	**UM**	**Corn stalks pellets**	**Biochar**	**Pyrolysis gas**
Relative masse	real	***1.00***	***0.237***	***0.763***
Carbon	real	0.4053	0.7267	30.55
Oxygen	real	0.3905	0. 489	49.66
Hydrogen	real	0.0540	0.0126	6.69
Ash	real	0.0502	0.2118	0
Humidity	real	0.10	0.00	13.11
L.H.V	MJ/kg	**14.98**	**25.60**	**11.68**
Carbon content	%	100	42.0	58.0
Energy content	%	100	40.50	59.50
CO2 footprint	kg.CO2/kWh	0.357	0.375	0.345
Carbon footprint	kg.C/kWh	**0.097**	**0.102**	**0.094**

Table 5: Corn stalks pellets for gasification

Feature	**UM**	**Corn stalks pellets**	**Biochar**	**Gasified Biomass**
Relative masse	real	***1.00***	***0.157***	***0.843***
Carbon	real	0.4053	0.6316	0.3632
Oxygen	real	0.3905	0.032	0.4573
Hydrogen	real	0.054	0.0167	0.0609
Ash	real	0.0502	0.3197	0
Humidity	real	*0.100*	*0,00*	*0.1186*
L.H.V	MJ/kg	**14.98**	**20.20**	**14.01**
Carbon content	%	100	21.17	78.83
Energy content	%	100	24	76
CO2 footprint	kg.CO2/kWh	0.357	0.413	0.342
Carbon footprint	kg.C/kWh	**0.097**	**0.113**	**0.093**

The model shown in figure 3 has a biochar output with **Cbch** carbon content and contains an **Ebch** energy.

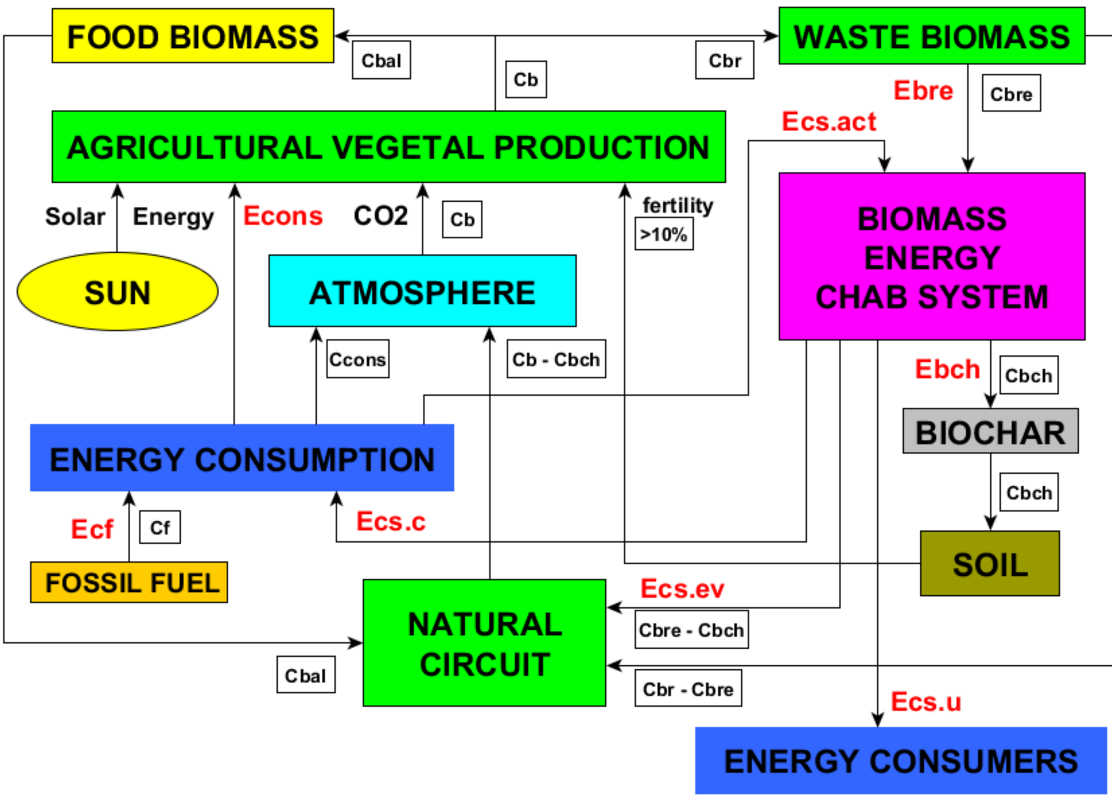

Fig. 3. Model of biomass energy system with CHAB concept

For BIOMASS ENERGY CHAB SYSTEM energy balance is:

$$\Delta Ebes = Ecs.inp - Ecs.out = 0 \tag{23}$$

Input energy is:

$$Ecs.inp = Ebre + Ecs.act \tag{24}$$

$$Ecs.inp = Kbe \cdot Ebr + Kact(Kbe \cdot Ebr) = (1 + Kact)(Kbe \cdot Ebr) \tag{25}$$

The relationship for the output energy is:

$$Ecs.out = Ecs.ev + (Esc.u + Ecs.c) + Ebch = (1 - \eta_{cs})(Ecs.out - Ebch) + (Esc.u + Ecs.c) + Ebch \tag{26}$$

Because at the carbon balance the carbon footprint for **Ecs.c** + **Ecs.u** is included in the exhaust outlet it results that:

$$\Delta Cbes = Cbre - (Csc.ev + Cbch) = Cbre - (Csc.ev + Kbch \cdot Cbre) = 0 \tag{27}$$

$$Csc.ev = Cbre(1 - Kbch) \tag{28}$$

In this case for ATMOSPHERE carbon balance is:

$$\Delta Catm = (Ccons + Cb - Cbch) - Cb = Ccons - Cbch \tag{29}$$

Carbon footprint in atmosphere is:

$$CFPatm = \frac{Ccons - Cbch}{Ecf + Ecs.c} = \frac{Cf - Kbch \cdot Cbre}{Ecf + Ecs.c} = \frac{Ecf \cdot CFPf - Kbch \cdot (Kbe \cdot Ebr) \cdot CFPbm}{Ecf + Ecs.c} \tag{30}$$

Two situations are analyzed: **CFPatm** = 0 or, for **Ecf = 0**, is obtained **CFPatm** <0.
For condition **CFPatm** = 0:

$$Ecf \cdot CFPf - Kbch \cdot (Kbe \cdot Ebr) \cdot CFPbm = 0 \tag{31}$$

If **Ecs.c** = 0 of the balance results **Econs** = **Ecf**.

$$(Ebr / EFENs) \cdot CFPf - Kbe \cdot (Kbch \cdot CFPbm) \cdot Ebr = 0 \tag{32}$$

To meet this condition, you must:

$$Kbe = \frac{CFPf}{CFPbm} \cdot \frac{1}{Kbch \cdot EFENs} \tag{33}$$

For gasification results **Kbe$_g$** ≥ 0.44, and for pyrolysis **Kbe$_p$** ≥ 0.23. When using gasification, more energy is available for external applications.
If the system energy **Ecs.c ≈ Ebr / EFENs** covers the energy requirement it results that **Ecf** = 0 and the carbon footprint is negative:

$$CFPatm = -\frac{Kbch \cdot (Kbe \cdot Ebr) \cdot CFPbm}{(Ebr / EFENs)} = -Kbch \cdot Kbe \cdot CFPbm \cdot EFENs \tag{34}$$

For **Kbe** = 0.67 with gasification **CFPatm$_g$** = - 0.124, and with pyrolysis **CFPatm$_p$** = - 0.814. Pyrolysis has to be noted the high negative value of the footprint, but there are a very little energy for the outside.

4. Conclusions

1. Original models for energy conversion systems of agricultural waste biomass were developed by burning, pyrolysis and gasification processes, for the determination of energy and carbon balance, as well as of the carbon footprint in the atmosphere. A power conection of vegetable production with energy generated by the system has been introduced to reduce positive carbon footprint.

2. The models were used to determine the regimes where the carbon footprint can be reduced to zero in the combustion process for different levels of useful energy needed for other applications.

3. The simulation was performed for residual biomass from corn with the highest total energy efficiency EFEN = 17.63 and the energy-producing biomass for EFENs = 9.68. An energy use factor Kbe $\in$ (0, 1) was used.

4. In the system with burning process if 50% of the harvested residual biomass is used, for a zero footprint, is obtained useful energy for other thermal applications of about 80% of the biomass used.

5. In system with gasification process for zero carbon footprint is necesary Kbe$_g$ ≥ 0.44, and for a Kbe$_g$ = 0.67 is a negative footprint CFPatm$_g$ = - 0.124 kg.C / kWh, relatively small, less biochor is obtained but available more power for other applications.

6. In system with pyrolysis process for zero carbon footprint is necesary Kbe$_p$ ≥ 0.44, and for a Kbe$_p$ = 0.67 is a negative footprint CFPatm$_p$ = - 0.814 kg.C / kWh, is a remarkable value due to the production of more biochar with a higher content of carbon.

7. Developed models are a useful tool for the design of energy conversion systems for biomass in general and especially for agricultural waste biomass. It is a very useful tool in the development of automated control systems, both as structure and optimal control algorithms.

8. Economic aspects will also be attached to become the most complete tool for developing biomass energy conversion systems.

References

[1]. S. Christoph, ”Biochar from agricultural and forestry residues – a complementary use of “waste” biomass”, J. Levine (edit), “U.S.-Focused Biochar Report, Assessment of Biochar's Benefits for the United States of America”, USBI and CEES, June, 2010, Colorado, USA;

[2]. E. Murad, ”CHAB din biomasă agricolă cu TLUD*”, Sesiunea de comunicări ştiinţifice - ICEDIMPH-HORTING*, 28 noiembrie 2013;

[3]. H. McLaughlin, “Combined Heat And Biochar: An alternate economic option for renewable biomass*”, 3rd Annual Conference of Heating the Northeast with Renewable Biomass*, 15 April 2011;

[4]. E. Murad, C. Dumitrescu, F. Dragomir, M. Popescu, „CHAB concept in sustainable development of agriculture”, *Procedings International Symposium ISB-INMA TEH 2016*, pp. 257-262, INMA Bucuresti, 2016, ISSN 2344 - 4118;

[5]. H. P Schmidt, et al, “European Biochar Certificate - Guidelines for biochar production”, 2012 Delinat Institute und Biochar Science Network, Version 4.2 of 13th June 2012;

[6]. J.F. Peters, D. Iribarren, J. Dufour, “Biomass Pyrolysis for Biochar or Energy Application's A Life Cycle Assessment”, *Envir. Sci. Technol.*, 2015, vol. 49(8) pp. 5195-5202;

[7]. L. Răus , G. Jităreanu, “The energetic efficiency of different tillage system and fertilization levels”, Soil Minimum tillage systems, 6th International Symposium, 27-29 June 2011 Cluj-Napoca, p. 32;

[8]. E. Murad, ”Conceptul CHAB în viticultură”*, Sesiunea de comunicări Stiinţifice ICDVV* Valea Călugărescă, 12 iunie 2014;

[9]. E. Murad, F. Dragomir, “Heat generators with TLUD gasifier for generating energy from biomass with a negative balance of CO_2”*, Proceedings of 2012 International Conference HERVEX*, 7-9 November 2012 Călimăneşti-Căciulata Romania;

[10]. E. Murad, “Biomass cogeneration systems with steam cycle for convective dryers with energy independence and negative balance of CO_2”, *CIEM – 2013*, UPB Bucharest, 7-8 November 2013;

[11]. J. Whitfield, “Combined Heat and Biochar Production”, Whitfield Biochar, USA, WA, Jan 2013;

[12]. E. Murad, “Power production a negative carbon balance with CHAB concept”, *International Conference HERVEX 2016*, Govora, 9-11 noiembrie 2016.

ISSN 1454 - 8003
Proceedings of 2017 International Conference on Hydraulics and Pneumatics - HERVEX
November 8-10, Băile Govora, Romania

HYDRAULICALLY CONTROLLED FERTIGATION EQUIPMENT WITH VOLUMETRIC INJECTION DEVICE

Gabriela MATACHE[1], Sava ANGHEL[1], Alina Iolanda POPESCU[1], Ana-Maria POPESCU[1], Gheorghe ȘOVĂIALĂ[1]

[1]The National Institute of Research & Development for Optoelectronics - Hydraulics and Pneumatics Research Institute, INOE 2000-IHP Bucharest

matache.ihp@fluidas.ro, sava.ihp@fluidas.ro, alina.ihp@fluidas.ro, ana-maria.ihp@fuidas.ro, sovaiala.ihp@fluidas.ro

Abstract: *Modern fruit growing pursues total control of plants development, ease of maintenance and harvesting works, automation of all field interventions. The technologies applied to intensive and super-intensive horticultural crops aim to ensure by watering water all that is necessary for the development of the plants, even by insulating the active area of the roots so that the plant depends only on the nutrients that are given by the watering water. We aim to control the growth of plants, sizing production, obtaining high quality products, maintaining and harvesting crops easily.*

Keywords*: Fertigation, injection device, fruit plantations*

1. Introduction

For fertilization application with irrigation water (fertigation), recommended dosages are applied weekly, or at most two weeks, correlated with foliar diagnosis and fruit production [1].
In the technique of water application by fertigation with drip irrigation systems, before applying fertilizer doses, first apply water for about 5 minutes, to flush the installation, then apply the water with dissolved fertilizers; after fertilizing, continue irrigation for another 5-10 minutes to entrain and infiltrate into the soil the last amount of nutrient solution, that could remain on the pipes and on the surface of the soil. [2]
The development of the fertigation equipment field with volumetric injection devices of double pump with membranes started with the implementation of the PD-1 dosing pump [3,4] at ICITID Baneasa Giurgiu whose scheme is presented in figure 1.

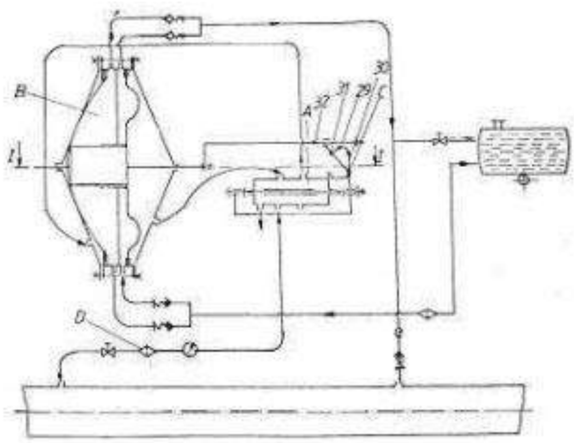

Fig. 1. Fertigation equipment with double volumetric pump type injection device with PD-1 membranes

The injection device, the main component of the fertigation equipment, consists of two membranes (B), directional control valve (A), and the exterior mechanism with swinging spring (C).[5]

Membranes separate four chambers with variable volumes. The active surfaces of the membranes in the outer chambers are larger than the active surfaces of the membranes in the inner compartments which determine appearance of the overpressure necessary for the primary solution injection in the same pipe from which is taken the water used as motion fluid. The directional control valve (A), depending on the position of the slide valve, establishes the water circuits in the two outer chambers. The displacement direction of the slide valve is determined by the position of the arm 31 of the outer mechanism component with swinging spring 29. The mechanism is located between the slide valve of the directional control valve and the movable assembly of the pump (moving the membranes).
Outside the injection device, the equipment consists of a fertilizer tank for preparing the primary solution, a four- check valves battery on the injection circuit, filters, and valves. In operation, the inner chambers vary in volume by making the fertilizer to be absorbed from the tank and discharged into the pipe through check valve battery.
The main inconveniences found in the operation of the equipment consist in the timing of the tilting mechanism, which changes the timing of the slide valve switching of the directional control valve, the degree of filling of the drive and injection chambers, the external positioning of the valves assembly for suction / discharge of the primary solution and of the elements which constitute the hydraulic circuits.

2. Presentation of the primary solutions injection device

Injection device realized through the execution of the contract 158/2014: Innovative technologies and equipment for the implementation in the irrigated agriculture of the modern fertigation concept (FERTIRIG), is a double pump with directional controlled valve hydraulically commanded.[6]
Injection device, [7,8] figure 2 was designed and realized in a compact way, in the body incorporating the piston-membranes mobile assembly, the hydraulic directional control valve, the driving of the directional control valve, the throttles of the drive chambers of the directional control valve, the suction / discharge valves block of the primary solution. The connection between the functional elements is achieved through the holes practiced in the device body and the movable assembly plunger, eliminating the external connections, except those related to the drive chambers of the directional control valve.
The schematic diagram of the fertilization equipment is shown in fig. 3.

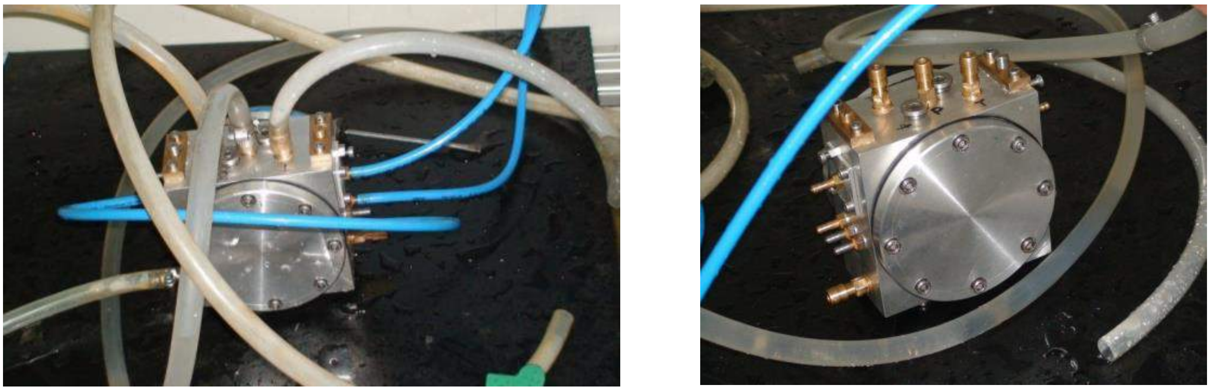

Fig. 2. Double pump type injection device with membranes

The mobile assembly, fig. 3-sect D-D, consists of piston, membranes, outer and inner flanges, special screws for fixing the membranes on the piston.
Primary solution suction / discharge valves assembly; each injection chamber is connected to an intake and discharge valve. The suction / discharge valves of the two injection chambers are interconnected and connected to the nozzles of the primary and discharge solutions.

In the construction of a 4-way, 2-position directional control valve, was chosen the alternative with slide valve, with O-rings seals, to allow the components to be executed in H8 / f7 tolerance fields, thus avoiding the extremely precise execution imposed at hydraulic directional control valves with classic slide valve, where the movements between the slide valve and the body are of the micron order. The versatile version of the directional control valve allows operation with irrigation water with a low filtration level.
The seals have been designed and made with as low as possible tightening, so that the friction forces of the movable elements are as small as possible.
The slide valve has a positive coating, the switching is done without loss of pressure.

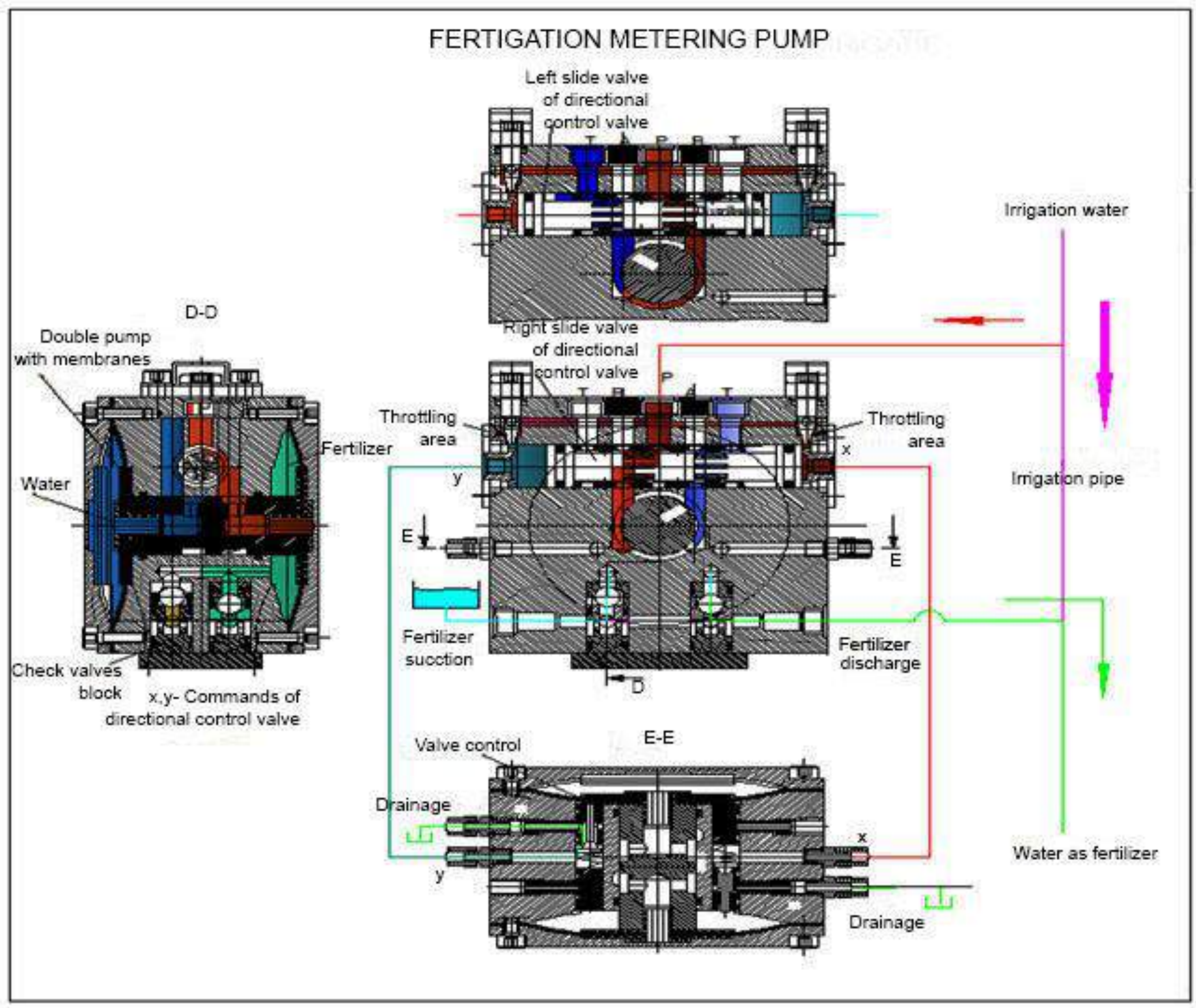

Fig. 3. The basic scheme of fertigation equipment

The control valves of the hydraulic directional control valve, fig.3 sect. E-E are cone-releasing valves, located in the water tank discharge holes in the drive chambers operated in the pump body, to ensure firm closure and opening and to reduce switching time for the directional control valve. The drive chambers are delimited by the outer surfaces of the membranes and the lids, and the injection chambers by the inner surfaces of the membranes and the body.

The operating principle

Depending on the position occupied by the slide valve of the directional control valve, fig. 4, the orifice P is connected to the orifices A or B, from which, by internal holes in the body and the piston, the pressurized water supply of the drive chambers is provided. Outside, holes A and B are plugged.

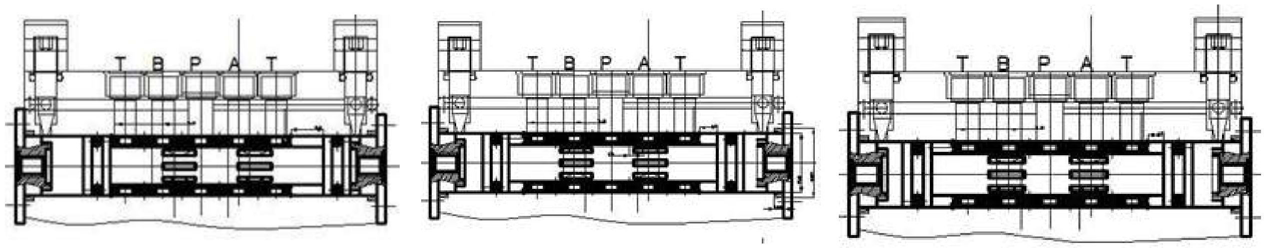

Fig. 4. Slide valve positions of the directional control valve

The T-holes alternately evacuate the liquid from the drive chambers (A to T or B to T) during the withdrawal phase of the membranes assembly (decrease the volume of the drive chambers).
Also from the P port, the Ccs-Ccd drive chambers of the hydraulic directional control valve are continuously supplied with pressurized water. The mobile assembly alternately operates through the internal flanges the pilot controlled valves, which shortly before reaching the end of the stroke, connect one of the drive chambers to the atmosphere, causing the switching of the slide valve of the directional control valve from the pressure drive chamber to the pressure discharge chamber.
The hydraulic switching of the slide valve is made by means of two identical hydraulic circuits, consisting of mechanically pilot controlled throttles and check valves, controlled on the end stroke of the mobile assembly, fig. 5. The slide valve of the directional control valve may take different positions in the directional control valve, depending on the fluid pressure on the ends (Pcs / Pcd - left / right control pressure). If the two valves are closed, the pressure on the ends is equal to the supply pressure (Pcs = Pcd) and the slide valve remains locked in the middle position. If one of the valves is unlocked, the liquid behind the throttle is removed to the outside, the Pcs or Pcd pressure falls only on the throttle, different pressures are applied to the ends of the slide valve and then the slide valve moves, being pushed in the direction of the lower pressure, switching the directional control valve.

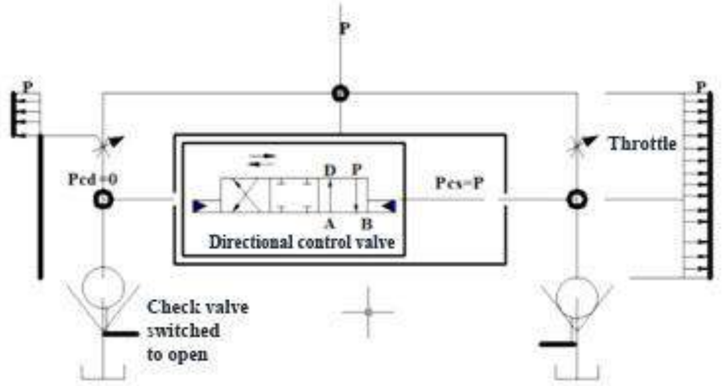

Fig. 5. Pressure circuit in control chambers of the directional control valve

When the mobile assembly reaches the end of the stroke, the inner flange, integral with the piston touches the end of the check valve, releases it and the pressure switches the slide valve, which changes the hydraulic connections with the membranes pump chambers, thus changing the direction of movement of the membrane shaft. After the assembly has reversed, the valve closes and locks the slide valve of the directional control valve in position. At the other end of the stroke is actuated the other valve that also changes the slide valve position, commanding the displacement in the opposite direction. The operation is repeated.

The throttles, which regulate the water flow that arrives into the drive chambers, keep the slide valve of the directional control valve in an equilibrium position and dictate the frequency of the mobile pump assembly.
The pressurized water supply of the left drive chamber causes the mobile assembly moving to the right, with the following effects:
- discharging of the moving fluid from the right drive chamber;
- aspiration of the primary solution in the right injection chamber;
- injection of the primary solution from the left injection chamber.

The volume reducing of the left injection chamber (implicitly increasing the pressure), causes the inlet valve ball to be seated and lifting the discharge valve ball out of the seat. Increasing the right injection chamber volume (implicitly producing a depression) causes the inlet valve ball to be lifted from the seat and seating the discharge valve ball. Injection chambers are alternately connected to the common suction connections (from the primary solution reservoir), respectively the discharge (in the supply pipe of the irrigation system), fig. 3.

3. The stand for testing

The experiments of the fertigation equipment under stand conditions were performed in the Environmental Protection Laboratory of IHP Bucharest.

3.1 The component of the testing stand

The test stand,[7] fig. 6, provides the hydraulic parameters (flow, pressure) necessary for the functioning of the fertigation equipment, simulating the irrigation system with which it works in the aggregate, being made up of the following components:
- pumping group with water recirculation used as working fluid;
- the water tank with the dimensions of 1130x900x785 and the useful volume of 0.6 m^3;
- the system for adjusting and monitoring the working parameters.

The WILO ECONOMY CO-2 MHI 206 / ER-RBI-CALOR pumping group, equipped with two high-pressure horizontal, without priming centrifugal pumps connected in parallel, provides a maximum flow of 10 m^3 / h and a height of maximum pumping capacity of 67 mCa. Pumping group is equipped with 2 "suction and discharge connections.
The pumping group consists of the following elements:
• Base frame: galvanized and fitted with vibration dampers with adjustable height for optimum sound insulation
• Piping system: suction and discharge connections of 2 ", all stainless steel pipes 1,4571, suitable for connection to all pipes in the installation technique, pipes are dimensioned according to the total hydraulic power of the pumping group
• Two parallel pumps of the MHI 2 series; all components of these pumps that come in contact with the liquid are 1,4301 stainless steel
• Reinforced fittings: each suction and discharge pump with CuZn closure fitting, Ni coated, DVGW marking and discharge retaining clack valve
• Pressure bottle with butyl rubber membrane, recognized as safe from the point of view of food law; designed for inspection and overhaul with CuZn ball valve, Ni-coated, with drainage and passage fitting according to DIN 4807
• Pressure sensor: 4 to 20 mA, located on the output pressure side for control of the central Economy controller
• Pressure display: through the pressure gauge on the outlet pressure side
• Control unit: The equipment is equipped with the Economy ER series regulator
• Components in contact with pumped fluid, corrosion-resistant

Fig. 6. Testing stand of fertigation equipment

The pumped fluids admitted are cooling water, drinking water and technological water. The admitted fluid is generally water without aggressive chemical or mechanical elements and without abrasive or long fiber components.

The water intake in the pumping group is made by an elastic connection element with an end type holender; discharge is done in the same tank, thus ensuring water recirculation.

Fertigation equipment is mounted in a bypass system, on a hydraulic circuit parallel to the group discharge pipe, similar from dimensional point of view and the hydraulic parameters point of view of the liquid transited with the main pipe in the drip or micro-sprinkler irrigation installations.

The connecting pipe of the injector device, fig. 7, includes connecting elements (nipples, sockets, reducing pieces, elbows) and elements that ensure the functionality, adjustment and monitoring of the working parameters (taps, Y path filter, check valve, pressure gauges, pressure reducer with pressure gauge, flow meter).

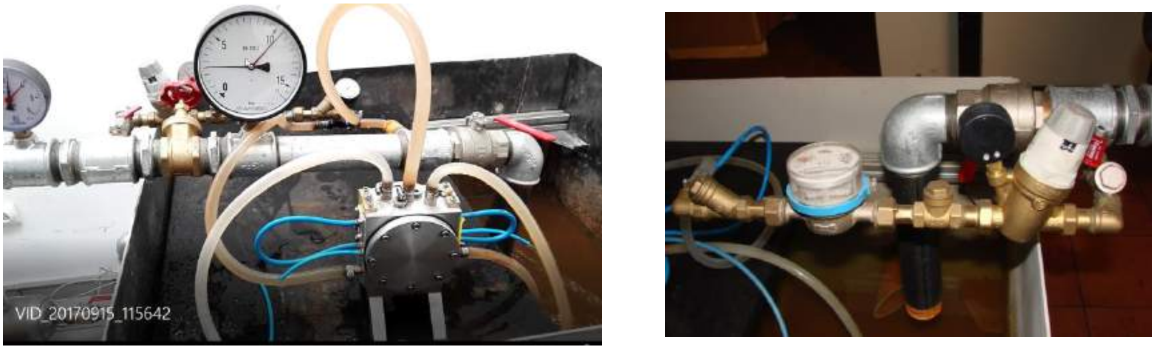

Fig. 7. The connecting pipe of the injector device

The injection device is provided with the following connections, fig. 8: The P-pressure connection, from which the drive chambers and control chambers of the directional control valve are fed; T_{cm} - water exhaust connections from the drive chambers; T_{cc} - water outlet connections from the control chambers of the directional control valve; A_f- the fertilizer aspiration connection; R_f - fertilizer discharge connection.

The pressure connection of the injection device is made from the downstream end of the line. Through the drive and control chamber tank connections, after performing the moving fluid function, the water is freely discharged into the stand tank. Through the A_f connection, the primary solution from the fertilizer tank B_f is absorbed, and the primary solution is injected through the R_f

connection. The circuit of the R_f connector is provided with a tap and pressure gauge to simulate and measure the injection pressure value.

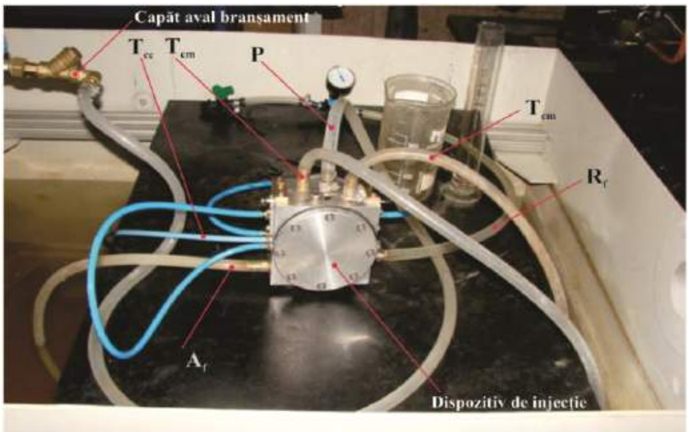

Fig. 8. Connection of the injection device in testing stand

The main discharge circuit of the pumping group is provided with:
- a pressure gauge located before the branching upstream point of the injection device, which measures the pressure value in the main pipe;
- path valve with slide valve, located on the main pipe between the branching point of the injection device, which causes a local pressure drop (which facilitates the injection process);
- path valve with sphere, located on the main pipeline, beyond the branching downstream point of the injection device, which can simulate the hydraulic resistance generated by the irrigation system distribution network.

After the injection device is branched, the values for the following parameters are adjusted:
- pressure of water upstream of the tap with slide valve, through which the pressure drop is created between
the connecting points, to facilitate the injection process, pressure measured by the manometer installed on the main pipe, upstream of the tap;
- working pressure of the injection device, regulated by pressure controller with pressure gauge;
- the flow in the main pipeline, by operation of the valve with sphere, mounted on the main pipeline, downstream of the injection point of the device.

Fig. 9. Laboratory graduated vessels for volumetric measurements

Fig. 10. Recipient for preparation of primary solution

Apart from the measuring and control instruments in the stand, the following were also used:
- recipients for volumetric measurements - laboratory graduated vessels, 500-1000 ml, fig. 9;
- the blank for the preparation of the primary solutions, fig. 10, with a capacity of 50 l, made of polyethylene resistant to corrosive action of chemical substances in fertilizers;

Considering the corrosive action of the fertilizers, in order not to affect the components of the test stand, the aspiration / discharge of the primary solution is made from / in the mixing vessel on a hydraulic circuit separated from the supply circuit with moving fluid of the injection device; the injection pressure value, at which the device operates uniformly and ensures the set parameters, is adjusted from the valve mounted on the discharge hose and is measured with the pressure gauge attached upstream of the tap.

3.2 Performed tests

The technical-functional characteristics achieved under stand conditions of the injection device, determined according to the methodology [4] are shown in Table 1.

Table 1: Technical-functional characteristics of the injection device

Pres. in the watering pipe, bar	**Working pressure of injection device, bar**	**Injection pressure, bar**	**Supply flow of injection device l/min**	**Exhaust flows from drive chambers 1 and 2, l/min**	**Volume of drive chambers 1 and 2, ml**	**Control chambers volume of directional valve 1 and 2, ml**	**Injected flow rate of primary solution, l/min**	**Frequency of mobile assembly, double strokes/min**	**Control chambers flow of directional valves 1 and 2, l/min**	**Efficiency of injection device η = $Q_{inj}/Q_{supply\ of\ inj.\ device}$, %**
3.7	**3.5**	**3.4**	**3.89**	**1.596/1.444**	**42/38**	**11.1/11.6**	**1.400**	**38**	**0.418/0.432**	**35.9**
4.0	3.0	2.5	4.22	1.720/1.650	19.5/19.0	9.5/8.0	0.570	98	0.465/0.392	13.5
3.8	3.0	2.4	2.35	0.712/0.736	15.0/15.5	9.5/9.5	0.265	95	0.451/0.451	11.2
2.8	2.6	2.3	2.34	0.647/0.647	17.5/17.5	14.5/14.0	0.235	74	0.536/0.518	10.0
2.8	2.0	1.5	2.31	0.612/0.616	17.5/17.6	15.5/15.5	0. 335	70	0.542/0.542	10.0

The device was equipped with balls injection valves, made of two types of material: steel (results shown on the first row of the table), respectively KETRON PEEK polyether-ketone.

4. Conclusions

Experiments lead to the following conclusions:
1. The minimum pressure at which the injection device operates uniformly and continuously, with the free discharge of the primary solution (without load) was 1.2 bar;
2. The injection device has been tested at preset working pressures in the range of 2-3.5 bar;
3. The minimum bypass flow rate that ensures device operation is 5 l / min;
4. The injection pressure is proportional to the supply pressure of the drive chambers and has values ranging from 3.4 to 1.5 bar;

5. To facilitate the injection process, a tap with slide valve (with fine flow adjustment) is installed between the connecting points of the device, generating a local pressure drop;
6. Injected primary solution flow rate is between 1.4-0.235 l / min (84-14 l / h); the fertigation equipment, depending on the preset working parameters, can administer both basic primary solutions, currently used in fertigation, as well as microelements, which are administered in very small doses.
7. The frequency of the mobile assembly is significantly influenced by the material from which the balls of the injection valves are made; the frequency decreases with the increase in the weight of the balls, with implications on the filling degree of the drive / injection chambers, the injection pressure and the flow rate of the injected primary solution;
8. The injection device was tested with a 0.2% primary solution prepared from the Magnisal chemical. Magnisal is a total water soluble fertilizer that contains 11% nitrogen as NO_3 and 16% magnesium as MgO; the solubility of the product is 173 g / 100 g water at a temperature of 0° C, 200 g / 100 g water at 100 ° C, 225 g / 100 g water at 200 ° C, 256 g / 100 g water at 300 ° C, 289 g / 100 g water at 400 ° C; concentration (%), pH and electrical conductivity (mS / cm) vary as follows: 0.1 / 5.56 / 0.88; 0.2 / 5.51 / 1.69; 0.3 / 5.37 / 2.52; 1.0 / 4.85 / 7.58; 5.0 / 4.06 / 29.9.
9. Equipment samples under operating conditions have validated the reliability of laboratory samples demonstrating the functionality and utility of the product.

References

[1] Z. Borlan, C. Hera, "Agrochemical tables and nomograms" („Tabele și nomograme agrochimice"), Ceres Publishing House, Bucharest,1982;

[2] C. Paltineanu, S. Dumitru, E. Chitu, N. Tanasescu, M. Butac, M.Militaru, P. Ignat, V.Mocanu, "Plum and apple in the soil-plant-atmosphere system, in soils with medium and light texture", (" Prunul si marul in sistemul sol-planta-atmosfera, in soluri cu textura medie si usoara"), Terra Nostra Publishing House, 2017, ISBN 978-606-623-073-5,

[3] I. Biolan, I. Paltineanu, V. Mardare, C. Fagarasanu, A. Galca, S. Biolan, Gh. Sovaiala, I. Serbu, Gh. Crutu, A. Vranceanu, Dosing pump (Pompa dozatoare) – Patent no. 102887/19.02.1991;

[4] I. Biolan, I. Serbu, Gh. Sovaiala, F. Mardare, "Techniques and technologies for crop fertigation" ("Tehnici si tehnologii de fertirigare a culturilor agricole"), Publisher: A.G.I.R., ISBN: 978-973-720-344-1, 2010;

[5] M. Avram, "Hydraulic and pneumatic drive systems. Classic and mechatronic equipment and systems" ("Acţionări hidraulice şi pneumatice – Echipamente şi sisteme clasice şi mecatronice"), Bucharest University Publishing House, ISBN 973-7787-40-4, 2005;

[6] Gh. Sovaiala et al, "Innovative technologies and equipment for the implementation in the irrigated agriculture of the modern concept of fertigation",("Tehnologii si echipamente inovative pentru implementarea in agricultura irigata a conceptului modern de fertirigatie"), PN-II-PT-PCCA-2013-4-0114, contract 158/2014, www.ihp.ro/fertirig

[7] Gh. Sovaiala, S. Anghel, G. Matache, A.-M. Popescu, P.-M. Carlescu, "Injector of primary solutions with hydraulic control", *Scientific Papers -Vol . 59/2016, Agronomy series,* pp. 131-134;

[8] Gh. Sovaiala, S. Anghel, G. Matache, A. I. Popescu, Testing in Operation Conditions of Fertigation Equipment, *"Hidraulica" Magazine*, no.3/2017, ISSN 1453-7303, pp.31-36.

RESEARCHES ON DRY EXTRUSION PROCESSING OF SOYBEAN SEEDS FOR THEIR SUPERIOR CAPITALIZATION IN ANIMAL FEED

Anişoara PĂUN[1], Carmen BRĂCĂCESCU[1], Dumitru MILEA[1], Alexandru ZAICA[1], Costin MIRCEA[1]

[1] National Institute of Research-Development for Machines and Installations Designed to Agriculture and Food Industry INMA Bucharest, Romania,

any_paun@yahoo.com; carmenbraca@yahoo.com; milea_dumitru57@yahoo.com; zaica_alexandru@yahoo.com; costinmircea@yahoo.com

Abstract: *The extrusion technology is one of the perspective and efficiency processes, combining hydrothermal and mechanical processing of raw material (soybeans seeds), allowing obtaining new-generation products and components with predetermined properties, with a new structure called instant products, which are successfully used in animals fodder ration. The paper presents the installation for soybean seeds superior capitalization IVSS (consisting of screw conveyor, supply system, extruder, cooling system, mobile belt conveyor and a unit for command and control) and the experimental research in the establishment of its optimal operating parameters. In conclusion, this installation for soybean seeds superior capitalization using seeds dry extrusion as processing method ensures: reduction of raw material processing losses on food chain, realization of complex fodder receipts, obtaining food products ready for consumption or creating components for them, having high thickening and water and fat retention capacity with increase assimilability and reduction of products microbiological contamination. Taking into consideration all these aspects, this project tries to transform typical farmer in professional livestock farmer*.

Keywords: *Dry extrusion, soybean seeds, animal feed*

1. Introduction

The quality of mixed fodder significantly influences the quality of animal products obtained. From this point of view, fodder producers and farmers worldwide are facing serious problems with food security, ensuring comfort for animals and the environment protection.
In our country too, it is noted that more and more livestock breeders are interested in providing a full-value food to farm animals, which includes rich fodder receipts that lead to increased milk and meat production.
By its amino acid content, soybean completes together with cereals the ration of these animals, which leads to the production of mixed fodder, balanced in terms of essential amino acids and makes possible to achieve performance and economic potential of the respective animals. [2, 3]
Progresses in livestock field have shown that fodder rations containing soybean may be supplemented with vitamins eliminating the need for adding animal protein in the ration. Soy grit is also an important protein component in animals fodder ration, especially for pigs. [1, 2]
Taking into account that raw materials to satisfy nutritional needs are necessary, one must consider the processing method used to obtain these ingredients, which can influence the animal's performances. Most commonly used is the heat treatment of soybeans. Taking into consideration that the anti-nutritional factors, in most cases, are proteins, the processing method can adversely affect soybean proteins. Therefore, it is important to obtain a product rich in nutrients (energy and usable proteins) and free of anti-nutritional factors.
Worldwide, there is a growing concern to produce fodder processing machines and installations flexible, with the highest yields possible, low specific energy consumption to allow livestock breeders produce their own fodder for their animals feed at low costs, fresh and in sufficient quantities [4, 5, 6].

Taking into account the importance of knowing extrusion processing of soybean seeds, this paper presents the extrusion technology to obtain feed ingredients, used by the installation for soybean seeds superior capitalization – IVSS, produced by INMA Bucharest.

2. Materials and methods

The installation for soybean seeds superior capitalization – IVSS (figure 1) with a productive capacity of 150÷200kg/h was designed as a support of farmers who want to approach a strategy on: choosing fodder recipes depending on the animals in the farm, using own fodder and not only, the technical base necessary to the farm, and in the same time they will meet the requirements according to which agriculture no longer serves only to produce wheat, corn, milk and other agricultural products, but it also provides environment conservation and product consumers food safety.

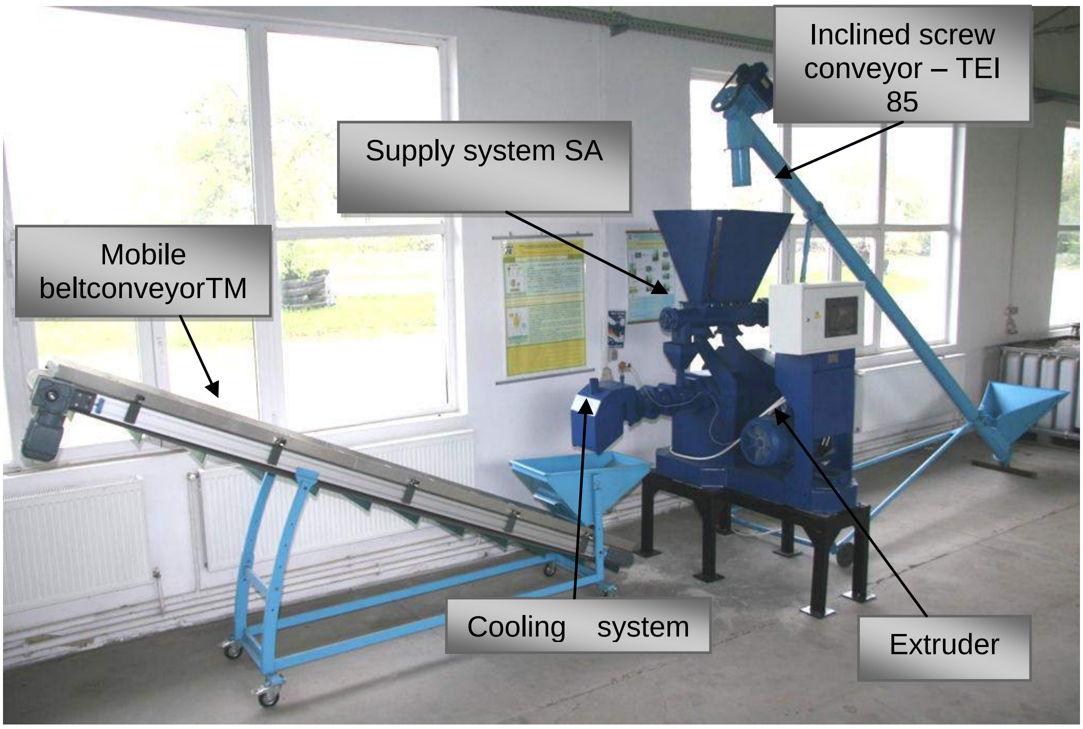

Fig. 1. Installation for soybean seeds superior capitalization – IVSS;

a) b)

Fig. 2. Material images (soybean seeds) at the installation inlet and outlet (final product “full fat soybean”)
a- Soybean seeds before processing; b- Final product “Full fat soybean”

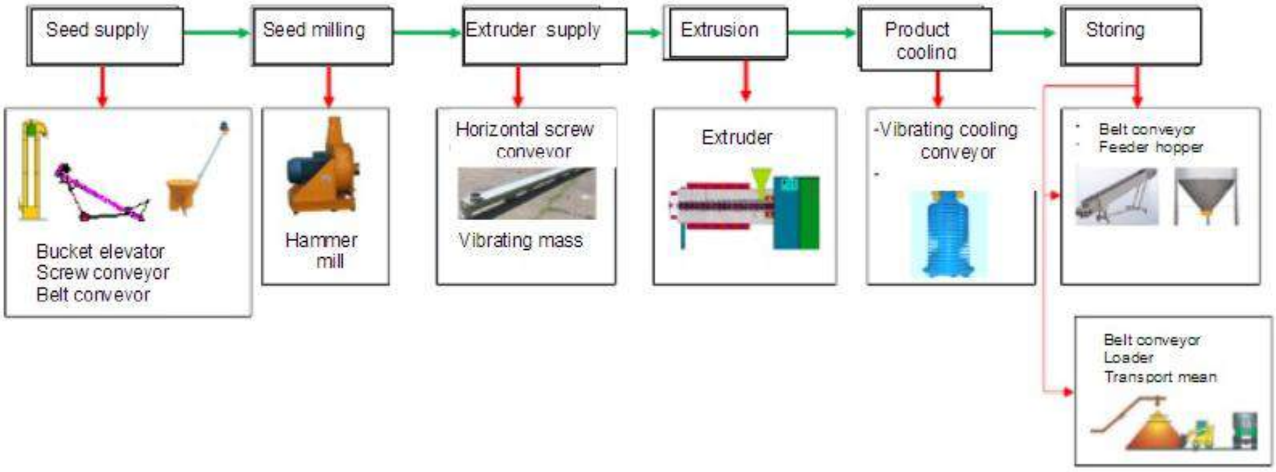

Fig. 3. Technological flow scheme of soybean seeds extrusion processing

During the extrusion process, the product can reach temperatures of approx. 140-150°C. As a result of the combination of temperature and pressure is ensured the distortion of anti-nutritional factors, oxidative enzymes and the release of oil from the cells by breaking the cell walls.

The main function of the extruder, besides transport, is to create a certain pressure necessary for the processed material to pass through the die orifice. The basic components that contribute to achieving this function are: the screw, the extrusion barrel and the die (Fig. 4).

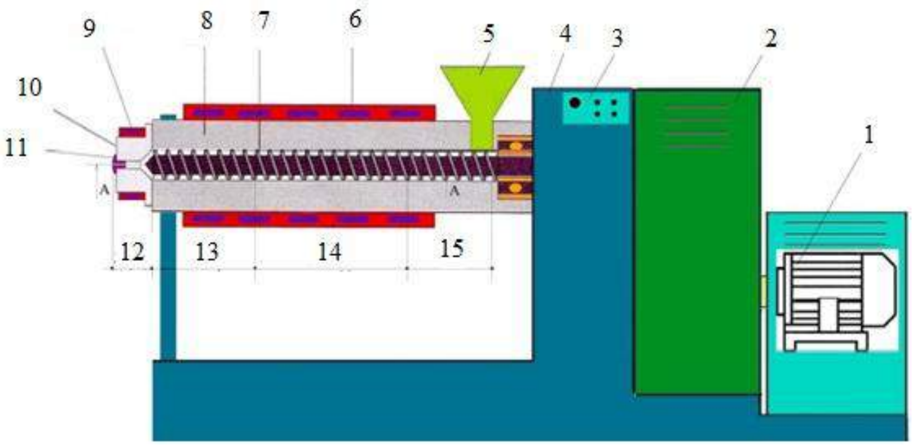

Fig. 4. Extruder scheme

1 - electric motor; 2- mechanical transmission; 3 - control panel; 4- frame; 5- supply hopper; 6- heating-cooling system for barrel; 7- screw; 8- barrel; 9- heating-cooling system for die; 10- die; 11- nozzle; 12- die section; 13- pressure section; 14- transition section; 15- feed section

The screw (7), beside the function of conveying the material from the supply hopper to the die entrance, influences, by its geometry, the mixing, shearing, the amount of mechanical energy dissipated in the heat and the pressure developed before the die.

According to the technological flow scheme in Figure 3, the product was introduced as a seed mass into the hopper of the inclined conveyor which transported it with the screw and discharged it into the feed system. From here, the seeds were dosed by a horizontal screw and discharged into the extruder feed funnel. The screw, the extruder main working element, picked up the raw material from the feed hopper, transported, processed and forced it to pass through the die hole at its end. The resulting expanded soybean was taken over by a belt conveyor and evacuated into storage hoppers.

The experimental researches were carried out at INMA Bucharest, both under laboratory and operating conditions. In the experimentation, we used soybean seeds, purchased from the cereal and industrial plants market, which underwent laboratory determinations on the physical characteristics that influence the extrusion process. For each sample we determined: product humidity, hectolitre mass, physical purity of different types of impurities removed, as shown in Table 1. In the case of soybean seeds used in the experiments, it was necessary to use the water for wetting the seeds as according to Table 1 the humidity was below 8%.

Table 1: Determinations of soybean seeds characteristics

No.	Characteristic	Parameter value		
		Sample 1	Sample 2	Sample 3*
1	Humidity, %	7.35	6.89	8.94
2	Hectolitre mass, kg/hl	69.53	69.14	61.96
3	Purity, %	99.49	98.85	86.52
4	Impurities: -oleaginous, % -non-oleaginous, %	 0.22 0.29	 0.68 0.47	 13.48 (total impurities)

*unconditioned seeds

The tests of the installation amounted to 115 hours of operation and were carried out in accordance with the specific procedures [2], using the following measuring devices: electronic balance and hectolitre balance, electronic humidometer, temperature transducer, tachometer and phase and frequency analyser (for the determination of the energy indices). At the same time, the proper functioning of the equipment and the measuring devices was checked and were measured the environmental conditions (ambient temperature and relative humidity) in which they were used.

Final product parameters were calculated using the following relations [7, 8]:

- *The expansion degree* characterized by:
  - final product *density*;
  - *apparent specific volume*

$$V_s = \frac{4}{\pi D_e L_{se}} \tag{1}$$

where*:*

D_e–outer diameter of expanded product;
L_{se} - specific average length (for 1g of extruded product).

- *Expansion index* characterized by:
  - *transverse expansion index (IET)*

$$IET = (D_e/D_m)^2 \tag{2}$$

where:

D_e– outer diameter of extruded product;
D_m – diameter of die hole

Table 2: Final product parameters

No.	Parameter	Parameter value		
		Sample 1	Sample 2	Sample 3
1	Outer diameter of expanded product, D_e [mm]	9.5	9.2	8.8
2	Specific average length (for 1g of extruded product), L_{se} [mm/g]	26.49	25.49	26.17
3	Apparent specific volume, V_S [g/mm^2]	5.5x10^{-3}	5.43x10^{-3}	5.53x10^{-3}
4	Diameter of die hole, D_m [mm]	7.8	7.8	7.8
5	Transverse expansion index, IET	1.48	1.39	1.27

3. Conclusions

The extrusion technology is one of the perspective and high efficiency processes that combine the hydrothermal and mechanical processing of raw material - soybean seeds, enabling new generation products and components with predefined properties, with a new structure: instant products.

In the case of soybean seeds processing by extrusion compared to traditional technologies, there are several advantages:

- products ready for consumption or components, which have a high water and fat retention capacity, are obtained;
- the degree of assimilation of raw material and use is higher;
- the degree of raw material microbial contamination and neutralization of the thermolabile anti-nutritive components is reduced.

Acknowledgments

This paper was financed with the support of National Agency for Scientific Research and Innovation, Programme NUCLEU, no. 8N/09.03.2016, Addendum No. 1/2016, Project PN 16 24 03 01 – “Innovative technology and installation for soybean seeds superior capitalization in animal feeding”.

References

[1] A. Păun, I. Pirnă, I. Cojocaru, P. Găgeanu, C. Brăcăcescu, “Optimization and implementation of technologies for concentrated fodder to improve the quality and chemical safety of products derived from livestock by providing the facility of obtaining concentrated fodder– IONC”, *Journal of INMATEH-Agricultural Engineering*, Vol.18, No.3, (2006), Bucharest, Romania: pp. 19-26;
[2] P. Halga& col., “Animal nutrition and feeding”, Alfa Publishing House, Iasi , Romania, 2005;
[3] J. Kaput, L. R.Raymond, “Nutritional genomics”, Wiley interscience, A John Wiley & Sons Inc. publication, 2006;
[4] A. Nedelcu, P. Găgeanu, L. Popa, R. Ciupercă, A. Zaica, Gh. Bunduchi, “Mechanical processing of camelina seeds for assuring the required conditions at superior capitalization of by-products”, Proc. of International Symposium ISB-INMA TEH' 2016, Agricultural and mechanical engineering, 27-29 oct.2016, Bucharest, Romania, pp. 757-762;
[5] A. Păun, P. Găgeanu, A. Danciu, “Impact of Technologies of Obtaining Concentrated Fodder Upon Animal Nourishment and Environment”, Bulletin of University of Agricultural Sciences and Veterinary Medicine Cluj-Napoca, Vol.66, No.1, 2009, pp.433-440;
[6] A. Zh. Koleva, “Dry pet food. Part 2, Hydrothermal processes for production”, Scientific Works of the University of Food Technologies-Plovdin, Bulgaria, 2012, Vol.59, pp.193-197;

[7] N. Cioica, G. Balc, V. Ionut, “Thermal transitions by directly expanded extruded maize grits”, Food processes and technologies, vol. XI, no.2, Agroprint Publishing Timisoara, 2005, pp. 255-260;
[8] G. Fodorean, C. Cota, N. Cioica, “Influence of rotation speed during extrusion to the properties and morphology of biopolymers blend”, Acta Technica Napocensis, September 2013.

ISSN 1454 - 8003
Proceedings of 2017 International Conference on Hydraulics and Pneumatics - HERVEX
November 8-10, Băile Govora, Romania

ANTIENTROPIC CONCEPT CHAB

Erol MURAD

EKKO OFFICE AG SRL,erolmurad@yahoo.com

Abstract: *To reduce the emission of CO2 and the environmental entropy, production of energy should be done with zero or negative carbon balance. The residual agricultural, forest and industry biomass can be converted in TLUD gasifier with the CHAB concept in heat and quality biochar with a negative entropic balance of -15 338 kJ / kWhth. Compared with the direct burning of biomass, which is theoretically a zero entropic balance, introducing biochar in agricultural soil produces negative entropy of -15.3 kJ/kg.bm.K, contributing to increased anti-entropic activity of agricultural soil and improves soil health, which enables plants to sequester carbon into the ground. This is known as the carbon multiplier effect.*

Keywords*: Entropy, biomass, CHAB concept, biochar, TLUD*

1. Introduction

The currently developped concept called CHAB (Combined Heat And Biochar production) consists in concurrently obtainingheat and biochar from biomass. Agricultural biochar amendment is a valuable contribution to agricultural soils, certified to increase their productive capacity. Biochar is produced from pyrolysis of biomass in different conditions with a specified temperature and oxygen supply. [1. 2. 3. 4]
Incorporation of biochar into the agricultural soil produces negative entropy variation of the environment, contributing economically and environmentally to atmospheric carbon sequestration for long periods, resulting in the absolute reduction of CO2 concentration in atmosphere. Biochar contributes directly to increasing soil fertility, which results in an increase in plant mass, which leads to a decrease of environment entropy, by fixing more CO2 through photosynthesis. This is known as carbon multiplier effect. [1.5.6]
It appears that using the concept CHAB has an anti-entropic nature, contributing directly to reducing both the environmental and agricultural soil entropy balance. A Monte Carlo analysisof the entropic balance, called Cross Entropy Method, enables optimization of processes used to obtain energy from renewable sources [7. 8. 9. 10]
Unlike energy production through biomass burning,in which in theory entropy remains constant, using the concept CHAB lowers the atmosphere and soil entropy. CHAB is an anti-entropic process. [9. 10.11]
Onecurrent application of the CHAB concept uses an anoxidic pyrolizor operating at 773 K in which, the exiting pyrolysis gas condensation produces bio-oil and syngas and a high proportion of biochar with VOC (Volatile Organic Componnents). Analysis shows that the system produces negative entropy. It appears that the greatest positive entropy is produced by the condenser unit. If possible the CHAB concept should avoid the condensation step. [12, 13]
This paper analyzes the entropic balance of the gasification process type TLUD (Top-Lit-Up-Draft) with CHAB concept for the production of heat and biochar. The gasifier TLUD can operate at a temperature of the mygratory pyrolysis front (MPF) higher than 973 K. It produces syngas with very little tar and does not have a condensation step,resulting at the output in a larger negative entropy value. [13]

2. TLUD gasifier with CHAB concept

The thermal system with CHAB concept shown in block diagram in figure 1 consists of TLUD gasification reactor, a gas burner and a biochar cooler. The analysis of the system entropy variation considers an isolated thermodynamic system which consists of three open subsystems.

ISSN 1454 - 8003
Proceedings of 2017 International Conference on Hydraulics and Pneumatics - HERVEX
November 8-10, Băile Govora, Romania

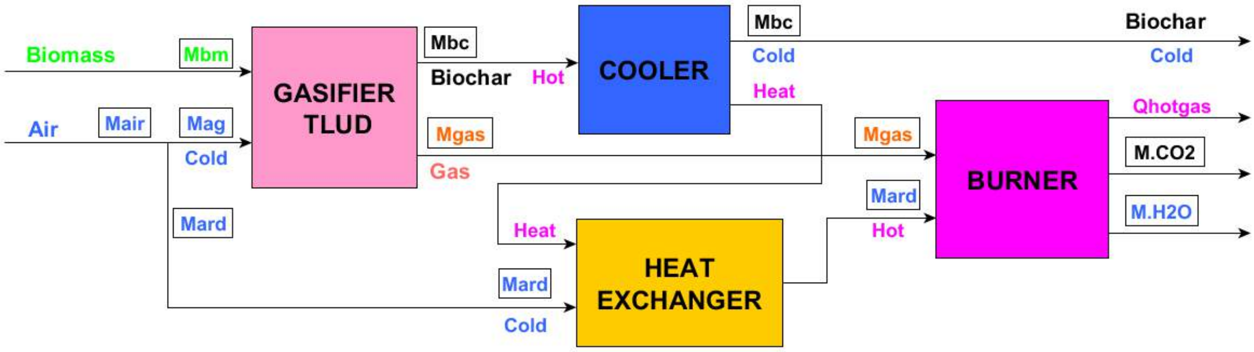

Fig. 1. Block diagram of CHAB concept thermal system

The batch input in the TLUD gasifier reactor is a M_{bm} (kg.bm) biomass at standard temperature 298Kwith known physical, chemical and energy characteristic. Initialize the ignition and gasification process by feeding an air mass input $M_{ag} = k_{ag} \cdot M_{bmg}$ (kg.air) at standard temperature. [3.4.14.15]
In gasification processes, some of biomass M_{bmg} is completely gasified and in reactor remains a warm biochar mass $M_{bc}$of average temperature Tbch.
The output warm biochar mass M_{bc} is:

$$M_{bc} = k_{BC} \cdot M_{bm} \quad (kg.bc)$$

The output mass of fully gasified biomass M_{bmg} is:

$$M_{bmb} = M_{bm} - M_{bc} = M_{bm} - k_{BC} \cdot M_{bm} \quad = (1 - k_{BC}) \cdot M_{bm} \quad (kg.bmg)$$

For further uses biochar is cooled to standard temperature 298K with a special cooler, which heats the air needed for combustion in the burner.
From gasification process result a mass of combustible gases M_{gas} (kg.gas):

$$M_{gas} = M_{bmg} + M_{ag} = (1 + k_{ag}) \cdot M_{bmg} \quad (kg.gas)$$

Produced gases M_{gas} are burned with a special burner with outdoor air intake mass M_{ard}:

$$M_{ard} = k_{ard} \cdot M_{ag} = k_{ard} \cdot k_{ag} \cdot M_{bmg} = k_{ard} \cdot k_{ag} \cdot (1 - k_{BC}) \cdot M_{bm} \quad (kg.air)$$

The combustion air is heated with the exit heat of biochar cooler, which makes the system emitting outdoor only the enthalpy Q_{hotgas} of fully gasified biomass M_{bmg}. [3. 14.15]
Theoretically, the ecological entropic balance burning biomass is null. The fully gasified biomass M_{bmg} releases an amount of water in the surroundings and the CO2 will be fixed by vegetation through photosynthesis, leading to a zero entropy variation. [6. 9]
The system with CHAB concept will return in environment the standard entropy of cold biochar. Depending on usage it can be positive if it is used as fuel for gasification, or negative if inserted into the agricultural soil.
The total entropy balance is:

$$\Delta S_{total} = S_R - S_C + S_{gent} = 0$$

where - S_R entropy generated by the reactor TLUD.
S_C - the entropy generated by the cooler. In this case the $S_C = 0$.
S_{gent} - entropy generated by the system.
With the entropy generated by the cooler being 0, the total entropic balance becomes:

$$\Delta S_{total} = S_R + S_{gent} = 0$$

3. Entropy balance of the TLUD gasifier

In general, in the analysis of entropic balances, absolute entropy, standard entropy and specific entropy are used. The entropy flow measurement is done using units specific to the different processes analyzed. This study uses specific entropy relative to one kilogram of biomass introduced reactor and measured kJ/kg.bm.K. [13. 16]
The entropy change ΔSR in gasifier TLUD, producing fuel gas and biochar (BC), considered as an independent subsystem, is null. The entropic balance is:

$$\Delta S_R = S_{inpr} - S_{outr} + S_{genr} = 0$$

where: S_{inpr}- entropy input in reactor.
S_{outr}- entropy output from reactor.
S_{genr} - entropy produced by the reactor.
In the present paper only the entropy input calculations will be explained.
The entropy input results from summing specific standard entropy S_{bm} of one biomass kilogram with the entropy S_{airg} of the air mass M_{ags} for gasification of a kilogram of biomass.

$$S_{inpr} = S_{bm} + S_{airg}$$

The standard enthalpy of biomass can be calculated with little approximation as the ratio of High Heating Value (HHV) (kJ/kg.bm) to the standard temperature of 298 K (25 C).

$$S_{bm} = \frac{HHV_{bm}\ (kJ / kg_{bm})}{298(K)}$$

The error of this approximation is within 3% for most biomass gasifiers. [12. 16.17.19]

HHV biomass can be determined experimentally with a calorimeter bomb, or if known chemical composition of biomass is known with semi-empirical models. The most used models are: Demirbaş (2000), Chang (2005), Azevedo (2005), Friedl (2005) and all. [17.18.19.20].
For this study, the data from experiments of doctoral thesis developed by S. Varunkumar were used. The chemical composition and Low Heating Value (LHV) for biomass pellets are given. These data are used to estimate the HHV value of biomass as 15.8 MJ/kg.bm. [7.15.17.20.21. 22]
Biochar entropy is calculated similar to that of biomass knowing the HHV value, or its experimentally determined value based on the chemical composition of biochar. In the analyzed experiment the high heating value of biochar HHV_{bc} = 27.8 MJ/kg.bc. [2.4.5. 14.15]
S_{ags} specific air entropy for of a kilogram of biomass gasification is:

$$S_{ags} = S_{airS} \cdot k_{ag} \cdot (1 - k_{BC})$$

where: Sags – standard air entropy. [23]
kag = 1.50.[15]
k_{BC} = 0.164. [15]
The heat losses of the reactor by convection and radiation are taken in consideration for the heated combustion air. The heat loss was determined experimentally to be 3% of the enthalpy of the biomass gasified. [15]

4. Cooler entropy balance

The biochar enters the cooler with a high temperature of 500 C and exits from the system with a low temperature. The heat taken up by cooling of the air is used to heat the combustion air, recovering some of the of the biomass source energy. Thus almost all the energy from gasified biomass Mbmg is found at the exit of the burner in the hot gases enthalpy.

5. Results and discussions

With the above considerations, calculations to determine the final entropy balance, as presented in tables 1 and 2have been performed. It appears that the overall balance of TLUD gasifier operating in CHAB concept with initial hypothesis conditions, is negative at - 3 353 kJ/kg.bm.K. By incorporating biochar in agricultural soil a environment entropy decrease with -15 299 kJ/kg.bm.K results.

Table 1: Gasifier TLUD with CHAB concept

Feature	M.U.	Value	Obs.
HHV pellets (BM)	MJ/kg.bm	**15.8000**	[20]
Standard input temperature	grade K	298.0000	[6]
Biomass input entropy	kJ/kg.bm.K	**53.0201**	
Input air entropy	kJ/kg.air.K	**6.8480**	[6]
A/F range	kg.air/kg.bmg	**1.5000**	[20]
Biochar yield	kg.bc/kg.bm	**0.1640**	[20]
Gasified biomass yield (BMG)	kg.bmg/kg.bm	**0.8360**	
Syngas mass	kg.gas/kg.bm	**2.0900**	
Carbon in biochar	kg.C/kg.bc	0.9100	[20]
Carbon of BM in BMG	kg.C/kg.bm	**0.1492**	[20]
HHV of biochar	MJ/kg.bc	**27.8000**	[20]
HHV of gasified biomass	MJ/kg.bmg	**13.4459**	
Specific heat of biochar	kJ/kg.bc.K	0.9500	[18]
Out reactor temperature	grade K	773.0000	[20]
Standard biochar entropy	kJ/kg.bc.K	**93.2886**	
Output biochar entropy	kJ/kg.bc.K	**36.5783**	
HHV output syngas	MJ/kg.gas	4.6000	[20]
Standard entropy syngas	MJ/kg.gas.K	11.5578	
Syngas specific heat	kJ/kg.gas	1.0000	[20]
Output syngas entropy	kJ/kg.gas.K	5.1025	
Heat loss - 3% of HHV.bm	kJ/kg.bm	474.0000	[20]
Heat loss entropy	kJ/kg.bm.K	1.5906	

(bm – biomass ; bmg – gasified biomass ; bc – biochar)

Table 2: Thermal system entropic balances

Feature	M.U.	Value
Balance reactor inputs		
Biomass mass	kg.bm	1.000
Input biomass entropy	kJ/kg.bm.K	53.0201
Input air entropy	kJ/kg.bm.K	8.5874
Total entropy inputs	kJ/kg.bm K	**61.6075**
Balance reactor outputs		
Output biochar entropy	kJ/kg.bm K	5.9988
Output syngas entropy	kJ/kg.bm K	10.6642
Thermal entropy loss	kJ/kg.bm K	1.5906
Total outputs entropy	kJ/kg.bm K	**18.2536**
Entropy generated in reactor	kJ/kg.bm K	**-43.3539**

Incorporating biochar in soil helps to increase crop production in same environmental conditions, which can decrease the environment entropy by sequestration in agricultural soil of about 0.153 kg.C/kg.bm or a 0.560 kg.CO2/kg.bm. This calculation confirms that the application of the CHAB concept can effectively contribute to decreasing the environment entropy.
Using the CHAB concept to achieve the same heat production, compared to the case of heat produced by directly burning biomass results in an average decrease of entropy by 15.338 kJ/kWhth.

Table 3: Environment entropic balance

Feature	M.U.	Value
Entropy of BC introduced in soil	kJ/kg.bm.K	**-15.299**
Carbon sequestered in biochar	kg.C/kg.bm	0.153
Carbon dioxide sequestered in soil	kg.CO2/kg.bm	**0.560**
Overall TLUD yield	real	0.912
Pellet burner yield	real	0.930
Burner energy with CHAB	MJ/kg.bm	10.143
Pellet burner energy	MJ/kg.bm	14.694
Specific entropy reduction	kJ/kWhth	**-15.338**

6. Conclusions

Using CHAB concept for the production of heat and biochar helps reduce the entropy of the environment so it is anti-entropic action, typical for the vegetation, contributing efficiently and directly to the sustainable development of agriculture and therefore for entire society.
The use of TLUD gasification process operating in CHAB conditions leads to a negative entropic balance of -43.353 kJ/kg.bm.K, a much higher entropy change than any other applications of the CHAB concept.
CHAB concept produces a unit of heat compared with the direct burning of biomass systems reducing the entropy with-15.338 kJ/ kWhth.
Compared with the direct burning of biomass with zero entropy balance, by introducing biochar in agricultural soil, a decrease of soil entropy with -15.3 kJ/kg.bm.K results, helping to increase the anti-entropic activity of agricultural soil.
An effective economic and ecologic optimization of similar thermal systems can be done by applying a Monte Carlo type analysis called the Cross Entropy Method.
This study may by used as a basis for advanced analysis of anti-entropic nature of energy production from biomass with CHAB concept.

References

[1].S. D. Joseph et al., “An investigation into the reactions of biochar in soil”, *Australian Journal of Soil Research*, 2010,48, 501–515;
[2].E. Murad, A. Culamet, G. Zamfiroiu, “Biochar- Economically and ecologically efficient technology for carbon fixing”, *International Symposium HERVEX 2011*,Călimăneşti, November 9-11, 2011;
[3].E. Murad, F. Dragomir, ”Heat generators with TLUD gasifier for generating energy from biomass with a negative balance of CO_2”, *International Conference HERVEX 2012*,Călimăneşti, November 7-9, 2012;
[4].E. Murad, “CHAB from agricultural biomass with TLUD”, *Scientific Symposium ICEDIMPH-HORTING*, November 28, 2013;
[5].E. Murad, “CHAB concept in viticulture”, *Scientific Symposium ICDVV* Valea Călugărescă, June 12, 2014;
[6].P. Wȕrtz, A. Annila,“Ecological succesion as an energy dispersal process”, *BioSystems*, no.100, 2010, 70-78;
[7].G. Deutscher, ”The Entropy Crisis”, Tel Aviv University, Israel, World Scientific Publishing Co,Pte,,2008;
[8].C. Loren, C. Jalocon, “Renewable energy portofolio planning using the cross-entropy method”, *Power and Energy Engineering Conference (APPEEC)*, 2013 IEEE PES Asia-Pacific, Dec., 2013;
[9].U. Lucia, “Entropy and exergy in irreversible renevable energy systems”, *Renevable and Sustainable Energy Reviews*, Vol, 20, April 2013, 559-564;

[10]. J.P. Meyn, ”Renevable energy sources in therms of entropy”, *European Journal of Physics*, Vol, 32, Number 1, 7 december 2010;
[11]. www.asas.ro/wcmqs/membri/asociati/MIHALACHE+Mircea,html, “Comportamentul anti-entropic al solurilor”;
[12]. K. Samiei, “Entropy analysis, as a tool for optimal sustainable use of biorefineries”, Master of Science Thesis, University College of Borås School of Engineering, Sweden, 16 November 2007;
[13]. K. Singh, E.W. Tollner, S. Mani, L.M. Risse and, K.C. Das, “Transforming solid wastes into high quality bioenergy products: entropy analysis“, *Proceedings of NAWTEC16, 16th North American Waste-to-Energy Conference*, May 19-21, 2008, Philadelphia, Pennsylvania, USA;
[14]. J. Thryner, “Combustion Phenomena in Biomass Gasifier Cookstoves”, Doctor Dissertation, Colorado State University, Fort Collins, Colorado Summer 2016;
[15]. S. Varunkumar, “Packed bed gasification-combustion in biomass based domestic stoves and combustion systems”, Doctor Thesis, Department of Aerospace Engineering, Indian Institute of Science, Bangalore – 560 012 (India), 17 Feb. 2012;
[16]. A. Blejan, ”Termodinamica tehnica avansata”, Ed, Tehnică, Bucuresti, 1996;
[17]. A.J. Callejon-Ferre, ”Prediction models for higher heating value based on the structural analysis of the biomass of plant remains from the greenhouses of Almería (Spain)”, *Fuel*, Vol. 116, 15 January 2014, pp. 377-387;
[18]. B.M, Jenkins, L,L, Baxter, T,R, Miles Jr., T,R, Miles, “Combustion properties of biomass”, Elsevier, *Fuel Processing Technology* 54,1998, 17–46;
[19]. E. Peduzzi, G. Boissonnet, F. Maréchal, “Biomass modeling: Estimating thermodynamic properties from the elemental composition”, Elsevier, *Fuel* no.181, 2016, 207–217;
[20]. M.J. Prins, “Thermodynamic analysis of biomass gasification and torrefaction”, Master of Science Thesis, Technische Universiteit Eindhoven, 2005;
[21]. P. Basu, “Biomass Gasification and Pyrolysis - Practical Design and Theory”, Elsevier, 2010;
[22]. K. Varmuza, B. Liebmann, A. Friedl, “Evaluation of the heating value of biomass fuel from elemental composition and infrared data”, University of Plovdiv „PaisiiHilendarski“ – Bulgaria Scientific Papers, vol. 35, book 5, 2007 – chemistry;
[23]. D.R. Lide, R. David, “Standard Thermodynamic Values at 25°C”, *CRC Handbook”,* 84th ed,; CRC Press: Boca Raton, Florida, 2003; pp. 5:5-5:60, 5:85-5:86.

ISSN 1454 - 8003
Proceedings of 2017 International Conference on Hydraulics and Pneumatics - HERVEX
November 8-10, Băile Govora, Romania

SPECIALIZED EQUIPMENT FOR CALIBRATION IN-LINE APPLIANCES FOR TESTING PHYSICAL PARAMETERS OF WATER QUALITY

Dumitru VLAD[1], Diana Mura BADEA[1], Valentina Daniela BAJENARU[1]

[1] National Institute of Research and Development in Mechatronics and Measurement Technique, Bucharest, Romania; didivlad2006@yahoo.com, dianamura@yahoo.com, valibajenaru@yahoo.com

Abstract: *In this paper we report on our experience in producing laboratory equipment (test stand) to determine the performance characteristics of on-line equipment for water analysis under controlled conditions. In this paper only reference is made to the physical parameters of drinking water. After building test bench facilities, an in-line sensor / equipment to determine performance characteristics using the comparison method should be considered. The performance characteristics to be determined are in accordance with the test procedures.*

Keywords*: Sensor test and in-line measurement, water drinking quality parameters*

1. Introduction

The quality conditions that drinking water must meet are rigorously established (regulated) by sanitary norms and standards. Sanitary norms are tables of a legal nature that include the limit values admitted for water quality indicators. [1]
Water quality standards are a set of rules defining the main quality characteristics that water has to meet, the methods of analysis, the units of measurement, the terminology of the symbols used, etc. [2].
Each country has its own standards and water quality standards. However, worldwide it tends towards a common basis, resulting from the experience and needs of all. [3]. The common basis is represented by a reference system, accepted in most countries, which includes the limit values allowed for the physical, chemical and biological composition of water, which ensures the safe use of water for a particular destination.
In recent years the development of IT and communications technologies have a more significant contribution in the water processing management and the technologies for water quality control are undergoing continuous improvements. These technologies not only must comply with strict rules, safety measures, and quality standards, social and environmental challenges but also face serious problems of obsolete infrastructure, network leaks and the quality of drinking water. On the other hand, supplying clean drinking water and protecting the health of the population of the adverse effects of any contaminated water intended for human consumption are fundamental requirements of the European Directive 98/83/EC, transposed into Romanian legislation law No. 458/2002 (amended and completed by law No. 311/2004 and the Governmental Ordinance No. 11/2011).
As a result, there is a market demand for drinking water management solutions considering that current technologies are far from satisfying the legal requirements in terms of monitoring, remote transmission and data processing for water quality. To know the water quality monitoring solution currently used is manual removal of samples, in certain specific points (especially the plug), transport to laboratory,measurements and issuing a report.

2. The current situation in the country

Drinking water quality monitoring can be achieved only in laboratories registered with the Ministry of Health. Registration is a process of recognition of the drinking water is done within the laboratories of DSP [4].

The manufacturers water quality monitoring is based on rigorous technical procedures and advanced control tools. Water monitoring is carried out in water plants (automated analyzers track each phase of water treatment to verify its effectiveness), in water tanks and on the distribution network, all these being coupled with laboratory analysis.
Annually about 120.000 indicators are analyzed on over 6.000 samples collected from the distribution network [5].
To know the water quality monitoring solution currently used is manual removal of samples, in certain specific points (especially the plug), transport to laboratory, measurements and issuing a report.
Sampling is currently in a period of time and the test results are known after 7 ÷ 10 days from the date of sampling. In this way, exceeding the maximum permissible content of chemical elements or physical is known only after the event, without being able to take swift action.
These laboratories equipment is not used in the field (expeditionary) and is not adaptable monitoring system water transport buses[6].

3. The current situation abroad

To highlight existing solutions on the market must mention two technical solutions for measuring parameters of drinking water. In-line measurement is made by placing measurement probes inside the pipes, and the on-line measurement of water sample is pumped from the water pipe to additional analytical tools pipeline. Currently for measuring on-line there are a variety of multi parameter probes used to determine several physic parameters such as: pressure, temperature, pH, turbidity, residual chlorine, total organic carbon (TOC), and turbidity [7].

4. General description of the product

Constructively, the adopted scheme of equipment for in-line calibration of apparatuses for determining the physical parameters of water quality is shown further (Fig.1).

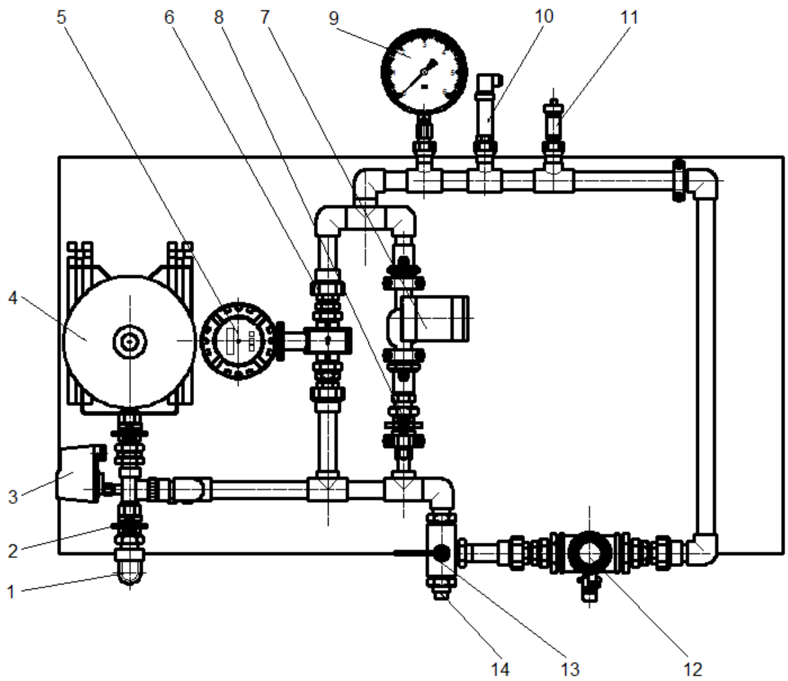

Fig. 1. General description

The equipment consists of the following components: water reservoir, 1 -sumersible pump, 2 - valve A, 3- pressure switch, 4- hydropneumatic accumulators in which the fluids are separated by balloon, 5 -electromagnetic flowmeter, 6- sense valve, 7- recirculating pump, 8 – valve B, 9 - pressure indicator, 10 - pressure and temperature transducer, 11 - ventilation valve, 12 - a bypass where the measuring probes and the monitoring system are mounted, 13 - 3-way pass valve, 14 – emptying path, pipes and fittings, elbows, mass support, etc.
Operation:
After mounting the calibrator in the by-pass where the measuring probes and the monitoring system are mounted, depending on the parameters determined, the stand provides two modes of operation:

A Closed system operation;
A pressure of 1.5 bar is provided in the hydropneumatic accumulator. With valve 2 in open position, valve 9 in open position and three-way valve having outlet path 14 closed, the water in the tank is pumped into the pipes at a pressure set by means of the pressure switch 3. At the moment of reaching the desired working pressure, the pump is disconnected by means of the pressure switch and closing valve 2. Air in the system is drained through the air valve. Start the water recirculation pump on the system at the flow rate it provides. We have the choice of three flow rates. The pressure and temperature transducer 10 together with the flow meter 5 provides information on each measured parameter by displaying the measured values on the control and control panel (laptop). The water passes through the bypass on which the calibrating apparatus is mounted and further returns to the tank by opening the three-way valve through the discharge head 14 after the calibration.

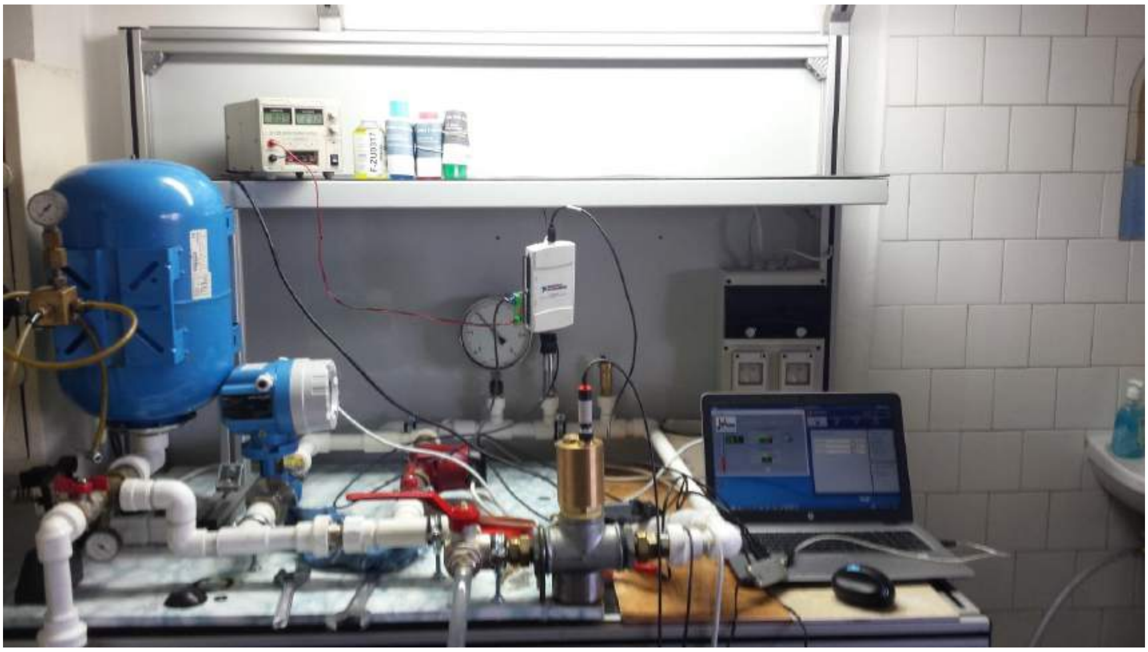

Fig. 2. Specialized equipment for calibration in-line

B Open system operation;
A pressure of 1.5 bar is provided in the hydropneumatic accumulator. With valve 2 in open position, tap 9 in the closed position and three-way valve having outlet path 14 open, tank water is pumped into the pipes at a pressure and flow comparable to those encountered in the water supply network. The air in the system is drained through the air vent valve. The pressure and temperature transducer 10 together with the flow meter 5 provides information on each measured parameter by displaying the measured values on the control and control panel (laptop). The water passes

through the bypass on which the calibration device is mounted, and then returns to the tank through the throttle tap 14 of the tap. The calibration of the appliance is carried out with the pump in operation.
Determining performance characteristics of sensors for analyzing the physical parameters of water in the laboratory, under controlled conditions, it can be described using the diagram as shown in Figure 3. [8]

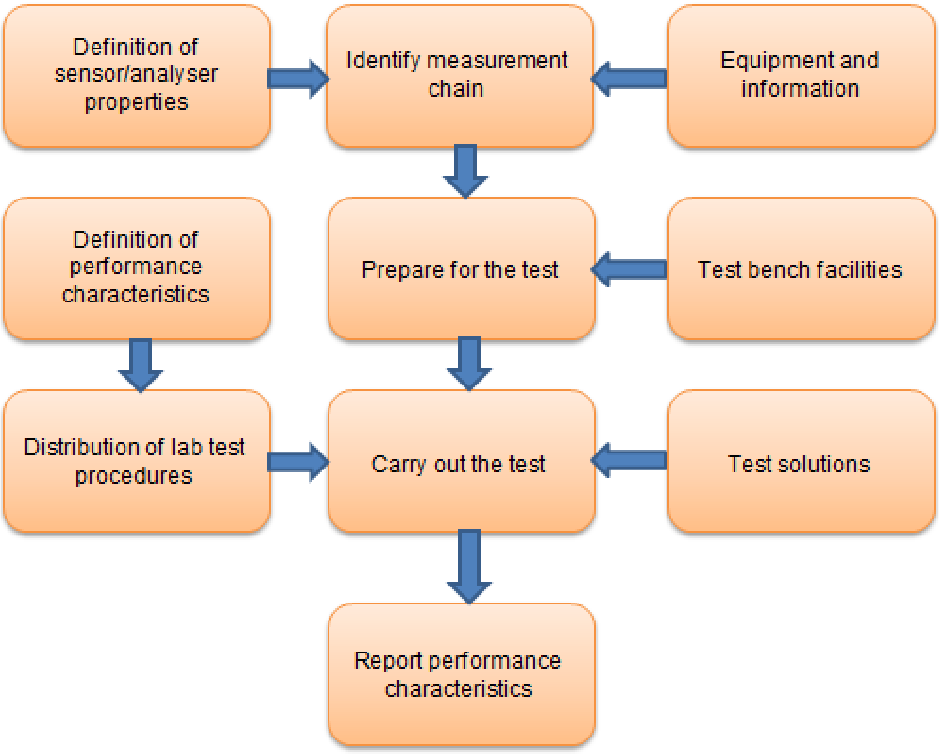

Fig. 3. Overview of test

<u>Technical specifications</u>

Fig. 4. Calibration test

The main technical characteristics of the specialized equipment for in-line calibration of the apparatuses for determining the physical parameters of the water quality are the following:

- Work environment: fluid (water);
- Pressure: minimum 0.7 bar and maximum 6 bar
- Working pressure: max. 3 bar
- Flow rate: F_{min} = 0.1887 mc /s; F_{max} = 0.55 mc /s; F_{work} = 0.25 mc /s
- Temperature: 25 ± 5 ºC
- Power supply: 50Hz; 1x230 V; 0 ... 24 VDC
- Pump: 0.016 mc /s - 0.09 mc /s
- Tank: 80 l

5. Conclusions

The experimental researches validated the constructive solutions chosen for the calibration stand in the field of physical parameters measurement of water quality, dynamic behavior of sensors, as well as the proposed test method for determining the main parameters influencing this behavior.
There are four series of measurements, three series with closed system operation and 1 series, in open system.
The experimental research on the behavior of the specialized equipment for the in-line calibration of the apparatuses for the determination of the physical parameters of the water quality, allowed the determination of the functional parameters, as well as the recording of the evolution of the physical parameters according to the variation of the pressure and the flow rate.

References

[1]. Law No.458 of the Romanian Parliament of 8 July 2002 on drinking water quality;
[2]. STAS 1342/91- Apă potabilă;
[3]. Current Online Water Quality Monitoring Methods and Their Suitability for the Western Corridor Purified Recycled Water Scheme – Roger O'Halloran, Shoshana Fogelman, and Huijun Zhao, October 2009;
[4]. Department of Public Health;
[5]. http://www.apanovabucuresti.ro/info-consumator;
[6]. EU-WFD 2003. Common implementation strategy for the Water Frame Work Directive (2000/60/EC),Guidance Document No. 7. Monitoring under theWater Framework Directive Produced by WorkingGroup 2.7 – Monitoring (2003);
[7]. FP7 – 217976/SecurEau - Security and decontamination of drinking water distribution systems following a deliberate contamination;
[8]. ISO 15839:2003 - Water quality-On-line sensors/analyzing equipment for water- Specification and performance tests.

ISSN 1454 - 8003
Proceedings of 2017 International Conference on Hydraulics and Pneumatics - HERVEX
November 8-10, Băile Govora, Romania

EXPERIMENTAL RESEARCH ON THE METHODS OF VALORIFICATION OF BIOMASS WASTE

Gabriela MATACHE[1], Ioan PAVEL[1], Petrin DRUMEA[1], Alexandru HRISTEA[1], Edmond MAICAN[2]

[1]Institute for Hydraulics and Pneumatics INOE 2000-IHP, fluidas@fluidas.ro

[2]UPB-ISB, e.maican@gmail.com

Abstract: *This paper presents the results obtained from testing a TLUD-type equipment, used to obtain biogas and biochar from biomass, developed and manufactured based on a patent elaborated under a research and development project by the staff of the Institute IHP. The paper presents solutions to increase the efficiency of burning boilers with gasification by recovering heat from flue gases discharged (which otherwise would be lost to the atmosphere) and reinserting it into the air circuit for gasification or combustion. The energy thus reintroduced into the combustion process can increase efficiency of gasification boilers by several percents, which means it saves large amounts of biomass and slows down global warming.*

Keywords: *Biomass, Combustion Processes, Thermal Energy, TLUD*

1. Introduction

One of the most important sources of fuel for humankind was wood. Essential for using this type of fuel is that energy can be recovered in a sustainable manner (being renewable). Worldwide there is a potential big enough for the use of wood for energy purposes. Many of Europe's forests can be used for energy purposes without compromising existing natural ecosystems. Harvesting and processing wood for energy purposes other than those involving large quantities of waste, often remain untapped. Thus, wood chips or sawdust, which can produce so-called pellets or briquettes are a valuable fuel. A big advantage of wood is that it retains the energy content in time, even in the first two to three years there is a relative increase, which is the period when drying occurs. This feature is important because if you do not have a properly degree of drying all wood humidity will be eliminated in the boilers with the price in the drop of the caloric power. Another disadvantage is the burn rate of the wet wood which decreases the temperature of the combustion, which leads to imperfect oxidation of all the combustible ingredients, the appearance of smoke, the clogging of the fumes canals and reducing the boiler life.
Gasification is the conversion of solid fuels into gaseous fuels, produced by partial oxidation using oxygen, air, water vapor or mixtures thereof in special equipment (gas-producing). The entire process takes place by partial combustion and heating of biomass with heat generated during combustion. The mixture of emerging has a high energy value which can be used, like other gaseous fuels, to produce heat or electricity.

2. Methodology

Wood boilers, gasification, with gasification, it runs on pyrolytic wood distillation process. When the air is limited, the wood turns into charcoal as it burns. At the same time appears the "wood gas", which is directed into the burner nozzle to be burned at the base of the boiler. This method of wood burning allows the effective use as fuel.

Combustion is a three-step process in every area of the boiler:

- Zone 1 - drying and gasification wood,
- Zone 2 - burning of the wood gas at the secondary preheating nozzle entrance,
- Zone 3 - lower combustion in uncooled combustion chamber.

Thus, the system for controlled combustion ensures a high efficiency - often up to 90%. Taking into account this, the boiler performance is continuously variable from 40% to 100%. Burning space typically includes the nozzles made of special refractory materials. The control of operating the boiler is made with an electronic controller, depending on the temperature.
In the gasification process there enters biomass and air and results fuel gas and ash with a neutral CO_2 balance.
The fuel gas with CO, H_2, CO_2, N_2 and tar can be used to:
- burning in a specialized burner from which results flue gases with high enthalpy containing, in very low concentrations PM and CO, hot gas that are used to:
  - processes of heating water, steam or air,
  - in internal combustion engines to produce electric energy.
- is filtered the content of tar and PM and is used in internal combustion engines to produce electric energy.

In Figure 1 is represented a block diagram of the procedure of energy recovery of biomass by thermo-chemical gasification.

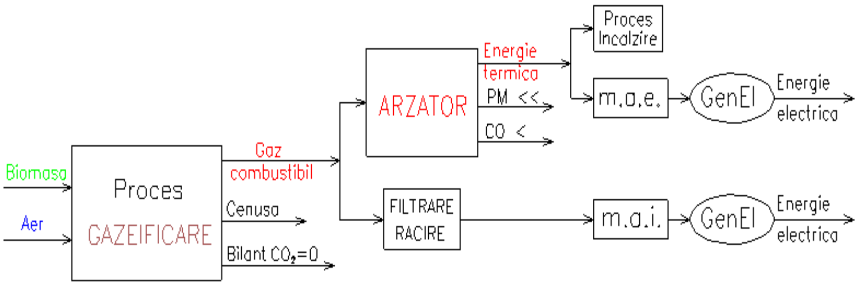

Fig. 1. Block diagram of the energy recovery from biomass via gasification

Given the high degree of automation of the gasification boilers, operation of such devices requires only minimum requirements. The content of the fuel compartment is sufficient for at least 4-10 hours of use on medium power. The boilers are designed for installation in systems with forced or gravitational circulation.
Gasification boilers can burn dry wood mass, wood waste naturally in a variety of forms, from chips to logs with lengths up to 80 cm and the a diameter of up to 30 cm, briquettes or pellets.

3. Energy module with micro-gasification process type TLUD

Functional diagram of a TLUD generator with coupled burner it is shown in Figure 2. The micro gasification process is supplied with air from a variable speed fan. In Figure 3 is represented a functional diagram of a TLUD generator at which the gasgen burner and separated from the gas producer. Gasgen is a combustible gas with low calorific power and for an efficient combustion are used specialized burners, FLOX type [1, 5, 9, 10].
Biomass is introduced into the reactor and rests on a grate through which passes, from the bottom up, the gasification air. Initialization process is made from the free top layer of biomass.
The heat is obtained by burning the hot gasgen resulted in pyrolysis phase; this is mixed with the preheated combustion air introduced into the combustion zone through orifices disposed at the top of the reactor. The mixture with high turbulence flame burns at the upper mouth of the generator with temperatures of 900-1000 ºC. To adjust the thermal capacity required the air flow rate Dag for gasification and Dard for combustion with two flaps, coupled mechanically or by varying fan speed. The TLUD is with a fixed bed biomass process and therefore the generator operates under rechargeable batch.
The gasification process is done with a light intensity with timetables specific consumption of 80 – 150 $kg._{bm}/m^2h$ which leads to reduced specific power for the reactor 250 – 350 kW/m^2. The slow process maintains a superficial velocity of the gasgen produced at very low values $v_{sup} \leq 0,06$ m/s resulting in reduced free ash entrainment and the concentration of $PM_{2.5}$ at output from the burner

of maximum 5 mg/MJ_{bm}; value of at least five times smaller than current rules imposed for thermal generators with solid fuel. [3, 5, 7, 9, 10]
Because it provides a very good mixing of gasgen with burning air at an optimum excess of 1.4 - 1.5, in the flue gases the CO concentration is less than 2%, or 0,8 g/MJ_{bm}; value under the standards required currently. These aspects make TLUD heat generator to be less polluting compared to other systems of the heat generation using solid fuel.

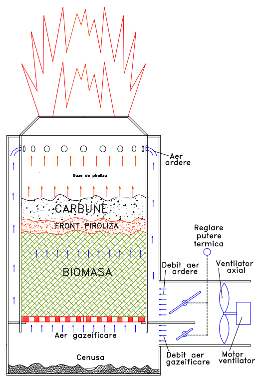

Fig. 2. Functional diagram of the TLUD generator with coupled burner

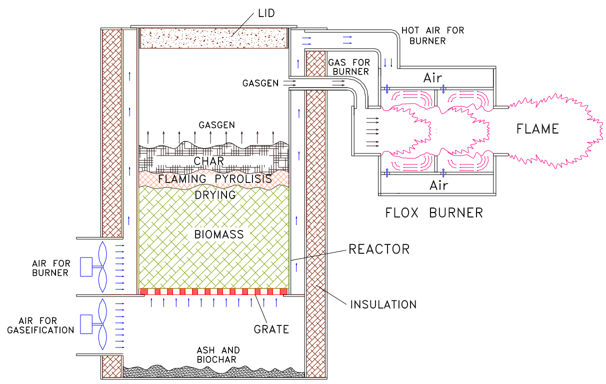

Fig. 3. Functional diagram of the TLUD generator with FLOX burner

This type of heat generator has been developed and used in stoves for preparing food in remote areas, operating very well with a wide variety of local biomass. An outstanding example is the environmental and energy performance is the portable stove produced by PHILIPS, in which the fan is powered by electricity produced by a Heat-generating semiconductor, mounted under the grill, being a typical generator thermal with energy independence.
In Figure 4 is a block diagram of a TLUD energetic module. Energetic inputs into the module are:

- biomass consumption C_{bm};
- air needed for gasification D_{ag} and for combustion D_{ard};
- the size of command u_{Pt} of thermal load.

The outputs from the energetic module are:

- biochar D_{ch} produced from pyrolysis and partly reduced;
- thermal power P_{th} of the flue gas at exit of the burner;
- concentration of C_{CO} in the combustion gases;
- concentration of solid particles PM in the combustion gases.

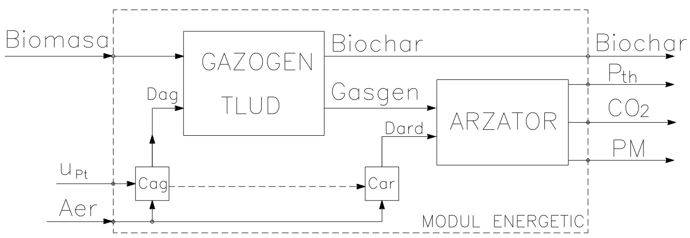

Fig. 4. Block diagram of the energetic module TLUD

In TLUD generator enters biomass gasification and combustion air and electricity. The electric energy consumption is not more than 0.3% of the thermal energy produced, aspect that recommended TLUD thermal generators in heating systems in energetic remote areas.
From the experiments carried out with modules TLUD it has been found that the conversion efficiency of the biomass entirely gasified in gasgen is in the range 92-95%. [1, 2, 4, 6, 8].

To achieve thermal performance and functional requirements imposed by current industrial consumers of thermal energy, to the heat generator TLUD it can be attach an automatic driving device type PLC.
Energy recovery is a topic addressed by most local development strategies, national and global, this is the basis of sustainable development.
The effects of energy recovery consist in:

- lower consumption of wood to heat a space, so lower costs for maintenance,
- resource conservation,
- the natural environment is more stable,
- rescued trees bring satisfaction, wellness and relaxation to people.

In a research project there were attempted to develop alternatives of TLUD gasifiers that aim to recover energy in the chimney (which is required by 150-200º C temperature), thus avoiding condensation and the tar deposit. So the proposed solutions focus on keeping constant the temperature imposed by chimney and the heat energy recovery of this area, that can be reintroduced partial in the combustion process or can be converted into electrical energy (E.g. for charging a battery by means of Peltier modules).

4. TLUD prototype testing

The biomass is introduced into the reactor and rests on a grill through which the primary air for gasification passes from bottom to top. Rapid pyrolysis reaches a point of incandescence at the top and continues down into biomass in the reactor. Rapid pyrolysis results in gas, tar and biochar. Tars pass through the incandescent charcoal layer, are cracked and completely reduced due to the heat radiated by the pyrolysis front and the upper flame. The resulting gas is mixed with the secondary combustion air, preheated by the reactor wall, introduced into the combustion zone through the orifices disposed at the top of the reactor. The mixture with high turbulence burns with flame at temperatures of about 900 ° C. The regulation of the thermal power is done by the variation of the primary and secondary air flows. The design solution shown in Fig. 5 has been filed as Patent No. A / 00286 / 27.04.2015 [12]

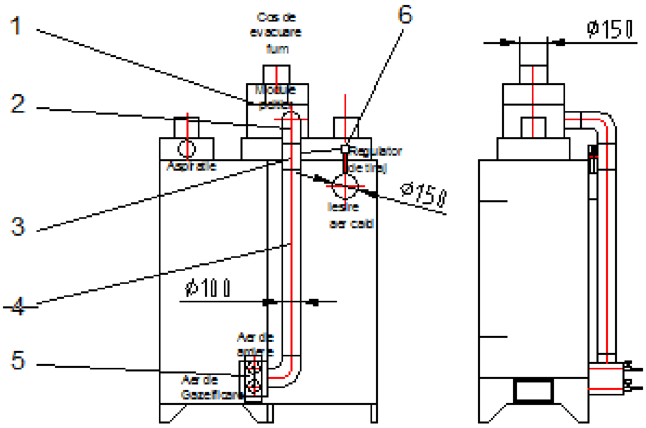

Fig. 5. Design solution of TLUD

In the tests, 15 kilograms of pellets were used as combustion material. The reactor allows the loading of two pellets.
The TLUD warm air prototype (Figure 6) was tested in the low power and maximum power mode. Tests were conducted at INOE 2000 IHP.
Recording the temperature variation at different points of the hot air generator is done with the help of Pt1000 temperature probes. They are connected to a data acquisition board via 4 ... 20 mA amplifiers, the voltage conversion for the analog input of the acquisition board is made with the help of resistors (Figure 9). An application made in LabVIEW is used to display and record the data (fig.10). The application displays numerically and graphically the temperature variation during

burning. When the recording stops, the application allows you to save the temperature values over time in a text file. These data can be processed later.

Fig. 6. The hot air generator prototype on the principle of TLU

The LabVIEW application (figure 7) contains the following function blocks: program loop with the possibility of setting the data acquisition interval, input block from the acquisition plate in which it is made and temperature scaling - output signal, numeric display, graph display, running time counter (seconds, minutes, hours), data entry in text file, graphical deletion (when starting a new sample), and a table display block.

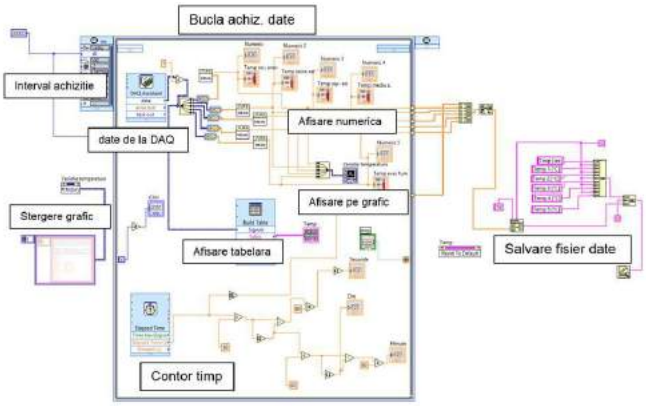

Fig. 7. LabVIEW data schematics acquisition program

4.1. Test 1 – Obtaining Gasification and biochar alternative

The contents of a pellet bag were introduced into the reactor. Initiation of the combustion process was done at the top of the material in the reactor, with commercial fire ignition lighters and from ignition to stabilized gasification entering about 12 minutes according to the data acquisition (Figure 8)

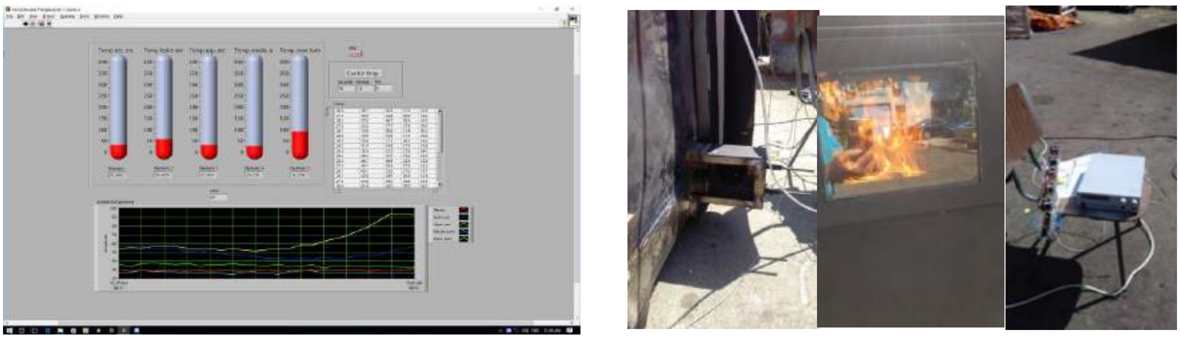

a b c

Fig. 8.

After entering the gasification regime, the flame has moved from the combustion material in the reactor to the burner. The gas produced in the reactor was mixed with the combustion air and a flame similar to the flame from the stove was produced (Fig. 8b). Several adjustments of the gasification and combustion air intake valves (Fig.8.a) have been made and the adjustability of the hot air generator power has been found. By opening them, the flame grows almost instantaneously. Thus, the correct operation of the TLUD type gasification principle (Top-Lit UpDraft) has been demonstrated [12].
As a result of the data acquisition (Fig. 8c) for the entire duration of the operation until the flame is blue and the hot air generator (stopping the fans and opening the supply door) to get the biochar, the graph of Fig. 9.

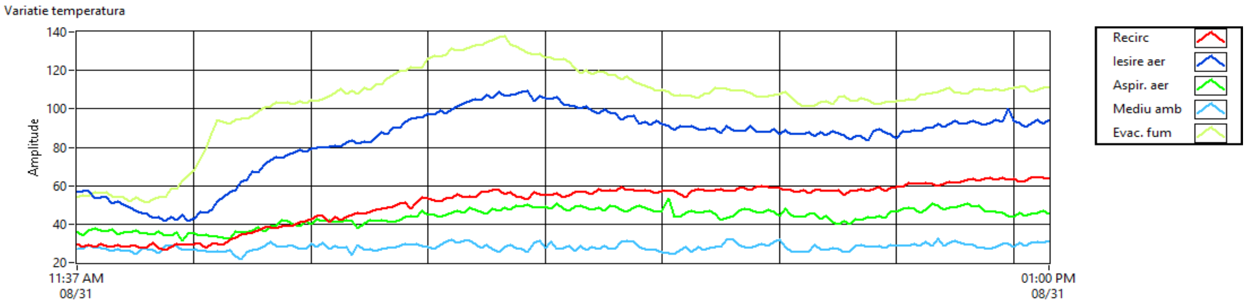

Fig. 9

The burning process lasted 83 minutes for a 15 kg pellet bag under minimal operating conditions and was interrupted when the flame was blue (signaling that the gasification of the matrix was complete and the gasification of the biochar commenced). Thus, approximately ¼ of the biochar (figure 10) was obtained from the volume of the material initially introduced for combustion.

Fig. 10. Biochar obtaining

A good adjustment of power from the hot air generator was achieved by adjusting the combustion air and gasification. The temperature of the heated air at the exit from the generator for the minimum operating condition was stabilized at about 90 ° C and the chimney temperature was about 120 ° C. The air flaps have been adjusted to approximately 1-2 mm opening.
Under these conditions it can be said that the generator cannot work below the test values, so it has a minimum operating power of 3kW

4.2. Test 2 - Gasification without making biochar with gasification of them gasification,.

Into the reactor were introduced the contents of a pellet bag. The initiation of the combustion process was done with commercial briquettes and from the ignition until the stabilized operation entered it took about 12 minutes according to the data acquisition (Figure 11).

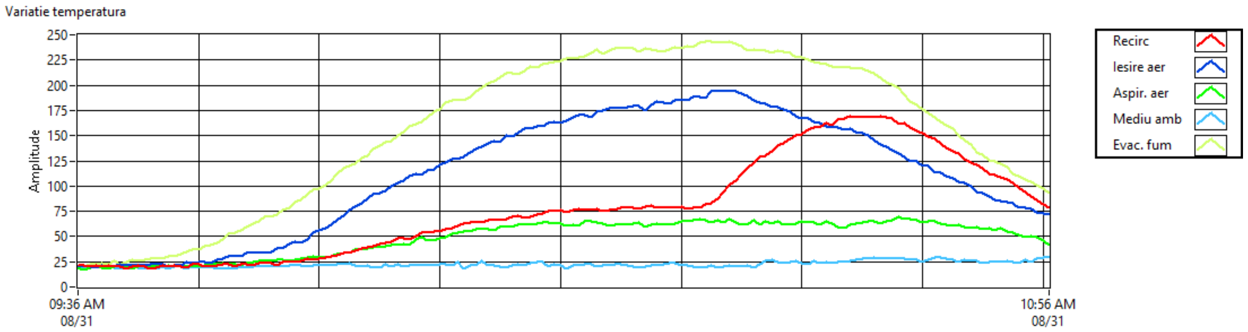

Fig. 11

Under the test conditions at maximum power with air flaps and gasification air open at more than 10 mm, an average heating air temperature of 175 ° C was obtained and the chimney temperature was approximately 230 ° C according to the graph of data acquisition.
In Test 2, the burning process was no longer interrupted to obtain the biochar (when its flame was blue) and thus a longer operating time and a higher energy amount with about ¼ of the reactor shutdown and biochar. The final result of total burning, including the batch, was a very small amount of ash of about 50 g. The generator can work very well in both ways; with the acquisition of biochar or burning it and getting energy. In both cases no emissions of smoke or fumes were found.
When the pyrolytic front reached near the bottom of the reactor and the thickness of the biochar layer decreased in the conditions of maintaining the flow of gasification and the minimum resistance created by the material, the burning process accelerated for a short time (until all combustion material including the biochar), although the burning process declined, the generator still supplied warm air for about 20 minutes due to thermal inertia.

5. Conclusions

The advantages of applying energy recovery solutions and increase efficiency on the gasification boilers are:

- superior recovery of the flue gases heat so their input temperature in the chimney is smaller, about 170...200°C compared to the 250°C of the existing boilers;
- complete combustion of gaszgen that leads to diminishing the specific loss by incomplete combustion;
- reducing the risk of carbon monoxide poisoning;
- the use of wood fuel with a moisture content greater than 20% as primary combustion air has a higher temperature;
- effectively increasing the efficiency of the boiler from 81 ... 86% to 90%;
- wood fuel saving for the same energy produced by other boilers;

The prototype tested responds to project objectives, works under different power regimes, on the TLUD principle and it can enter into an industrial design process, after which it can be manufactured and delivered to the market.
It has been found that the smoke fan is high for operating conditions less than those obtained at test 1, but for maximum power at test 2 it is well-sized. An improvement could be obtained if the electronic control panel it can provided an electronic mount for the variation of the fan speed. Thus, the hot air generator can be shown to operate from a minimum power of 3 kW up to a maximum power of 24 kW by regulating the air inlet and exhaust gas intake flaps.
If it is desired to introduce hot air into the greenhouse at a lower temperature than that provided by the generator, it is possible to adapt a mixture of hot air from the generator with fresh air from the atmosphere until the desired optimal temperature for entering the greenhouse is obtained.
Besides energy recovery of waste, it is also aimed:

- replacing fossil fuels such as fuel oil, fuel gas and coke (conservation / protection of resources);
- reducing the impact of CO_2 emissions on climate (climate protection);
- reducing the dependence of global markets of energy connected with the cost reduction;
- increase the degree of flexibility of waste management by reducing the amount of residual waste.

Arguments in support of biomass use:

- diversifying of energy supply;
- replace conventional fuels with high emissions of CO_2;
- contribute to waste recycling;
- protects and creates jobs in rural areas;
- possibility of adjusting, automation and control of the system depending on the objective requirements or heated building;
- high efficiency system.

Acknowledgements

This paper has been developed in INOE 2000-IHP, as part of a project co-financed by the European Union through the European Regional Development Fund, under Competitiveness Operational Programme 2014-2020, Priority Axis 1: Research, technological development and innovation (RD&I) to support economic competitiveness and business development, Action 1.2.3 – Partnerships for knowledge transfer, project title: *Eco-innovative technologies for recovery of biomass wastes*, project acronym: ECOVALDES, SMIS code: 105693-594, Financial agreement no. 129/23.09.2016.

References

[1]. P. Basu, “Biomass Gasification and Pyrolysis : Practical Design and Theory”, Academic Press, 2010;
[2]. A. Belonio, “Rice husk gas stove handbook”, College of Agriculture, Central Philippine University, 2005;
[3]. A. Belonio, “Dual- reactor rice husk gasifier for 6-ton capacity recirculating-type paddy dryer”, Central Philippine University, Iloilo City, Philippines;
[4]. Knoef H.A.M Editor, “Handbook Biomass Gasification Second Edition”, BTG Biomass Technologies Group, Nederlandes, 2012;
[5]. H. Mukunda, et al., “Gasifier stoves – science, technology and field outreach”, *Current Science*, vol. 98, no. 5, 10 March 2010;
[6]. E. Murad, “Optimisation of biomass gasification load regime”, *International Conference ENERGIE - MEDIU CIEM 2005*, UPB, Bucharest, October. 2005;
[7]. E. Murad, A. Culamet, G. Zamfiroiu, “Biochar-Economically and ecologically efficient technology for carbon fixing”, *Simpozion HERVEX 2011*, 9-11 November, Călimăneşti , ISSN 1454-8003;
[8]. E. Murad, Gh. Achim, C. Rusănescu, “Valorificarea energetică şi ecologică a biomasei tăierilor din livezi”, *Sesiunea de comunicări ştiinţifice – ICEDIMPH-HORTING*, 20 September 2012;
[9]. J. Porteiro, D. Patino, et al, “Experimental analysis of the ignition front propagation of several biomass fuels in fixed-bed combustor”, *Fuel* 89, 2010, pp. 26-35;
[10]. S. Varunkunar, „Packed bed gasification-combustion in biomass domestic stove and combustion systems”, PhD. thesis, Department of Aerospace Engineering Indian Institute of Science, Bangalore, India, Feb. 2012;
[11]. Financial Agreement no. 67/2014 “Utilizarea resurselor energetice regenerabile pentru cresterea independentei energetice a mimiserelor si solariilor”, PN-II-PT-PCCA-2013-4-0221.

ISSN 1454 - 8003
Proceedings of 2017 International Conference on Hydraulics and Pneumatics - HERVEX
November 8-10, Baile Govora, Romania

A NEW AUTOMATED DEVICE FOR TURBINED WATER AERATION

Florentina BUNEA[1], Adrian NEDELCU[2], Corina Alice BĂBUȚANU[3]

[1] National Institute for Research and Development in Electrical Engineering ICPE-CA, florentina.bunea@icpe-ca.ro

[2] adrian.nedelcu@icpe-ca.ro

[3] corina.babutanu@icpe-ca.ro

Abstract: *The paper studies a new system for air injection inside turbines draft tube, with a beneficial effect on the aquatic environment, leading to a maximum transfer of the dissolved oxygen (DO) into the discharged water with a minimum energy consumption. To achieve this goal, it is necessary to obtain an interphase contact area as large as possible, achievable by dispersing the air introduced in the discharged water as fine bubbles. In order to have a lower influence over the hydraulic circuit, and to affect as little as possible the turbine efficiency, the studied device is noninvasive. Preliminary experiments were developed using a small scale laboratory set-up regarding to solutions for water aeration in dispersed gas-liquid, turbulent and with an adverse pressure gradient flows. Finally, it is developed an automatic control system of aeration device so that it operates with a minimum energy consumption and also reaching the level of dissolved oxygen required by the user. The device will only work when there is a deficiency of oxygen in the water and will permanently ensure compliance with the water quality norms related to the dissolved oxygen content of the water in the downstream rivers of the hydro power plants (HPP).*

Keywords*: Environmental friendly turbines, turbine aeration, water quality, dissolved oxygen, automatic control system*

1. Introduction

On the international level the main energy suppliers and hydroelectric equipment manufacturers in Europe (Voith, General Electric, Andritz) and SUA (Tennessee Valley Authority) have responded to environmental concerns regarding HPP operation since 1950 and has initiated research aimed at reducing their environmental impact. Several methods for the modernization of hydraulic turbines have been implemented in this respect. The efficiency of these aeration methods from air-water oxygen transfer point of view is analyzed and compared in the literature [1], [2], highlighting the main aeration parameters: turbine geometry, air quantity, the type and place of the air intake. Although in some studies of turbine aeration systems carried out at different hydro power plants, the results were not in line with expectations, research continues because of the significant importance of aeration on ecosystems. As a consequence of these issues, HPP operators are trying to optimize the ratio of water quality improvement measures and energy efficiency.
Regarding the level of DO in hydro power plants (HPP) downstream the rivers, there are intense concerns of hydraulic turbine manufacturers and HPP users. Reduced DO content in rivers is a pollution factor, which may in some cases reach up to 0-2 mg / l DO, provided that the minimum level required for aquatic life is about 5 mgDO / l. This value varies depending on temperature / climate, pressure, organic substances, flora and fauna, which leads to the need for individual case studies.
In the United States of America (especially on the Tennessee, Saluda and Provo rivers - where real environmental disasters have been encountered), the turbines have been upgraded to respond the needs of the environment and the authorities (Water Resource Agencies) have developed [2] strategies and control systems to improve turbine performance in terms of environmental impact. During the summer months, at Deer Creek Reservoir, the DO in the discharged water from the plant was up to 0 ÷ 2 mg / l; this low oxygen value affects the fish over a distance of 3 ÷ 5 km. The criteria established by the US Environmental Protection Agency in 2006 that water has to satisfy are: minimum 3 mg / l for fish survival, an average of 6.5 mg / l for 30 days

to protect the fish reproduction/development and at least 4 mg/l for cold water-sensitive invertebrates.

In Bakun, Malaysia, [3], 88% of the reservoirs contained zero DO in water deeper than 4 m (Fig. 1), and river water quality is affected up to 3-5 km in downstream of hydro power plants. In order not to affect the environment, the development of an aeration system is essential in such an area.

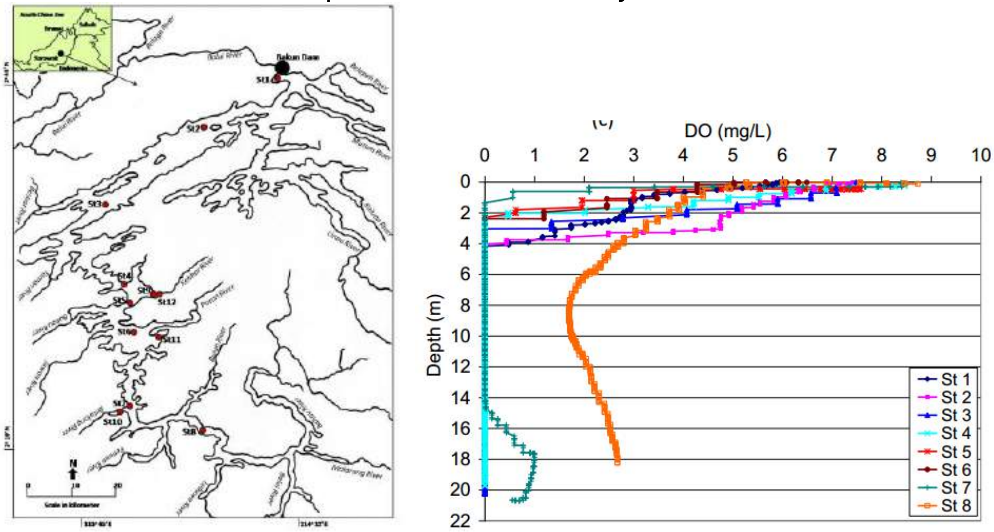

Fig. 1. Reservoirs in Bakun – Malaysia [3]

The results of water quality monitoring in Danshuei River, China [4] indicate a high concentration of phosphorus and nitrogen and reduced DO in water.

Generally, to increase the DO level by 1 mg/l, an air volume equal to 1% of the volume of flowing water is required [5]. On the other hand, in order not to affect sensitively the hydraulic performance, the air flow rate must not exceed 3% of the flow rate of the turbined water (relation 1). Current turbine water aeration methods affect the performance of hydropower on the one hand due to flow disturbance through introduction of air and on the other hand due to the energy consumption required for injection of air (e.g. a compressor station).

$$Q_{air} < (1 \div 3\%)\ Q_{water} \tag{1}$$

This is a sensitive issue for manufacturers and users of hydraulic turbines, since injecting an extra amount of air into the turbine circuit can reduce the efficiency of the turbine; therefore, air injection (mode and place of introduction, quantity, etc.) becomes important for the balance between turbine efficiency and environmental factor.

The efficiency of aeration in HPP is usually expressed by the void fraction

$$\phi = \frac{Q_{air}}{Q_{water}}, \tag{2}$$

where Q_{air} is air flow rate, respectively Q_{water} is the water flow rate. Thus, in order to increase the effect of aeration, other parameters should also be considered: air-water interface area, pressure gradient, air retention time in the water, the DO gradient upstream and downstream turbine, distribution of gas bubble size in water, and, as the case may be, the standard aeration efficiency will be calculated.

2. Laboratory study of rotational biphasic flows with adverse pressure gradient

The test bench on which the testing of rotational biphasic flows with adverse pressure gradient was conducted [6] aims at studying and testing the small-scale aeration devices, on the basis of which will be designed the aerators that can be mounted in hydraulic turbines. Emphasis is on the quality of the aeration process, respectively on the increase of the air-water interphase area, the retention time, the pressure drop on the aeration devices, their geometry and their dimensioning, etc.

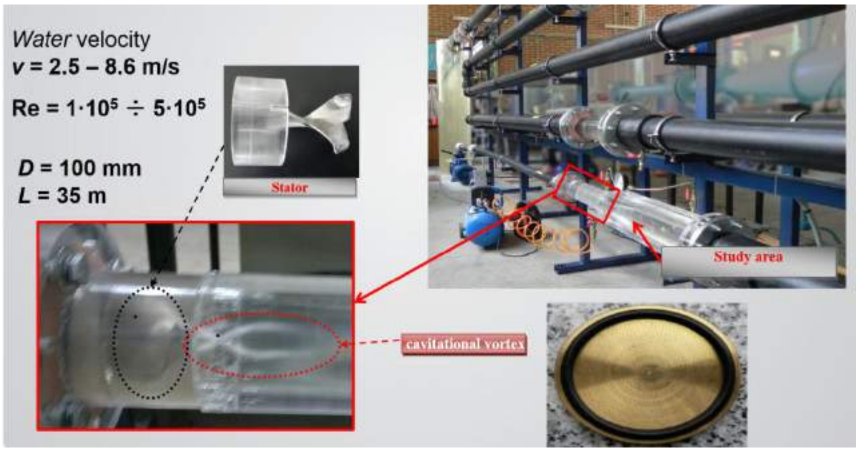

Fig. 2. Test bench for study of rotational biphasic flow with adverse pressure gradient

The test bench (Fig. 2) is made in a close loop and consists of a supply tank, from which, by means of a pump, clean water is introduced into a pipe line. The test bench is designed to simulate flow parameters in hydraulic turbines for the entire operating range of the turbine. To simulate rotational flow, the stand is provided with a transparent area, conical to the inside and parallelipipedic to the outside, made of transparent material, consisting of a stator and a divergent area. In the study area Reynolds numbers between Re = 1 10^5 ÷ 5 10^5 are covered. The study area also includes a dispersed air injection device located downstream of the stator.
The test bench is dimensioned to ensure the minimum contact time in which a particle travels from the inlet to the outlet draft tube of a Francis hydraulic turbine (at least 10 s) and an average water velocity of 3 m/s.

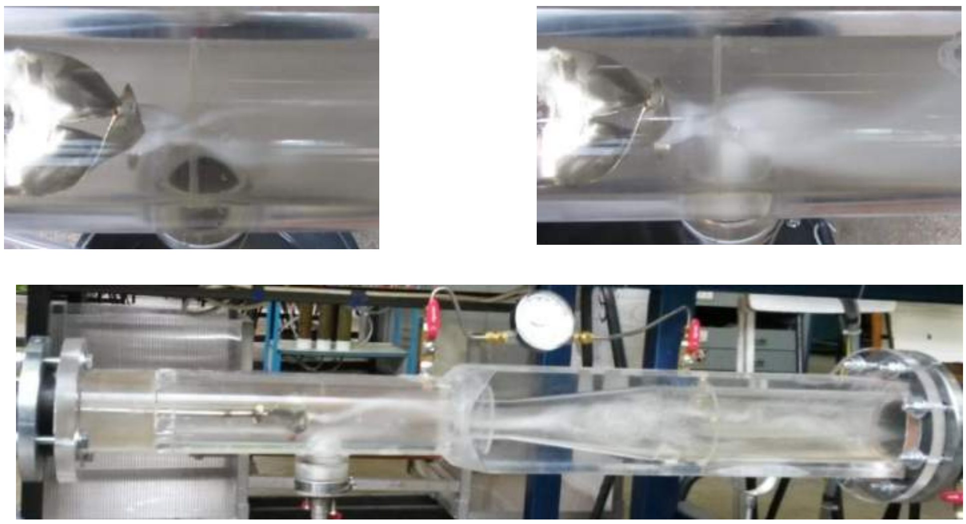

Fig. 3. Visualization area of rotational biphasic flow

With the increase of the water flow rate, the rotation impressed by the stator forms a cavitational vortex (Fig. 3). By introducing dispersed air into the study area, it is possible to study the water disperse aeration in rotational turbulent flows. Injection of the air will be controlled in accordance with the DO deficiency in the water through a non-invasive aeration device located on the pipe wall so as not to influence the flow in the hydraulic circuit. The test bench allows the study reliably of complex phenomena such as turbulent gas-liquid dispersed flows with adverse pressure gradient,

where the mass transfer through the interface is a dynamic process associated with the interface dynamics and the interface area varies along the flow [7].
The test bench is equipped with a dispersing aeration device, with interchangeable plates, through which air bubbles of different sizes is injected. Thus, four perforated metal plates with orifices of 0.1mm (MP01), 0.2mm (MP02), 0.3mm (MP04) and 0.5mm (MP05) were tested under the following conditions:

- For each perforated plate, the air flow rate injected into the circuit (Q_{air} = 5, 8, 10, 12 l/min) was varied, and the water flow (Q_{water} = 1110 l / min) was kept constant
- for each perforated plate, the air flow rate injected into the circuit (Q_{air} = 5 l / min) was kept constant, and the water flow rate (Q_{water} = 330, 882, 1044, 1110 l / min) was varied.

Table 1 [8] shows the ratio between the injected air flow rate and the flow rate of water flowing through the laboratory setup, so that the relationship (1) is respected and the aeration process covers as much as possible the oxygen deficiency in the water.

Table 1: Void fraction (%) for tested MPs

Q_{water} (lpm)	MP 01				MP 02				MP 03				MP 05				Obs.
	Q_{air} (lpm)				Q_{air} (lpm)				Q_{air} (lpm)				Q_{air} (lpm)				
	5	8	10	12	5	8	10	12	5	8	10	12	5	8	10	12	
330	1.51				1.51				1.51				1.51				Non cavitational vortex
882	0.57				0.57				0.57				0.57				Incipient cavitational vortex
1044	0.48				0.48				0.48				0.48				Developed cavitational vortex
1110	0.45	0.7	0.9	1.1	0.45	0.72	0.9	1.1	0.45	0.72	0.9	1.1	0.45	0.72	0.9	1.1	Developed cavitational vortex

The entire procedure for determining standard air efficiency is described extensively in [8].

Table 2: SAE variation depending on air and water flow

Q_{water} (l/min)	MP 01				MP 05			
	Q_{air} (l/min)				Q_{air} (l/min)			
	5	8	10	12	5	8,5	10	12
330	377				408			
882	992				1017			
1044	1117				1018			
1110	1112	1797	2176	2759	1083	1826	1899	2041

Table 2 shows the standard aeration efficiency (SAE) for 0.1, respectively 0.5 mm orifices plates resulting from aeration tests.
For a better understanding of the behavior of the injected air controlled in a site hydraulic turbine, flow visualizations from the inside of the turbine were performed, in the air injection area, through the proposed demonstration model. Although the demonstration model for turbulent water aeration is not shown in this paper (existing a patent application for it), fig. 4 shows two photographic captures within the suction cone when the turbine was running at a relatively high flow rate of 57.1% and a 1% voids fraction. For this, an borescope camera with a 90° x 8 mm x 440 mm (67°) HOPKINS lens and a "Techno LED Nova 150" light source, 100 - 240 VAC, 50/60 H.

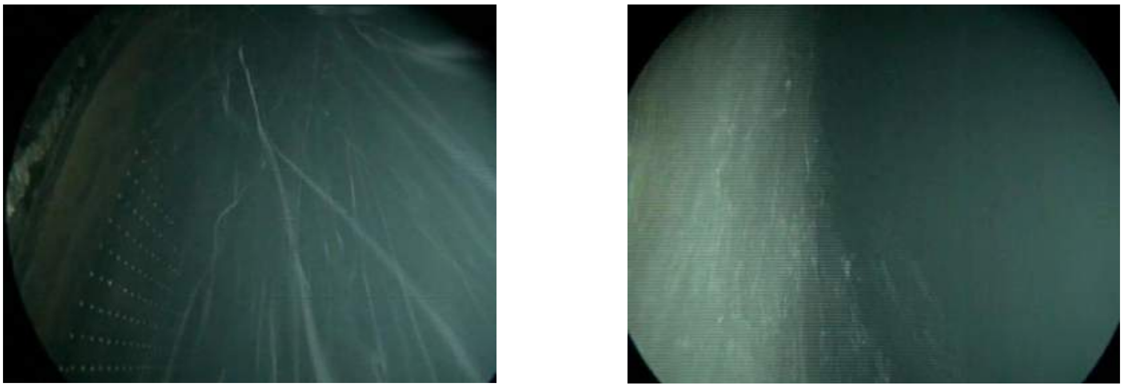

Fig. 4. Photographic captures in the injection area from a hydraulic turbine

$$f_{injection} = \frac{n}{3} \quad (3)$$

These visualizations allowed validation of the air distribution injected inside the flow section. The injected air does not remain in the boundary layer of the wall but is distributed about one-third (out of) the draft tube section. The frequency with which air is injected in the presence of the rope vortex depends on the turbine rotational speed after the relationship (3).
Details about aeration process influence over the operation of a small hydro turbine - generator unit, are presented in [9]. The paper presents the frequency analysis of vibration signals recorded during a turbine-generator unit in operation, while different air flow rates are injected downstream the runner. From the dynamic behavior point of view, this paper show that the controlled injecting air into water downstream the runner has no negative influence over the operation of the unit.

4. Integration of the aeration device into an automated water aeration system

The automation of the aeration system discussed in this paper is required to control the air fraction injected into the hydraulic circuit, depending on dissolved oxygen in the water and the turbine operating regime. Air injection control also reduces shocks
A LabView program it was developed to help to integrate the aeration device into an automated water aeration system, by simulating the device in different operation modes. In situ measurements' results were used in simulation.
The aeration device will only work when the dissolved oxygen measured in turbined water is lower then the limit set by operator ($OD_m \geq OD_i$) to comply with river water quality regulations.
Figure 5 shows the conceptual block diagram of the automated aeration system for turbined water.
The algorithm for automatic adjustment of the oxygenation process is based on the pressure level in the draft tube cone. The algorithm follow the steps described below

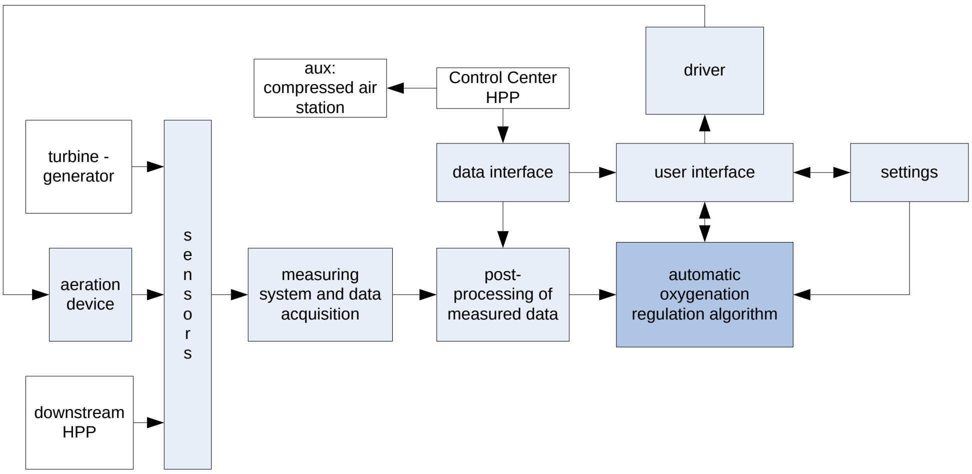

Fig. 5. Conceptual block diagram of the automated aeration system

- Air velocity at inlet after the realtion (4):

$$v = \sqrt{\frac{|dp| \cdot 2g}{\rho_{air}} \cdot \frac{|dp|}{dp}}, \text{ with } dp = p_{atm} - p_{asp} \tag{4}$$

- Computes Q_{air} for different varying degrees of opening of the inlet valve, as follows

$Q_{air\ min} = Q_{water}\ \phi_{min}$
$Q_{air\ max} = Q_{water}\ \phi_{max}$
$Q_{air\ h\phi} = Q_{water}\ h_{\phi}$

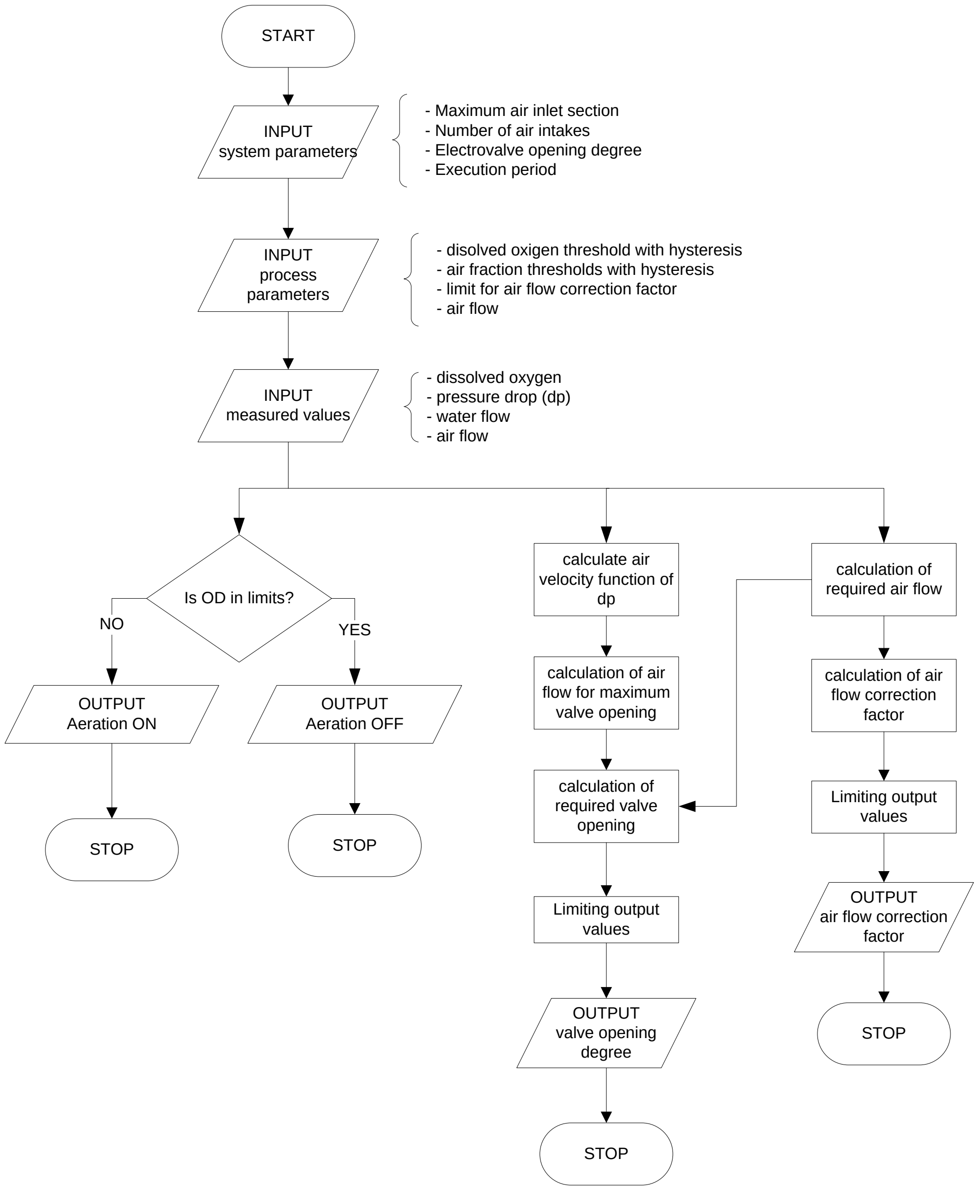

Fig. 6. Logic scheme of the algorithm for automation of the oxygenation process

The logic scheme of the automatic regulation of the aeration process is shown in Fig. 6.
Input variables:

- OD_m [mg/l] – Dissolved oxygen measured from the downstream turbine water
- p_{asp} [bar] – Relative pressure measured on the wall of the turbine CON ASPIRATOR
- Q_{water} [m^3/h] – Turbinated water flow rate

- Q_{air} [m^3/h] – Measured injected air flow rate

Output variables:

- *S* [ur] – opening degree of the air inlet valve
- Q_{air_fcor} – air flow rate correction factor

Parameters:

- OD_i [mg/l] – Dissolved oxygen level required downstream of HPP
- $\pm h_{OD}$ [mg/l] – hysteresis value for OD_i threshold to start/stop the aeration device
- $\phi = \frac{Q_{air}}{Q_{water}}$ [%] – the minimum / maximum permitted air fraction to be introduced into the hydraulic circuit
- h_ϕ [%] – hysteresis value for minimum and maximum air fraction thresholds to start/stop the aeration device
- Φ correction factor – limiting factor of the air intlet valve opening

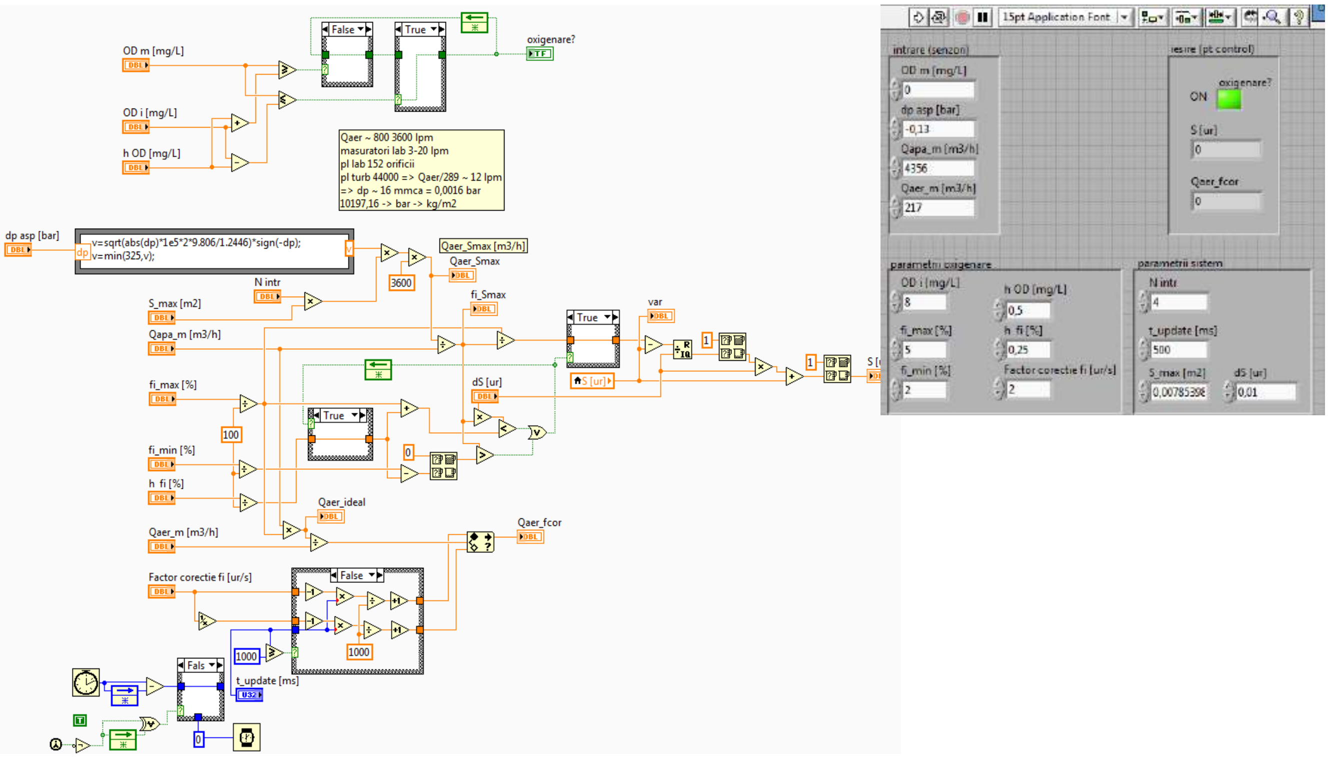

Fig. 7. LabView implementation of the automatic aeration algorithm

In order to verify the stability of the algorithm, a test program was developed in which the input variables are automatically generated. This helps to check the limits imposed on the output variables. Figure 8 shows the pressure difference variation ($dp = p_{asp} - p_{atm}$) as well as the response of the algorithm: the valve opening degree (S) and the air flow rate correction factor (Q_{water_fcor}).

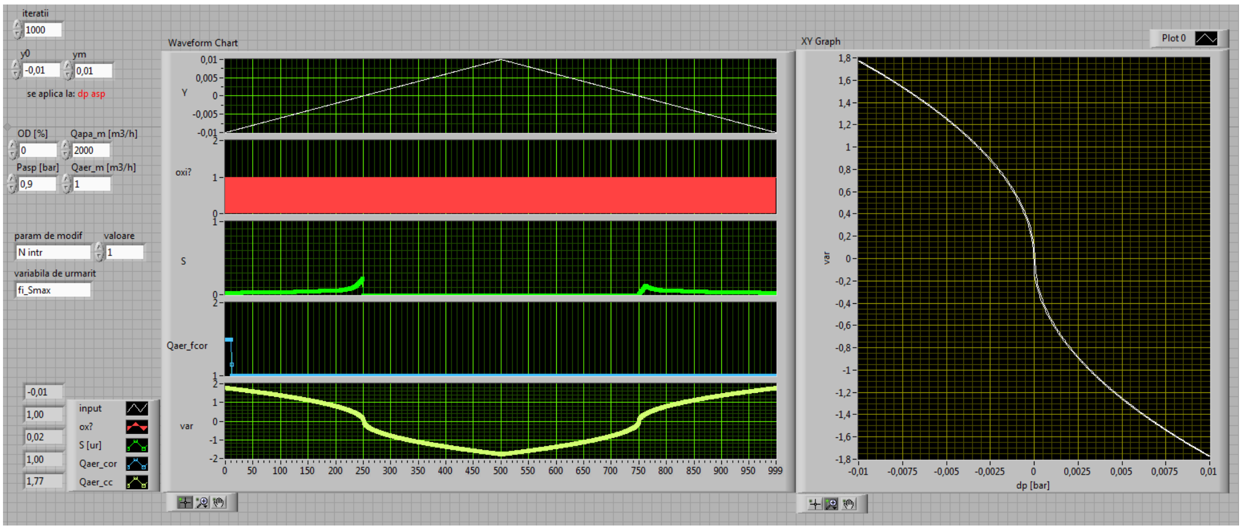

Fig. 8. Stability check of the algorithm

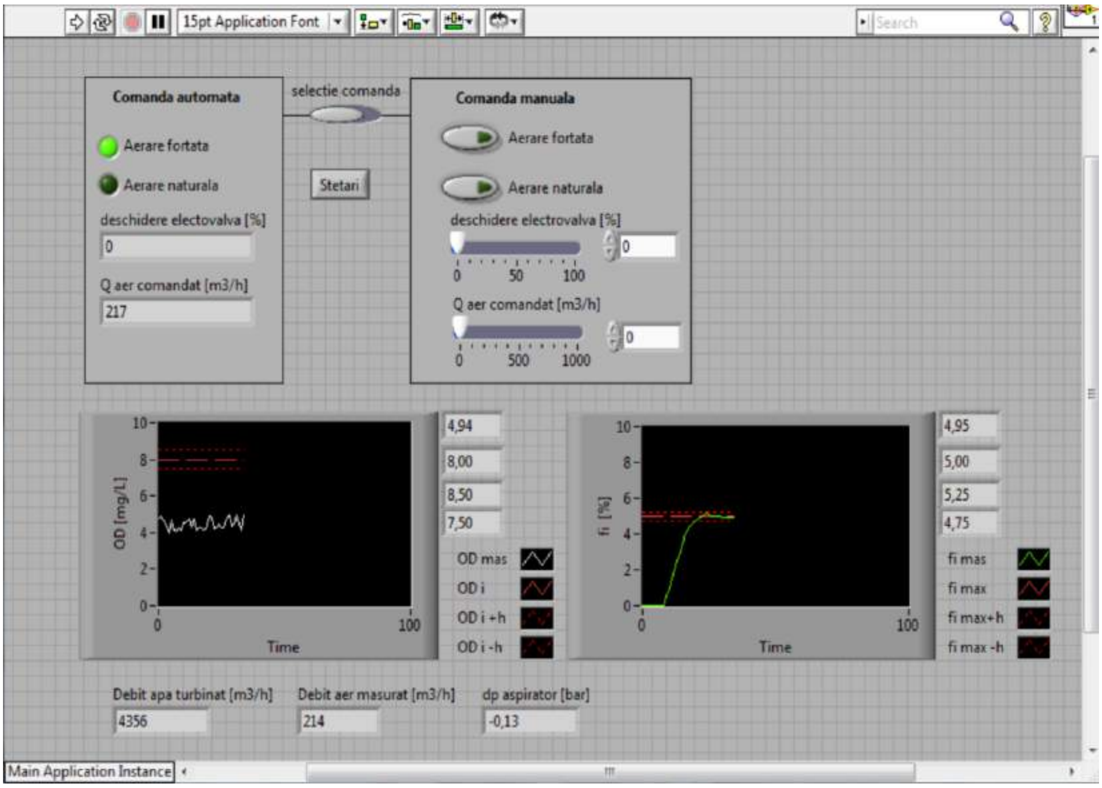

Fig. 9. Graphical user interface of the automated aeration system

Figure 9 shows the graphical user interface of the automated water aeration system, which allows the operator to monitor the automatic aeration process (shown in Fig. 6), configuration of the parameters, the connection with the data communication interface and manual override of the aeration process.

5. Conclusions

Because, at the moment, there is no water aeration solution easy to implement, without damaging the energy performance and efficient from the aeration point of view, makes it difficult to comply with current legislation if the HPP water is poor in dissolved oxygen. This can lead to real ecological disasters.

In this paper is study a disperse nonintrusive aeration solution in turbulent flows corresponding with hydraulic turbines flow. Models of air injection devices are tested at reduced scale, and different void fraction ($\phi \leq$ 1-3%) are injected into the hydraulic system. For this it was developed a test bench for study of rotational biphasic flow with adverse pressure gradient where the flow parameters are in according with flow parameter from the draft tube turbine: water mean velocity, air-water contact time, rotational flow with cavitational vortex, adverse pressure gradient.
After laboratory study of the aeration devices behavior, a real scale aeration equipment is implemented and tested in situ on a Francis turbine, currently being patented and protected by copyright. Finally, an automated system for controlling the aeration device is developed, in order to operate with minimum energy consumption and to reach the level of dissolved oxygen imposed by the user. The aeration equipment works only when, in turbined water there is an oxygen deficiency, to ensure constant compliance with water quality standards, relating to the dissolved oxygen content of river water downstream of hydropower plants.
We appreciate that hydraulic turbines fitted with the proposed equipment will become *environmental friendly turbines* because it can be proven that the turbined water through them will consistently meet the ecological quality requirements

Acknowledgments

The work has been funded by the Executive Agency for Higher Education, Research, Development and Innovation (UEFISCDI), PN-II-PT-PCCA-2013-4 program, ctr. no. 88/2014, ECOTURB project.

References

[1] Rohland K., Foust J., Lewis G. & Sigmon J., 2010, *Aeration Turbines for Duke Energy's New Bridgewater Powerhouse*, Hydro-Review, pp. 58-63, ISSN 0884-0385;
[2] Papillon B., Sabourin M., Couston M., Deschenes C., *Methods for air admission in hydroturbines*, Proc.of the XXIst IAHR Symp. on Hydraulic Machinery and Systems, Lausanne, sept. 9-12, 2002;
[3] Lee N., Yee L.T., Grinang J., *Physico-chemical characteristics în the filling phase of Bakun Hydroelectric Reservoir, Sarawak, Malaysia,* „International Journal of Applied Science and Technology", University of Malaysia Sarawak ,Vol. 2 No. 6, pp. 92-101, June 2012;
[4] Liu W.C., Liu S.Y., Hsu M.S., Kuo A.Y*., Water quality modeling to determine minimum în stream flow for fish survival in tidal rivers*, „Journal of Environmental Management", 52, pp. 55–66, 2005;
[5] March P.A., Brice, T.A., Mobley, M.H, Cybularz, J.M., *Turbines for solving the DO dilemma*, „Hydro Review", 11(1), U.S., 30-36, 1992, ISSN 0884-0385;
[6] Bunea F., Ciocan G.D*., Stand pentru studiul curgerilor bifazice, rotaționale, cu gradient advers de presiune*, Patent application registration, OSIM no. A/00704/29.09.2015;
[7] Bunea F., Ciocan G.D., Nedelcu A., Bucur D.M., Dunca G., Chihaia R., *Experimental setup for the study of new aeration devices in hydraulic turbines*, Environmental Engineering and Management Journal, May 2017, Vol.16, No. 5, pp.1033-1040, ISSN:1582-9596;
[8] Bunea F., Nedelcu A, Ciocan G.D., "Prediction of water aeration efficiency in high turbulent flow", Desalination and Water Treatment, 2017, no. 85, 55-62, DOI: 10.5004/dwt.2017.20774;
[9] Bucur D.M., Dunca G., Bunea F., Călinoiu C., Aeration process influence over the operation of a small hydro turbine - generator unit, 10th International Symposium On Advanced Topics In Electrical Engineering (ATEE), 23-25 March 2017, Bucharest, Publisher: IEEE, DOI: 10.1109/ATEE.2017.7905045

ISSN 1454 - 8003
Proceedings of 2017 International Conference on Hydraulics and Pneumatics - HERVEX
November 8-10, Băile Govora, Romania

HIGH EFFICIENCY ELECTRIC MOTOR

Mihail POPESCU[1], Constantin DUMITRU[1]

[1]National Institute for R&D in Electrical Engineering ICPE-CA Bucharest, office@icpe-ca.ro

Abstract: *Electric motors are a significant consumer of electricity, so over time they have been improved. From the point of view of energy consumption, the main parameter of an electric motor is the efficiency. This paper describes an electric motor that combines two electric machines, a transformer and an electric motor, in order to improve the efficiency.*

Keywords: *Electric machine, high efficiency, permanent magnet, reduced loss*

1. Introduction

Since the start of the industrial revolution, global energy consumption has been steadily increasing, thus encouraging and accelerating the growth of the human standard of living. One of the indicators of a nation's economic development is the per capita energy consumption index. For example, the United States, which accounts for about 5% of the global population, consumes about 25% of the world's energy.
At global level, the largest amount of energy is consumed by electrical machines (about 80% of the whole electricity that is used) used in the production, transport and distribution of electricity, the operation of industrial and household equipment and so on.

2. Existing legislation in the field of increasing the electric machines efficiency

With the reduction of the fossil fuels reserves and the increasing demand for electricity, an action to improve the efficiency of electromechanical conversion processes has been initiated. This approach led to a gap in European standardization (CEI and CENELEC) compared to the national standardization of some states (Canada and USA).
The comparison between the two approaches regarding the increasing of the electric motors efficiency is shown below:

USA-Canada	**European Union**
Written e - PACT laws Minimum efficiency for 2, 4 and 6 poles and 60 Hz motors is provided in the power range of 1-200 HP (0.75-150 kW):	Voluntary obligations developed by CEMEP for 2 and 4 poles and 50 Hz motors with short-circuit rotor in range 1.1-90 kW: - classification of yields (Eff3, Eff2, Eff1); - big discounts on the market for Eff3 engines.
The efficiency should be selected from the NEMA MG1 rough steps values.	There is no degradation of the exact value for efficiency.
The yield is an average value of a number of engines of the same construction. It is permissible that the output of a single engine to be down to 2 steps in the table.	Tolerances allowed after CEI 60034-1 - 15% loss on motors < 50 kW; - 10% loss on motors > 50 kW.
IEEE 112B Measurement Process with Modified Execution Conditions.	Verification by individual measurement according to IEC 60034-2 by the loss separation method.
Efficiency is proven through accredited measurement laboratories.	The proof based on the manufacturer's declaration is the Eff 1 ÷ 3 label.

Regarding the recommendations of CEI and CENELEC, the Technical Committee 2/CEI has developed the standard 60034-30-1: "Maşini electrice rotative. Partea 30-1: Clase de randament pentru motoarele asincrone trifazate cu rotor în scurtcircuit, cu o singură turaţie (Cod IE)".

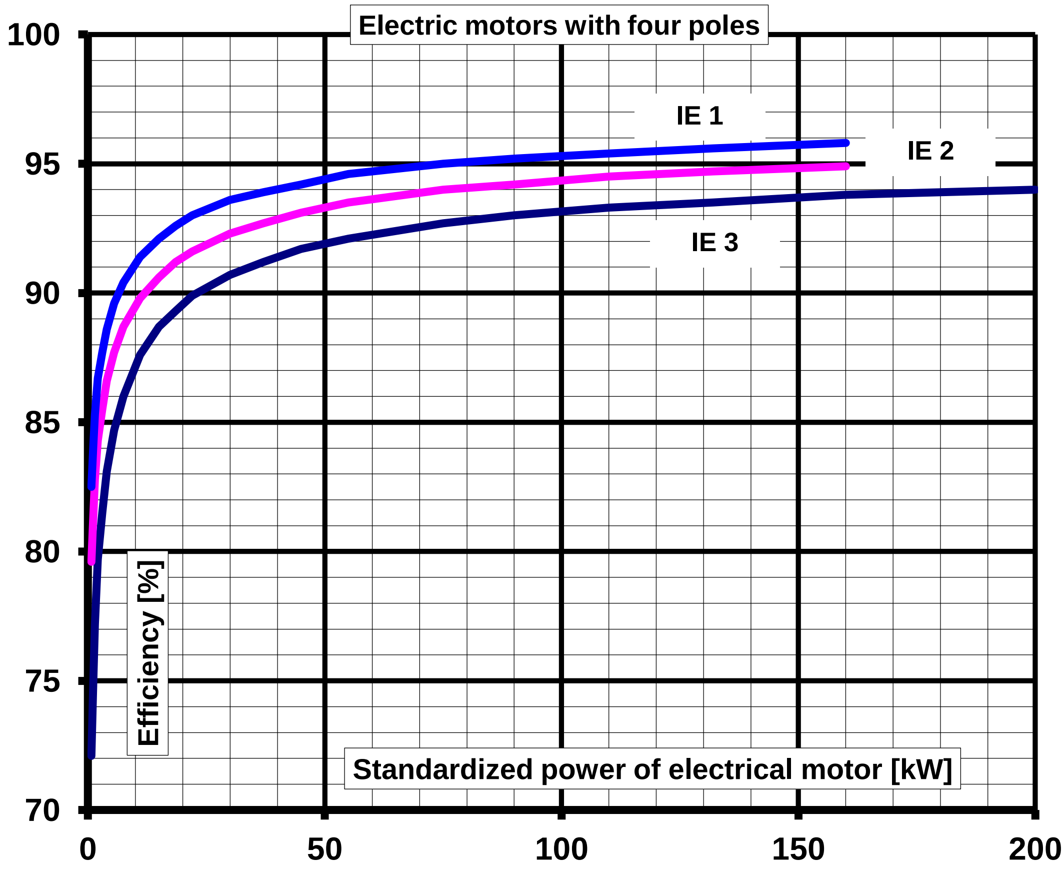

Fig. 1. The variation of the efficiency of electric motors according to efficiency classes IE1, IE2, IE3

3. Operating regimes of electric machines

An electrical machine can operate in several types of operating regimes:

a) In **motor regime**, the electrical machine absorbs power from the grid at the stator winding terminals and supplies mechanical power to the shaft. This mode of operation is the most used, the balance of power being shown in the figure below:

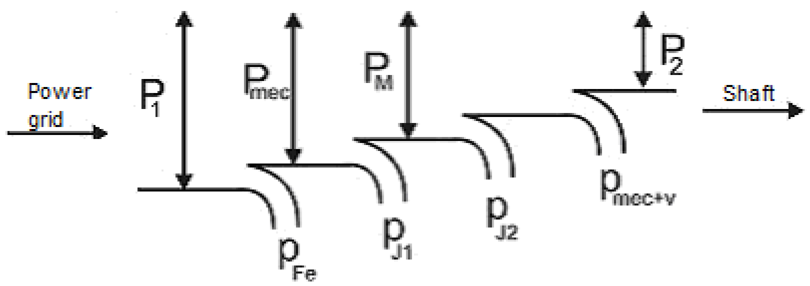

Fig. 2. The balance of power of an electric motor

where:
P_1 - the electrical power absorbed by the stator winding;

P_M – electromagnetic power (transferred to the rotor by electromagnetic field);
P_{mec} – mechanical power;
P_2 – power to the shaft;
p_{J1} – Joule effect losses from stator winding;
p_{Fe} – losses in the ferromagnetic core;
p_{J2} – Joule effect losses from rotor winding;
p_{mecv} – mechanical and ventilation losses.

b) Operation in the generator regime.
If the electric machine is driven by an auxiliary motor at a speed ***n*** and the magnetic circuit is driven by a magnetic field whose value can be changed by changing the value of the electric current through the inductor winding, than the operating regime changes. So, that electrical machine works in the generator regime.
In this operation regime, the machine receives mechanical power on the shaft (from auxiliary motor) and delivers electrical power to the stator winding terminals. The power balance is shown in the figure below:

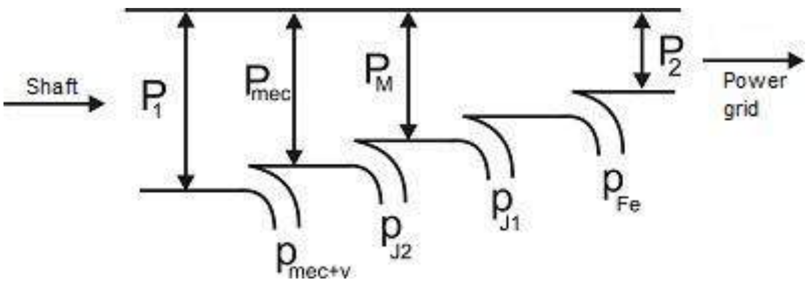

Fig. 3. The balance of power of an electric generator

c) Brake operation regime
In this case, an electromagnetic brake is applied and the machine is trained externally in the opposite direction to the stator field (W<0, s>1). The machine receives mechanical power on the shaft, electrical power on the stator winding terminals and, after the losses are covered, the entire output power is dissipated on the rotor.

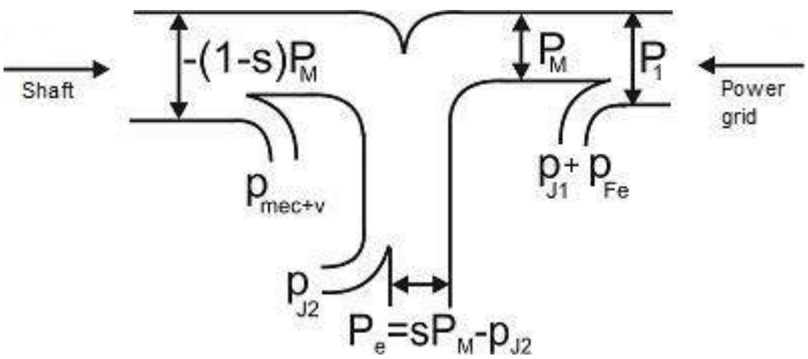

Fig. 4. The balance of power in brake operation regime

4. Solutions to reduce the losses in electric machines

Until now, a series of technical solutions have been developed to reduce the losses of the electric machines. Among them, the followings are presented:

- Use of copper in the asynchronous motors rotor winding; this solution leads to a decrease in the electrical resistance value in the rotor circuit and implicitly of the associated Joule effect losses;
- Insertion of permanent magnets into the rotor magnetic circuit, thus ensuring the magnetization of electric machines;

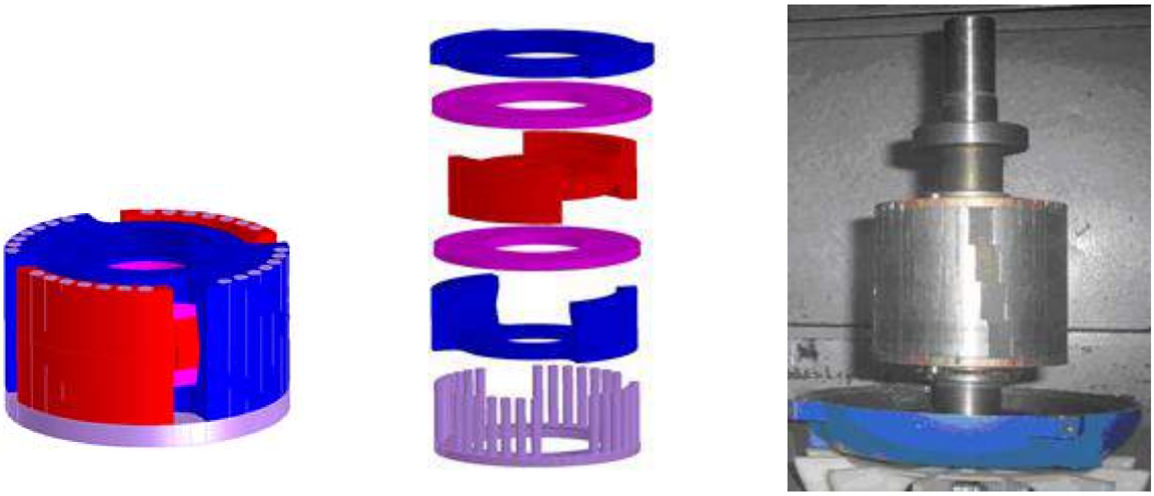

(a) (b) (c)

Fig. 5. Inductor construction details
Two assembled modules (a), expanded view (b) and physical construction (c)

The motor with permanent magnets has a squirrel cage that provides self-starting, combining the advantages of the synchronous motor, related to the absence of the main Joule effect losses in the rotor, with the self-starting advantages of asynchronous motor with the rotor winding in short-circuit. In this way, exploitation and production losses can be reduced.
Since is no longer necessary to provide reactive magnetizing current of the magnetic circuit, the presence of permanent magnets presents advantages over normal asynchronous motors. The load factor and Joule losses decrease.
- The use of special windings in the stator's electrical circuit adapted to the demands of the electric motors and made by combinations between the coils of each phase and multiple star / delta connections.

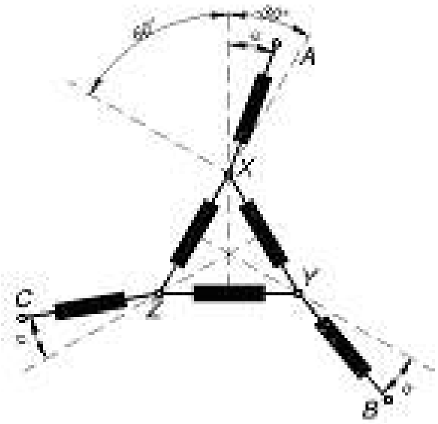

Fig. 6. Combination star-delta winding. Defining the spatial relative position

Combined star – triangle windings had long been used to reduce triangular start - up current for step - wise start - up of asynchronous motors, especially fast 2 - pole motors, which drive large inertial loads.

For achieving this winding, it is assumed that in the notches uniformly distributed at the periphery of the electrical machine armature, two distinct winding systems are located - one connected in a triangle and the other connected in a star. It is also considered that the phases of the star are connected in series with the triangle. Otherwise, there are extreme demands in the electric machine.

Transient torque (Δ) [Nm]

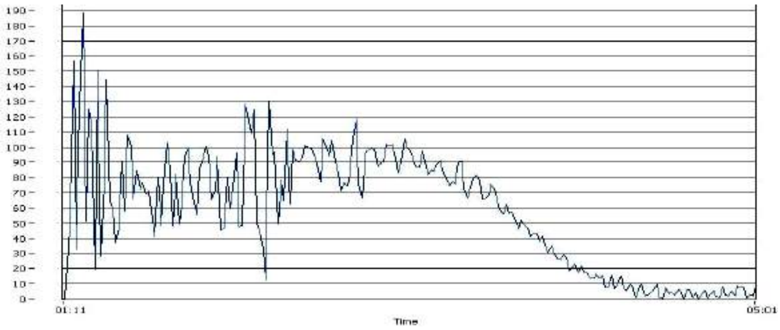

Transient torque (Δy) [Nm]

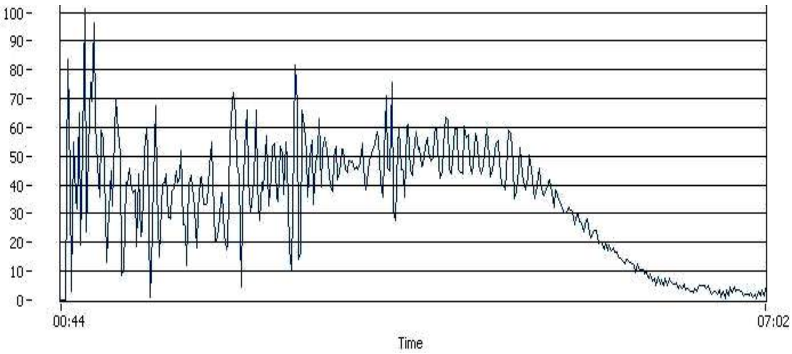

Transient torque (Y) [Nm]

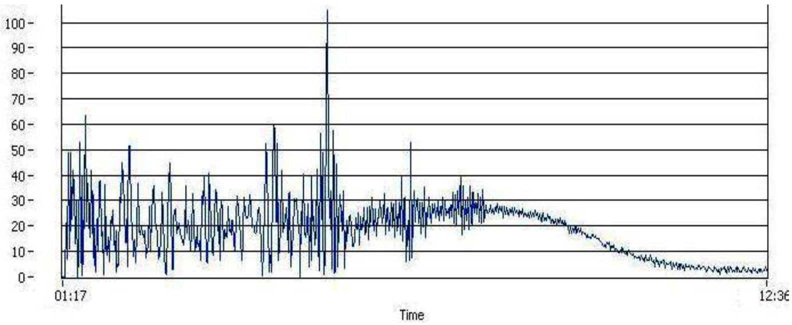

Fig. 7. Transient start-up regime for three combinations

For a 4 kW - 1500 rpm electrical motor provided with such windings, by using these 6 connection, were obtained in load function 4 / 3.25 / 2.5 / 2 / 1.75 / 1.35 kW.

5. The proposed solution for transverse geometry

A group of researchers from INCDIE ICPE - CA proposed and achieved within a research contract (NUCLEU no. PN 16110102/2016 contract) a new transverse geometry of the electrical machine.
The technical solution has several advantages, as follows:
- the active materials used in its construction are those currently marketed and used in the manufacture of electric transformers;

- the ferro-silicon sheet has smaller thicknesses of 0.1 ... 0.3 mm than the one used in the current electric machines, namely 0.5 mm;
- due to the reduced sheet thickness, the hysteresis losses and eddy currents are lower;
- the sheets used have oriented crystals and presents a higher value for magnetic saturation, namely 1.85...2T, compared to the classic values of 1.6 to 1.8T.

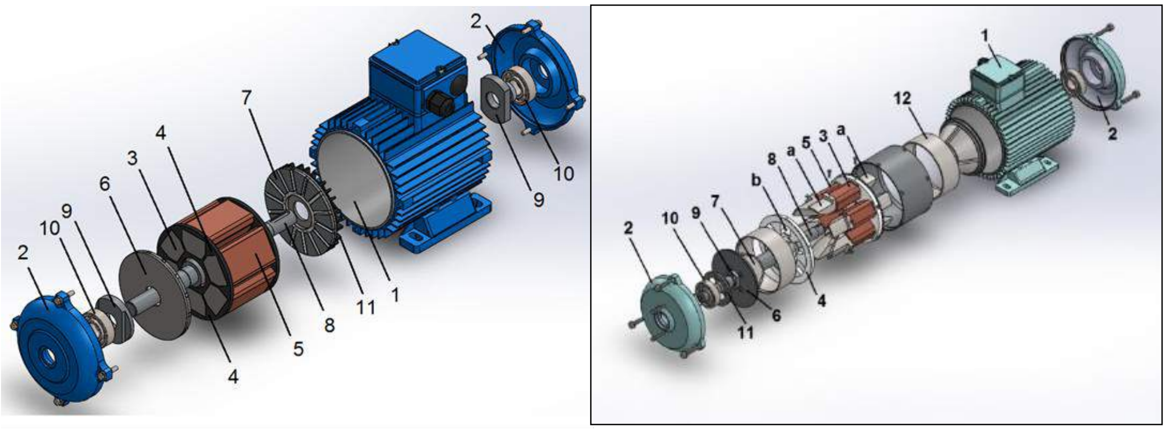

Fig. 8. The exploded machine assembly with modified transverse geometry with axially and conically air gap

The magnetic circuits have the form of columns while the stator windings are in the form of cylindrical coils along the columns. This solution has also the advantage of removing the front ends of the coils; as it is known, they do not contribute to the creation of mechanical torque in the shaft in the case of motors, and respectively to the increase of the supply voltage in the generator operation regime. At the same time, for winding operations, the winding is not inserted into the slots, so a significant number of device, tools and verifiers are eliminated, and the execution time is reduced.

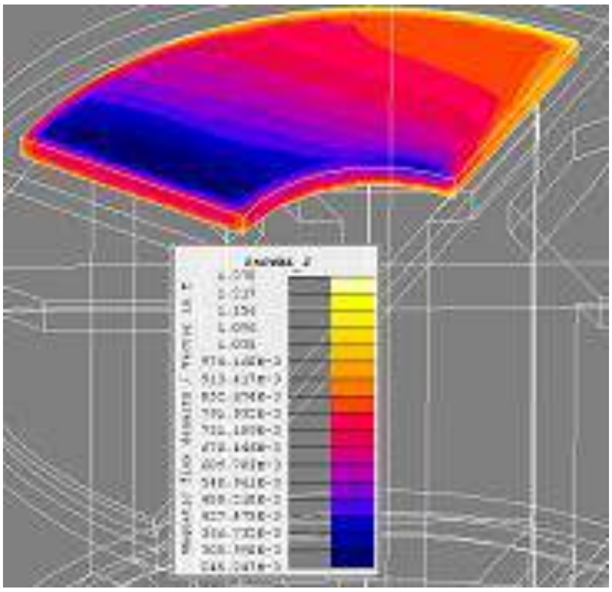

Fig. 9. Map of magnetic induction distribution inside the motor with axial air gap

Fig. 10. Electric motor with axial air gap

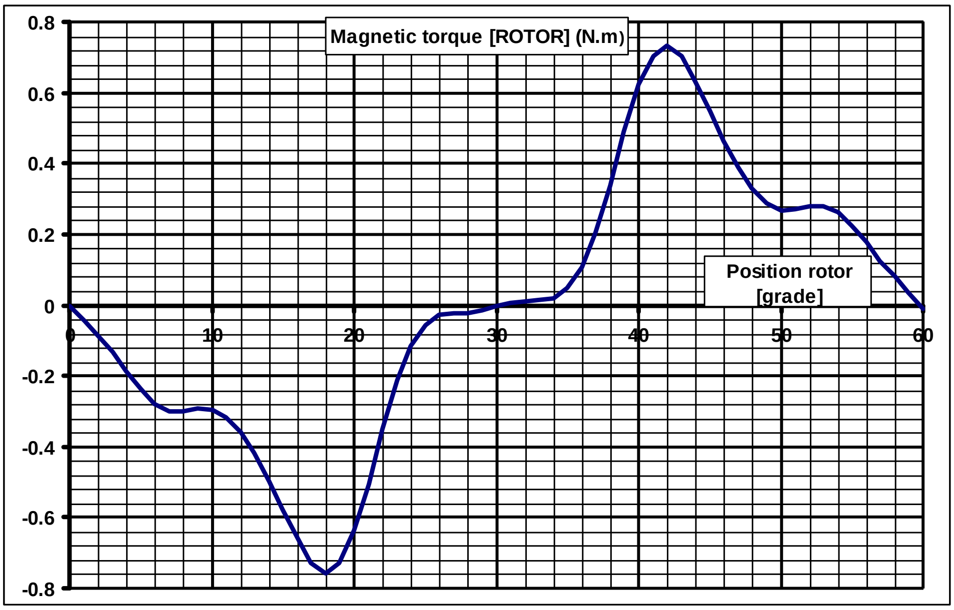

Fig. 11. Mechanical torque generated by permanent magnets at the shaft of axial drive machine with axial air gap

The magnetic rotor circuit, achieved of two subassemblies, is made of a number of magnets and possibly magnetic flux concentric pieces.

6. Conclusions

Over time, increasing electric motor performance has been an important concern for mankind. Different technical solutions have been applied, which generally refer to the increase of the consumptions of the active materials, respectively to the decrease of the electro - magnetic loads.
By comparing the solutions applied so far to the one promoted by INCDIE ICPE-CA, it was found that the value of the efficiency can be increased in the conditions of using existing active materials.
Taking into account the proposed transverse geometry and the advantages stated above, it results that higher-performance electric machines can be obtained. Eliminating the losses in the electric machine leads to obtaining a return in a higher class.

References

[1] "Geometrie transversala utilizata pentru masini electrice cu intrefier axial", A/01020/ 19.12.2016;
[2] "Maşina electrica cu magneţi permanenţi şi întrefier conic", A/00887- 30.10.2017;
[3] http://www.novatorque.com;
[4] T. Tudorache, I. Melcescu, V. Bostan, G. Colț, M. Popescu, M. Predescu, "Electromagnetic analysis of a hybrid permanent magnet generator", Revue Roumaine des Sciences Techniques, Editura Academiei Române.

ISSN 1454 - 8003
Proceedings of 2017 International Conference on Hydraulics and Pneumatics - HERVEX
November 8-10, Băile Govora, Romania

OPEN SCIENCE IN CLOUD TECHNOLOGY

Alexandru MARIN[1], Laura BOANȚĂ[2]

[1] University POLITEHNICA of Bucharest, alexandru.marin@upb.ro

[2] University POLITEHNICA of Bucharest, laura.boanta@upb.ro

Abstract: *The OSTEC project proposes an open IT environment for the scientific community to store and reuse data and scientific results. At European level, the Cloud Initiative is an important step in the evolution of "big data" exploitation by researchers. OSTEC project proposes the implementation of open access technology and scientific services, making possible to displace, exchange and reuse their data without discontinuities at global scale, for interdisciplinary research approaches.*

Using ICI's cloud infrastructure, the project proposes to create a research data warehouse in our country and an associated cloud platform for storage, exchange, management, use and re-use of data. UPB will develop a management model for cloud platform data and services, for project development and sustainability with a governance proposal outlining and overseeing the future development of the cloud platform and interconnection at EOSC, based on its social and economic impact, demonstrated by INCE's contribution. The project will exemplify a demonstration pilot, conducted by ICPE-CA and INCDMTM, by using a pre-defined service portfolio, offered to the scientific community. In this way, the institutional capacity of the consortium of the OSTEC project will be increased and concretized through the development of a training and education strategy, as part of a process of long life learning mechanism of RDI staff from public or private organizations.

Finally, we follow the development of standards and an incentive framework to address both the OSTEC consortium organizations and other stakeholders, destined to develop the capabilities necessary to operationalize an open science platform in cloud technology in Romania and its interconnection with EOSC.

Keywords*: Open Science, Cloud Technology, “Big Data” Mining, FAIR Services, Open Access*

1. Introduction

On 12 June 2017, the European Commission organised the EOSC Summit, Europe’s moment of commitment to the European Open Science Cloud (EOSC) [1]. The Summit was a success in many respects. The Summit brought together, from all over Europe, 110 players that are key for the implementation of the EOSC. Participation was highly representative, including scientific fields, national scientific infrastructures, research funders and ministries of Member States and Associated Countries.
At the Summit, 110 key participants reviewed five key areas of EOSC implementation, based on specific input papers:
1. data culture, data stewardship: practical and policy tools;
2. adoption and implementation of FAIR data principles [2];
3. research data infrastructures and services;
4. sustainable funding & governance;
5. high-performance computing, big data and super connectivity.

The Summit provided strong support for the implementation of the EOSC and marked a step change in the initiative. There was strong agreement on data culture, on the need for FAIR data and on the need to develop and gear supporting infrastructure of services; there were agreements and no fundamental objections on the much-debated issues of services, governance and financing. The intents of the input papers were broadly shared and further specified. This all supported the need to act immediately and swiftly in the next few months to keep the momentum achieved by the 'coalition of doers'. Participants demonstrated a strong sense of commitment towards the implementation of the EOSC. They agreed that the EOSC is a truly common European project

which will ensure long term sustainability and support Europe to become a key player in research data.
The EOSC Summit also marked a clear division of labour between research policy makers and funders (Member States and the EC), and implementing stakeholders such as national infrastructures, projects and initiatives. Both scientific stakeholders and Member States must be engaged in the making of the EOSC via dedicated channels.
Based directly on the results of the Summit, DG Research and Innovation drafted the EOSC Declaration. Straight after the Summit, all session Chairs and Rapporteurs worked hard to draw conclusions from the event. They revisited the input papers to factor in the commitments and introduced several clarifications. The Declaration is composed of 33 high level statements meant to capture our common understanding on the required Data culture & FAIR data, Research data services & architecture, Governance and funding to make the EOSC a reality by 2020.

2. EOSC Declaration

RECOGNISING the challenges of data driven research in pursuing excellent science;
GRANTING that the vision of European Open Science is that of a research data commons, widely inclusive of all disciplines and Member States, sustainable in the long-term;
CONFIRMING that the implementation of the EOSC is a process, not a project, by its nature iterative and based on constant learning and mutual alignment;
UPHOLDING that the EOSC Summit marked the beginning and not the end of this process, one based on continuous engagement with scientific stakeholders, the European Commission;
PROPOSES that all EOSC stakeholders consider sharing the following intents and will actively support their implementation in the respective capacities:

2.1 Data culture and FAIR data

[Data culture] European science must be grounded in a common culture of data stewardship, so that research data is recognised as a significant output of research and is appropriately curated throughout and after the period conducting the research. Only a considerable cultural change will enable long-term reuse for science and for innovation of data created by research activities: no disciplines, institutions or countries must be left behind.

[Open access by-default] All researchers in Europe must enjoy access to an open-by-default, efficient and cross-disciplinary research data environment supported by FAIR data principles. Open access must be the default setting for all results of publicly funded research in Europe, allowing for proportionate limitations only in duly justified cases of personal data protection, confidentiality, IPR concerns, national security or similar (e.g. 'as open as possible and as closed as necessary').
[Skills] The necessary skills and education in research data management, data stewardship and data science should be provided throughout the EU as part of higher education, the training system and on-the-job best practice in the industry. University associations, research organisations, research libraries and other educational brokers play an important role but they need substantial support from the European Commission and the Member States.
[Data stewardship] Researchers need the support of adequately trained data stewards. The European Commission and Member States should invest in the education of data stewards via career programmes delivered by universities, research institutions and other trans-European agents.
[Rewards and incentives] Rewarding research data sharing is essential. Researchers who make research data open and FAIR for reuse and/or reuse and reproduce data should be rewarded, both in their career assessment and in the evaluation of projects (initial funding, review of performance and impact). This should go hand in hand with other career policies in universities and research institutions (appointments, promotions etc.).

[FAIR principles] Implementation of the FAIR principles must be pragmatic and technology neutral, encompassing all four dimensions: findability, accessibility, interoperability and reusability. FAIR principles are neither standards nor practices. The disciplinary sectors must develop their specific notions of FAIR data in a coordinated fashion and determine the desired level of FAIR-ness. FAIR principles should apply not only to research data but also to data related algorithms, tools, workflows, protocols, services and other kinds of digital research objects.
[Standards] The EOSC must be underpinned by minimal and rigorous global standards for open research data, as well as standards for EOSC based services for collaboration through the EOSC (e.g. to facilitate inter-disciplinarity and avoid fragmentation). These standards (technical, semantic, legal and organisational) must combine long-term sustainability with optimal freedom of local implementation. They should be jointly defined by the research communities, taking into account existing instruments (e.g. EU Rolling Plan on ICT Standardisation). Cross-disciplinary agreements/protocols will lead to specific standards, inspired directly by relevant domain specific needs. Variations across scientific disciplines and their specific efforts of making research data open and FAIR should be respected.
[FAIR Data governance] The design and implementation of FAIR principles must be built upon inclusive stakeholder participation (e.g. researchers from different scientific disciplines, EU Member States and the European Commission). Policy will go hand in hand with the implementation of technical and human resources, and a social infrastructure including education and training. To make FAIR data a reality, it is imperative to engage stakeholders and relevant multipliers, based on a solid stakeholder engagement strategy, on inter-institutional arrangements, well-established frameworks and decision making flows. Data governance needs to be agreed upon and the division of responsibilities be charted, ensuring transparency, representativity and accountability. European and national scientific research organisations, publishers and other actors must align their data-related business processes, responsibilities and expectations to achieve commonly agreed goals.
[Implementation & transition to FAIR] Implementation of FAIR principles requires careful prioritisation and orchestration. The FAIR Data Action Plan 2018-2020 is an important collaborative instrument for the embedding of FAIR principles in the first phase of the EOSC.
The plan will not necessarily suggest any specific technology, standard or implementation solution. For an even transition of data from different levels of maturity to FAIR, existing activities to make data FAIR (e.g. GO-FAIR) must be complemented by new initiatives that embed FAIR principles in all the phases of data life cycle.
[Research data repositories] Trusted research data repositories play a fundamental role in modern science. Scientist must be able to find, re-use, deposit and share data via trusted data repositories that implement FAIR data principles and that ensure long-term sustainability of research data across all disciplines. Data repositories must be easy to find and identify, and provide to users full transparency about their services.
[Accreditation/certification] Scientists must be assured that the European and national scientific research infrastructures where they deposit/ access data conform to clear rules and criteria (e.g. certified) and that their data is FAIR compliant. An accreditation or certification mechanism must be set in place based on agreed processes and an accreditation or certification body must maintain an up-to-date and accessible catalogue of certified repositories. Experience from existing accreditation processes must be taken into account.
[Data Management Plans] A key element of good data management is a Data Management Plan (DMP); the use of DMPs should become obligatory in all research projects generating or collecting publicly funded research data, based on online tools conforming to common methodologies. Funder and institutional requirements must be aligned and minimum conditions for DMPs must be defined. Researchers' host institutions have a responsibility to oversee and complete the DMPs and hand them over to data repositories.

[Technical implementation] While FAIR data must be implemented as part of good data governance at this highest possible level (e.g. certification, institutional implementation and support, as describe above), researchers also need handy tools to make data FAIR.
These include:
[Citation system] A data citation system should be put in place to reward the provision of excellent open data. This will assist both the assessment of researchers and their projects, and help implementing the findability, accessibility, interoperability and reusability of research data.
[Common catalogues] There must be catalogues (e.g. for datasets, services, standards) based on machine readable metadata and identifiable by means of a common and persistent identification mechanism that will make research data findable via an 'EOSC Portal'.
[Semantic layer] Research data must be both syntactically and semantically understandable, allowing meaningful data exchange and reuse among scientific disciplines and countries.
[FAIR tools and services] Easy access must be available to a common set of FAIR tools and services, to guide the curation of FAIR data for re-use and to assess FAIR compliance.
[Data expert organisations] The Research Data Alliance, CODATA, DDI Alliance and other organisations active in the research communities must be used as forums to reach consensus on practical implementation of FAIR data principles at European and global level.
[Legal aspects] It is essential for the success of EOSC to clarify and address the legal uncertainty of Open Access to research data, as well as the correct legal implementation of the FAIR principles. Legal barriers to access and reusability of research data must be identified and overcome and the underpinning legal framework must be made simpler and more coherent.
Conversely, issues of ownership must be addressed, particularly where institutions have created services and resources. All these measures should allow easier integration of research data across different legal frameworks, policy implementation plans and strategies.

2.2 Research data services and architecture

[EOSC architecture] The EOSC will be developed as a data infrastructure commons serving the needs of scientists. It should provide both common functions and localised services delegated to community level. Indeed, the EOSC will federate existing resources across national data centres, European e-infrastructures and research infrastructures; service provision will be based on localto-central subsidiarity (e.g. national and disciplinary nodes connected to nodes of pan-European level); it will top-up mature capacity through the acquisition of resources at pan-European level by EOSC operators, to serve a wider number of researchers in Europe. Users should contribute to define the main common functionalities needed by their own community. A continuous dialogue to build trust and agreements among funders, users and service providers is necessary for sustainability.
[Implementation] Resources, components and initiatives of pan-European relevance will be federated on the basis of objective criteria, agreed by stakeholder-driven governance, such as organisational readiness and technical capacity to deliver EOSC main functionalities: provision of core common services, certification activities, joint-procurement initiatives, definition of minimum quality standards of service (based on clear Service Level Agreements SLAs), identity provisioning and management, common cataloguing data and computing/analytic services and tools.
[Legacy] The EOSC should incentivise the re-use of existing building blocks, state-of-the-art services and solutions delivered by past and ongoing projects, local, national and European, as opposed to subsidizing actions aiming at reinventing the wheel. It should facilitate learning from the past, adopting best practices, tailoring scientific community needs through live use cases and leveraging the network effect.
[User needs] Users should see the EOSC as a one-stop-shop to find, access, and use research data and services from multiple disciplines and platforms. Services and functionalities shall be user driven and determined by clear use cases. Intermediary users and other brokers of end-users' demand – IT departments, umbrella associations, community networks – should assist data scientists and ICT specialists in the identification of key requirements for EOSC services.

[Service provision] Research Data Infrastructures, e-infrastructures and commercial operators will develop and provide services based on user needs, and discontinue provision when not justified by the level of adoption. Services will be offered at highest Technology Readiness Levels (TRLs) and kept future-proof based on a cutting-edge cloud based environment. In order to avoid lock-in by individual service providers, the EOSC should foster fair competition of public, PPP and private providers on clear value propositions of highly professional services.
[Service deployment] The EOSC shall support different deployment models (e.g. Infrastructure as a Service, Platform as a Service, Software as a Service), to meet the needs of communities at different levels of maturity in the provision and use of research data service. The EOSC shall support the whole research lifecycle by strong development at platform level that facilitate the provision of a wide set of software, infrastructure, protocols, methods, incentives, training, services. Software sustainability should be treated on an equal footing as data stewardship.
[Thematic areas] The EOSC shall promote the co-ordination and progressive federation of open data infrastructures developed in specific thematic areas (e.g. health, environment, food, marine, social sciences, transport). The EOSC will implement a common reference scheme to ensure FAIR data uptake and compliance by national and European data providers in all disciplines.
[Research infrastructures] The role of ESFRI [3] and EIROFORUM research infrastructures and organisations in the EOSC will be enhanced, Member States and the European Commission made significant investment; research infrastructures should be 'the steward of the community of standards' and provide scientists with a ramp-up for the utilisation of the EOSC.
[EU-added value and coordination] The EOSC must implement policy hand in hand with technology. Condition of national and European measures is required to link the initiative to national strategies, to maximise the added value of inter-disciplinarity by making data FAIR, and to preventing duplication of efforts and investments. Over time, coordination will provide
European added value by minimizing overlap and reducing fragmentation of infrastructures and services, helping long-term sustainability.
[High Performance Computing and the EOSC] European commitment to HPC is clearly demonstrated by the signature of the EuroHPC Declaration by eight Member States since March 23, 2017. The Member States agreed to work together and with the European Commission in the context of a multi-government agreement called EuroHPC for acquiring and deploying by 2022/2023 a pan-European integrated exascale supercomputing infrastructure that will support data-intensive advanced applications and services. It is a response to the surging demand from scientists, industry and the public sector for access to leading-edge computing capacity to cope with vast amounts of data produced in almost all scientific and engineering domains. This supercomputing and data infrastructure could support the European Open Science Cloud by providing data access and advanced computing and data management services. The EC plans to propose, by end of 2017, a legal instrument that provides a procurement framework for the exascale supercomputing and data infrastructure.
[Innovation] The EOSC should create a level playing field for businesses and innovative SMEs to develop, and co-develop with publicly funded institutions, added-value services for researchers. Funding should support the migration of cutting-edge solutions to the EOSC, increasing European added value by fostering innovation.

2.3 Governance and funding

[Governance model] A long-term, sustainable research infrastructure in Europe requires a strong and flexible governance model based on trust and increasing mutuality. As interdisciplinarity is one of the main objectives of the EOSC, the governance model should be based on representativity, proportionality, accountability, inclusiveness and transparency.
[Governance framework] The EOSC governance framework will be co-designed, stakeholder driven and composed of three main layers: 1) institutional, including EU Member States and

European Commission 2) operational, including a governance board and relevant working committees (e.g. thematic and functional) and 3) advisory, including a stakeholder forum.
[Governance board] A governance board will coordinate the efforts of stakeholders endorsing the EOSC Declaration, with the broad mandate to reach practical agreements for the implementation of an EOSC Roadmap by 2020. The board will have an advisory role and an implementing role of the decisions by Member States and European Commission concerning the programming, financing and towards the setting up of a long-term governance and business model for the EOSC. It will make best use of the outcomes of past and current projects (e.g. EOSCpilot, eInfraCentral and EOSChub) and independent expert advice and studies.
[Coordination structure] A coordination structure, funded by Horizon 2020, will help the governance board to manage the implementation, according to agreed rules and methods of stakeholder participation. The structure and its participating entities should be accountable for the responsibilities assumed, based on an objective assessment of their level of readiness in delivering the EOSC main functionalities.
[Long-term sustainability] The European Commission, Member States and Research Funders will use existing and future resources strategically, to ensure long-term sustainability of open research data and research infrastructures, facilitating inter-disciplinarity.
[Funding] Over time, a co-funding mechanism mixing different revenue streams for the EOSC will be set up, to increase the accountability of the governance, building trust, sharing resources and building long-term capacity for European research data. Early implementation of the EOSC will pilot innovative business models and support an integrated data and service platform for European research.
[Global aspects] The EOSC will be European and open to the world, reaching out over time to relevant global research partners. It will increase the global value of open research data and support stakeholder engagement, including researchers and citizens. It will gradually widen the initiative to federated network of infrastructures and nodes from global research partners. The EOSC Stakeholder Forum will have an important role in this sense.

3. EOSC Declaration Action List

3.1 Data culture

European science must be grounded in a common culture of data stewardship, so that research data is recognised as a significant output of research and is appropriately curated throughout and after the period conducting the research. Only a considerable cultural change will enable long-term reuse for science and for innovation of data created by research activities: no disciplines, institutions or countries must be left behind.
OpenAIRE [4] offered to help to involve research libraries for policy alignment and for a user-driven approach that also reach the 'long tail of research'.

3.2 Skills

The necessary skills and education in research data management, data stewardship and data science should be provided throughout the EU as part of higher education, the training system and on-the-job best practice in the industry. University associations, research organisations, research libraries and other educational brokers play an important role but they need substantial support from the European Commission and the Member States.
The League of European Research Universities (LERU) offered to raise awareness and help develop training activities for staff and doctoral students.
CESSDA [5] offered to help coordinate and organise trainings across ERICs.

3.3 FAIR Data governance

The design and implementation of FAIR principles must be built upon inclusive stakeholder

participation (e.g. researchers from different scientific disciplines, EU Member States and the European Commission). Policy will go hand in hand with the implementation of technical and human resources, and a social infrastructure including education and training. To make FAIR data a reality, it is imperative to engage stakeholders and relevant multipliers, based on a solid stakeholder engagement strategy, on inter-institutional arrangements, well-established frameworks and decision making flows. Data governance needs to be agreed upon and the division of responsibilities be charted, ensuring transparency, representativity and accountability.
European and national scientific research organisations, publishers and other actors must align their data-related business processes, responsibilities and expectations to achieve commonly agreed goals.
OpenAIRE offered to facilitate open science of coordination based on a network of 34 countries we want to see EOSC have a stronger commitment.

3.4 Implementation & transition to FAIR

Implementation of FAIR principles requires careful prioritisation and orchestration. The FAIR Data Action Plan 2018-2020 is an important collaborative instrument for the embedding of FAIR principles in the first phase of the EOSC. The plan will not necessarily suggest any specific technology, standard or implementation solution. For an even transition of data from different levels of maturity to FAIR, existing activities to make data FAIR (e.g. GO-FAIR) must be complemented by new initiatives that embed FAIR principles in all the phases of data life cycle.
The Swiss National Science Foundation offered to coordinate policies on what repositories can be used (freedom for researchers).

3.5 Research data repositories

Trusted research data repositories play a fundamental role in modern science. Scientist must be able to find, re-use, deposit and share data via trusted data repositories that implement FAIR data principles and that ensure long-term sustainability of research data across all disciplines. Data repositories must be easy to find and identify, and provide to users full transparency about their services.
The Austrian Science Fund offered to work to extend Re3Data to better understand the data repository landscape.
The German Research Foundation (DFG) offered to contribute and fund updating of Re3Data.

3.6 Data Management Plans

A key element of good data management is a Data Management Plan (DMP); the use of DMPs should become obligatory in all research projects generating or collecting publicly funded research data, based on online tools conforming to common methodologies. Funder and institutional requirements must be aligned and minimum conditions for DMPs must be defined. Researchers' host institutions have a responsibility to oversee and complete the DMPs and hand them over to data repositories.
The Netherlands Organisation for Scientific Research (NWO) offered to contribute to coordination of criteria for Research Data Management.

3.7 User needs

Users should see the EOSC as a one-stop-shop to find, access, and use research data and services from multiple disciplines and platforms. Services and functionalities shall be user driven and determined by clear use cases. Intermediary users and other brokers of end-users' demand – IT departments, umbrella associations, community networks – should assist data scientists and ICT specialists in the identification of key requirements for EOSC services.

PLAN-E & eScience Center offered to help support scientists to translate scientific requirements into practical services and infrastructural components.
GEO offered to contribute as a broker for interdisciplinary domains: a) climate changes, b) disaster risk reduction & c) sustainability development goals strategic targets to help define and serve concrete user needs.

3.8 Service deployment

The EOSC shall support different deployment models (e.g. Infrastructure as a Service, Platform as a Service, Software as a Service), to meet the needs of communities at different levels of maturity in the provision and use of research data service. The EOSC shall support the whole research lifecycle by strong development at platform level that facilitate the provision of a wide set of software, infrastructure, protocols, methods, incentives, training, services. Software sustainability should be treated on an equal footing as data stewardship.

3.9 Thematic areas

The EOSC shall promote the co-ordination and progressive federation of open data infrastructures developed in specific thematic areas (e.g. health, environment, food, marine, social sciences, transport). The EOSC will implement a common reference scheme to ensure FAIR data uptake and compliance by national and European data providers in all disciplines.
PLAN-E offered to help and promote implementing FAIR principles for data and software across all domains.

3.10 Governance model

A long-term, sustainable research infrastructure in Europe requires a strong and flexible governance model based on trust and increasing mutuality. As interdisciplinarity is one of the main objectives of the EOSC, the governance model should be based on representativity, proportionality, accountability, inclusiveness and transparency.
GEO offered to contribute to the development of governance by providing & sharing their lessons.

4. Open Science in Cloud Technology – OSTEC project

Open Science in Cloud Technology - OSTEC is a Romanian initiative, materialized within a project that proposes an open IT environment for the scientific community to store and reuse data and scientific results. At European level, the Cloud Initiative is an important step in the evolution of "big data" exploitation by researchers. OSTEC project targets the implementation of open access technology and scientific services, making possible to displace, exchange and reuse their data without discontinuities at global scale, for interdisciplinary research approaches [6].

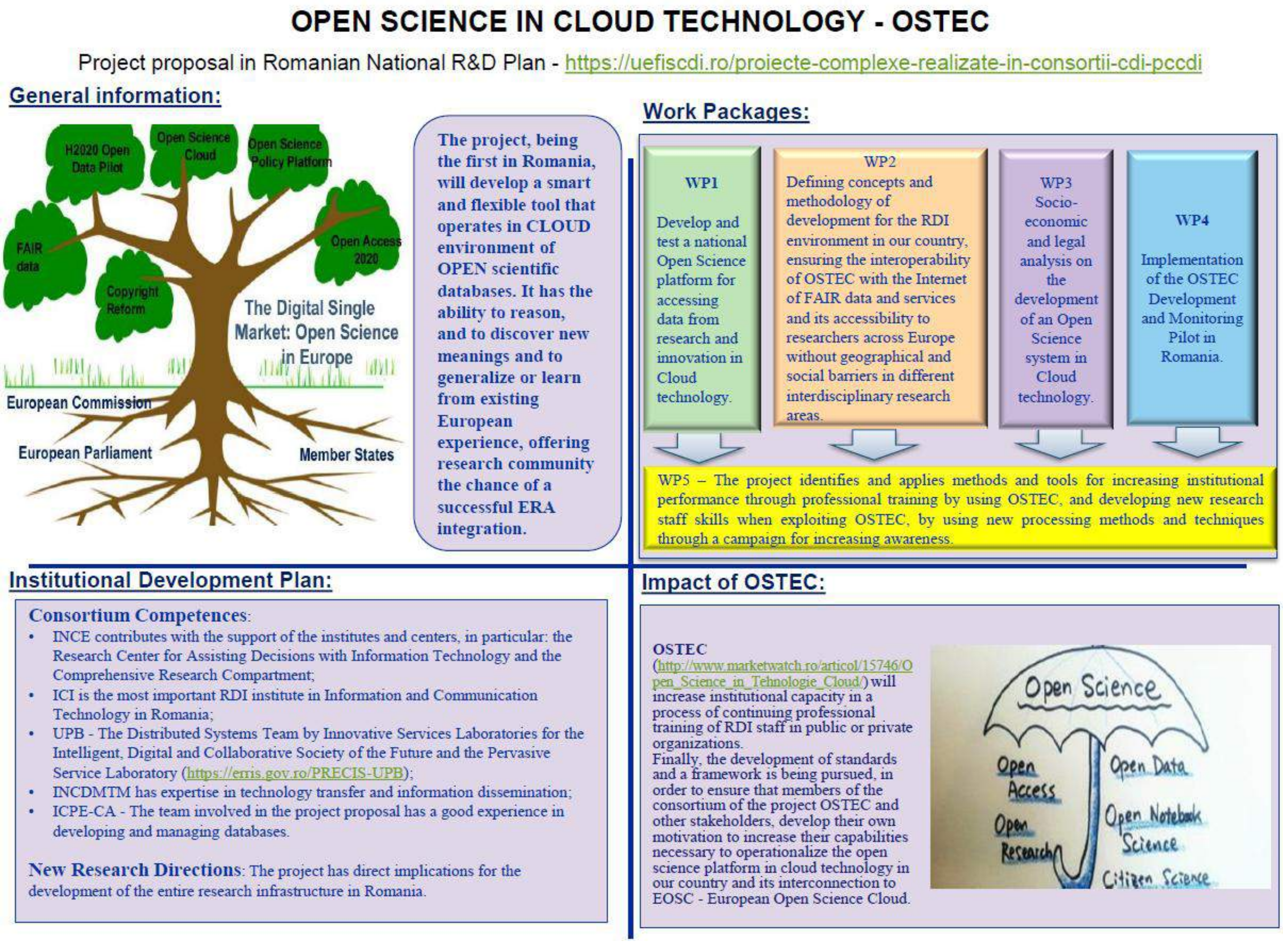

5. Conclusions

There is no way back now, but that does not mean that everything is already written in stone. The European Commission will work with Member States, with the EOSCPilot and to make the most of the INFRA-EOSC Call, and with research funders regarding open research data policies and tools in support of the EOSC.

Stakeholder engagement with the initiative will continue and there will be plenty of occasions in future to engage and make their voice heard. The DG is working with the EOSCPilot project to ensure that the EOSC implementation takes centre stage at the First stakeholder engagement event, to be held on 28-29 November 2017 in Brussels. This event could serve as the first, pilot meeting of a future EOSC Stakeholder Forum in support of the EOSC initiative.

The Commission also announced how it plans to support the EOSC in WP 2018- 2020 to the Research infrastructures Programme Committee (27 June 2017); the draft was pre-published on 3 October. This support is provided mainly by the Call INFRA-EOSC; the Call covers all the future key functions of the EOSC, with an overall budget of 270-300 million Euro. The Call is a central piece in the implementation strategy. Moreover, several research funders expressed a desire to work jointly to make the most of open, FAIR research data policies, to support their uptake and implementation. The Commission will work with them in this respect, to ensure full implementation of the 'data culture' and 'FAIR data' action areas of the Declaration.

Finally, the Commission is strongly committed to working with Member States and Associated Countries to start discussions of concrete proposals on governance via the Roadmap on the basis of the draft Declaration. The Roadmap will put forward proposals for governance and funding - including a proposal for the future Executive Board of the EOSC. The Commission will work with the Council via the ERAC Standing Working Group on Open Science & Innovation ('ERAC OSI'),

1) to gather essential Member State input on the EOSC Roadmap, especially on the design of governance and on funding levels (MS requested this explicitly), and 2) to ensure that the initiative is aligned with national strategies for scientific data infrastructures.

References

[1] https://ec.europa.eu/research/openscience/index.cfm?pg=open-science-cloud;
[2] https://www.nature.com/articles/sdata201618;
[3] https://ec.europa.eu/research/infrastructures/index_en.cfm?pg=esfri;
[4] https://www.openaire.eu/;
[5] https://www.cessda.eu/;
[6] http://www.marketwatch.ro/articol/15746/Open_Science_in_Tehnologie_Cloud/.

ISSN 1454 - 8003
Proceedings of 2017 International Conference on Hydraulics and Pneumatics - HERVEX
November 8-10, Băile Govora, Romania

MODERN TRENDS IN THE DESIGN AND MODERNIZATION OF HYDRAULIC DRIVES

Zygmunt DOMAGAŁA[1], Krzysztof KĘDZIA[1]

[1] Wrocław University of Science and Technology, Mechanical Faculty, Department of Operation and Maintenance of Logistics, Transportation and Hydraulic Systems

e-mail: zygmunt.domagala@pwr.edu.pl, krzysztof.kedzia@pwr.edu.pl

Abstract: *The article describes modern trends in the design of hydraulic drives. It contains two examples of this approach and the didactic and research offer of the Laboratory of Hydraulic Drives and Vibroacoustics of Machines.*

Keywords*: Hydrostatic drive system, design, modelling and simulation, simulation model verification*

1. Introduction

Hydraulic drives and controls are widely used around the world. The properties of working fluids enable design simpler, cheaper and more aesthetically pleasing machine designs, replacing mechanical drive. It is difficult to imagine today's work machine (e.g. excavator, loader, dump truck, etc.) without hydraulic components and controls.
Energy saving, energy efficiency of machines and equipment, reduction of CO_2 emissions are the terms we meet more and more often. On the energy efficiency of industrial machinery and equipment, where energy consumption is highest and where it can save the most money- do we pay the same attention on it?
Therefore the criterion of energy efficiency of hydrostatic systems is becoming more and more important. For this reason, intensive work is underway to reduce the demand for hydrostatic power and to reduce the already existing power losses.
Concept development is also an important stage in the design process of the hydraulic drive system. A qualitative part of the concept is a schematic diagram of a system, consisting of contractual symbols representing individual assemblies (elements) of the system. The schematic of the system can be created in many ways. One of them is to adapt existing solutions or peek into what the competition is doing. Such approaches are not reprehensible. They are used by many companies and engineers. However, in market conditions, when we have to meet sometimes sophisticated customer expectations, they turn out to be in many cases wrong.
To design a schematic diagram of a hydraulic system that works well and satisfies the customer, it is good to use some method to support creative thinking at the stage of its generation.
The illustrated solutions illustrate the approach to the hydraulic drive design.

2. Design of a new hydraulic power unit

In order to design a schematic of a hydraulic system that works well and satisfies the customer, it is good to use a method that support creative thinking at the stage of its generation.
One of them is a functional approach to this problem, based on the functional classification of hydraulic systems.
The analysis of many existing systems has shown that there are two groups of functions:
- **basic functions** that result directly from the operating conditions of the final object, or more specifically the actuator (work unit) (e.g. pressure regulation, torque, system load, speed synchronization,

ISSN 1454 - 8003
Proceedings of 2017 International Conference on Hydraulics and Pneumatics - HERVEX
November 8-10, Băile Govora, Romania

- **auxiliary functions**, which generally result from the specificity of hydrostatic systems (e.g. technological overload protection, inertial protection, protection against uncontrolled movement, etc.).

First group includes basic functions (useful), resulting from tasks assigned to machines and/or equipment. In this group are many functions, but the most important function of which is speed control of the actuator. It is possible to do in two main ways:

a) throttle control (Fig.1)

b) volume control (Fig. 2)

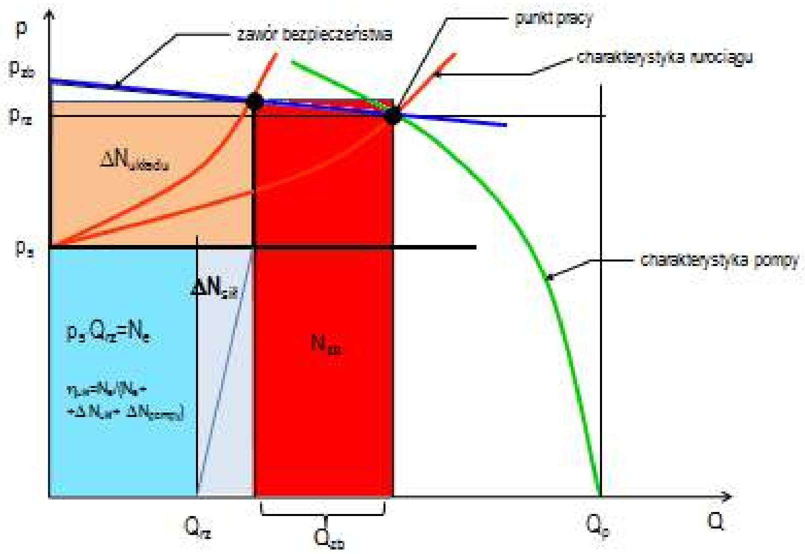

Fig. 1. Characteristics of the system with partially open throttle valve

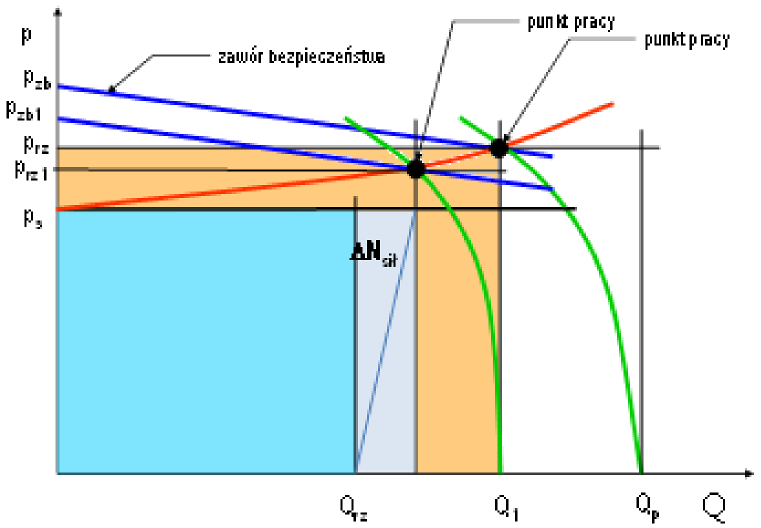

Fig. 2. Characteristics of the system with volume control

According to the authors, both methods of speed regulation of the actuators generate large losses. For this reason, inverters have become increasingly important in electric motors. Particularly they have important role in the drive fans and rotary pumps. The use of an inverter entails many benefits, primarily financial. The use of inverters in applications with fans and pumps entails reduced electricity consumption and no need for additional automation devices.

Based on the analysis, it was decided to build a prototype hydraulic power supply in which the generator was to be a gear pump driven by an electric motor. The rotational speed of the pump was to be provided by the inverter and the entire propulsion system was to replace the piston pump with a constant pressure regulator. The built-in power supply has been tested for energy efficiency.

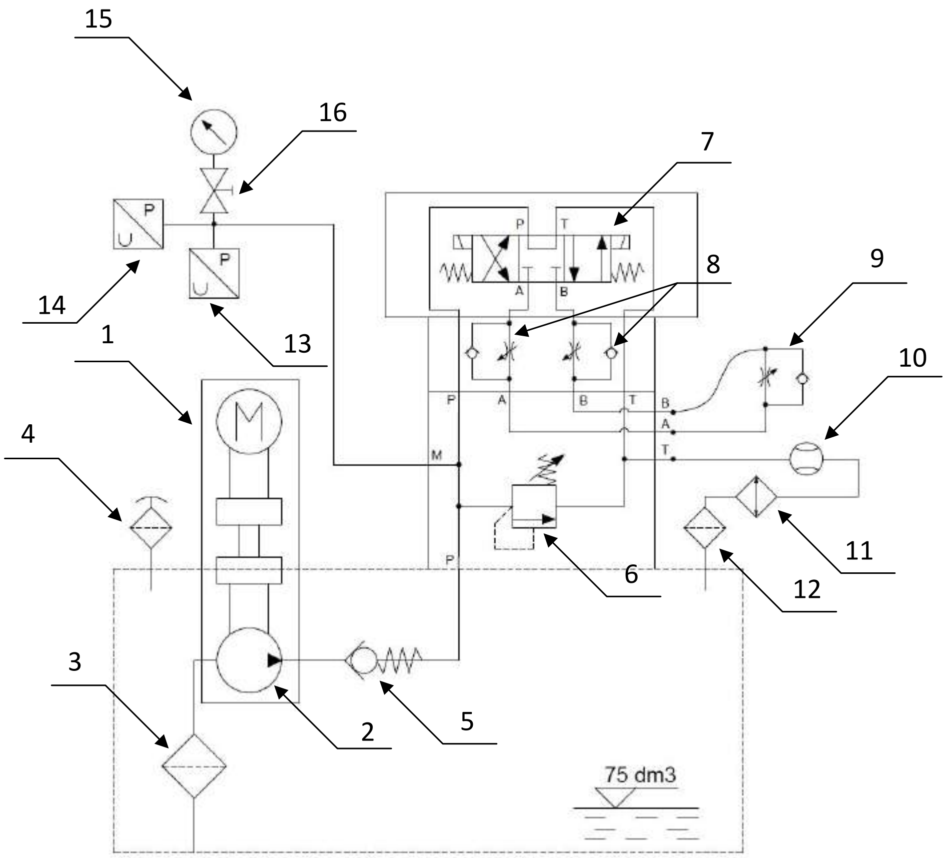

Fig. 3. Hydraulic diagram of the tested power unit: 1 - electric motor 4 kW, 2 - external gear pump, 3 - inlet filter, 4 - vent filter, 5 - check valve, 6 - maximum valve, 7 - 8 - throttle valves, 9 - throttle valve, 10 - flow meter, 11 -CSL oil cooler, 12 - sump filter, 13 - pressure transducer

The dependence of the hydraulic power of the generator as a function of the fluid demand of the hydraulic receiver shown in Fig. 4 is best illustration of the energy efficiency of the hydraulic power supply. With maximum liquid demand, power demand in "eco" mode is about 20% lower than in "normal" mode. This is even more evident with minimal demand for liquid receivers. In this case, the power demand in the "eco" mode is only 23% of the power required by the "normal" mode.

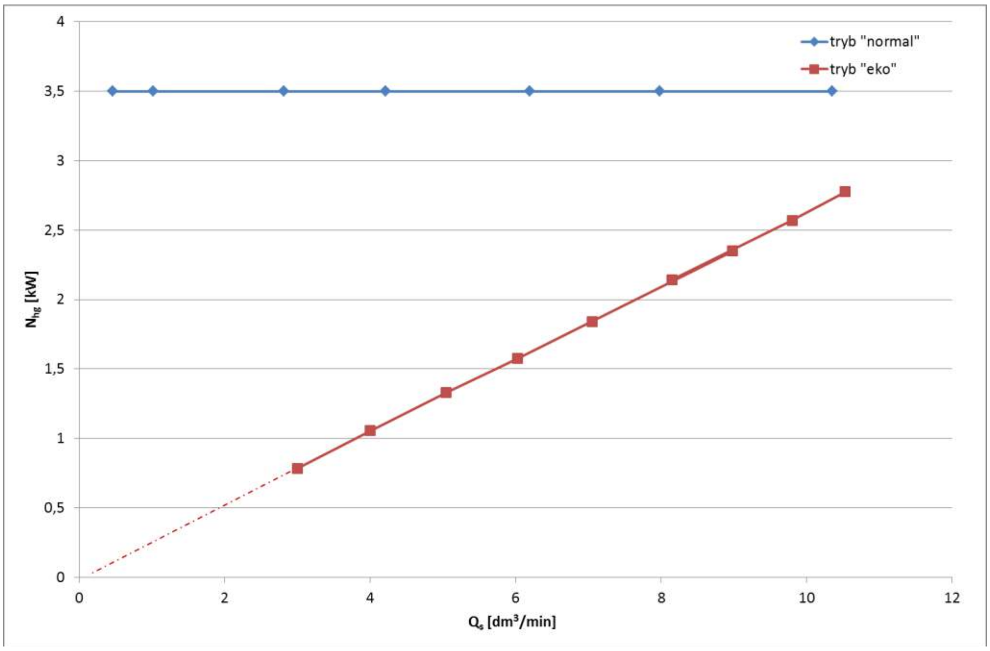

Fig. 4. Dependence of the hydraulic power of the generator as a function of the demand for liquid by the hydraulic receiver

The main purpose of the research was to determine the energy efficiency of a prototype power supply with an electronic control system. The economic aspects of this type of solutions are obvious. The price of the complete electronic control unit is lower than the equivalent system using a variable-output pump (Table 1).

Table 1. Comparison of different solution

Pump with variable displacement					
Name (symbol)	Price	Output	Producer	Max. pressure	r.p.m range
Axial piston pump (PFR-206)	7182 PLN	5,8 cm^3/rev	ATOS	35 MPa	600-1800 rev/min

Total amount of money: 7182 PLN

Suggested solution					
Name (symbol)	Price	Output	Producer	Max. pressure	r.p.m range
Gear pump (PS2A-04D-10N)	720 PLN	6 cm^3/rev	Contarini	25 MPa	650-3500 rev/min
Inverter (SINAMICS V20)	1755 PLN	-	Siemens	-	-

Total amount of money: **2475 PLN !!!**

During the test it was found that in the "eco" operating mode, below the rotational speed of 500 rpm of the electric motor driving the pump, the pressure in the pump discharge manifold starts to change dynamically and the amplitude values of these changes reach 20% of the value determined for operation in this mode.
Main savings are achieved by properly programming the pump's running cycle during slow movements or idling.

3. Modernization of hydraulic drive

In the opencast mines for transporting conveyor belt drive stations, caterpillar trackers of special construction are used. Drive stations and other equipment are often several times larger than conveyors. The aim of the study was to improve the technical parameters of the hydrostatic transport system of the conveyor. By measuring the selected parameters of the system,

the obtained results were verified on a real object, using the mathematical model of the driving drive.
In the opencast mines for transporting conveyor belt drive stations, caterpillar trackers of special construction are used. Drive stations and other equipment are often several times larger than conveyors. The aim of the study was to improve the technical parameters of the hydrostatic transport system of the conveyor. After measuring the selected parameters of the system, the developed mathematical model of the drive system has been verified.

Fig. 5. TUR 600 transporter

The primary source of energy for hydrostatic drives is the Diesel IC engine, which drives the hydraulic gear units through the distribution gear. Two variable displacement hydrostatic motors were used for each track, driving the planetary gear of the crawler wheel.
The hydrostatic drive system of the caterpillar consists of:

- multi-piston variable displacement pump and alternating discharge direction,
- two hydraulic motors of variable flow, connected in parallel to the supply line circuit,
- flow control elements.

The pump is equipped with a constant power regulator, while the hydraulic motors in the overflow valves limit the maximum torque transmitted by the drive system. The diagram of the described hydrostatic drive is shown in Fig. 6.
The high cost of experimental research and the technical difficulties of their implementation led to the use of an analytical method to determine the drive load values of caterpillar drive based on discrete mathematical model, which was then verified in the Bełchatów Mine.
MATLAB with the Simulink software was used to model the equations. Simulink is an interactive package designed for modeling, simulation and dynamic analysis of continuous, discrete and mixed circuits.
The results obtained were compared with the results of the measurements. Measurements were made in real conditions on the lignite coal mine KWB Bełchatów.

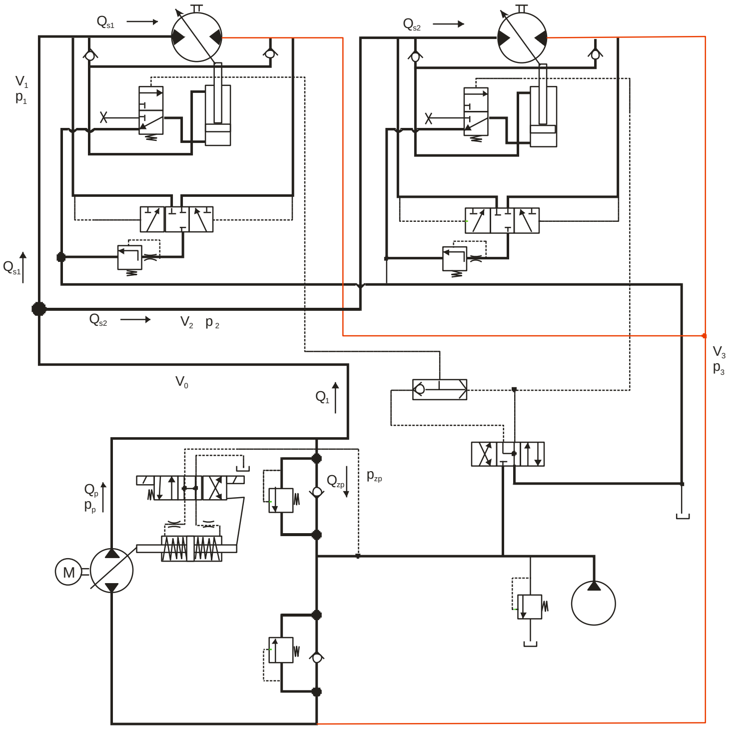

Fig. 6. Scheme of the hydraulic drive system

The measurement program included the determination of parameters for given cycles of load:

- travel forward without load with a right turn,
- slow travel (speed of maneuver v=5-7km/h) forward with load (mass 246T),
- travel with the highest speed (transport speed v = 10 km/h) forward and turn in both directions.

Fig. 7. shows the recorded pressure function in the hydrostatic drive system for the TUR600 transporter during operational measurements. This conveyor was loaded with 245 ton and moved in 3 degrees inclination.

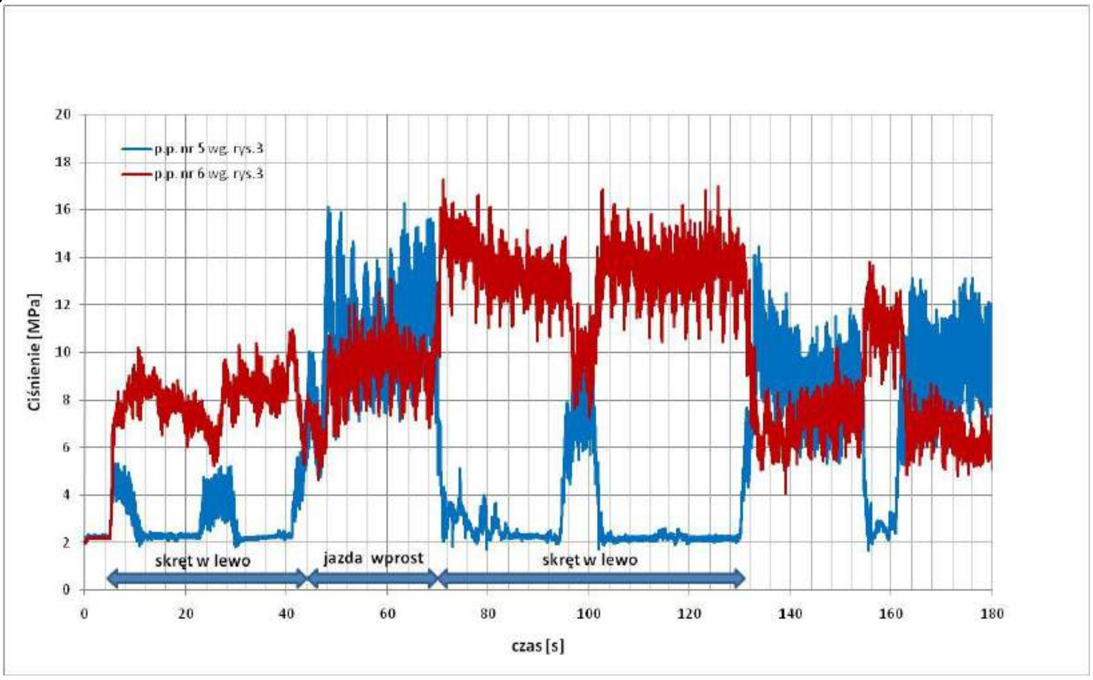

Fig. 7. Pressure function recorded in the hydrostatic drive system of the TUR600 transporter during operational measurements.

Comparing the results of the simulations with experimental results (Fig. 7) it can be stated that they differ in terms of pressure values. Analysis of the mathematical model and the simulation of experimental results showed that the differences were due to incorrect initial parameters or boundary conditions for simulation.
Firstly, it was assumed that the engine speed is 1450 rpm. This assumption is based on the Cummins engine characteristics. In this rotation range, the engine has the greatest torque. According to the Technical Operating Document, which was obtained at the KWB Bełchatów, the nominal engine speed is 1800 rpm and the Cummins engine is set to this value. So regardless of the load, the engine speed is 1800 rpm.
The second assumption that turned out to be wrong was the pressure in drainage line of the crawler drive system. For simulation tests it was assumed that the pressure was 1 MPa. The experimental measurements show that it is 2.4 MPa.
By measuring the pressure values in the drive hydraulic system, the missing data were obtained, from which some values in the simulation model (eg pressure on the suction line of the pump) were verified. Measurements also allowed for verification and comparison of real and simulation results.

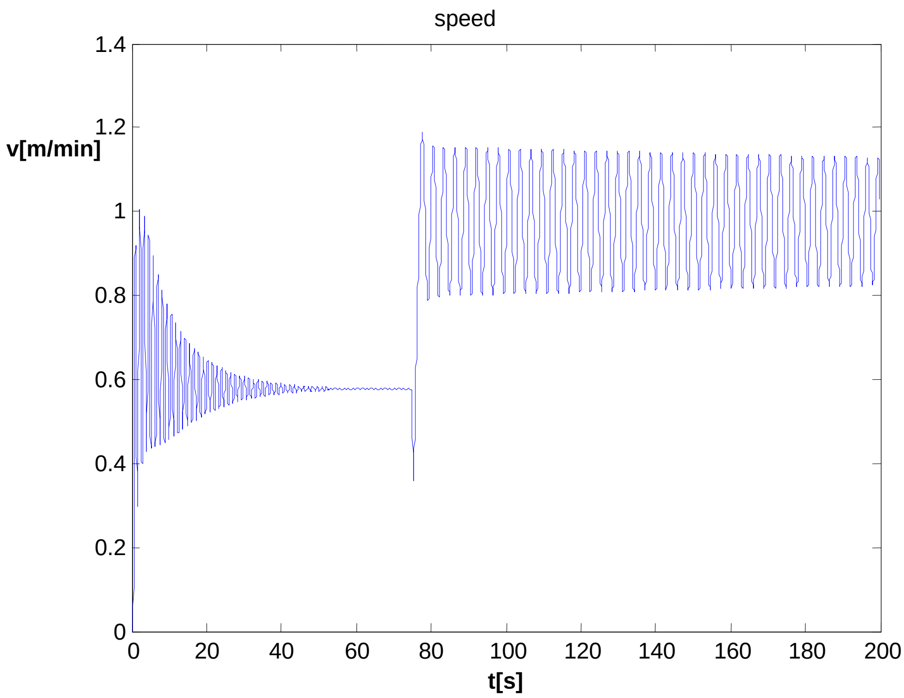

Fig. 8. Speed of conveyor: M_n = 2260kNm, qs_1 = 500cm^3/rev, qs_2 = 1000cm^3/rev, ratio of planetary gear i=400.

The picture above (Fig. 8) shows the results of the research with optimal parameters. The conveyor moves on every terrain (inclination angle, type of soil, wind effect on the machine and transported load), reaching the expected maneuverability.
The conclusions:
• The designed hydraulic drive system did not meet the design requirements,
• The operation of the system will effectively improve the replacement of one of the hydraulic motors in the crawler drive to a higher power motor (qs = 1000cm3 / rev).

Verification of simulation models requires appropriate staff, equipment and skills. In our Department there is a laboratory which has all these qualities.

4. Laboratory of Hydraulic Drives and Vibroacoustics of Machines

Laboratory of Hydraulic Drives and Vibroacoustics of Machines is one of the most advanced in the field of hydraulics and vibroacoustic diagnostics on the national and European level. In the laboratory, in addition to a wide range of courses dedicated to students of the Faculty of Mechanical Engineering of Wrocław University of Science and Technology, are also carried out research on the needs of master's theses, doctoral dissertations and research projects as well as professional measurements on external orders, including industrial ones. The Laboratory is the only one in the country entitled to attestation of hydraulic components and systems in terms of radiated noise. The interdisciplinary research team consists of experienced academics of Wrocław University of Science and Technology who conduct scientific and development researches in the field of hydrostatic drive for decades. As a result of numerous projects, the research team of the Laboratory boasts the industrial implementations and important prizes and awards. The team of the Laboratory continues in developing didactic and research offer, trying to take care of the highest possible professionalism in the performance of tasks. One of the many activities of the Laboratory is also conducting trainings in hydraulic drive and control systems for the engineering staff of enterprises through the implementation of proprietary training programs.

4.1. Fields of Laboratory activities

In the field of hydraulic systems, machinery and equipment vibroacoustics are carried out the research regarding [6]:

- analysis and synthesis of hydraulic, microhydraulic and pneumatic structures,
- design and modernization of hydraulic and electro-hydraulic systems,
- design and modernization of hydraulic components,
- miniaturization of hydraulic components design,
- automation of hydraulic systems control,
- durability testing of hydraulic components,
- identification of vibroacoustic energy propagation in the environment,
- use of vibroacoustic signals for diagnostic purposes,
- synthesis of vibroacoustic machinery and signals,
- location of vibration and noise sources in hydraulic components and systems and noise reduction,
- passive and active methods to reduce noise and vibration of machines and equipment with hydraulic systems,
- simulation of dynamic phenomena in hydraulic components and systems,
- optimization of hydraulic components and systems,
- identification of phenomena associated with the flow of fluid in the hydraulic systems,
- modeling of viscous and compressible fluid flow with thermodynamic changes,
- calculation of multiphase flows, e.g. cavitation.

4.2. Equipment of the Laboratory

The laboratory is equipped with a stand for testing hydraulic systems Hydro-Prax (Rexroth), a new generation of components controlled by electromagnetic coils, proportional elements: directional valves, throttle valves, pressure control valves, check valves, load-sensing valve, and actuators – hydraulic motors and cylinders [2]. Furthermore, in the system can be used timers, pressure switches or inductive proximity sensors to implement sequential hydraulic circuits (Fig. 9).
The laboratory has extensive facilities for the design, construction and testing of components, pneumatic systems and controls enabling the creation of many individual sets for teaching and research in the field of pneumatic and electric automation, such as systems with timers, limit switches, pressure and logic elements (Fig. 10).

Fig. 9. Educational stand with hydraulic components and electrical and proportional control panel

Fig. 10. Test rigs with a set of elements for pneumatic control systems

Additionally, in the Laboratory of high powers, unique test rigs are dedicated for testing seals, cylinders, valves, including proportional spool valves, servos and for studying cavitation, type of flow, obliteration and dynamic testing of hydraulic components and systems. Acoustic reverberation chamber for vibroacoustic tests meets the requirements of ISO 9000 and enables attestation of machines and devices for vibration and noise, while a set of instruments for measuring the noise emission with the use of energetic methods with a probe and acoustic holography allow to identify the noise source and the measurement of sound power by ISO 9614 (Fig. 11 and 12).

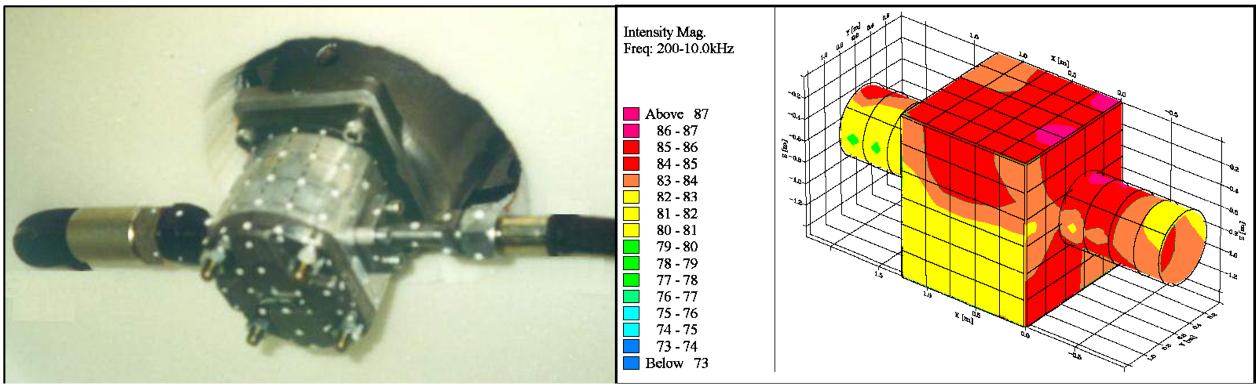

Fig. 11. Localization of noise sources in the external gear pump (acoustic probe) [3]

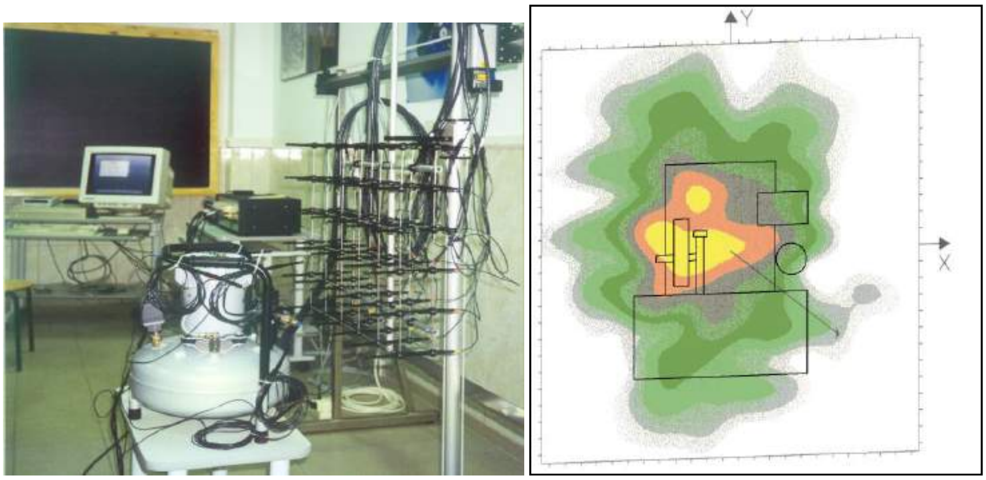

Fig. 12. Localization of noise sources in the compressor (acoustic holography)

The linear hydrostatic drive simulator Hydropax ZY25 should also be described. It is a research unit of the propulsion system with reciprocating movement meeting the actual working conditions of devices with this drive type. The simulator consists of a hydraulic unit, control unit and the control program (Fig. 13).

Fig. 13. Linear hydrostatic drive simulator

Finally, equipment and wide range of educational offer of Laboratory of Hydraulic Drives and Vibroacoustics of Machines makes it the perfect base to put into practice the knowledge acquired during the academic lectures. The didactic offer is addressed to students of various courses and specializations in the field of vibroacoustics, hydraulic and pneumatic drive and control, but also can successfully serve the students of other fields i.e. related to electronics. In addition, the laboratory provides the opportunity to conduct advanced research and measurements at the request of the industry. Laboratory employees strive to continually improve the didactic and research offer in order to provide services at the highest possible level.

References

[1] W. Kollek, Z. Kudźma, M. Stosiak, "Symulator liniowego napędu hydrostatycznego źródłem nowych możliwości badawczych”, *Międzynarodowa Konferencja Naukowo-Techniczna "Napędy i Sterowania Hydrauliczne i Pneumatyczne"*, Wrocław 2005;

[2] W. Kollek, M. Łabik, „Koncepcja laboratorium napędów i sterowań hydraulicznych i pneumatycznych”, *Napędy i Sterowanie*, nr 2, 2000, s. 54-57;.

[3] W. Kollek, P. Osiński, „Gerauscheuntersuchungen der Zahnradpumpen mit Hilfe der energetischen Methode”, W: Innovation und Fortschritt in der Fluidtechnik, Viertes Deutsch-Polnisches Seminar. Technische Universitaet Warszawa, Fakultaet fuer Mechatronik. Institut fuer Automatik und Robotik, Sopot, 20-21 September 2001;

[4] P. Osiński, M. Stosiak, „Badania wybranych właściwości wibroakustycznych symulatora liniowego napędu hydrostatycznego”, *Hydraulika i Pneumatyka*, nr 1, 2015, s. 17 – 22;

[5] *** Documentation SYHCE-1-1X, Manesmann Rexroth, 1995;

[6] *** Internet website of Laboratory of Hydraulic Drives and Vibromechanics of Machines www.lhiw.pwr.edu.pl;

[7] Z. Domagała, K. Kędzia, “Analysis, modelling and verification of the phenomena occurring in a hydraulic prop during dynamic load”, Czasopismo Techniczne = Technical Transactions. 2017, R. 114, z. 2, s. 139-153, 16 rys., bibliogr. 8 poz.;

[8] Z. Domagała, K. Kędzia, “Analysis of hydraulic drive system equipped with a hydraulic cylinder with long stroke”, *Hydraulika a Pneumatika* (Žilina). 2014, Roc. 16, cis. 1, s. 13-16, 7 rys., bibliogr. 7 poz.;

[9] K. Kędzia, “An algorithm for the determination of the control parameters of a multisource drive system”, Czasopismo Techniczne = Technical Transactions. 2017, R. 114, vol. 3, s. 173-182, 5 rys., 1 tab., bibliogr. 22 poz.

ISSN 1454 - 8003
Proceedings of 2017 International Conference on Hydraulics and Pneumatics - HERVEX
November 8-10, Băile Govora, Romania

RESEARCH CONCERNING DESIGNING SPECIFICATIONS AND COMPONENTS FOR AN ECO-INNOVATIVE TECHNOLOGIES IMPLEMENTATION MODEL

Irina RADULESCU[1], Florica COSTIN[2], Maria DUMITRACHE[2], Alexandru Valentin RADULESCU[1]

[1] University POLITEHNICA of Bucharest, e-mail address: irena_sandu@yahoo.com

[2] S.C. ICTCM S.A. Bucharest, e-mail address: coca.costin@gmail.com

Abstract: *The development of Romanian clean technologies market is due to legislation, which obliges polluting companies and intensive resources consumers to retrofit. It is the key-role of research institutes to aid and built various consortia, in order to develop solutions and clean process technologies. State and private companies have developed own solutions and green technologies in their research - development - innovation departments. Creating a model for the implementation of eco – innovative technologies is a part of an extensive research, being a component of a virtual hub for eco-innovation, in order to increase the organizational competitiveness in recycling of waste electrical and electronic equipment and the involvement of public and private entities in promoting eco-innovation for the development of green economy. The eco - innovative technologies implementation model represents a tool to achieve this goal, its interactive approach leading to obtain a friendly eco - profile for the user organization, that can be visualized by potential partners and also, to the eco - innovative technology improvement by selecting the best solution, considering the ecological and technological points of view.*

Keywords*: eco-innovation, technology, implementation model*

1. Introduction

National and international economies are focused on sustainable directions concerning goods and services production and consumption, in order to keep a clean environment without harming it, no natural resources depletion or damage of ecosystems.

There are developed and improved many friendly environmentally practices as reducing or eliminating waste levels and pollutants emissions, improving waste treatment, reducing raw materials demand and natural resources usage [1].

European Union highlights ideas for sustainable consumption and production, as overall objective in the EU Sustainable Development Strategy (EU SDS), “by addressing social and economic development within the carrying capacity of ecosystems and decoupling economic growth from environmental degradation and Improving the environmental and social performance of products and processes and encouraging their uptake by business and consumers”.

Between all directions to follow by European Union countries one refers to “increase global market share in the field of environmental technologies and eco – innovations” [2].

Eco-innovation is more and more present in organizations activities for a sustainable consumption and production, “that will contribute to improving the environmental performance of products and increase the demand for more sustainable goods and production technologies”. Its definition emphasizes the society commitment on environment protection, being “any innovation that makes progress towards the goal of sustainable development by reducing impacts on the environment, increasing resilience to environmental pressures or using natural resources more efficiently and responsibly”[1].

The 10-year strategy proposed by the European Commission on 3 March 2010: *Europe 2020* – represents an advancement of the EU economy, aiming "smart, sustainable, inclusive growth" for all European countries, focused also on greater coordination of national and European policy.

The most important instrument is represented by the Eco-innovation Action Plan (EcoAP), which development is oriented on “specific bottlenecks, challenges and opportunities for achieving

environmental objectives through innovation", by complementing other Europe 2020 Flagship Initiatives. The development of EU capacities for a sustainable growth represents an Europe 2020 Strategy priority, also their transition towards a green economy represents a target for the Eco-innovation Action Plan [3].
Main ideas developed for promoting resources efficiency intend to connect economic growth to a rational use of resources; that is the purpose of the Roadmap to a resource efficient Europe, that supports "the shift towards a low-carbon economy, an increased use of renewable energy sources, the modernization our transport sector and promotes energy efficiency".
Analyzing the relationship between the Eco-innovation Action Plan and technologies, the first one is defined like a "tool to identify and implement measures for the deployment of key environmental technologies". It is important to strengthen the cooperation between European Union and Member States, by involving the disseminations of new innovative technologies and promoting appropriate skills development; these are done by using business environment, especially the small and medium enterprises (SMEs), to obtain "the development of a strong and sustainable industrial base able to compete globally"[3].
According to European Council environment targets and to the Kyoto Protocol, in terms of Romanian involvement in eco-innovation, our country aligns to Members States to the implementation of energy-climate change package, that requires the development of "a new economic model to integrate environmental concerns into the production process and the resulting products" [2].
Romanian efforts are increased at eco-innovation level of enterprises by the participation in the "Framework Programme for Competitiveness and Innovation 2007-2013", the Eco-innovation component. The purpose to improve the competitiveness and innovation capacity of the European Community companies is achieved by supporting projects, that aim first application or reproduction on the market of eco –innovative techniques, products or services relevant to the European Union. A sub-program regarding entrepreneurship and innovation provides a 430 million euros budget, for investment activities in eco-innovation projects and facilitating the access to finance for the SMEs creation and development.
The importance of eco –innovation and attracting investments in new green technologies are relevant for the achievement of sustainable economic growth. Romania had some recent ecological improvements, but it is still lagging behind the European Union average, due to the poor encouragement and insufficient funds, also difficult legislation for the small and medium enterprises (SMEs) and eco-innovative companies.
However, data show that the SME segment is interested in obtaining grants for eco –innovation, on account of limited ability to access capital markets. Recent analysis of implemented projects reveals that more than 50% focuses on improvements processing facilities, equipment to increase productivity, optimization of the costs of raw materials, utilities, reducing CO2 emissions and creation of approximately 470 new jobs.
The development of Romanian clean technologies market is due to legislation, which obliges polluting companies and intensive resources consumers to retrofit. It is the key-role of research institutes to aid and built various consortia, in order to develop solutions and clean process technologies. Also, state and private companies have developed own solutions and green technologies in their research - development - innovation departments [4].

2. The development of the eco-innovative technologies implementation model

Creating a model for the implementation of eco – innovative technologies is a part of an extensive research, being a component of a virtual hub for eco-innovation in order to increase the organizational competitiveness in recycling of waste electrical and electronic equipment and the involvement of public and private entities in promoting eco-innovation for the development of green economy.
The eco - innovative technologies implementation model represents a tool to achieve this goal, its interactive approach leading to obtain a friendly eco - profile for the user organization, that can be visualized by potential partners and also, to the eco - innovative technology improvement by selecting the best solution, considering the ecological and technological points of view.

It is offered for the user an useful tool to verify his own eco-innovation technology, by drawing his own profile and by analyzing the influence factors in action; there are also presented several successful examples from Romanian industry concerning the eco-innovation technologies applied by companies and innovation centers with activities in the field [5].
By identifying Romanian successful examples and presenting them in the eco – innovation Library of the EcoInnEWaste platform - authors provide the opportunity for an analysis of a relatively wide large range of eco - innovative technologies. It is a chance for entrepreneurs to be informed and to find possible solutions, compatibility or cooperation possibility with other companies involved in waste field.

2.1 The methodology

The first step involves the successful log-on on the EcoInnEWaste hub platform, by entering the name and the password for an authorized user; this allows to access the Tool: *Implementing Eco-Innovative Technology.*
The structure of the model proves its usefulness by clear specifications in designing its components, friendly design of the interfaces, so a lot of business environment issues can have their answers (for producers, users, suppliers or companies interested in Waste of Electrical and Eelectronical Equipments problems), [5].
The development of the eco – innovative technologies implementation model is based on the analysis of Romanian enterprises with successfull green technologies and on the possibility to bring their influence factors to a common denominator. Thus, the model steps to be taken are following the imposed design specifications:

- Specifying the eco-innovation appliance areas:
- preventive eco-innovative technologies;
- Innovative eco-innovative technologies;
- eco-innovation technologies in Research – Development - Innovation;
- monitoring, surveillance and control,
- specifying the factors that have led to the adoption of eco-innovative solutions;
- specification of the existing resources (human, material, financial)- it is important to hire highly qualified personnel for the entity who has the appropriate technical and material endowment for eco - innovation;
- specification of the eco-innovative activity share in the entity's activities, that is necessary to determine the degree of possible involvement in eco-innovation projects;
- specification of the certification systems at the entity level: quality management and environmental management applied at the entity level;
- specification of the entity 's experience in eco - innovative activities;
- specification of the main developed eco - innovative solutions;
- specification of the costs and results of the implementation of eco-innovative solutions;
- specification of the relevance of the implementation results of eco - innovative solutions.

The information management interface for eco - innovative technologies is represented by a screen; the user registers by specifying his organization data, having the possibility of selecting answers for each step (ticking the buttons), the number of the chosen situation being automatically passed to the corresponding box on the screen. This situation is presented in Figure 1, the information to select being written in Romanian, due to the fact the device is offered to the Romanian business environment.

3. Results and discussions concerning the eco-innovative technologies implementation model

As a result of design specifications, the interfaces were friendly designed, so, by clicking one of the presented options, the page with successful / good practice models for the appropriate eco-innovative technologies can be opened, in pdf format.

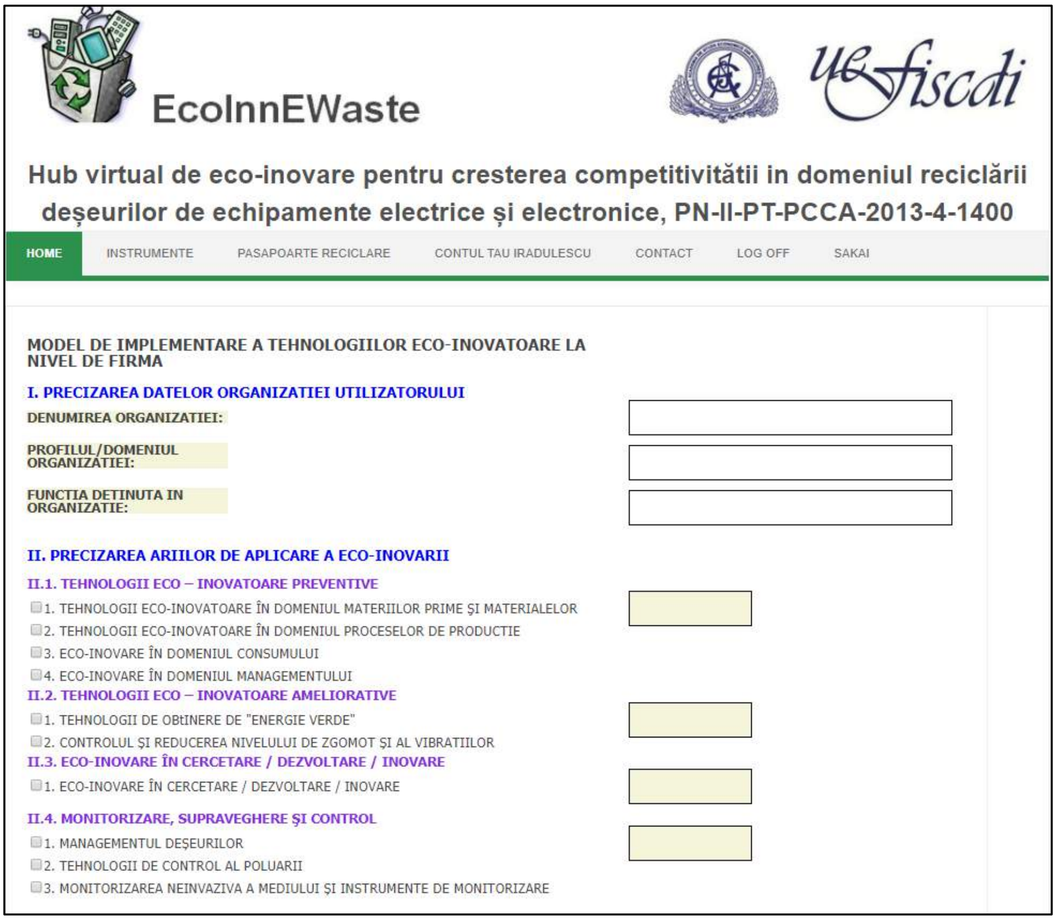

Fig. 1. The Interface of the eco - Innovative technologies implementation model

Design specifications aim to complete the steps mentioned above, to record the data and to obtain the user's profile, in order to be visualised. So, it is possible to obtain an user-friendly "business card" by providing information to application owners, also for data management for the users interested in this domain. With the user's consent, this profile can be made public, after that being possible to establish business rellations, the user can be contacted by potential partners / collaborators in the field or himself can represent a model to follow for other users.
There is an wide range of areas where eco-innovative technologies can be applied, design specifications were made for, ready to take account in viewing profiles.
Areas of eco-innovative technologies that can be consulted and they give business information include (Figure 2):

- Technologies for sieving and recycling household waste;
- Technologies for water treatment and purifying;
- Research - Development – Innovation;
- Waste sorting systems;
- Technologies for terrestrial works, power stations, environmental protection;
- Research - development in engineering and technology;
- Systems to obtain "green energy";
- Exhaust and industrial filtration installations;
- Integrated industrial ecology services (integrated waste management services);
- Absorbent petroleum products;
- Waste management - treatment and co-processing, energy recovery, WEEE treatment, incineration disposal, recycling, medical waste management, sorting and transfer stations;
- Noise and vibration monitoring;

- Decontamination technologies;
- SIP Integrated Construction System, EVOTHERM thermal insulation system;
- Complex technological equipment for refineries, chemical and petrochemical plants, power plants, environmental engineering;
- Heating systems;
- Environmental Engineering;
- Energetic services;
- Containers for chemical industry, surface coating and galvanotechnics, water and air purification;
- Design and execution of electrical installations, automation (intelligent buildings and industrial automation) and electricity;
- Ecological reconstruction services;
- Technologies for monitoring and control the pollution of environmental factors;
- Applications for industrial automation;
- Technology Information Centers, Technological and Business Incubators.

Fig. 2. Profiles visualization to access a good practice model for eco - innovative technologies

The eco - innovative technologies implementation model also offers a component structure that allows the access and the visualization of a model for choosing the optimal version of an eco - innovative technology, by two - steps design specifications within the application.
First step introduces the user in a model worksheet by learning how to analyse and obtain an optimal version of an eco – product: *"eco product application model"*. It provides the explanation of file completion for the product case, having the possibility to materialize several functions, taking into consideration several possible versions of product design and construction, analyzing the

possibilities and product functions. This is a demonstration how to choose the optimal variant to obtain an eco - innovative product.

In the case of an eco - technology the situation is similar, being presented in the second step: the second workheet - *"eco technology application"* - provides the workspace for the algorithm presented in the previous worksheet, with the cell connections made ready for the calculations of user's data. This interface guides the user in solving the problem, allowing to introduce the specific influence factors of own eco-technology, guiding the user towards an optimal choice of eco-innovative technology, (Figure 3 and Figure 4).

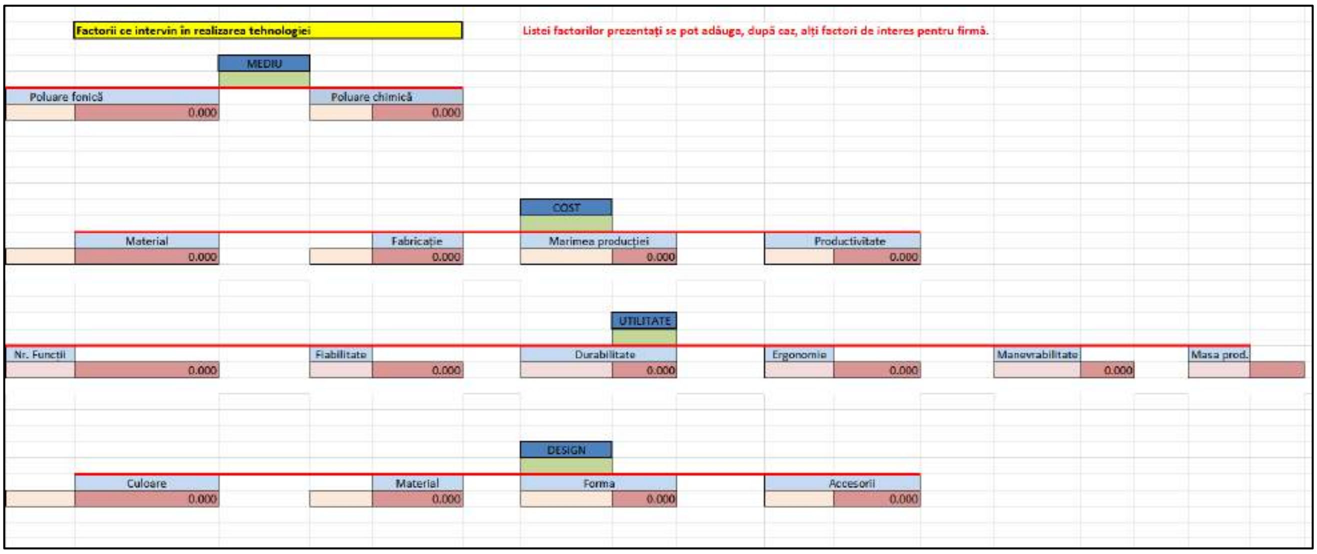

Fig. 3. Influence factors involved in achieving the eco-innovative technology

Analiza variantelor tehnologiei

Factori	Pondere		Varianta 1		Varianta 2		Varianta 3		Varianta...		Varianta "n"	
de influență			Punctaj		Punctaj		Punctaj		Punctaj	Pondere	Punctaj	Pondere
(utilizatorul îi alege)	(fracție)	zecimale	(de la 1 la 4)	Pondere	(de la 1 la 4)	Pondere	(de la 1 la 4)	Pondere	(de la 1 la 4)		(de la 1 la 4)	
(1)	(2)	(3)	(4)	(5)	(6)	(7)	(8)	(9)	(10)	(11)	(12)	(13)
Poluare fonică		0.000		0.000		0.000		0.000		0.000		0.000
Poluare chimică		0.000		0.000		0.000		0.000		0.000		0.000
Material		0.000		0.000		0.000		0.000		0.000		0.000
Fabricație		0.000		0.000		0.000		0.000		0.000		0.000
Mărime producție		0.000		0.000		0.000		0.000		0.000		0.000
Productivitate		0.000		0.000		0.000		0.000		0.000		0.000
Număr de funcții		0.000		0.000		0.000		0.000		0.000		0.000
Fiabilitate		0.000		0.000		0.000		0.000		0.000		0.000
Durabilitate		0.000		0.000		0.000		0.000		0.000		0.000
Ergonomie		0.000		0.000		0.000		0.000		0.000		0.000
Manevrabilitate		0.000		0.000		0.000		0.000		0.000		0.000
Culoare		0.000		0.000		0.000		0.000		0.000		0.000
Material		0.000		0.000		0.000		0.000		0.000		0.000
Forma		0.000		0.000		0.000		0.000		0.000		0.000
Accesorii		0.000		0.000		0.000		0.000		0.000		0.000
SUMA				0.000		0.000		0.000		0.000		0.000

Varianta optimă este: Varianta.....

La analiza variantelor tehnologiei sunt enumerați toți factorii, cu ponderile lor totale.
Pentru fiecare variantă propusă se va aprecia fiecare factor cu o notă, apoi se va calcula ponderea corespunzătoare aferentă, ca produs între notă și ponderea inițială.
Prin însumarea ponderilor factorilor variantelor analizate se va alege varianta optimă - varianta cu cea mai mare valoare a sumei ponderilor factorilor.

Fig. 4. The analysis of technology versions

The eco - innovative technologies implementation model applies a relatively new method used in the innovative products and services management for obtaining best managerial decision, in a rapid manner, with minimal risk, [6], [7]. It is necessary to achieve technologies versions or enhancements by using morphological analysis based on functions involved, describing their performance. This is the path to improve enterprise technology and to find its optimal version, but the SMEs manager must know all information related to specific parameters and influence factors involved in the analyze and he must decide about the optimum solution (the variant with the highest value of the influence factors shares sum).

4. Conclusions

The model of implementation of eco-innovative technologies at company level is based on research on Romanian business environment, by assessing the level of the environment protection and eco-innovation technology level, identifying successful examples and drawing up possible ways to follow up new possible users. By presenting the methodology and the component structure of the eco - innovative technologies implementation model, authors invite users to access the tool to discover succesful eco-innovative examples, also to choose optimal eco-innovative technologies variants for their own companies. Specifying components, planning interfaces and design specifications have the role to build an easy-to-access and user-friendly interactive environment tool, that provides current and useful information about eco-innovation technologies, at national level, with the possibility to be extended at international level.

Acknowledgments

This work was supported by MEN –UEFISCDI, Joint Applied Research Projects programme, project number PN-II-PT-PCCA-2013-4-1400, contract 320/2014.

References

[1] http://ec.europa.eu/environment/waste/weee/index_en.htm
[2] http://ec.europa.eu/environment/ecoap/about-action-plan/objectives-methodology/index_en.htm
[3] http://ec.europa.eu/europe2020/index_en.htm, Innovation for a sustainable Future - The Eco-innovation Action Plan (Eco-AP), Ecoinnovation Action Plan_En_CELEX-52011DC0899-EN-TXT.pdf, 2011.
[4] http://www.anpm.ro/deseuri-de-echipamente-electrice-si-electronice
[5] http://www.ccib.ro/
[6] A. Filipoiu, C. Radu, C. Berbente, “Severity assessment for aeronautical risk analysis”, (“Evaluarea severității pentru analiza riscurilor aeronautice “), U.P.B. Sci. Bull., Series D, Vol. 74, Iss. 4, ISSN 1454-2358, Bucharest, 2012.
[7] A.C. Filipoiu, C. G. Alionte, I.D. Filipoiu, D. Comănescu, A.Comănescu, I. Geantă, ”6435 Method Used For Risk Analysis With Application In Airport Management” (“Metoda 6435 folosită pentru analiza riscurilor cu aplicație în managementul aeroportului”), The 20th INTERNATIONAL DAAAM SYMPOSIUM "Intelligent Manufacturing & Automation: Theory, Practice & Education", ISSN 1726-9679, Vienna, 2009.

ISSN 1454 - 8003
Proceedings of 2017 International Conference on Hydraulics and Pneumatics - HERVEX
November 8-10, Băile Govora, Romania

THE FAILURE OF PUBLIC UTILITIES, A MEASURE OF EARTHQUAKE IMPACT ON POPULATION

Ștefan-Nicolae TRACHE[1], Dan BURLACU[1]

[1] "Alexandru Ioan Cuza" Police Academy – Fire Officers Faculty,
tkstefan@gmail.com, burlacudan92@gmail.com

***Abstract**: "Prevenim, protejăm, salvăm" – "We prevent, we protect, we save" says the motto of the Romanian firefighters, which presents the everyday struggle and "raison d'être" – reason for being of the rescue services that plan and act for the well-being of the citizens that they protect. One of the types of risk that firefighters are called to address is the earthquake, which in itself poses an immense task for the emergency preparedness system, but given the disruptions that this type of event causes, the population affected by it finds itself threatened even after the end of its this type of risk's manifestation, by the failure of the systems that insure everyday commodities. That is the issue that is addressed in this paper, of the importance of taking into account the public systems that provide necessary support for everyday life, which can be disrupted in the event of a major seismic activity manifestation.*

***Keywords**: Earthquake, Public Utilities, Failure, Response*

1. Introduction

One of the less emphasized sides of the impact that a major earthquake can have on population is that of the lack of basic living means such as sanitization, drinking water supplies, food and heat. In the surreal hypothesis that following a major earthquake there would be no casualties, but only infrastructure loses, loss of lives would follow. If even the most basic needs that we often overlook in our daily lives, such as waste management, would suffer an interruption, or even an overload, the consequences that follow could be dire, especially in correlation with the lack of sanitization means that could lead to the onset of epidemics.
Public utilities whose infrastructures do not suffer damage directly from seismic activities could still cease to function due to lack of fuel caused either directly through the stop of fuel production, or indirectly through the hindrance of transport from production site to, say, thermal power station or heating plants.
Major cities are consumer oriented establishments that are dependent at least on the transport infrastructure to link them to the production sites of various goods, for sustaining day to day activities and in the case of a major disruption caused by a significant earthquake, population safety and well-being is certainly the main concern of public authorities. Given this fact, this paper hopes to provide insight on the necessity of public utilities failure management in case of a major earthquake and shed light on the way that this failure might be used to assess the immediate impact on population of such event and help the decision making process of authorities in restoring temporal normal conditions in a short time span.

2. Public utilities failure impact on population

Day to day life as we know it, with its routine and comforts depends on the public utilities that are made available to us in the areas that we work, live and study. The lack of these utilities can lead to serious problems in a society that has developed such a strong dependence upon these comforts and the way things take place on a daily basis. As such, in the event of a major earthquake, the disruption of the same utilities becomes the main author of public unsettlement and strives. In the following, comes a brief evaluation of the chain of events that concur in aggravating an already unstable situation, marked by confusion, panic and rupture in the quotidian, powered to even further lengths by the failure of the following:

2.1. Water supply network

Water used for drinking and cooking is generally provided by a system of pipes and pumps or is available as bottled water. Rarely in urban settings are people dependent on private wells or get their water supply directly from a natural source. Given the important role that water has in everyday life and the amount of it needed daily for drinking and sanitization, a discontinuation of residential water supply will influence the bottled water demand, which, in turn, may over run the supply and cause uncontrolled migration and public safety violations.
In the event of a long-term disruption of water supplies, poor hygiene and waste management may lead to the onset single cases of diarrheal diseases, typhoid fever, infection with different types of parasites [1], or may result in the outbreak of epidemics.

2.2. Sewage

Tightly linked with the lack of water supply is personal hygiene and in the particular case of an earthquake, the excreta disposal process may be affected by the lack of infrastructure and/or means of due sanitization.
Even if the housing infrastructure resists an earthquake, the sewage disposal one can fail and result in indoor flooding and, if the problem persists, the inadequate sewage system may lead to health problems and disease outbreaks. Lack of education of the population regarding proper excreta disposal when sewage services are unavailable would speed up the disease spreading process.
Odor pollution and water supply contamination may be other possible threats to communities' well-being provoked by the affected sewage infrastructure, in correlation with poor education regarding community living and care for the environment. In this situation, information about proper excreta management should be popularized.

2.3. Waste management

Following a major earthquake, the waste management facilities may suffer major damages which could hinder the normal processes, or the personnel may not be able to work as usual, resulting in a reduction or stop of waste collecting activities, or even the transport infrastructure damage may prevent normal functioning of the waste management agencies.
Improper storage or the accumulation of household waste may lead to disease outbreaks, a reduction of living comfort by odor pollution and animal attacks caused by the various creatures that may thrive on garbage and are drawn to the area.

2.4. Electricity

Failure of electricity delivering systems, either by stop of production or by failure of transport infrastructure would cause the population to resort on power generators, dependent on fuel. Lack of electricity in an area could lead to panic, a rise in crime rates, and if the problem persists, more complications may result in communications failures because of the loss in functionality of TVs, radios, computers and phones, even mobile ones or the inability of people to buy goods because of the loss of power of banks and mobile pay means. A more urgent need that would arise in the unfortunate event that the electricity is cut off for an extended period of time is that of food preservation, given the fact that all cooling apparatus would stop working. In the same manner, the hospitals and blood banks may be unable to deliver their services to the more than ever in need population, due to the lack in power.

2.5. Natural gas

Depending on the season of year that a major earthquake might critically affect natural gas delivery systems to a major city, the consequences would be more or less dire. Used either as fuel for food preparation and heat generation, natural gas is a public utility that can be replaced by the use of electrical power, if that is available. In the event that homes would rely on natural gas for heating, the means for electrical heating might not be available and distributors might be overwhelmed by the growing request.

Another problem that may arise on a local plane due to the failure of natural gas transport infrastructure is the formation of explosive gas clouds that can be easily triggered by sparks and cause a lot of damage. Given the odorless nature of natural gas, and in the hypothesis that there isn't enough odorant in its composition for allowing facile identification of such clouds, their neutralization or avoidance could become a potentially tedious task without the use of readily available gas detectors.

2.6. Transportation

Transportation, be it public or private, can be disrupted in many ways following an earthquake. Evidently, the infrastructure that would be the most affected would be roads. Either by debris pile up or by the asphalt crumbling, the formation of sink holes or the failure of bridges, both public and private transport would be affected to some degree. Transportation is crucial both for providing assistance for the earthquake victims, and for evacuating affected areas. Access to hospitals would be cut off and survival supplies delivery would not be possible.
Another major inconvenient caused by a severe transportation disruption is the cutoff of fuel delivery to local gas station, in which case power generators might be affected and cause further complications of an already unstable situation.
In the case of a major loss of a city's housing capabilities, transportation is crucial for the population to move to relatives or find housing in unaffected areas.

3. Utilization of public utility failure as a measure of earthquake impact on population

In the passing of time, given humanity's frequent encounter with the destructive power of earthquakes and the need of cataloguing earthquakes' impact on settlements for the purpose of anticipating an adequate response in the event of similar manifestations, in the condition of little or none information available in the aftermath, there have been proposed several scales [2] for the expression of an earthquake's intensity.
Similar to the intensity scale, a scale or table, if you will, to measure immediate impact on population and to help authorities prioritize needs and develop quick and effective strategies for the reestablishment of temporal normal conditions might come in great use, and a representation of such a tool is found in Table 1.

Table 1: Earthquake assessment by public utilities failure

Code	Affected public utility	Authorities' priority
I	Natural gas	Provide alternative means of heating / food preparation Detect and seal leaks Aid companies in making critical repairs
II	Transportation	Asses alternative routes Clean debris Provide shuttles
III	Waste management	Designate and inform about waste storage areas Provide and promote immunization against infectious diseases [3]
IV	Sewage	Provide mass communication and enforcement of hygienic rules Provide basic sanitization materials Set up temporary public showers
V	Electricity	Insure public safety Provide power islands Aid companies in making critical repairs
VI	Water supply network	Provide and rationalize drinking water Insure public safety Set up temporary water purification stations Provide mass communication about dietary choices to avoid dehydration

This choice of hierarchy was used by reason of emergency that each public utility failure has. In that regard, a failure of natural gas providing utilities has the least impact on population day to day activities, given that other means of heating and food preparation can be used. In the case of the transportation infrastructure failure, the impact increases as time passes from the event and resources diminish. As such, it does not call for such an immediate response. Waste management utilities failure can become of major importance with the passing of time because of the potential outbreaks that it can cause. It doesn't call for an immediate response, but more of a reorganization and allocation of resources on behalf of the public authorities.
Moving into the higher end of threats, the sewage infrastructure failure poses an immediate threat due to the potentially rapid disease spread rate that it could generate because of high population concentration. Not only that, but in correlation with unfortunate weather, it can lead to flooding, especially in urban areas, which are heavily dependent on the sewage infrastructure for the drainage of meteoric waters.
Today's society is dependent on electricity for almost every aspect of its daily business. That is why a failure of the electricity infrastructure is so high on the list. With possible complications like rises in criminal rates, depletion of fuel for power generators, the impossibility of provision of medical care and banking services, the failure of the electricity infrastructure presents authorities with multiple urgent tasks.
The biggest threat to population well-being after a major earthquake in terms of utilities failure is the loss of access to drinking water. In this case, people may resort to using water directly from natural sources like rivers, lakes or ponds, which, without proper treatment, may result in the widespread of diseases. Another side effect of this issue might be a rise in criminality and the reason that this is the number one emergency is because water plays such an important role in daily life and conditions many other activities.

4. Interdependencies

As is the case often times, when a major earthquake occurs, there is not just one system failing, but series of failures result in the cascading of effects. For example, the failure of the natural gas and drinking water delivery infrastructure may result in the impossibility of boiling the water obtained from natural sources, thus leading to disease spread. The failure of electricity and transportation systems may lead to total blackouts given the impossibility for fuel delivery. The failure of the waste management system may be caused by the failure of the transport infrastructure, by limiting access of waste management companies. The failure of both sewage and water supply would quickly lead to a growing deterioration of public health. The list of interdependencies goes on and on and given the fact that the failure of only six public utilities systems were taken into account, one can study the dependencies and outcomes caused by the failures of each combination of systems, but such a study exceeds the compass of this article.

5. Conclusions

Given the above stated scenarios and the importance that education plays in all of these to keep population safe and secure in the aftermath that major seismic activity can cause in an area, emergency preparedness for earthquakes should encompass the information needed not only to survive during an earthquake and in the moments that follow, but also that needed to prevent the spread of disease and to live in restrictive conditions, within a community, for an indefinite period of time. As we have stated, not only the earthquake itself poses a threat to population, but also the disruption that it can bring to systems that provide basic necessities. Also, authorities must take into consideration courses of action in the event of different public utilities system failure, and have at hand a variety of plans of action for the quick, partial or full restoration of their functions.
As much as it implies a response from the authorities and a change in behaviour of the population, the failure of public utilities provides a measurement of the impact the earthquake had on

communities, by damage inflicted upon the public utilities services and level of effort needed for the restoration of normal conditions.

References

[1] Máire A. Connolly, ed., “Communicable disease control in emergencies: a field manual”, World health organization, 2005;
[2] Roger M.W. Musson, Gottfried Grünthal, Max Stucchi, "The comparison of macroseismic intensity scales", *Journal of Seismology* 14.2 (2010); pp. 413-428;
[3] Rebecca Tooher, et al., "Vaccinations for waste-handling workers. A review of the literature", *Waste management & research* 23.1 (2005); pp. 79-86.

ISSN 1454 - 8003
Proceedings of 2017 International Conference on Hydraulics and Pneumatics - HERVEX
November 8-10, Băile Govora, Romania

TECHNOLOGY TRANSFER. STAGES FOR IMPLEMENTATION. SELECTING AND IMPLEMENTING "THE BEST PRACTICES". FACTORS WHICH INFLUENCE THE TECHNOLOGY TRANSFER ACTIVITIES

Diana Mura BADEA[1], F.T. TANASESCU[2], Dumitru VLAD[1], Valentina Daniela BAJENARU[1]

[1] National Institute of Research and Development in Mechatronics and Measurement Technique, Bucharest, Romania

[2] Comitetul Electrotehnic Roman, comisia6@icpe.ro

Abstract: *In this paper we introduce a model for Benchmarking analise witch can be applied to products/technologies/services/processes, or only to some of them. It can be applied to the manufacturing process of products and services. A significant example of this is the take-up of new products/technologies/services superior to competition and the level of market resulting from the research activities of universities and/or research institutes.*

Keywords*: Benchmarking, new products, new technologies, new services*

1. Introduction

The Technology Transfer Center pays particular attention to the transfer of state-funded scientific research results, to the development of firms and their increased competitiveness, a priority of European research [1].
Technology Transfer does not just mean selling a patent, but it also adds everything the scientific research can provide to a company: knowledge transfer, personal training, training sessions, joint projects and activities, access to laboratories and innovation platforms, technical assistance, services.
Technological Transfer is carried out within TT entities established within the academic environment (universities or research institutes), entity with or without legal personality, specialized in transfer, marketing, industrial property, dimensioned to perform a range of activities which will be included in the Regulation for its organization and operation.
The Shift of a Knowledge Transfer is generally performed after a certain TT scheme, but there may also be some customized phases for a particular application.

2. Steps in conducting a Technology Transfer

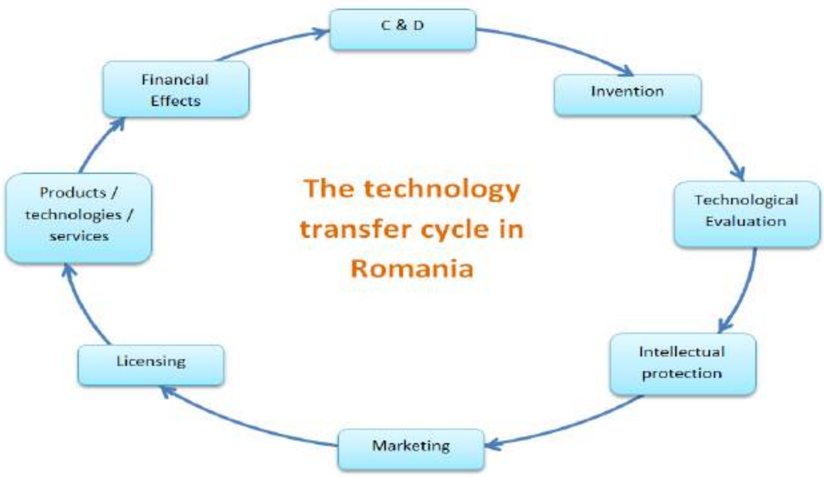

Fig. 1. Steps (stages) that go from the research/idea phase to capitalizing on the outcome

Generally speaking, the patterns encountered internationally foresee the same steps with a nuance difference signaled at the starting point: some believe that research is the basis of a patent from which the process begins, others that the idea of a future patent lies at the heart of research.
In the following, the steps will start from research, the patent being a result of C-D activity. It is the process through which the knowledge, products and technologies developed by government-funded public research are passed on to companies to accelerate their development as well as increasing competitiveness.
The goal of TT is to support the economy and enable companies to become as competitive as possible.

2.1 Step 1. Research

Throughout the research, a number of elements are considered to be new, less known, and through which new products, new technologies, or ideas can be built to provide services.
The researcher who benefited from public funding for his project has a moral duty to commercialize the scientific result obtained by giving him a scientific and economic recognition through the benefits of the patent and attracting additional funds to the institution in which he works.
The company engaged in the transfer of a new product / technology / knowledge is interested in taking a patent to increase its competitiveness on the market, superior technical and economic effects.

2.2 Step 2. Presenting the patented idea (description) to the Technology Transfer Center (TTC)

In a first step, the researcher will present TTC with the idea that should be patented, the novelty resulting from the research that has been developed and the impact it may have on its application.
TTC will ask the virtual inventor for the necessary information, submitting a note with technical and economic elements that justify the development of a patent. This note will be confidential and will be recorded as such, TTC responding to its secret [2].
The researcher must work with TTC in the next stages of evaluation and patenting, all documents and discussions of a confidential nature, including written documents or records.

2.3 Step 3. Technological evaluation of the invention and establishment of the conditions for elaboration of a patent

At this stage, we assess the impact of this invention, the technical and economic effects, the market and competitors in the field of the patent, comparisons with the patent literature and the retention of the elements of originality, marketing potential, possible licensing strategies, company licensing or start-up development -up, the final form of the Patent for Invention is to be submitted to the Patent Organization (OSIM). Without disclosing the secret of the invention to be developed, TTC may consult with OSIM Intellectual Property Specialists or OSH professionals in clarifying some of the Intellectual Protection issues at which the process begins. All documents drawn up are confidential and recorded as such [3].
It is not appropriate for the researcher or members of the research team to publish works or to support communications on this subject that would betray the secret of the invention until the release of the patent.

2.4 Step 4. Intellectual Protection. Patent

The patent application is filed with the State Office for Inventions and Trademarks - OSIM. Once patented, it is granted for a certain period of time when the rights of the inventor after the patent are protected. To reconcile the rights of the participants to the commercialization of the Patent. From now on the patent is public and any information about it can be made for marketing. The patent can also be registered with the European Patent Office.

2.5 Step 5. Marketing

TTC develops a market study identifying partners who may be interested in taking over the patent, competitors who make the same product / technology and their technical and economic performance, the existence of companies that want to diversify their profile, distribution networks, workforce level and their ability to leverage their patent, material resources, ability to promote a new product on the market. The analysis also takes into account the possibility of developing the patent at start-ups, in which case parallel assessments of advantages, disadvantages and risks are made.

2.6 Step 6. Licensing

The licensing of a patent is granted through the conclusion of a licensing agreement concluded between TTC (licensor) and the Company that is interested in taking over the patent (the licensee). The agreement fixes the rights that the patent owner grants, the financial benefits of this act. The same agreement ends also when the patent is taken over by a start up. By understanding between partners, a number of information can circulate between partners under confidentiality. The agreement specifies the rights and obligations of the partners, the exclusivity or the exclusivity of the Patent.

2.7 Step 7. Comercialization of the Patent

The company that licensed the patent agrees to its purchase, develops its production / application, develops manufacturing lines, launches the product, receives licensor assistance when it is provided in the contract, improves workforce, diversifies itself or in collaboration with the patent owner, the initial invention and the development of products adjacent to the subject of the patent.

2.8 Step 8. Economic Effects, Breaking the Income of the Patent

The revenue resulting from the sale of a patent is shared between the TTC, the beneficiary of the patent and the inventor / inventor usually one third if not otherwise agreed. In Romania the rights to the inventor are at least 30%. The money for the other parties is foreseen for development, new research, development of activities, etc., according to the interests of the Parties.

3. Selecting and implementing "The Best Practices”

Dissemination of the results obtained in research activities by specialized institutes, universities and some innovative enterprises is a moral and material obligation of these entities to use them in industry and economy.
Through the extended benchmarking process and / or through own actions of the interested entities, an industrial research is carried out which highlights the solutions offered by the research results and from which the best solution is chosen as the "best practice".
As a result, universities and institutes in the field accomplish through the research process technical solutions that are "best practices" while other entities (SMEs) through internal analyzes or as a result of their own strategic development policies aim to take over and to implement "best practice".
In this technology transfer activity and / or in the benchmarking process, the following main actors are involved:

- ✓ entities doing research through products/technologies/equipment /services;
- ✓ entities that from objective needs want to take over and implement these results;
- ✓ entities in the form of technology transfer centers created within universities and / or institutes that have extensive attributions in technology transfer, and are bridges between academia and industry.

The realization of the technological transfer depends on several issues that are related to the policies of the entities that generate the best solutions and want their capitalization in the industrial environment as well as the policies and strategies of the entities that want to take over and implement by transferring them [4].

Among the main issues of technology transfer policies can be listed:

- the existence and development of an adequate infrastructure for innovation;
- increasing the technical and professional skills and competences of the personnel (especially in the entities that take over the technological transfer);
- a possibility to allocate funds to support the commercialization of research results (this concerns both the transferring entity and the receiving entity, since each stage of the transfer requires staff costs, licenses, patents, property rights, expenses equipment materials, organization of production, distribution network expenses, etc.);
- protection systems, regulations and legal framework for property rights, innovation results, etc.

It should be underlined that the interaction between the entities that generate "best practice" and users is essential for the success of the technological transfer. For this reason, the importance of technology transfer centers as liaison points is special and the organization of these centers, their competencies as well as their attributions must be considered and established with much responsibility.
The success of the technological transfer is conditioned by the technical competence but also by the abilities that must lead to the identification of the "best practice" but also of the partner (s) whose product / technology / equipment / service is needed and to which the technology fits and is it is possible to implement it (in terms of resources, technical, development, etc.).

4. Factors which influence actions in technological transfer

In view of the emergence of such difficulties and important barriers to the transfer of research and development results in industry and economy, a number of factors that directly influence the technological transfer actions
and which have a significant technical, financial, economic, social impact on these actions. A list of principles of these factors must primarily focus on the comparative benchmarking analysis, focusing primarily on those qualitative elements from which we present some more important:

- Factors related to the Technology Transfer request
    - Potential Market (global)
    - Stability of TT demand
    - The life cycle of the technology
- Market Acceptance Factors
    - The necessary promotion effort
    - Distribution network
- Factors related to competition
    - Competitive partner position
    - Direct and existing competition
    - The price of technology
- Factors related to economic risks
    - Product development stage
    - Functional feasibility
    - Recovering the investments made both for the initial realization of the technology and for the exploitation after the takeover.
- Environmental factors
    - Impact of technology / technological process on the environment
    - Impact on society
    - Safety in operation of the product / equipment / installation
- Various other elements
    - The sale or location of machines, machines, etc.
    - Concession of a trademark or other intellectual property rights (design, model, etc.)

- Selling to the person who receives the technology of raw materials, materials, components, subassemblies necessary for the manufacture and exploitation of the acquired technology / license.

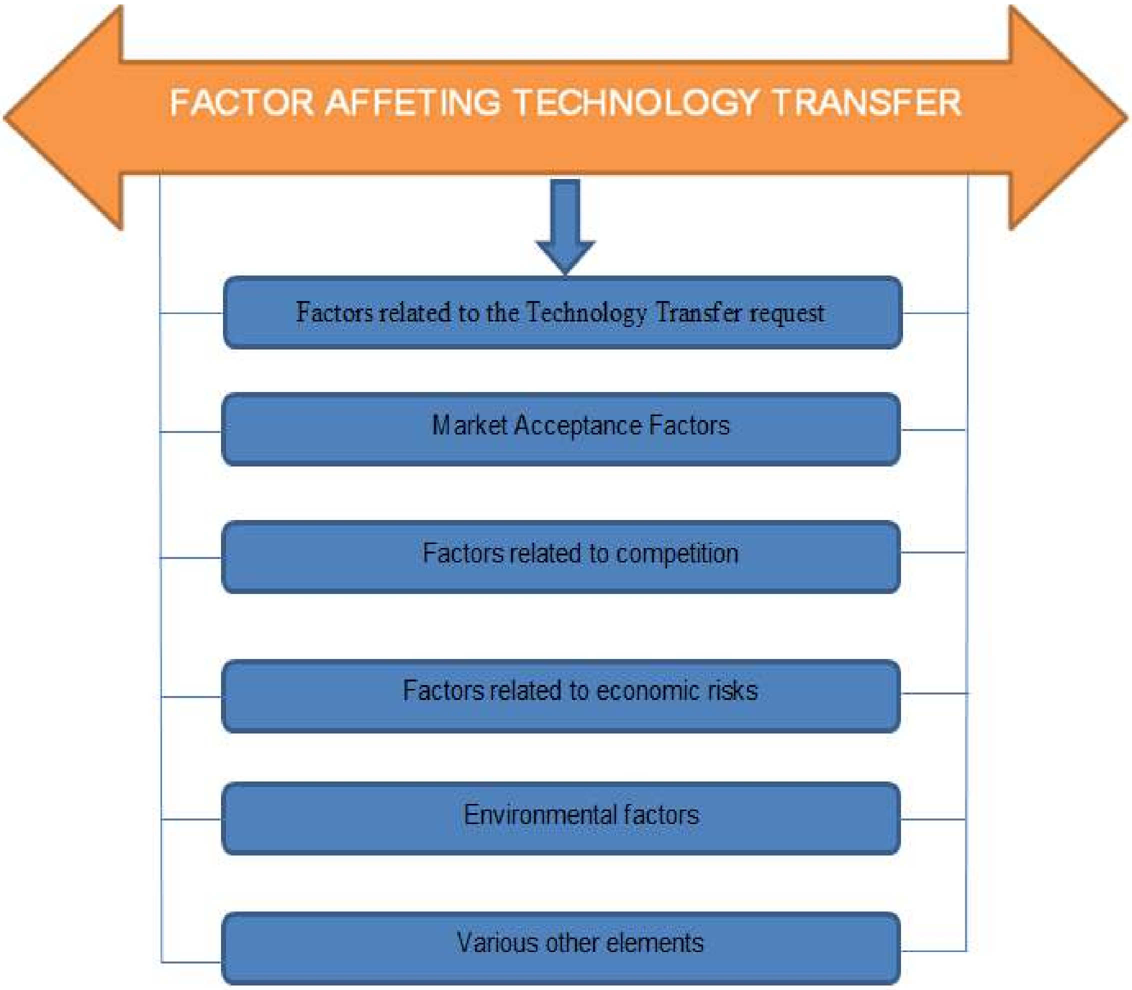

Fig. 2. Factor affeting technology transfer

5. Conclusions

Some important measures are needed to support TT activities:

- ✓ realization of financial instruments (loans, venture funds, public-private capital);
- ✓ communicating the results obtained in CDs through the websites of the developers, periodically, to SMEs even to multinational companies;
- ✓ the initiation of periodical publications summarizing the results of research by universities, institutes (public or private), innovative entities, individuals, etc;
- ✓ Informal transfer of knowledge through a structured network for this purpose;

Developing (more) broader, at least annual, programs of technical and scientific events focusing on topics such as:

- ✓ research results;
- ✓ trends in the development of high market products;
- ✓ European and international market trends lectures on certain technologies (from research, design, training, etc. manufacturing, production organization, commercial issues, marketing distribution strategic and operational, management, etc.).

References

[1] Comanescu, D., M., ş.a., "Benchmarking. Analize and Competitivity" („Benchmarking. Analizã şi Competitivitate"), University Publishing, Bucharest, 2008;
[2] Scurtu, V., Russu C., "Benchmarking – Application and theory", Economical Publishing; Bucharest, 2006;
[3] Armstrong, M, "Human resources management. Practice manual" ("Managementul resurselor umane. Manual de practica"), CODECS Publishing; Bucharest, 2003;
[4] European Commision DG III, "Benchmarking. Introduction and principles of the basic industry applied in organizational benchmarking" ("Benchmarking. Introducere şi principii de Industrie baza aplicate în benchmarkingul organizational");

ISSN 1454 - 8003
Proceedings of 2017 International Conference on Hydraulics and Pneumatics - HERVEX
November 8-10, Băile Govora, Romania

INNOVATION ECOSYSTEM MODEL FOR COMMERCIALIZATION OF RESEARCH RESULTS AND THE NEW HORIZON 2020 COMMISSION WORK PROGRAMME.

Gabriel VLĂDUŢ

IPA-SA CIFATT, Craiova, Dolj, Romania, 0040/251 418 882, office@ipacv.ro ; www.ipacv.ro

Abstract: *Innovation means Creativity and Added value recognise by the market.*
The first step in creating a sustainable commercialization of research results, Technological Transfer – TT mechanism, on one hand is to define the "technology" which will be transferred and on other hand to define the context in which the TT mechanism work, the ecosystem.
The focus must be set on technology as an entity, not as a science or a study of the practical industrial arts and certainly not any specific applied science. The transfer object, the technology, must rely on a subjectively determined but specifiable set of processes and products. Focusing on the product is not sufficient to the transfer and diffusion of technology. It is not merely the product that is transferred but also knowledge of its use and application.
The innovation ecosystem model brings together new companies, experienced business leaders, researchers, government officials, established technology companies, and investors. This environment provides those new companies with a wealth of technical expertise, business experience, and access to capital that supports innovation in the early stages of growth.
The Commission Work Programme 2018 released on 24 October 2017 lays the groundwork for concrete actions that will complete the work on President Juncker's 10political guidelines. The boost of jobs, growth and investment through the Circular Economy Action Plan is at the core of the Commission's agenda for the year ahead.

Keywords*: Innovation, Innovation Ecosystem model, Technology Transfer Centres, Technology Transfer Value Chain, Technology Readiness Level (TRL).*

1. Introduction

When we talk about innovation, we often focus on individuals. In business, we generally identify good innovators and nurture their ability to generate creative practical solutions to new problems. There is less focus on the kinds of structures that promote a culture of innovation. In business, we generally identify good innovators and nurture their ability to generate creative practical solutions to new problems.
If your organization relies heavily on individual innovation or institutional innovation, consider creating your own innovation reef, where creative problem-solving experts develop a network of individuals skilled in bringing new ideas to market.

Research and Innovation looking at the market
Valorization of the research results; transfer of knowledge to the market

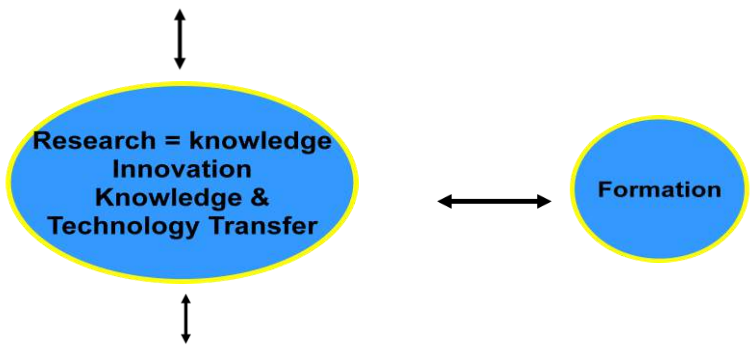

The market looking at research and innovation as engine for competitiveness and growth

There are essential elements to creating this in your company:
Get the right people involved. The innovation network has to include upper-level management that can fund projects, leaders who have had success with past innovations, technical experts, and external consultants.
Cultivate the network. This extended group should have opportunities to mix together in productive ways. Hold regular meetings, events, and talks where innovators from across an organization can get together and share their experience. Lead innovators need to meet regularly with a variety of groups within a company that are working on innovative projects to help connect together groups that are undergoing similar problems.
Educate others. In order for best innovation practices to diffuse through an organization, it is important to develop those ideas before projects begin. The innovation network should implement a company-wide education program on how to develop good ideas and how to transform good ideas into actionable plans to bring those ideas to market. These lessons should be delivered both to the future leaders within the company (which many companies do well) as well as broadly to the rank-and-file who will ultimately play a significant role in innovation success (which fewer companies do well).
Measure the results (with clears indicators). Innovation is a process that is best managed with a long term perspective, not necessarily measured in long time increments (e.g., months, years) but rather in completion of targeted goals. This requires separating the innovation process into three implementable stages: 1) identification of goals and exploration activities, 2) short term deliverables and 3) near term development.

2. The necessary steps for developing the financing instruments afferent to the innovation and technological transfer entities

The 48 ITT entities accredited in Romania exist and function with results (more or less good). Before analysing the activity of these entities, the used criteria for their accrediting/re-accrediting is recommended to be analysed together with the given tasks, the existent financing, the regulation onto which basis they activate and their monitoring indicators as well.
These entities have been monitored under this whole period and those failing to activate or which had an inappropriate (non-conformity) activity, had their accrediting withdrawn. A part of them have notable results both nationally, internationally and at the European level as well. Examples of networks in which a part of the entities activate:

- Enterprise Europe Network
- DTC – Danube Transfer Centres.

The establishment, accrediting and monitoring of ITT entities or the introduction of new ITT types of entities (e.g.: HUBs / co-working spaces, business accelerators, innovation labs, techno-pools/cities of sciences, etc.) should also be done under the existent regulation (with the necessary completions and amendments), so that no parallel would be created which in turn cannot lead to the expected results, respectively a unitary method should be ensured, with unitary indicators and objectives.

3 .The necessary steps to establish the financing instruments afferent to the innovation and technological transfer entities.

- Defining the assessment indicators for the ITT entities accredited in accordance with the stated regulation, from the point of view regarding to innovation, technological transfer and trading/commercialising the financing research results from public funds.
- The activity analysis of the ITT entities accredited under the defined indicators.

- The selection of ITT entities and scientific and technological parks with the potential and results from the point of view regarding the innovation, technological transfer and commercialising the financing research results from public funds.
- Identifying the type of ITT entities missing (e.g. HUBs/co-working spaces, business accelerators, technological development centres, techno-pools/cities of science, etc.)
- Coherent mapping of development regions with RIS /SMART specialization strategy nationally / regional, underlining the existent entities and the need for new ones.
- The establishment of new ITT entities in accordance with the existent regulation (with the necessary completions and amendments), based upon the identification necessity and proved competences.
- Defining the functioning indicators under which the activity of these entities will be monitored (supervised).
- Proper amendment of the current regulation.
- Development and implementation of training (induction) programs for the staff within the selected ITT entities in order to provide specific ITT services.
- Development and implementation of a coherent funnel type financing program for the ITT entities based upon marked achieved results from public funds financed research results traded point of view.
- Implementing the open innovation concept and specific instruments afferent to efficient and effective functioning of open innovation arena type platforms.
- The study underlined special programs (financed by INFRATECH program - 2004-2008) dedicated to these ITT entities have allowed their staff to enter in contact with similar existent organisations at European level. The financing stopping from the INFRATECH program interrupted these links in the case of some ITT entities.

4. The necessary steps in the innovation development

- Creating a functional and efficient innovation ecosystem.
- Developing all the weak links / the incipient/missing links, mainly the ones regarding to the innovation financing (structural / national / regional funds financing, business angels, venture capital, risk capital, etc.)
- Developing a continuous entrepreneurship training system
- Functional links between the ministries on one part and between the central and regional level on the other part (in coherence with The National Strategy RDI 2014-2090, RIS3 and Smart Specialization Strategy).
- Creating some effective and efficient partnerships, including the public-private ones between actors competing to innovation at central and regional level (Ministries, Regional Development Agencies, City Halls, County Councils, ITT Entities, Technological and Scientific Parks, Universities, Research Centres, Patron and Professional Associations, Competitiveness Clusters/Pools).
- Developing a real business environment partnership – Research-Development-Innovation which should identify the opportunities and necessities.
- Concrete action plans for Smart Specialization Strategies implementation at the level of all the development regions of Romania.
- Specific financing instruments for commercializing the public funds financed R&D results.
- Regional / Partner structures in favour of innovating SMEs from which ITT entities should take part (e.g. Competitiveness Clusters/Pools – Regional Development Agencies – Local Administration – Increase Pools – ITT Entities – Training Centres, etc.)
- Market indicators regarding the efficiency of innovation and technological transfer which should be found in the functioning indicators of the entities.

5. Objectives which should be followed for innovation development

- The innovation should address firstly to the development necessities of the innovating SMEs with the activity based on a large added value contributing to economic growth, export development and establishment of new jobs.
- Stimulation of innovative and creative enterprise development, start-ups, spin-offs and competitiveness clusters/pools in order to support those becoming robust, mature, generators of jobs, resistant to economic risks and sustainable.
- Supporting the technological and knowledge transfer towards the innovative firms.
- Stimulating the development and introducing new products to be manufactured along with the systems, services, performing organisational management based upon the R&D results.
- Stimulating the testing of invention patents (better before patenting).
- Creating the favourable conditions for private sector implication growth within the research-development-innovation activity.
- The research and innovation should be addressed to the real needs of the market; the markets to be oriented towards R7D, as means to increase competitiveness.
- The research should offer solutions to market needs, to develop knowledge, innovation should be applied and transfer the results for economic units use.
- Creating a real partnership regarding research-innovation-market for the identification of needs and finding solutions in order to increase competitiveness (social cohesion).
- Innovation management should be comprised in a continuous training system and in an entrepreneurial training.
- Motivating people to innovate; promoting an entrepreneurial culture by acquiring the necessary skills for a creative enterprise.
- Promoting the entrepreneurial spirit and innovation in small and middle sized companies/firms, especially in new ones.
- Developing the entrepreneurship and internationalizing the SMEs business.
- Increasing and applying the skills; an efficient skill flow, development of networks helping to increase, disseminate skills, with an efficient intellectual property rights system.
- Applying the innovation as a solution to social and global challenges; promoting the entrepreneurial spirit in economy and cost-efficient technologies.
- Coherent policies between: idea generators (innovation, research), finance innovation, regional development, regional centres, advertising, research and new technology valuing in the market use, entrepreneurial training.
- Regional development policies through innovation, RIS and 3S.
- Reinserting vouchers for innovation as development instruments.
- Databases resulted from research and technology quotations in accordance with international standards.

Value chain of value-added services

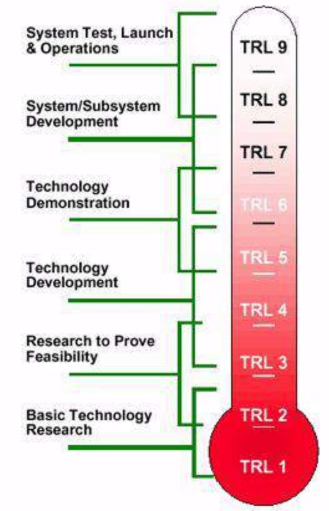

In order to increase the efficiently of the TTC's, meaning every TTC to efficiently use its specific key resources (physical, intellectual, human and financial), the Business Models of the corresponding TTC must be cantered on one of the three stages of the value chain of value-added services depending of their own resources. [1]

Technology readiness levels (**TRL**) are a method of estimating technology maturity of Critical Technology Elements of a program during the acquisition process. They are determined during a Technology Readiness Assessment that examines program concepts, technology requirements, and demonstrated technology capabilities.
The use of TRLs enables consistent, uniform discussions of technical maturity across different types of technology (see Figure 1).

Fig. 1. The stages of the value chain of value-added services, respectively the knowledge and TT value chain in comparison with the Technology Readiness Levels (TRL

6. Transferring the results to the market

- Indicators regarding the efficiency of technological transfer and innovation
- Accredited (certified) and trained staff (Technological Transfer and Innovation, technologies brokers, intellectual property)
- Entrepreneurial training program
- Promoting, training a culture of innovation, of mass.

7. Policies for competitiveness growth through R&D&I and technological transfer

The necessary mechanisms for a minimum innovative system functioning are presented in figure 2 (eco-innovative system). With black – what is very well integrated; with purple – what we need to increase. A transfer centre of research results towards the market may function only in an ecosystem with all the links being functional.

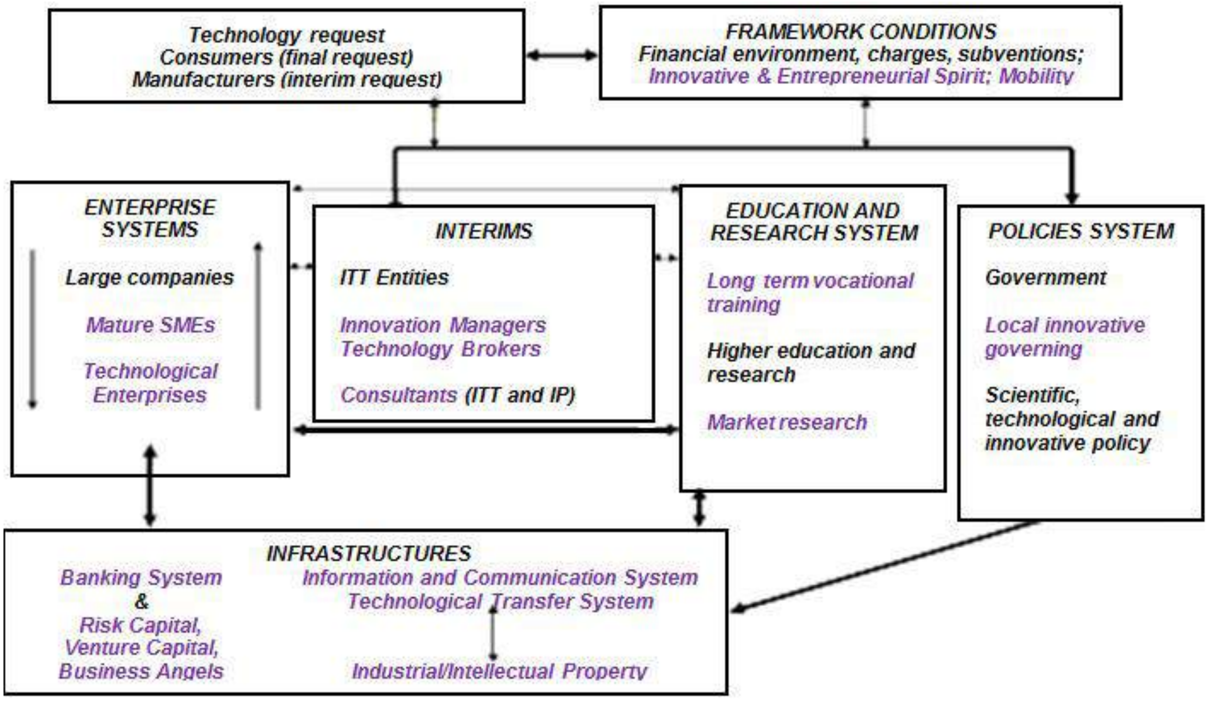

Fig. 2. The necessary mechanisms for a minimum innovative functioning ecosystem

Ecosystem model for the transfer of research results towards the economic environment
No interpretation of the concept regarding to *technologic transfer, spin-off entity or entrepreneurial university* may be used against the idea that the university is an ”Alma Mater” for its students, researchers and professors functioning on academic freedom principles in what regards to knowledge exploitation and access to idea distribution towards the students and the business environment.
The main challenges approached, are linked to insufficient concentration of R&D&I in the excellencies pools capable to compete globally, those of weak element integration within the R&D&I triangle, insufficient trans and inter disciplinary research focused on the innovation needs, lack of some governing and managing models for the European level education and research, by high costs of EU patenting and low mobility of researchers.
One of the pursued objectives consists in the encouragement of partnerships for addressing the local business communities. I believe that there are a number of principles behind the success of an ITT entity: focusing on strong regional points; their functioning in a coordinated network; high reputation and powerful brand; their commercial/trading focus and the independent operation.

8. Partner/Supplier Innovation

Many organizations around the world today don’t stand alone as independent entities. Pretty much any organization you can think have today is somehow aligned with or supplied to another organization. By opening up information and innovating with suppliers and partners both parties will win. Suppliers and partners will be able to provide better products and services that customers are asking for and the organizations will be able to dramatically improve forecasting while dramatically reducing wasted resources and time spent. The earlier the company can bring partners and suppliers into the innovation process the more effective the relationship will be. Innovation is no longer something that can be done by a few people or a single department.

9. Innovation Culture.

I want to stress that there are different ways to analyze innovation ecosystem. You can think about best practices. You can think about frameworks or key pillars that form a system. You can think about historical development and trends that could be analyzed considering successful examples. But I would like to start from one particular issue. This issue is Culture. Innovation Culture.
I personally believe that without innovative culture institutions, based on a functional and efficient eco-system, with infrastructure and funds, the business incubators, clusters, science parks, technology centres, companies simply will not work.

10. Understanding the Innovation Economy

The innovation economy is the economy that transforms knowledge into products, processes and services that fuel competitiveness and economic growth, create employment and wealth, and generate significant improvements in the region's standard of living.
It describes the large and diverse array of participants and resources that contribute to and are necessary for ongoing innovation in a modern economy. This included entrepreneurs, investors, researchers, university faculty, venture capitalists as well as business development and other technical service providers such as accountants, designers, contract manufacturers and providers of skills training and professional development. Sustaining an innovation economy means evolving, adapting, re-imagining and reinventing to create and utilize new ideas and information into both existing and new products and services.

11. Innovation Ecosystem model - Principles and considerations

The model has at its basis the following principles and considerations:

- The establishment/generating of start-ups and spin-offs based upon some developed technologies within Universities and RDI Institutions/Organisations, continuous training, business development methods.
- Banking" department organised as a foundation, to finance the activity by venture capital and business angels.
- A "finance magnet, project generator" department
- All departments need to collaborate with a unitary strategy under a tightly linked University/R&D Entity management.
- The management also ensures the interfacing with the Universities, R&D Entities, Business Environment, Central and Local Administration.
- The departments (total or by fields) may function independently also as profit centres or in a collaboration form under a University/R&D Entity regulation.
- The ITT Entities correlation with the place and attribution defining:
  - Technological development
  - Technological and business incubator
  - Virtual Centre, expanding ITT communication and services towards companies/firms by internet techniques.
  - Technological and Business Park; Competitiveness Cluster; Technological transfer and innovation.

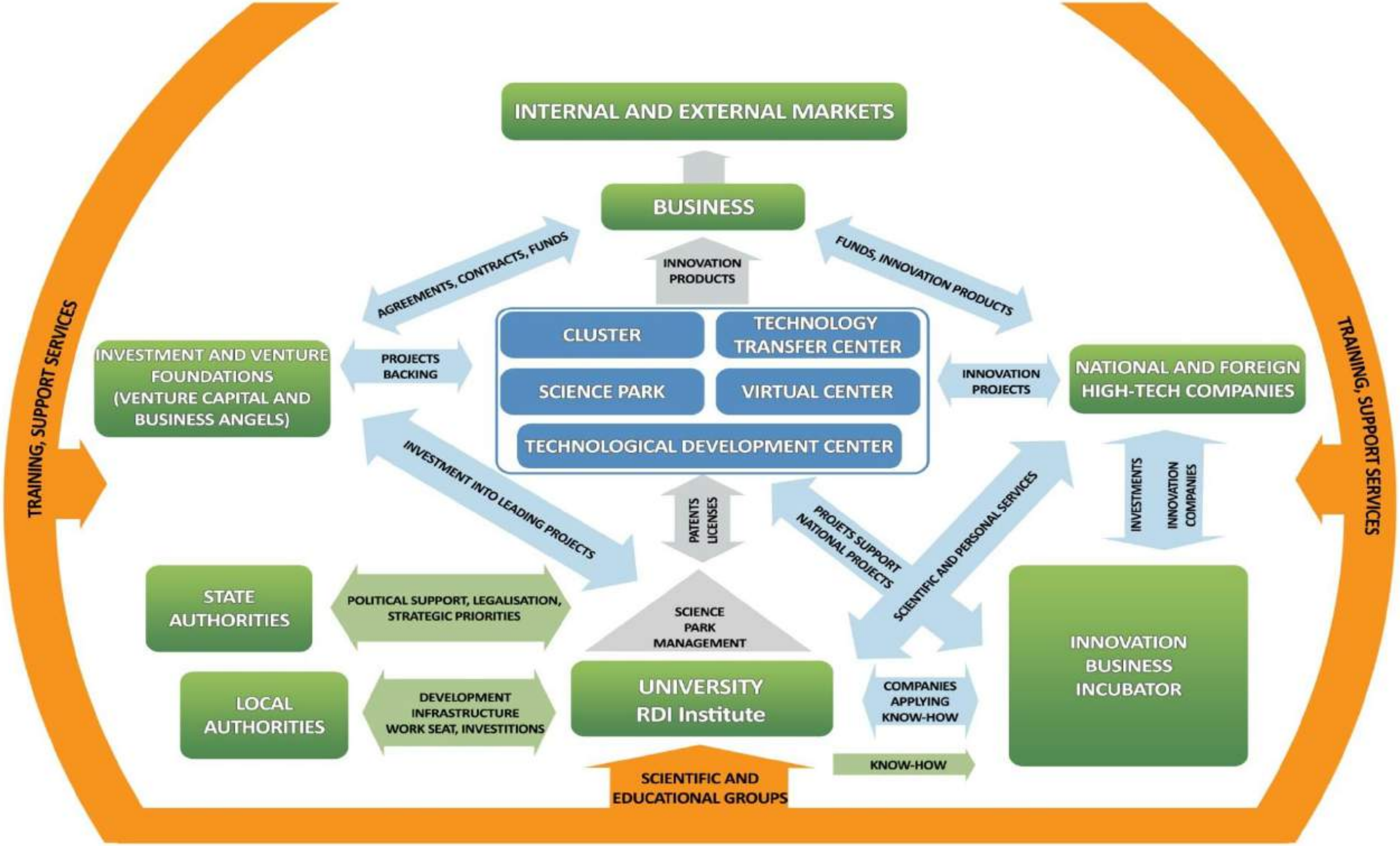

Fig. 3. Ecosystem model for research results transfer towards the economic environment

The link, ITT Entity – Scientific Park – Competitiveness Cluster/Pool with Specialists, High-Tech Companies / with export capacities, Investors, is present in figure 4.

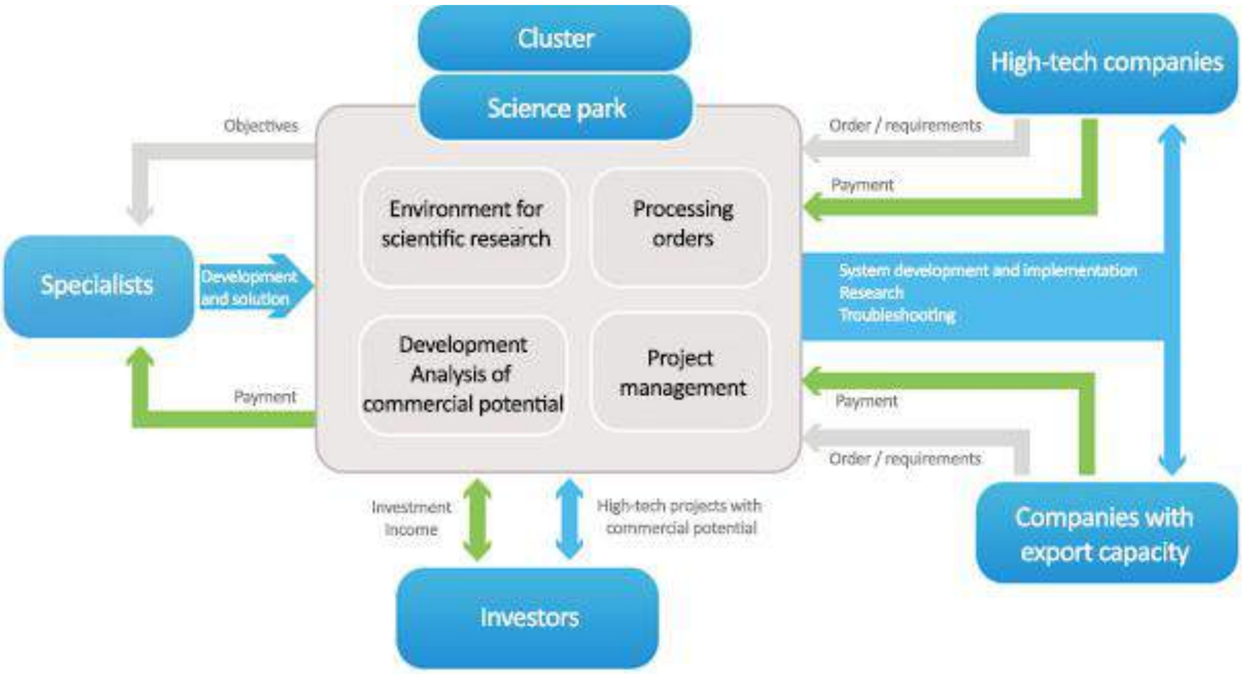

Fig. 4. The link of ITT Entity – Scientific Park – Competitiveness Cluster / Pool with Specialists, High-Tech Companies / with export capacities, Investors

The management of ITT Entities is done in company development steps. Whilst companies develop themselves, they could also be moved in other structures, locations, with adequate spaces, all offering consultancy services, competitiveness, business development, innovation and research.

The flexibility of these ITT Entities from the perspective of offered services and permanent adaptation to market requests, including the staff training requirements, is essential for the efficiency of these ITT Entities and for the commercialization of market results. The presented structures may also work complementary, separately but with a common strategy.

Technological development centre

Are specialized centres (as infrastructure and expertise in staff) for developing new technologies based upon research results (sometimes even from the fundamental research phase). Collaboration with the business environment is essential for the development and commercialization of new solutions.

Technological transfer centre

The technological transfer and commercialization centre plays a major role in the protection and commercialization (trading) of industrial property goods from the Universities and R&D&I Organisations / Institutions, awarding licenses for technology developers and innovative firms, as well as assisting in start-ups initiations, companies which commercialize or produce upon new technologies.

From economy perspectives, as a whole, there’s a risk that a valuable industrial property to remain unused without specific market transfer mechanisms.

The technological transfer offers a great potential for additional incomes.

Technological and business incubator

A technological and business incubator represents a company/department which helps new companies and start-ups to develop their business, helps in business by providing support services in technologies, information, management support, business internationalization, innovation and office spaces.

Technological and scientific park

The technological and scientific parks are large scale projects which host already matured companies on the market having development services integrated in order to expand companies including the laboratories.

They make available delimited terrains/areas, with the necessary infrastructure (water-sewage, electrical energy, gas) and spaces for transportation and warehousing.

Innovative Cluster / Competitiveness Pool

The innovative cluster represents a group of legal personalities constituted upon an association agreement, concluded between organisations from the science and innovation field and/or higher education institutions, on one part, and economic agents, local public administration authorities, paternal or professional associations, on the other part, having the purpose of developing the scientific research activity regarding knowledge and technological transfer of scientific results, valuing them through economic activities.

Project and program department

Starting from the participating companies' structure, the development needs on both sides considering the regional / national / international calls, the department brings up the awareness in what regards the partners, achieves partnerships and attracts financings.

Project financing foundation

The project financing foundation is a bank managed as a foundation which operates under mechanisms as venture capital, risk capital and business angels with the projects proposed by start-up companies, SMEs, Universities, R&D Centres, based upon some reintroducing criteria regarding the invested capital.

This type of foundation magnetises finances from diverse donors and offer opportunities. The bank and sponsors relations need to be permanently considered with the integration in management structures regulating also through public policies and development strategies.

Lack of financing the innovative ideas, patents residing in the idea phase / embryonic inventions represents a barrier in the technological transfer.

The Universities / R&D centres identify and validate the development value and together with the specialist in venture capital / risk capital, permanently supported by consultancy and expertise activities, bring ideas on the market. At this point, commercial, innovative companies intervene with their identification of the potential and bring equipment, systems and services into manufacturing.

Entities management

Entities management represents a key piece which ensures the compatibility, methodology and communication instruments between all the actors, on both sides being an interface with the business environment. In essence, besides the management function it also includes the facility function.

It should have the skill to communicate with the two large groups: the research and respectively the business environment, meaning that it needs to master their specific and motivational language in equal measure.

Scientific and educational groups

They have the role to know the real state on the market and in research, forming trends and methodologies, identify research themes which once outsourced may be applied on the market, research groups, identifying the research results and communicating them to the business groups.

On the other part, it's essential to train all specialists working in all of these entities and infrastructures with the business environment included as well (both professional and entrepreneurial). The continuous training, practical activity and specialists selecting may be interest themes of the business environment.

Learning in SMEs

As environmental problems came more and more into focus, concepts as eco-innovative entrepreneurship, new business strategy that incorporates sustainability throughout all business operations based on life cycle thinking and in cooperation with partners across the value chain.

SMEs are restricted in the efficient use of technology for learning and in adequate management learning approaches. The managers should understand the importance of using other forms of learning like mobile ones, webinars, access to on-demand learning resources and social learning supported by social media.

Problem-based learning-PBL is an exciting alternative to traditional classroom learning. With PBL, the teacher presents you with a problem, not lectures or assignments or exercises. Since you are not handed "content", your learning becomes active in the sense that you discover, work with content that you determine to be necessary to solve the problem. The teacher acts as facilitator / mentor, rather than a source of "solutions"

Local administration

Has the role to offer spaces, locations, in order to develop the activities, support for clusters and technological and scientific parks, presenting local and regional strategies for development so that the technological needs for development are identified.

On the other part, the local administration is a beneficiary of the development studies performed by the university, departments and/or entities.

Central administration

The link needs to be bi-univocal both as beneficiary of public policies and as generator, identifier of market needs.

R&D Entity /University

Have two collaboration paths with this structure by The Entity Management Department – offering research results and receiving research-innovation themes as necessity, respectively the scientific and educational groups – offering scientific and educational services and receiving scientific and educational themes as necessity.

The R&D Entity / University is the organism which manages the activity, measures the results on the market, creates methods and functioning regulations, and controls the activity.

National and International High-Tech Companies

Usually they have their own research-development and innovation groups.

At the same time, they need a powerful training component to know and offer research themes sometimes fundamental and of large perspective.

The expertise and high level competences are absolutely necessary.

These companies may be interested by research results, technological transfer and new themes generators with potential market results.

To become a partner of the technological and scientific park, a partnership agreement may be signed. Likewise, these companies may also be members in the competitiveness clusters / pools or may conclude partnership agreements with the R&D institutions / organisations or may activate independently and collaborate punctually in accordance with the necessities. A partnership agreement foresees:

- The mutual participation to the achievement of innovative projects in the field of high-end technologies, new efficient ways to manufacture and implement competitive high-end technology products on internal and international markets.
- Development of mutual investment programs in the innovation sectors of the economy in order to magnetise direct foreign investments
- Representation and defending the mutual interests deriving from statutory aims of the contractual parties.
- Promoting the efficient development of innovative structures in the technological and scientific park.

Innovation promoting activity – Innovative projects competition

The competition is organised in collaboration with the entities from the eco-innovating structure, innovative companies, business development and innovation funds and professional associations.

The purpose of the competition is to find the best suited technological activity for commercializing and developing the innovative activity, to create partnerships, to attract young people, students, the scientific and business community to participate at the technological transfer promoting cooperation between scientists, businessmen / businesswomen and government for the innovative development of economics and it integration in the European and global space with high-end technology.

The competition focuses on innovative businesses oriented projects which have a scientific and practical value and which can be introduced in production and used in the economic activity with the proper social or economic effect.

12. How do you Measure Innovation Results and Outcomes

If we define innovation as "people creating new value and capturing value in a new way," there are basically some focal points to measure it:

- Past / current innovation performance
- The demonstrated ability to create and capture sustainable and profitable value from innovation
- Future/expected innovation potential
- Effective/efficient innovation capacity
- The activated capacity to realize the firm's full growth and innovation potential

Innovation management covers many aspects from business intelligence to idea generation to managing intellectual property and working with innovation partners. To focus on the whole chain in a more balanced way, it is recommended that companies utilize a diagnostic tool to assess the quality of the different links.

The Assessment report provides a comprehensive picture of your firm's innovation management performance and capacity. The report has a main section with key information on firm's innovation management performance and a section with valuable detailed information on the company. It presents performance scores and compares them with the scores of the Growth Champions and the average for your benchmarking class.

The evaluation assesses five dimensions: Innovation Strategy, Innovation Organisations and Culture, Innovation Life Cycle Processes, Enabling Factors and Innovation Results. The "spider" diagram shows your performance on each dimension.

Based on standard compliant assessment tools and the largest benchmarking database on innovation management, companies can compare their innovation management capabilities and performances against the average scores of thousands of direct or indirect competitors.

.

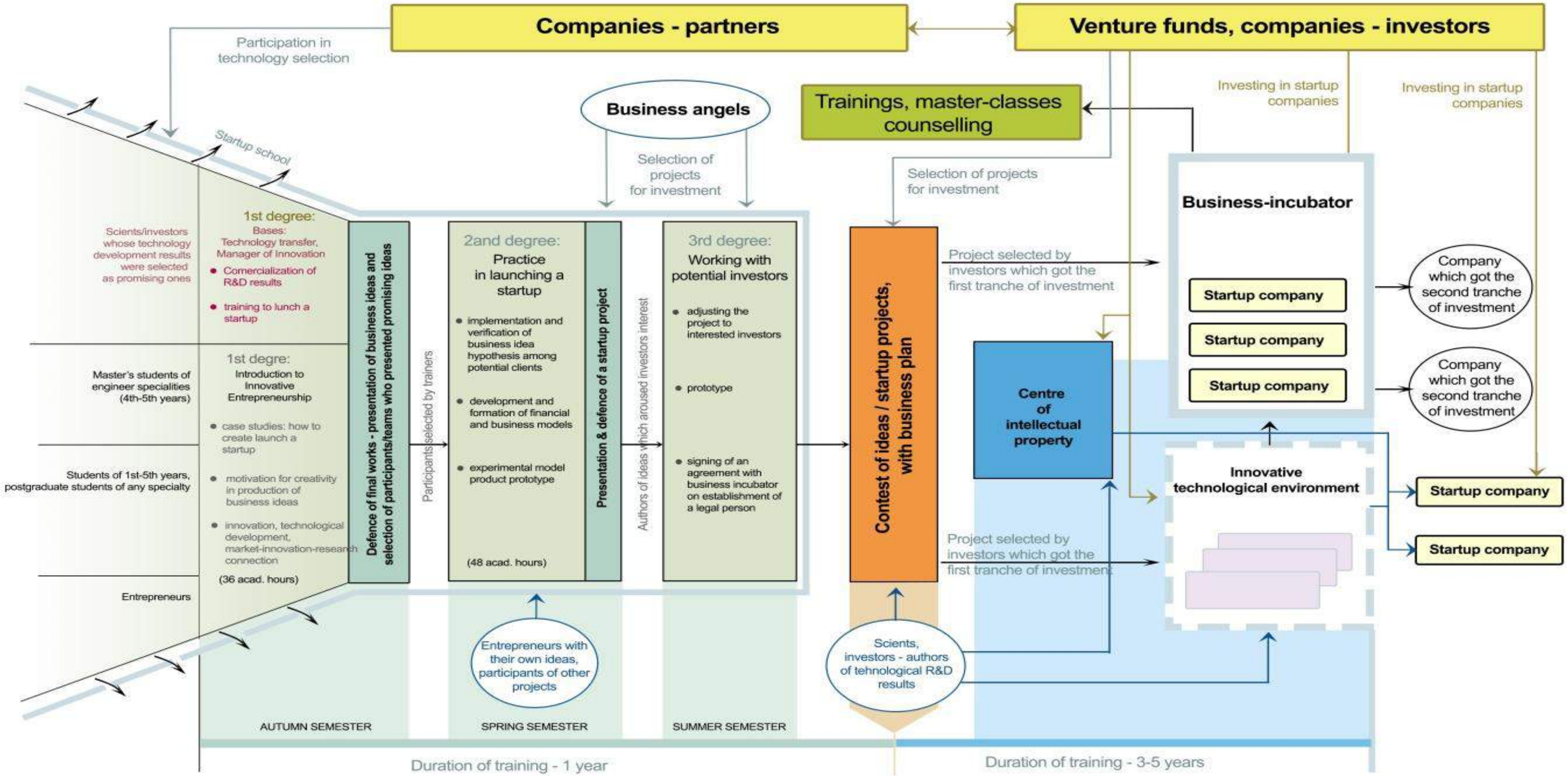

Fig. 5. Forming entrepreneurships; selection of projects to create start-ups/spin-offs

The advantages:
For high-end technology companies:
- Development of new technological solutions and creating new competitive products
- Reducing the innovative cycle and implementing the idea into the product
- Reducing the risk of creating and manufacturing non-competitive products
- Attracting competitive specialist to promote intensive scientific products

For investments and risk funds:
- Availability of implemented innovative projects ready to be promoted on the market
- Availability of innovative projects in an incomplete implementation phase
- Innovative development ”bank”; Profitable developments fields
- High-end technology logic efficiency warranty and profitability of invested developments
- Reducing the invested funds, full payment period
- Implementation potential of the end result on large scale
- Interaction with the state at governmental level

Projects coordinated in a transparent manner:
- Investor and project managers
- Investment fund control, target use
- Development and implementation process control

For research-development entities and scientists:
- Financial and technological conditions to achieve and promote innovative ideas on the market
- Obtaining the copyrights – remuneration for the developed and patented use, popularity amongst business and scientific circles

For faculties and departments:
- High certification training and graduating specialists with practical and theoretical knowledge application.
- Developing a laboratory scientific basis with high-end equipment
- University and students’ involvement in innovative businesses.

For government:
Nationally:
- Accelerating the innovative economic development
- Preventing the ”brain exodus”; Increasing the nation’s life quality
- Increasing the foreign investments and possibilities of exportation

Locally:
- New high-end tech jobs
- Increase the standard living level
- Consolidating the staff component in the technical and scientific potential of the region
- Attracting regional investments; improving regional infrastructure.

Horizon 2020: Commission Work Programme: towards EU's future in 2025 and beyond
The Commission Work Programme 2018 released on 24 October lays the groundwork for concrete actions that will complete the work on President Juncker's 10 political guidelines. The boost of jobs, growth and investment through the Circular Economy Action Plan is at the core of the Commission’s agenda for the year ahead.
The work programme shows how the Commission plans to give practical effect to the political priorities set out by the President. It provides a multiannual overview to help stakeholders and the other EU institutions plan their work with the Commission.
Europe is visibly regaining its strength. The European Union is now in its fifth year of an economic recovery that reaches every single Member State. With growth now above 2% for the EU as a whole – and 2.2% for the euro area – Europe's economy has grown faster than that of the United States over the last two years. Almost 8 million jobs have been created during this mandate,

thanks in part to the work of the EU Institutions, the contribution of the European Fund for Strategic Investments, the Youth Guarantee, the European Structural and Investment Funds, and the monetary policy of the European Central Bank. Confidence and trust in the European Union is returning. Leaders in Rome in March declared their will to make the European Union stronger and more resilient, through even greater unity and solidarity and the respect of common rules.
Europe now has a window of opportunity – but one that will not stay open forever. To make the most of the current momentum, the Commission is tabling its work programme for the next 14 months to the end of 2018. This builds on the Roadmap for a More United, Stronger and More Democratic Union, which President Juncker presented alongside his State of the Union address on 13 September 2017. It will help keep Europe on track by continuing to deliver on its positive agenda, and it will ensure that Europe's focus remains firmly on the big things, where European action has a clear and demonstrable added value.
On the Participant Portal
http://ec.europa.eu/research/participants/portal/desktop/en/funding/reference_docs.html#h2020-work-programmes-2018-20
you can find all the H2020 reference documents starting with legal documents and the Commission work programmes for research and innovation up to model grant agreements and guides for specific actions and horizontal issues. The documents are grouped by categories. It also includes reference documents of other EU programmes, as 3rd Health, Consumer, COSME and Research Fund for Coal and Steel programmes.

- Legislation
- Work Programmes
  - ✓ Main WP
    - Future and Emerging Technologies (FETs) 2018-20
    - Information and communication technologies (ICT) 2018-20
    - Nanotechnologies, advanced manufacturing and processing 2018-20
    - Innovation in SMEs 2018-20
    - Secure, clean and efficient energy 2018-20
  - ✓ General Annexes to the Main WP
  - ✓ European Research Council
  - ✓ Euratom
- Grant agreements, contracts and rules of contest
- Guidance
- Templates & forms
- Expert names (annual lists)

13. Conclusions

The first step in creating a sustainable commercialization of research results, Technological Transfer – TT mechanism, on one hand is to define the “technology” which will be transferred and on other hand to define the context in which the TT mechanism work, the ecosystem.
The innovation ecosystem model brings together new companies, experienced business leaders, researchers, government officials, established technology companies, and investors. This environment provides those new companies with a wealth of technical expertise, business experience, and access to capital that supports innovation in the early stages of growth. It is necessary to develop an IT system to allow ecosystem to insert data and connect each to other. The monitoring and measurement of the performance of the ecosystem is mandatory.
It is necessary to consider education, **entrepreneurial culture**, and personal formation, on each stage of development of eco-innovation models. Meanwhile development models should work in innovative eco-systems, and functional complex that creates competitiveness and added value.
I want to remember a quote by Victor Hwang (author of Innovation Rainforest) who said that “*E**conomies thrive when culture overcomes social barriers and fosters connectivity, trust, and collaboration between diverse people…***” Think about that.

References

[1] S. Fulga, Al.Marin, Al. Hadăr, D. M. Badea, G. Vlăduţ, B. Ciocănel, D. Bucur, I. Ivan, L. Boanţă, "Business models for increasing technological transfer effectiveness", *Forum for Innovation*, Bucharest, 2016, Conference;
[2] ***, How to Create an Innovation Ecosystem, Art Markman, Harvard Business Review, https://hbr.org/2012/12/how-to-create-an-innovation-ec;
[3] J. Morgan, "The Innovation Ecosystem for the Future of Work", Forbes, http://www.forbes.com/sites/jacobmorgan/2015/08/12/innovation-ecosystem-future-of-work/#2c1f3d5b6079;
[4] V. Ryzhonkov, "Innovation Ecosystems: Why Culture is the Key Element", https://worldbusinessincubation.wordpress.com/2013/11/05/innovation-ecosystems-why-culture-is-the-key-element/;
[5] ***, The Massachusetts Innovation Economy, http://masstech.org/innovation-ecosystem;
[6] ***, How do you Measure Innovation Results and Outcomes? http://www.innovationmanagement.se/imtool-articles/how-do-you-measure-innovation-results-and-outcomes/;
[7] I. Hamburg, G. Vlăduţ, E. O'Brien, "Fostering Eco-innovation in SMEs through Bridging Research, Education and Industry", *Forum for Innovation*, Bucharest, 2016, Conference;
[8] G. Teodorescu, G. Vlăduţ, "Integral Innovation and Innovation Management Assessment", Forum for Innovation, Bucharest, 2016, Conference;
[9] ***, The Commission Work Programme 2018.

http://hervex.ro